
**CEDR Transnational Road Research Programme
Call 2013: Energy Efficiency –
Materials and Technology**

funded by Germany, Norway, UK,
Austria and Slovenia



Conférence Européenne
des Directeurs des Routes
Conference of European
Directors of Roads



Functional Durability-related Bitumen Specification (FunDBitS)

Identified correlations between bitumen and asphalt properties

Deliverable No D.1
April 2015

Czech Technical University in Prague (CTU), Czech Republic
University of Kassel (UoK), Germany
Belgian Road Research Centre (BRRC), Belgium
Slovenian National Building & Civil Engineering Institute (ZAG), Slovenia
Transport Research Laboratory (TRL), UK
École Polytechnique Fédérale de Lausanne (EPFL), Switzerland
European Asphalt Paving Association (EAPA), Belgium
Laboratório Nacional de Engenharia Civil (LNEC), Portugal
ASMUD, Turkey
Vienna University of Technology (TU Vienna), Austria
Nynas NV, Belgium

CEDR Call 2013: Energy Efficiency – Materials and Technology

FunDBitS Functional Durability-related Bitumen Specification

Identified correlations between bitumen and asphalt properties (Interim Report)

ITERIM REPORT

Due date of deliverable: 30/05/2015
Actual submission date: 31/12/2015

Start date of project: 01/05/2014

End date of project: 31/09/2015

Authors this deliverable:

Cliff Nicholls, TRL, UK
Jan Valentin & Lucie Soukupova, CTU, Czech Republic
Konrad Mollenhauer, UoK, Germany
BRRC, Belgium
Marjan Tušar, ZAG, Slovenia
Nicolas Bueche & Sara Bressi, EPFL, Switzerland
Carsten Karcher, EAPA, Belgium
Fátima Batista & Margarida Sá da Costa, LNEC, Portugal
Gülay Malkoc, Asmud, Turkey
TU Vienna, Austria
Hilde Soenen, Nynas NV

PEB Project Manager: Gerhard Eberl (ASFINAG), Austria

Table of contents

Executive summary	i
1 Introduction.....	1
1.1 BiTVal project	1
1.2 Current need.....	1
1.3 FunDBitS project organisation	2
2 Data.....	4
2.1 Conferences reviewed	4
2.2 Other sources	4
2.3 Data form.....	4
2.4 References	4
3 Bitumen tests.....	6
3.1 Bending Beam Rheometer (BBR) Test	6
3.2 Binder Fatigue Test	7
3.3 Capillary Viscometer Test	8
3.4 Coaxial Cylinder Viscosity Test.....	9
3.5 Cone and Plate Viscosity Test	11
3.6 Creep Zero Shear Viscosity Test	11
3.7 Direct Tensile Test (DTT).....	14
3.8 Complex shear modulus and phase angle by Dynamic Shear Rheometer (DSR) Test	15
3.9 Elastic Recovery Test	16
3.10 Force Ductility Test.....	16
3.11 Fraass Breaking Point Test.....	18
3.12 Fracture Toughness Test (FTT)	19
3.13 Multiple Stress Creep and Recovery (MSCR) Test	20
3.14 Oscillatory Squeeze Flow Rheometer	21
3.15 Oscillation Zero/Low Shear Viscosity (ZSV/LSV) Test	23
3.16 Penetration Test	25
3.17 Penetration Index	25
3.18 Repeated Creep Test	26
3.19 Softening Point (Ring and Ball) Test	28
3.20 Tensile Test.....	29
3.21 Vialit Pendulum Test.....	30
4 Binder conditioning regimes.....	31
5 Permanent deformation (rutting)	33
5.1 Asphalt test methods for permanent deformation.....	33
5.1.1 General	33
5.1.2 Wheel tracking test.....	33
5.1.3 Cyclic compression test according to EN 12697-25.....	34
5.1.4 SUPERPAVE shear tester.....	35
5.1.5 Simple Performance Tests (SPT)	35
5.1.6 Coaxial Shear Test (CAST)	36
5.1.7 Carleton in-situ shear strength test.....	36
5.2 BitVal findings on permanent deformation	37
5.3 Relationship found between bitumen properties and asphalt resistance to permanent deformation.....	38
5.3.1 General	38
5.3.2 Capillary Viscometer Test.....	38
5.3.3 Coaxial Cylinder Viscosity Test	40
5.3.4 Cone and Plate Viscosity Test.....	40

5.3.5	Creep Zero Shear Viscosity (ZSV) Test.....	40
5.3.6	Complex shear modulus and phase angle by Dynamic Shear Rheometer (DSR) Test	41
5.3.7	Elastic Recovery Test.....	61
5.3.8	Multiple Stress Creep and Recovery (MSCR) Test.....	61
5.3.9	Oscillation Zero/Low Shear Viscosity (ZSV/LSV) Test.....	85
5.3.10	Repeated Creep Test	86
5.3.11	Ring and Ball (R&B) Softening Point Test.....	89
5.3.12	PG grading.....	96
5.4	Binder ageing effect on permanent deformation	107
5.5	Overall uncertainty of correlations.....	107
5.6	References for permanent deformation.....	107
6	Stiffness.....	111
6.1	Asphalt test methods for stiffness	111
6.2	BitVal findings for stiffness.....	111
6.3	Relationship found between bitumen properties and asphalt stiffness	112
6.3.1	General	112
6.3.2	Dynamic Shear Rheometer (DSR)	139
6.3.3	Bending Beam Rheometer (BBR).....	153
6.3.4	Direct Tensile Test (DTT)	153
6.3.5	Needle penetration	153
6.3.6	PG grading.....	160
6.4	Binder ageing effects on stiffness	172
6.5	Effects of different additives and modifiers.....	177
6.6	Overall uncertainty of correlations.....	194
6.7	References for stiffness	194
7	Low temperature cracking.....	197
7.1	Asphalt test methods for low temperature cracking.....	197
7.1.1	General	197
7.1.2	Test procedures with uniaxial loading.....	197
7.1.3	Test procedures with non-uniaxial loading at low temperatures.....	199
7.1.4	Test procedures addressing fracture energy approaches	200
7.2	BitVal findings for low temperature cracking	200
7.3	Relationship found between bitumen properties and asphalt low temperature cracking	202
7.3.1	Binder-Mix relationship reported for TSRST	202
7.3.2	Binder-Mix relationship reported for other uniaxial test methods on asphalt mixtures	221
7.3.3	Binder-Mix relationship reported for results of IDT.....	222
7.3.4	Binder-Mix relationship reported for results of fracture energy assessments	224
7.3.5	Relationship between binder low-temperature properties and site cracking	225
7.4	Ageing effect on low temperature cracking	227
7.5	Overall uncertainty of low temperature cracking	228
7.6	References for low temperature cracking.....	228
8	Fatigue cracking	231
8.1	Asphalt test methods for fatigue cracking	231
8.1.1	Other test protocols for fatigue testing.....	232
8.2	BitVal findings for fatigue cracking.....	249
8.3	Relationship found between bitumen properties and asphalt fatigue cracking.....	250
8.3.1	Correlation between binder and asphalt properties in fatigue resistance ..	250
8.3.2	Polymer modified binders effect on asphalt fatigue resistance.....	274

8.3.3	Fatigue life of unconventional mixtures.....	321
8.3.4	Fatigue life and healing effect.....	331
8.4	Binder ageing effect on fatigue cracking	333
8.5	Overall uncertainty of fatigue cracking	337
8.6	References for fatigue cracking	357
9	Binder/aggregate interaction	360
9.1	Asphalt test methods for binder/aggregate interaction	360
9.2	BitVal findings for binder/aggregate interaction.....	361
9.3	Bitumen tests correlating with binder/aggregate interaction	362
9.3.1	General	362
9.3.2	Tests conducted on compacted mixtures	363
9.3.3	Tests conducted on loose coated aggregate	370
9.4	Binder ageing effect on binder/aggregate interaction	373
9.5	Overall uncertainty for binder/aggregate interaction.....	373
9.6	References for binder/aggregate interaction	373
10	Conclusions	375
11	Acknowledgement	376
Annex A:	Relevant papers identified.....	1

Executive summary

This report presents an extensive review of existing knowledge available worldwide in the field of bitumen testing, bitumen durability assessment and the relation between bitumen and asphalt mixture properties. The results are shown for plenty of technical or scientific papers summarizing their contents and providing basic comments. The attention in this respect was paid to identifying possible contexts and relationships between the assessments done for the binder and the final composite material. Based on the results presented in this report it is then possible to more deeply analyze, verify and delimitate possible correlations for selected properties or performance-related characteristics. It is of course always important to focus also on the conditions of the tested material. A key role in this connection plays unambiguously ageing and how this phenomenon is presently included in bitumen or asphalt mixture assessment or how it should be reflected in the future if durability of asphalt pavements might be better defined and predicted.

The report is divided into 10 chapters providing a complex work based on analysing more than 560 papers or research studies related to the bitumen testing and the relations between binder properties and asphalt mixture characteristics. These papers and studies are selected for the time period of 2007 to 2014 providing a kind of follow-up to the earlier European BitVal project. For this reason the BitVal findings and conclusions are included in different parts of this report.

The first chapter provides the actual needs and motivation factors, why better and more advanced assessment of bitumen durability is needed. These demands are not only based on some requests or desires to technically or scientifically better understand the road material bitumen and thereof resulting asphalt composite but from the simple need understand better the long-term behaviour being able to predict and plan life-time, to correctly improve the materials and to achieve a life-cycle oriented approach. In this relation the FunDBitS mission and project structure is explained and summarized. Following chapter provides then the approach to get proper data, how to gather them and later sort and analyse.

Third chapter gives a good overview about the bitumen tests which are presently available. The resented list and description of bitumen test should not be understood as full-range and exhausting summary of what is world-wide available. Presented tests are either applied in Europe according to EN standards, or are under discussion, or are known to European bitumen and asphalt experts and have been experimentally used or at least analyzed. The use of some of them is of course very limited because of laboratory equipment needed or simply because of lack of experience and relevant data. The chapter provides traditional empirical tests known for decades (like penetration or softening point) which are often criticized for limited information they do provide about the real behaviour of bitumen. They are simple and with limited relation to the real behaviour of an asphalt pavement (asphalt layers) but they provide still a good way to classify bituminous binders. Of course their limitations become visible as soon as we start to speak about functional binders modified or treated by various modifiers and additives. In all these cases more advanced performance-based or performance-related tests are needed and for the future even an approach combining mechanical behaviour and chemical characteristics will be needed and will lead to introduction of a new attitude introducing mechano-chemistry. Nevertheless, this is not part of FunDBitS project and the assessments which have been done and will be provided later by the follow-up reports. In terms of functional testing the reports therefore provides a summarized description of tests which are available for assessing permanent deformation, stiffness, fatigue or bitumen behaviour in low temperature range related to cracking.

Chapter 5 to 9 are related to the key identified aspects of bitumen and asphalt mixture behaviour. These five groups of performance-related characteristics are structured always in a same way and were applied for the analysis of all relevant papers and studies as described earlier. For each of this behaviour type applicable and potentially usable test methods are described. As a second step the relation of the assessed characteristics and the conclusion and key findings of BitVal project is identified and described to provide for the future a good continuity between both projects. Finally from the extensive analysis found or potentially existing relations between bitumen behaviour or properties and the asphalt mixture performance and characteristics are provided. This part of the report is divided according to the original structuring of the FunDBitS project in the areas of:

- Permanent deformations.
- Stiffness.
- Low temperature cracking.
- Fatigue life.
- Bitumen / aggregate interactions (adhesion and cohesion phenomena).

These five selected areas are believed to seamlessly cover the term of durability of either the bituminous binders or related asphalt mixtures. Of course each of the related characteristics is influenced also by the natural ageing of bitumen which should be in the future considered even more than is specified in technical standards and product-related characteristics today.

1 Introduction

1.1 *BiTVal project*

It has long been recognised that the binder properties alone do not determine pavement performance. Other parameters, such as aggregate characteristics, mixture design, manufacture and laying are also considered as important. A process needed to be followed to ensure that, for the second generation of bitumen standards, the performance relationships of a binder property were assessed before a specification was developed. The basic sequential steps were as follows:

- (1) Identify the binder properties linked to the performance requirements of asphalt pavements.
- (2) Select and standardise appropriate (new) test methods to measure these properties.
- (3) Collect data and ensure field validation for establishing (new) binder specifications.
- (4) Review the grading system according to the (new) specification.

CEN TC336 working groups addressed steps (1) and (2). To address step (3), FEHRL proposed to organise a European project on validation of the new EN test methods, and this was presented and discussed at the BiTSpec seminar in June 2003.

The FEHRL Board agreed that the first phase of the project, named BiTVal, should go ahead as a desk study, analysing information gathered from all sources, and additional work needed would be identified during this process. Ten national research organisations from across Europe (LNEC, CEDEX, ISTU, TRL, LCPC, BAST, NPRA, VTI, LCPC, BRR, IBDiM and ZAG), which had to find their own funding, comprised the consortium undertaking the research supported by European stakeholders EAPA, CEN TC336, FEHRL and Eurobitume.

This BiTVal project represented a significant effort, requiring support and participation from industry and authorities in many countries. It was expected to:

- Deliver the appropriate answers for assessing the suitability of test methods.
- Establish their relevance and correlation to the asphalt pavement performance.
- Give the required level of confidence in the future specification system to be used during many years in the whole of Europe.

The key outputs of the BiTVal project were a database, covering publications of the identified bitumen properties and their relationship to asphalt properties and/or road performance, and a FEHRL report to TC336 WG1 summarising the P-R aspects for each test method, together with recommendations for their use in 2nd generation standards. However, it is now several years since the BiTVal report was published.

1.2 *Current need*

More than 80 % of the European Road Network is paved with asphalt materials. Energy efficient asphalt pavements can be built by using durable pavement materials in order to avoid or postpone maintenance and rehabilitation works. In order to improve the durability of asphalt materials, performance-based specifications were introduced for relevant asphalt mixtures. The asphalt types consist of aggregate particles in a specific grading and bitumen, the viscoelastic properties of which largely predetermine the mechanical asphalt properties. Although the durability of asphalt mixtures is highly dependent on the properties of the bituminous binder, these are specified based on empirical test procedures (Softening Point

Ring and Ball, penetration) which were devised around 100 years ago. It is well known that these test methods do not allow a prediction of asphalt mix performance, particularly for polymer-modified binders which are often used in heavily-loaded asphalt materials. In addition, the ageing of bitumen (which has a crucial effect on binder properties and thus on pavement performance), its durability and recyclability are not taken into account by European specifications in terms of performing functional testing after short- or long-term ageing. To cover these aspects, functional performance-based bitumen test procedures were developed in the past and are widely applied for evaluating the binder's effects on the asphalt mixture's performance. For asphalt mixtures, performance-based specifications were introduced with EN 13108-series in 2006, whilst performance-based bitumen specifications are still not implemented in EN 12591 (paving grade bitumens), EN 14023 (polymer modified bitumens) and EN 13924 (hard paving grade bitumens). In EN 14023 latter, standard specific performance-based test methods are discussed only as a guideline.

During the BitVal project, an extended study was performed in order to evaluate correlations between bitumen and asphalt mixture properties. Resulting from that research, bitumen characteristics were researched for which good correspondences with performance-based asphalt mixture properties could be found. However, due to the limited number of research results available and discrepancies between the test conditions in both the bitumen and asphalt test procedures, it was too early to draw firm conclusions for specifications from those results.

In the meantime, performance-based asphalt test procedures were applied Europe-wide in order to evaluate the mechanical properties of asphalt mixtures. Since the introduction of performance-based test methods in the EN 12697-series, in particular, Parts 12 (water sensitivity), 24 (fatigue), 25 (rutting resistance), 26 (stiffness) and 46 (low-temperature cracking) have harmonised the relevant test methodologies within Europe. In order to find correlations between binder and asphalt mixture properties, a lot of research has been conducted internationally since then which should allow stronger proposals to draft specifications for paving grade and polymer-modified bitumens that will broadly improve the durability, and thus the energy efficiency, of asphalt pavements. Furthermore, asphalt producers who improved the asphalt mixture properties during mix design were also forced to conduct tests on bitumen performance characteristics in order to establish quality control for their products. Therefore, data from the asphalt industry are available which will allow the correlation of asphalt and binder performance-based characteristics to be determined.

1.3 FunDBitS project organisation

Functional Durability-related Bitumen Specification (FunDBitS) is a project from the CEDR Transnational Road Research Programme Call 2013 for Energy Efficiency: Materials and Technology funded by Germany, Norway, the United Kingdom, Austria and Slovenia. The consortium undertaking the research is led by Czech Technical University in Prague with ten further partners, these being University of Kassel, Belgian Road Research Centre, Slovenian National Building and Civil Engineering Institute, TRL Limited, École Polytechnique Fédérale de Lausanne, European Asphalt Pavement Association, Laboratório Nacional de Engenharia Civil, Turkish Asphalt Contractors Association, Vienna University of Technology and Nynas NV. As such, the consortium has representatives across Europe and across the industry.

In the FunDBitS project, the data that has become internationally available since the BitVal project are being reviewed in order to develop performance-based bitumen characteristics which may be introduced into bitumen specification standards EN 12591, EN 14023 and EN 13924. The correlations found may also be applied for special binder products containing various additives or modifiers (e.g. waxes or crumb rubber). By having all stake-holder

parties involved in the project, including national road research laboratories, universities, asphalt industry and bitumen producers, the required discussions on the feasibility of test procedures and the results for the specification will shorten the later discussions in CEN TC336 committee and its working/task groups, in particular CEN TC336 WG1/TG5 'Framework P-R Specification for Bituminous Binders'. In particular, the new data sources will be evaluated for proposing a system for performance-based bitumen specifications. These will be based on:

- proposed changes of EN 12591, EN 14023 and EN 13924 for bitumen characteristics applied for performance-based specifications;
- changes of bitumen test procedures in order to be more precise on test conditions and to improve the test precision;
- proposed changes for EN 13108 including suitable bitumen performance characteristics for selected asphalt mixture types.

When the next 5-year reviews for the bitumen specification standards are scheduled in 2015, the results of FunDBitS will be available. However, this report gives the initial findings of the FunDBitS project.

2 Data

2.1 Conferences reviewed

Papers from the following international conferences that took place between 2007 and 2014/15 were included in the review:

- Association of Asphalt Paving Technologists (AAPT)
- Australian Road Research Board (ARRB)
- Environmentally Friendly Roads (ENVIROAD)
- Eurasphalt & Eurobitume
- European Asphalt Technology Association (EATA)
- European Pavement and Asset Management Conference (EPAM)
- Four Point Bending (4PB) workshop
- International Conference on Bearing Capacity of Roads, Rail and Airfields (BCRRA)
- International Conference on Bituminous Mixtures and Pavements
- International Conference on Sustainable Pavement Engineering and Infrastructures
- International Conference on Transport Infrastructures (ICTI)
- International Conference on Warm Mix Asphalt
- International Road Federation (IRF)
- International Society for Asphalt Pavements (ISAP)
- International Union of Laboratories and Experts in Construction Materials (RILEM)
- Maintenance and Rehabilitation of Pavements and Technological Control (MAIREPAV)
- Road Engineering Association of Asia and Australasia (REAAA)
- Transport Research Arena (TRA)
- Transportation Research Board (TRB)

The papers found to be potentially relevant are given in Annex A.

2.2 Other sources

In addition, some national conferences were also reviewed together with international and national journals. Again, the papers found to be potentially relevant are given in Annex A.

2.3 Data form

In the review, papers which covered details of both binder and asphalt properties were identified and the data form, as shown in Figure 2-1, completed on a page of an Excel spreadsheet. The data from the spreadsheets were then incorporated into a database that can be searched for papers covering specific pairs of data.

2.4 References

Because of the number of papers reviewed, references will be given by chapter using the Harvard system. However, the FunDBitS reference will also be given for continuity.

REVIEWER		REFERENCE	
Name:		Title:	
Affiliation:		Authors:	
		Source:	

Binder properties	Mixture properties
-------------------	--------------------

<p style="text-align: center;">Elevated service temperature properties</p> <table border="1" style="width: 100%; border-collapse: collapse;"> <tr><td>Complex modulus</td><td>DSR</td><td></td></tr> <tr><td></td><td>other</td><td></td></tr> <tr><td>Dynamic viscosity</td><td>Cone&Plate</td><td></td></tr> <tr><td></td><td>Coaxial cylinders</td><td></td></tr> <tr><td></td><td>Capillary viscosimeter</td><td></td></tr> <tr><td></td><td>other</td><td></td></tr> <tr><td>Low Shear Viscosity</td><td>Oscillation method</td><td></td></tr> <tr><td></td><td>Creep method</td><td></td></tr> <tr><td></td><td>other</td><td></td></tr> <tr><td>Softening point</td><td>R&B</td><td></td></tr> <tr><td>Creep stiffness</td><td>Repeated Creep Test</td><td></td></tr> <tr><td>Compliance and recovery</td><td>MSCR test</td><td></td></tr> <tr><td></td><td>Elastic recovery</td><td></td></tr> </table> <p style="text-align: center;">Intermediate and/or low service temperature properties</p> <table border="1" style="width: 100%; border-collapse: collapse;"> <tr><td>Complex modulus</td><td>DSR</td><td></td></tr> <tr><td></td><td>other</td><td></td></tr> <tr><td>Penetration</td><td>Penetration</td><td></td></tr> <tr><td>Low temperature stiffness</td><td>BBR</td><td></td></tr> <tr><td></td><td>Direct Tensile Test</td><td></td></tr> <tr><td></td><td>other</td><td></td></tr> <tr><td>Cohesion</td><td>Force ductility</td><td></td></tr> <tr><td></td><td>Direct Tensile Test</td><td></td></tr> <tr><td></td><td>Fracture toughness test</td><td></td></tr> <tr><td></td><td>other</td><td></td></tr> <tr><td>Fatigue</td><td>Binder fatigue test</td><td></td></tr> <tr><td></td><td>other</td><td></td></tr> </table>	Complex modulus	DSR			other		Dynamic viscosity	Cone&Plate			Coaxial cylinders			Capillary viscosimeter			other		Low Shear Viscosity	Oscillation method			Creep method			other		Softening point	R&B		Creep stiffness	Repeated Creep Test		Compliance and recovery	MSCR test			Elastic recovery		Complex modulus	DSR			other		Penetration	Penetration		Low temperature stiffness	BBR			Direct Tensile Test			other		Cohesion	Force ductility			Direct Tensile Test			Fracture toughness test			other		Fatigue	Binder fatigue test			other		<p style="text-align: center;">Ageing/Weathering</p> <table border="1" style="width: 100%; border-collapse: collapse;"> <tr><td rowspan="5">short term ageing</td><td>RTFOT</td><td></td></tr> <tr><td>TFOT</td><td></td></tr> <tr><td>RFT</td><td></td></tr> <tr><td>Modified German RFT</td><td></td></tr> <tr><td>other</td><td></td></tr> <tr><td rowspan="5">long term ageing</td><td>PAV</td><td></td></tr> <tr><td>RCAT</td><td></td></tr> <tr><td>Modified German RFT</td><td></td></tr> <tr><td>Modified RTFOT</td><td></td></tr> <tr><td>other</td><td></td></tr> <tr><td colspan="2" style="text-align: center;">State binder</td><td></td></tr> <tr><td>Pure</td><td></td><td></td></tr> <tr><td>Modified</td><td></td><td></td></tr> <tr><td>Unaged</td><td></td><td></td></tr> <tr><td>Short term aged</td><td></td><td></td></tr> <tr><td>Long term aged</td><td></td><td></td></tr> <tr><td>Recovered</td><td></td><td></td></tr> <tr><td colspan="2" style="text-align: center;">Type of modification</td><td></td></tr> <tr><td>SBS</td><td></td><td></td></tr> <tr><td>EVA</td><td></td><td></td></tr> <tr><td>Elvaloy</td><td></td><td></td></tr> <tr><td>Crum rubber</td><td></td><td></td></tr> <tr><td>PPA</td><td></td><td></td></tr> <tr><td>other</td><td></td><td></td></tr> </table>	short term ageing	RTFOT		TFOT		RFT		Modified German RFT		other		long term ageing	PAV		RCAT		Modified German RFT		Modified RTFOT		other		State binder			Pure			Modified			Unaged			Short term aged			Long term aged			Recovered			Type of modification			SBS			EVA			Elvaloy			Crum rubber			PPA			other			<p style="text-align: center;">Elevated service temperature properties</p> <table border="1" style="width: 100%; border-collapse: collapse;"> <tr><td>Stiffness</td><td>Stiffness test</td><td></td></tr> <tr><td>Permanent deformation</td><td>Wheel tracking test</td><td></td></tr> <tr><td></td><td>Cyclic compression test</td><td></td></tr> <tr><td></td><td>other</td><td></td></tr> </table> <p style="text-align: center;">Intermediate and/or low service temperature properties</p> <table border="1" style="width: 100%; border-collapse: collapse;"> <tr><td>Stiffness</td><td>Stiffness test</td><td></td></tr> <tr><td>Strength</td><td>Indirect tensile test</td><td></td></tr> <tr><td></td><td>Direct tensile test</td><td></td></tr> <tr><td></td><td>other</td><td></td></tr> <tr><td>Low temperature cracking</td><td>Thermal stress restrained specimen test</td><td></td></tr> <tr><td></td><td>Crack propagation test</td><td></td></tr> <tr><td></td><td>other</td><td></td></tr> <tr><td>Fatigue cracking</td><td>Fatigue test</td><td></td></tr> <tr><td>Adhesion</td><td>Aggregate/Binder affinity</td><td></td></tr> <tr><td></td><td>Particle loss of Porous Asphalt (Cantabro)</td><td></td></tr> <tr><td></td><td>other</td><td></td></tr> <tr><td>Water sensitivity</td><td>Indirect tensile test + conditioning</td><td></td></tr> <tr><td></td><td>Duriez</td><td></td></tr> <tr><td></td><td>AASHTO T283 (Modified Lotmann)</td><td></td></tr> <tr><td></td><td>other</td><td></td></tr> <tr><td>Scuffing test (ravelling)</td><td>Scuffing test</td><td></td></tr> </table> <p style="text-align: center;">Precision</p> <table border="1" style="width: 100%; border-collapse: collapse;"> <tr><td>Binder test</td><td></td></tr> <tr><td>Mix test</td><td></td></tr> </table> <p style="text-align: center;">Correlations</p> <table border="1" style="width: 100%; border-collapse: collapse;"> <tr><td>Binder/Mix</td><td></td></tr> <tr><td>Binder/Field</td><td></td></tr> <tr><td>Mix/Field</td><td></td></tr> </table> <p style="text-align: center;">Relevance</p> <table border="1" style="width: 100%; border-collapse: collapse;"> <tr><td>High</td><td></td></tr> <tr><td>Moderate</td><td></td></tr> </table>	Stiffness	Stiffness test		Permanent deformation	Wheel tracking test			Cyclic compression test			other		Stiffness	Stiffness test		Strength	Indirect tensile test			Direct tensile test			other		Low temperature cracking	Thermal stress restrained specimen test			Crack propagation test			other		Fatigue cracking	Fatigue test		Adhesion	Aggregate/Binder affinity			Particle loss of Porous Asphalt (Cantabro)			other		Water sensitivity	Indirect tensile test + conditioning			Duriez			AASHTO T283 (Modified Lotmann)			other		Scuffing test (ravelling)	Scuffing test		Binder test		Mix test		Binder/Mix		Binder/Field		Mix/Field		High		Moderate	
Complex modulus	DSR																																																																																																																																																																																																																						
	other																																																																																																																																																																																																																						
Dynamic viscosity	Cone&Plate																																																																																																																																																																																																																						
	Coaxial cylinders																																																																																																																																																																																																																						
	Capillary viscosimeter																																																																																																																																																																																																																						
	other																																																																																																																																																																																																																						
Low Shear Viscosity	Oscillation method																																																																																																																																																																																																																						
	Creep method																																																																																																																																																																																																																						
	other																																																																																																																																																																																																																						
Softening point	R&B																																																																																																																																																																																																																						
Creep stiffness	Repeated Creep Test																																																																																																																																																																																																																						
Compliance and recovery	MSCR test																																																																																																																																																																																																																						
	Elastic recovery																																																																																																																																																																																																																						
Complex modulus	DSR																																																																																																																																																																																																																						
	other																																																																																																																																																																																																																						
Penetration	Penetration																																																																																																																																																																																																																						
Low temperature stiffness	BBR																																																																																																																																																																																																																						
	Direct Tensile Test																																																																																																																																																																																																																						
	other																																																																																																																																																																																																																						
Cohesion	Force ductility																																																																																																																																																																																																																						
	Direct Tensile Test																																																																																																																																																																																																																						
	Fracture toughness test																																																																																																																																																																																																																						
	other																																																																																																																																																																																																																						
Fatigue	Binder fatigue test																																																																																																																																																																																																																						
	other																																																																																																																																																																																																																						
short term ageing	RTFOT																																																																																																																																																																																																																						
	TFOT																																																																																																																																																																																																																						
	RFT																																																																																																																																																																																																																						
	Modified German RFT																																																																																																																																																																																																																						
	other																																																																																																																																																																																																																						
long term ageing	PAV																																																																																																																																																																																																																						
	RCAT																																																																																																																																																																																																																						
	Modified German RFT																																																																																																																																																																																																																						
	Modified RTFOT																																																																																																																																																																																																																						
	other																																																																																																																																																																																																																						
State binder																																																																																																																																																																																																																							
Pure																																																																																																																																																																																																																							
Modified																																																																																																																																																																																																																							
Unaged																																																																																																																																																																																																																							
Short term aged																																																																																																																																																																																																																							
Long term aged																																																																																																																																																																																																																							
Recovered																																																																																																																																																																																																																							
Type of modification																																																																																																																																																																																																																							
SBS																																																																																																																																																																																																																							
EVA																																																																																																																																																																																																																							
Elvaloy																																																																																																																																																																																																																							
Crum rubber																																																																																																																																																																																																																							
PPA																																																																																																																																																																																																																							
other																																																																																																																																																																																																																							
Stiffness	Stiffness test																																																																																																																																																																																																																						
Permanent deformation	Wheel tracking test																																																																																																																																																																																																																						
	Cyclic compression test																																																																																																																																																																																																																						
	other																																																																																																																																																																																																																						
Stiffness	Stiffness test																																																																																																																																																																																																																						
Strength	Indirect tensile test																																																																																																																																																																																																																						
	Direct tensile test																																																																																																																																																																																																																						
	other																																																																																																																																																																																																																						
Low temperature cracking	Thermal stress restrained specimen test																																																																																																																																																																																																																						
	Crack propagation test																																																																																																																																																																																																																						
	other																																																																																																																																																																																																																						
Fatigue cracking	Fatigue test																																																																																																																																																																																																																						
Adhesion	Aggregate/Binder affinity																																																																																																																																																																																																																						
	Particle loss of Porous Asphalt (Cantabro)																																																																																																																																																																																																																						
	other																																																																																																																																																																																																																						
Water sensitivity	Indirect tensile test + conditioning																																																																																																																																																																																																																						
	Duriez																																																																																																																																																																																																																						
	AASHTO T283 (Modified Lotmann)																																																																																																																																																																																																																						
	other																																																																																																																																																																																																																						
Scuffing test (ravelling)	Scuffing test																																																																																																																																																																																																																						
Binder test																																																																																																																																																																																																																							
Mix test																																																																																																																																																																																																																							
Binder/Mix																																																																																																																																																																																																																							
Binder/Field																																																																																																																																																																																																																							
Mix/Field																																																																																																																																																																																																																							
High																																																																																																																																																																																																																							
Moderate																																																																																																																																																																																																																							

Comments:

Abstract:

Figure 2-1: Worksheet for single paper

3 Bitumen tests

3.1 Bending Beam Rheometer (BBR) Test

The BBR was developed from the SHRP project in the USA, where it has been used for at least 20 years and for over 15 years elsewhere. The European Standard for the BBR is EN 14771:2012.

The BBR is a three-point bending-beam test, designed to characterise the low-temperature behaviour of bituminous binders. The test determines the flexural creep stiffness of bituminous binders in the range of 30 MPa to 1 GPa by means of the bending beam rheometer. The bending beam rheometer is used to measure the mid-point deflection, in three-point bending, of a beam of bituminous binder. A constant load is applied to the mid-point of the test specimen for a defined loading time and the deflection is measured as a

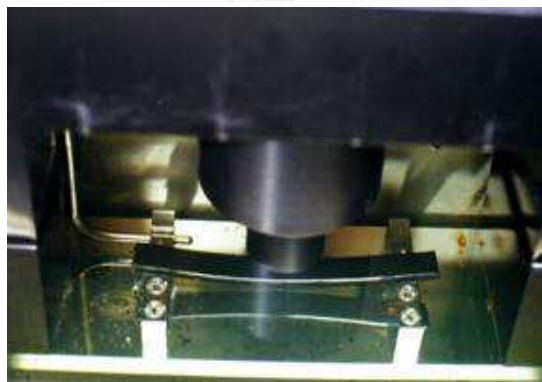
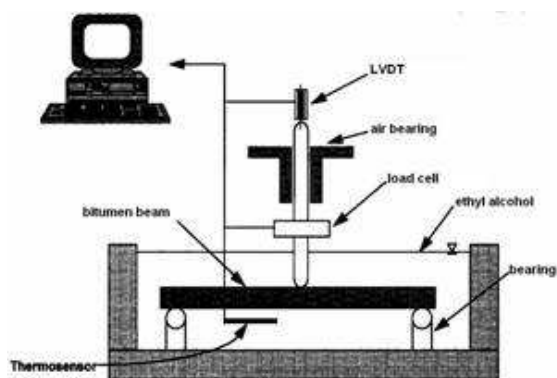


Figure 3-1: BBR experimental setup

function of time. A low temperature liquid bath (ethyl alcohol) is used to control the temperature (Figure 3-1). The creep stiffness S of the test specimen for the specific loading times is calculated from the bending stress and strain. In addition to the creep stiffness, the logarithmic creep rate, generally known as the m -value, is determined. The m -value represents the slope of tangent to $\log S - \log t$ graph at $t = 60$ s (Figure 3-2).

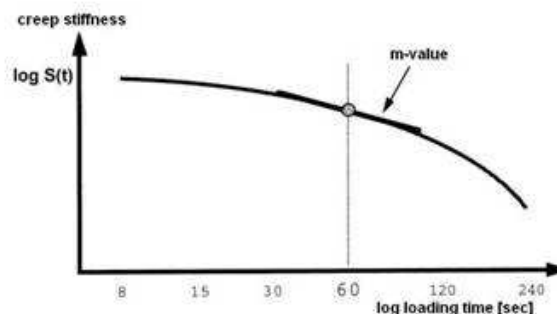


Figure 3-2: BBR definition of the m -value

The test has been standardised in the USA as ASTM D 6648-01.

The precision given in EN 14771 is repeatability, r , of 9 % of the mean value and reproducibility, R , of 27 % of the mean value for the creep stiffness and a repeatability, r , of 4 % of the mean value and reproducibility, R , of 13 % of the mean value for the m -value.

There is a broad correlation with the Fraass breaking point (Section 3.11) for paving grade bitumens and also some suggestion with PMBs. However, the interpretation of the m -values found for some multigrade binders and for certain types of PMBs is not necessarily consistent with that for paving grade bitumen.

3.2 Binder Fatigue Test

There is currently no European standard with only some laboratory test methods existing in a few laboratories around the world. In the test, a fatigue crack is induced by applying continuous oscillatory shear loading with a rheometer, as describe in Section 3.8. It has been shown that the DSR can only be used to evaluate fatigue properties in a narrow stiffness or temperature region. The fatigue phenomena due to the repeated traffic loads imposed on binders is reputed to produce large deformations. Therefore, binders have to be tested in the non-linear region in order to accumulate significant damage.

All the tests are made with parallel plate geometry in order to compare the fatigue responses of binders for:

- The linear region of strain for one temperature and frequency, with the number of cycles needed to reduce the initial value of G^* by 50 % being recorded.
- The non-linear region for one temperature and frequency, the change of G^* versus the strain level between 5 % and 50 % being recorded.
- The non-linear region for one temperature and the same initial stress level, the change of G^* versus the cycle number being recorded.

However, the failure mechanism inside the film of bitumen depends on the temperature at which the test is carried out and on the size of the gap (Figure 3-3).

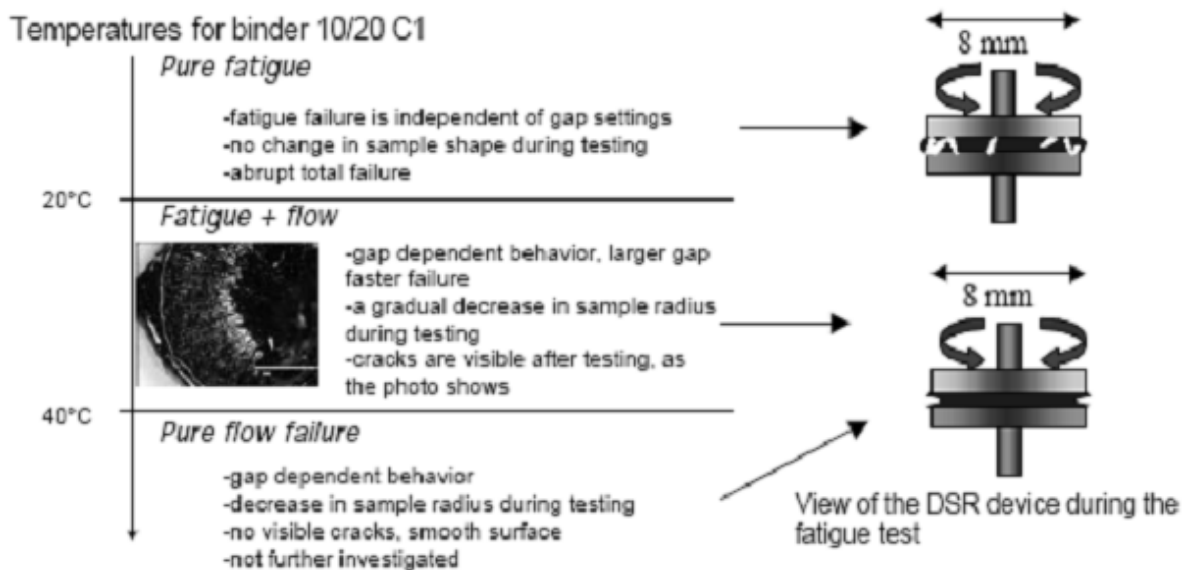


Figure 3-3: Schematic phenomena taking place in the DSR during fatigue testing

In order to observe fatigue cracking when the stiffness of the binder is high (10 MPa to 50 MPa with frequencies between 10 Hz and 50 Hz), it is necessary to ensure that the measurements are not biased by the compliance of the equipment. In this stiffness range, repeated sinusoidal oscillations, with controlled-stress as well as controlled-strain deformations, lead to an abrupt decrease in modulus after a certain number of loadings (**Chyba! Nenalezen zdroj odkazů.**).

The different penetration grades cannot always be compared at a constant temperature because the stiffness of the binders needs to be high. For this situation, the test can be adapted by comparing binders at a constant value of G^* . The test can also be adapted by conducting the test at the same temperature but with rest periods. In this case, the criterion is to retain the cumulative dissipated energy ratio for each binder.

There is no known equivalent standardised method for the binder fatigue test. The repeatability and reproducibility of the tests and the confidence are not known to have been determined.

Although many test methods measure related properties and therefore there will be some relationship, no formal correlation has been found in the papers reviewed between the binder fatigue test and other bitumen tests.

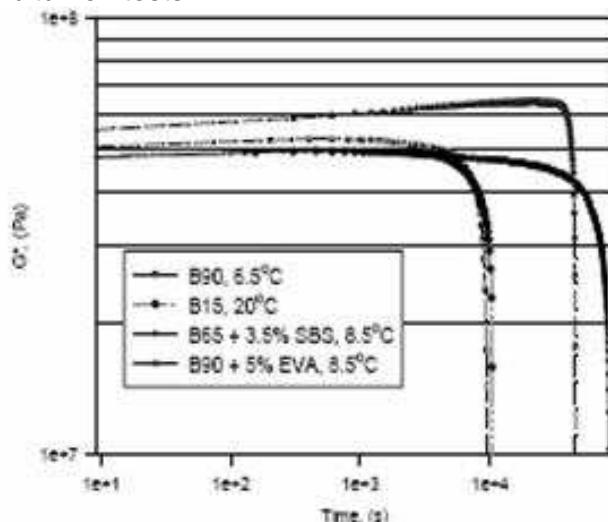


Figure 3-4: Different binders fatigue results at the same initial strain level

3.3 Capillary Viscometer Test

There are two European Standard tests for measuring viscosity with capillaries.

Standard EN 12595:2007 specifies a method for the determination of kinematic viscosity of bituminous binders at 60 °C and 135 °C, in the range from 6 mm²/s to 300 000 mm²/s. Results from the method can be used to calculate dynamic viscosity when the density of the test material is known or can be determined. This method is usually used to determine the viscosity of unmodified bitumen at 135 °C.

Standard EN 12596:2007 specifies a method for the determination of dynamic viscosity by vacuum capillary of bituminous binders at 60 °C, in the range from 0,0036 Pa.s to 580 000 Pa.s. This method is usually used to determine viscosity of unmodified bitumen at 60 °C. Preparation of samples and cleaning the tubes takes a lot of effort. These methods are not suitable for measuring modified bitumen.

Standard EN 12595 has been standardised elsewhere in the world as ASTM D 2170-95 and EN 12596 as ASTM D 2171-94.

The precision values are given in Table 3-1.

Table 3-1: Precision values in EN 12595 and EN 12596

Standard	Temperature (°C)	Range	Repeatability, <i>r</i> (% of mean)	Reproducibility, <i>R</i> (% of mean)
EN 12595	135	< 600 mm ² /s	4	6
		≥ 600 mm ² /s	4	9
EN 12596	60	< 2000 Pa.s	6	12
		≥ 2000 Pa.s	6	10

The dynamic viscosity at 60 °C measured with the capillary viscometer test to the Australian standard AS 2341.02 was correlated with other binder properties for multigrade binders. A good correlation is reported with $G^*/\sin\delta$ at a frequency of 10 rad/sec and 60 °C before and after RTFO-ageing. The correlation with the Ring and Ball softening point was good after RTFO-ageing, but not before.

3.4 Coaxial Cylinder Viscosity Test

The test method described in the standard EN 13702-2:2003 was developed for modified binders, but it is suitable for all types of bituminous binders. In EN 13702-2, recommended test conditions are:

- temperature 60 °C with shear rate 1 s⁻¹,
- temperature 100 °C with shear rate 100 s⁻¹ and
- temperature 150 °C with shear rate 100 s⁻¹.

There is no known equivalent standardised method for the coaxial cylinder viscosity test. The cone and plate viscosity test to EN 13702-1 (Section 0) can be used as an alternative.

EN 13702-2 proposes the following precision data at least until results of further round robin tests are available:

- Difference between two results under repeatability conditions > 5 % in one case in twenty.
- Difference between two results under reproducibility conditions > 15 % in one case in twenty.

Table 3-2: Test results of two binders with modifications

Binder	D 70			D 200		
	Base	+ 4 % SBR	+ 4 % SBS	Base	+ 4 % SBR	+ 4 % SBS
Penetration at 25 °C (0,1 mm)	80	67,5	57,5	173	136	104
Softening Point R&B (°C)	43,8	47,8	50,7	36,2	41,8	50,4
Dynamic viscosity at 60 °C (Pa.s)	216	260	334	93,2	216	296
After TFOT						
Change in weight (%)	0,046	0,015	0,012	-0,143	-0,176	-0,269
Penetration at 25 °C	60	61,5	46,5	102	85,5	89
Softening Point R&B (°C)	48,1	50,7	53,3	43,3	49,1	54,4
Dynamic viscosity at 60 °C (Pa.s)	298	470	534	202	370	389
Stiffening Indexes						
dPen25 (%)	25	8,9	19,1	41	37,1	14,4
dTR&B (°C)	4,3	2,9	2,6	7,2	7,3	4,1
Hardening index	1,4	1,8	1,6	2,2	1,7	1,3

It has been stated that “Originally, the penetration was related to the steady state dynamic viscosity, which is difficult to measure below the ‘Ring and Ball’ temperature. The correlation between the penetration and the dynamic viscosity has been reconfirmed repeatedly”.

The rheological property changes of two different paving grade binders (D 70 and D 200) modified by two different elastomers (SBS and SBR) during the laboratory-ageing test (TFOT) have been measured. The results are given in Table 3-2. It is not specified which test was used to measure the dynamic viscosity. However, linear regression on the results in Table 3-2 gives a good correlation between dynamic viscosity at 60 °C and R&B softening point ($R^2 = 0,95$), but the number of binders considered is too small to derive a meaningful correlation coefficient.

Experimental data on the classical tests for a larger number of binders, including PMBs, has been found. The data, reproduced in Table 3-3, show the dynamic viscosity in combination with penetration and R&B softening point. Simple regression of these data gives a weak correlation between R&B softening point and logarithm of dynamic viscosity at 60°C with $R^2 = 0,48$.

Table 3-3: Classical test results from several binders

Binder	Binder Penetration (0,1 mm)	Softening Point (°C)	Dynamic Viscosity (Pa.s)
35 Pen grade	31	56,4	1 000
50 Pen grade	52	51,2	381
70 Pen grade	59	49,4	255
PMB 1	49	59,6	2 850
PMB 2	44	64,0	300
PMB 3	46	58,4	1 370
PMB 4	42	61,6	2 080
PMB 5	51	77,6	42 200
PMB 6	47	59,4	1 480
PMB 7	70	79,2	6 760
PMB 8	105	83,4	60 000
PMB 9	193	78,8	2 270
MG	40	61,8	2 680
WAX 1	46	67,4	335
WAX 2	44	65,6	144
WAX 3	51	59,4	1 140

The properties of multigrade bitumen have also been studied. Although the method of viscosity measurement is not specified, the correlations in Table 3-4 were found. The correlations show that the binder property that is most closely correlated to the dynamic viscosity is the Ring and Ball softening point (after RTFOT).

Other references all contain some data on the dynamic viscosity in combination with other rheological properties (although, in most of these references, the dynamic viscosity is measured with a Brookfield viscometer rather than the coaxial cylinder method). A general conclusion from these references is that a correlation is observed between dynamic viscosity and R&B softening point temperature, but the number of binders considered in each paper is too small to draw quantitative conclusions on the degree of correlation.

To summarise, the most significant study of the relation between the dynamic viscosity and other rheological properties is the one discussed in reference [2.16]. This study, which involves a high number of PMBs, shows that the correlation between the dynamic viscosity and the R&B softening point is rather weak.

Table 3-4: Correlations for multigrade bitumen

Property	Correlated with	Correlation coefficient >0,9
Viscosity at 60 °C after RTFOT	Softening point (after RTFOT)	Yes
	Penetration (after RTFOT)	No
	Penetration index (after RTFOT)	No
	$G^*/\sin \delta$ (after RTFOT)	No (0,58)
	δ (after RTFOT)	No
	G^* (after RTFOT)	No
	Viscosity at 60°C (before RTFOT)	Yes
Viscosity at 60 °C before RTFOT	Softening point (before RTFOT)	No
	Penetration (before RTFOT)	No
	Penetration index (before RTFOT)	No
	$G^*/\sin \delta$ (before RTFOT)	No (0,68)
	δ (before RTFOT)	No
	G^* (before RTFOT)	No

3.5 Cone and Plate Viscosity Test

The test method described in European Standard EN 13702-1:2003 was developed for modified binders, but it is suitable for all types of bituminous binders. In EN 13702-1, recommended test temperatures are 60 °C, 100 °C and 150 °C and the shear rate is set at $0,05 \text{ s}^{-1}$, but the diameter and the angle of the cone are not prescribed.

There is no known equivalent standardised method for the cone and plate viscosity test. However, the coaxial cylinder viscosity test to EN 13702-2 (Section 3.4) can be used as an alternative.

The European standard EN 13702-1 proposes the following precision data, at least until results of further round robin tests are available:

- Difference between two results under repeatability conditions > 5 % in one case in twenty.
- Difference between two results under reproducibility conditions > 15 % in one case in twenty.

The coaxial cylinder viscosity test and cone and plate viscosity test are similar tests with the conclusions already given in Section 3.4.

3.6 Creep Zero Shear Viscosity Test

The test is a binder creep test, designed to measure zero shear viscosity (ZSV, notated as η_0). ZSV is also referred to as the first Newtonian viscosity and is believed to be a suitable indicator to evaluate the partial contribution of the bituminous binder (including polymer modified binders) to the rutting resistance of asphalt. The test is conducted at elevated service temperatures, these being significant for rutting.

In a low shear creep test, ZSV is the inverse of the slope of the compliance curve in the steady state flow regime, where the slope becomes constant (Figure 3-5) according to Equation (3.1).

$$\frac{dJ(t)}{dt} = \frac{1}{\eta_0} \quad (3.1)$$

A procedure to perform the test in a shear rheometer has been defined. The reproducibility of the results when following the test protocol was investigated. It was concluded that the test is suitable for conventional, multigrade and lightly modified binders. For highly modified binders, it was concluded that the steady state creep flow cannot be attained within a reasonable creep period and, hence, ZSV cannot be measured.

A draft test method was prepared by CEN TC 336/WG1/TG1, “High Temperature Performance”, that, at the time of writing, was at CEN Enquiry stage. In this test method, the parallel plate geometry is recommended with a diameter of 20 mm or greater, a 2 mm gap and the conditions given in Table 3-5. The cone and plate geometry is also appropriate. The draft also specifies a range of the viscosity (100 to 50 000 Pa.s) beyond which the test is not applicable. The upper limit is in accordance with the conclusion discussed above.

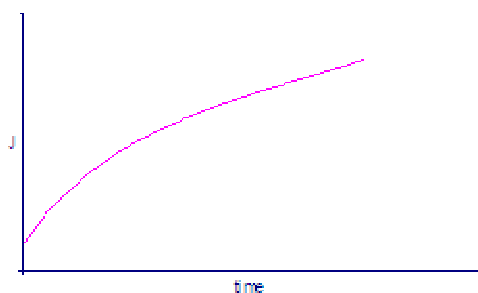


Table 3-5: Test conditions recommended by the draft European test method

Type of binder	Stress (Pa)	Time (h)	Temp. (°C)
Non modified	50	1	60
Polymer modified	10 – 50	4	60

Figure 3-5: Compliance curve measured in a low shear creep test

The average viscosity over the last 15 min (900 s) is derived from the compliance curve according to Equation (3.2).

$$\eta_i = \frac{\Delta t}{\Delta J} = \frac{900}{(J_{end} - J_{15 \text{ min before end}})} \quad (3.2)$$

If, at the end of the recommended creep time, the viscosity is still increasing by more than 5 % per 15 min, the creep time should be extended to a maximum of 8 h. If the viscosity increases by less than 5 % per 15 min, it is recorded as the steady state viscosity. If the test results are independent of the stress level (linear range), this steady state viscosity is accepted as the ZSV.

There is no equivalent standardised test. An alternative to the creep test for measuring the ZSV is the oscillation ZSV test (Section 3.15). However, the draft test method for the oscillation test has been designed to determine the equi-viscous temperature for a low shear viscosity (LSV) of 2000 Pa.s, while the creep ZSV test determines the ZSV (which is also actually a low shear viscosity) at a given temperature.

Precision was estimated in a round-robin exercise conducted by CEN TC336 WG1/TG1 involving 9 laboratories. Five binders were tested (2 pure bitumens and 3 PMBs). The resulting precision is given in Table 3-6.

Table 3-6: Precision data of the ZSV by the creep test method

Statistic	Bit A	Bit B	PMB 1	PMB 2	PMB 3
Overall mean (Pa.s)	190	10481	3355	11908	904788
Repeatability coefficient of variation (%)	5,3	11,7	6,1	7,7	36,6
Reproducibility coefficient of variation (%)	15,1	17,4	12,3	17,3	91,4

PMB3 should not be considered because its overall mean ZSV value is outside the range of applicability mentioned in the draft test method (ZSV range from 100 to 50000 Pa.s). The round robin established the limit of viscosity outside which the test is not applicable. This limit is reflected in the standard.

ZSV by the creep test and ZSV by the oscillation test theoretically determine the same binder property, so the results from both tests have been compared by various researchers [2.26 to 2.29]. Both tests give the same results for unmodified binders as well as for some binders with low polymer content. However, the results often differ for highly modified binders. The reason for this is that either:

- the steady state is not reached within a reasonable time of testing in the creep test (hence the draft standard for the test specifies an upper limit for the measurable ZSV); or
- the frequency is not sufficiently low to obtain the low frequency plateau in the viscosity curve in the oscillation test.

However, at the high concentration of polymer (high viscosity) when the two methods diverge, the standard for the creep test excludes its use.

Correlations between ZSV by the creep test and other binder properties related to permanent deformation were investigated for a set of 15 binders. The creep period was one hour, regardless of whether or not the creep flow had reached steady state. Table 3-7 shows the correlations obtained for the unmodified binders. ZSV by the oscillation method, the SHRP parameter of $G^*/\sin\delta$, the repeated creep test and the static creep test have all been found to correlate closely to the traditional rheological properties of penetration and R&B softening point.

Table 3-7: Correlations between various bitumen tests for unmodified binders [2.27]

Linear correlation coefficients	ZSV oscillation 0,001 Hz	Logarithmic (tests after 1 day storage)				Static Creep Test 25 Pa	Temperature	
		$G^*/\sin(\delta)$		RCT			PG grading (°C)	R&B (°C)
		0,001 Hz	1,59 Hz	25 Pa	300 Pa			
Log(pen @ 25°C)	0,94	0,94	0,96	0,94	0,95	0,94	0,94	0,96
R&B (°C)	0,98	0,98	0,98	0,98	0,98	0,98	0,95	1,00
PG grading (°C)	0,97	0,97	0,99	0,98	1,00	1,00	1,00	0,95

Table 3-8 shows the correlation coefficients obtained for modified binders. For these binders, the static creep test has a good correlation only with the ZSV by the oscillation method, with

the SHRP parameter of $G^*/\sin\delta$ when measured at a very low oscillation frequency of 0,001 Hz, and with the repeated creep test.

Table 3-8: Correlations between various bitumen tests for modified binders [2.27]

Rheological test, after 1 day (logarithmic) at 50 °C	Logarithmic					
	ZSV oscillation 0,001 Hz	$G^*/\sin(\delta)$ 0,001 Hz	$G^*/\sin(\delta)$ 10 rad/s	RCT 25 Pa	RCT 300 Pa	Static creep
ZSV oscillation @ 0,001 Hz	1,00	0,94	0,02	0,99	0,77	0,94
$G^*/\sin(\delta)$ @ 0,001 Hz	–	1,00	0,03	0,94	0,75	0,92
$G^*/\sin(\delta)$ @ 10 rad/s	–	–	1,00	0,02	0,00	0,01
RCT @ 25 Pa	–	–	–	1,00	0,75	0,96
RCT @ 300 Pa	–	–	–	–	1,00	0,80
Static creep	–	–	–	–	–	1,00
SHRP grading	–	–	–	–	–	–
High PG temperature	0,46	0,49	0,21	0,50	0,09	0,31
Traditional tests:						
Log(pen @ 25 °C)	0,00	0,00	0,85	0,00	0,00	0,10
R&B (°C)	0,53	0,51	0,25	0,59	0,19	0,47

3.7 Direct Tensile Test (DTT)

The Direct Tensile Test (DTT) is a procedure used to measure the strain at failure and stress at failure in an asphalt binder test specimen pulled at a constant rate of elongation. It can be used with unaged or aged material (Figure 3-6). The test apparatus is designed for testing within the temperature range from -36 °C to +6 °C. This test method was developed for binders at temperatures where they exhibit brittle or brittle-ductile failure. This failure will result in a fracture of the test specimen as opposed to a ductile failure in which the specimen stretches without fracturing. The test is not applicable at temperatures where failure is by ductile flow. Strain at failure is used as the criterion for specifying the low temperature properties of asphalt binders in accordance with the SHRP binder classification in conjunction with the BBR test (Section 3.1).

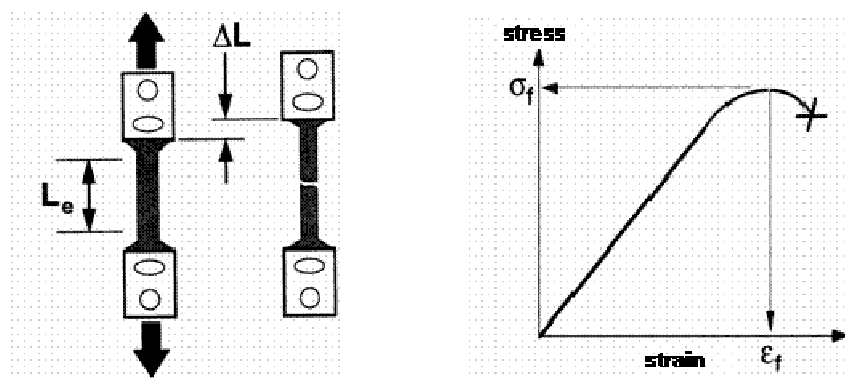


Figure 3-6: DTT measurement principle

The direct tensile test is not yet standardised in Europe. However, the test has been standardised in AASHTO standards TP3-98 [2.28] and T314 [2.29].

The precision is not known to have been determined.

Although many test methods measure related properties and therefore there will be some relationship, no formal correlation has been found in the papers reviewed between the direct tensile test and other bitumen tests. Nevertheless, the combination of the BBR (Section 3.1) and DTT results can be used to determine a critical thermal cracking temperature.

3.8 Complex shear modulus and phase angle by Dynamic Shear Rheometer (DSR) Test

EN 14770:2012, the European Standard for the DSR-test, describes a procedure for the determination of the complex shear modulus and phase angle using a dynamic shear rheometer (Figure 3-7). The test is performed in oscillatory shear, in stress or in strain controlled mode, over a range of temperatures and frequencies (Figure 3-8). The rheometer is fitted with parallel plates, with a constant gap. Temperature control encompasses both plates. Parallel plates with a diameter between 8 mm and 25 mm and gap settings from 0,5 mm to 2,0 mm are recommended.

The test consists of performing isothermal frequency sweeps at discrete temperature steps. The time between two frequency sweeps shall be sufficient to allow for thermal equilibrium in the sample. Isotherms of G^* (Pa) and δ ($^\circ$) against frequency (Hz) are the basic test results.

The test has been standardised in the USA as AASHTO TP5-97.

The precision statement from EN 14770 indicates that tests under reproducibility conditions have been carried out using the AASHTO test according to SHRP protocols, which are similar to EN 14770, and also by RILEM using nominally the same method on a range of binders. The test is approximately as precise as the softening point test (Section 3.19). In particular, the results from the RILEM exercise on the measurement of complex modulus and phase angle for rotational DSRs with parallel plate sample geometries of 25 mm, 1 mm gap and 8 mm, 2 mm gap, indicated that:

- Reproducibility of G^* may be practically achieved in the range below 10 %, independent of the type of binder (pure or modified) and its state (original or aged by RTFOT or PAV).



Figure 3-7: Dynamic Shear Rheometer

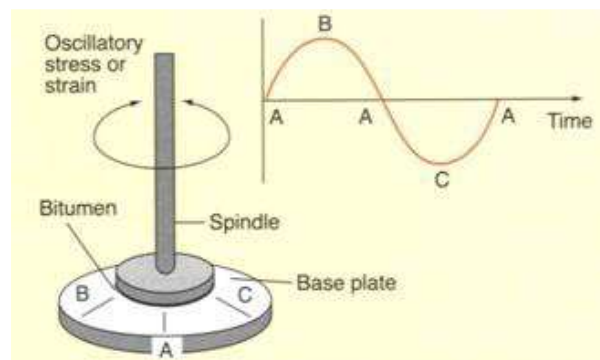


Figure 3-8: Schematic of DSR mode of test

- Reproducibility of phase angle may be practically achieved in the range below 5 %, independent of the type of binder (pure or modified) and its state (original or aged by RTFOT or PAV).

Penetration has been correlated with DSR measurements, as described in Section 3.16.

It is generally considered that, for paving grade bitumens, the R&B softening point is equivalent to a penetration of $800 \times 0,1$ mm. From the relationship between $\log(G^*)$ and $\log(\text{pen})$, it is possible to calculate the value of G^* which equates to 800 pen ($G^*_{800 \text{ pen}}$). Measurement of G^* at more than one temperature enables a relationship between G^* and temperature to be established and it is then possible to determine the temperature which corresponds to $G^*_{800 \text{ pen}}$, nominally the R&B softening point.

It has been found that the stiffness of the binder can be predicted from the penetration index and R&B softening point for paving grade bitumens. At very low testing frequency, the ratio $G^*/\sin\delta$ is related to the oscillation ZSV because ZSV is defined by equation (3.3).

$$\eta_0 = \frac{1}{\omega J''} = \frac{G^*}{\omega \sin \delta} \quad (3.3)$$

Hence, there is also a relation with creep ZSV.

3.9 Elastic Recovery Test

The elastic recovery test was developed in the past to determine the elasticity of polymer modified bituminous binders. In Europe the test is described by EN 13398 (compare to AASHTO T 51 as used in USA) using standard ductilometer and moulds for ductility test. The elastic recovery is evaluated by the percentage of recoverable strain measured after elongation during a conventional ductility test. Unless otherwise specified, the test shall be run at the temperature of $(25 \pm 0,5)$ °C or $(10 \pm 0,5)$ °C and with a speed of 50 mm/min. The test specimen is elongated by the given speed to a deformation of 200 mm (AASHTO T 51 considers also elongation of only 100 mm). Immediately after reaching the required prolongation (the time has to be no longer than 10 s) the test specimen is cut into two halves at the midpoint and left in the water bath in undisturbed conditions for 30 minutes (AASHTO T 51 requires 60 minutes). After this time period the elongated halves of the test specimen are moved back to each other so they touch. The length of the elongated and recovered test specimen is measured and finally the elastic recovery calculated by following equation (3.4):

$$R_E = \frac{d}{L} \times 100 \quad (3.4)$$

where d is the distance between both half bitumen fibres and L is the elongation distance.

If the elongated bitumen sample parts before reaching the distance of 200 mm such test specimen can be used for calculating elastic recovery by modifying the defined equation and noting this matter of fact in the testing protocol.

3.10 Force Ductility Test

The method and calculation of the deformation energy are described in EN 13589:2010 and EN 13703:2003. The device consists of a water bath with temperature control and a traction device. The bitumen specimen is fixed onto the traction device (Figure 3-9). The specimen is elongated with a constant speed of $(50 \pm 2,5)$ mm/min. Usually, the test temperature is 5 °C but, depending on the brittleness of the specimen, the test temperature can be increased in steps of 5 °C. The maximum testing time is determined by the length of the water bath. The testing time is about 20 min for a water bath of a length of 1000 mm.

Preparation time for the specimen is approximately 4 h (including the cooling). The primary use of the force ductility test is to distinguish between modified and unmodified bitumen. The deformation energy between 200 mm and 400 mm is the specification criterion (Figure 3-10).

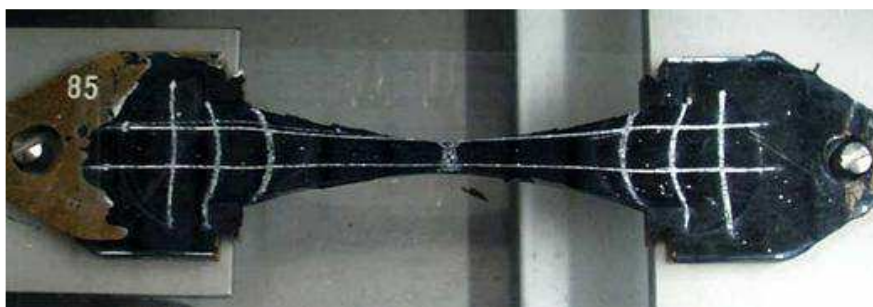


Figure 3-9: Force ductility specimen

There is no known equivalent standardised method for the force ductility test. However, the tensile test, EN 13587:2010, and the Vialit test, EN 13588:2008, are also used for assessing the cohesive properties of bitumen. Some correlation has been found between the tensile test and the force ductility test. Generally, deformation energies measured by the tensile test are lower than values measured by force ductility at 5 °C or 10 °C. The sequence of the tested bitumen is almost the same for both methods. However, a systematic study comparing the three methods is missing.

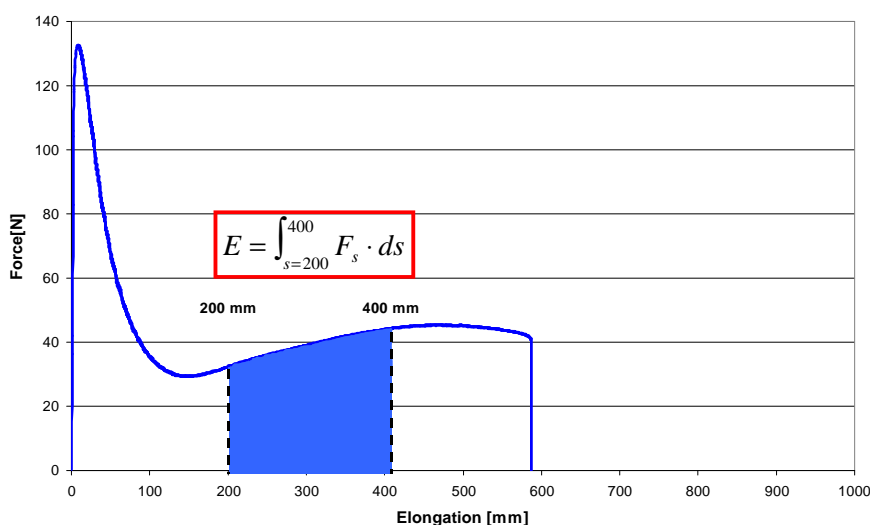


Figure 3-10: Deformation energy (EN 14023)

Precision data was determined by a European Round-Robin-test under participation of 18 laboratories in 2002. The data were in accordance with EN 13703 [2.35]. The repeatability is 0,11 J/cm² for E_{0.2-0.4} < 1 J/cm² and 8 % for E_{0.2-0.4} > 1 J/cm² while the reproducibility is 0,39 J/cm² for E_{0.2-0.4} < 1 J/cm² and 33 % for E_{0.2-0.4} > 1 J/cm².

Correlation between the maximum energy of the force ductility curve and penetration has been found. The force ductility curve gives qualitative information on the cohesive and elastic properties of polymer modified bitumen. These properties are determined by the polymers in terms of their type, distribution, concentration and network (Figure 3-11).

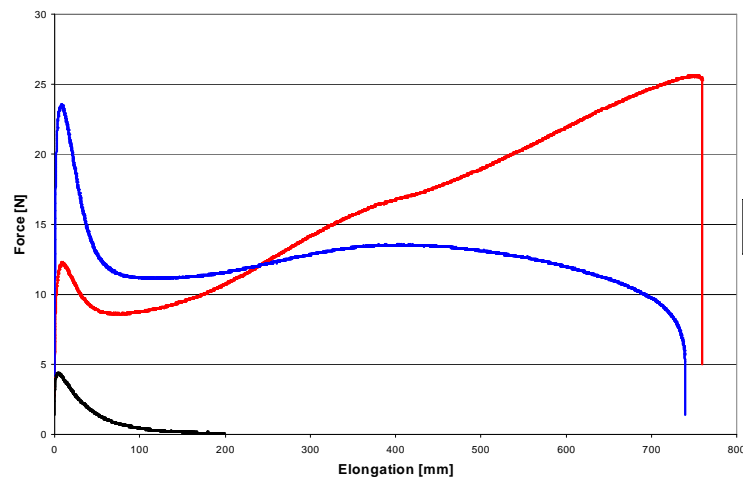


Figure 3-11: Force ductility curves for three different PMB binders

The force ductility device can also be used for the determination of the elastic recovery, EN 13398:2010.

3.11 Fraass Breaking Point Test

The Fraass breaking point test provides a measure of the brittleness of bitumen and bituminous binders at low temperatures. A sample of bituminous binder is applied to a metal plate at an even thickness. This plate is submitted to a constant cooling rate and flexed repeatedly until the binder layer breaks (Figure 3-12). The temperature at which the first crack appears is reported as the Fraass breaking point.

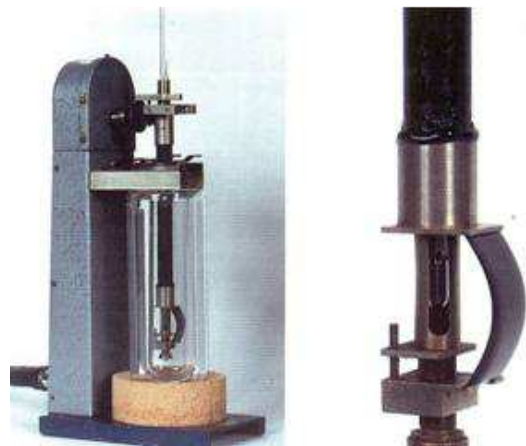


Figure 3-12: Fraass breaking point

The European Standard for Fraass breaking point is EN 12593:2007.

The precision given in EN 12593:2007 is repeatability, r , of 3 °C and reproducibility, R , of 6 °C.

There is a broad correlation of the Fraass breaking point test with the BBR (Section 3.1) for unmodified bitumen and also some suggestion with PMBs.

3.12 Fracture Toughness Test (FTT)

The resistance to fracture of a material is known as its fracture toughness. Fracture toughness generally depends on temperature, environment, loading rate, the composition of the material and its microstructure, together with geometric effects (constraint). Fracture toughness is a critical input parameter for fracture-mechanics based on fitness-for-purpose assessments.

Various measures of “toughness” exist, including the widely used but qualitative Charpy impact test. Although it is possible to correlate Charpy energy with fracture toughness, a large degree of uncertainty is associated with correlations. It is preferable to determine fracture toughness in a rigorous fashion, in terms of K (stress intensity factor), CTOD (crack tip opening displacement), or J (the J integral).

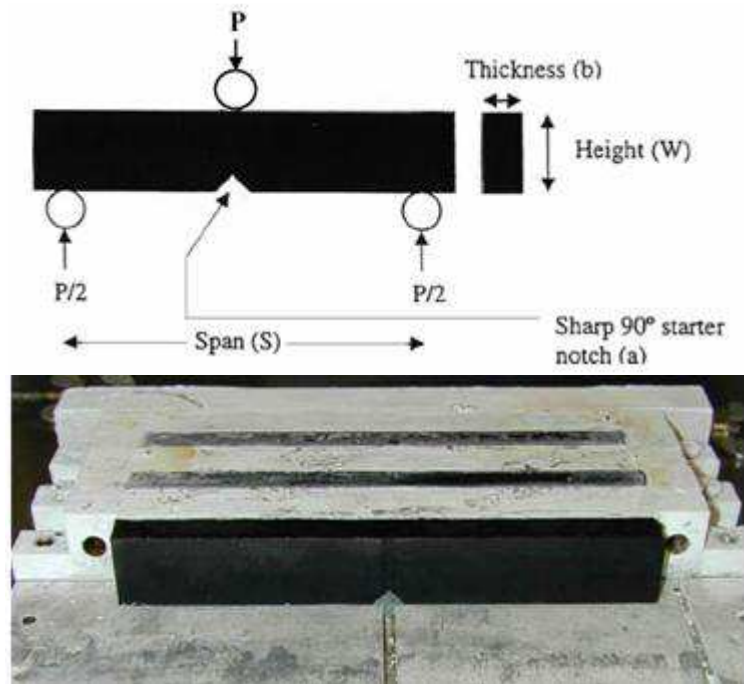


Figure 3-13: FTT test layout and specimen preparation

Standards exist for performing fracture mechanics tests, with the most common specimen configuration shown in Figure 3-13 (the single-edge notch bend, SENB, specimen). A sharp fatigue notch is inserted in the specimen, which is loaded to failure. The crack driving force is calculated for the failure condition, giving the fracture toughness.

There are no standards for the fracture toughness of bitumen. However, National Standards have been developed for fracture toughness testing of metals. In particular:

- The UK BS 7448 includes four parts, for testing of metallic materials, including parent materials, weldments, high strain rates (dynamic fracture toughness testing, still in preparation) and R -curves (for ductile tearing). BS 7448: Part 2 is the first Standard worldwide to apply specifically to weldments.
- A series of American ASTM Standards cover K , CTOD, J testing (including R -curves), together with a summary of applicable terminology.
- The European Structural Integrity Society (ESIS) has published procedures for R -curve and standard fracture toughness testing of metallic materials.

Although different Standards have historically been published for determining K , CTOD and J , the tests are very similar, and generally all three values can be established from one test. None of these standards specifies tests on bitumen specifically.

No precision data are published for FTT on bitumen yet.

Although many test methods measure related properties and therefore there will be some relationship, no formal correlation has been found in the papers reviewed between the fracture toughness test and other bitumen tests.

3.13 Multiple Stress Creep and Recovery (MSCR) Test

The multiple stress creep and recovery test is at present stage under European normalization (prEN 16659) and is a method used to determine the presence of elastic response in bitumen and bituminous binders under shear creep and recovery at two stress levels, at a specified temperature.

The presence of the elastic response is determined by measuring the percent recovery (%R) and non-recoverable compliance (J_{nr}) of the binder. The percent recovery at multiple stress levels is intended to determine the presence of elastic response and stress dependence of bituminous binders. Non-recoverable creep compliance has been shown to be an indicator of the resistance of bitumen to permanent deformation under repeated load.

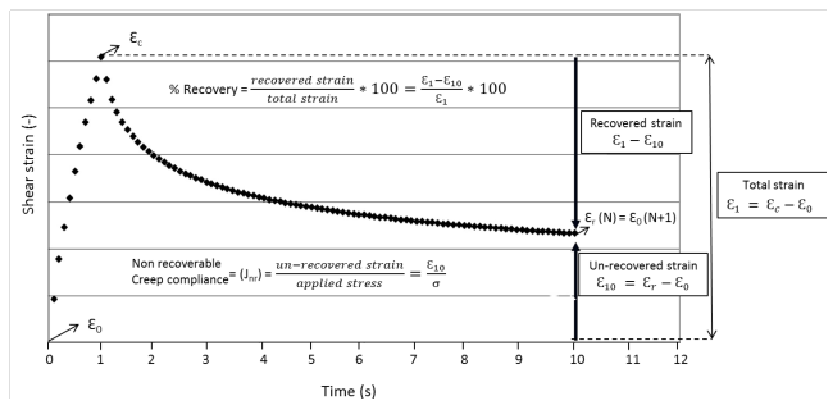


Figure 3-14: Typical creep-recovery cycle

The test can be conducted at different temperatures, 40°C, 50°C, 60°C or 70°C as appropriate, but other test temperatures may be used for comparative purposes. Sample preparation and apparatus are in accordance with EN 14770, using the 25 mm parallel plate geometry with a 1 mm gap setting. The sample is loaded at constant stress for 1 s, then allowed to recover for 9 s. Ten creep and recovery cycles are run at 0,100 kPa creep stress followed by ten more cycles at 3,200 kPa creep stress (see Figure 3-14 and Figure 3-15).

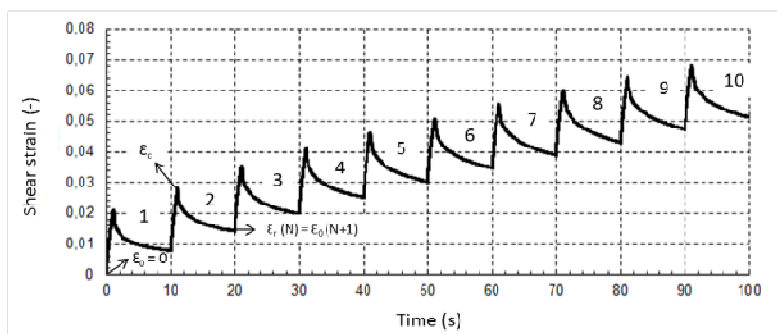


Figure 3-15: Typical creep-recovery curve after 10 consecutive cycles

For percent recovery (defined as the recovered strain in a specimen during the recovery part of a cycle) the following calculations are considered:

- Percent recovery for each of the ten cycles at creep stress of 0,100 kPa and 3,200 kPa, for $N = 1$ to 10:

$$R_N(0,1\text{ kPa}, N) = \frac{\varepsilon_1 - \varepsilon_{10}}{\varepsilon_1} \times 100 \quad (3.5)$$

$$R_N(3,2\text{ kPa}, N) = \frac{\varepsilon_1 - \varepsilon_{10}}{\varepsilon_1} \times 100 \quad (3.6)$$

- Average percent recovery at 0,100 kPa and 3,200 kPa and percent difference in recovery between the two stress levels:

$$R_{0,1\text{ kPa}} = \sum \frac{[(R_N)(0,1\text{ kPa}, N)]}{10} \text{ for } N = 1 \text{ to } 10 \quad (3.7)$$

$$R_{3,2\text{ kPa}} = \sum \frac{[(R_N)(3,2\text{ kPa}, N)]}{10} \text{ for } N = 1 \text{ to } 10 \quad (3.8)$$

$$R_{diff} = \frac{(R_{0,1\text{ kPa}} - R_{3,2\text{ kPa}}) \times 100}{R_{0,1\text{ kPa}}} \quad (3.9)$$

For non-recoverable creep compliance (defined as the residual strain in a specimen after a creep and recovery cycle divided by the stress applied) the following calculations are considered:

- Non-recoverable creep compliance for each of the ten cycles at creep stress of 0,100 kPa and 3,200 kPa, for $N = 1$ to 10, expressed in kPa^{-1} :

$$J_{nr}(0,1\text{ kPa}, N) = \frac{\varepsilon_{10}}{0,100} \quad (3.10)$$

$$J_{nr}(3,2\text{ kPa}, N) = \frac{\varepsilon_{10}}{3,200} \quad (3.11)$$

- Average non-recoverable creep compliance at 0,100 kPa and 3,200 kPa and percent difference in non-recoverable creep compliance between the two stress levels:

$$J_{nr,0,1\text{ kPa}} = \frac{\sum [(J_{nr})(0,1\text{ kPa}, N)]}{10} \text{ for } N = 1 \text{ to } 10 \quad (3.12)$$

$$J_{nr,3,2\text{ kPa}} = \frac{\sum [(J_{nr})(3,2\text{ kPa}, N)]}{10} \text{ for } N = 1 \text{ to } 10 \quad (3.13)$$

$$J_{nr-diff} = \frac{(J_{nr,3,2\text{ kPa}} - J_{nr,0,1\text{ kPa}}) \times 100}{J_{nr,0,1\text{ kPa}}} \quad (3.14)$$

3.14 Oscillatory Squeeze Flow Rheometer

The compressional rheometer is able to measure complex shear modulus (G^*), storage modulus (G') and loss modulus (G'') without the need for delicate air bearings and motor necessary for a typical controlled stress rheometer.

The sample is loaded between two parallel plates, the upper of which is driven by an oscillatory force in the axis normal to the plate surfaces as shown in the schematic in Figure 3-16. The force is generated by a linear motor and the displacement measured by a linear transducer. Temperature control is through Peltier elements placed in thermal contact with the lower plate. In addition, the sample and upper plate are covered by an insulated cover and the internal space is filled with water (c. 3 ml) to minimise thermal gradients. There is a Pt 100 in good thermal contact with the lower plate to sense the temperature, and another sensing the water temperature above the upper plate to ensure that the whole system is at thermal equilibrium.

This is a new technique for measuring bitumen properties and is less expensive and more robust than the dynamic shear rheometer because of its mechanical simplicity. It also does not need a water bath, computer or air supply.

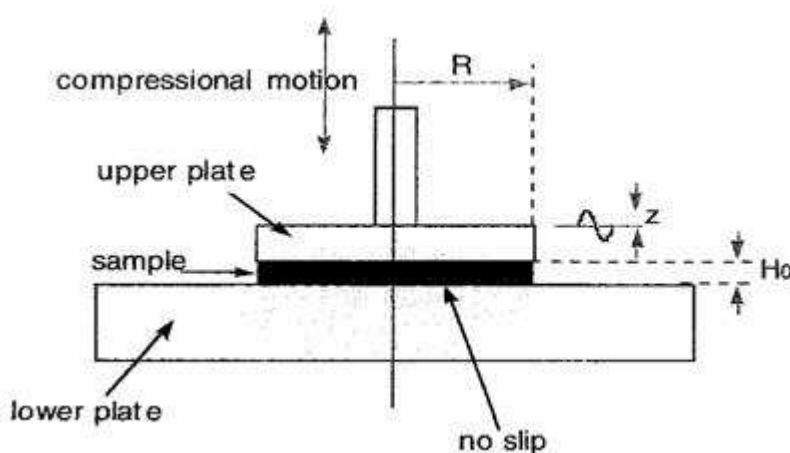


Figure 3-16: Schematic of operation of compressional rheometer

This test is currently not included in any CEN standard test method because it has only recently been introduced. However, it has been concluded that, on the basis of both the quality of the data and the speed with which measurements can be made, this instrument combines the measurement of the rheological properties of bitumens, with the ability to rapidly predict traditional properties. As such, it offers potential as a quality assurance tool.

There are no current standards for the oscillatory squeeze flow rheometer, although it could be incorporated into the European Standard for the DSR, EN 14770 [2.30] (Section 3.8).

Of 58 measurements on 21 bitumens, only three failed to meet the most rigorous comparison between measured and predicted values of penetration. That is, the difference between them should be within the reproducibility of the penetration test itself. For bitumens which met CEN specifications in terms of penetration and softening point gradings, the softening point could be predicted accurately to within the reproducibility of the softening point test.

The oscillatory squeeze flow rheometer was designed as an alternative to the dynamic shear rheometer (DSR). Penetration has been correlated with DSR measurements, as described in Section 3.8. Measurements have been made using the compressional rheometer at 25°C and 0,4 Hz to evaluate this relationship for the oscillatory squeeze flow rheometer test. Similarly, the R&B softening point, an equiviscous temperature, can be calculated using the DSR test (Section 3.8). It has been concluded that measurement of G^* at 25°C and 0,4 Hz can be used to predict bitumen penetration in approximately 12 min, and both penetration

and softening point may be predicted in approximately 22 min if an additional measurement of G^* at 60 °C and 0,4 Hz is made.

3.15 Oscillation Zero/Low Shear Viscosity (ZSV/LSV) Test

It is possible to perform an oscillation test as an alternative to the creep zero shear viscosity test (Section 3.6) in order to determine the zero shear viscosity (ZSV, again notated as η_0). In the frequency domain, ZSV is related to the loss compliance $J''(\omega)$ by [2.48] according to Equation (3.15).

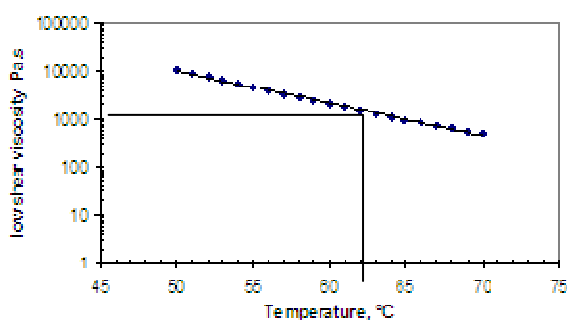
$$J''(\omega) - \int_0^{\infty} \omega [J_{de}(\infty) - J_{de}(t)] \cos \omega t dt = \frac{1}{\omega \eta_0} \quad (3.15)$$

Consequently, when the oscillation frequency tends to zero, the zero shear viscosity can be found in accordance with Equation (3.16).

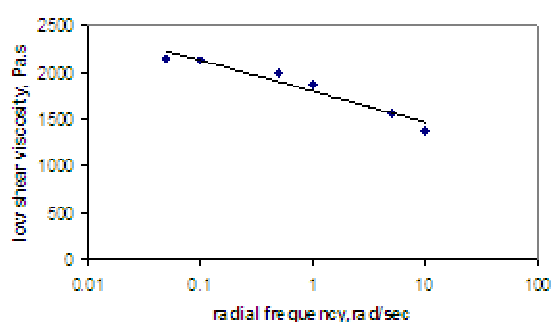
$$\eta_0 = \frac{1}{\omega J''(\omega)} = \frac{G^*}{\omega \sin \delta} \quad (3.16)$$

The test is performed by means of a dynamic shear rheometer in oscillation mode. In 2004, a draft test method was prepared by Technical Committee CEN TC 336 WG1/TG1, "High Temperature Performance". At the time of writing, the draft was at CEN Enquiry stage. In this draft, the term ZSV is replaced by Low Shear Viscosity (LSV) because it is practically not possible to measure at zero shear. The same comment is also applicable to the creep ZSV. This test is also not performed at zero shear, but at a low shear rate. Instead of measuring the LSV at a given temperature, an equi-viscous temperature based on LSV is determined (temperature at which LSV equals 2000 Pa.s). The test is performed in two steps (Figure 3-17):

- Step 1 consists of a temperature sweep at a frequency of 0,1 rad/s. The temperature at which the viscosity attains the value of 2000 Pa.s is a first approximation of the equi-viscous temperature (EVT1)
- In step 2, a frequency sweep is performed at the temperature EVT1, down to a very low frequency (e.g. from 10 down to 0,01 rad/s) to obtain the LSV at EVT1. The difference between this LSV and 2000 Pa.s allows the increase in temperature with respect to EVT1, required in order to obtain a LSV of 2000 Pa.s, to be determined. The correction of EVT1 by this increase in temperature leads to equi-viscous temperature EVT2.



Step 1: Temperature sweep at 0,1 rad/s



Step 2: Frequency sweep at EVT1

Figure 3-17: Principle of measurement of equi-viscous temperature for 2000 Pa.s LSV

Step 2 may not be necessary for pure binders because the viscosity of these binders reaches a plateau at sufficiently low frequencies. Therefore, $EVT2 \approx EVT1$. For heavily modified binders, $EVT2$ can be significantly higher than $EVT1$.

No equivalent standardised tests are currently known to exist. However, the test is related to the creep ZSV test (Section 3.6).

Two round robin tests have been carried out by CEN TC 336/WG1/TG1, in which 15 laboratories participated. Five binders were studied, including two pure bitumen and three PMBs. The outcome of these tests is given in Table 3-9.

Oscillation ZSV is related to $G^*/\sin\delta$, as shown in Equation (3.17), when measured at the same low frequency, because both properties are theoretically interrelated and measured using the same type of test equipment (i.e. DSR).

$$\eta_0 = \frac{1}{\omega J''} = \frac{G^*}{\omega \sin \delta} \quad (3.17)$$

Table 3-9: Precision values for the oscillation zero shear viscosity test

Parameter	Statistic	Bit A	Bit B	PMB 1	PMB 2	PMB 3
EVT1 (at 2000 Pa.s)	Overall mean (°C)	44,7	69,3	60,8	67,5	60,6
	Repeatability std. dev. (°C)	0,7	0,7	0,7	1,0	0,6
	Reproducibility std. dev. (°C)	0,7	1,0	1,5	1,6	1,9
EVT2	Overall mean (°C)	45,4	70,9	63,1	71,6	66,7
	Repeatability std. dev. (°C)	0,6	0,8	0,7	0,7	0,7
	Reproducibility std. dev. (°C)	1,0	1,8	2,2	2,5	2,3

The relation with creep ZSV was already discussed in Section 3.6.

Correlations of ZSV by oscillation at a temperature of 50°C with other binder properties have been reported. Table 3-7 and Table 3-8 in Section 3.6 show the linear correlation coefficients obtained. It is observed that oscillation ZSV (or LSV) at 0,001 Hz correlates closely with the results from the repeated creep test. The correlations with $G^*/\sin\delta$ at 0,001 Hz and with the creep ZSV were also good.

Correlation data between the equi-viscous temperatures by the oscillation zero shear viscosity test and other bitumen tests have not yet been reported.

3.16 Penetration Test

The penetration of a standard needle into a conditioned test sample is measured (Figure 3-18). The European standard for needle penetration is EN 1426:2007.

For penetrations up to $500 \times 0,1$ mm, the operating parameters are a test temperature of 25°C, an applied load of 100 g, and a duration of loading of 5 s.

For penetrations above $500 \times 0,1$ mm, the test temperature is reduced to 15 °C

but the operating parameters of the applied load and the duration of loading remain unchanged. There is also a test at 15 °C with a higher load and longer loading time.



Figure 3-18: Penetration test

The precision for paving grade bitumen is given in Table 3-10. These precision data are not necessarily applicable at other conditions or for modified bitumen.

For unmodified bitumens, the penetration test correlates well with the stiffness of the bitumen measured, using the DSR, at the same temperature (25 °C) and at a frequency of 0,4 Hz, with the equivalent loading time. In rheological terms, a good correlation has been identified between $\log(G^*)$, the complex shear modulus and $\log(\text{pen})$.

Table 3-10: Precision for penetration test

Temperature	Operating conditions		Penetration in 0,1 mm	Repeatability, <i>r</i>	Reproducibility, <i>R</i>
	Load	Duration			
25 °C	100 g	5 s	< 50	2	3
			≥ 50	4 % of mean	6 % of mean
15 °C	100 g	5 s	≥ 50	5 % of mean	8 % of mean
5°C	200 g	60 s	< 50	2	4
			≥ 50	9 % of mean	13 % of mean

It is generally considered that, for paving grade bitumens, the R&B softening point is equivalent to a penetration of $800 \times 0,1$ mm.

Although many other test methods measure related properties and therefore there will be some relationship, no formal correlation has been found in the papers reviewed between the penetration index and other bitumen tests.

3.17 Penetration Index

The penetration index, *PI*, is a measure for the temperature susceptibility of a bitumen that can be derived mathematically either from the penetration values at two temperatures or from the standard penetration and softening point values, as given in Equations (3.18) and (3.19) respectively.

$$PI = \frac{\log(\text{pen}@T_1) - \log(\text{pen}@T_2)}{T_1 - T_2} \quad (3.18)$$

$$PI = \frac{1952 - 500 \log(\text{pen}) - 20 SP}{50 \log(\text{pen}) - SP - 120} \quad (3.19)$$

However, SP in Equation (3.18) is the ASTM (unstirred) softening point which will generally be 1,5°C higher for unmodified bitumen than the EN 1427 (stirred) value.

The values of PI range from around -3 for highly temperature susceptible bitumens to around +7 for highly blown bitumens with low temperature susceptibility. For paving grade bitumen used for highways, the typical range is -1,5 to +1,0.

The calculation of the penetration index has not been standardised.

The precision of the measure is dependent on the precision of the measurement of the penetration and softening point or on the two values of penetration.

Although many test methods measure related properties and therefore there will be some relationship, no formal correlation has been found in the papers reviewed between the penetration index and other bitumen tests.

3.18 Repeated Creep Test

The repeated creep test was designed to determine the resistance of the binder to permanent deformation under conditions of repeated loading and unloading cycles. The test is conducted at elevated service temperatures, which are significant for rutting.

An AASHTO test protocol has been published in NCHRP report 459 [2.51]. According to this protocol, the test is performed using a dynamic shear rheometer at low stress level (between 25 and 300 Pa at the outer edge of the plates). The loading time is typically 1 s, but 2 s or 3 s could also be used. The ratio between loading time and unloading time has to be 1:9 (e.g. 9 s unloading for 1 s loading). The sample is subjected to 100 cycles and the strain is measured as a function of time. The test data of cycles 50 and 51 are fitted using the four-element Burgers model (Figure 3-19). This model yields the value of the viscosity η_0 of the serial dashpot of Burger's model, which is responsible for the permanent deformation component. The creep stiffness G_v , calculated from Equation (3.20), is proposed as an indicator for the resistance to permanent deformation.

$$G_v(t) = \frac{\eta_0}{t} \quad (3.20)$$

where t is the total loading time.

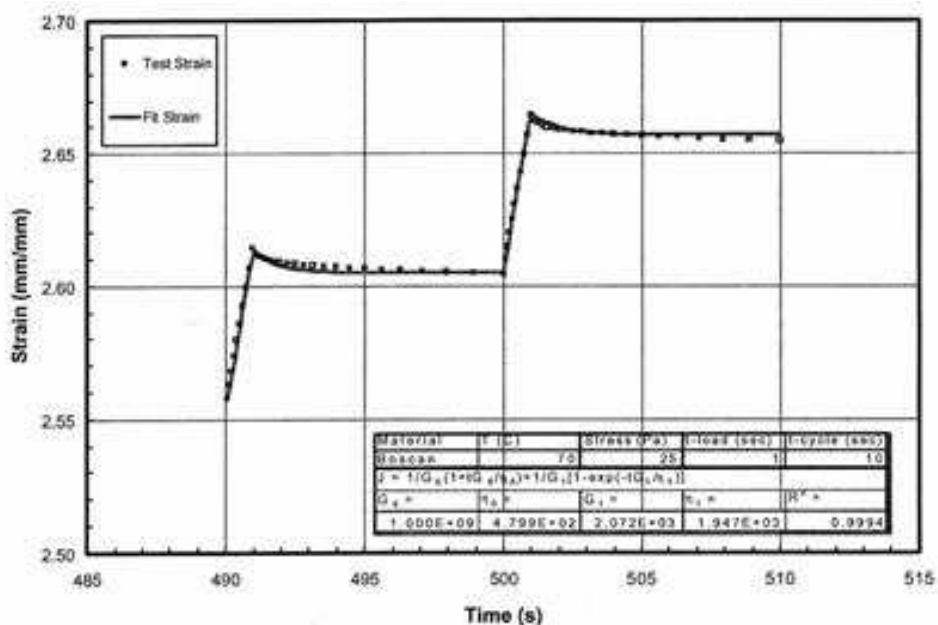


Figure 3-19: Determination of the viscosity η_0 using Burger's model

The repeated creep test has not yet been standardised in Europe.

The precision is not known to have been determined.

The data of the repeated creep test are fitted using Burger's four-parameter model. The viscosity of the serial dashpot in Burger's model theoretically equals the ZSV (Sections 3.6 and 3.15). A comparison was made between the ZSV derived from fitting the repeated creep test with Burger's model and the results from both the creep ZSV and oscillation ZSV tests. The observed systematic under-estimation of ZSV with the repeated creep test was explained by the creep cycles being too short to attain steady state shear flow. The same conclusion was drawn in a comparison of the results from oscillation ZSV to the ZSV derived from the repeated creep test.

The results of the repeated creep test have been compared with the oscillation ZSV test and the creep ZSV test for a total of 13 pure and modified binders. Figure 3-20 shows the range of accumulated strain. The accumulated strain correlated reasonably well with ZSV.

Correlations between the repeated creep test and other bitumen tests have also been reported in (see Table 3-8 and Table 3-9). A good correlation is reported with ZSV by the oscillation test, $G^*/\sin\delta$ at 0.001 Hz and with the creep ZSV.

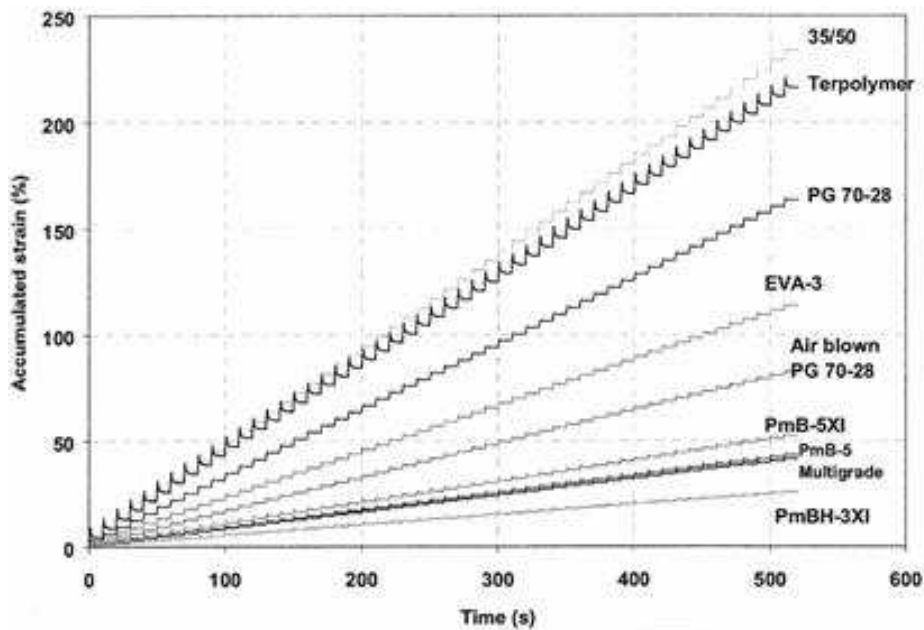


Figure 3-20: Repeated creep tests at 60°C and a stress level of 50 Pa

3.19 Softening Point (Ring and Ball) Test

Softening Point (Ring and Ball) Test is a method for the determination of the softening point of bitumen and bituminous binders, in the range 30°C to 150°C. Two horizontal discs of bituminous binder, cast in shouldered brass rings, are heated at a controlled rate in a liquid bath while each supports a steel ball (Figure 3-21). The European standard for softening point is EN 1427:2007.

The softening point is reported as the mean of the temperatures at which the two discs soften enough to allow each ball, enveloped in bituminous binder, to fall a distance of $(25,0 \pm 0,4)$ mm.

Some equivalent standards to EN 1427, including ASTM D36-95, do not include stirring the liquid bath, without which the result will generally be 1,5°C higher for unmodified bitumen; this difference may not apply to modified binders.

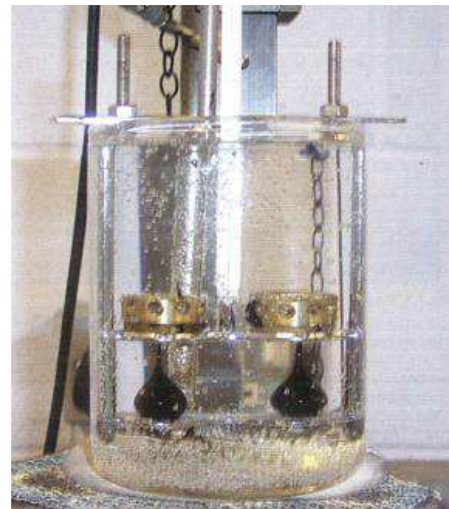


Figure 3-21: Softening point test

The precision quoted in EN 1427 is:

- Repeatability, r , of 1°C and reproducibility, R , of 2°C for unmodified bitumen in water.
- Repeatability, r , of 1,5°C and reproducibility, R , of 3,5°C for modified bitumen in water.
- Repeatability, r , of 1,5°C and reproducibility, R , of 5,5°C for oxidised bitumen in glycerol.

It is generally considered that, for paving grade bitumens, the R&B softening point is equivalent to a penetration of $800 \times 0,1$ mm.

Although many test methods measure related properties and therefore there will be some relationship, no formal correlation has been found in the papers reviewed between the softening point test and other bitumen tests.

3.20 Tensile Test

The tensile test is performed at a constant stretching speed and temperature and was originally intended for polymer modified bitumens. Test specimens are elongated until failure or up to a given proportional elongation over their initial length. The European standard for the test is EN 13587:2010.

The procedure is based on similar methods used on other materials such as rubber or plastics. The tensile properties measured are useful as indicators for quality assessment of the materials. One of them, the conventional energy (calculated in accordance with EN 13703:2003, has been chosen as the specification criterion to evaluate the cohesion characteristics of polymer modified bitumens.

Different test temperatures (ranging from $-20\text{ }^{\circ}\text{C}$ to $+20\text{ }^{\circ}\text{C}$) and speeds (1, 10, 50, 100 and 500 mm/min) can be used. The test temperature is kept within $\pm 0,5\text{ }^{\circ}\text{C}$ by means of a temperature chamber. Test equipment also includes appropriate attachment jaws for a correct clamping of the specimens, force and elongation measurement devices.

Binder specimens are cast using dumbbell-shaped moulds of fixed dimensions (H2 type). However, other geometries are allowed given the difficulties found when preparing and working with this type of specimen. The results obtained from different geometries are not equivalent.

The tensile force applied and the elongation of each specimen is recorded during the test, so that the force against elongation curves can be obtained. The tensile properties normally reported are stress and proportional elongation at:

- the flowing threshold;
- fracture;
- 400 % elongation; and
- the maximum elongation if fracture is not reached.

Further calculations from the curves include the conventional (or cohesion) energy at 400 % elongation, which is the quotient of the deformation energy at this point and the initial cross section of the specimen.

There are no known equivalent standardised methods.

In accordance with EN 13703, the repeatability for the conventional energy, in J/cm^2 , corresponding to an elongation of 0,2 m (400 %), $E'_{0,2}$ is 10 % and the reproducibility is 30 %.

The tensile test has several common features with the direct tensile test (DTT) (Section 0) despite the procedures being intended for different purposes. In the DTT, a ductile-brittle transition temperature is sought whereas, in the tensile test to EN 13587:2010, a sample is rejected if a brittle break occurs. The tensile test is similar to the force-ductility test where the elastic/rubbery properties are tested with the elongation in these tests normally being $> 100\%$. DTT is a low temperature test and the result is a temperature whereas the tensile test is an elongation test and the result is an elongation and force. Nevertheless, the specification for the main components of the equipment for both tests, except the attachment devices, are compatible, making it possible to use the same basic equipment with most of the test machines and temperature chambers available on the market for both tests with the necessary modifications. A single stretching speed of 1 mm/min is required for both tests and the test temperature range is common to both procedures.

Similarly defined, but not equivalent, tensile properties can be measured through the force ductility test to EN 13589:2008 (Section 3.9). Although readily available and less costly than the tensile test equipment (providing the ductilometer has not also to be purchased), the force ductility apparatus has the drawbacks of a fixed stretching speed of 50 mm/min and a narrower test temperature range of 5 °C to 25 °C.

EN 13703:2003 for deformation energy states two calculation procedures for the conventional energy, depending on the method followed. Different specification limits have to be fixed for each test result.

3.21 Vialit Pendulum Test

The Vialit pendulum test assesses the degree of cohesion of the bituminous binder. The general layout is shown in Figure 3-22 and the apparatus used for carrying out the test is shown in Figure 3-23. The procedure, which is standardised in EN 13588:2008, involves placing a thin film of binder between two steel cubes and measuring the energy required to remove the upper block. The cracks appear in the bitumen film and not at the steel-bitumen interface. It is of greatest significance in situations where aggregate is placed in direct contact with traffic stresses, for example in surface dressings and the chippings in hot rolled asphalt surface courses. The maximum impact energy is usually increased by polymer modification, as is the overall energy across the entire temperature range. Its significance for other materials has yet to be fully evaluated.

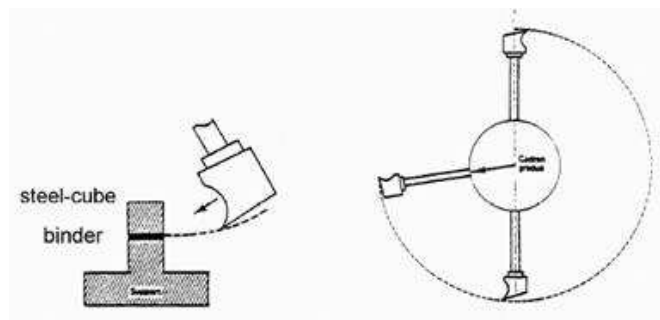


Figure 3-22: Schematic of the Pendulum test

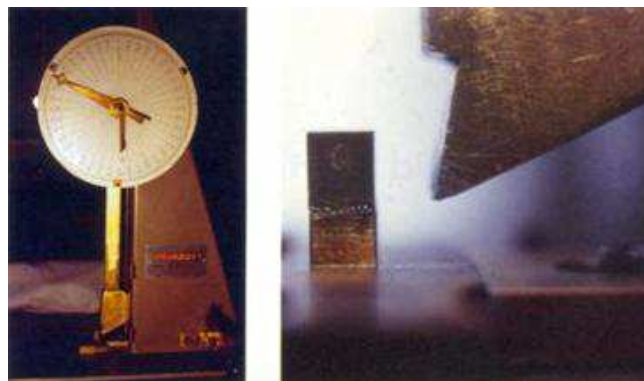


Figure 3-23: Vialit pendulum test

No equivalent methods have been identified.

The following precision data are the best currently estimated and are proposed until results of further round robin tests are available.

For unmodified bitumens:

- Repeatability: difference between 2 successive results < 0,06 J/cm².
- Reproducibility: difference between 2 single results < 0,18 J/cm².

For modified bitumens:

- Repeatability: difference between 2 successive results < 0,10 J/cm².
- Reproducibility: difference between 2 single results < 0,36 J/cm².

Although many test methods measure related properties and therefore there will be some relationship, no formal correlation has been found in the papers reviewed between the Vialit pendulum test and other bitumen tests.

4 Binder conditioning regimes

One of the key phenomena related naturally to bitumen and asphalt mixtures is ageing. As generally known there are two key regimes of ageing:

1. Short-term ageing covering several hours and related to asphalt mix production, transport, paving and compaction.
2. Long-term ageing counted in several years which is related to operational stage of the asphalt layer in the pavement.

During the short-term (thermic) ageing high temperatures are applied and the asphalt mix is due to uncompacted state showing higher specific surface area which facilitates thermal damage of metastable molecules and partly evaporation of some volatile compounds of the bitumen. As a result if overheating asphalt mix mainly during the production and at the same time sufficient amount of available oxygen the oxidative processes can start and degradation processes are accelerated. This usually can lead to an early bitumen hardening. Approximately 50 % of the total ageing arises already during the period of asphalt production and paving. The crucial part of the remaining ageing potential occurs in the asphalt pavement within 10 to 12 years. After that period usually the oxidative potential is saturated, i.e. the asphalt mix reaches its limiting ageing and further ageing is very slow or even not important anymore. The ageing procedure is in time always non-linear; the asphalt mix ages mostly during the first year, then the process is slowed-down. After 2 years in operation the rate of ageing is always considerably lower than total average ageing rate. Therefore studying and considering the sources of short-term ageing and the possibilities to limit consequences of this part of overall ageing with respect to the pavement life-time is important and should be taken into account if asphalt mix and its performance is studied. Especially in terms of its stiffness, low-temperature cracking or fatigue behaviour.

For bituminous binders short-term ageing is simulated according to EN 12607 series, whereas the key (reference) test procedure is specified by EN 122607-1 (Rolling Thin Film Oven Test – RTFOT). Additionally Thin Film Oven Test – TFOT or Rotating Flask Test – RFT can be used as well nevertheless for these tests some limiting factors have been repeatedly identified and discussed by studies and research works in the past. Long-term ageing is since the concluding recommendations of Strategic Highway Research Program finished almost 20 years ago in the U.S. simulated by Pressure Ageing Vessel – PAV according to EN 14769. Generally it is believed that applying this test method the aged bitumen corresponds to the binder properties after 7-10 years in a pavement (if standard procedure with 20 hours ageing is used). Another type of accelerated long-term ageing is Rotating Cylinder Ageing Test – RCAT or modified RTFOT or even TFOT test. The modification is related either to the conditions in the test heating chamber (e.g. applying ozone instead of natural fresh heated air) or repeating the standard procedure 2 or 3 times. In general bitumen ageing is fully standardized in Europe and applied to the binders regularly. Probably the only task is to concentrate during bitumen characterization.

The ageing process cannot be directly measured, therefore the evaluation of ageing level on test specimens or laboratory produced bulk asphalt mixtures needs to define a suitable test method determining particular mechanical or functional properties and comparing the gained results with the control (unaged) asphalt mixture. This comparability is provided by several bitumen tests as well as by qualitative or quantitative tests on asphalt mixtures. In the latter case the question remains if compacted test specimens or bulk asphalt mixture should be aged and tested. At the same time further extensive research is needed to understand better how the used test conditions (time and temperature) do in reality simulate real age of the asphalt layers. It might be even different if mixtures from the base layer or from the surfacing are aged.

Ageing of asphalt mixture in short-term or long-term regime is described by the American AASHTO R 30-02. Two possibilities are considered: (a) bulk asphalt mixture which is aged either 2 hours at 154 °C or 4 hours at 135 °C to simulate short-term ageing, (b) leaving compacted test specimens for 5 days at 85 °C in the heating chamber. In Europe several research projects in the last few years focused partly on asphalt ageing. In Re-Road project several possible procedures were described and compared including the experience from U.S. but also some national procedures or even RILEM coordinated testing. CoRePaSol project integrated ageing of cold recycled asphalt mixtures in the recommendations for European wide harmonized guidelines for cold recycled mixtures. With respect to CEN committees and their activities actually the prEN 12697-52 is in preparation and review. In terms of short term ageing the preferred procedure is heating bulk asphalt mixture for 4 hours at 135 °C. For long-term ageing the standard defines at least four procedures:

- bulk asphalt mixture conditioned at 60 °C for 14 days,
- bulk asphalt mixture conditioned at 85 °C for 9 days,
- accelerated ageing of bulk asphalt mixture using PAV where the mix is conditioned for 20 hours at 90 °C,
- ageing of Marshall test specimens at 85 °C for 5 days.

Several other test procedures are available or have been developed. In general for all procedures (mainly if long-term ageing is assessed) the question remains what exactly is simulated by the particular test method and what effect is reached after the ageing procedure is done. At the same time it becomes more and more obvious that including ageing conditioning to either bulk asphalt mixture or compacted test specimens is crucial for better understanding of performance behaviour of an asphalt pavement. As stressed earlier this is important mainly for fatigue life testing, stiffness behaviour or crack initiation and propagation in an asphalt layer. From many later analysed and summarized papers and/or research studies it is obvious that predominantly testing on fresh (unaged) asphalt mixtures is done. On the other hand for bituminous binders ageing behaviour has been studied and standardized in the last 10-20 years more intensively.

5 Permanent deformation (rutting)

5.1 Asphalt test methods for permanent deformation

5.1.1 General

Permanent deformation is the irreversible structural change in an asphalt layer caused by high pressure on the surface at elevated service temperatures. The relevant European asphalt tests are EN 12697-22, Wheel tracking and EN 12697-25, Cyclic compression test. In the USA, the SUPERPAVE shear tester (SST) is used to evaluate the resistance to permanent deformation.

5.1.2 Wheel tracking test

The wheel tracking test is used to measure the rut formed by repeated passes of a loaded wheel at constant elevated service temperature. EN 12697-22 describes three types of test devices (extra-large size device, large size device and small size device).

- Extra-large size device: The specimens have dimensions (700 x 500) mm and a height of either 30 mm, 50 mm, 60 mm, 75 mm or 100 mm. A wheel fitted with a pneumatic tyre without a tread pattern and having a track width of 110 mm travels 700 mm over the specimen in 2,5 s. The rolling load applied to the test specimen is 10 kN at the centre of the test specimen.
- Large size device: The specimens have dimensions (500 x 180 x 50) mm or (500 x 180 x 50) mm. A wheel fitted with a 400 x 8 pneumatic tyre without a tread pattern and having a track width of 80 mm travels 410 mm over the specimen with a frequency of 1 Hz. The rolling load applied to the test specimen is 5 kN at the centre of the test specimen.
- Small size device: The block specimens have minimum dimensions of (260 x 300) mm or cylindrical specimens with a diameter of at least 200 mm. A treadless tyre with an external diameter between 200 and 205 mm and a rectangular cross profile with a track width of 50 mm travels 230 mm over the specimen with a frequency of 26,5 load cycles/min. The rolling load applied to the test specimen is 700 N.

The number of load cycles (i.e. two load passes) with extra-large size device is between 14 000 and 30 000 while with large size devices it is between 30 000 and 100 000. Two procedures are available for small size devices: Procedure A with 1000 load cycles and Procedure B with 10 000 load cycles. The conditioning and testing of samples is in air unless using Procedure B with small size devices, when the conditioning and testing of samples can be in either air or water.

The results are represented as proportional rut depth against number of load cycles except for small devices, which gives the results as wheel tracking rate and rut depth in the case of Procedure A and as wheel-tracking slope and rut depth besides proportional rut depth in case of Procedure B.

Other laboratory-scale accelerated loaded wheel tests commonly used are the following:

- Asphalt Pavement Analyser (APA): Oscillating beveled aluminium wheels apply a repetitive load through high-pressure hoses to generate the desired contact pressure. The loaded wheel oscillates back and forth over the hose. While the wheel moves in the forward and backward directions, the linear variable differential transducers (LVDTs) connected to the wheels measure the depression at regularly specified intervals. Usually, three replicates of specimens are tested in this machine. Rut evaluation is typically performed by applying 8000 load cycles. The wheel load is usually 445 N, and

the hose pressure is 690 kPa. APA testing can be performed using chamber temperatures ranging 5°C to 71°C. Rutting and moisture-induced damage evaluations can be performed on either cylindrical or beam specimens. This machine is capable of testing in both dry and wet conditions (Chowdhury & Button, 2002).

- Hamburg Wheel Tracking Device (HWT): This equipment was originally developed in Germany, but has been adapted to other configurations in countries such as USA. The basic idea is to operate a steel wheel on a submerged, compacted HMA slab or cylindrical specimen. The original HWT uses a slab with dimensions of 320 × 260 × 40 mm³. The slab is usually compacted at 7 ± 1 percent air voids using a linear kneading compactor. The test is conducted under water at constant temperature ranging from 25°C to 70°C. Testing at 50°C is the most common practice. The sample is loaded with a reciprocating motion of the 47 mm wide steel wheel using a 705 N force. Usually, the test is conducted at 20 000 cycles or up to a specified amount of rut depth. Rut depth is measured at several locations including the center of the wheel travel path, where usually it reaches the maximum value. One forward and backward motion comprises two cycles (Chowdhury & Button, 2002).
- French Rutting tester (FRT): This equipment was developed in France, and has also been adopted in other countries/laboratories. The test specimen is an asphalt slab with typical dimensions of 180 × 500 mm². The FRT can apply wheel loads simultaneously on two test slabs. Loading is accomplished by applying a 5 kN wheel load using a smooth pneumatic tire pressurized at 600 kPa. The pneumatic tire passes over the slab center at the rate of 120 times per minute. For rut susceptibility evaluation, the test is conducted at a higher temperature range, typically 50-60°C. FRT rut depth is defined by the deformation expressed as a percentage of the original slab thickness. The rut depth is measured across the width of the specimen. The typical number of cycles used with the FRT is 6000 (Chowdhury & Button, 2002). Large size device of EN 12697-22 was adopted from the original FRT.

5.1.3 Cyclic compression test according to EN 12697-25

EN 12697-25 describes two test methods for determining the resistance to permanent deformation of asphalt: the uniaxial cyclic compression test and the triaxial cyclic compression test. The specimens may be either prepared in the laboratory or cored from a pavement.

- In the uniaxial cyclic compression test, a cylindrical test specimen with height of 60 mm and diameter of 150 mm, maintained at elevated conditioning temperature, is placed between two parallel loading platens. In order to achieve a certain confinement, the diameter of the loading platen is smaller than that of the sample. The standard allows for two different uniaxial cyclic compression test procedures:
 - 1st) The upper platen has a diameter of 100 mm (due to inclination the contact area with the specimen has a diameter of 96 mm) and the lower platen is larger than the specimen. The specimen is subjected to a cyclic axial block--pulse pressure, with frequency 0,5 Hz (1 s loading and 1 s rest period) and a typical stress of 100 kPa.
 - 2nd) The upper platen has a diameter of 56,4 mm and the lower platen is larger than the specimen as well. The specimen is subjected to a cyclic axial haversine loading with a pulse duration of 0,2 s (equivalent to a loading frequency of 5 Hz) and a rest period of 1,5 s between the loading pulses, and a typical stress of 350 kPa for the maximum pulse load pressure and of 80 kPa for the minimum rest load pressure.

In both cases there is no additional lateral confinement pressure applied.
- In the triaxial cyclic compression test, a cylindrical test specimen, maintained at elevated conditioning temperature (typical between 30 °C and 60 °C), is placed between two parallel loading platens. When the nominal maximum aggregate size is less than or equal to 16 mm, the specimen has a minimum height of 50 mm and a minimum diameter

of 50 mm. A specimen with nominal maximum aggregate size greater than 16 mm has a minimum height of 80 mm and a minimum diameter of 80 mm. The specimen is subjected to a cyclic axial pressure (σ_A) and a static lateral confinement pressure (σ_C). The cyclic axial pressure can be a block-pulse or haversine with a frequency from 1 Hz to 5 Hz.

During the test, the change in height of the specimen is measured at specified numbers of load applications. The results are represented in a creep curve. The test does not allow quantitative prediction of rutting, but makes it possible to rank various mixtures in terms of resistance to permanent deformation.

5.1.4 SUPERPAVE shear tester

The SUPERPAVE shear tester (SST) is a servo-hydraulic machine that can apply both axial and shear loads at constant temperatures to a cylindrical (150 x 150) mm specimen using closed-loop control. The current SST protocols consist of different modes of operation. Two of the commonly used modes are the frequency sweep at constant height (FSCH) and the repeated shear at constant height (RSCH). In each mode, different types of information are available. The FSCH test involves the application of a sinusoidal shear strain with a certain peak amplitude (e.g. 0,4 $\mu\text{m}/\text{mm}$) at a fixed temperature of interest at each of the following frequencies: 10; 5; 2; 1; 0,5; 0,2; 0,1; 0,05; 0,02; and 0,01 Hz. The generated response parameters are the complex shear modulus (G^*), the phase angle (δ), the recoverable shear modulus (G'), and the loss shear modulus (G''). The RSCH test consists of applying 5000 cycles of a haversine shear load with a shear stress level of (68 ± 5) kPa: the axial load is varied automatically during each cycle to maintain constant height of the specimen to within 0,0013 mm. The test involves the repeated application of a 0,1 s load pulse followed by a 0,9 s rest period during which the permanent deformation is recorded and used for comparisons. The protocol followed is in accordance with AASHTO provisional standard TP7-94, which contains a detailed description of the SST test in the different modes of operation. The information obtained from the SST using different modes of operation is used conventionally by researchers to compare generated data for any proposed mixture of unknown performance with another mixture with known performance under the same conditions at identical temperatures.

5.1.5 Simple Performance Tests (SPT)

In the framework of NCHRP Project 9-19, simple performed tests to evaluate the permanent deformation of HMA mixture were developed, as follows:

- **Dynamic Modulus:** The dynamic modulus test procedure is similar to ASTM D 3497 with some modifications. In the proposed test method, dynamic modulus (E^*) and phase angle (δ) are measured from the sinusoidal axial load application on a cylindrical Superpave Gyratory Compactor (SGC) specimen at a single temperature ($T_{\text{eff}} = 25$ to 40°C) and design loading frequency (0.1 to 10 Hz). Here, the complex modulus is calculated by dividing the stress by the axial strain. The phase angle is the angle lagging by the axial strain from the axial stress. The concept is similar to the FSCH test by SST equipment. The specimen used for this test is 100 mm in diameter and 150 mm in height (Chowdhury & Button, 2002).
- **Flow Number:** Flow number is the number of load repetitions at which shear deformation begins under constant volume (Figure 5-1). In this test protocol, the SGC compacted cylindrical specimen is subjected to repetitive axial load in a triaxial environment at a single temperature. The load is applied for a duration of 0,1 s, followed by a rest period of 0,9 s. Usually, a 69-207 kPa stress is applied and the cumulative permanent axial and

radial strains are recorded throughout the test. The specimen dimension is the same as that of the dynamic modulus test (Chowdhury & Button, 2002).

- Flow Time: Flow time is defined as the postulated time when shear deformation starts under constant volume. In this test protocol, the SGC compacted cylindrical specimen is subjected to static axial load in a triaxial environment at a single temperature. The applied stress and the resulting permanent axial and radial strains are recorded throughout the test to calculate the flow time (Chowdhury & Button, 2002).

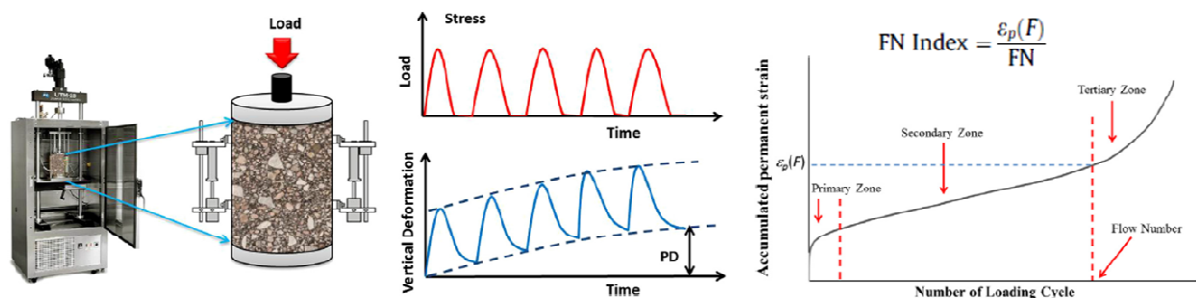


Figure 5-1: Flow Number test setup and configuration [source: Zang *et al.*, 2013]

5.1.6 Coaxial Shear Test (CAST)

The Co-Axial Shear Test (CAST) is a dynamic, axial loading system to determine the complex shear modulus (G^*) of asphalt concrete. The test was first developed at EMPA in 1987 and further developed. Tests are performed in a conventional, temperature controlled, servo-hydraulic tension-compression machine. The specimens were cored in the center to produce donut shaped asphalt concrete specimen of approximately 150mm outer diameter and 55mm inner diameter and 50mm in height (Figure 5-2). The specimen is glued to a central steel cylinder and an outer steel ring with epoxy resin. The shear load is applied perpendicular to the specimen's circular surface by the steel cylinder with lateral confinement provided by the metal ring surrounding the specimen. This format allows loading along the same axis as that of traffic loading while the lateral confinement simulates a semi-infinite in-situ situation (Poulikakos *et al.*, 2007).



Figure 5-2: Cut view of a CAST specimen at EMPA [source: Poulikakos *et al.*, 2007]

5.1.7 Carleton in-situ shear strength test

The Carleton in-situ shear strength test (CISST) facility is a device for measuring the in-situ shear strength. A torque is applied to a loading platen bonded to the asphalt surface with a strong epoxy resin. The torque and the angle of twist at failure are measured.

5.2 *BitVal findings on permanent deformation*

The BitVal project identified and reviewed eight binder tests as having a potential relationship with asphalt permanent deformation (Capillary Viscometer Test; Cone and Plate Viscosity Test; Creep Zero Shear Viscosity Test; Dynamic Shear Rheometer Test; Oscillation Zero Shear Viscosity Test; Repeated Creep Test; Softening Point Test by Ring and Ball method), which are described in Chapter 3). Six of the tests were designed for measuring the viscosity of the binder at elevated service temperatures, the exceptions being the R&B softening point test and the dynamic shear rheometer DSR test for measuring G^* . However, the R&B softening point test could be excluded because the R&B softening temperature is not capable of correctly ranking PMBs in accordance with their rutting sensitivity. The capillary viscometer test is also not appropriate because the test only applies to unmodified binders.

The number of references found was limited for the coaxial cylinder test and the cone and plate viscosity test. This lack does not mean that the test results would necessarily correlate poorly with permanent deformation. The main reason is probably that these test geometries are less used than the more commonly used parallel plates.

The DSR test is relevant for permanent deformation when the complex modulus is considered at elevated service temperatures and at low frequencies. The DSR test is then equivalent to the oscillation test for zero shear viscosity ZSV (see below).

The validity of the creep ZSV test can be regarded as an indicator for permanent deformation. However, questions remained concerning:

- The precision of the results for PMBs with a high polymer content. This concern was also the conclusion of the round robin test conducted by CEN TC336 WG1/TG1. It should be further investigated if the reproducibility can be improved by refining the test protocol (e.g. by fixing criteria for stopping the creep test).
- The duration of the creep test. From a practical point of view, a creep period of 8 h or more is not desirable. Shorter creep periods may lead to good correlations with asphalt rutting, but this assumption can only be demonstrated by actually performing asphalt tests and looking at correlations with creep tests after various creep periods.
- The large deformations applied. With creep periods of hours and more, the deformations become very large and outside the range of deformations normally encountered in asphalt mixtures. It is not clear to what extent this difference in range also has an impact on the degree of correlation.

It should be noted that the creep test will always be limited to binders with a ZSV below a maximum value, because of the precision and the duration of the test.

The oscillation ZSV test was then the most interesting candidate because:

- Good correlations had been reported, coming from three different sources.
- The test is relatively simple and the duration is acceptable (depending on how low the test frequency is).

It had not yet been shown which exact test conditions (temperature and frequency) will give results that correlate best with asphalt rutting. However, the following guidelines generally applied:

- the correlation will be best if the test temperature is as close as possible to the temperature at which rutting occurs; and
- test frequencies from 0,01 Hz to 0,001 Hz lead to a good correlation, while still being practically feasible.

For the equi-viscous temperature based on the oscillation ZSV, as described in the European draft test method, the precision data are satisfying, including for the PMBs. Correlations with asphalt tests had not yet been reported, but the correlations were expected to be good because the oscillation ZSV at a given temperature correlated closely with asphalt rutting tests at the same temperature. However, it was an important recommendation for future work because the validation of the test method depends on the demonstration of this correlation.

The repeated creep test was also an interesting candidate, for which good correlations with asphalt rutting tests had been reported. However, the validation of this test still required some work, including the estimation of the precision under conditions of reproducibility. Nevertheless, it had already been reported in the USA that the reproducibility of the test was not good because the test requires very high standards for the DSR equipment. Therefore, it was questionable to invest more research into following this trail.

5.3 Relationship found between bitumen properties and asphalt resistance to permanent deformation

5.3.1 General

Besides the tests addressed within BitVal project, other tests to characterize bitumen properties were also considered in the framework of the present study. Among these, all the tests referred in chapter **Chyba! Nenalezen zdroj odkazů.** are considered, as long as they are referred as bitumen properties related with permanent deformation of bituminous mixtures. Besides, new/recent tests relating bitumen and asphalt performance are also attended.

In the present of state-of-art review, relationships between bitumen properties and asphalt resistance to permanent deformation were analyzed according to the test used to determine the bitumen properties. In a following step, the results achieved in this phase will be mainly addressed by highlighting the correspondent binder property.

According to the issued data form (section **Chyba! Nenalezen zdroj odkazů.**), in the case of permanent deformation of bituminous mixtures, the main relevant bitumen properties at elevated service temperatures conditions are the following:

- Complex modulus;
- Dynamic viscosity;
- Low shear viscosity;
- Softening point;
- Creep stiffness;
- Compliance and recovery.

5.3.2 Capillary Viscometer Test

5.3.2.1 Paper 559 (Reyes Lizcano et al., 2009)

This paper describes an investigation to quantify the effect of polymer modification to Colombian asphalt on hotmix asphalt performance. Mixes prepared with binders with varying percentages of styrene-butadienestyrene (**SBS**) were studied. An oil-based additive was necessary to lower the mixing temperature to a manageable level for polymer contents above 3 %. Tests conducted included traditional binder and mix design tests, as well as dynamic characterization of the mixes using the Nottingham Asphalt Tester.

The modified asphalts showed lower thermal susceptibility and greater consistency than the base asphalt. The increment in the modifying agent improves resistance to plastic strain that

can occur at high temperatures, **based on the increment in the softening point**. Additionally, the asphalt elasticity is improved. Dynamic characterization of mixes produced with the modified binders showed that the binder modified with 3 % SBS presents a **higher dynamic modulus**, which translates into a lower rutting risk. All the mixes with modified asphalts showed **higher permanent deformation resistance** than mixes with unmodified binders.

In this study the base asphalt was mixed with different percentages of polymer (3 %, 5 %, 7 %, 9 %, 11 %, and 13 %). To obtain a modified asphalt that can be mixed and compacted, it was necessary to add an additive that would soften (lower the viscosity of) the asphalt to manageable levels.

To evaluate the behavior of the mixtures under cyclical loads produced by traffic, the mixtures were subjected to dynamic tests using the Nottingham Asphalt Tester (NAT). A cyclic uniaxial load without confinement was used in this study (Repeated Load Axial Test, or RLA). The procedure followed is described in European Norm prEN 12697-25. The binders selected for these tests were conventional asphalt C, asphalt with additive A, and modified asphalts M1, M3, and M5. All tests were conducted at a temperature of $(40 \pm 1) ^\circ\text{C}$.

Table 5-1: Characteristics of the various virgin and modified binders studied

Characteristic	Asphalt							
	Conventional	Modified						Asphalt with Additive
		C	M1	M2	M3	M4	M5	
Polymer Content (%)	-	3	5	7	9	11	13	-
Additive Content (%)	-	5	15	30	40	55	65	1,7
Penetration 100 g, 5 s, at 25°C, (0.1 mm)	72	66	84	117	124	150	147	75
Cinematic Viscosity at 135°C, (cSt)	291,9	633,2	713,7	475,7	572,4	778,6	867,4	269,1
Softening Point [Ball and Ring], (°C)	48,6	53,8	57,8	59,8	61,8	61,0	60,0	47,0
IP* [INV E-724]	-0,6	0,4	2,1	3,7	4,3	5,0	4,7	-1,0
Elastic Recovery using a Ductilometer (%)	0	67,1	77,6	81,4	83,3	82,9	82,4	0
Specific Weight at 25°C	1,0177	1,0166	1,0159	1,0126	1,0105	1,0046	1,0008	1,0163
Residual Penetration at 25°C after the RTFOT (0.1 mm)	33	39	47	67	79	98	104	38
Mass Reduction (%)	1,95	1,84	1,66	1,78	1,84	1,94	1,78	2,27
Retained Penetration (%)	46	59	56	57	64	66	71	51
Softening Point of the Residual after the RTOFT (°C)	58	62	63	65,8	65,0	63,5	62,0	55,5
Absolute Viscosity at 60°C (cP)	159000	412000	499000	482000	432000	193000	146000	135000
Absolute Viscosity at 80°C (cP)	14167	31567	32500	24706	20636	16417	16133	12571
Absolute Viscosity at 100°C, (cP)	2420	5261	5400	4046	4175	3783	3912	2217
Absolute Viscosity at 120°C, (cP)	668	1322	1487	1270	1388	1350	1430	605
Absolute Viscosity at 140°C, (cP)	238	505	575	520	620	613	655	220
Absolute Viscosity at 160°C, (cP)	115	210	260	260	310	320	345	90
Absolute Viscosity at 180°C, (cP)	-	110	153	155	195	190	210	-

The term "Penetration Index" is not applicable to modified asphalts, since by definition its use is limited to conventional asphalts (Newtonian). However, in this study the term is used as an empirical method to show the reduction in the thermal susceptibility of asphalts.

Table 5-2: Repeated load axial test results

Number of Load Cycles	Binder Used in the Mix								
	C	C	M1	M1	M3*	M5	M5	A	A
	Strain (%)								
10	0.5776	0.5284	0.4206	0.3880	0.4385	0.4717	0.4162	0.4630	0.4725
100	0.7610	0.7012	0.5726	0.5114	0.5499	0.5879	0.5337	0.6035	0.6504
1000	1.0175	0.9072	0.7814	0.6577	0.7149	0.7677	0.7037	0.8179	0.9158
1400	1.0619	0.9371	0.8106	0.6803	0.7409	0.7977	0.7308	0.8583	0.9575
1800	1.0999	0.9599	0.8344	0.6936	0.7622	0.8175	0.7506	0.8891	0.9904
3600	1.2162	1.0290	0.9056	0.7367	0.8191	0.8831	0.8098	0.9909	1.0960

* Two tests were conducted, but one was discarded due to problems during testing.

Conclusion: Modified asphalts present better behavior under permanent strain tests, which is consistent with the literature.

5.3.3 Coaxial Cylinder Viscosity Test

(No papers)

5.3.4 Cone and Plate Viscosity Test

5.3.4.1 Paper 171 (Mogawer et al., 2012)

See section 5.3.12.3.

5.3.5 Creep Zero Shear Viscosity (ZSV) Test

5.3.5.1 Paper 023 (Dueñas et al., 2012)

The results from Figure 5-3 show that there is certain linearity between different data, in both strain and slope, although there are some points, especially the crumb rubber binder with significant deviations.

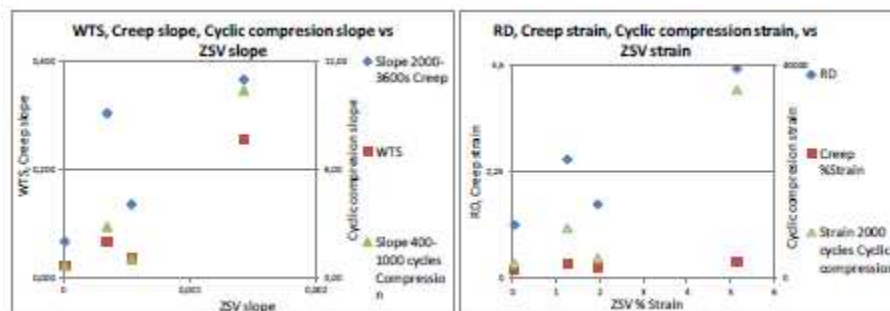


Figure 5-3: Relations between Wheel tracking mix test (WTT), cyclic compression mix test (CCT) Creep test, and binder creep test

5.3.5.2 Paper 042 (Robertus et al., 2012)

See also sections 5.3.6.1, 5.3.8.4 and 5.3.11.2.

Figure 5-19 shows the relationship between wheel tracking rate and ZSV for unaged binders. There is no correlation ($R^2=0,49$) when considering all binders. However, considering only rheological simple binders, NPGs and SPs, a very good correlation ($R^2=0,93$) is found. This correlation is furthermore independent of temperature.

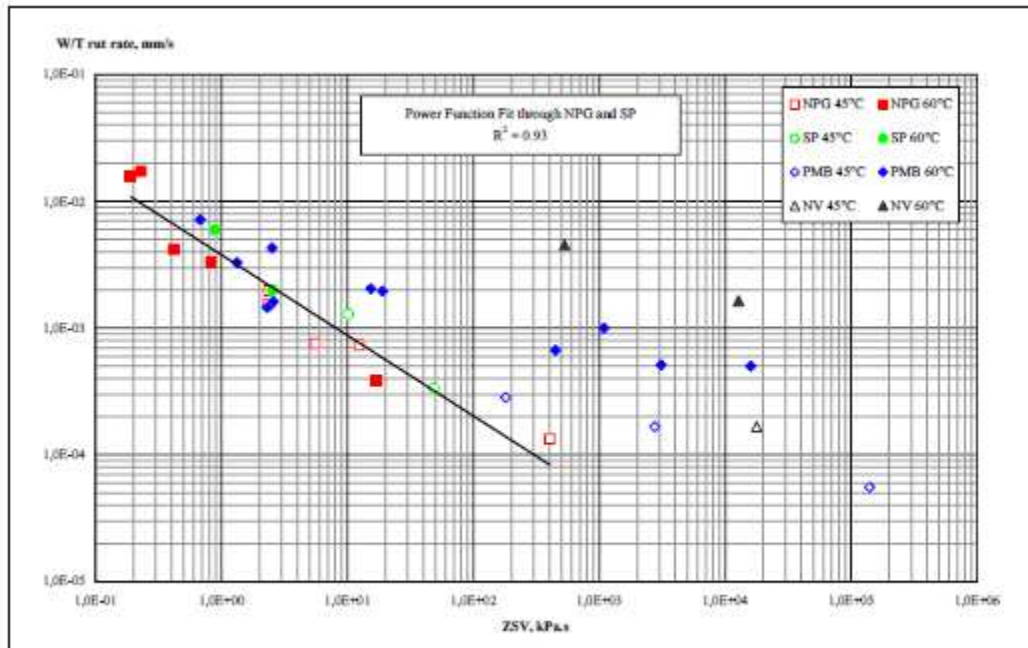


Figure 5-4: Wheel-tracking rut rate vs ZSV of unaged binders at 45°C and 60°C

5.3.5.3 Paper 067 (Guericke & Schlame, 2008)

See also sections 5.3.6.5 and 5.3.11.3.

Results of rut tests with a SMA standard mixture involving 11 different unmodified and polymer modified binders are shown in Figure 5-5. In an earlier test programme the viscosity at 60°C was measured with DSR in oscillation mode at a low shear rates and extrapolated to zero (Guericke & Schlame, 2000). The good correlation of Zero Shear Viscosity with rut depth in asphalt was encouraging to refine the method. For this test programme the mode of extrapolation to ZSV was a preliminary one and has been improved during the later standardization process, with the result reported in this paper.

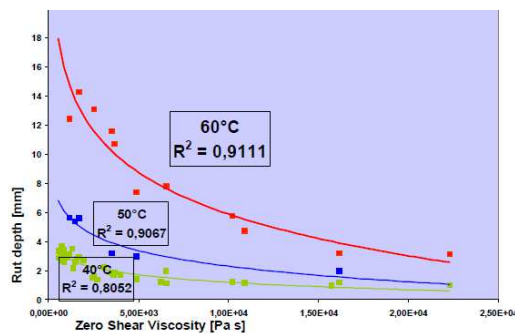


Figure 5-5: Rut depth (Hamburg Wheel-tracking Test) in SMA at 40 °C, 50 °C and 60 °C vs ZSV at 60 °C after short-term ageing (RFT)

5.3.6 Complex shear modulus and phase angle by Dynamic Shear Rheometer (DSR) Test

5.3.6.1 Paper 042 (Robertus et al., 2012)

See also sections 5.3.5.2, 5.3.8.4 and 5.3.11.2.

The relationship between wheel-tracking rut rate and Stiffness Modulus G^* (1,59 Hz) at 45 and 60 °C of the original binders is shown in Figure 5-6. For unmodified (rheological simple) binders G^* correlates well with rut rate ($R^2 = 0,94$). However, for rheological complex binders (i.e. most PMBs) there is clearly no correlation between rut rate and G^* . In fact the contribution of these binders to rutting resistance is generally largely underestimated by G^* . For example PMB3, which is a commonly used binder in Germany, has at 60 °C the same value for G^* as NPG1 (± 7 kPa) but a factor 2 lower rut rate. PMB5 with a lower value for G^* at 60 °C (± 4 kPa) has even a factor 6 lower rut rate than NPG1. This trend/picture remains when $G^*/\sin\delta$ or data of the short term aged binder is plotted.

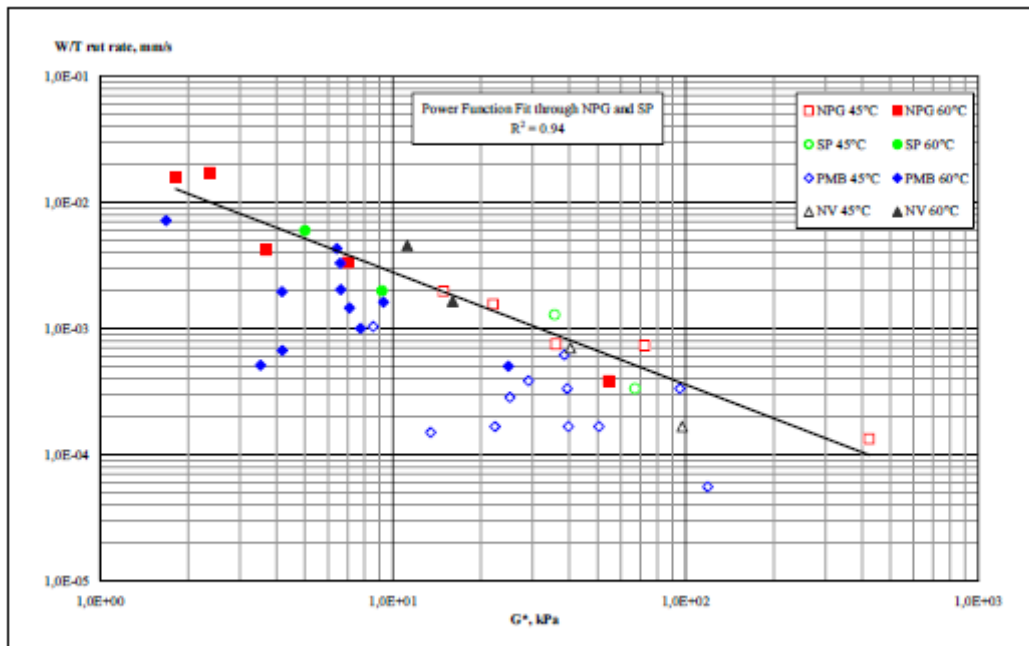


Figure 5-6: Wheel tracking rut rate vs stiffness modulus (1,59 Hz) of unaged binders at 45 °C and 60 °C

5.3.6.2 Paper 043 (Morea, 2012)

If the R_r measurements (WTT) are represented as a function of the bitumen LSV (original or aged) determined at each test temperature, see Figure 5-7, all asphalts follow a similar tendency. It was observed how improves the rutting performance in the WTT (minor R_r) when the LSV is increased. In addition Figure 5-7 shows that R_r drastically changes in the region of low LSV values. Considering the temperatures range, the different types of asphalts and the gradations studied, it is observed that notable changes in rutting resistance appear when the original bitumen binder has LSV values lower than 500 Pa.s, see Figure 5-7 left. Similarly strongly changes in the rutting behaviour take place for aged bitumen LSV values lower than 1000 Pa.s. Based on this observation, the CEN/TS 15324:2006 LSV value of 2000 Pa.s can be taken as a safer threshold for the aged asphalt condition.

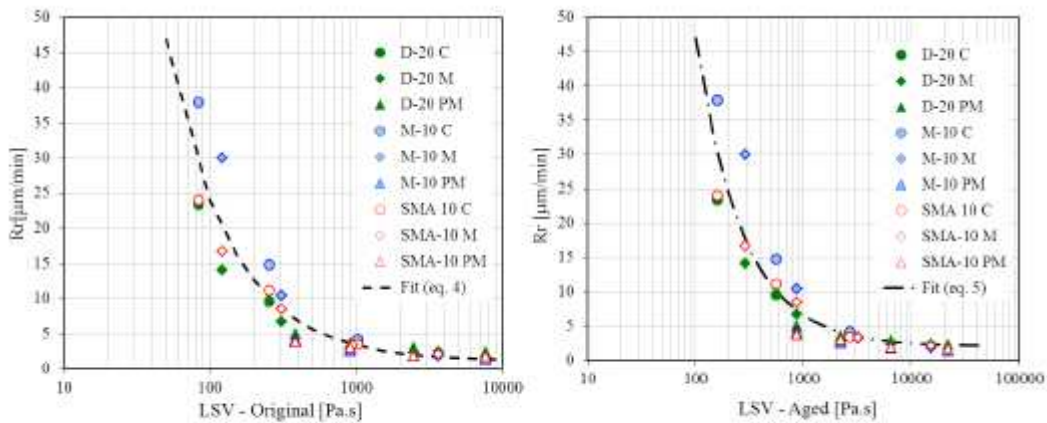


Figure 5-7: Rr of D-20, M-10 and SMA-10 asphalt vs. bitumen LSV (left: original, right: aged)

5.3.6.3 Paper 047 (Gungor & Sađlik, 2012)

As it is seen on the $G^*/\sin\delta$ -strain and ZSV-strain graphics drawn according to the test results, the value of ZSV provides a higher degree correlation with the occurred permanent strains (Figure 5-8). In this sense, it can be said that the value of zero shear viscosity represents the viscoelastic behavior of the bitumen better.

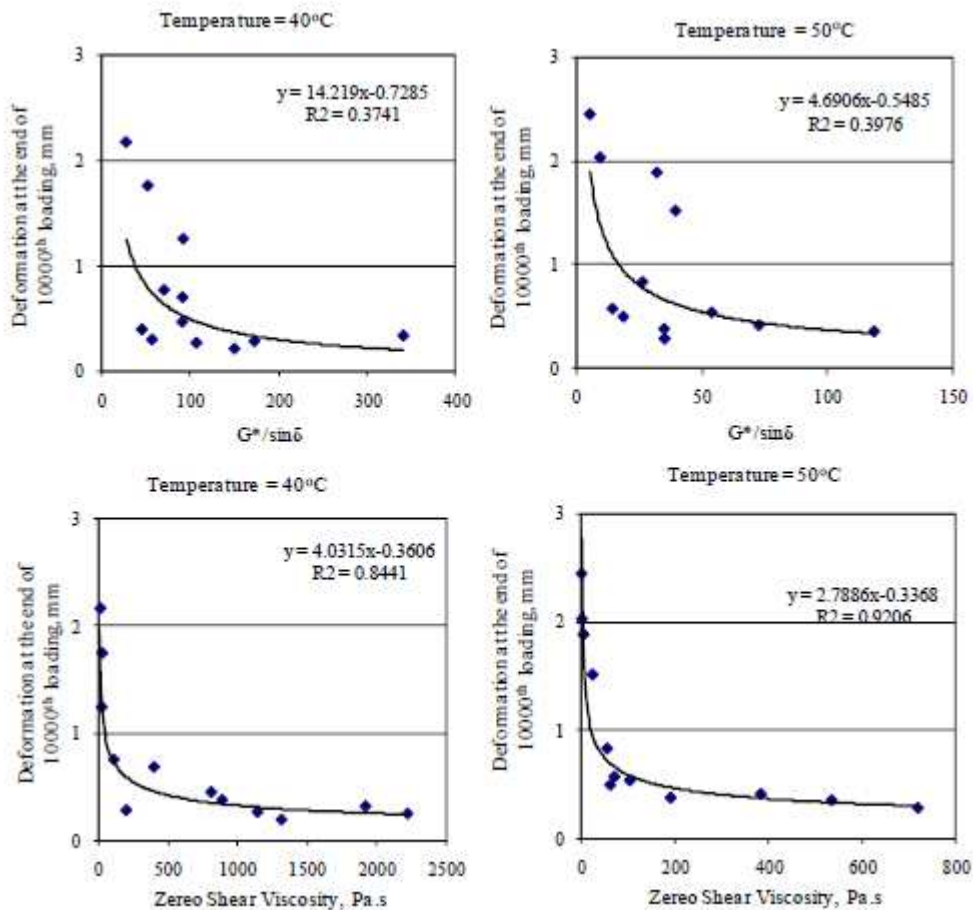


Figure 5-8: ZSV vs deformation and $G^*/\sin\delta$ vs deformation at 40 °C and 50 °C

5.3.6.4 Paper 061 (Beckedahl et al., 2008)

To determine the correlation between $G^*/\sin\phi$ and rut depth as well as between resilient modulus and rut depth, comparison of adequate test results have been carried out for different asphalt type. The DSR test appears to be a good tool to investigate the effect of binders for example on rutting behaviour of asphalt in laboratory binder tests. To determine the correlation the relation $G^*/\sin\phi$ and the rut depth are opposed in the Figure 5-9 (left) and a corresponding regression curve and regression coefficient have been produced. The determined regressions coefficients show a satisfy correlation for different asphalt type. By means of resilient modules the strength of asphalt can be characterised at different temperature. Asphalt with high strength at high temperature will show high resistance against rutting. Thus, asphalt with high resilient modules at high temperature will cause a low rut depth. To confirm this prediction the rut depth are compared with resilient modules at 50 °C for different asphalt type (Figure 5-9 right). The comparison show good correlation. As expected the slope of the regression curve for adequate asphalt types are different because of their different mix composition. In general a good correlation has been determined between binder and asphalt test, but to make an authentic correlation the comparison shall be carried out with more than three test results.

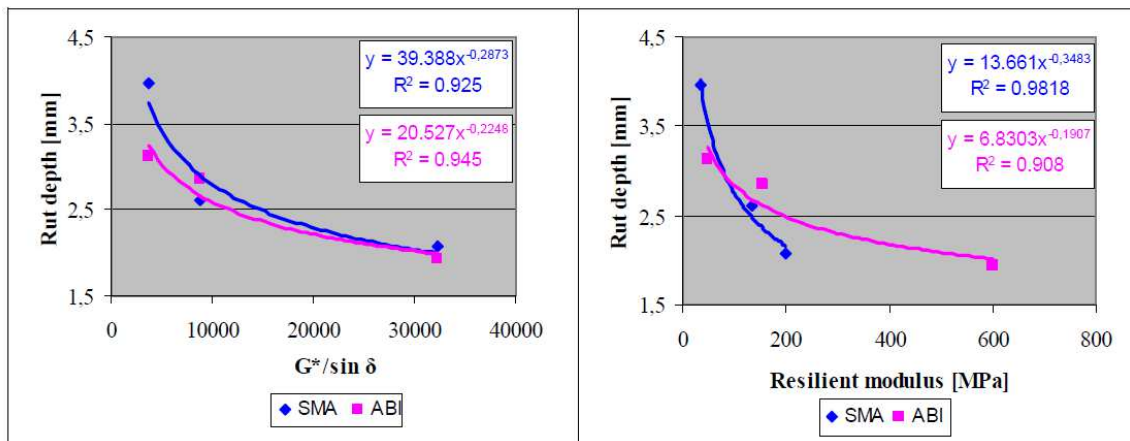


Figure 5-9: Correlation of rut depth and relation $G^*/\sin\phi$ (60 °C) (left) and Correlation of rut depth and resilient modulus (50 °C) (right)

5.3.6.5 Paper 067 (Guericke & Schlame, 2008)

See also sections 5.3.5.3 and 5.3.11.3.

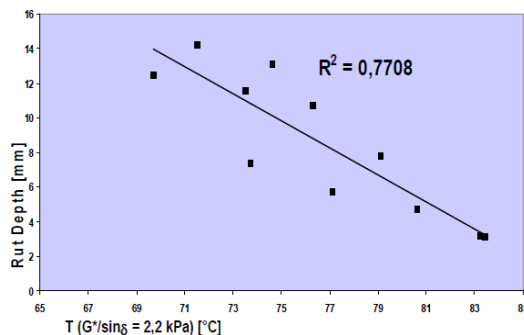


Figure 5-10: Rut depth (Hamburg Wheel-tracking Test) in SMA at 60 °C vs T ($G^*/\sin\delta=2,2$ kPa) after short-term ageing (RFT)

5.3.6.6 Paper 124 (Zeleeuw et al., 2011)

See also sections 5.3.8.5 and 5.3.12.1.

This paper is about the performance of different WMA additives. Figure 5-11 presents the master curve of asphalt binders at a reference temperature of 21,1 °C. Frequency sweep tests at testing temperatures of 4,4 °C; 21,1 °C; 37,8 °C and 54,4 °C were utilized to generate this master curve. It is shown that the binder type Sasobit® terminal blend measured the highest shear modulus values comparing to other asphalt binders, particularly under lower frequency ranges. Again, this binder sample should exhibit better permanent shear deformation performance.

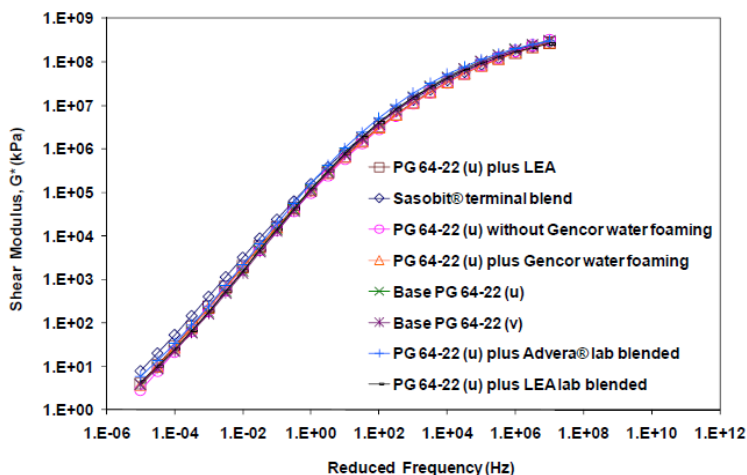


Figure 5-11: Bitumen master curve

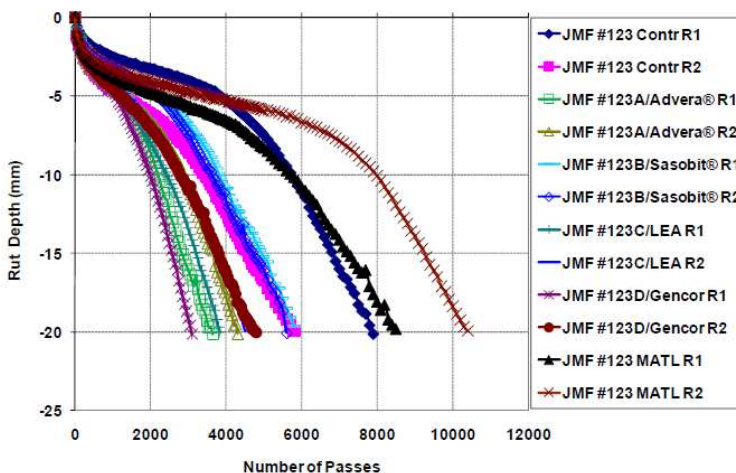


Figure 5-12: Hamburg test results: rut depth

At a given temperature, increasing Fn values indicate increasing permanent deformation resistance potential. Figure 5-13 shows the Flow Number test results for all asphalt mixtures tested under 50 000 microstrain at three temperatures (i.e., 45,8 °C; 51,8 °C and 57,8 °C). It is evident from this figure that the Fn test is highly dependent on testing temperatures. Overall, the Fn values decreased with an increase in testing temperature. This is apparent for viscoelastic materials where asphalt binder softening occurs upon temperature increase. The MATL mix design replication tested at 51,8 °C measured the highest Fn, likely because the mix was laboratory aged before testing. On the other hand, the lowest Fn was observed for WMA/Gencor at all testing temperatures. The contractor’s HMA and WMA/Sasobit® also measured higher Fn values.

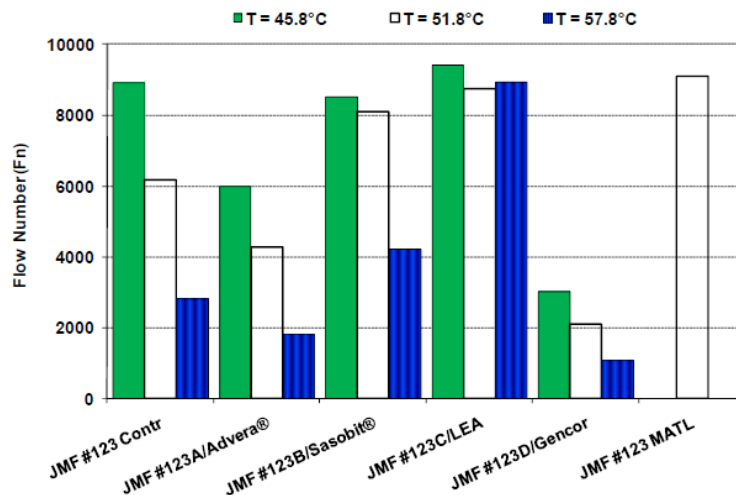
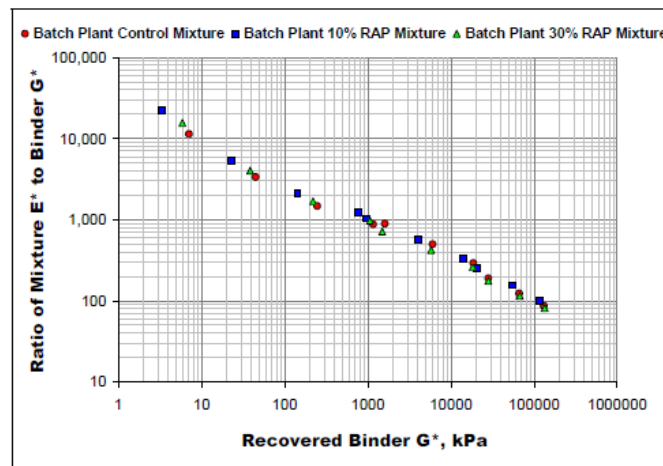
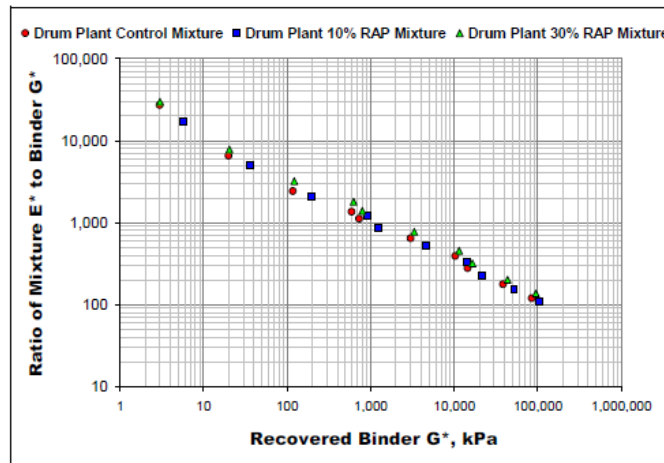


Figure 5-13: Flow number test results: Fn

5.3.6.7 Paper 135 (Mogawer *et al.*, 2012)

A partial master curve was developed for the recovered binder from each mixture over the range of reduced frequencies used in the dynamic modulus testing. This master curve was developed from frequency sweep data collected with the Dynamic Shear Rheometer (DSR) at temperatures of 10 °C; 22 °C; 34 °C and 46 °C using frequencies ranging from 0,1 to 100 rad/sec. The resulting data were fit to the Christensen-Anderson model (9) to allow the recovered binder modulus to be computed at the temperatures and loading frequencies used in the mixture dynamic modulus testing. The ratio of the measured mixture dynamic modulus to the recovered binder shear modulus was then calculated. Figure 5-14 shows plots of the ratio of the measured mixture dynamic modulus to the recovered binder shear modulus for the mixtures from the two plants. These plots indicate that there is a power law relationship between the binder shear modulus and the ratio of the mixture dynamic modulus to the binder shear modulus.





(b)

Figure 5-14: (a) Plot of ratio of mixture E^* to binder G^* - batch plant; (b) Plot of ratio of mixture E^* to binder G^* - drum plant

5.3.6.8 Paper 171 (Mogawer *et al.*, 2012)

See section 5.3.12.3.

5.3.6.9 Paper 214 (Centeno *et al.*, 2008)

This paper assesses rutting susceptibility of five different modified asphalts in bituminous mixtures using rheology and wheel tracking tests.

Table 5-3: Results of rheology characterization by SUPERPAVE method

Asphalt/modifier	PG	Failure temperature, °C	G^* , kPa	δ , °	$G^*/\sin \delta$, kPa (at PG Temp.)	Classification
AC-20 Salamanca	70	71.3	2.527	80.8	2.56	5
Elvaloy	76	81.9	3.054	58.8	3.57	1
EVA	76	80.1	3.373	75.1	3.49	2
Oxidized	76	79.0	2.828	71.6	2.98	3
SBS	76	77.5	2.370	67.8	2.56	4

In Table 5-3 is possible to see that all modified asphalts are classified like PG 76-YY. The failure temperature and the angle of phase (δ) are different. It is important to notice that the phase angle is different for all asphalts; since this parameter offers an idea of how much elastic recovery can present the asphalt (asphalt with smaller angle of phase expects great elastic recovery).

Table 5-4: Results of rheology characterization by refined SUPERPAVE method

Asphalt/modifier	PG	Failure temperature, ° C	G*, kPa	δ , °	$G^*/(1-(1/\sin \delta \tan \delta))$, kPa (at PG Temp.)	Classification
AC-20 Salamanca	70	72.3	2.527	80.8	3.02	5
Elvaloy	88	91.5	1.167	61.2	3.13	1
EVA	76	81.1	3.373	75.1	4.65	4
Oxidized	76	81.7	2.828	71.6	4.36	3
SBS	76	81.8	2.370	67.8	4.24	2

Results showed in Table 5-3 and Table 5-4 shows clearly that Refined SUPERPAVE specification gives more importance to the phase angle comparing to SUPERPAVE specification. It is important to note that Refined SUPERPAVE specification classifies the asphalt modified with Elvaloy as PG88-YY, a great difference with the classification given before. The other modified asphalts was near to being classified as PG82-YY. With this results it is easy exemplified the differences between both methods.

Table 5-5: Results of rheology characterization by ZSV method

Asphalt/modifier	PG	Failure temperature, ° C	Classification
AC-20 Salamanca	70	71.3	5
Elvaloy	94	94.9	1
EVA	76	76.1	4
Oxidized	76	81.2	3
SBS	76	81.3	2

Table 5-6 – Results of rheology characterization by Repaeted Creep

Asphalt/modifier	Test temperature, ° C	Average elastic recovery at 100 Pa, %	Average elastic recovery at 3200 Pa, %	Difference between elastic recovery	Cumulative total deformation (20 cycles), %	Classification
<i>Specified values</i>			<i>15 min.</i>	<i>70 max.</i>		
AC-20 Salamanca	70	2	0 (-6)	8	13683	5
Elvaloy	76	75	68	7	1339	1
EVA	76	27	0 (-3)	30	18260	3
Oxidized	76	26	0 (-3)	29	9608	4
SBS	76	32	11	21	8886	2

In Table 5-5 are shown the results ZSV characterization method. As it was observed with Refined SUPERPAVE method, the classification of asphalt modified with Elvaloy changed. It goes from PG 76-YY to PG 94-YY. SBS modified and Oxidized asphalt were near to be classified as PG 82-YY. EVA modified asphalt has a failure temperature near to 76 °C.

As it had been indicated before, Repeated Creep serves as complement of other methods for asphalt classification. For this study, it was considered as a complement of SUPERPAVE method. Then, the analysis of different asphalts by Repeated Creep indicates if asphalt has a minimum elastic recovery and if it is susceptible to different stress levels. In Table 5-6 is possible to observe that only Elvaloy modified asphalt fulfils the proposed specified value for average elastic recovery at 3200 Pa. It is important to notice that Elvaloy modified asphalt was the only one which changes its PG with Refined SUPERPAVE and ZSV specifications. In the same table it is also possible to appreciate that all analyzed asphalts fulfil the value specified for the difference between elastic recoveries at both levels of stress.

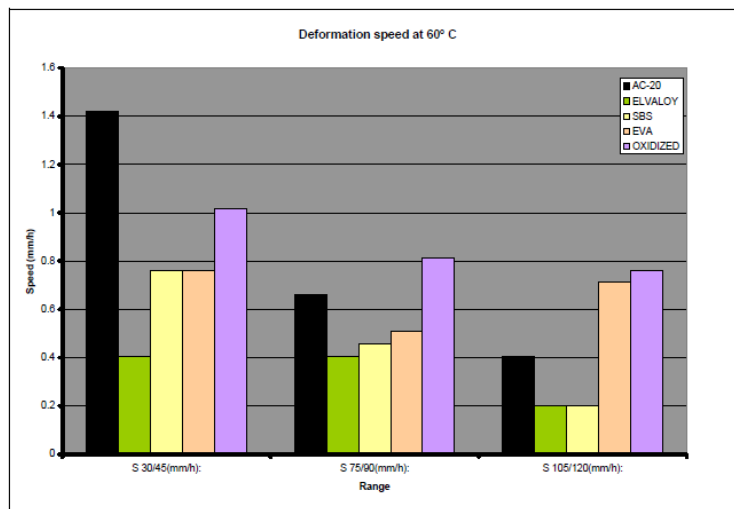


Figure 5-15: Speed of deformation at 60 °C for different asphalt mixtures

The Spanish standard NLT-173 (8), Resistance to the plastic deformation of the bituminous mixtures by means of the wheel tracking tests, was taken as the device for assessing rut resistance of 15 cm. diameter specimens made in laboratory with the gyratory compactor. In the Spanish standard NLT-173, it is specified that the testing specimen must be quadrangular of 30 cm. by side and compacted with vibratory equipment. For this study it was chosen to use specimens of 15 cm. diameter, compacted with SHRP gyratory compactor. This change was made due to the unavailability of vibratory equipment and because the SHRP gyratory compactor simulates better the field compaction. The Spanish wheel tracking device is composed by an environmental chamber. Inside this chamber there's a frame with a movable car where the specimens are placed. These specimens pass in a swinging movement, under a rubber surface wheel for a period of 120 minutes, at rate of 21 cycles per minute. This machine was jointly constructed between SURFAX S.A. de C.V. and the San Nicholas Hidalgo Michoacan University.

Tests at high PG temperature:

The maximum PG temperatures, at which tests were run, were defined by the SUPERPAVE rheology characterization method. Thus virgin asphalt was tested at 70°C, whereas the other asphalts (the modified ones) were tested at 76°C. It's important to consider this, because these temperatures would be different if other rheology method were chosen.

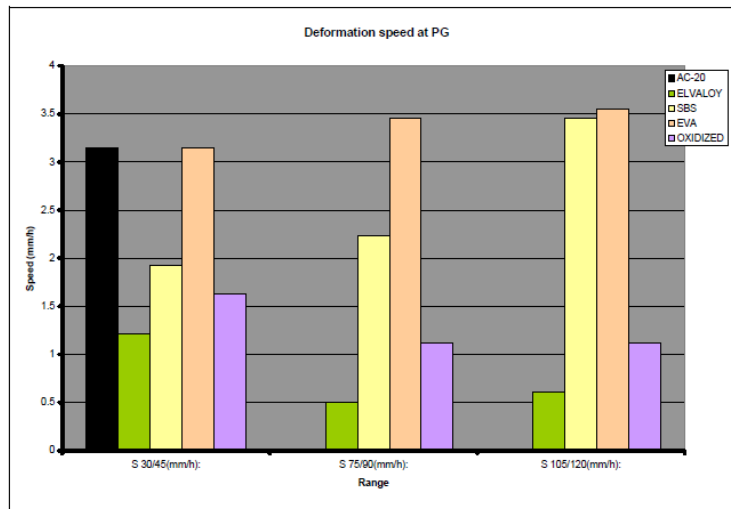


Figure 5-16: Speed deformation at high PG temperature for different asphalt mixtures

In Figure 5-16 it is possible to observe that the speed of deformation for the three intervals is smaller for the mixture made with Elvaloy, followed by oxidized asphalt, SBS, EVA and finally AC-20. It is important to precise that for AC-20 it was not possible to collect deformation data after 75 minute. The deformation was extremely great and the machine was stopped around the 70 min. by the friction between the tire and the specimen rut. That's why, it was considered that AC-20 mixture fails. In general, it is possible to assert that the mixtures with better results at the high PG Temperatures were in first place the mixtures with Elvaloy, followed by oxidized asphalt, SBS, EVA and finally AC-20.

Tests at failure temperature plus 3 °C:

The failure temperature of an asphalt is defined as the temperature to which the $G^*/\sin d$ is equal to 2,2 kPa (for an asphalt aged in RTFO), in the specification defined in SUPERPAVE. If the rheology characterization predicts correctly the performance of mixture to rutting, when the test is run above the failure temperature, the plastic deformation that will appear on a specimen will be remarkably superior that the presented under that temperature.

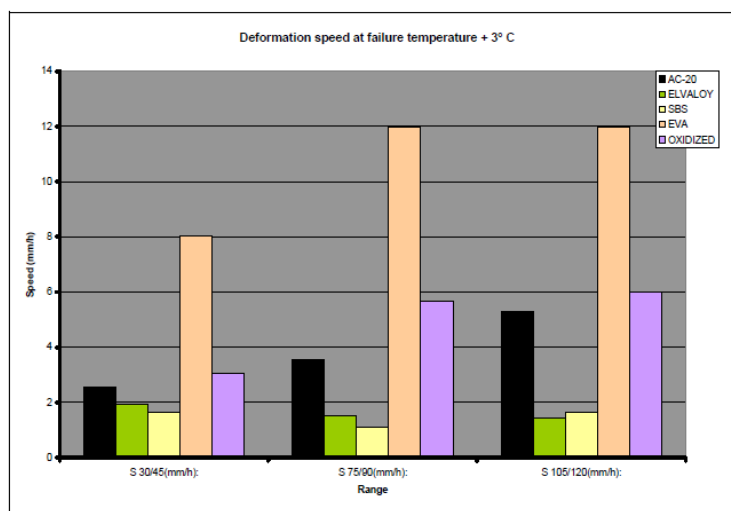


Figure 5-17: Speed of deformation at failure temperature +3 °C for different asphalt mixtures

The graphic presented in Figure 5-17 shows that there are 3 asphalts more susceptible to rutting than the other 2. Checking up the results, the SBS has the smallest deformation speed followed by Elvaloy, AC-20, oxidized asphalt and finally EVA.

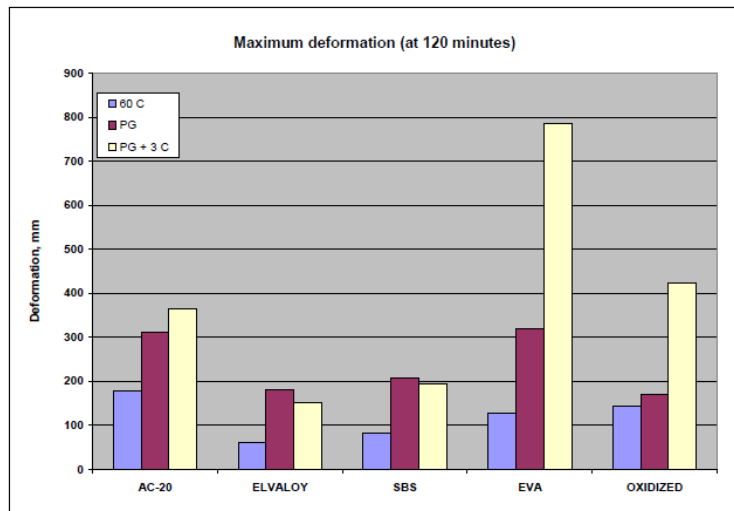


Figure 5-18: Maximum deformation at different temperatures

Figure 5-18 shows the deformation at 120 minutes. The general trend is Elvaloy and SBS present the less deformation, followed by oxidized, AC-20 and EVA. This trend is similar to the speed of deformation at all test temperatures.

5.3.6.10 Paper 308 (Tan et al., 2014)

Unified evaluation index (R_J) was used in this study to evaluate the high-temperature performance of several asphalt binders: 5 bitumens and 2 modified bitumens – Table 5-7. R_J is inversely proportional to compliance (J) and is expressed by the following equation:

$$R = \frac{1}{J} = \frac{G^*}{\sin \delta} (1 - \cos \delta)$$

At high-temperature levels, the higher the R_J value, the better the deformation resistance of the asphalt binder.

Table 5-7: Properties of the studied bitumens

Index	Unit	A-50	B-70 I	B-70 II	C-90	D-110	E	F
Penetration (25°C, 100 g, 5 s)	0,1 mm	57	69,7	80,1	84,6	120	109,8	78,8
Softening point (Ring and Ball)	°C	48,7	47,8	46,5	45,8	44,8	84,8	89,5
Ductility (cm/min, 10°C)	Cm	23,7	31,2	35,7	43,9	63,7	-	-
Ductility (cm/min, 5°C)	cm	-	-	-	-	-	62,7	39,1

In order to obtain R_J , dynamic shear tests were conducted at 60°C, using a 25-mm diameter parallel plate geometry and 1-mm gap. The frequency was 10 rad/s. The controlled stress was different for the different binders tested and it was low enough to keep the binders in the linear viscoelastic domain. Figure 5-19 shows R_J values of the studied bitumens. The high-temperature performance ranking of the studied binders in terms of R_J , is: F > E > A-50 > B-70I > B-70II > C-90 > D-110.

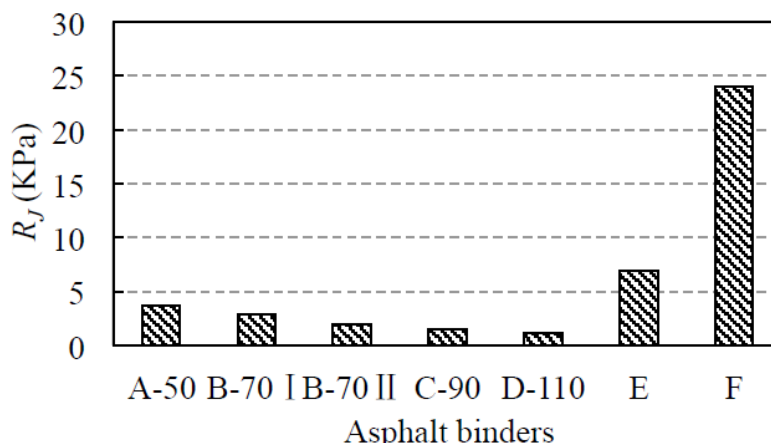


Figure 5-19: R_j of bitumens at 60 °C

Asphalt mixtures were tested by the wheel tracking test. Laboratory-compacted slabs (300 mm × 300 mm × 50 mm) were subjected to repeated wheel loads while the resultant rut depth was monitored at 60 °C. Dynamic stabilities of the studied mixtures are given in Table 5-8. The high-temperature performance ranking of the studied asphalt mixtures is: F > E > A-50 > B-70I > B-70α > C-90 > D-1.

Table 5-8: Dynamic stability of asphalt mixtures

Bitumen	A-50	B-70 I	B-70 II	C-90	D-110	E	F
Dynamic stability (time/mm)	2420	2250	1545	900	864	2801	8554

Figure 5-20 shows the correlation between the R_j and dynamic stability. The relationship of the two parameters is approximately linear. The R-square value for fitting the relationship between dynamic stability and R_j is 0,9866. That is, the unified R_j index can effectively evaluate the high-temperature performance of asphalt binders.

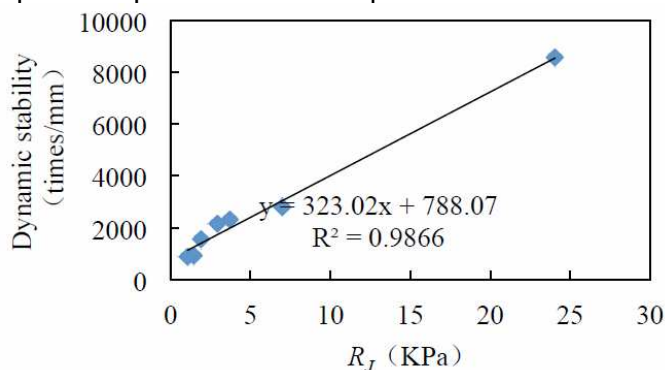


Figure 5-20: Correlation between R_j and dynamic stability

In order to study the applicability of the unified index further, it was made a comparison with $G^*/\sin\delta$, G_v and accumulated strain obtained from the RCRTs. As shown in Table 5-9, the rankings of the studied asphalt binders evaluated by R_j , G_v and accumulated strain are the same. That is, F > E > A-50 > B-70 I > B-70 II > C-90 > D-110. This ranking is also the same as for the high-temperature performance ranking of the studied asphalt mixtures evaluated by dynamic stability. For $G^*/\sin\delta$, the high temperature performance ranking of the neat asphalt binders is the same as the ranking for the neat asphalt mixtures, but for the modified

asphalt binder, the rankings are not the same. This finding also indicates that $G^*/\sin\delta$ is not suitable for modified asphalt binders.

Table 5-9: High-temperature performance of bitumens evaluated by different indices and dynamic stability of asphalt mixtures

Bitumen	A-50	B-70 I	B-70 II	C-90	D-110	E	F
R_J (KPa)	3,709	2,923	1,910	1,487	1,068	6,975	24,034
$G^*/\sin\delta$ (KPa)	3,472	2,747	1,830	1,434	1,035	3,165	9,469
G_V (Pa)	396,4	311,7	195,0	172,0	100,3	1514,3	3378,3
Accumulated strain	24,53	31,05	49,81	57,21	98,77	0,08	0,03
Dynamic stability (time/mm)	2420	2250	1545	900	864	2801	8554

In order to determine which index is the best among all the indices, grey rational analysis was performed to compare the high-temperature evaluation indices. The coefficient of correlation is a measure of the strength of the relationship between the variables, that is, how well changes in one variable can be predicted by changes in another variable. The larger the coefficient, the better is the relationship between the index for the asphalt binder and the index for the mixture. Table 5-10 presents the grey rational analysis results of the high-temperature evaluation indices and the dynamic stability.

Table 5-10: Grey rational analysis of asphalt high-temperature evaluation indices and dynamic stability of asphalt mixtures

Item	X_1	X_2	X_3	X_4
Indices	$G^*/\sin\delta$ (60°C)	G_V (60°C)	Accumulated strain (60°C)	R_J (60°C)
Coefficient	r_1	r_2	r_3	r_4
Neat asphalt	0,8925	0,9016	0,6839	0,8935
Modified asphalt	0,5936	0,8449	0,7395	0,8990

Table 5-10 shows that for the neat asphalt binders the coefficient ranking is r_2 then r_4 then r_1 then r_3 , and for the modified asphalt binders the coefficient ranking is r_4 then r_2 then r_3 then r_1 . So, for the neat asphalt binders, the correlation between G_V and dynamic stability is the highest, and for the modified asphalt binders, the correlation between R_J and dynamic stability is the highest. Although R_J is not the best indicator for evaluating the high-temperature performance of all the studied binders, it is still better than $G^*/\sin\delta$ and accumulated strain. Furthermore, compared to G_V , the test time to obtain R_J is much less than to obtain G_V . So, the established unified evaluation R_J index is a good high-temperature evaluation index for asphalt binders.

5.3.6.11 Paper 425 (Dreessen *et al.*, 2009)

See section 5.3.6.11.

5.3.6.12 Paper 428 (Beckedahl *et al.*, 2009)

Two binders were studied, one conventional (conv) and the other was a special high polymer modified bitumen (PmB 25H) - Table 5-11.

Table 5-11: Properties of the polymer modified bitumen (PmB 25H)

Bitumen property	Softening point [°C]	Needle penetration at 25 °C [1/10 mm]	Ductility at 25 °C [cm]	Elastic recovery [%]
PmB 25H	91,3	23,0	55,0	87,0

Tests were conducted according to EN 14770, 2006, with temperature sweeps (ranged from 46 °C to 82 °C), using a 25 mm plate-plate set up and under controlled strain conditions at a frequency of 1,59 Hz. $G^*/\sin \delta$ of PmB 25H showed very high value (about 9 times more) compared to conventional binder at 60 °C (Figure 5- 21).

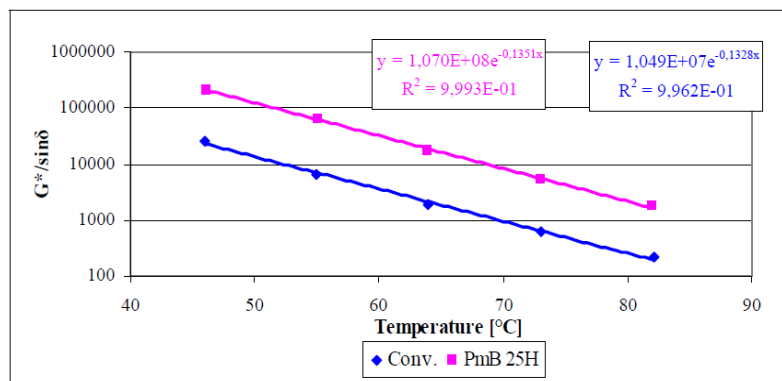


Figure 5-21: Comparison of $G^*/\sin \delta$

The wheel-tracking test after the German Standards, with steel wheels in a water-controlled device at 50 °C conducted in stone mastic asphalts, brought the results of Figure 5-22. The results of the innovative asphalt PmB25H stand out positively against the conventional asphalt. Hence it can be classified as an asphalt mixture with high rutting resistance.

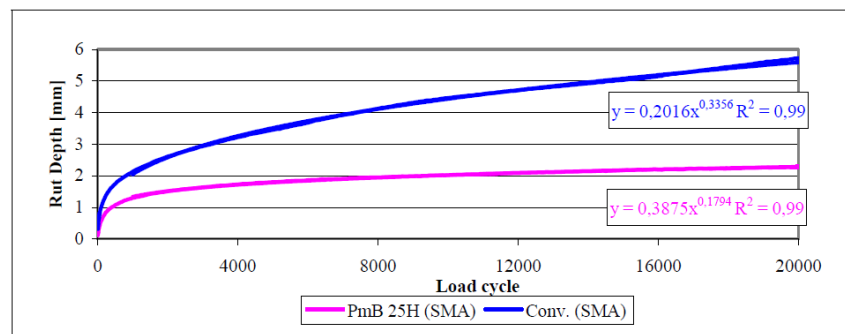


Figure 5-22: Results of Wheel Tracking Test (50 °C, Water, Steel Wheel)

5.3.6.13 Paper 476 (Wagner *et al.*, 2008)

Experimental study on the effects of FT paraffin modification, considering 2 binders:

1. Neat binder
2. PmB 45/80-50

Wax content was varied from 2 to 6 %.

The following binder properties are measured:

- Viscosity (using rotational viscosimeter) in range of production temperatures
- $G^*/\sin \delta$ (DSR) in range of service temperatures
- BBR in low temperature range

Asphalt mixture tests:

- WTT and Triaxial Cyclic Compression Tests
- TSRST tests

The binder tests show a lower viscosity at production temperature (wax molten), a higher stiffness at service temperatures and less resistance to thermal cracking at low temperatures. This is reflected in asphalt mixture tests: less permanent deformation, but more susceptible to low temperature cracking.

5.3.6.14 Paper 511 (Mollenhauer *et al.*, 2011)

On average, the results of the performance tests made on the laboratory prepared mixes were the same as on the plant mix. From this study, it is concluded that it is possible to do an initial type testing study with laboratory prepared mixtures and that there is no significant impact from the laboratory mixing procedure, as long as the European standard for laboratory mixing EN 12697-35 is correctly followed.

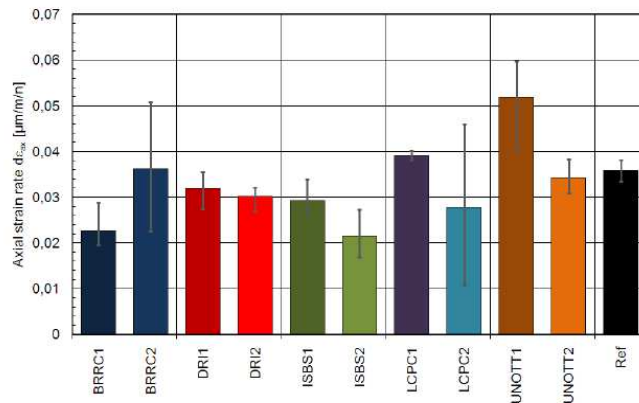
Resistance against permanent deformation:

For analysing the effect of various laboratory mixing procedures as well as the mixing time on the resistance against permanent deformation or rutting, cyclic triaxial stress tests (CTST) according to EN 12697-25-B were conducted.

Table 5-12: Results of the cyclic tri-axial stress tests

Specimen	Axial strain rate	Axial strain	Radial strain rate	Radial strain	Stiffness Modulus	Poisson Ratio
	$d\varepsilon_{ax}$	ε_{ax}	$d\varepsilon_{rad}$	ε_{rad}	S_{Mix}	μ
	[($\mu\text{m}/\text{m}$)/ n]	[‰]	[($\mu\text{m}/\text{m}$)/ n]	[‰]	[MPa]	[-]
BRRC131	0,02883	5,990	-0,00283	0,0355	646	0,25
BRRC132	0,01977	7,407	-0,00789	0,1356	643	0,38
BRRC133	0,01955	5,721	-0,00539	0,1265	679	0,33
BRRC243	0,03529	5,862	-0,00613	0,1775	688	0,28
BRRC244	0,05075	7,597	-0,00813	0,1065	614	0,28
BRRC245	0,02261	6,338	-0,00792	0,0412	554	0,36
DRI112	0,03552	7,632	-0,00621	0,2307	709	0,28
DRI114	0,02739	7,449	-0,00496	0,2990	705	0,29
DRI18	0,03282	8,028	-0,00805	0,0975	731	0,31
DRI226	0,03218	7,084	-0,01332	-0,1528	760	0,39
DRI227	0,03116	7,346	-0,00489	0,2740	701	0,27
DRI229	0,02694	7,259	-0,00292	-0,0080	706	0,25
ISBS111	0,02762	7,516	-0,00597	0,1270	641	0,30
ISBS115	0,03397	8,280	-0,00463	0,3952	658	0,27
ISBS17	0,02628	7,818	-0,00777	0,1626	694	0,34
ISBS210	0,02019	5,283	-0,00509	0,0973	691	0,32
ISBS212	0,02728	6,220	-0,00509	0,1183	676	0,29
ISBS28	0,01682	6,216	-0,00839	0,1061	678	0,42
IFSTTAR14	0,03911	9,854	-0,00205	0,6869	659	0,21
IFSTTAR15	0,03818	9,911	-0,00255	0,6595	606	0,23
IFSTTAR16	0,04017	10,410	-0,00507	0,4569	570	0,26
IFSTTAR24	0,04593	9,045	-0,00175	0,5240	583	0,22
IFSTTAR25	0,01072	5,717	-0,00851	0,0270	646	0,52
IFSTTAR26	0,02679	6,937	-0,00668	0,0565	662	0,32
UNott11	0,05577	15,056	-0,00697	0,5913	613	0,26
UNott12	0,05982	7,952	-0,00329	0,7472	538	0,23
UNott17	0,04012	8,900	-0,00530	0,0505	659	0,26
UNott217	0,03096	7,714	0,00008	-0,0175	614	0,20
UNott220	0,03833	7,563	-0,00667	-0,0469	624	0,28
UNott222	0,03342	8,955	-0,00583	0,2245	615	0,28
Ref7	0,03342	7,025	-0,00355	0,2202	688	0,25
Ref14	0,03810	7,935	-0,00912	-0,3361	709	0,31
Ref15	0,03597	6,869	-0,00655	0,2186	665	0,29

For the axial strain rate $d\epsilon_{ax}$ (compare Figure 5-23), the prolonged mixing time results generally in lower mean axial strain rates. Only for BRRC results, the longer mixing times results in a higher strain rate. However, the three replicates for the samples BRRC2, IFSTTAR2 and UNott1 show high scattering of the test results.



note: index 1 stands for normal mixing times and 2 for double mixing times

Figure 5-23: Mean axial strain rate results

Multiple recycling:

Performance testing is necessary to validate the mix design. Preparing the test specimens with laboratory mixed material was acceptable for the mix studied in the lab mixing study. The validity of predicting the asphalt performance using mixing laws was less convincing as shown in the multiple recycling study. It may be acceptable as a first estimation, but performance testing on the final mix remains necessary.

5.3.6.15 Paper 513 (Šušteršič *et al.*, 2013)

Rutting vs $G^*/\sin \delta$:

Recycling waste polymers rationally and efficiently has become one of the priorities of road pavement industry in recent years. Therefore, in this study waste PMMA/ATH powder was incorporated in an asphalt mixture. In one case waste PMMA/ATH was used as an asphalt binder modifier and in other case as a partial replacement for fine aggregate fraction. Basic performance characteristics of asphalt mixtures were evaluated by measuring material properties such as rutting potential and stripping resistance. Binder characteristics were determined also on artificially aged samples. With both modification methods, improved performance characteristics of asphalt mixture were achieved which can increase road pavement durability.

Paving bitumen (70/100 grade) was employed to prepare PMMA/ATH modified bitumen. The optimum concentration of PMMA/ATH was 25 % by weight of total binder (wet process). Asphalt concrete mixtures with maximum aggregate size 8 (AC-8) was selected to incorporate with waste PMMA/ATH powder (dry process): The same amount of waste PMMA/ATH powder as it was used in asphalt binder modification was also used for the dry process. The volumetric ratio of filler and waste powder was 5:1. Binder content in asphalt mixtures was as follows: 5.8 wt % in reference and modified (A) mixture; whereas 6.8 wt % was necessary for the wet process in modified (B) mixture.

Rheological tests were carried out under conditions of linear viscoelastic response with Anton Paar Physica MCR 301, equipped with parallel plates (PP25 and PP08), specifically designed for bitumen characterization. Mechanical spectra were determined from oscillatory shear measurements at 20 °C. The temperature sweep tests were performed to examine

temperature dependence of rutting parameter. Rutting parameter is defined at frequency 10 rad/s at the ratio of complex shear modulus (G^*) and sinus of phase angle (δ). For a sufficient rutting resistance, a higher complex modulus values and low phase angle are desirable.

Rutting as a common distress mode of asphalt mixtures was estimated by means of standard procedure EN 12697-22. Slab specimens (305 x 305 mm in cross sectional area and 45 mm in height) were made from typical batch of asphalt concrete by rolling machine. The rutting test was performed using wheel load (0.7 MPa of contact pressure) at 50°C under dry conditions. Rutting properties are reported at testing temperature 50°C, since a pavement surface temperature is thought to rise up to 50°C. Wheel passes with frequency of 26.5 load cycles per minute at the center of specimen. After total of 10,000 load cycles, the proportional rut depth (PRD) was calculated. Cylindrical and slab specimens of reference asphalt mixture were made at temperature 145°C, whereas modified mixtures (A) and (B) were compacted at 160°C.

Table 5-13: Performance indexes of reference and modified asphalt binder in unaged and aged condition (RTFOT)

	Unaged		RTFOT aged		RTFOT + PAV aged	
	Reference	Modified (B)	Reference	Modified (B)	Reference	Modified (B)
Softening point (°C)	46.2	53.6	54.2	61.8	66.6	74.2
Penetration, 0.1 mm at 25 °C	78	55	40	26	21	17
Fraass breaking point (°C)	-11	-15	-11	-13	-2	-7
$G^*/\sin(\delta)$, kPa at 50 °C	3,860	10,890	14,022	38,700	79,428	170,945

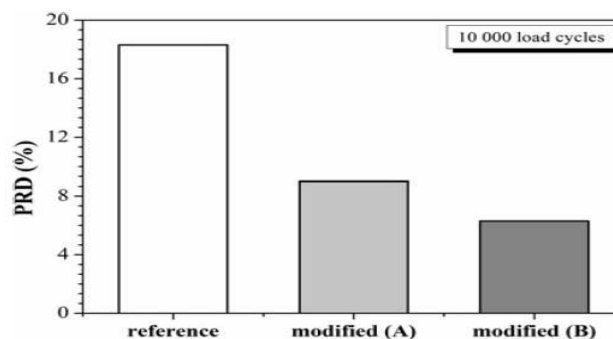


Figure 5-24: Proportional rut depth (PRD) for reference mixture, modified mixture (A) and modified mixture (B)

Conclusion: Positive effects of PMMA/ATH addition: to bitumen on mechanical properties in high, intermediate and low temperatures were identified by standard test methods and rheological measurements. From these results it could be concluded that the waste particles retard oxidative reactions in bitumen.

5.3.6.16 Paper 533 (Renken, 2012)

Wax modified binders have been tested using Asphaltan B (MW), Sasobit (FT), Licomont BS 100 (FSA). In total 12 binder combinations were used in an asphalt binder layer type AC16 B S and an asphalt concrete (dense mix) for top layers type AC11 D S. The mix AC16 B S was made with 30/45 and with 25/55-55 A and the asphalt mix AC11 D S with 50/70 and with 25/55-55 A.

Table 5-14: Bitumen grades and type of modification

Basisbitumen	Art der Modifikation			
	ohne (Referenz)	Montanwachs	FT-Wachs	Fettsäureamid
50/70	x	x	x	x
30/45	x	x	x	x
25/55-55 A	x	x	x	x

In situ investigations

Additionally, a SMA variant from the road was added to this research program, as compensation for the SMA which was initially foreseen in the laboratory investigation.

Permanent deformation properties

In this project, the permanent deformation was measured by a wheeltracking test and a pressure-swell test. For both tests, standard protocols exist in the German standard: TP Asphalt-StB. The wheel tracking test is performed according to TP Asphalt-StB Teil 22 (referring to EN12697-22), and the uni-axial dynamic compression test according to TP Asphalt-StB, Teil 25 B1, Einaxialer Druck-Schwellversuch - Bestimmung des Verformungsverhaltens von Walzasphalt bei Wärme (based on EN12697-25 B, but without the radial stress).

Table 5-15: Conventional binder properties: softening point (EP) – Penetration (Pen) and Fraass (BP)

Art des Zusatzes	Art und Sorte des Basisbitumens								
	50/70			30/45			25/55-55 A		
	EP [°C]	Pen [1/10 mm]	BP [°C]	EP [°C]	Pen [1/10 mm]	BP [°C]	EP [°C]	Pen [1/10 mm]	BP [°C]
Basis	50,4	55	-12,6	54,1	39	-11,4	62,3	46	-17,3
Asphaltan	71,2	45	-9,8	74,8	29	-9,1	71,1	45	-18,5
Sasobit	83,1	41	-9,8	84,2	27	-8,9	81,5	40	-16,2
Licomont	93,5	46	-12,2	93,5	33	-10,5	97,4	45	-16,4
Abkürzung	EP: Erweichungspunkt Ring und Kugel			Pen: Penetration			BP: Brechpunkt nach Fraaß		

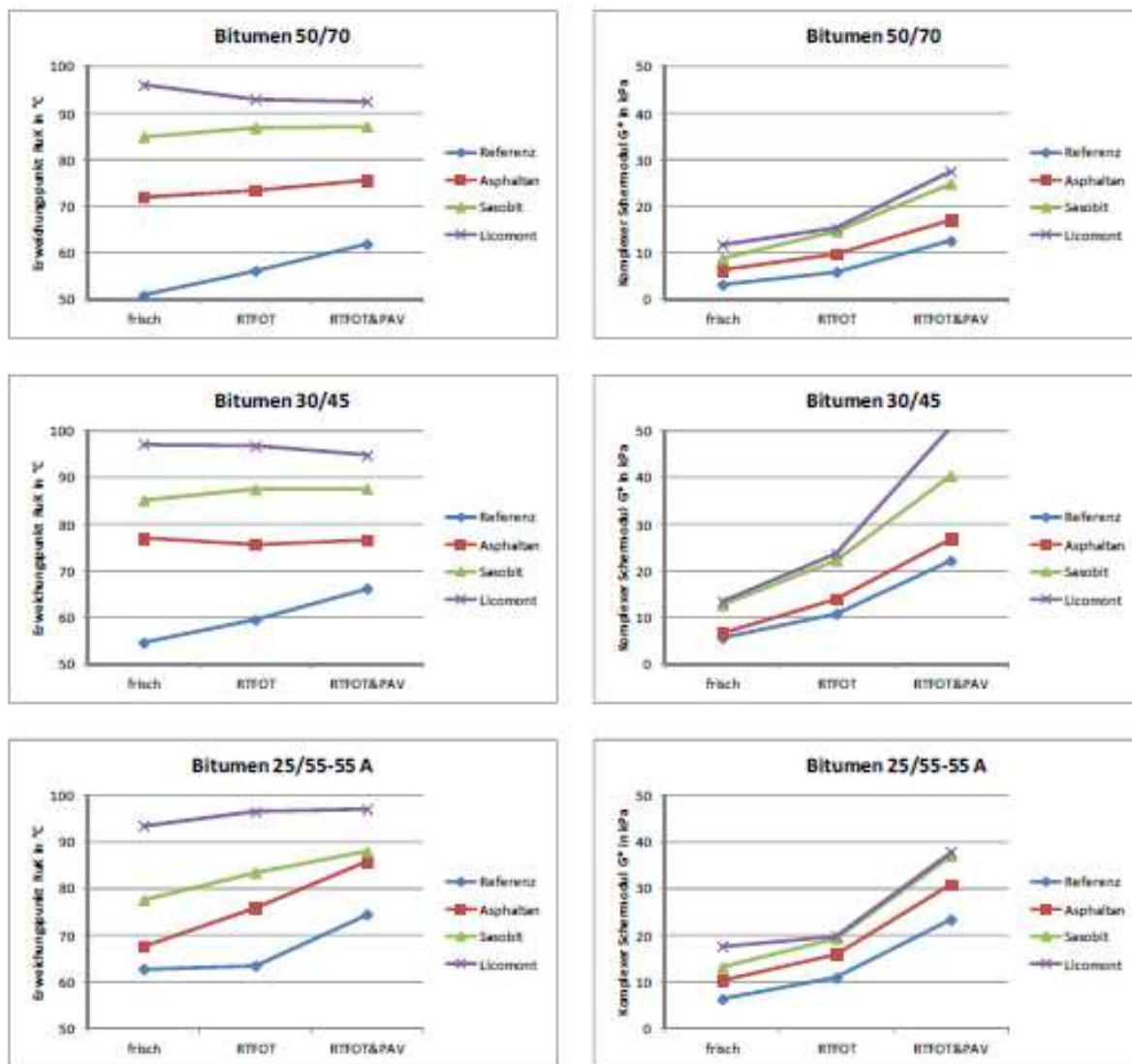


Figure 5-25: Softening point (left) and Complex modulus G^* @ $T = 60^\circ\text{C}$; $f = 1,59\text{ Hz}$ (right) for 3 binders and their modification with 3 waxes, fresh and aged

The wheel tracking tests were executed in air at a temperature of $T = 60^\circ\text{C}$. The rut depth after 10000 cycles is plotted here.

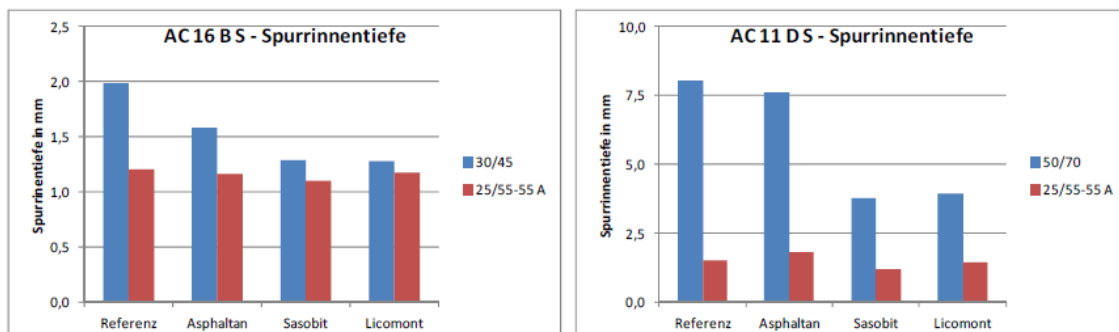


Figure 5-26: Rut depth for both asphalt mixes with and without wax modification

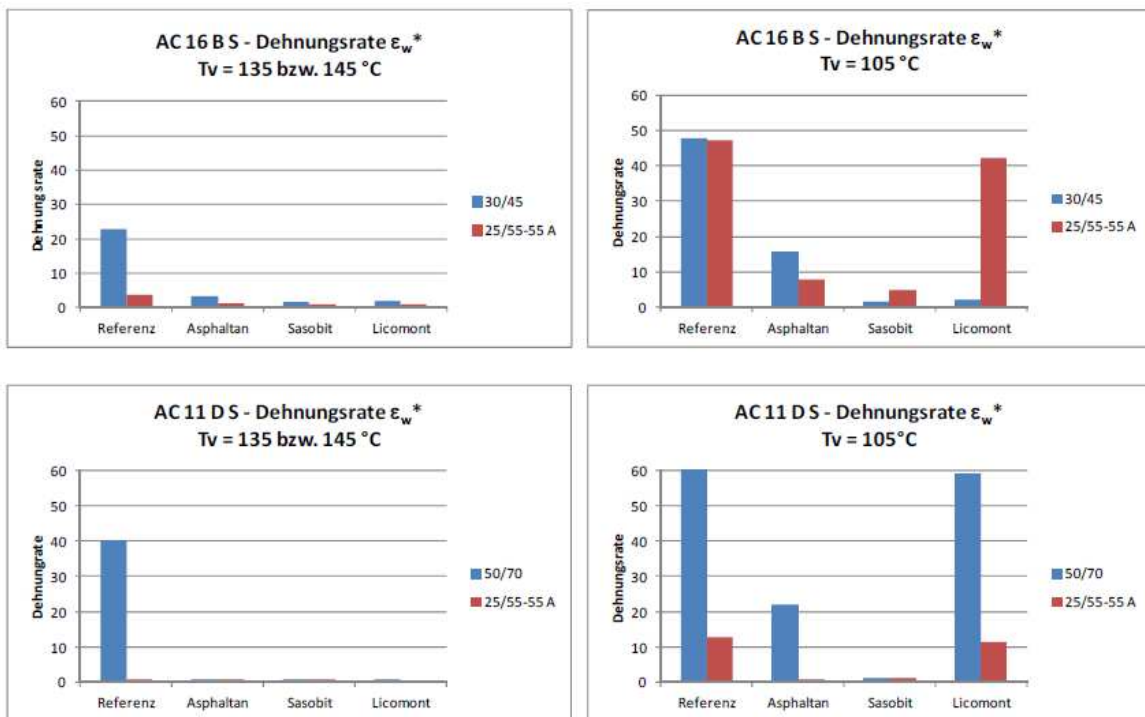


Figure 5-27: Creep rate from the dynamic compression test for the asphalt mixes with and without max modification

The resistance against permanent deformation is positively influenced by the use of additives that change the viscosity of the binder. This is shown by the results of the wheeltracking tests performed at $T = 60\text{ °C}$ and the uni-axial dynamic compression tests performed at $T = 50\text{ °C}$.

From the compression tests, it was also demonstrated that the reduction of the compaction temperature by 20 Kelvin (penbitumen) respectively 30 Kelvin (PmB), the deformation sensitivity can increase substantially in some cases.

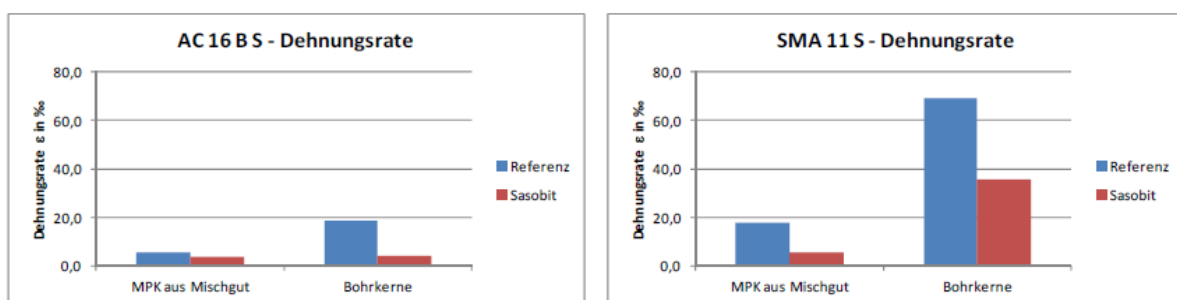


Figure 5-28: Creep rate in the inflection point determined in the cyclic compression test for asphalts produced with and without wax modification

From Figure 5-28 one can conclude that the asphalt binderlayer AC 16 has a higher resistance against permanent deformation than the SMA, and the creep rate, determined on Marshall compacted samples is lower than determined on cores from the road. The lab samples are apparently much stiffer.

Conclusions:

The temperatures to achieve equal viscosities, vary in a range of the compaction temperature ($T_v = 135\text{ °C}$ for bitumen resp. $T_v = 145\text{ °C}$ for PmB) and depending on the wax

type and binder type, in an order of magnitude of maximum 10 Kelvin. In the range of the application temperature, the influence of binder type (pen grade bitumen vs. PmB) on the dynamic viscosity is much bigger than the influence of the type of wax modification.

5.3.7 Elastic Recovery Test

5.3.7.1 Paper 234 (Hrdlicka et al., 2007)

See section 5.3.10.2.

5.3.8 Multiple Stress Creep and Recovery (MSCR) Test

5.3.8.1 Paper 023 (Dueñas et al., 2012)

A linear dependency between the elastic recovery of the binder, measured as a recovered strain percentage upon MSCR test, and the mixture elastic recovery from the Creep tests, has been found, with a good correlation. Furthermore, the rut depth parameter from the wheel-tracking test decreases exponentially with the elastic recovery of the mixture. Then a higher elastic character of the binder provides for a better resistance to rutting. Nevertheless, with respect to the non-recovered part of the Compliance, which could be envisaged as responsible for the accumulation of strain, a good agreement was found for the binders and the mixtures, except for the crumb rubber case. This could be explained by the lower penetration of this binder. Thus, the elastic recovery is ascertained to better correlate binders and mixtures rutting performance (see Table 5-16 and Figure 5-29).

Table 5-16: Mix properties: Creep test calculated Recovery (%), non-recovered Compliance and WTT Rut depth. Binder properties: MSCR recovery RE (%) and non-recovered Compliance

	Neat 50/70	CRMB	PMB	hvpMB
Creep Test Recovery %	26,3	37,0	52,7	66,1
Creep Test Jnr*10 ⁵ , 1/Pa	2,620	1,838	0,943	0,535
RD WTT, mm	4,436	2,519	1,571	1,165
MSCR Recovery %	1	15	40	82
MSCR Jnr, 1/Pa	4,524	0,396	0,618	0,084

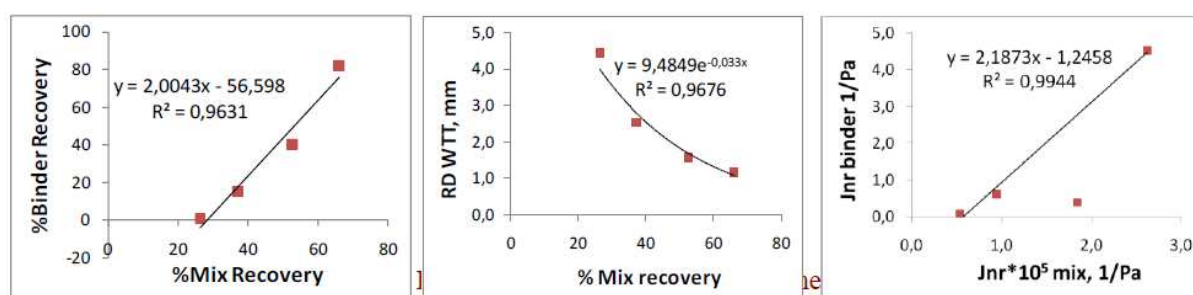


Figure 5-29: Representation of Mix properties (Creep test calculated Recovery (%), non-recovered Compliance and WTT Rut depth) versus binder properties (MSCR recovery RE (%) and non-recovered Compliance)

5.3.8.2 Paper 028 (Hase et al., 2012)

Correlations between the binder characteristics and the asphalt characteristic values are drawn up by using simple regression analyses in order to determine requirement values for binder regarding rheological characteristic values. The analysis results in the outcome that the “rates of strain” determined by using the uniaxial compression tests correlates best with

the binder characteristics “average, percent recoveries with 1600 and 3200 Pa” determined by using the MSCR test (Figure 5-30). A further good correlation exists between the above mentioned asphalt characteristic (rate of strain) and the phase angle at 50 °C after RTFOT aging (Figure 5-30).

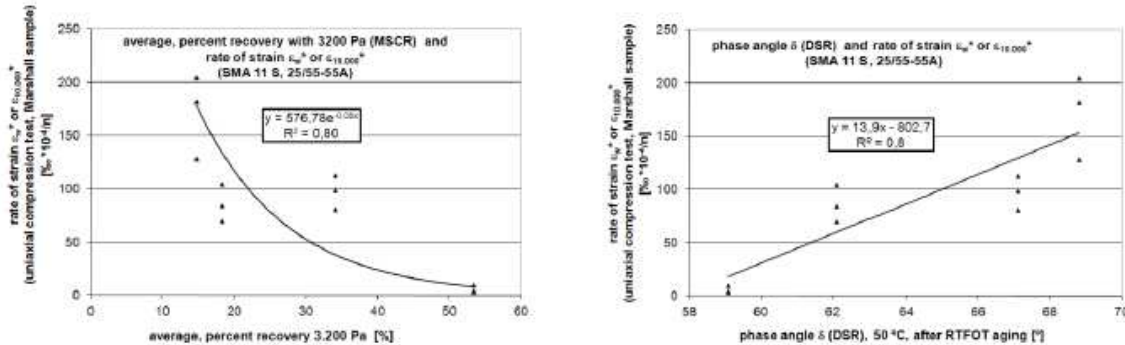


Figure 5-30: Correlation between binder and asphalt characteristics

5.3.8.3 Paper 035 (Dressen & Gallet, 2012)

The Jnr values of neat and polymer modified binders at the stress level of 25600 Pa appears to linearly correlate far better to WTT (Table 5-17) than $G^*/\sin \delta$ and the softening point. The correlation coefficients are stress level related, with trends starting to show up at 3200 Pa. Correlations are more evident at higher stress values above 6400 Pa, when the binders start deviating from their linear behavior (R^2 going as high as 0,90 in a couple of cases). The dependence on the number of passes is somehow blurred by the fact that the soft binder 70/100 failed in the rut tester before 30000 cycles, other asphalt mixes featuring a good resistance against rutting, below 5 mm rut depth at 30000 cycles. One should not forget also the uncertainties linked to the rut depth determination itself.

Table 5-17: Correlation coefficients of Jnr values at several stress level and WTT rut tester

Jnr [Pa-1]	Cycles of French Rutting tester at 60 °C			
	1000	3000	10000	30000
100	0.2186	0.1857	0.1074	0.3604
1600	0.3441	0.3468	0.2925	0.3028
3200	0.6350	0.6374	0.4916	0.4453
6400	0.8498	0.9025	0.8483	0.5674
12800	0.8787	0.9008	0.8050	0.7149
25600	0.8475	0.8059	0.6410	0.7711

5.3.8.4 Paper 042 (Robertus et al., 2012)

See also sections 5.3.5.2, 5.3.6.1 and 5.3.11.2.

Figure 5-31 and Figure 5-32 present wheel tracking rut rate against Jnr at 45 °C and 60 °C of unaged and RTFOT aged binders respectively. There appears a single good correlation for all binders independent of temperature. The correlation is even better when aged properties are considered ($R^2 = 0,79$ unaged vs 0,90 aged).

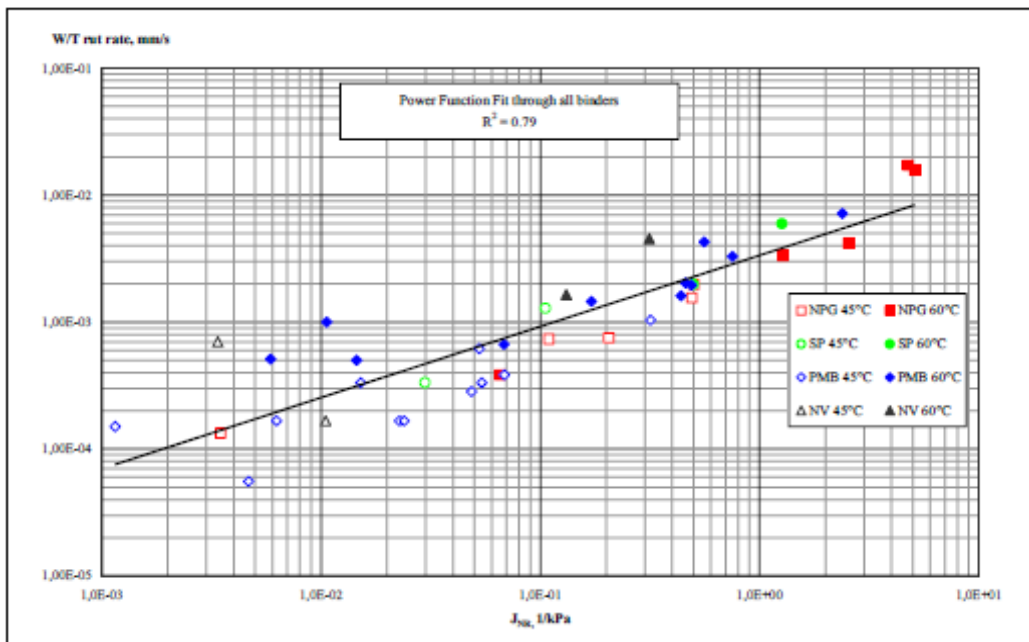


Figure 5-31: Wheel tracking rut rate against Jnr of unaged bitumen at 45 °C and 60 °C

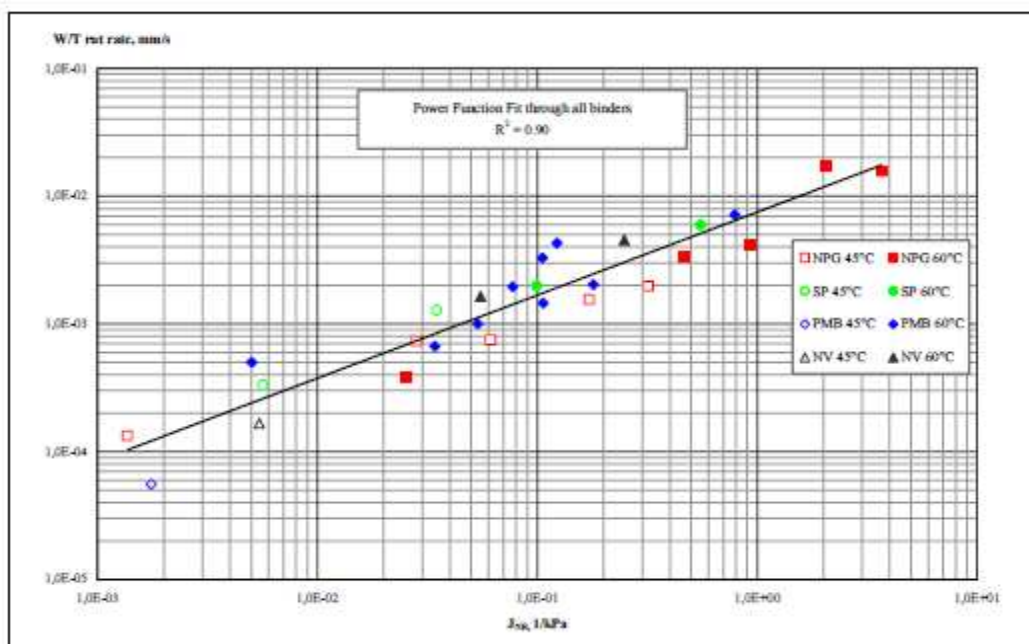


Figure 5-32: Wheel tracking rut rate vs Jnr of RTFOT aged bitumen at 45 °C and 60 °C

5.3.8.5 Paper 124 (Zeleeuw *et al.*, 2011)

See also sections 5.3.6.6 and 5.3.12.1.

This paper addresses the performance of different WMA additives. The Multiple Stress Creep Recovery (MSCR) test method is used to determine the presence of elastic response in an asphalt binder under creep and recovery at two stress levels at a specified temperature. MSCR tests were conducted using the Dynamic Shear Rheometer (DSR) at the project location pavement design temperature using RTFO residue per AASHTO TP 70-09. The DSR testing included 25 mm parallel plate geometry at 1 mm gap setting. The creep test lasted for one-second followed by a nine second recovery. Ten creep and recovery cycles

were performed at two shear stress levels (i.e., 0,1 kPa and 3,2 kPa) in order to quantify the elastic response of asphalt binder samples. The test excluded rest periods between creep and recovery cycles. The total time required for completion of the creep and recovery test was 200 seconds. The non recoverable compliance (J_{nr}), percent recovery, and the percent difference in non recoverable compliance ($J_{nr\text{diff}}$) of the asphalt binder samples were determined.

Table 5-18: Summary of MSCRT test results: J_{nr} and $J_{nr\text{diff}}$

Asphalt Binder ID	Test Temperature (°C)	Non-recoverable Compliance (J_{nr}) (1/kPa)		$J_{nr\text{diff}}$ (%)
		0.1 kPa	3.2 kPa	
PG 64-22 (u) plus LEA	52	0.597	0.635	6.44
	58	1.530	1.670	9.15
	64	3.680	4.140	12.50
	70	8.420	9.510	12.95
Sasobit® terminal blend	58	0.667	0.865	29.69
	64	1.595	2.300	44.20
	70	3.520	6.050	71.88
PG 64-22 (u) without Gencor water foaming	76	6.630	13.380	101.81
	52	0.496	0.532	7.27
	58	1.348	1.493	10.69
PG 64-22 (u) plus Gencor water foaming	64	3.132	3.425	9.38
	70	6.990	7.571	8.32
	52	0.489	0.519	6.18
PG 64-22 (u) plus Gencor water foaming	58	1.288	1.391	8.01
	64	3.200	3.512	9.74
	70	7.149	7.895	10.44
Base PG 64-22 (u)	52	0.587	0.598	1.90
	58	1.521	1.593	4.74
	64	3.854	4.104	6.48
Base PG 64-22 (v)	70	8.669	9.356	7.93
	52	0.597	0.604	1.13
	58	1.581	1.661	5.09
PG 64-22 (u) plus Advera® lab blended	64	3.759	4.082	8.58
	70	8.741	9.265	6.00
	52	0.532	0.540	1.61
PG 64-22 (u) plus LEA lab blended	58	1.428	1.493	4.55
	64	3.481	3.700	6.29
	70	7.981	8.483	6.30
PG 64-22 (u) plus LEA lab blended	52	0.638	0.654	2.63
	58	1.720	1.782	3.57
	64	4.026	4.160	3.34
	70	8.889	9.349	5.18

Table 5-19: AASHTO M320-09 table 3 high temperature specification requirements

Traffic Loading	Non-recoverable Compliance (J_{nr}) at 3.2 kPa ($J_{nr3.2}$)	Percent Difference in Non-recoverable Compliance ($J_{nr\text{diff}}$)
Standard Traffic (S)	≤ 4.0	Maximum 75%
Heavy Traffic (H)	≤ 2.0	
Very Heavy Traffic (V)	≤ 1.0	

At a given temperature, increasing F_n values indicate increasing permanent deformation resistance potential. Figure 5-34 shows the Flow Number test results for all asphalt mixtures tested under 50,000 microstrain at three temperatures (i.e., 45,8 °C; 51,8 °C; and 57,8 °C). It is evident from this figure that the F_n test is highly dependent on testing temperatures. Overall, the F_n values decreased with an increase in testing temperature. This is apparent for viscoelastic materials where asphalt binder softening occurs upon temperature increase. The MATL mix design replication tested at 51,8 °C measured the highest F_n , likely because

the mix was laboratory aged before testing. On the other hand, the lowest Fn was observed for WMA/Gencor at all testing temperatures. The contractor's HMA and WMA/Sasobit® also measured higher Fn values.

Table 5-20: AASHTO M320-09 table 3 (MSCR) PG grade test results

Asphalt Binder ID	Table 3 PG Grade	Recommended Traffic Levels
PG 64-22 (u) plus LEA	PG 58-22H	Standard Grade (S) less than 10 million ESALs
Sasobit® terminal blend	PG 58-22V	
PG 64-22 (u) without Gencor water foaming	PG 58-22H	
PG 64-22 (u) plus Gencor water foaming	PG 58-22H	Heavy Grade (H) 10 to 30 million ESALs
Base PG 64-22 (u)	PG 58-22H	
Base PG 64-22 (v)	PG 58-22H	Very Heavy Grade (V) greater than 30 million ESALs
PG 64-22 (u) plus Advera® lab blended	PG 58-22H	
PG 64-22 (u) plus LEA lab blended	PG 58-22H	

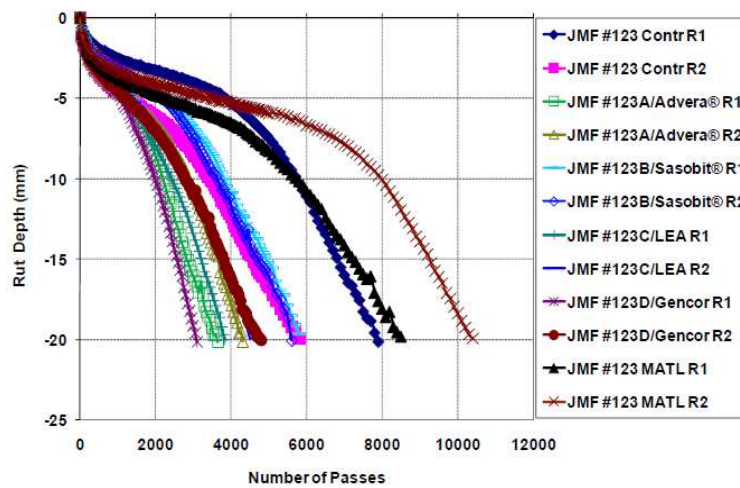


Figure 5-33: Hamburg test results: rut depth

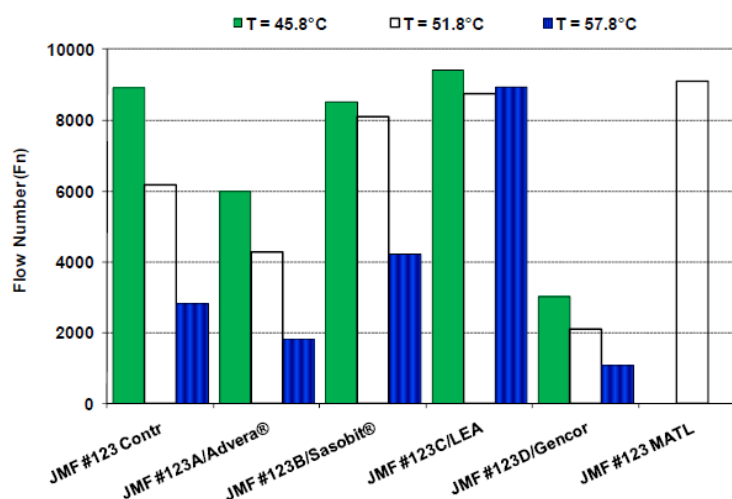


Figure 5-34: Flow number test results: Fn

5.3.8.6 Paper 153 (Willis et al., 2012)

See also section 5.3.12.2.

This paper presents results from laboratory evaluation of high polymer plant-produced mixtures (HPM).

Table 5-21: Non-recoverable creep compliance at multiple stress levels

Mixture	Test Temperature, °C	$J_{nr0.1}$ (kPa ⁻¹)	$J_{nr3.2}$ (kPa ⁻¹)	$J_{nr\text{diff}}$ (%)	Performance Grade
Control - Surface	64	0.98	1.37	39.8	64-22 H
Control - Base	64	1.68	1.95	16.1	64-22 H
HPM - Surface	64	0.004	0.013	200.7	Not Graded
HPM - Base	64	0.004	0.013	200.7	Not Graded

Note: $J_{nr0.1}$ = average non-recoverable creep compliance at 0.1 kPa; $J_{nr3.2}$ = average non-recoverable creep compliance at 3.2 kPa; $J_{nr\text{diff}}$ = percent difference in non-recoverable creep compliance between 0.1 kPa and 3.2 kPa.

Table 5-22: Requirements for non-recoverable creep compliance (AASHTO MP 19-10)

Traffic Level	Max $J_{nr3.2}$ (kPa ⁻¹)	Max $J_{nr\text{diff}}$ (%)
Standard Traffic "S" Grade	4.0	75
Heavy Traffic "H" Grade	2.0	75
Very Heavy Traffic "V" Grade	1.0	75
Extremely Heavy Traffic "E" Grade	0.5	75

Note: The specified test temperature is based on the average 7-day maximum pavement design temperature.

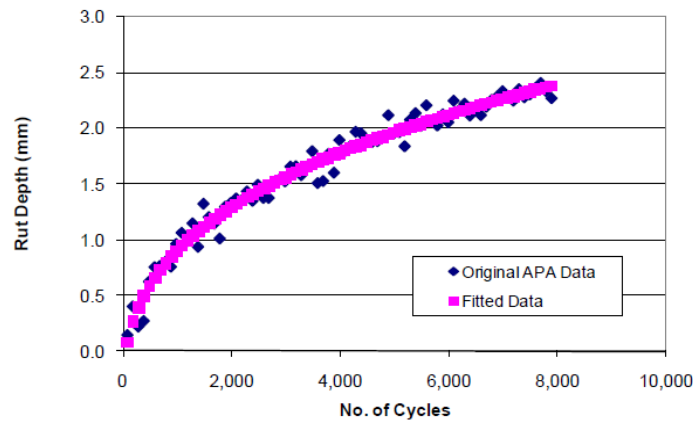


Figure 5-35: Example rate of rutting plot for two samples in centre mould

Table 5-23: Rutting test comparison

Mixture	APA Rut Depth, mm	F_n , cycles	APA Ranking	F_n Ranking
Control - Surface	3.07	164	3	3
Control - Base	4.15	129	4	4
HPM - Surface	0.62	4825	1	1
HPM - Base	0.86	944	2	2

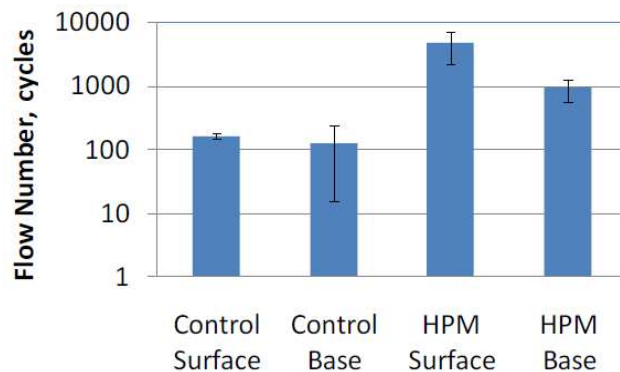


Figure 5-36: Flow number results

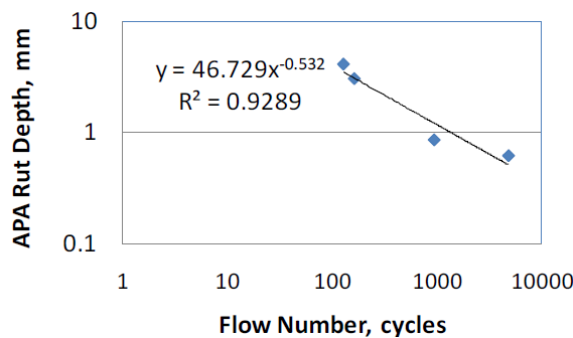


Figure 5-37: Rutting test comparisons

5.3.8.7 Paper 185 (D'Angelo *et al.*, 2007)

The new test and criteria will have to be performance related and blind to modification. The results from these binder tests were compared against hot-mix rutting results from the Asphalt Pavement Analyzer, the Hamburg Wheel Tracking, the ALF test sections and actual roadway sitesmance related and blind to modification.

The MSCR test is conducted at 11 stress levels from 25 to 25 600 Pa. Each stress level is repeated for 10 cycles and then increased to the next level.

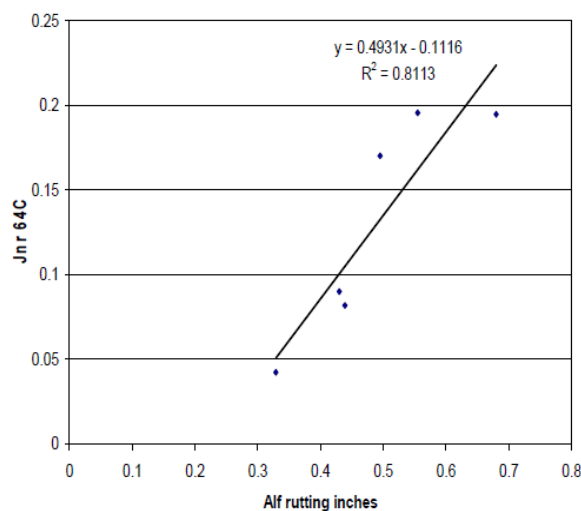


Figure 5-38: MSCR vs Lab rutting test – Correlation between ALF rutting performance and Jnr obtained using MSCR

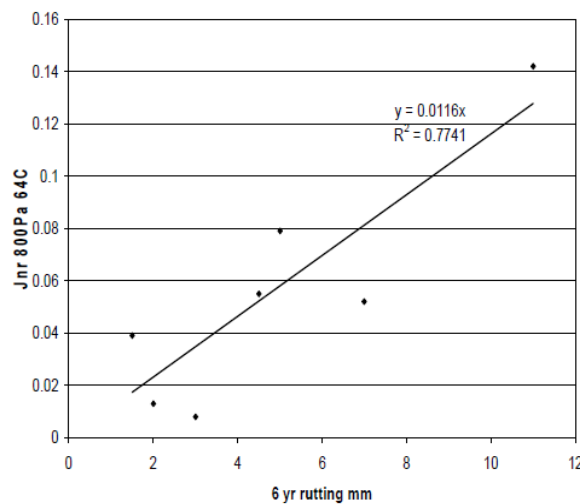


Figure 5-39: MSCR vs field rutting (6 yr rut in mm) – Correlation between the new MSCR binder parameter Jnr and field rutting data from MSDOT test sections of polymer modified asphalt binders

Table 5-24: Jnr of neat binders at the continuous grade temperature

Binder grade	Continuous grade	Jnr @3200Pa
58-28	61,8-30,8	0,302
64-22	66,1-	0,40
70-22	70,24	0,35
70-22	73-	0,317

The binder criteria currently used to specify the high temperature properties (SHRP criteria G*) are specifically intended to be run in the linear viscoelastic range and therefore can not determine the stress dependency on binder materials. The multi step creep and recovery test can be run at multiple stress levels and can characterize the stress dependency of polymer modified binders.

Conclusions:

A property called non recoverable compliance Jnr was developed based on the nonrecovered strain at the end of the recovery portion of the test divided by the initial stress applied during the creep portion of the test. The Jnr value normalizes the strain response of the binder to stress which clearly shows the differences between different polymer-modified binders.

Non-recoverable compliance can be related to rutting in different rut testers and the roadway. This parameter can be developed into high temperature binder criteria that will be blind to binder modification. The final step in the development of a binder specification for rutting will be the tie to actual pavements. Pavements sections will be evaluated to relate non-recoverable compliance of binders determined at various stress levels to field rutting.

5.3.8.8 Paper 191 (Masad et al., 2009)

This paper presents a Plasto-Viscoelastic approach to analyze the MSCR test results. The approach relies on identifying the viscoelastic response (recoverable with time) and the actual permanent strain (irrecoverable). A nonlinear viscoelasticity theory is employed in this approach to analyze the recoverable response. By developing a Plasto-Viscoelastic method to analyze the MSCR binder test results, the idea was to propose an index to characterize the resistance of asphalt binders to permanent deformation.

The MSCR test involves applying 11 shear stress levels (25, 50, 100, 200, 400, 800, 1600, 3200, 6400, 12800, and 25600 Pa) using a DSR.

In the study, 4 modified binders, and 5 ALF binders were tested. These ALF binder results were compared with permanent deformation data of ALF asphalt mixtures. The ALF experiment is a full-scale test of asphalt pavement sections including the same aggregate type and gradation but different asphalt binders (test sections 10 m – speed 19 km/h – temp = 64 °C).

Some conclusions:

Asphalt binders varied in their nonlinear viscoelastic response during loading and recovery. The viscoelastic response of some asphalt binders remained linear throughout the MSCR test. Other binders, however, exhibited nonlinear response during loading and/or recovery. The recovered strain decreased after a certain level of accumulation of permanent strain. This decrease was marked by a reduction in the nonlinear viscoelastic parameter (2 g).

The results of the new method for characterizing resistance of asphalt binders to permanent deformation conformed well to asphalt mixture permanent deformation.

5.3.8.9 Paper 314 (Willis *et al.*, 2014)

This research project designed and compared the performance of seven open-graded friction course (OGFC) mixtures which contained six different ground tire rubber (GTR) modified binders and a styrene-butadiene-styrene (SBS) modified binder. These mixtures (Table 5-25) were compared namely for rutting susceptibility.

The six rubber products modified a standard PG 67-22 binder. It should be noted that all of the GTR modified asphalt binders were able to achieve a high temperature performance grade of at least 76 °C. Once the modified binder had been created and mix designs completed, OGFC specimens were fabricated for performance testing. The specimens were subjected to Asphalt Pavement Analyzer testing (GDT115; testing @ 64 °C for 4 h) and to Hamburg testing (AASHTO T324; testing @ 50 °C for 20 000 passes), whose results are presented in Figure 5-40 and Figure 5-41, respectively.

Table 5-25: Modified binders properties

OGFC mix ID	Modified binder ID	% modified binder on the mix	m-Value (-12°C)	PG	True Grade	Softening Point % Diff	Jnr % Diff
Control	SBS with fibers ⁽¹⁾	5,75	-	-	-	-	-
20 Mesh	-20 Ambient	6,33 (10% of rubber by weight of binder)	0,315	82-22	83,1-24,6	16,4	85,8%
Crackermill	-30 Crackermill		0,306	82-22	82,8-23,1	12,4	50,9%
Cryohammer	-30 Cryohammer		0,307	82-22	82,2-23,2	15,9	34,2%
MD-105-TR	MD-105-TR		0,317	76-22	77,9-25,6	0,8	26,1%
MD-400-TR	MD-400-TR		0,316	76-22	80,4-24,2	17,2	19,2
MD-400-AM	MD-400-AM		0,294	82-16	82,1-20,8	13,8	30,5%

(1) Cellulose fibers necessary for the control design were added at a rate of 0,3 %by weight of the mix.

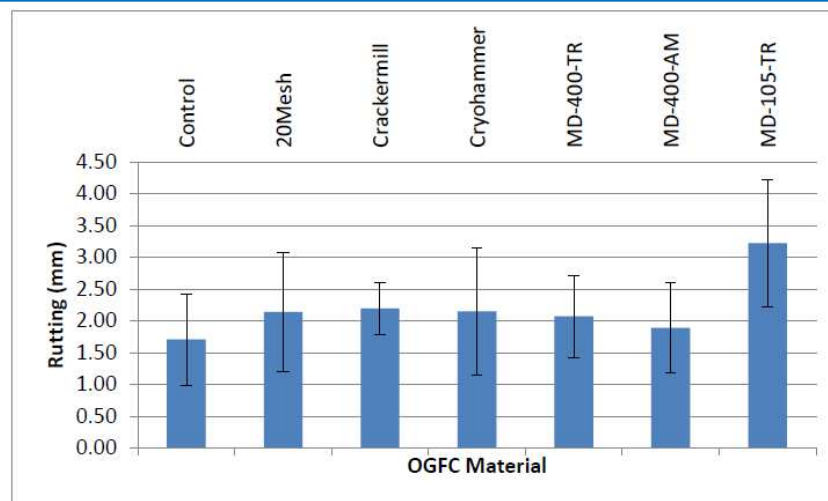


Figure 5-40: Average rut depth from APA testing

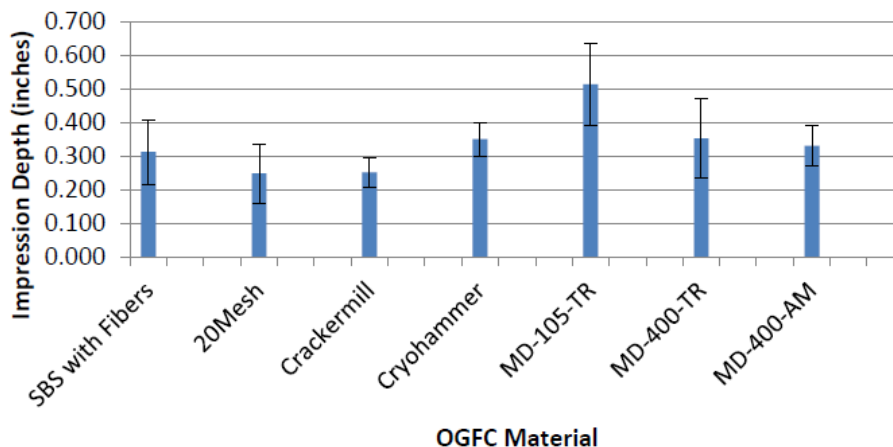


Figure 5-41: Average Hamburg impression depths

5.3.8.10 Paper 319 (Wu *et al.*, 2014)

This study investigates the performance of HMA with and without recycled asphalt shingles (RAS) based on the evaluation of field cores drilled from four experimental pavement sections that were constructed in September 2009. Two sections (1 and 4) of HMA without RAS (the control 1 section) and two sections (2 and 3) with 3 % RAS were paved as 50 mm thick overlays. All sections contained 15% recycled asphalt pavement (RAP). The virgin binder used is PG 64-22.

The performance of the asphalt mixtures and the recovered asphalt binders were evaluated via laboratory experiments, namely, with respect to rutting. Eight field cores (six with a 100 mm and two with 150 mm diameter), for each of the four sections were obtained for testing in January 2013. After performance tests the bituminous binder was extracted. The recovered binder is considered as the rolling thin-film oven (RTFO) binder for the high temperature PG tests, multiple stress creep and recovery (MSCR) tests, and the monotonic fatigue and thermal cracking tests. The MSCR tests were conducted at 52,2 °C, according to the climate temperature of the project from the Long-Term Pavement Performance (LTPP) binder program. Table 5-26 summarizes the mix characteristics of each section, as well as the PGs of the original and recovered binders.

Table 5-26: Summary of mixtures of the four sections and its PG grades

Sections	Asphalt mixture			Performance grade of binders		
	Added material	Binder content, %	Air void content, %	Original	Recovered	
					True grade	PG grade
1 (Control)	15% RAP	5,6	2,3	64-22	73,4-17,0	70-16
2	15% RAP + 3% RAS	5,6	3,3		79,7-19,6	76-16
3	15% RAP + 3% RAS	6,4	1,0		73,6-17,4	70-16
4	15% RAP	5,4	3,3		74,4-14,4	70-10

In 2011, the four sections following three years of post-construction service were in excellent conditions. All sections exhibit only minimal rutting, showing an average rut depth of 1,8 mm and 2,0 mm, respectively, for sections 1,2 & 3 and section 4.

Figure 5-42 (a) and (b) show the results of the MSCR binder tests in terms of non-recoverable compliance ($J_{nr3.2}$) and percentage of recovery ($R_{3.2}$), respectively. The lower J_{nr} and higher R 13 values indicate better rutting resistance of the binder.

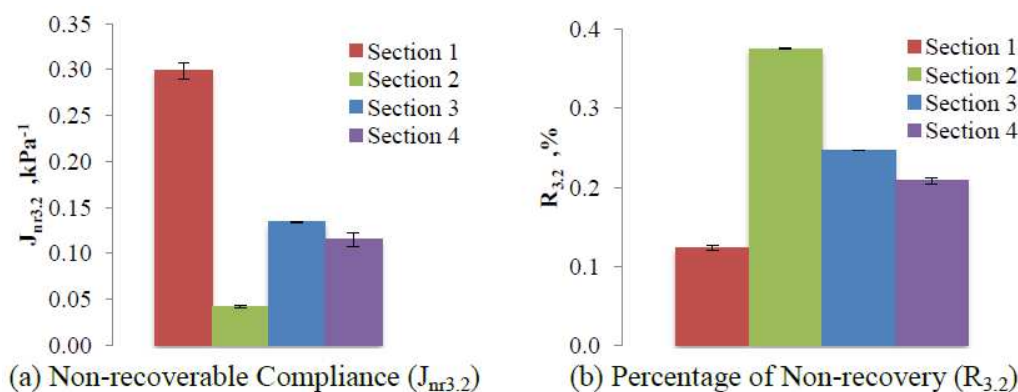


Figure 5-42: MSCR test results of recovered binder at 52,2 °C

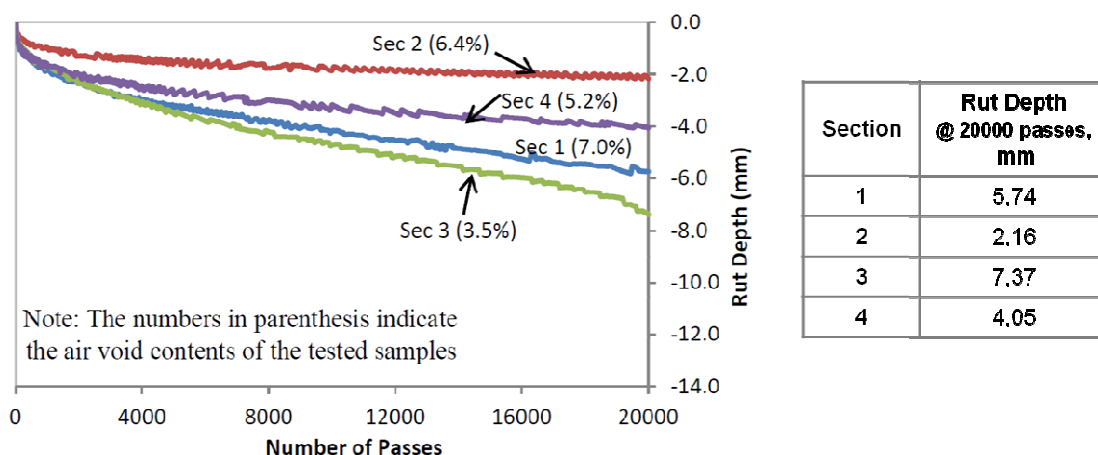


Figure 5-43: HWTD test results of field cores in the four sections

Figure 5-43 shows the HWTD test results for the field cores from the four sections tested at 50 °C. The requirements of the HWTD test specify that for binders with a high temperature PG of 70, the minimum number of passes to reach the rut depth of 12,7 mm at the test

temperature of 52,2 °C should be 15 000. In this study, all the mixtures show rut depths of less than 12,7 mm after 20 000 passes.

The HWTD test results suggest that mixtures with RAS exhibit better rutting resistance than mixtures without RAS, which is consistent with the MSCR binder test results.

5.3.8.11 Paper 330 (Bower *et al.*, 2014)

The properties of asphalt binder and mixtures (field cores) were characterized as well as the early-stage field performance from WMA pavements and HMA control pavements in the state of Washington. Four different WMA projects were evaluated, including Sasobit® (organic additive), and three water foaming technologies - Aquablack™, Gencor® and ALmix water injection (Table 5-27). The aggregate gradation of WMA and HMA for each project during the construction was the same.

Table 5-27: Summary of the four project sections

Project Contract	7474	7419	7755	7645
WMA	Aquablack™	Sasobit®	Gencor®	ALmix Water Injection
Production Temperature (°F)	HMA (325) WMA (275)	HMA (330) WMA (276)	HMA (295) WMA (260)	HMA (300) WMA (250)
Binder PG Grade	64-28	76-28	64-28	64-28
Asphalt Content (%)	5,2 (5,2)	5,5 (5,1)	5,8 (5,1)	5,4 (5,3)
RAP (%)	20	15-20	20	15-20
Anti-stripping (%)	Superbond (0,25)	None	None	Polarbond (0,50)
Overlay Thickness (in.)	3,0	3,0	1,8	1,8

The original and recovered binders from the field cores, of WMA and HMA, were tested with respect to the Performance Grade (Table 5-28).

Table 5-28: Performance Grades of original and recovered binders

Projects	PGs		
	Original	Recovered	
		HMA	WMA
Aquablack™	64-28	70-22 (73,5-22,2)	70-22 (71,9-22,6)
Sasobit®	76-28	76-22 (80,6-24,7)	76-22 (80,8-22,5)
Gencor®	64-28	70-22 (74,2-23,9)	70-22 (71,2-22,4)
Water Injection	64-28	70-22 (75,6-24,7)	70-22 (70,7-26,7)

Note: The PGs in parenthesis indicate the continuous PGs.

The recovered binders were tested by the MSCR test, at 64 °C, according to AASTHO TP70. Table 5-29 presents MSCR results - non-recoverable compliance (J_{nr}) and percentage of non-recovery (% Non- ϵ_r) - in terms of mean, standard deviation and effect size. The effect size method of statistical analysis was adopted to compare the performance of WMA and HMA technologies. The effect size is determined by the difference in the means of two groups divided by the pooled standard deviation. An effect size of 1,6 was used in this study to determine if there was a difference in the material properties using WMA technologies.

As shown in Table 5-29, the Aquablack™, Gencor®, and water injection WMA binders have higher J_{nr} and % Non- ϵ_r than their corresponding HMA binders, indicating lower resistance to rutting. However, for Sasobit® binder, the effect size results indicate no difference in J_{nr} but significant difference in % Non- ϵ_r . For the Aquablack™, Gencor®, and water injection binders, the susceptibility of the binders to rutting may be due to the reduced production temperature and aging. However, the addition of the Sasobit® additive might stiffen the binder and offset the effect from reduced aging.

Table 5-29: Asphalt binder MSCR and Asphalt mixture HWTD test results

Project	Asphalt binder MSCR test results						Asphalt mixture HWTD test results		
	J_{nr} (1/psi)			% Non- ϵ_r			Rut Depth (mm)		
	HMA	WMA	Effect Size	HMA	WMA	Effect Size	HMA	WMA	p -value
	Mean / (σ)	Mean / (σ)		Mean / (σ)	Mean / (σ)		Mean	Mean	
Aquablack™	1,23 (0,11)	1,71 (0,11)	5,35	94,2 (0,30)	95,5 (0,22)	5,77	3,64	3,21	0,23
Sasobit®	0,28 (0,01)	0,27 (0,03)	0,62	39,6 (1,13)	34,8 (1,47)	4,18	1,80	1,85	0,58
Gencor®	1,01 (0,07)	2,10 (0,02)	22,96	93,4 (0,25)	97,1 (0,22)	19,76	3,16	4,17	0,00
Water Injection	0,84 (0,04)	1,76 (0,04)	27,39	80,0 (0,35)	90,2 (0,32)	37,41	2,66	3,92	0,00

The wheel tracking results, with the Hamburg wheel tracking device (HWTD), – 50°C, 20.000 passes, AASHTO T324 – for WMA and HMA mixtures are shown in Table 5-29. The p -values indicate that there is no statistically significant difference between the Sasobit® and Aquablack™ sections with their corresponding HMA mixtures. The water injection and Gencor® mixtures had significantly larger rut depths than their corresponding HMA control mixtures. It should be noted that, however, all the mixtures performed well within the acceptable level of rut depth, which is typically 12,5 mm after 20.000 passes. The differences in rut depths of these mixes are very small.

The rutting performance of the field cores and early-stage field performance of WMA pavements and HMA control pavements are summarized in Table 5-30.

Table 5-30: Rutting performance test results of asphalt mixtures and of early-stage field cores

Project	Rut Depth (mm)			
	Asphalt mixtures (field cores)		Early-stage field cores	
	HMA	WMA	HMA	WMA
Aquablack™	3,64	3,21	3,30 (σ =2,03)	2,79 (σ =1,52)
Sasobit®	1,80	1,85	4,32 (σ =1,02)	4,32 (σ =0,76)
Gencor®	3,16	4,17	3,30 (σ =1,02)	3,05 (σ =0,76)
Water Injection	2,66	3,92	2,54 (σ =0,18)	2,79 (σ =1,27)

5.3.8.12 Paper 425 (Dreessen *et al.*, 2009)

Table 5-31 presents the properties of the studied binders. The polymer modified binders A–G are commercial grades produced according to Styrelf® crosslinking process as presented in

multiple pending patents. The polymer content ranges from 2% to 5%. The experimental polymer modified binders have been produced with the 70/100 binder. The binder 70/100 + 3% SBS XL was cross-linked in situ. The other two modified binders are physical blends. The special grade is a multigrade bitumen produced by a blend of different refining bases, according to the Ornital[®] proprietary recipe. It is used as a reference for a non-polymer modified binder designed for its anti-rutting characteristics.

Table 5-31: Properties of the binders

Binders	Before RTFOT		After RTFOT		
	R&B, °C (EN 1426)	Penetration @ 25 °C, 1/10mm (EN 1427)	R&B, °C (EN 1426)	Penetration @ 25 °C, 1/10mm (EN 1427)	G*/sin δ @ 60°C (EN 1477)
Pure binders					
70/100	45,0	76	47,2	64	2,3
35/50A	51,0	41	58,0	28	14,3
35/50 B	53,6	37	58,4	25	21,3
35/50 C	52,4	37	58,0	29	9,5
35/50 D	50,8	41	56,2	24	56,2
20/30 A	58,7	23	65,6	14	38,7
20/30 B	57,0	23	62,6	16	22,6
Polymer modified binders					
70/100 + 3% SBS	58,2	41	62,0	35	10,5
70/100 + 3% SBS XL	63,6	36	68,0	29	13,9
70/100 + 3% EVA	62,0	28	66,0	21	19,7
PmB A	56,0	55	62,6	34	13,8
PmB B	55,0	58	60,8	38	35,6
PmB C	67,4	34	67,6	26	24,3
PmB D	66,4	42	70,4	21	48,0
PmB E	67,2	28	72,2	17	29,3
PmB F	71,2	26	75,0	14	53,8
PmB G	65,4	25	70,7	22	19,8
Special binders					
10/20	64,6	14	74,0	10	12,5
Special grade	61,0	35	66,6	27	40,6

The aged binders, obtained after RTFOT (EN 12607-1), were submitted to MSCR test, carried out in a dynamic shear rheometer using a 25 mm parallel plate geometry with a 1 mm gap. The test was run at 60 °C for a better comparison with the French rutting test carried out at the exact same temperature. The samples were loaded at constant stress for 1 s, then allowed to recover for 9 s. Complementary to the procedure described in AASHTO and ASTM the tests were performed at 11 stress levels ranging from 25 Pa to 25600 Pa.

Figure 5-44 shows that at high stress levels, above around 3200 Pa, the binder resistance to deformation starts to decrease as shown by a sharp increase in J_{nr} , whereas binder compliance remains very constant at low stress level. Increasing stress level, the binder sensitivity to stress becomes significant and the differences due to the binder origin or fabrication process in binder responses become more obvious.

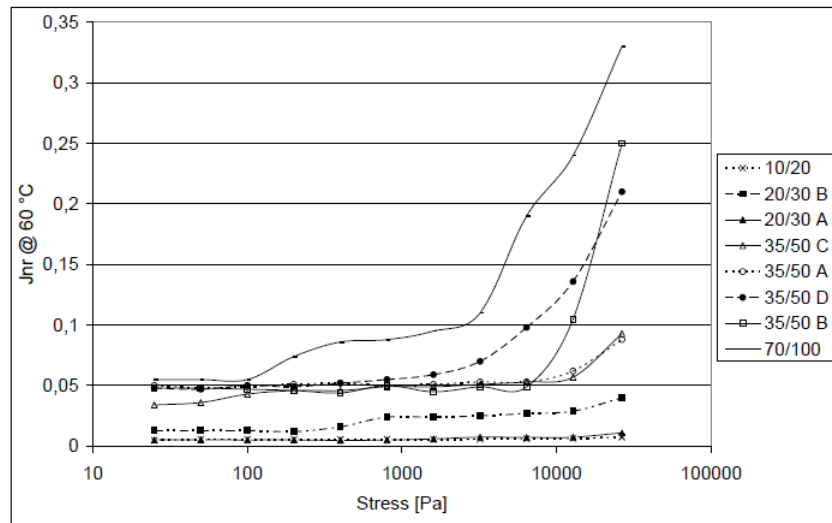


Figure 5-44: J_{nr} values at several stress levels for pure binders

The same tendency could be seen for the polymer modified binders (Figure 5-45) but their J_{nr} values are generally much lower (below 0,1) and the binder sensitivity to stress even starts at higher stress level, above 6400 Pa. This high stress level compared to the ones published elsewhere could be explained by the testing temperature of 60 °C. The ASTM test method recommends testing at the SHRP high critical temperature, which is significantly higher and therefore leads to a softer binder more stress susceptible.

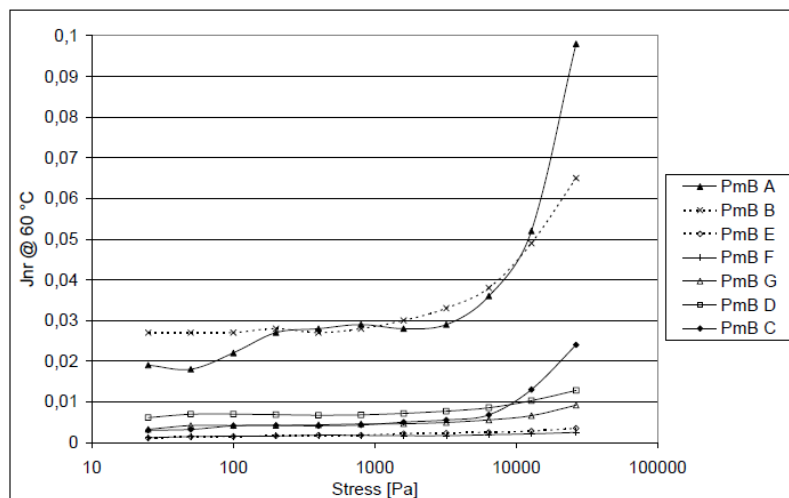


Figure 5-45: J_{nr} values at several stress levels for polymer modified binders

Figure 5-46 shows a clear influence of the addition of polymers to primary binder. The three modified binders by SBS crosslinked or not, and EVA have similar stress dependencies. The increase in the SBS modified binders J_{nr} values above 10000 MPa is not significant. Wider differentiation between PmB's would require testing at higher temperature as recommended in the ASTM protocol

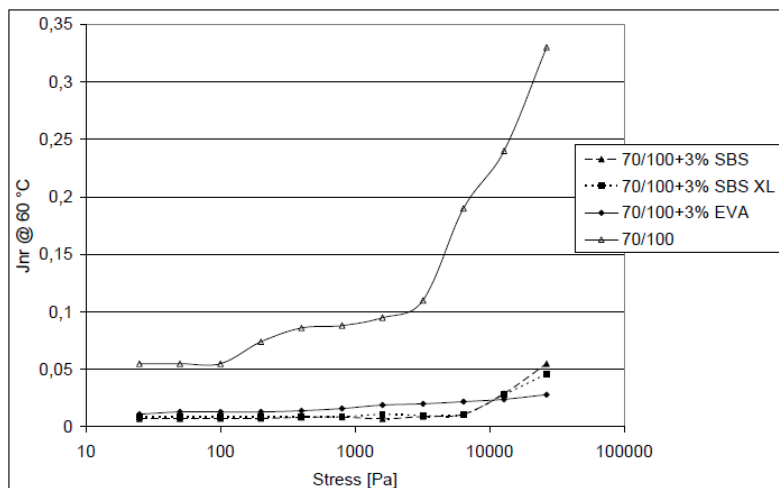


Figure 5-46: Influence of J_{nr} values due to polymer modification

The comparison (Figure 5-47) of several binders within the same penetration range shows no significant difference between the Special grade, PmB C and PmB D until 6400 Pa stress application. At higher stress level, the more highly polymer modified binder has less stress susceptibility. Contrarily, the unmodified binder 35/50 A is constantly at a higher J_{nr} level so that it clearly differentiates from the modified and special binders.

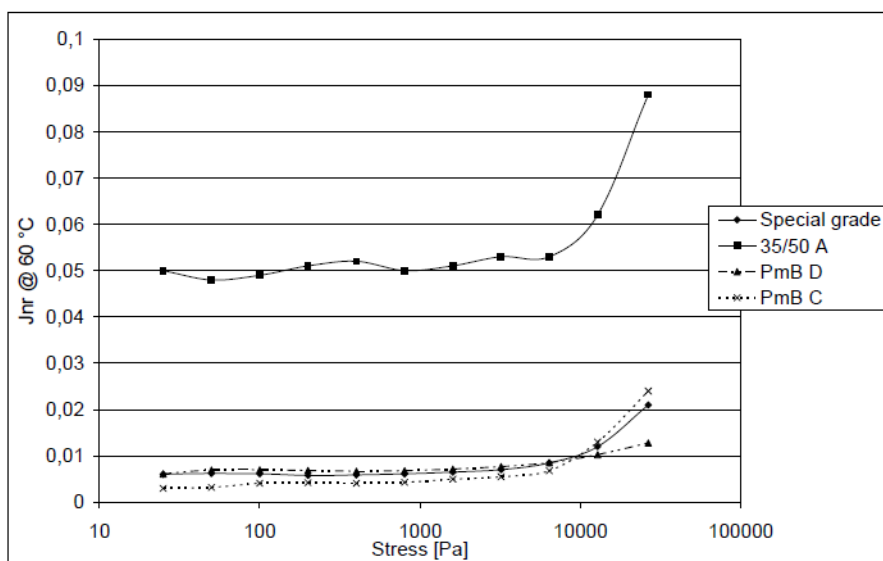


Figure 5-47: Comparison of several binders of same penetration range

Table 5-32 shows that there is no correlation between J_{nr} values at several stress levels and the other widely used binder parameters like softening point, penetration, $G^*/\sin\delta$, G^* and the phase angle δ . In particular, no better correlation could be pointed out with the characteristics measured at the same 60 °C temperature like G^* and δ , than with softening point and penetration. The correlation coefficients are slightly better at higher stress.

Optimized rut resistant asphalt concrete wearing course EB 10 according to standard EN 13108-1 was produced, fitting into the third class, with a rut depth less than 5 % after 30000 cycles at 60 °C. The asphalt concrete was laboratory mixed according to EN 12697-35, and then compacted using a roller compactor (EN 12697-33) to produce slabs with the dimension of 500x180x100 mm. Wheel tracking tests were run, using the French LCPC rut tester

according to EN 12697-22, at 60 °C, with rut depth profiles after 100, 300, 1000, 3000, 10000 and 30000 passes of a rubber tire with a load of 500 daN and frequency of 1 s⁻¹.

Table 5-32: Correlation coefficients, R², of binder parameters with J_{nr} at several stress levels

J _{nr} at stress	Softening point	Penetration	G*/sinδ	G*	δ
25600	0,7459	0,4645	0,4511	0,5242	0,5698
12800	0,7824	0,5722	0,5508	0,6309	0,5717
6400	0,7727	0,5801	0,5801	0,6564	0,6005
3200	0,7722	0,5433	0,5919	0,6814	0,3756
800	0,4756	0,4501	0,5388	0,6350	0,1341
100	0,3444	0,3015	0,3804	0,4600	0,0853

Correlations were made between binder properties and rutting performance of several binders (7 pure, 6 polymer modified and 2 specials binders). The results are shown in Table 5-28. The J_{nr} values at the stress value of 25600 Pa appears to linearly correlate far better to French rutting than the Superpave G*/sin δ criterion and the traditional test method for softening point.

The correlation coefficients of J_{nr} values at several stress levels and French rutting (Figure 5-48) are stress level related. Trends start to show up at 3200 Pa, whereas correlations are more pronounced at the higher stress values 6400 and 12800 Pa. There is also a dependency in the number of passes which can easily be explained by the fact that the soft binder 70/100 failed in the rut tester before 30000 cycles. Nearly all of the other asphalt mixes are characterized by a good resistance against permanent deformation

Table 5-33: Correlation coefficients of J_{nr} values at several stress levels and French rutting

J _{nr} [Pa-1]	Cycles of French Rutting tester at 60 °C			
	1000	3000	10000	30000
100	0,2186	0,1857	0,1074	0,3604
1600	0,3441	0,3468	0,2925	0,3028
3200	0,6350	0,6374	0,4916	0,4453
6400	0,8498	0,9025	0,8483	0,5674
12800	0,8787	0,9008	0,8050	0,7149
25600	0,8475	0,8059	0,6410	0,7711

Binders giving better rut performing asphalt mixes are those staying longer in the linear region. Possibly, due to the fixed temperature of the study (60 °C), higher stress levels were necessary to influence the binder resistance to deformation than in previous published papers, where the testing temperatures selected as the PG grade high end, were generally higher.

There is no correlation between J_{nr} and R&B softening point or penetration (Figure 5-49). Moreover, those figures demonstrate that binders having similar penetration or softening point can have very different J_{nr}. This latter parameter better differentiates binder properties.

According to the authors, further development work would need to involve a wider range of binders and mixes, and binder testing at various temperatures, on one hand to seek for an even better binder differentiation or look at other related parameters like “equi J_{nr}

temperatures”, and on the other hand to evaluate MSCRT precision. It should also include a comparison with low shear viscosity to understand how those two very different tests compare in terms of asphalt rutting performance predictors.

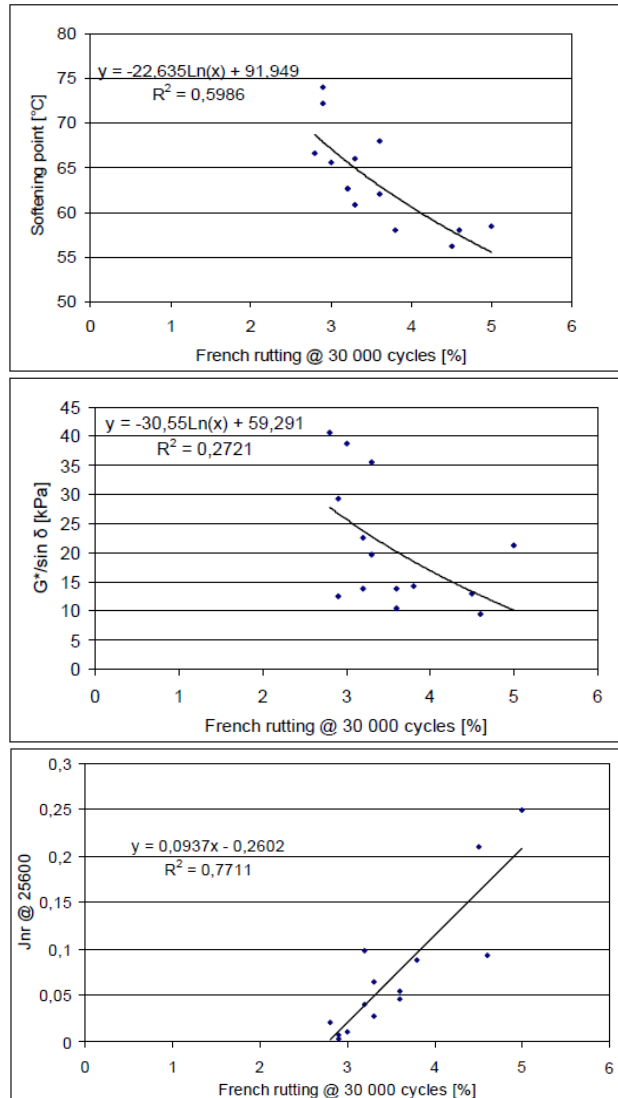


Figure 5-48: Correlation of softening point, $G^*/\sin \delta$ @ 60 °C and J_{nr} at 25600 Pa with rutting

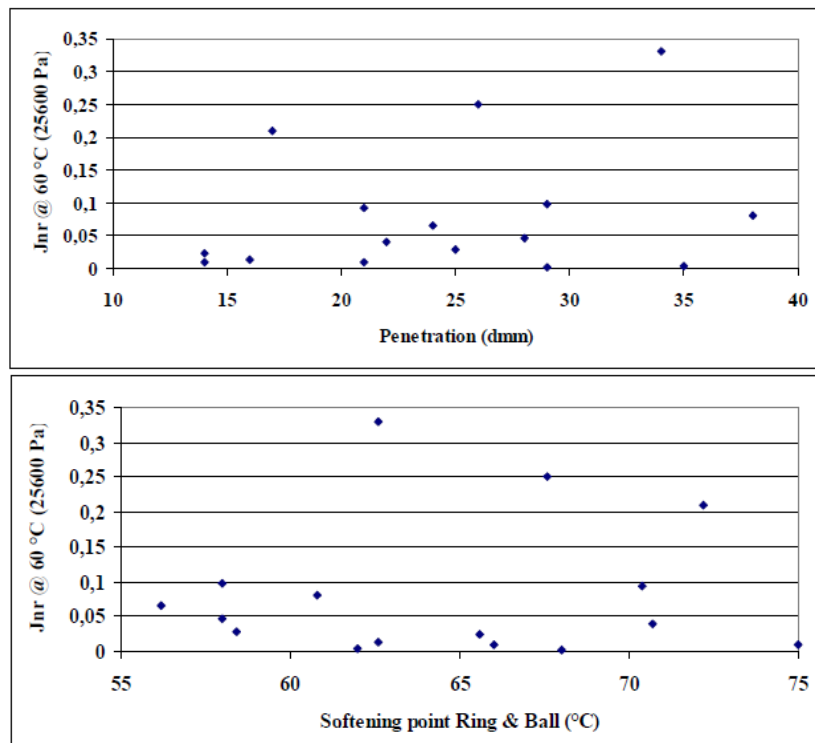


Figure 5-49: Differentiation by J_{nr} of binders with similar penetration or softening point

5.3.8.13 Paper 455 (Romagosa *et al.*, 2010)

Paper contains data on effect of PPA (as stand-alone modifier or combined with SBS) on:

- Conventional binder properties (PEN, R&B, viscosity at 60 °C)
- SHRP properties ($G^*/\sin\delta$ and m-value of BBR)
- MSCR (J_{nr} and % Recovery)

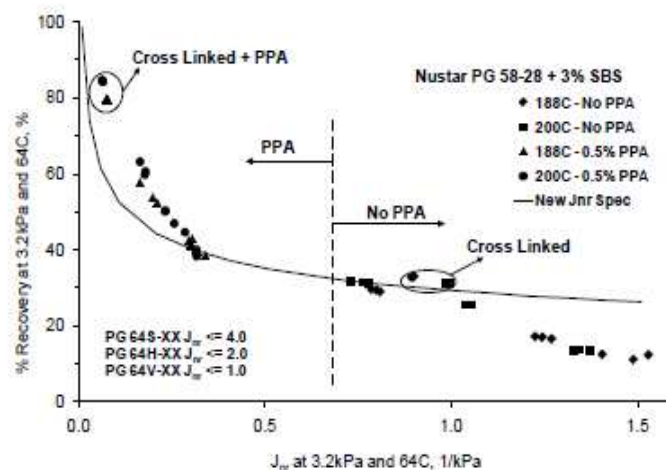


Figure 5-50: Effect of lend optimization variables on the newly proposed MSCR based high temperature PG grade

The tests demonstrate a stiffening effect at high temperatures, but little impact on low temperature properties => range between high and low PG grade temperatures becomes larger.

Effect of blending temperature and blending time are investigated:

- longer blending times lead to superior performance of the binder;
- MSCR properties show more clearly the effect of these parameters than SHRP parameter $G^*/\sin \delta$.

Paper also discusses impact of PPA on some asphalt properties:

- Fatigue resistance: no negative impact observed
- Water sensitivity (Lottman and Hamburg WTT): depends on type of aggregate binder and combination with adhesivity dopes and adhesion promoters like hydrated lime => shall be tested on the asphalt mixture
- Storage stability: generally a positive impact, bu shall be tested

Paper contains no data on permanent deformation of asphalt mixtures, to correlate with MSCR or other binder tests.

5.3.8.14 Paper 456 (Bennert & Martin, 2010)

Experimental study, considering 3 binders:

1. Neat binder
2. SBS (4,25 %) modified binder
3. SBS (2,75%)+ PPA (0,5 %) modified binder

For each binder, binder properties are measured and compared to asphalt mix performance (same grading, different binder):

- Binder tests performed: MSCRT
- Asphalt mixture tests: Stiffness, fatigue, permanent deformation (Repeated load permanent deformation test), moisture sensitivity (TSR)

MSCR tests showed a better performance for binder 2 than for binder 3 (especially higher % Recovery).

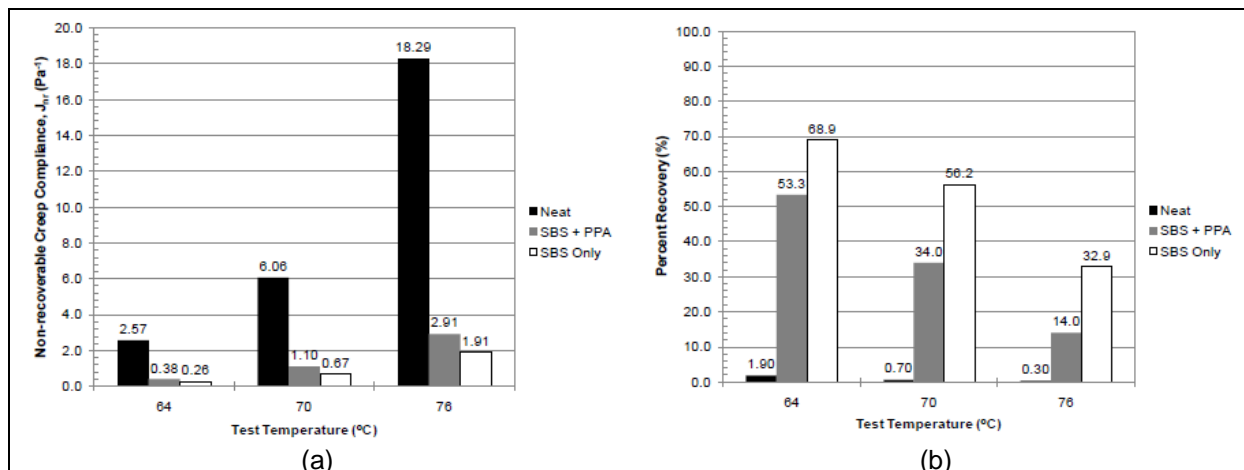


Figure 5-51: (a) Non-recoverable creep compliance properties of bituminous binders in study

However, in the mixture tests (repeated load permanent deformation in uniaxial compression), both mixtures showed the same high resistance to permanent deformation.

In general, the mixture tests showed similar performance with binders 2 and 3, which leads to the conclusion that SBS content can be lowered by adding PPA.

5.3.8.15 Paper 502 (Dreessen *et al.*, 2009)

The current binder characteristics G^* and δ are measured in the linear range. But the rutting is the plastic deformation of an asphalt mix caused by heavy traffic loads under low speed. This is a high strain failure in the pavement and leads to a non-linear response. So multiple stress testing is needed to describe the binder properties in the non-linear range. One of the promising candidates is the multiple stress creep recovery test (MSCRT) under current development in the USA. The MSCRT is measured in a dynamic shear rheometer at various stress levels.

This paper presents a study on the rutting resistance of several mixtures and the corresponding binders. Relations between the behavior of mixtures and binders are discussed through the use of the different analysis methods DSR (G^* , δ), MSCRT and the French wheel-tracking test for the mixtures. The influence of parameters, such as binder nature, penetration grade, nature and level of polymer modification are also discussed and related to the resistance performances of both binders and mixtures.

The non-recoverable creep compliance J_{nr} could be considered as a better alternative method to replace the $G^*/\sin \delta$ and/or R&B softening point for the prediction of the rutting due to better correlation to the French rutting test at 60 °C . The value normalizes the strain response of the binder to stress which clearly shows the differences between different binders.

It differentiates binders having penetrations, softening points or $G^*/\sin \delta$ in the same range.

Table 5-34: Overview polymer modified binders and their properties

Binder	Before RTFOT aging		After RTFOT aging		$G^*/\sin \delta$	J_{nr} @ 60°C		
	R&B	Penetration	R&B	Penetration		100 Pa	12800 Pa	26500 Pa
70/100 + 3% SBS	58,2	41	62,0	35	10,5	0,072	0,029	0,055
70/100 + 3% SBS XL	63,6	36	68,0	29	13,9	0,088	0,028	0,046
70/100 + 3% EVA	62,0	28	66,0	21	19,7	0,013	0,024	0,028
PmB A	56,0	55	62,6	34	13,8	0,022	0,052	0,098
PmB B	55,0	58	60,8	38	35,6	0,027	0,049	0,066
PmB C	67,4	34	67,6	26	24,3	0,0041	0,013	0,024
PmB D	66,4	42	70,4	21	48	0,007	0,0103	0,0128
PmB E	67,2	28	72,2	17	29,3	0,0015	0,0028	0,0035
PmB F	71,2	26	75,0	14	53,8	0,0015	0,0021	0,0025
PmB G	65,4	25	70,7	22	19,8	0,0042	0,0066	0,0092

The criterion J_{nr} can characterize modified as well as unmodified binders and gives better correlation to the French rutting test at 60 °C than the current $G^*/\sin \delta$ value for the SHRP specifications and softening point and penetration for the classical testing. **It has to be mentioned that this study was only carried out at the temperature of 60 °C to compare the resulting values with the French rut tester run at the same temperature.** Possibly, due to this fixed temperature, higher stress levels are necessary to influence the binder resistance to deformation than in previous published papers.

Summary stresses that for $J_{nr} > 6400 \text{ Pa}^{-1}$ it is needed to have good correlations.

Table 5-35: Correlation coefficients of Jnr values at several stress levels and French rutting

Rut cycles Jnr [Pa-1]	Rut cycles			
	1000	3000	10000	30000
100	0,2186	0,1857	0,1074	0,3604
800	0,3642	0,3571	0,2756	0,3547
1600	0,3441	0,3468	0,2925	0,3028
3200	0,6350	0,6374	0,4916	0,4453
6400	0,8498	0,9025	0,8483	0,5674
12800	0,8787	0,9008	0,8050	0,7149
25600	0,8475	0,8059	0,6410	0,7711

5.3.8.16 Paper 510 (Hase, 2011)

Same paper in German as paper 28: discussed in section 5.3.8.2.

5.3.8.17 Paper 517 (Laukkanen et al., 2014)

In this study the Multiple Stress Creep Recovery (MSCR) test method is used to investigate the creep recovery behavior of various bituminous binders and its relation to asphalt mixture rutting. Frequency sweep and MSCR tests were conducted on three unmodified and six elastomer and/or wax modified binders, and the resulting data were used to calculate the values of various binder rutting parameters. These binders were also used to manufacture asphalt slabs for mixture rutting simulations in the LPC wheeltracking device.

Table 5-36: The LVE rutting parameters of the studied binders

Binder	High PG temperature		G* _{sinδ} at 1.59 Hz		G* _{sinδ} at 0.01 Hz		ZSV from the simplified Cmas model		ZSV from the simplified Carreau model		LSV at 0.01 Hz	
	°C	Rank	kPa	Rank	kPa	Rank	kPa s	Rank	kPa s	Rank	kPa s	Rank
B1	80 ^a	3	1.11 × 10 ²	2	1.22 × 10 ⁰	3	2.29 × 10 ¹	4	1.92 × 10 ¹	3	1.94 × 10 ¹	3
B2	68	8	1.15 × 10 ¹	8	9.53 × 10 ⁻²	8	1.57 × 10 ⁰	8	1.51 × 10 ⁰	8	1.52 × 10 ⁰	8
B3	65	9	6.90 × 10 ⁰	9	5.32 × 10 ⁻²	9	8.65 × 10 ⁻¹	9	8.42 × 10 ⁻¹	9	8.47 × 10 ⁻¹	9
E4	70 ^a	5	2.24 × 10 ¹	5	4.45 × 10 ⁻¹	5	1.50 × 10 ¹	5	7.30 × 10 ⁰	5	6.92 × 10 ⁰	5
E5	73 ^a	7	1.60 × 10 ¹	6	1.92 × 10 ⁻¹	7	3.39 × 10 ⁰	7	2.99 × 10 ⁰	7	3.06 × 10 ⁰	7
E6	74 ^a	6	1.32 × 10 ¹	7	2.62 × 10 ⁻¹	6	1.34 × 10 ¹	6	4.44 × 10 ⁰	6	3.90 × 10 ⁰	6
W7	77 ^a	4	7.27 × 10 ¹	4	5.94 × 10 ⁻¹	4	6.31 × 10 ¹	3	1.16 × 10 ¹	4	9.23 × 10 ⁰	4
EW8	89 ^a	2	1.04 × 10 ²	3	2.45 × 10 ⁰	2	n.d.	1-2	1.49 × 10 ⁰	2	3.29 × 10 ¹	2
EW9	93 ^a	1	1.80 × 10 ²	1	6.49 × 10 ⁰	1	n.d.	1-2	9.63 × 10 ²	1	9.10 × 10 ¹	1

All the parameters are evaluated at 50 °C (except for the high PG temperature)

n.d. not determined because of unrealistically high predicted value

^a Value extrapolated from the measurement data using Eq. (1)

Table 5-37: Average values of the MSCR test parameters calculated from the test data

Binder	R ₁₀₀	R ₃₂₀₀	J _{nr100}	J _{nr3200}	R _{diff}	J _{nrdiff}	γ _{acc}	Rank		
	%	%		Rank		kPa ⁻¹			kPa ⁻¹	Rank
B1	25.1	24.4	7	0.051	0.052	4	2.7	1.0	1.699	4
B2	7.0	4.1	8	0.709	0.744	8	41.7	4.9	24.503	8
B3	4.8	1.9	9	1.178	1.248	9	61.4	6.0	41.125	9
E4	52.7	49.6	5	0.140	0.151	5	5.8	7.6	4.977	5
E5	35.2	29.5	6	0.282	0.315	7	16.1	11.8	10.377	7
E6	70.2	58.5	4	0.145	0.211	6	16.7	46.3	6.902	6
W7	92.4	67.7	3	0.004	0.027	3	26.8	523.7	0.865	3
EW8	94.1	88.6	1	0.003	0.006	2	5.8	144.5	0.199	2
EW9	91.7	84.2	2	0.001	0.003	1	8.2	136.4	0.107	1

Table 5-38: Values of the asphalt mixture rutting indicators and corresponding rankings

Binder	Rutting rate		Power-law fit			
	mm/10 ³ loading cycles	Rank	<i>a</i>	<i>b</i>	Rank	<i>R</i> ²
B1	0.0159	3	0.635	0.152	3	0.926
B2	0.0746	8	0.480	0.261	8	0.992
B3 ^a	n.d.	9	n.d.	n.d.	9	n.d.
E4	0.0163	4	0.603	0.173	4	0.957
E5	0.0419	6	0.688	0.195	7	0.989
E6	0.0307	5	0.623	0.183	5	0.992
W7	0.0437	7	0.830	0.192	6	0.973
EW8	0.0119	2	0.765	0.141	2	0.896
EW9	0.0077	1	0.424	0.132	1	0.955

n.d. not determined

^a WTT failed due to the softness of the binder

Table 5-39: Coefficients of determination for the linear and power-law relationships between

	<i>T</i> _{RRB}	<i>G</i> [*] /sin δ at 1.59 Hz	High PG temperature	<i>G</i> [*] /sin δ at 0.01 Hz	ZSV from the simplified Cross model	ZSV from the simplified Carreau model	LSV at 0.01 Hz	<i>J</i> _{acc200}	γ _{acc}
Rutting rate (mm/10 ³ loading cycles)									
Linear	0.498	0.401	0.656	0.331	0.752 ^a	0.202	0.337	0.976 (0.985) ^b	0.975 (0.985) ^b
Power law	0.674	0.758	0.876	0.910	0.894 ^a	0.575	0.912	n.d.	n.d.
Parameter <i>b</i> from the power law model									
Linear	0.632	0.502	0.768	0.430	0.738 ^a	0.273	0.434	0.982 (0.984) ^b	0.982 (0.984) ^b
Power law	0.750	0.741	0.878	0.890	0.877 ^a	0.684	0.891	n.d.	n.d.

n.d. not determined since high correlation was already found for linear correlation

^a Correlations do not include data for binders EW8 and EW9, see Table 3

^b The value in parentheses is the coefficient of determination calculated for the data collected during the round robin study [45]

It was found that the non-recoverable creep compliance parameter (J_{nr3200}) and the accumulated strain at the end of the MSCR test (CACC) correlate very strongly with each other and that they both have a superior capability of predicting asphalt mixture rutting compared to other rheological binder rutting indicators. An effort was made to explain the manifested nonlinear viscoelastic properties of the modified binders with their expected microstructural characteristics.

As expected, modified bituminous binders were discovered to be much more rut resistant compared to unmodified binders of the same penetration class. However, it was also observed that highly modified binders, and especially binders modified with wax, are more stress sensitive compared to unmodified and moderately modified binders. This is believed to be due to the rupture of the physical network that the modifying agent forms in them. A detailed investigation of the creep-recovery data revealed that the modification of bitumen significantly changes the way the material response develops under repeated creep-recovery loading. For unmodified binders the strain response is not changed with successive creep-recovery loadings, but for elastomer and wax modified binders the effects of delayed elasticity and the rupture of crystalline microstructure, respectively, can be observed. These kinds of changes in material response are not captured by the standard MSCR test parameters, but they can provide a deeper understanding of the influence of different modifiers and their microstructural characteristics on the binder rutting performance.

Overall: MSCR test highly recommended as binder parameter for rutting characterization of both unmodified and modified bituminous binders.

5.3.8.18 Paper 563 (Tabatabaee & Tabatabaee, 2010)

The present study assesses the performance of binders modified with a wide range of crumb rubber content using these newly developed test methods. Additional binder and mixture performance tests were used to compare and validate the results. The results showed that the new tests performed well in predicting performance. Current Superpave criteria also showed good conformance with mixture test results for CRM binders. Tests results suggest that the MSCR can complement current rutting prediction testing.

The MSCR test was carried out on all RTFO-aged CRM binders at temperatures from 52-88°C according to ASTM D 7405-08a. The average non-recoverable creep compliance (J_{nr}) and the average percent of recoverable strain were calculated at the end of the 1 sec creep plus 9 sec recovery time. The loading was done in 10 cycles at 100 Pa followed by 10 cycles at 3200 Pa. A comparison of the results at the two stress levels shows the degree of nonlinear behavior of the material.

Table 5-40: Results from binder and mixture laboratory permanent deformation tests

Binder Type	MSCR at 64°C				G*/sinδ at 64°C (kPa)		UDC test at 40°C J (1/Pa)
	100 Pa Stress level		3200 Pa Stress level		Original Binder	RTFO Aged	
	J_{nr} (1/Pa)	Recovery (%)	J_{nr} (1/Pa)	Recovery (%)			
A	0.00117	21	0.04993	6	0.9	2.4	2.77E-05
A3%	0.00078	35	0.03626	13	2.7	5.6	6.65E-06
A6%	0.00034	48	0.01412	32	3.7	7.9	4.26E-06
A9%	0.00024	60	0.01204	39	5.7	10.8	4.57E-06
A12%	0.00008	76	0.00393	63	7.6	15.1	4.23E-06
A15%	0.00005	84	0.00275	72	10.9	17.5	3.30E-06

The results show that compliance significantly decreased as rubber content increased, indicating much better rut resistance in highly modified CRM binders. The amount of improvement in J_{nr} follows a similar trend for both stress levels. It was also observed that the stress dependency increased as temperature increased.

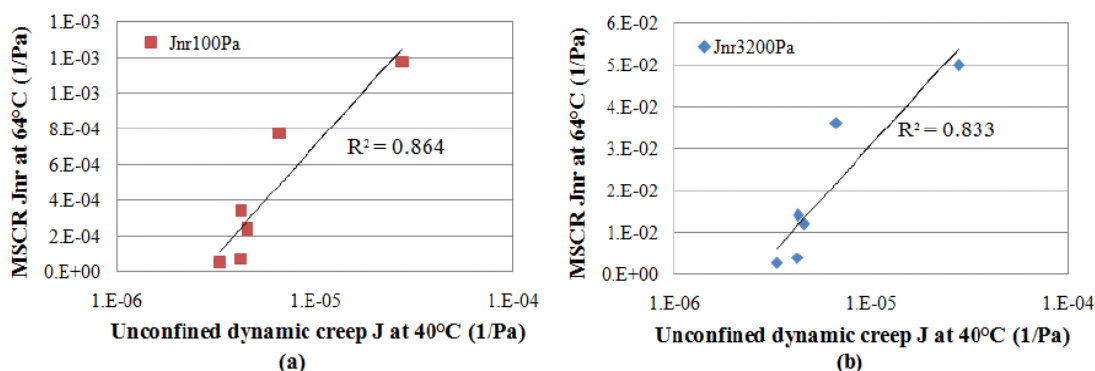


Figure 5-52: MSCR vs mixture compliance from unconfined dynamic creep test

Conclusion:

The MSCR test showed that rubber caused a significant increase in binder elastic recovery, reducing permanent deformation and thus improving rut resistance. A comparison of the two stress levels showed that CRM binders were stress sensitive, showing less recovery at 3200 Pa for each binder but more improvement as rubber content increased. Jnr from the MSCR correlated well with the compliance from the mixture test results.

5.3.9 Oscillation Zero/Low Shear Viscosity (ZSV/LSV) Test**5.3.9.1 Paper 214 (Centeno et al., 2008)**

See chapter 5.3.6.9.

5.3.9.2 Paper 500 (de Visscher & Vanelstraete, 2009)

The task group of CEN TC336 WG1/TG1, responsible for the high temperature binder test methods, developed a new test procedure, published in document prCEN/TS_15324. The procedure leads to the determination of a temperature, at which the viscosity measured at very low shear rate is 2000 Pa.s (EVT: equiviscous temperature). In this paper, this test procedure was used to measure the EVT of a series of 12 binders (pure bitumen, different types of PmBs, semi-blown bitumen and waxy bitumen). Recommendations on possible improvements of the test are given, which is another step forward towards a European standard test that satisfies the general need for a reliable binder indicator for rutting. Tables 3 and 4 shows correlations of EVT with wheel tracking and cyclic triaxial compression tests on asphalt mixtures, compared to other binder characteristics. EVT1 (measured at $f=0,01$ Hz) is a first estimation, while EVT2 is a correction for lower frequencies which is claimed to be necessary in the case of PmBs.

Table 5-41: Comparison of correlation coefficients with wheel tracking test results

	Rut depth (wheel tracking test)								
	$T_{R\&B}$	LSV @ 10^{-3} Hz	LSV @ 10^{-2} Hz	LSV @ 1 Hz	η_0 (RSCT)	$G^*/\sin\delta$ @1.59 Hz	$G^*/\sin\delta$ @ 10^{-3} Hz	EVT2	EVT1
All, except PmBs	0,85	0,82	0,85	0,90	0,83	0,89	0,82	0,85	0,86
All binders	0,61	0,81	0,84	0,77	0,73	0,64	0,78	0,49	0,83

Table 5-42: Comparison of correlation coefficients with cyclic triaxial compression test results

	Cyclic triaxial compression test								
	$T_{R\&B}$	LSV @ 10^{-3} Hz	LSV @ 10^{-2} Hz	LSV @ 1 Hz	η_0 (RSCT)	$G^*/\sin\delta$ @ 1.59 Hz	$G^*/\sin\delta$ @ 10^{-3} Hz	EVT2	EVT1
All, except PmBs	0,83	0,81	0,84	0,88	0,82	0,88	0,81	0,83	0,83
All binders	0,72	0,81	0,72	0,51	0,87	0,46	0,80	0,77	0,76

EVT1 correlates well with the results from the wheel tracking tests, but EVT2 overestimates the rutting potential of the PmBs. While it was the intention to improve the correlation with asphalt rutting by estimating the EVT at a frequency as low as possible, it appears that the frequency is too low, compared to the loading frequency of the wheel tracking test according to EN12697-22 (large device).

The correlation of EVT2 with the results from the cyclic triaxial compression test (performed according to EN12697-25 at a frequency of 1 cycle per second) is better and equivalent to that found for EVT1. It could still be improved by estimating EVT2 at a frequency of for example 0,001 Hz instead of 0,0001 Hz.

The main conclusion is that the EVT based on low shear viscosity may be a valuable binder indicator for rutting, but the frequency of 0,0001 Hz to which EVT2 is related seems to be too low. A frequency of 0,001 Hz or 0.01 Hz would lead to better correlations with asphalt tests. As EVT1 is related to a frequency of 0,01 Hz, it could even be considered to limit the test procedure to the determination of EVT1 for PmBs as well as for pure binders.

This paper compares EVT to MSCR (developed later):

- Strong point of EVT: measurements are made in the temperature range appropriate for the binder.
- Weak point: EVT is measured at low strain levels and therefore can't capture the nonlinear behaviour of the binder, like the MSCR test developed later.

5.3.10 Repeated Creep Test

5.3.10.1 Paper 214 (Centeno et al., 2008)

See chapter 5.3.6.9.

5.3.10.2 Paper 234 (Hrdlicka et al., 2007)

The bitumen modifiers assessed in this study include: Styrene-Butadiene-Styrene (SBS), Styrene-Butadiene-Rubber (SBR), Tire Rubber (TR), and Elvaloy. The modifier types and binder properties used in this study are summarized in Table 5-43.

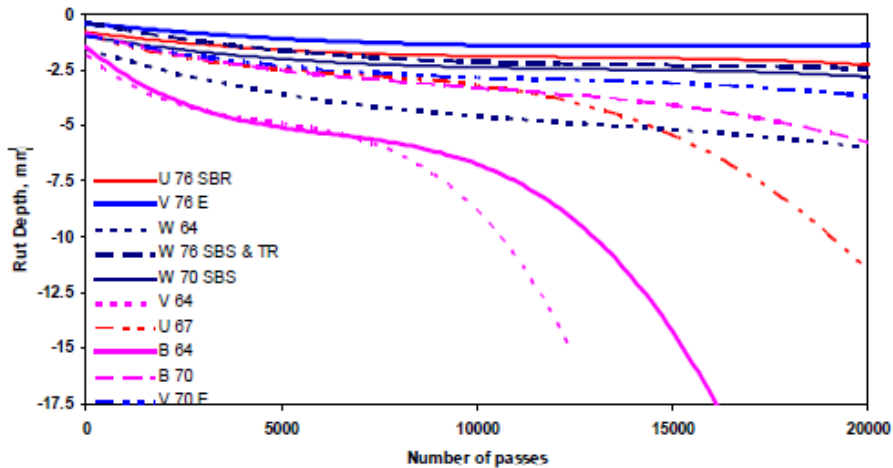
Table 5-43: Rheological properties of bituminous binders

Asphalt Producer	Wright Asphalt			Ultrapave		Valero Armor		
	64-22	70-22	76-22	67-22	76-22	64-22	70-22	76-22
PG grade	64-22	70-22	76-22	67-22	76-22	64-22	70-22	76-22
Modifier	0%	3.0% SBS	SBS+TR	0%	3.5% SBR	0%	2.0% Elvaloy	3.5% Elvaloy
Rotational Viscosity, @ 135°C	0.53	1.4	2.133	0.587	1.367	1.025	0.855	5.122
Softening Point, F	0.23	137	153	N/T	N/T*	N/T	N/T	N/T
Penetration @ 25 °C	61	56	52	N/T	N/T	N/T	N/T	N/T
G*/sind @ 76°C @ 10rad/sec, kPa	1.75	1.517	1.329	2.5	3.02	1.78	1.5	2.34
Phase Angle @ 76°C	84.6	74.2	69.1	81.1	70.7	81.7	78.2	72.2
Specific Gravity @ 60°F	1.04	1.038	1.039	N/T	N/T	N/T	N/T	N/T
Elastic Recovery @ 10°C	N/A	52.5	62.5	N/T	N/T	N/T	54.7	54.7
RTFO Aging	N/T							
G*/sind @ 76°C @ 10rad/sec, kPa	4.47	3.388	2.958	6.35	10.6	4.16	3.59	6.53
Phase Angle @ 76°C	79.8	69.8	66.8	85.2	85.4	85.3	73.2	67.2
Change in mass	0.02	0.019	0.02	N/T	N/T	N/T	N/T	N/T
PAV Aging	N/T							
G*/sind @ 31°C @ 10rad/sec, kPa	1978.9	2184.8	2374.8	3086	2585	N/T	N/T	N/T
S, -12 °C @ 60sec	147.2	1.335	107.4	122	114	N/T	N/T	N/T
m, -12 °C @ 60sec	0.3137	0.3283	0.3135	0.325	0.317	N/T	N/T	N/T

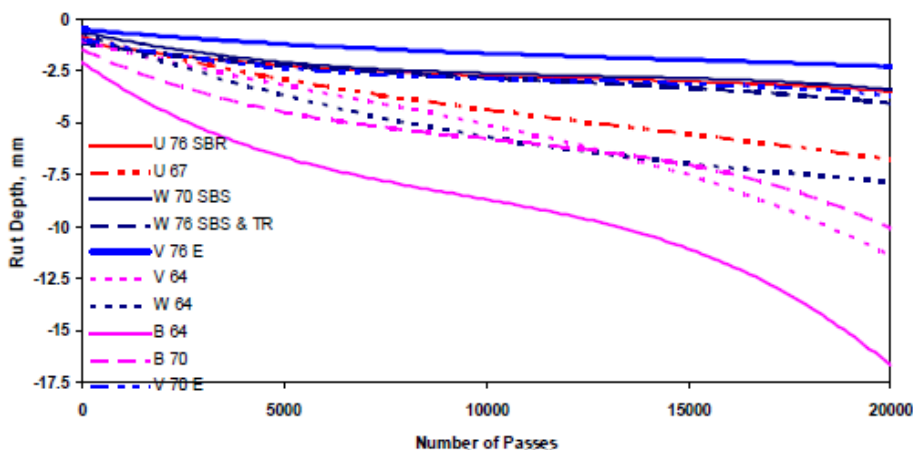
Two mix designs used were Type-D and Coarse Matrix High Binder (CMHB-C), both of them with the same binder content.

The HWTB tests were performed, at the test temperature of 50 °C, on compacted specimens with (150 ± 2) mm in diameter by (62 ± 2) mm in height, until 20,000 cycles. The results are reported in Figure 5-53. Deformations obtained at the end of 20,000 cycles are summarized in Table 5-44 for all tested locations: center of the specimen and center of the slab (interface of two specimens).

Repeated creep tests were performed at 52 °C, 64 °C and 76 °C, using a 25-mm diameter parallel plate geometry and 1-mm gap. The shear stress was 100 Pa. The loading and unloading times were set at 1 s and 9 s, respectively. The tests were conducted for a total of 100 repeated cycles. See results in Table 5-44 and trend lines in Figure 5-54.



a) Type D Mix



b) CMHB-C Mix

BinderType	Abbreviation
Wright Asphalt PG 64-22	W 64
Wright Asphalt PG 70-22 3.5% SBS	W 70 SBS
Wright Asphalt PG 76-22 SBS & TR	W 76 SBS & TR
Ultrapave PG 67-22	U 67
Ultrapave PG 76-22 3.5% SBR	U 76 SBR
Valero Armor PG 64-22	V 64
Valero Armor PG 70-22 2% Elvaloy	V 70 E
Valero Armor PG 76-22 3.5% Elvaloy	V 76 E
BASF PG 64-22	B 64
BASF PG 70-22 2% SBR	B 70

Figure 5-53: HWTB rut depth for Type D and CMHB-C mix design at the center of specimen

Table 5-44: DSR accumulated strain and HWTD rut depth data

	52 Degrees Acc Strain	52 Degrees Acc Strain	Center of Specimen Deformation	Center of Specimen Deformation	Maximum Deformation	Maximum Deformation	Center of Slab Deformation	Center of Slab Deformation
Wright Asphalt 76-22 (SBS + TR)	0,33	0,49	2,7	4,1	3,0	5,4	2,6	4,2
Wright Asphalt 70-22 (3.5% SBS)	0,45	0,36	2,9	3,4	2,8	4,9	2,7	4,6
Wright Asphalt 64-22	1,31	2,43	4,0	8,0	4,4	6,1	4,0	6,1
Valero Armore 64-22	2,34	3,50	14,2	9,3	17,0	12,7	16,4	12,0
Valero 76-22 (3.5% Elvaloy	0,28	0,61	2,3	2,6	2,3	3,4	1,6	2,0
Valero 70-22 (2% Elvaloy)	0,73	1,83	4,7	10,6	5,4	13,0	3,9	13,0
Ultra Base (67-22)	1,45	1,47	9,2	7,2	14,4	11,1	13,3	7,6
Ultra 76-22 (3.5% SBR)	0,55	0,54	2,5	3,5	3,2	3,9	2,8	3,0
BASF 0% SBR	7,01	6,30	17,8	15,0	17,8	16,7	17,1	16,7
BASF 2% SBR	2,83	3,70	10,1	9,2	11,0	9,5	7,4	8,2

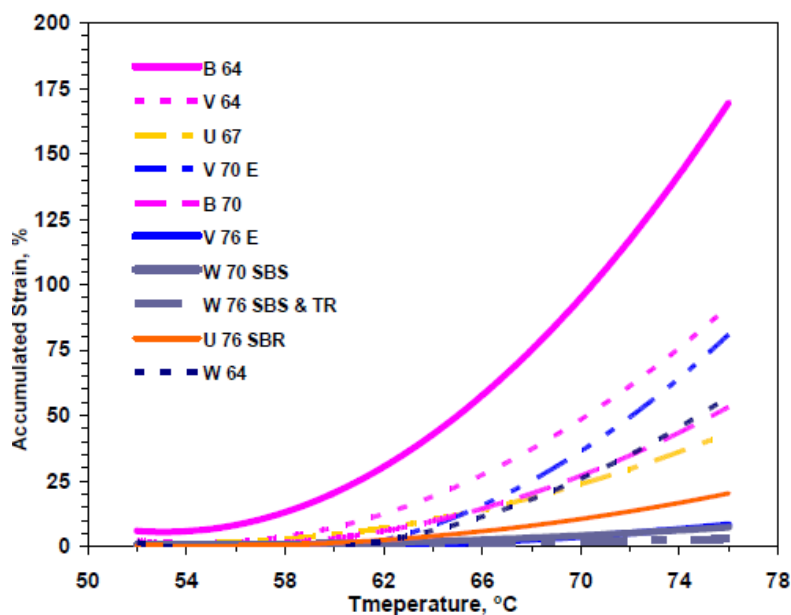


Figure 5-54: Percent accumulated strain at a shear stress of 100 Pa after 100 creep and recovery cycles

A typical example of relationship between accumulated strain and rut depth is shown in Figure 5-55 for unaged and aged (RTFOT) binder.

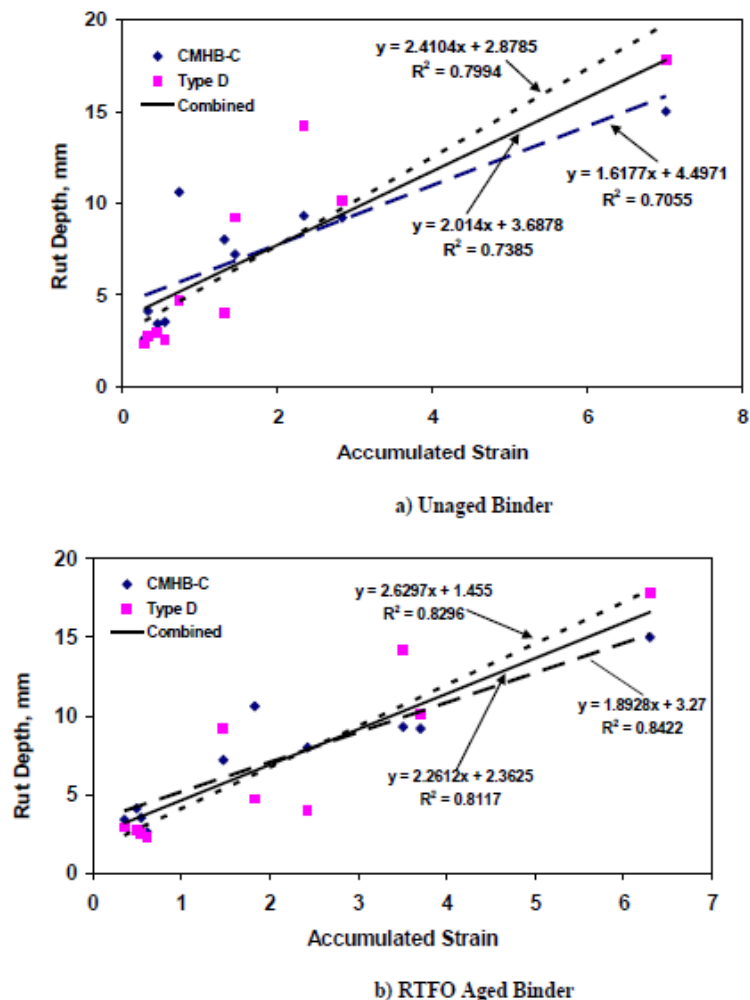


Figure 5-55: HWT center specimen deformation vs accumulated strain at 52 °C

The Prediction Sum of Squares (PRESS) technique was used to validate the relationship between accumulated strain and rut depth. PRESS is a variation of data splitting technique to evaluate the precision of a model used for performance prediction. A more detailed analysis is presented in the paper.

5.3.10.3 Paper 308 (Tan *et al.*, 2014)

Repeated creep recovery tests (RCRT) were conducted at 60 °C, using a 25-mm diameter parallel plate geometry and 1-mm gap. The shear stress was 30 Pa. The loading and unloading times were set at 1 s and 9 s, respectively. The tests were conducted for a total of 100 repeated cycles.

See results in section 5.3.6.10.

5.3.11 Ring and Ball (R&B) Softening Point Test

5.3.11.1 Paper 026 (Eckmann *et al.*, 2012)

Due to the wheel-tracking tests results a continuous decrease of the rut depth after 30 000 loading cycles with increasing polymer contents have been observed. A similar trend is followed by indicators usually associated with the high temperature performance of the corresponding bituminous binders such as, for instance, the softening point or rheological indicators based on $|G^*|$ and δ . Figure 5-56 illustrates some possible correlations.

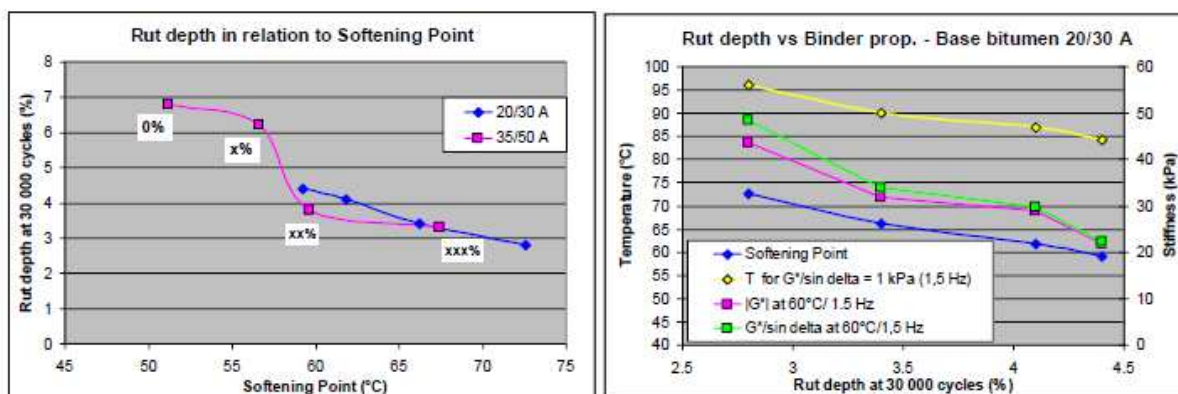


Figure 5-56: Rut depth vs. softening point (left) and rut depth vs. binder G^* characteristics (right)

Since test conditions applied in binder testing (even in so-called “rheological” tests) are markedly different from the stress and strain conditions prevailing in mechanical asphalt mix testing (and even more so from those encountered in an actual pavement), such correlations can of course not be generalised and need to be re-established for every new asphalt mix formulation and type of binder. In addition, they are often questioned, especially in the case of polymer modified binders, due to the poor reproducibility of binder tests (as an effect, for instance, of the thermal history undergone by the test sample) or to specific test artefacts (highly modified soft bitumen may, for instance, lead to artificially high values of the softening point). In the present case, the correlations shown in Figure 5-56 may however be given some extra credit due to the fact that all modified binders have been made from bitumen of the same origin and that modification occurred via a cross-linking process which confers the binder a nearly mono-phasic structure. The rut depths measured for the asphalt mix based on 35/50 bitumen at x% and xx% of polymer could be respectively over- and underestimated.

5.3.11.2 Paper 042 (Robertus *et al.*, 2012)

See also sections 5.3.5.2, 5.3.6.1 and 5.3.8.4.

Figure 5-57 shows the relationship between wheel tracking rut rate at 60 °C and Softening Point of the fresh binders. As is known this correlation is very poor ($R^2=0,68$) when considering all binders. However, when looking only at the five normal paving grades (NPGs) and the two special bitumens (SPs) one can distinguish an almost perfect correlation ($R^2=0,95$). A similar picture develops when Softening Point after RTFOT ageing is used. Apparently the more complex rheological nature of the modified bitumens removes the straight forward traditional correlation between rutting and Softening Point. Interestingly, for highly modified PMBs and FT wax modified bitumen, Softening Point underestimates the actual rutting propensity of these binders when compared with normal paving grades. The Softening Point of some PMB with low modification appears to coincide with the NPG correlation suggesting they do follow the “normal” trend. This confirms that for unmodified binders and some low polymer content PMBs the contribution to deformation susceptibility can be accurately described by Softening Point.

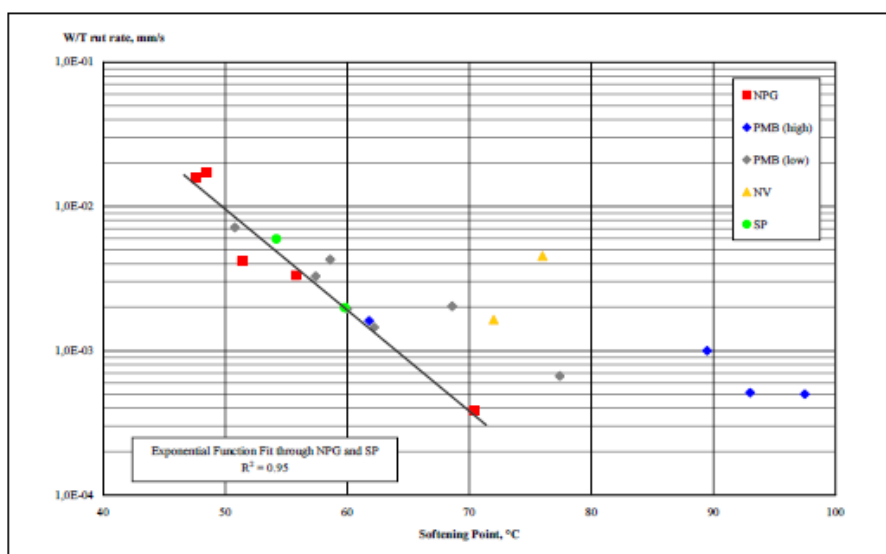


Figure 5-57: Wheel tracking rut rate at 60 °C vs softening point of unaged binder

5.3.11.3 Paper 067 (Guericke & Schlame, 2008)

See also sections 5.3.5.3 and 5.3.6.5.

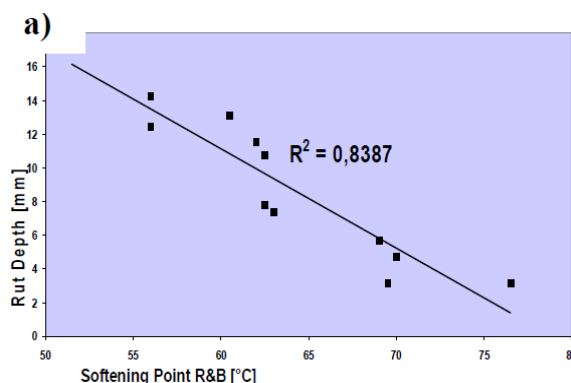


Figure 5-58: Rut depth (Hamburg Wheel-tracking Test) in SMA at 60 °C vs softening point R&B after short-term ageing (RFT)

5.3.11.4 Paper 234 (Hrdlicka et al., 2007)

See section 5.3.10.2.

5.3.11.5 Paper 259 (Kim et al., 2013)

This paper compares the performance of warm-recycled asphalt mixture using polyethylene wax-based WMA additive to hot-recycled asphalt mixture (Table 5-45 and Figure 5-59).

Table 5-45: Bitumen binder properties

ID	Binder content	Binder composition	Penetration (25°C), 0,1mm	Softening point, °C	Ductility, mm	PG grade
HMA LEADCAP 0%	5,1%	RAP 25,2% + Virgin asphalt 74,2%	44	54,2	14,9	64-18
WMA LEADCAP 1,5%	5,2%	RAP 25,2% + Virgin asphalt 73,3% + LEADCAP 1,5%	48	54,1	21,0	64-18

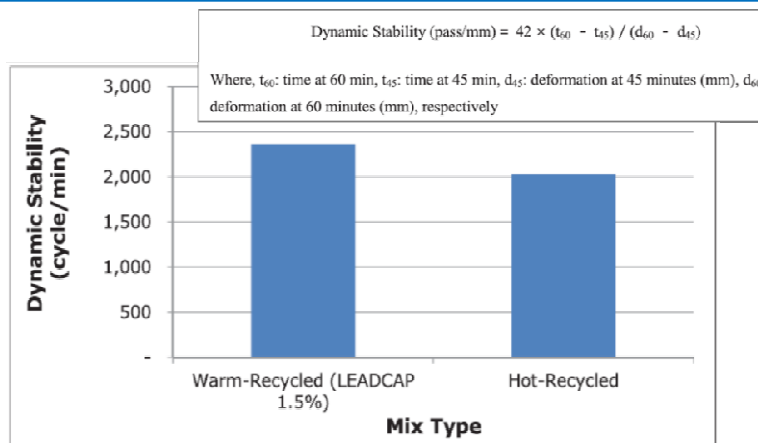


Figure 5-59: Wheel tracking test (KS F 2374:2010), 40 °C, slabs 30x30x5cm³, 42 pass./min.

5.3.11.6 Paper 261 (Kedoudja *et al.*, 2013)

This paper compares the performance of HMA containing different percentages of an industrial waste (NBR - acrylonite butadiene rubber) and a 35/50 pen grade bitumen (Table 5-46).

Table 5-46: Bitumen binder properties

Bitumen		Penetration (ASTM D5), 0,1mm	Softening Point (ASTM D36), °C	Ductility (ASTM D113-79), mm
35/50	Before RTFOT	43	50,6	> 100
	After RTFOT (ASTM D2872)	27,2	59,4	28

A static creep test (Figure 5-60 and Figure 5-61) was carried out in order to evaluate deformations under constant stress (0,14 MPa) and constant temperatures (40°C and 60°C).

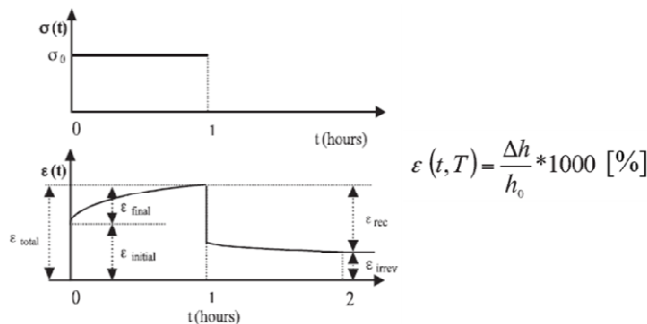


Figure 5-60: Static creep test: applied stress and measured deformation

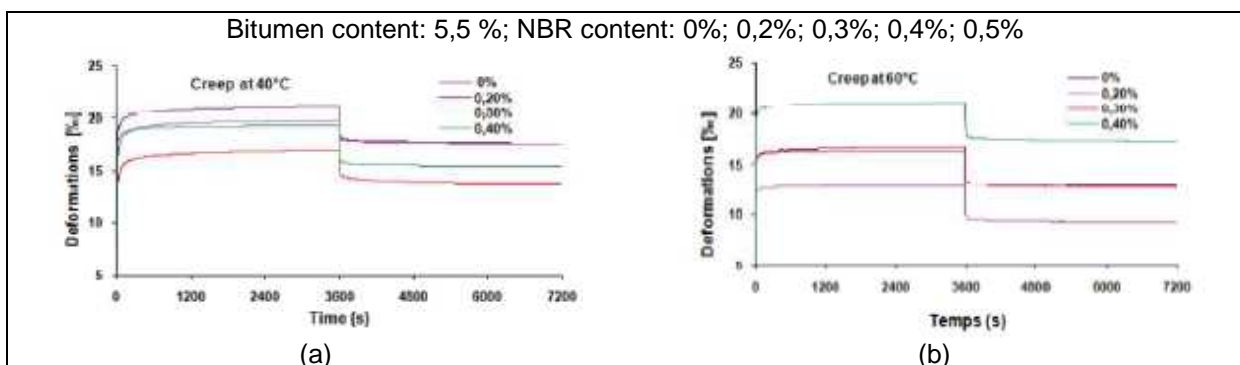


Figure 5-61: Curves of creep recovery: (a) at 40 °C ; (b) at 60 °C

5.3.11.7 Paper 308 (Tan *et al.*, 2014)

See section 5.3.6.10.

5.3.11.8 Paper 314 (Willis *et al.*, 2014)

See section 5.3.8.9.

5.3.11.9 Paper 425 (Dreessen *et al.*, 2009)

See section 5.3.8.12.

5.3.11.10 Paper 505 (Tusar *et al.*, 2009)

Within the framework of the SPENS project and Within Task 1 (Investigation of the Performance of the Conventional and Polymer Modified Bitumen) the objective is to find performance based binder criteria founded on correlations between binder tests and critical asphalt performance tests.

Table 5-47: A selection of binder and asphalt mixture properties

Binder								
Test ↓	Unit ↓	A	B	C	D	E	F	G
Penetration	dmm	82	30	29	68	44	74	54
Penetration mod. I	dmm	147	43	42	104	66	141	88
Softening point	°C	47.6	62.2	67.6	71.2	66.8	49.6	54.8
Fraass Break Point	°C	-17.5	-9.5	-10	-12	-14	-19.5	-18.5
Kinematic viscosity	mm ² /s	599	1370	2234	713	2055	416	596
Dynamic viscosity	Pa s	271	2697	5184	1405	5029	181	528
Penetration/RTFOT	dmm	53	23	25	44	32	51	41
Soft. point/RTFOT	°C	53.4	68.4	73.6	75.4	75.2	56.2	60.8
Dyn. visc./RTFOT	Pa s	666	7819	15758	1902	8886	825	2373
Elastic recovery	%	46		74	99	89		
Deformation energy II	J/cm ²	2.2		12.6	4.3	9.1		
Deformation energy III	J/cm ²	0.1		1.8	2.2	3.6		
Cone Plate viscosity IV	Pa s	227	2022	3219	1407	2624	141	460
Cone Plate viscosity V	Pa s	0.219	0.587	0.734	0.286	0.691	0.133	0.176
Ekviscous temp. VI	°C	145	162	167	151	168	138	144
Coaxial cyl. visk. VII	Pa s	1.69	4.74	6.93	1.89	5.42	1.08	1.97
Coaxial cyl. visk. VIII	Pa s	0.43	0.80	1.26	0.42	1.17	0.21	0.38
Asphalt test								
on SMA/basalts								
Wheel tracking rut	mm	2.45	1.86	1.53	1.54	1.33	2.48	1.98
IT-CY stiffness, 15°C	MPa	1657	4413	4031	2174	3218	1369	2279
Asphalt test								
on AC/basalts								
IT-CY stiffness, 15°C	MPa	1974	4163	4121	2171	2823	1696	3043
Asphalt test								
on AC/limestone								
IT-CY stiffness, 15°C	MPa	2494	9132	5297	4320	4572	2225	4934
Asphalt test								
on PA/basalts								
IT-CY stiffness, 15°C	MPa	838	2670	2889	1435	1975	969	1987

I: Penetration at 35°C with total weight of 50 g; II: At 10°C and speed 50 mm/min; III: At 25°C and speed 50 mm/min; IV: At 60°C; V: At 150°C; VI: According to ASTM D 1559 (2382); VII: At 120°C; VIII: At 150°C.

A combination of fundamental binder test methods, e.g. the complex shear modulus measured with DSR and methods characterizing the binder during severe stress have been suggested to be asphalt mixture performance related.

Table 5-48: Correlation coefficient, R², in linear regression between binder and asphalt test results

Binder test ↓	Asphalt mix test			
	SMA/wheel tracking	AC(basalts)/stiff.	AC(limest.)/stiff.	PA(basalts)/stiff.
Penetration	0.43	0.88	0.67	0.97
Penetration mod. I	0.58	0.87	0.70	0.96
Softening point	0.90	0.23	0.22	0.37
Fraass Break Point	0.5	0.55	0.55	0.57
Kinematic viscosity	0.57	0.50	0.19	0.58
Dynamic viscosity	0.66	0.44	0.18	0.56
Penetration/RTFOT	0.53	0.89	0.72	0.94
Soft. point/RTFOT	0.94	0.25	0.23	0.40
Dyn. visc./RTFOT	0.44	0.67	0.25	0.75
Elastic recovery	0.47	0.00	0.03	0.00
Deformation energy II	0.48	0.93	0.78	0.97
Deformation energy III	0.86	0.08	0.50	0.23
Cone Plate viscosity IV	0.72	0.54	0.30	0.66
Cone Plate viscosity V	0.57	0.57	0.34	0.63
Ekviscous temp. VI	0.68	0.54	0.36	0.61
Coaxial cyl. visk. VII	0.50	0.67	0.32	0.73
Coaxial cyl. visk. VIII	0.55	0.51	0.20	0.58

See table 1 for notes.

From table 4.46 (table 2 in the original paper) it seems to be a fairly good correlation between the wheel tracking rut depth and the softening point even though there are four polymer modified binders in the study. These results are in contrast with the conclusion drawn in the BitVal report Nicholls (2006), but in line with the current European specification for polymer modified bitumen.

5.3.11.11 Paper 520 (Zaumanis *et al.*, 2014)

Recycling agents

Six different recycling agents are used in the study. Measured kinematic viscosity and the specific gravity, along with some basic characteristics obtained from manufacturers are included in Table 5-49.

Table 5-49: Overview recycling agent properties and description

Recycling agent	Kin. visc. at 135 °C (cSt)	Specific gravity	Engineered ^a or generic ^b	Petroleum or organic	Refined or waste	Molecular structure	Polarity
WV oil	5.17	0.924	Generic	Organic	Waste	Ring and strand	Non ^c
WV grease	4.28	0.924	Generic	Organic	Waste	Ring and strand	Mild
Organic oil	5.43	0.947	Engineered	Organic	Refined	Ring and strand	Very ^d
Distilled tall oil	5.60	0.950	Generic	Organic	Refined	Ring and strand	Mild
Waste engine Oil	3.86	0.872	Generic	Petroleum	Waste	Aliphatic	Slight
Aromatic extract	9.20	0.995	Generic	Petroleum	Refined	Aromatic ring	Very
Virgin binder	474	1.020	Generic	Petroleum	Refined	Ring and strand	Mixed ^e

^a A proprietary formulation to optimize performance available through controlled sales network

^b A non-proprietary oil with established properties available globally from a wide variety of suppliers and manufacturers

^c Products with very few if any polar compounds

^d Products with high percentage of polar compounds

^e Reference to the mixture of oil fractions with different degrees of polarity comprising asphalt cement

The experimental plan of the study including mixture and binder test methods as well as respective standards is summarized in Figure 5-62. The results are linked to performance-related properties. Six different recycling agents were added to extracted RAP binder at 12 % dose.

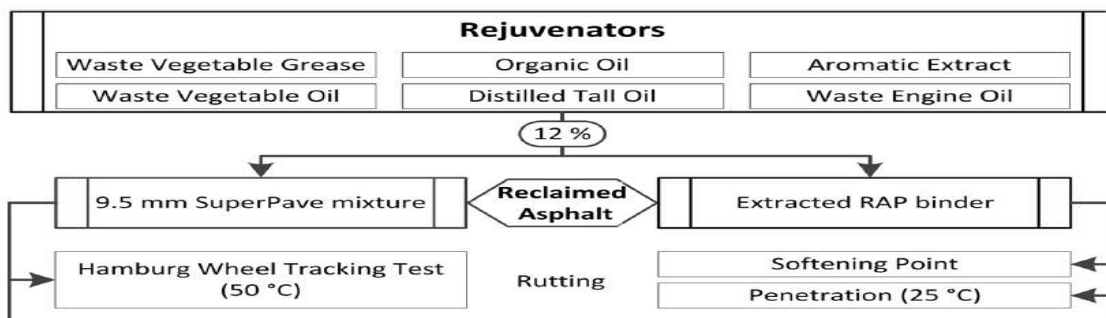


Figure 5-62: Schematic view

Hamburg wheel tracking test (WTT)

Hamburg wheel tracking test samples were prepared by gyratory compactor using 150 mm molds to approximately 60,5 mm height. Four samples (two pairs) are necessary to perform the WTT according to AASHTO T324 in water. 50 °C test temperature was chosen based on the test procedure of Texas DOT, where the test is used for acceptance of mixtures. The samples prepared for Hamburg WTT were also used for evaluation of the mixture workability by calculating the number of gyrations to 8 % air voids according ASTM D6925.

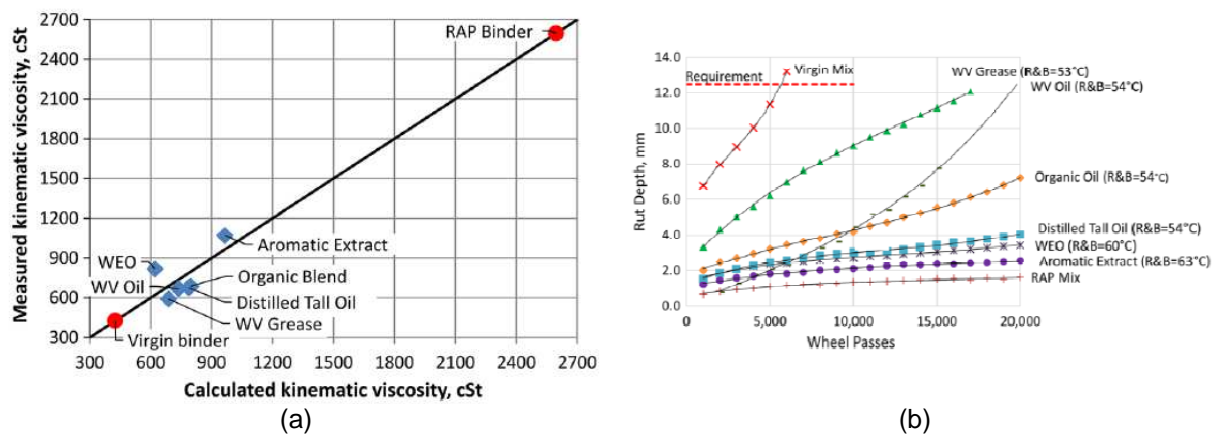


Figure 5-63: (a) Calculated kinematic viscosity, cSt; (b) Hamburg wheel tracking test results

It is clear that all recycled mixtures show high rutting resistance and only the “virgin mix” fails the requirement. Since none of the rejuvenated mixtures has rutting problem, while some of them do have similar penetration and only slightly higher softening point, it is possible that other factors are contributing to the unsatisfactory performance of the virgin mix.

The correlation between binder penetration from and Hamburg WTT rut depth at 10 000 passes is illustrated in figure. The virgin mixture is not included in the figure since it exceeded the maximum rut depth before reaching 10 000 wheel passes. The high correlation ($R^2 = 0,97$) with exponential regression suggests that excessive rutting due to binder softening should not be an issue if the recycling agent dose is calculated according to penetration results.

The following conclusions can be drawn from the research:

1. All six products can reduce the binder viscosity to the level of virgin binder at intermediate temperature (25 °C), but at increased temperature as measured by softening point and kinematic viscosity tests, the binder viscosity remains higher than that of a virgin binder.
2. The organic additives require lower dose than the petroleum additives to provide similar softening effect on RAP binder.

- Penetration test is a good measure of predicting rutting resistance of rejuvenated mixture due to binder softening. Thus it can be used as a reference point to determine the optimum dose of recycling agent for designing rut resistant mixtures. Another advantage of the penetration test is that results can be predicted by only two data points using a simple exponential equation as shown in the study.

5.3.11.12 Paper 533 (Renken, 2012)

See section 5.3.6.16.

5.3.11.13 Paper 559 (Reyes Lizcano et al., 2009)

See section 5.3.2.1.

5.3.12 PG grading

5.3.12.1 Paper 124 (Zeleeuw et al., 2011)

See also sections 5.3.6.6 and 5.3.8.5.

Table 5-50: AASHTO M320-09 Table 3 (MSCR) PG Grade Test Results

Asphalt Binder ID	Table 3 PG Grade	Recommended Traffic Levels
PG 64-22 (u) plus LEA	PG 58-22H	Standard Grade (S) less than 10 million ESALs
Sasobit® terminal blend	PG 58-22V	
PG 64-22 (u) without Gencor water foaming	PG 58-22H	
PG 64-22 (u) plus Gencor water foaming	PG 58-22H	Heavy Grade (H) 10 to 30 million ESALs
Base PG 64-22 (u)	PG 58-22H	
Base PG 64-22 (v)	PG 58-22H	Very Heavy Grade (V) greater than 30 million ESALs
PG 64-22 (u) plus Advera® lab blended	PG 58-22H	
PG 64-22 (u) plus LEA lab blended	PG 58-22H	

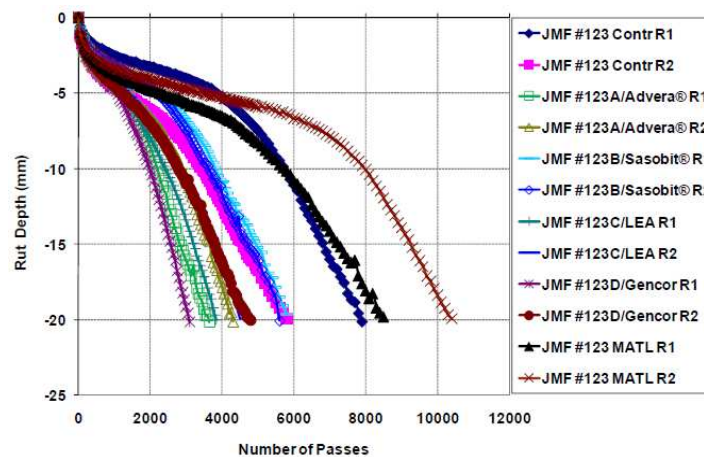


Figure 5-64: Hamburg test results: rut depth

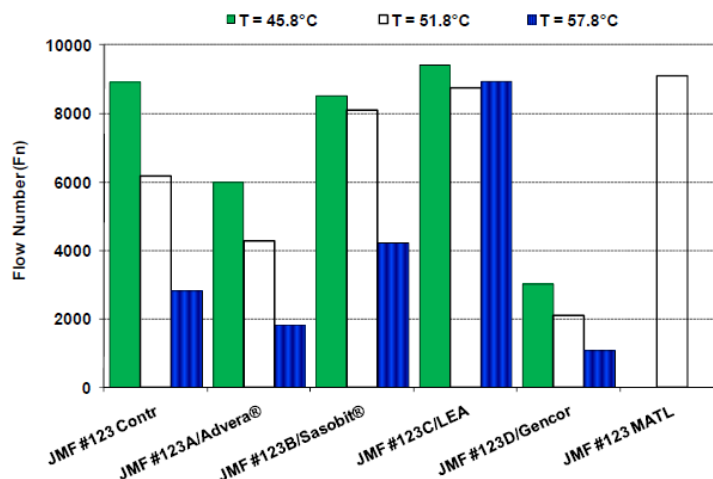


Figure 5-65: Flow number test results: Fn

At a given temperature, increasing Fn values indicate increasing permanent deformation resistance potential. Figure 5-34 shows the Flow Number test results for all asphalt mixtures tested under 50,000 microstrain at three temperatures (i.e., 45,8 °C; 51,8 °C and 57,8 °C). It is evident from this figure that the Fn test is highly dependent on testing temperatures. Overall, the Fn values decreased with an increase in testing temperature. This is apparent for viscoelastic materials where asphalt binder softening occurs upon temperature increase. The MATL mix design replication tested at 51,8 °C measured the highest Fn, likely because the mix was laboratory aged before testing. On the other hand, the lowest Fn was observed for WMA/Gencor at all testing temperatures. The contractor's HMA and WMA/Sasobit® also measured higher Fn values.

5.3.12.2 Paper 153 (Willis *et al.*, 2012)

See section 5.3.8.6.

5.3.12.3 Paper 171 (Mogawer *et al.*, 2012)

The purpose of this study was to evaluate the effect of a bio-modified binder on the performance and workability of asphalt mixtures designed with and without a high Reclaimed Asphalt Pavement (RAP) content. The four mixtures that were designed and evaluated were: a control mixture incorporating virgin materials (PG52-28 binder), the control mixture incorporating 40 % RAP, the control mixture incorporating the bio-modified binder (PG52-28 Bio-modified binder) and the control mixture incorporating the bio-modified binder and 40 % RAP (see Table 5-51 on binder properties). The performance of each mixture was evaluated namely for moisture susceptibility/rutting potential (Hamburg Wheel Tracking Device), whose results are shown in Table 5-52.

Table 5-51: Performance grade binder testing results

	PG52-28 Virgin	PG52-28 Bio-Modified	AASHTO M320 Specification
PG Grade	PG58-28	PG52-28	-
Continuous Grade	59.4-30.4	56.8-31.3	-
Viscosity at 135°C (Pa•S) AASHTO T316	0.242	0.220	<3 Pa•S
Viscosity at 165°C (Pa•S) AASHTO T316	0.077	0.067	-
G*/sinδ (kPa) Original AASHTO T315	1.194 @ 58°C 0.563 @ 64°C	1.854 @ 52°C 0.851 @ 58°C	1.0 kPa min.
G*/sinδ (kPa) - RTFO Residue AASHTO T315	3.028 @ 58°C 1.360 @ 64°C	2.347 @ 58°C 1.085 @ 64°C	2.2 kPa min.
G* sinδ (kPa) - PAV Residue AASHTO T315	6,210 @ 13°C 4,547 @ 16°C	6,006 @ 13°C 3,969 @ 16°C	5,000 kPa max.
Creep Stiffness @ 60s S (MPa) AASHTO T313	199 @ -18°C 411 @ -24°C	181 @ -18°C 458 @ -24°C	300MPa max.
Slope @ 60s m-value AASHTO T313	0.321 @ -18°C 0.268 @ -24°C	0.378 @ -18°C 0.292 @ -24°C	0.300 min.

Table 5-52: Overlay test and Hamburg wheel tracking device test results

Mixture	Average Overlay Test (OT) Cycles to Failure	Stripping Inflection Point from HWTD	Average Rut Depth at 10,000 Cycles (mm)	Average Rut Depth at 20,000 Cycles (mm)
Control	1,004	16,800	1.64	5.21
40% RAP	37	NONE	0.75	0.89
Control + Bio-Modified Binder	1,200	11,700	4.72	n/a
40% RAP + Bio-Modified Binder	523	NONE	1.30	1.71

n/a = Testing did not reach 20,000 cycles due to the maximum rut depth exceeding 20 mm.

5.3.12.4 Paper 230 (Alvarez *et al.*, 2008)

This paper addresses the durability of Porous Friction Courses (PFC), namely by the HWTT. Three different mixtures were evaluated: two produced with AR and one with PG binder (Figure 5-66 and Figure 5-67).

Mixture	Highway	Location	Asphalt Type	Optimum Asphalt Content (OAC) (%)	Aggregate Type and Proportion (%)	Other Materials
US-281- AR	US 281	San Antonio, Tx	AC-10 w/ 16% crumb rubber	8.1	Sandstone ¹ , 50 Limestone ² , 50	None
US-290-AR	US 290	Paige, Tx	AC-10 w/ 17 % crumb rubber	8.3	Sandstone ¹ , 100	None
I-35-PG	IH 35	San Antonio, Tx	PG 76-22S	6.1	Sandstone ¹ , 52 Limestone ² , 47	Lime (1%), fibers (0.3%)

¹The same sandstone was used in all three mixtures. ² The limestone used in the US-281-AR and I-35-PG mixtures is similar.

Figure 5-66: Mixtures description

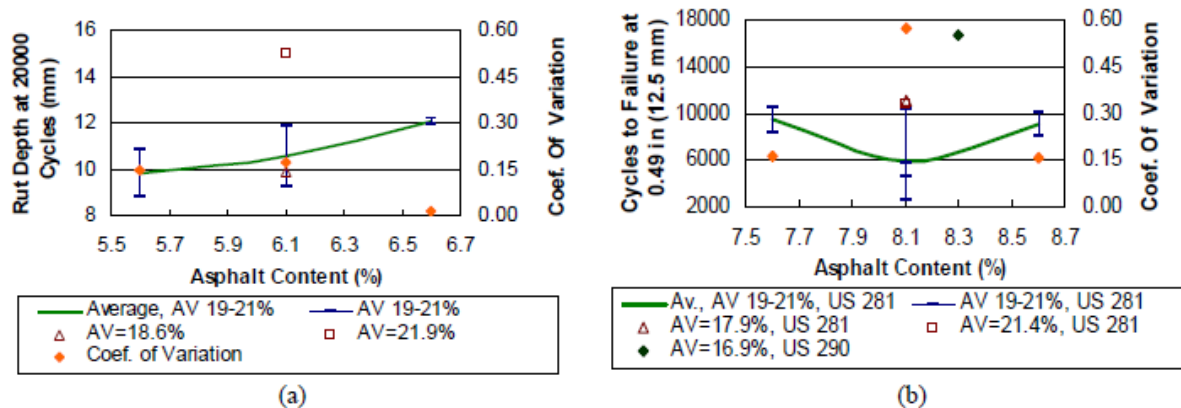


Figure 5-67: Hamburg Wheel-Tracking test results for (a) I-35-PG and (b) US-281-AR and US-290-AR mixtures

The results obtained on I-35-PG and US-281-AR demonstrate that variability plays an important role in HWTT results and makes it difficult to assess the impact of asphalt content on the rut resistance of these mixture systems. These results agree with previous studies that indicate that the variability in the HWTT results should be included in evaluating dense-graded HMA. Data collected in this study suggest that a coefficient of variation of approximately 0,15 is a representative value, although extreme values of 0,57 and 0,02 suggest that this index can vary substantially.

5.3.12.5 Paper 235 (Azari *et al.*, 2008)

This paper addresses the rutting of HMA produced with six different asphalt binder types. Asphalt pavement lanes were built with HMA and two different thicknesses (Table 5-53). All pavements consist of an AC (HMA) layer on an unbound, dense-graded, crushed aggregate base over a uniformly prepared AASHTO A-4 subgrade soil. The total thickness of the surface and base layer was 660 mm.

Table 5-53: Binder types and AC layer thickness in ALF experiment

Binder ID	Binder type	Lane No.	AC layer thickness (mm)	PG grade	Binder description
Control	PG 70-22	2	100	70-22	An unmodified PG 70-22 asphalt binder (considered as the Control)
		8	150	70-22	
AB	Air Blown	3	100	70-28	An air-blown asphalt binder
		10	150	70-28	
SBSLG	SBS LG	4	100	70-28	Styrene-Butadiene-Styrene modified asphalt binder with linear grafting
		11	150	70-28	
SBS64	SBS 64-40	9	150	70-34	SB and SBS blended binder
CR-TB	CR-TB	5	100	76-28	A terminal-blend crumb rubber
Elvaloy	Terpolymer	6	100	70-28	An ethylene terpolymer binder
		12	150	70-28	

Flow number tests were performed on three Plant-Produced & Lab-compacted (PP) replicate samples (PP1, PP2 and PP3) for each one of the six binder type considered and on three Lab-Produced & Compacted (LP) replicate samples (LP1, LP2 and LP3) for three binders. Specimens were prepared with average diameter of 100 mm and average height of 150 mm.

Tests were conducted at target test temperature of 64 °C and with confining pressure of 35 kPa, contact pressure of 41 kPa and target deviator stress of 827 kPa.

Figure 5-68 (a) shows permanent deformation versus loading cycles for PP HMA specimens. Two of the three CR-TB specimens failed (reached permanent deformation of 90 000 microstrains or 13 mm) after 6 500 and 8 500 cycles. Two of the SBSLG specimens failed after 6 500 and around 10 000 cycles. Other samples failed after less than 3 000 loading cycles. The permanent deformation property of SBS64-40 was marginally worse than Control and those of AB and Elvaloy were marginally better than Control. The permanent deformation results clearly show that SBSLG and CR-TB samples performed better than other binders while there was not a significant difference between the other four binders.

Figure 5-68 (b) includes average flow number (FN) for PP and LP HMA specimens. The LP specimens for Control and SBSLG binders have significantly lower FN than PP specimens. CR-TB and SBSLG have the highest FN for PP specimens (4 800 and 4 000 respectively). Flow numbers for other binders were between 1 000 and 2 000. Although the average stiffness of PP specimens for Control binder is less than stiffness of LP specimens (**Chyba! Nenalezen zdroj odkazů.**), the flow number of PP specimens is higher than LP. Furthermore, the flow number of PP specimens of SBSLG is higher than that of LP specimens while their stiffness values are comparable. This indicates that there are other factors involved in permanent deformation other than stiffness.

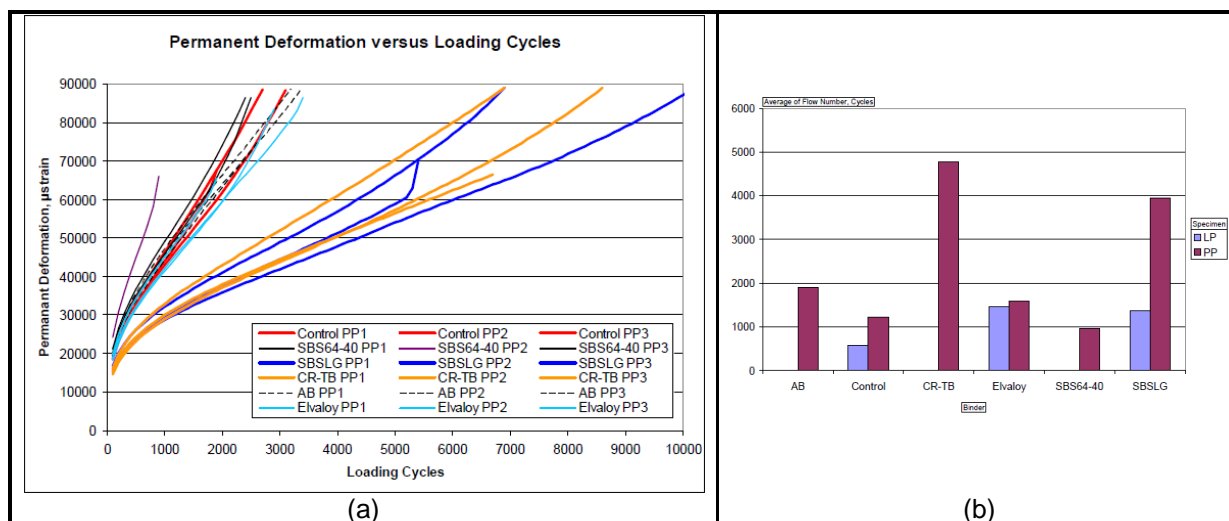


Figure 5-68: Flow Number test results: (a) Permanent deformation versus loading cycles for plant-produced HMA using six different binders; (b) Average FN

Figure 5-69 (a) shows the rutting in AC and base layer. The lowest AC rutting observed was by CR-TB binder (Lane 5) which was 9 mm after 50 000 loading passes. The next lowest rutting observed was by SBSLG binder. The AC rutting observed for this binder after 50 000 loading cycles was 13 and 14 mm for 100 and 150 mm thick HMA, respectively. The highest AC rutting was recorded for lane with SBS64 binder after 50 000 loading cycles (21 mm). The rutting performance of other binders were somewhere in between. It was expected to observe a rather consistent rutting for the base layer for all lanes; however, the rutting varied between 7 and 21 mm. This is rather unexpected since all lanes have the same base type and the base thickness is also similar. The base rutting varied between binders, however, for each binder it did not significantly vary with thickness.

Figure 5-69 (b) shows the AC rutting of ALF lanes at different loading cycles. It shows that lane with 100 mm CR-TB had less rutting at all loading cycles and thus consistently performed better than other lanes. The lane with SBS64-40 binder had the highest final rutting recorded. This binder performed well until around 7 000 cycles but developed rutting at higher rates afterwards. Similar trends can be observed for lanes with 100 mm thick Elvaloy and 150 mm thick AB. All other lanes showed a rather consistent performance throughout the testing period. The lane constructed with 150 mm Control binder performed poorly while 100 mm thick Control lane performed average. The lane with 150 mm thick Elvaloy performed much better than 100 mm thick Elvaloy. Other binders had comparable performance with 100 and 150 mm thick layers. In general, for the same binder the thicker layer exhibited more rutting.

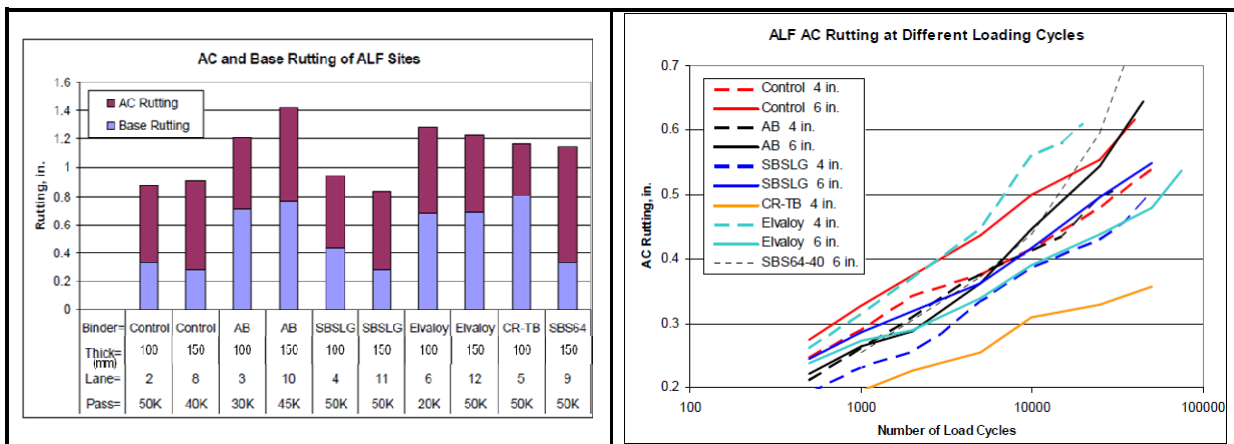


Figure 5-69: Measured rutting @ 64 °C of ALF sites: (a) Total rutting of AC + Unbound base layer; (b) AC rutting at different cycles

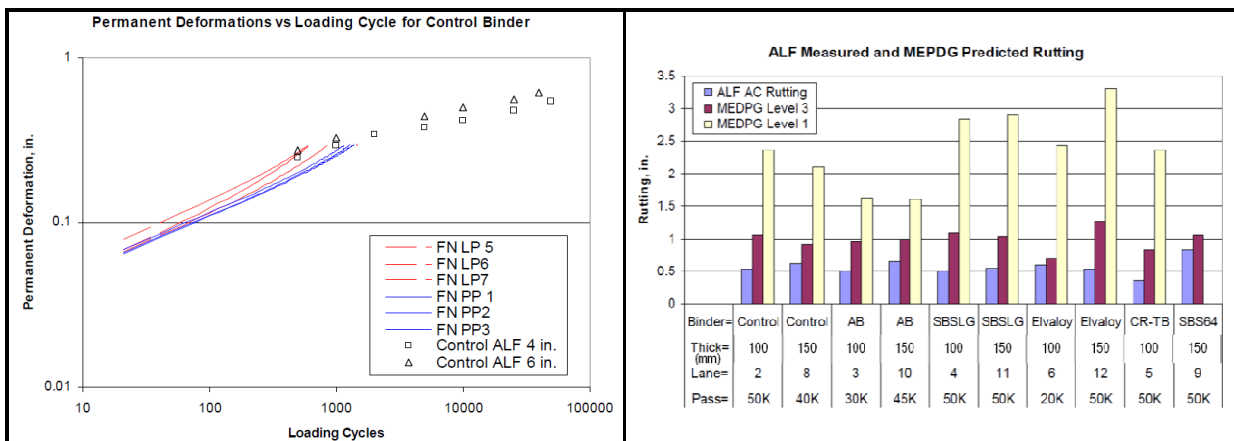


Figure 5-70: (a) ALF Rutting and Flow Number Test Data for LP and PP Specimens of Control Binder; (b) ALF Measured AC Rutting and Predicted AC Rutting using MEPDG Level 1 and Level 3

Comparisons between data from FN tests and ALF rutting data were made. Figure 5-70 (a) shows ALF rutting versus loading cycles for lanes with Control binder as well as permanent deformation from flow number test (for cycles up to Flow Number) for LP and PP specimens in a log-log plot. As shown by the lines in Figure 5-70 (a), the LP specimens performed worse than PP specimens (higher permanent deformations) and the variability between three replicates was higher for LP than PP specimens. FN test results for six ALF binders shows that a good relationship exists between initial rutting of ALF lanes (for cycles up to FN), however, for higher loading cycles the slope of the line through field rutting data differed from

the slope of the permanent deformations from flow number test data as shown in Figure 5-70 (b). This indicates that while FN correlates with initial rutting rather well, the fitted curve cannot be directly extrapolated to predict rutting beyond flow number.

MEPDG software runs were performed at two levels; level 1 and level 3: At level 1, SPT measured E^* values were entered for mix stiffness calculations. At level 3, HMA stiffness is estimated using binder and mix properties. Binder PG was entered from table 5-22. Predicted AC rutting for each lane for MEPDG level 1 and level 3 and the actual ALF measurements are shown in Figure 5-70 (b). The data in this figure shows that the predicted rutting using MEPDG level 3 is 10 % to 130 % higher than the rutting measured in the ALF lanes. The MEPDG level 1 AC rutting predictions, however, are significantly higher than measured rutting for all binders. The measured rutting for the lane with CR-TB binder is 9,1 mm and the level 1 MEPDG prediction is 60,2 mm which is 6.6 times the measured rutting. The closest level 1 predicted rutting to ALF rutting is for the lane with 150 mm AB binder. The ALF measured AC rutting was 16,5 mm and the MEPDG level 1 prediction was 41,1 mm (prediction is 2.5 times measured). For other lanes, the difference is somewhere in between.

The following conclusions were drawn from rutting analysis of the six different HMA studied:

1. The ALF lanes constructed with SBSLG and CR-TB binders performed better than other lanes both in field rutting and SPT flow number despite the fact that their mix was less stiff than mixes prepared with Control and AB binders.
2. The MEPDG predicted least rutting for the lanes constructed with AB binder (best rutting performance) mainly due to the high mix stiffness. However, between the six binders, the mix prepared with AB was ranked third in flow number and fourth in ALF rutting performance.
3. Mixes with Elvaloy and SBS64-40 binders had low flow numbers and performed poorly in ALF rutting. MEPDG also predicted high rutting for lanes constructed with these binders due to their low mix stiffness.
4. MEPDG rutting predictions of ALF sites showed mixed results. The level 3 predictions were generally higher than measured ALF rutting but were in the same ball park. The level 1 prediction, however, was significantly higher than the ALF measured rutting.
5. MEPDG level 1 rutting predictions were significantly higher than level 3.
6. MEPDG level 3 stiffness using NCHRP 1-37A stiffness prediction equation significantly over-estimated stiffness of ALF lanes.
7. The main reason for MEPDG level 1 rutting over-prediction was the calibration of NCHRP 1-37A permanent deformation model which was apparently performed using predicted stiffness using NCHRP 1-37A stiffness equation rather than tested $|E^*|$ using SPT.
8. ALF experiment clearly showed that stiffness alone cannot explain field rutting.

5.3.12.6 Paper 259 (Kim *et al.*, 2013)

See section 5.3.11.5.

5.3.12.7 Paper 292 (Lacroix & Kim, 2014)

In this paper several methods of predicting the rutting resistance of asphalt mixtures are evaluated. The applied prediction models comprised mixtures characterization regarding their stiffness and rutting resistance using, respectively, the dynamic modulus ($|E^*|$) test and the Triaxial Stress Sweep (TSS) test. Furthermore, these predictions are compared to common current tests, such as APA and HWTT. The mixtures and field performance data come from the NCAT 2009 Test Track. The mixtures are taken from the surface (layer 1), intermediate (layer 2), and base (layer 3) layers of six sections of the NCAT Test Track, as listed in Table 5-54.

Two of the methods for predicting the rutting resistance involved:

- The dynamic moduli $|E^*|$ of the mixtures in confined and unconfined conditions. The ranking of the mixtures predicted from both conditions is good compared to the observed ranking from the track, but is more reasonable with the confined data.
- The Viscoplastic (VP) material-level model, following the shift model (Choi and Kim, 2013), which requires a reference test to characterize the permanent strain mastercurve. The reference tests are Repeated Loading Permanent Deformation (RLPD) tests with a loading history of 1,26 s pulse and 10 s rest period for 600 cycles. The stress state is 690 kPa deviatoric stress and 69 kPa confining stress at 54 °C. Other tests, referred to as TSS tests, are performed at different temperatures, pulse times, rest periods, and multiple deviatoric stress levels. The deviatoric stress levels used for all the TSS tests are 485, 690, and 897 kPa and confined at 69 kPa. The protocol requires performing TSS tests at low, intermediate, and high temperatures based on climate (i.e., 26 °C, 44 °C and 54 °C). The low and intermediate temperature tests are performed using 0,4 s haversine pulse with 1,6 s rest. The high temperature tests are performed with 1,26 s pulse and 10 s rest.

The predicted rut depths are biased 2.5 mm higher than those measured in the field when using all three layers (175 mm) of asphalt to predict the rut depth, but the ranking matches the field quite well.

Table 5-54: Summary of NCAT Test Track asphalt mixtures

Mix ID	Mix Description	NMSA (mm)	WMA	Rap content (%)	Binder Grade	$ E^* $ Air Voids (%)	VP ⁽¹⁾ Air Voids (%)	Binder content (%)
NCAT-C1	Control HMA	9,5	-	0	PG 76-22	4.3	6.9	6.1
NCAT-C2	Control HMA	19	-	0	PG 76-22	6.1	7.2	4.4
NCAT-C3	Control HMA	19	-	0	PG 67-22	7.4	7.4	4.7
NCAT-O1	OGFC - Open graded friction Course	9,5	-	0	PG 76-22	18.3	18.3	5.1
NCAT-O2	Same as NCAT-C2	19		15	PG 76-22	5.1	6.3	4.4
NCAT-O3	Same as NCAT-C3	19		0	PG 67-22	8.3	8.3	4.7
NCAT-FW1	WMA, Double-barrel green foaming technology	9,5	Foam	0	PG 76-22	4.9	7.7	6.1
NCAT-FW2		19	Foam	0	PG 76-22	6	7.1	4.7
NCAT-FW3		19	Foam	0	PG 67-22	7.7	7.7	4.7
NCAT-AW1	WMA, Additive technology	9,5	Additive	0	PG 76-22	3.9	6.3	6.4
NCAT-AW2		19	Additive	0	PG 76-22	6.2	7.1	4.6
NCAT-AW3		19	Additive	0	PG 67-22	6.1	6.1	5
NCAT-R1	HMA-Rec	9,5	-	50	PG 67-22	4.7	7.4	6
NCAT-R2		19	-	50	PG 67-22	6.1	7.1	4.4
NCAT-R3		19	-	50	PG 67-22	5	5	4.7
NCAT-RW1	WMA-Rec, Double-barrel green foaming technology	9,5	Foam	50	PG 67-22	5	7.9	6.1
NCAT-RW2		19	Foam	50	PG 67-22	5.8	6.9	4.7
NCAT-RW3		19	Foam	50	PG 67-22	5.8	5.8	4.6

(1) Viscoplastic (VP) material-level model, which is used within a layered viscoelastic continuum damage (LVECD) pavement model to predict the rut depth beneath the center of the moving wheel load with a realistic temperature profile and loading history.

Figure 5-71 show the results obtained.

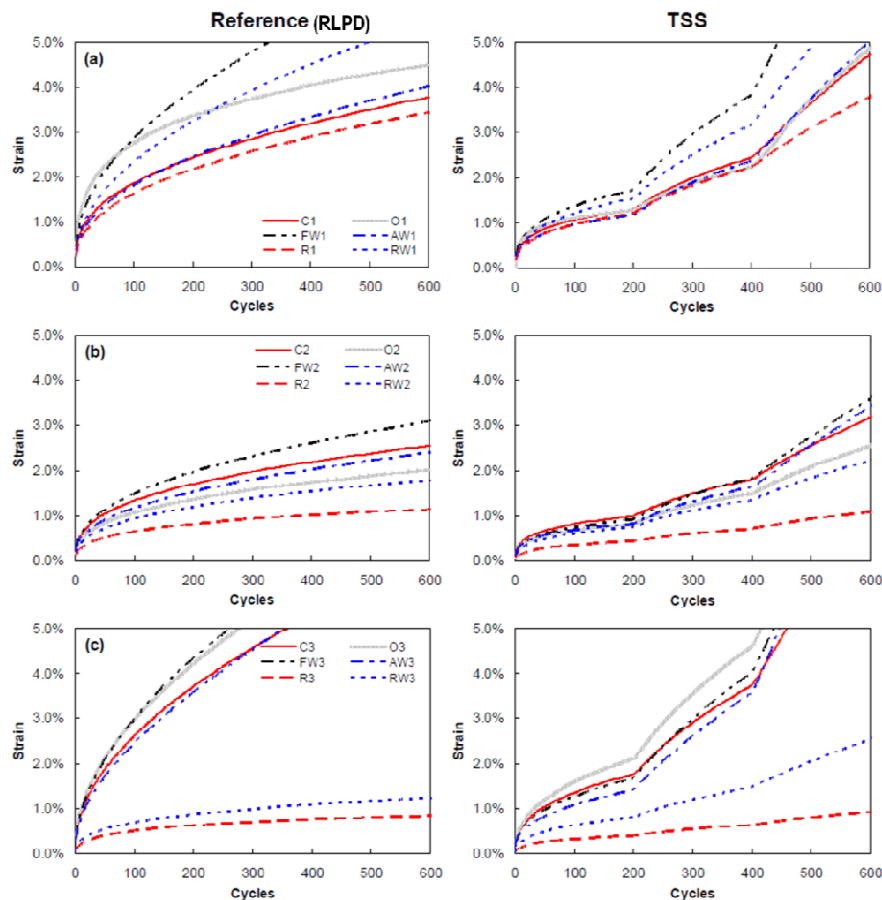


Figure 5-71: Averaged results for VP protocol reference and TSS tests for (a) surface, (b) intermediate, and (c) base layer mixtures at 54 °C

The comparison of laboratory test measurements and rankings for the APA, HWTD, and RLPD of surface mixtures are presented in Figure 5-72. The APA test is run at ~7% air void content at 64 °C by applying 690 kPa to a pneumatic hose for 8 000 cycles. The HWTD test is performed by applying a 703 N wheel load to a specimen with 7% air void content at 50 °C in a water bath for 10 000 cycles. The RLPD results are the strains measured at the end of the test (e.g. 600 cycles of repeated loading) multiplied by the specimen height. The rut depths for the APA and HWTD are measured at the end of the tests. The HWTD has the same ranking as the field results. The APA and RLPD tests rank poorly compared to the field results. The R and RW mixtures have very high relative APA rut depths, which is unusual considering that high $|E^*|$ values due to high RAP contents generally reduce permanent deformation. The HWTD test for the surface mixtures has a high correlation of 0,88 to the field rut depth, suggesting it is a good candidate to predict field rutting. The RLPD test has a correlation of 0,26 and APA has -0,22; both results suggest that these tests are poor candidates for field ranking. Figure 5-72 (e) confirms these observations showing a linear trend for the HWTD but more scattered results for the APA and RLPD tests. The errors in Figure 5-72 (f) show that the bias is small, i.e. evenly scattered on both sides of the line, for RLPD and APA, but biased lower for the HWTD. The mixtures have different rankings and correlations depending upon the test used, which shows the difficulty in capturing the critical rutting parameters. Furthermore, these tests can be used to rank the mixtures. If these tests are used for performance-related specifications, they need to be sensitive enough to distinguish between relatively small changes in mixtures properties such as asphalt content

and air void content. HWTd tests are known to have high variability, which makes this goal difficult, so further options are evaluated.

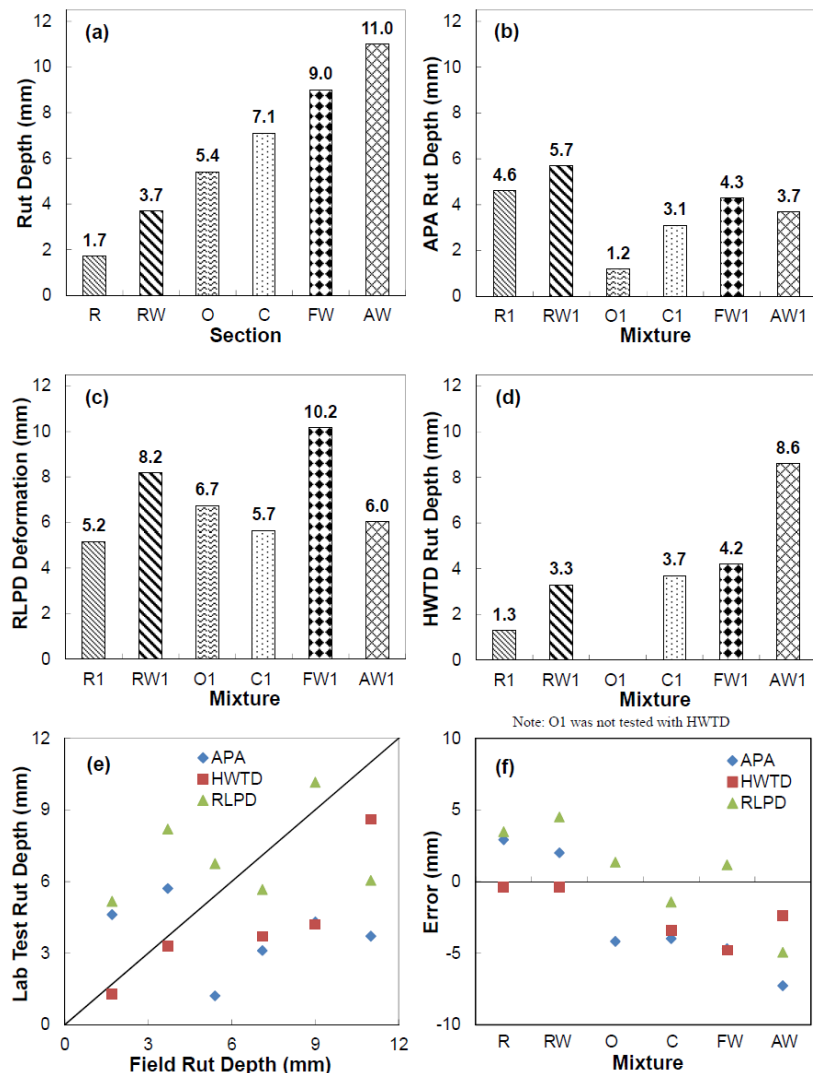


Figure 5-72: Comparison of ranking of (a) measured field rut depths with rutting predictions from (b) APA, (c) RLPD, and (d) HWTd with (e) line-of-equality and (f) residual error

5.3.12.8 Paper 314 (Willis *et al.*, 2014)

See section 5.3.8.9.

5.3.12.9 Paper 319 (Wu *et al.*, 2014)

See section 5.3.8.10.

5.3.12.10 Paper 329 (Kim *et al.*, 2014)

This paper addresses the influence of the mixing/production temperature (STAT - short-term aging temperature) on the performance of SBS-modified WMA mixtures, namely on two high-temperature properties: Rut depth in WT tests; and Strength against deformation (S_D) in simple compression tests. The experimental design included the use of one base asphalt (PG64-22), four SBS brands (S1, S2, S3 and S4) and three WMA additives (Pewboil, P_{ew} ; Leadcap, L_{cp} ; and Evotharm, E_{vt}), as synthesized in Table 5-55. The PG grade of each binder was measured using a dynamic shear rheometer (DSR) and a bending beam rheometer (BBR), as it is also shown in Table 5-55.

Table 5-55: Binder types, DRS and BBR test results and PG grades

Mixture type	Modifier polymer	Additive	Binder composition	DSR pass/fail temperature ^a (°C)		PG grade
				High ^b	Low ^c	
HMA	None	None	AP (base asphalt)	68,2	-15	64-22
	SBS: S1 (L-401), S2 (L-501), S3 (L-512) or S4 (K 1192)	None	AP + 4,5% SBS	80,7	-13	76-22
WMA	None	P _{ew}	AP + 1,7% P _{ew}	66,7	-14	64-22
		L _{cp}	AP + 1,5% L _{cp}	66,4	-14	64-22
		E _{vt}	AP + 0,5% E _{vt}	69,7	-14	64-22
	SBS: S1 (L-401), S2 (L-501), S3 (L-512) or S4 (K 1192)	P _{ew}	AP + 4,5% SBS + 1,7% P _{ew}	81,1	-15	76-22
		L _{cp}	AP + 4,5% SBS + 1,5% L _{cp}	78,4	-16	76-22
		E _{vt}	AP + 4,5% SBS + 0,5% E _{vt}	79,7	-14	76-22

(a) Represent the highest temperature for the binder to pass the minimum stiffness ($G^*/\sin \delta$), and the lowest failure temperature in the stiffness limit in DSR test; (b) Represent the lowest value within each binder group; (c) Represent the highest value within each binder group.

The mix design was performed using the same aggregate (13 mm dimension) for all mixtures. The optimum asphalt content (OAC ranging from 5,3 % to 5,6 %) of HMA was first determined by mix designed and then the OAC was used for WMA with a minor modification. Bituminous mixtures were produced at different STA temperatures and times: 160 °C and 1h for HMA-normal; 175 °C and 1h for HMA-PMB (with SBS); 125 °C, 135 °C or 145 °C and 2h for WMA (normal/unmodified or polymer modified binders).

Wheel-tracking tests (WTT) were performed using a steel wheel applying a pressure of 689,4kPa. WTT were performed for 2 520 passes at the speed of 42 pass/min for 1 hour at 60 °C (Figure 5-73, Table 5-56).

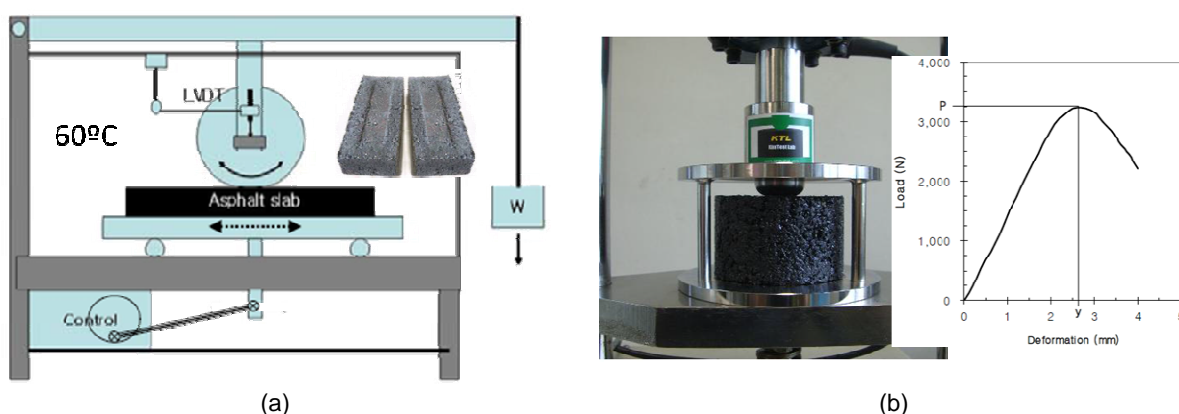


Figure 5-73: High-temperature performance-related tests settings: (a) Wheel-tracking test; (b) S_D test

The strength against deformation or deformation strength (S_D) at a high service temperature (60 °C) has showed a high correlation with WT rut depth; the higher values of S_D representing a stronger rut resistance of the mixture. Simple compression tests were performed applying a static load on the top of specimen at 30 mm/min through a round-

edged loading head. The 100 mm-diameter specimen was submerged in 60 °C water for 30 minutes before placing in the test holder (Figure 5-73, Table 5-56).

Table 5-56: WT rut depth and S_D of unmodified or SBS-modified HMA and WMA mixes

Mixture type	Modifier polymer	Additive	WT rut depth (mm)					S_D (MPa)				
			125°C	135°C	145°C	160°C	175°C	125°C	135°C	145°C	160°C	175°C
HMA	None	None	9,21	7,76	7,49	4,97	-	2,95	3,39	3,28	3,73	-
HMA	SBS: S1, S2, S3 or S4	None	-	-	-	-	3,27	-	-	-	-	4,863
WMA	None	P_{ew}	7,82	5,91	4,96	-	-	3,01	3,67	3,82	-	-
		L_{cp}	8,74	6,01	5,72	-	-	2,95	3,43	3,54	-	-
		E_{vt}	7,62	6,64	6,47	-	-	3,26	3,61	3,48	-	-
		Mean	8,06	6,19	5,72	-	-	3,07	3,57	3,61	-	-
WMA	SBS: S1, S2, S3 or S4	P_{ew}	5,12	4,44	3,32	-	-					
		L_{cp}	5,20	3,88	3,59	-	-					
		E_{vt}	4,94	3,46	3,69	-	-					
		Mean	5,08	3,92	3,53	-	-	4,058	4,421	4,485	-	-

5.4 Binder ageing effect on permanent deformation

In some analysed papers (e.g. Paper 234 - Hrdlicka *et al.*, 2007), the ageing effect on test results used for interpretation of permanent resistance of bituminous mixtures was evaluated. The synthesis will be included in deliverable report D2.

5.5 Overall uncertainty of correlations

Currently, there is a number of tests for evaluation of permanent deformation behaviour of bituminous mixtures (see section **Chyba! Nenalezen zdroj odkazů.**). Therefore, precision of available tests is needed. Some papers identified during this study contain scattering data for the results given (e.g. Paper 230 - Alvarez *et al.*, 2008 - where a relatively high coefficient of variation was obtained for HWTT results). Besides, some papers where uncertainty of correlations is addressed were identified as well. Some examples of these are: Paper 042 - Robertus *et al.*, 2012 - where a correlation between wheel tracking rut rate and J_{nr} is evaluated; Paper 047 - Gungor & Sağlik, 2012 - where correlations between deformation and ZSV and $G^*/\sin\delta$ are assessed; Paper 067 - Guericke & Schlame, 2008 - where the binder softening point is correlated with the correspondent asphalt rut depth (HWT).

In deliverable D2, the available precision data resulting from test repetitions and for correlations between different tests/properties will be used both for evaluating repeatability precision parameters and to recommend possible correlations.

5.6 References for permanent deformation

Zhang, J.; Alvarez, A.E.; Lee, S.I.; Torres, A.; Walubita, L.F. (2013). Comparison of flow number, dynamic modulus, and repeated load tests for evaluation of HMA permanent deformation, *Construction and Building Materials* 44, 391–398.

Chowdhury, A.; Button, J. (2002). Evaluation of superpave shear test protocols, Report No.FHWA/TX-02/1819-1, 112p.

Poulikakos, L.; Takahashi, S.; Partl, M.N. (2007). Coaxial Shear Test and Wheel Tracking Tests for Determining Porous Asphalt Mechanical Properties, *Road Materials and Pavement Design*, 8:3, 579-594.

Reported Papers:

- Paper 023 **Dueñas, A.P.; Lepe, A.P.; Martinez, E.M.; Ibañez, V.C. (2012).** Relationships between zero shear viscosity, low shear viscosity and MSCRT tests and EN 12697-22 rutting test. *E&E2012*.
- Paper 026 **Eckmann, B.; Mazé, M.; Largeaud, S.; Dumont, S.F. (2012).** The contribution of cross-linked polymer modified binders to asphalt performance. *E&E2012*.
- Paper 028 **Hase, M.; Oelkers, C.; Schindler, K. (2012).** Influence of differences in quality polymer modified bituminous binder same variety on the mechanical behaviour of asphalt, Part 1: Deformation behaviour under heat. *E&E2012*.
- Paper 035 **Dressen, S.; Gallet, T. (2012).** MSCRT: Performance related test method for rutting prediction of asphalt mixtures from binder rheological characteristics. *E&E2012*.
- Paper 042 **Robertus, C.; van Rooijen, R.; Thimm, L. (2012).** A comparison of binder tests that relate to asphalt mixture deformation. *E&E2012*.
- Paper 043 **Morea, F. (2012).** Performance of asphalt mixtures at different temperatures and load, their relation with the asphalt low shear viscosity (LSV). *E&E2012*.
- Paper 047 **Gungor, A.G.; Sağlik, A. (2012).** Evaluation of rutting performance of neat and modified binders using zero shear viscosity. *E&E2012*.
- Paper 061 **Beckedahl, H.J.; Sivapatham, P.; Neutag, L. (2008).** Impacts of the compaction degree of asphalt mixes on the asphalt pavement performance. *E&E2008*.
- Paper 067 **Guericke, R.; Schlame, K. (2008).** A new "Softening Point" - Based on asphalt pavement performance figures. *E&E2008*.
- Paper 071 **Ballié, M.; Chailleux, E.; Dumas, P.; Eckmann, B.; Leroux, C.; Lombardi, B.; Planche, J.-P.; Such, C.; Vaniscote, J.-C. (2008).** Characteristics of bituminous binders and their consequences on the mechanical performance of asphalts. *E&E2008*.
- Paper 124 **Zeleeuw, H.; Paugh, C.; Corrigan, M.R. (2011).** Warm-mix asphalt laboratory permanent deformation performance in state of Pennsylvania: Case study. *TRB2011*.
- Paper 135 **Mogawer, W.S.; Austerman, A.J.; Bonaquist, R. (2012).** Determining influence of plant type and production parameters on performance of plant-produced RAP mixtures. *TRB2012*.
- Paper 153 **Willis, J.R.; Taylor, A.J.; Tran, N. (2012).** Laboratory evaluation of high polymer plant-produced mixtures. *TRB2012*.
- Paper 171 **Mogawer, W.S.; Fini, E.H.; Austerman, A.J.; Booshehrian, A.; Zada, B. (2012).** Performance characteristics of high rap bio-modified asphalt mixtures. *TRB2012*.
- Paper 185 **d'Angelo, J, R Kluttz, R Dongré, K Stephens and L Zanzotto (2007).** Revision of the Superpave high temperature binder specification: The multiple stress creep recovery test. *AAPT2007*.
- Paper 191 **Masad, E, C-W Huang, J d'Angelo and D Little (2009).** Characterization of asphalt binder resistance to permanent deformation based on nonlinear visco-elastic analysis of multiple stress creep recovery (MSCR) test. *AAPT2009*.

- Paper 214 **Centeno, M.; Sandoval, I.; Cremades, I.; Alarcón, J. (2008).** Assessing rutting susceptibility of five different modified asphalts in bituminous mixtures using rheology and wheel tracking test. *TRB2008*.
- Paper 230 **Alvarez, A.E.; Martin, A.E.; Estakhri, C.; Izzo, R. (2008).** Evaluation of Durability Tools for Porous Friction Courses. *TRA2008*.
- Paper 234 **Hrdlicka, G M.; Tandon, V. (2007).** Estimation of hot mix asphalt concrete rutting potential from repeated creep binder tests. *TRB2007*.
- Paper 235 **Azari, H; Mohseni, A.; Gibson, N. (2008).** Verification of rutting predictions from mechanistic empirical pavement design guide using accelerated loading facility data. *TRB2008*.
- Paper 259 **Kim, Y.; Lee, M.; Lee, J.; Cho, D.; Kwon, S.; Oliveira, J. (2013).** Evaluation of warm-recycled asphalt mixtures containing polyethylene wax-based WMA additive. *14th REAAA Conference 2013*.
- Paper 261 **Kedoudja, S., Samia, S.; Smail, H. (2013).** Influence of the modification process of the bituminous concrete by the NBR on the mechanical characteristics. *REAAA2013*.
- Paper 280 **Buss, A F, Y Kuang, R C Williams, J Bausano, A Cascione and S A Schram (2014).** Influence of warm-mix asphalt additive and dosage rate on construction and performance of bituminous pavements. *TRB2014*.
- Paper 292 **Lacroix, A.; Kim, Y.R. (2014).** Performance Predictions of Rutting for the NCAT Test Track. *TRB2014*.
- Paper 308 **Tan, Y.; L Shan, L.; Li, X. (2014).** A Unified evaluation index for high- and low-temperature performance of asphalt binder. *TRB2014*.
- Paper 314 **Willis, J.R.; Rosenmayer, T.; Carlson, D. (2014).** Effect of ground tire rubber on open-graded mixture performance. *TRB2014*.
- Paper 319 **Wu, S.; Zhang, K.; Wen, H.; DeVol, J.; Kelsey, K. (2014).** Performance evaluation of hot-mix asphalt containing recycled asphalt shingles in Washington State. *TRB2014*.
- Paper 329 **Kim, S.; Lee, S.-J.; Youn, Y.; Kim, K.-W. (2014).** Evaluation of optimum short-term aging temperature for SBS-modified warm-mix asphalt mixtures. *TRB2014*.
- Paper 330 **Bower, N; Wen, H.; Wu, S.; Willoughby, K.; Weston, J.; DeVol, J. (2014).** Evaluation of the performance of warm mix asphalt in Washington state. *TRB2014*.
- Paper 425 **Dreessen, S.; Pascal, J. P. (2009).** Seeking for a relevant binder test method for rutting prediction. *ENVIROAD2009*.
- Paper 428 **Beckedahl, H.J.; Sivapatham, P.; Janssen, S. (2009).** Heavy loaded asphalt bus lane test sections in the city of Wuppertal - comparison of in situ and lab-test rutting. *ENVIROAD2009*.
- Paper 455 **Romagosa, E E. R Maldonado, D Fee, R Dongré and G Reinke (2010).** Polyphosphoric acid binder modification. *Asphalt Paving Technology 2010*.
- Paper 456 **Bennert, T, and J-V Martin (2010).** Polyphosphoric acid in combination with styrene-butadiene-styrene block copolymer – Laboratory mixture evaluation. *Asphalt Paving Technology 2010*.

- Paper 476 **Wagner, M, M P Wistuba and R Blab (2008).** Low viscous asphalt mixtures – A critical review of FT paraffin modified mixture properties using performance-based test methods. *TRA2008*.
- Paper 500 **de Visscher, J, and A Vanelstraete (2009).** Equiviscous temperature based on low shear viscosity: Evaluation as binder indicator for rutting and critical discussion of the test procedure. *ATCBM2009*.
- Paper 502 **Dreessen, S, J P Planche and V Gardel (2009).** A new performance related test method for rutting prediction: MSCRT. *ATCBM2009*.
- Paper 505 **Tusar, M, M R Turk, W Bankowski, L Wiman and B Kalman (2009).** Evaluation of modified bitumen, high modulus asphalt concrete and steel mesh as materials for road upgrading. *ATCBM2009*.
- Paper 510 **Hase, M (2011).** Bindemittel und die Gebrauchseigenschaften von Asphalt. *Asphaltstraßentagung 2011*.
- Paper 511 **Mollenhauer, K, V Mouillet, N Piérard, T Gabet, M Tušar and A Vanelstraete (2011) & De Visscher, J.; Mollenhauer, K.; Raaberg, J.; Khan, R. (2012).** Chemical and physical compatibility of new and aged binders from RA % Mix design and performance of asphalt with RA. *Re-Road Deliverables D2.3 and D2.4, 2011 & 2012*.
- Paper 513 **Šušteršič, E; M Tusar, A Zupanciv (2013).** Asphalt concrete modification with waste PMMA/ATH. *Materials and Structures 2013*.
- Paper 517 **Laukkanen, O-V, H Soenen, T Pellinen, S Heyrman and G Lemoine (2014).** Creep-recovery behavior of bituminous binders and its relation to asphalt mixture rutting. *Materials and Structures 2014*.
- Paper 520 **Zaumanis, Mallick and Frank (2014).** Evaluation of different recycling agents for restoring aged asphalt binder and performance of 100 % recycled asphalt. *Materials and Structures 2014*.
- Paper 533 **Renken, P (2012).** Walzasphalte mit viskositätsabsenkenden Additiven – Entwicklung und Optimierung der Eignungs- und Kontrollprüfungsverfahren und Bestimmung der Einflüsse auf die performance- orientierten Asphalteigenschaften. DAV/DAI, AiF-Forschungsvorhaben Nr. 15589 N, http://www.asphalt.de/site/startseite/literatur/infomaterial_download/forschungsberichte/
- Paper 559 **Reyes Lizcano, F, C Lizarazo, A Figueroa, M Candia, G Flintsch and S W Katicha (2009).** Dynamic characterization of hot-mix asphalt mixtures using modified and conventional asphalts in Colombia. *TRB2009*.
- Paper 563 **Tabatabaee, N, and H A Tabatabaee (2010).** Multiple stress creep and recovery and time sweep fatigue tests: Crumb rubber modified binder and mixture performance. *TRB2010*.

6 Stiffness

6.1 Asphalt test methods for stiffness

The stiffness of asphalt is a structural property that can be used in the design of pavements but which varies with temperature and frequency, as with many asphalt properties. The relevant European asphalt test is EN 12697-26:2012, Stiffness, containing several options (two-, three and four-point bending, indirect tension, direct tension-compression and direct tension) that give mutually consistent resultants. The scope states that the test method is used to rank asphalt mixtures on the basis of stiffness, as a guide to relative performance in the pavement, to obtain data for estimating the structural behaviour in the road and to judge test data according to specifications for asphalt.

6.2 BitVal findings for stiffness

The BitVal project identified and reviewed six binder tests that were considered as having a potential relationship with asphalt mixture stiffness. Of these tests:

1. The BBR test can be discounted at that time because there were only two papers with diametrically opposing conclusions with regard to the ability of that test to reflect potential asphalt stiffness, if only because the testing was carried out under different conditions. However, because this divergence neither proved nor disproved any relationship, further work could make it relevant.
2. The DSR is covered by many papers which, in general, supported there being a relationship between the binder stiffness and asphalt stiffness. The relationship is particularly strong when using the same temperature and frequency conditions for both the binder and the mixture. However, the relationship is also dependent on the aggregate skeleton of the mixture.
3. The data on the Fraass test was limited to data from a single paper and, therefore, insufficient to draw conclusions at that time. However, the Fraass brittle temperature would not be expected theoretically to be related to mixture stiffness.
4. Penetration was found to correlate well with mixture stiffness, especially at the same temperature and loading time, although generally not as well as the DSR binder stiffness which is able to evaluate binder stiffness over a large range of temperatures and frequencies. The relationship was less good for PMBs than for paving grade bitumen. Nevertheless, it had potential for initial assessments because the test is simpler to perform than the DSR.
5. The penetration index generally had a marginally worse correlation with the mixture stiffness than the penetration whilst being a more complicated measure, so there appeared no justification to use it as the binder measure for asphalt stiffness.
6. The R&B softening point generally has a significantly worse correlation with the mixture stiffness than the penetration, so there appears no justification to use it as the binder measure for asphalt stiffness.

Therefore, the best options for identifying the potential binder contribution to asphalt stiffness were DSR binder stiffness and/or penetration, with the former being able to evaluate stiffness for many temperature/frequency combinations that are encountered in practise but is also more complex.

There were sufficient data from the papers identified to validate the relationship between DSR binder stiffness and the mixture stiffness, particularly when using the same temperature and frequency conditions. However, the durability implications and any relationship to pavement performance are effectively missing. Furthermore, several of the papers indicated that DSR binder stiffness after RTFOT was less well correlated with mixture stiffness than the results from unaged binder. Therefore, there is justification to undertake further research

in order to understand the measures required to identify long-term changes in mixture stiffness from binder properties, although such research would take some time to reach any conclusion.

There were sufficient data from the papers to support the use of the penetration test as a simple surrogate for the potential for mixture stiffness, at least for paving grade bitumens. Because it is a pragmatic test, the limitations in the relationship for durability and field performance would have to be accepted. Penetration could also be used as a simple quality control test.

6.3 Relationship found between bitumen properties and asphalt stiffness

6.3.1 General

6.3.1.1 Paper 128 (Zezelew *et al.*, 2012)

Figure 6-2 presents the comparison of laboratory measured and predicted $|E^*|$ using the three models in arithmetic and logarithmic scales. A total of 570 data points were used involving only WMA mixtures tested at four temperatures and six loading frequencies. In order to meet one of the stated objectives, the control HMA mixtures (both plant produced and MATL mix design replication) were not included in the $|E^*|$ prediction analysis. In these figures, over-prediction of $|E^*|$ was observed when the Witczak 1-37A and 1-40D models were utilized. The over-prediction is pronounced with higher modulus values that correspond to the asphalt mixtures tested at high loading frequencies and low test temperatures. In the logarithmic scale, the Hirsch model predicted $|E^*|$ with the highest coefficient of determination ($R^2 = 0,9005$) and the lowest error ($Se/Sy = 0,3154$) followed by the Witczak 1-40D model ($R^2 = 0,8453$ and $Se/Sy = 0,3934$) and the Witczak 1-37A model ($R^2 = 0,8074$ and $Se/Sy = 0,4388$). Better predictions were obtained using the Witczak 1-37A model following the Hirsch model when the arithmetic scale is considered. These findings are consistent with the model developers with high correlation coefficient and low error in logarithmic scale for the Witczak 1-40D and Hirsch models. Comparisons of the predictive models amongst various WMA technologies (i.e. foam, chemical, and organic) are also shown in Figure 6-1.

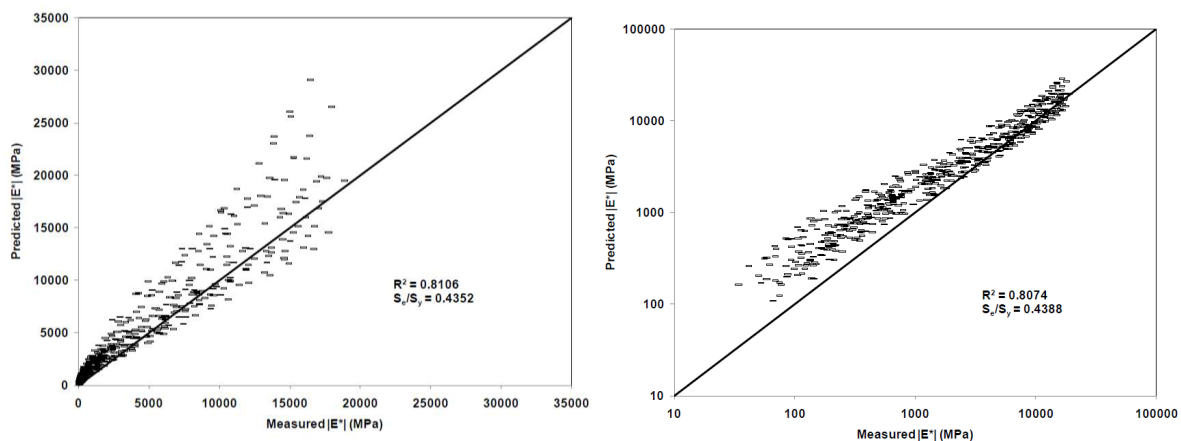


Figure 6-2(a): Comparison of measured and predicted $|E^*|$ by Witczak 1-37A model in arithmetic and logarithmic scales

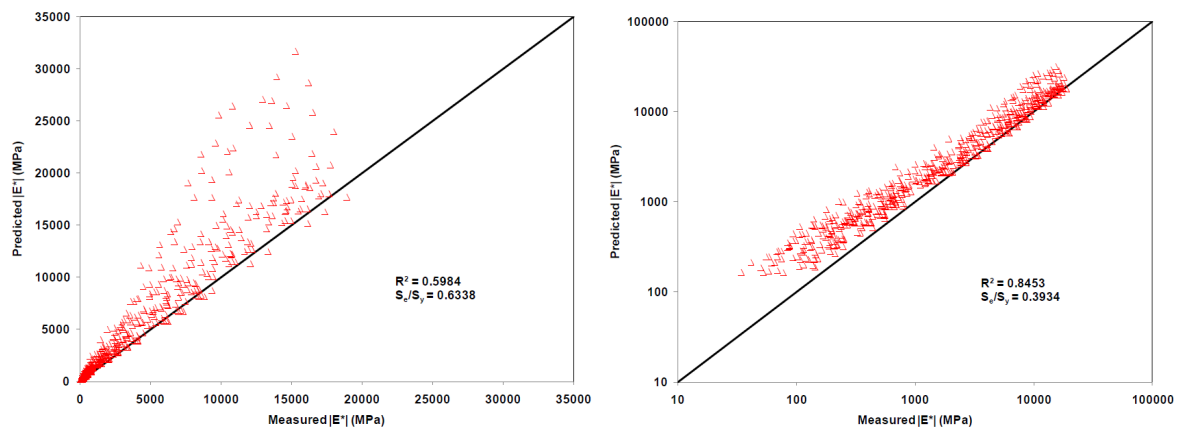


Figure 6-2(b): Comparison of measured and predicted $|E^*|$ by Witzak 1-40D model in arithmetic and logarithmic scales

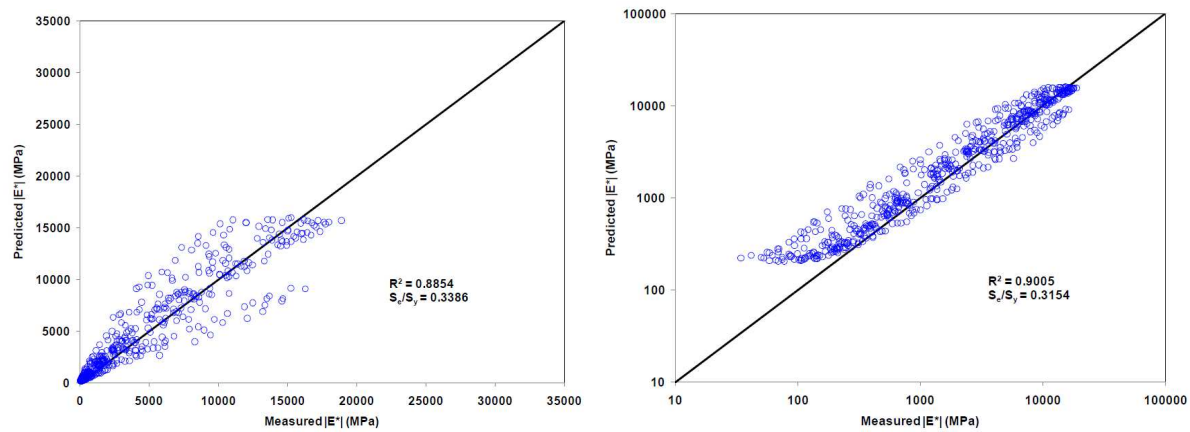


Figure 6-2(c): Comparison of measured and predicted $|E^*|$ by Hirsch model in arithmetic and logarithmic scales

6.3.1.2 Paper 037 (Iwanski and Mazurek, 2012)

Table 6-1: Significance of bitumen properties on asphalt at the compaction temperature of 125 °C with significance level $\alpha = 0,1$

	Resilient modulus of elasticity (MPa)	Air voids content (%)
Penetration index	non significant	significant
Complex modulus (Pa)	significant	non significant
Phase angle (°)	significant	non significant
Low shear viscosity (LSV) (Pa·s)	significant	non significant

The results in Table 6-1 indicate that the visco-elastic properties of the bitumen play a major role on changes in value of the resilient modulus of elasticity at 20 °C. Only for the penetration index did this factor not play a significant role, while others factors had a significant influence whilst the penetration index had a significant effect on the air voids content.

6.3.1.3 Paper 022 (Cope et al., 2007)

Penetration grade bitumen (40/60) was blended with vegetable oil to produce bitumen/oil blends. Normal groundnut cooking oil ranging from 0 % to 10 % by mass was used as vegetable oil mixed with bitumen. As expected, the vegetable oil blended very easily with the bitumen showing noticeable increase in viscosity as the oil content was increased.

Table 6-2: Effect of blending oil with bitumen on penetration, softening point and viscosity

Oil content (%)	Penetration (dmm)	Softening point (°C)	Viscosity (Pa.s) at:			Temperature at 0.2 Pa.s (°C)
			120°C	150°C	180°C	
0	56	50.4	1.074	0.231	0.074	160 *
2	89	46.6	0.844	0.200	0.064	156
4	121	44.3	0.723	0.172	0.060	152
6	155	41.1	0.607	0.151	0.053	149
8	222	37.2	0.504	0.131	0.046	146
10	285	33.7	0.429	0.117	0.044	143

* mixing temperature selected based on BS EN 12697-35.

DSR tests were performed under the following test conditions: controlled strain mode of loading, test temperatures ranging from 0 °C to 80 °C, with 0,01 Hz to 10 Hz test frequency, parallel plate geometries (8mm diameter with 2mm gap for low temperatures, and 25mm diameter with 1mm gap for high temperatures), strain amplitude kept within the LVE response (0,5 % to 10 %) depending on G* values. The rheological properties of the blends were measured in terms of complex shear modulus G*, and phase angle δ. The DSR rheological data for all the blends are presented in the form of master curves of at a reference temperature of 25 °C.

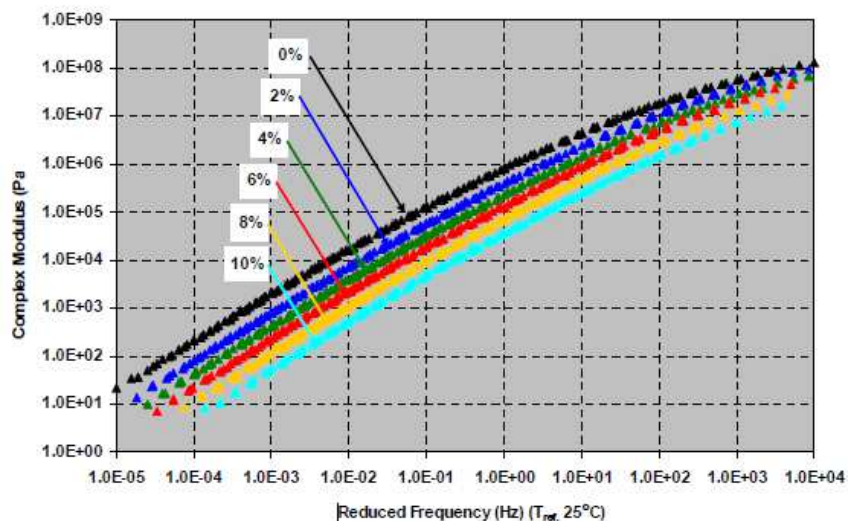


Figure 6-2: Complex modulus G* master curves at 25 °C reference temperature for all bitumen/oil blends investigated

As expected, the G* master curves in Figure 6-2 for all binder blends approach a similar, common limiting stiffness value (glassy complex modulus) at high frequencies and a viscous 45° asymptote at low frequencies. The shape of the master curves does not differ amongst the blends. The G* master curves show a consistent decrease in stiffness at any one loading frequency (or temperature) as the oil content is increased. Using time-temperature equivalency this behaviour can be considered to be analogous to moving from a lower to a higher penetration grade binder. The phase angle δ is generally considered to be more sensitive to the chemical structure and morphology of the binder and, therefore, more sensitive to the degree and type of modification of the bitumen than G*. In terms of the

viscoelastic response, the phase angle master curves show no clear distinction between the response of the various binders other than that related to relative binder stiffness.

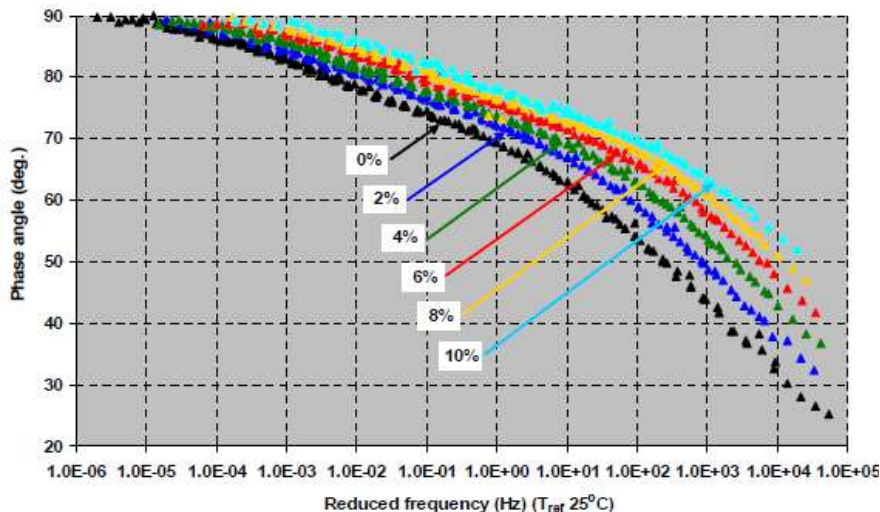


Figure 6-2: Phase angle δ master curves at 25 °C reference temperature for all the bitumen/oil blends investigated

The bitumen/oil blends were then used to manufacture 4 conventional Dense Bitumen Macadam specimens 14 with 4,9 % binder content. Two of the specimens were compacted immediately, whilst the other two were kept in a loose state in an oven set at the mixing temperature for a period of 4 hours prior to compaction (to simulate short term mix ageing).

Indirect tensile stiffness moduli at 20°C were then measured on the initial samples and the procedure repeated following 20°C water immersion for periods of two and four weeks. A very consistent step wise reduction in stiffness is recorded as the oil content in the mix is increased which is exactly what would be expected from gradually using softer binder grades. More importantly, the figure 5 also shows that there was no significant trend in the change in stiffness between the aged and unaged specimens and hence blending even large proportions of oil with the bitumen does not adversely affect the ageing properties of the mix.

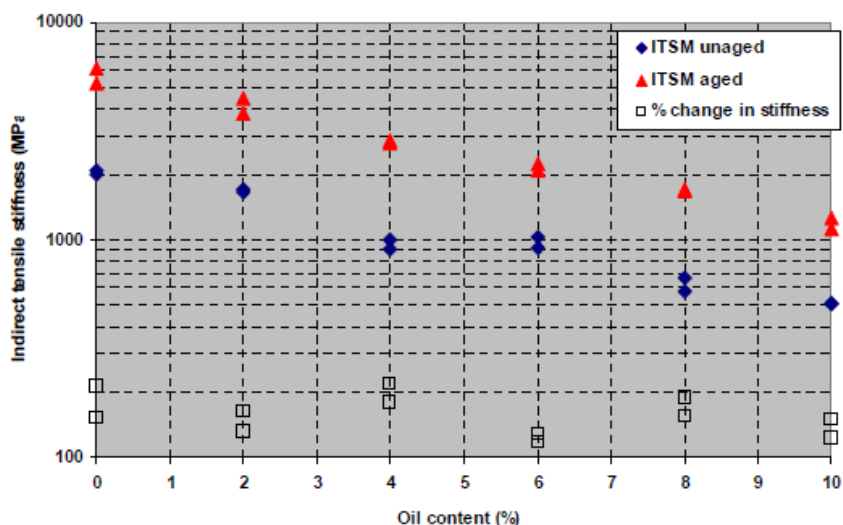


Figure 6-2: ITSM values of asphalt mixes at different oil contents

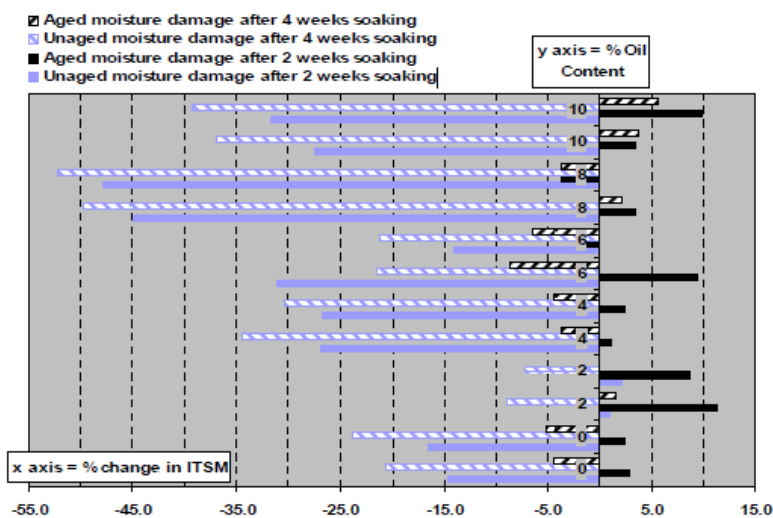


Figure 6-2: Comparison of initial ITSM values against retained values after water immersion for periods of 2 and 4 weeks

Significant improvements that short term oven aging imparts on the retained stiffness values of all mixes should be noted for all binder options. This seems to imply that the large reductions following moisture conditioning in the unaged specimens caused by the introduction of the oil. Because of the relatively poor precision of modulus determinations on asphalt mixtures, modulus predictions using the Hirsch model might be almost as reliable as independent modulus measurements made on the same mixture (Figure 6-2).

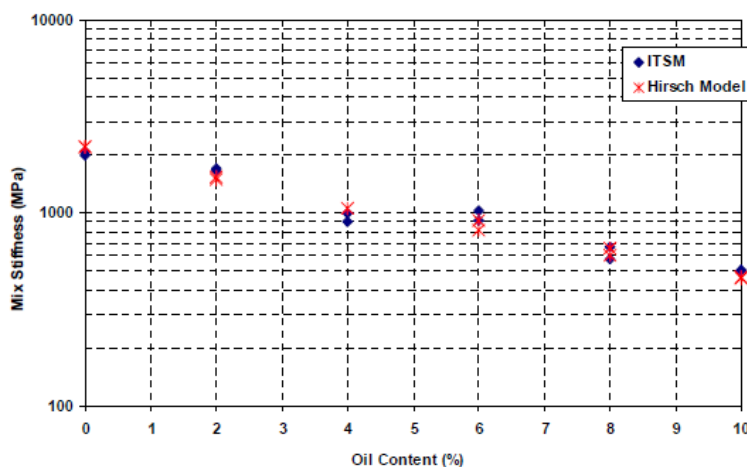


Figure 6-2: Comparison of measured ITSM values v.s. the mix stiffness values predicted using the Hirsch model

6.3.1.4 Paper 034 (Dreessen et al., 2012)

A comparative experimental durability study on the highway A9 near Sion was conducted between 1988 and 2002. An intense campaign of monitoring the surface conditions and laboratory tests on materials was realized on 16 comparative sections of 300 m made with commercial PMBs. Samples were collected at various times during the life time of the highway. Comparison sections with SBS (N°11 and N°1 1a) and with bitumen 80/100 (section N°15), with same pen grade as SBS are described. AC 16 is used for the surface layer.

Laboratory analysis was carried out on bitumen and mix taken from wearing course samples after 2, 8, 14 and 19 years of service. The mix was heated in a microwave oven at a

temperature of 80 °C. Binder was then recovered using toluene according to the standard procedure. Binders were characterised using standard bitumen testing, BBR and elastic recovery test. In order to characterise the chemical composition of binders, infra-red spectroscopy (FTIR - Fourier-Transform Infra Red) and Size Exclusion Chromatography (GPC - Gel Permeation Chromatography) were used. Figure 6-2 presents the conventional characterization results for the extracted straight-run bitumen and PMB, showing the evolution of penetration, softening point and Fraass breaking point values during service life.

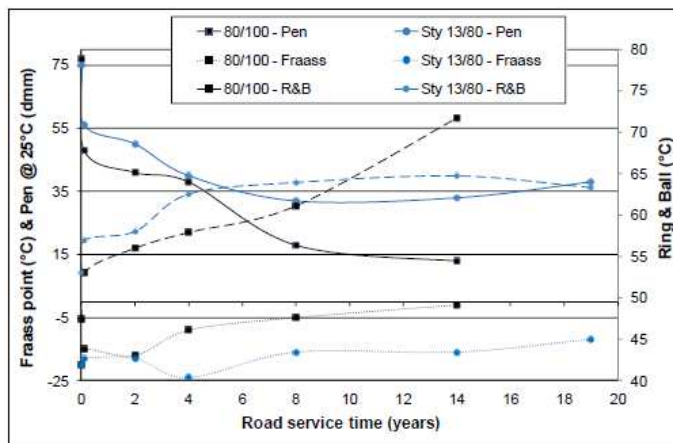


Figure 6-2: Evolution of penetration, R&B and Fraass during road service time

Figure 6-2 confirms the strong binder aging effect during the mixing, transportation and paving steps. This is evidenced by a strong initial penetration drop (20 to 30 dmm), and a softening point increase (around 8 °C). The conventional binder curve demonstrates a continuous rise in softening point and a constant decrease in penetration during road service. Contrarily, the PMB evolution stabilizes after 8 service years, as both penetration and ring and ball plateau. Aging effect seems much lower for the PMB than for the straight-run bitumen. The pure binder Fraass brittle point loses about 14 °C during road life after 14 years, whereas the crosslinked PMB lost much less (6 °C) during an even longer time period of 19 years. The same tendency is found for BBR results. The increase in the temperature at which the stiffness is 300 MPa is limited to only 4 °C for the PMB, as opposed to 12 °C for the straight-run bitumen. The limiting m-value temperature evolves more than the iso-stiffness for the straight-run bitumen.

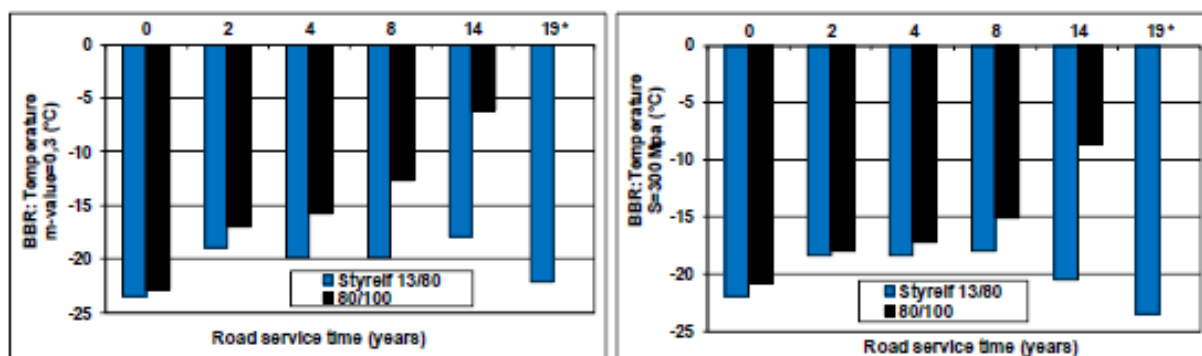


Figure 6-2: Evolution of limiting iso-stiffness and m-value BBR temperature

Some samples taken from the 19 year old surface were sawed along their depth: bitumen from the top 15 mm and from the bottom 25 mm were extracted separately for SL and EL. Standard tests were carried out on top, bottom and wholly recovered binder. Values are compared to the initial binder aged under different process: 0 year, 0 year extracted from the

road, after RTFOT , after 40h in PAV and aged for 19 years in a can in a controlled atmosphere (table 3). Wholly recovered binders after 19 years provided us with information concerning the specific features of binders. Plasticity range remains high in particular as the Fraass point remains low. Elastic recovery is well above the RTFOT reference value. It was noted that there was a moderate hardening of the binder retrieved from samples taken from the surface subjected to traffic.

Table 6-3: PMB (Styrelf 13/80) properties after 19 years extracted from the pavements compared to initial binder aged with different process (NB: 'X'=brittle material, '/' = not tested)

Characterization	0 year (initial)	0 year (extracted)	RTFOT	PAV 40h	19 years (can aged)	Slow Lane			Emergency Lane		
						Who.	Top.	Bot.	Who.	Top.	Bot.
Penetration at 25°C [1/10mm]	75	56	52	27	68	38	24	44	46	26	62
Softening point (R&B) [°C]	53	56,9	57,9	71	56,4	63,3	68,1	61,2	61,2	67,3	57,8
PI Pfeiffer [-]	0,6	0,7	0,7	1,5	1,1	1	0,8	0,9	1	0,9	1,1
Fraass breaking point [°C]	-20	-18	/	/	-15	-12	-10	-16	-18	-12	-17
Plasticity range [°C]	73	75	/	/	71	75	78	77	79	79	74
Elastic recovery at 25°C [%]	82	77,3	78	X	80	69,0	X	73,8	76,0	X	82,5

The average measured value when extracting the entire thickness does not take the heterogeneity of the layer into account. Bitumen from the upper layer is equivalent to PAV 40h for penetration but have a slightly lower softening point. There is no difference with traffic as it is climate which has a greater influence in this area. Bitumen extracted from slow lane aged more than from emergency lane. This may be due to pumping of water by traffic or to a physical chemical ageing process induced by repeated pressure. It should be noted that the binder not subjected to the least constraint (EL bottom) shows similar characteristics to bitumen which was stored for 19 years in a can.

In order to compare the mechanical performances of asphalt mix, fatigue and modules tests were carried out using trapezoidal specimens. For the modules strain values of 40 microstrains at the following frequencies was used: 1, 3, 10, 25, and 40 Hz in a range of temperatures, between -10 °C and 30 °C in stages of 5 °C.

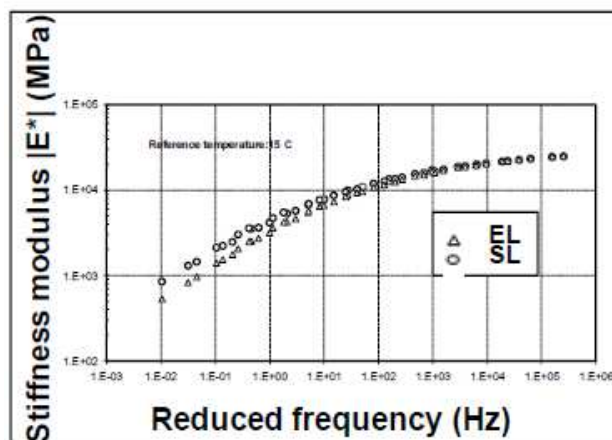


Figure 6-2: Master curve of stiffness modulus -SL (subjected to traffic) and EL after 19 years

6.3.1.5 Paper 049 (Kamal et al., 2010)

Effect of PMBs on rutting was shown by this study focused mainly on elastic characteristics of asphalt concrete. Indirect tensile tests were carried out using Universal Testing Machine (UTM-5P) according to ASTM D4123 and resilient behavior of asphalt concrete mixes A (coarser with optimum bitumen content of 4,2 %) and B (finer with optimum bitumen content of 4,3%) for wearing coarse with straight-run bitumen 60/70 and Elvaloy modified bitumen (PMB) were evaluated over a range of stress levels (100 kPa, 300 kPa and 500 kPa) at 25 °C, 40 °C and 55 °C with standard loading time (0. 1 s followed by 0.9 s rest period).

At low temperature and stress level (25 °C, 100 kPa) no definite trend was observed at high temperature (40 °C & 55 °C) and stress levels (300 kPa & 500 kPa) modified mixes (A & B) showed high resilient modulus. Coarse gradations showed high resilient modulus for conventional and PMB mixes at all temperatures and stress levels. Resilient modulus in case of both bitumen types increases with stress level up to 40 °C, then reduces dramatically.

Table 6-4: Test Results for conventional 60/70 bitumen and PMB

Tests	Conventional 60/70	PMB	Standard AASHTO
Softening Point Test	48 °C	59 °C	T-53
Penetration	62	51	T-49
Ductility (cm)	47	44	T51

Stiffness modulus specimens were tested at test pulse period of 1000 ms, pulse width of 450 ms. A total number of 120 samples (30 samples each for mix A and B with 60/70 and PMB) were prepared.

Table 6-5: Resilient modulus for mix A & B (conventional)

Temperature (°C)	Stress (kPa)	Resilient Modulus (MPa)	
		Conv "A"	Conv "B"
25	100	2880	2790
40	100	2352	1286
55	100	734	684
25	300	4874	4454
40	300	2666	1621
55	300	1050	938
25	500	6738	6186
40	500	3255	1889
55	500	681	557

Table 6-6: Resilient modulus for mix A & B (PMB)

Temperature (°C)	Stress (kPa)	Resilient Modulus (MPa)	
		PMB "A"	PMB "B"
25	100	2886	2340
40	100	2259	1710
55	100	1108	1059
25	300	5498	5385
40	300	2891	1814
55	300	1280	1156
25	500	5923	5456
40	500	3923	2422
55	500	926	754

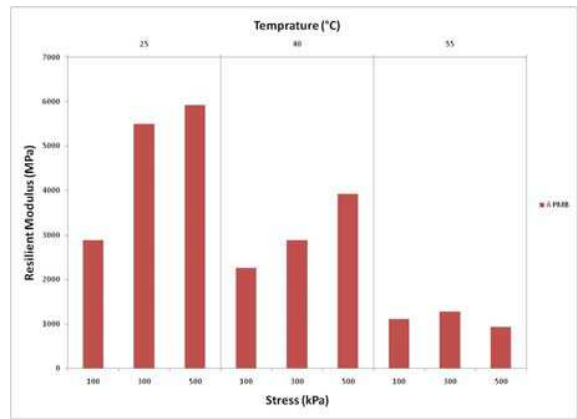
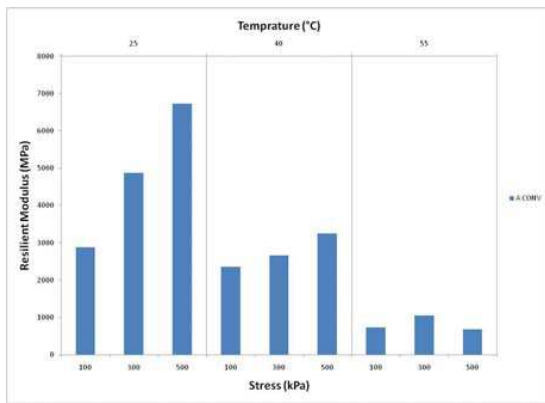


Figure 6-2: Resilient modulus vs stress @ 25, 40 & 55 °C; class A (left – 60/70; right – PMB)

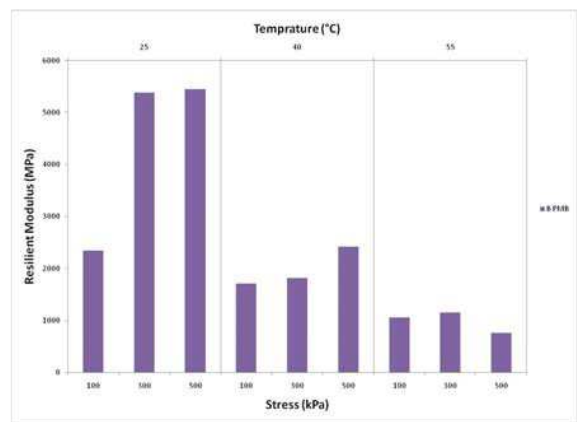
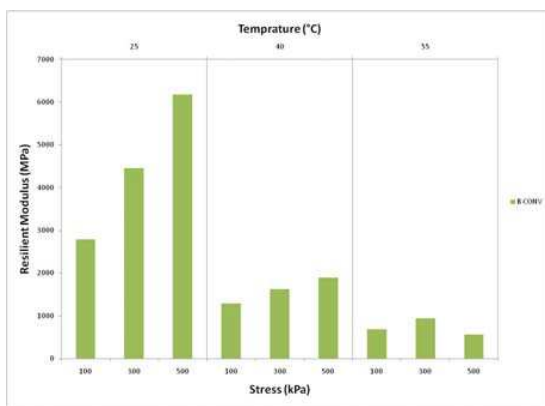


Figure 6-2: Resilient modulus vs stress @ 25, 40 & 55 °C; class B (left – 60/70; right – PMB)

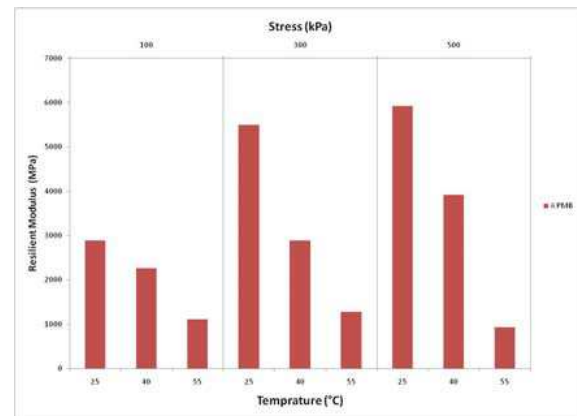
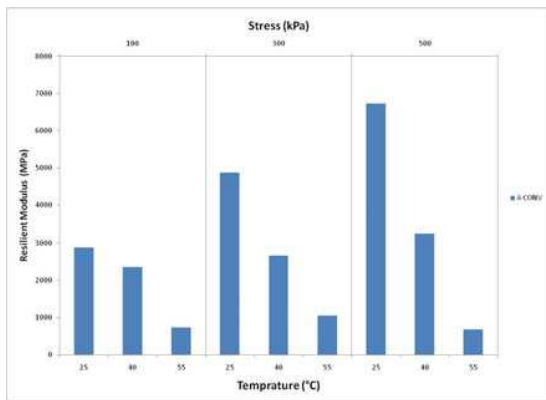


Figure 6-2: Resilient modulus vs temperature @ 100, 300 & 500 kPa; class A (left – 60/70; right – PMB)

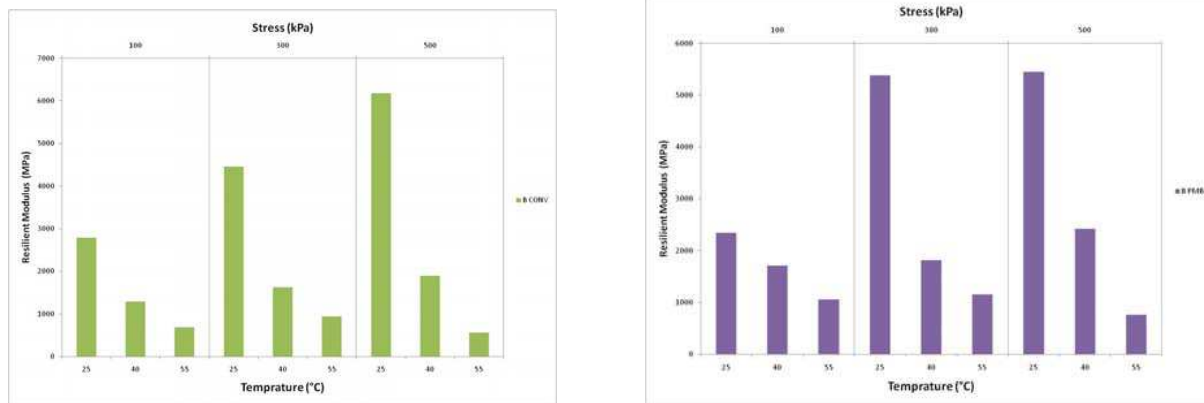


Figure 6-2: Resilient modulus vs temperature @ 100, 300 & 500 kPa; class B (left – 60/70; right – PMB)

At low temperatures and short loading durations, they exhibit elastic behavior and the stiffness of a mixture depends only on the binder properties and Voids in Mineral Aggregates (VMA) of the mix. The stiffness in this region may be termed as elastic stiffness. At higher temperatures or longer loading times, the stiffness is highly influenced by other parameters associated with the mineral aggregate. This may be referred to as “viscous stiffness” and depends on the type, grading, shape and texture of aggregate, the confining conditions and the method of compaction in addition to the bitumen stiffness and the VMA.

It was further confirmed that stiffness decreases with the increase in temperature. It can be observed from the figures that M_r increases with increase in stress at the same temperature whereas it decreases with an increase in temperature. **The mix stiffness is dependent largely on binder stiffness.** It can be also stated that coarse mix (A) has less area of coverage for bitumen and offers higher stiffness than mix B (fine graded mix) and the obvious reason is due to reinforcement provided by bitumen mortar between the aggregate particles. This is valid for straight-run bitumen as well as for PMB. VMA also affects the stiffness characteristics of asphalt mixtures (coarser mix has higher VMA percentage than mix B).

It may be noted that the bitumen modification has a significant role at higher temperatures and stress levels. It can also be observed that at lower temperature and stress levels i.e. at 25°C and 100 kPa, elastomeric properties of PMB mixes are more dominant by bitumen modification. In general it can be argued that mixes with bitumen modification would exhibit better elastic properties when subjected to load and temperature conditions.

Low temperature and stress level regimes:

- At low stress levels (100 kPa) the interlocking mechanism was not observed to be initiated which resists further deformation over the temperature regimes tested. Binder fines mortar exhibited a more dominant behavior.
- At low temperatures and stress levels (25°C & 100 kPa) no definite trend was observed where as in mixes with PMB exhibit lower resilient modulus than the mixes with conventional bitumen. This behavior may be attributed towards modification of bitumen which enhances the elastomeric properties of mixes with PMB.

High temperature and stress level regimes:

At 40 °C, and stress levels 300 and 500 kPa, modified mixes showed higher modulus.

At high temperatures and stress levels (55 °C and 5 00 kPa), a shift in the behavior of all mixes was noted. The resilient modulus of the mixes based on the test results at 25 °C and 40 °C increases with increase in stress levels, whereas the same was observed to decrease at higher stress and temperature levels i.e. 55 °C and 500 kPa. This behavior is expected since asphalt mix is a viscoelastic material thereby expressing that it acts as a viscous fluid at higher temperatures. This shift in the behavior may imply that a threshold temperature barrier exists somewhere between 40 °C and 55 °C where the resilient modulus starts to decrease with an increase in stress level.

6.3.1.6 Paper 070 (Gauthier et al., 2008)

Experimental study on stiffness and fatigue evaluation involving six asphalts with the same aggregate size distribution was performed. Stiffness evaluation was done using the bending test on trapezoidal cantilever beam with a temperature and frequency sweep. Three different bitumen were considered (B1 = 35/50, B2 = semi-blown special bitumen and B3 = cross linked SB modified bitumen). The studied asphalt mix was a 0/6 mm dense asphalt concrete.

Table 6-7: Material characteristics

Asphalt reference	Bitumen characteristics			Asphalt characteristics	
	Bitumen nature	Penetration (dmm)	Ring&Ball softening point (°C)	Bitumen content (% of agg. weight)	Void content (%)
F10	Bitumen 1	38	53	6,85	3,3
F11				5,35	6,5
F20	Bitumen 2	35	62,8	6,35	3,4
F21				5,35	6,8
F30	Bitumen 3	36	63,4	6,85	3,5
F31				5,35	5,7

The complex modulus tests have been performed in bending mode in the small strain linear regime (strain < 50 µm/m). Trapezoidal cantilever specimens (height 250 mm, thickness 25 mm, large based 56 mm and small base 25 mm) have been tested according to the European standard. Dynamic modulus is investigated for 6 frequencies (1, 3, 10, 25 30 40 Hz) and 8 temperatures (-10, 0, 10, 15, 20, 30, 40, 50 °C) on 4 specimens of each one mixture. Dynamic modulus data are presented (figure 3) in both Cole-Cole and Black plots.

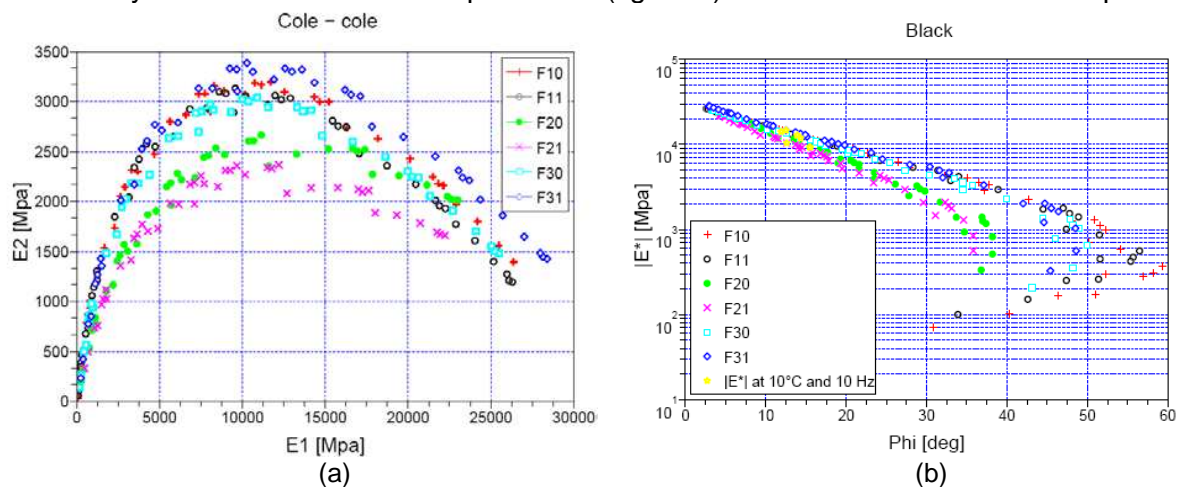


Figure 6-2: Complex modulus data (a) Cole-Cole diagram (b) Black diagram

Materials F10, F11, F30 and F31 are very similar in the considered range of temperature. Materials F20 and F21 appear less stiff due to the change of bitumen. The Black diagram

exhibits a lower thermal dependency on these two mixes. In order to predict the thermal increase coupled to the thermal dependency during fatigue tests, a rheological model was fitted on laboratory data (Table 6-8). The viscoelastic behaviour and thermal dependence of the E^* value are described by the Huet and Sayegh model proposed in 1963 and modified by Sayegh for asphalt behavior.

$$E(\omega, \theta) = E_0 + \frac{E_\infty - E_0}{1 + (i \omega \tau(\theta))^{-h} + \delta (i \omega \tau(\theta))^{-k}}$$

Table 6-9: Huet Sayegh model parameters

Material	E0 [MPa]	E∞ [MPa]	Δ	K	h	T _{ref}	C1	C2
F10	31,42	30918	2,37	0,637	2,39	0,27	22,91	148,31
F11	34,97	30353	2,13	0,19	0,61	0,45	23,95	155,78
F20	0,07	50374	2,78	0,10	0,41	7,10-3	24,64	161,66
F21	0,53	51037	2,71	0,08	0,40	9,10-3	21,74	157,26
F30	17,83	30976	0,07	0,58	0,19	3,10-3	26,52	174,84
F31	43,55	31425	2,50	0,21	0,62	0,66	25,13	166,00

In the table differences in terms of E_∞ remains extrapolated values of the model because no experimental data in that range of temperature have been tested as shown in figure 3(a). On figure 3(b) on the y log axis the extrapolation to a phase angle equal to zero indicated qualitatively similar E_∞ values.

Another step of the analysis is to take into account the effect of the self-heating of the specimen during cyclic tests due to the viscoelastic dissipation and the thermal dependency of the material. The thermal correction is based on a numerical estimation of the stiffness decrease due to thermal dissipation. The thermomechanical framework had been implemented in the multi purpose finite element code Cast3M.

6.3.1.7 Paper 071 (Ballié et al., 2008)

More than 160 mechanical physical characteristics of ten binders (pure bitumens, polymer modified and special bitumens) were analyzed. These binders are representative of the current use in the French market. A multidimensional statistical analysis was used for data exploitation. As a guide, in Figure 6-2 we plotted the penetration and R&B softening point of each of the 10 adopted binders. It can be noted that the selected products are well distributed throughout the area occupied by bituminous binders. Just one product has an extreme behaviour (denoted R), and is outside the commonly encountered population.

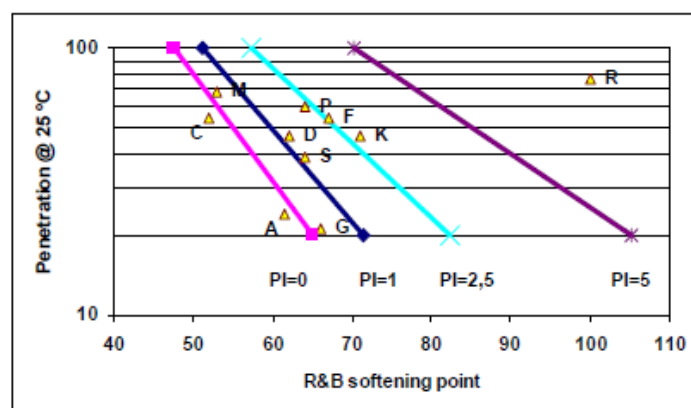


Figure 6-2: Penetration and softening point diagram for different binders

The laboratory tests were conducted on binders before ageing, after RTFOT artificial ageing and after extraction from the asphalts. The used type of asphalt was 0/14 SCAC, tested for fatigue, complex modulus and water resistance.

The multidimensional statistical processing tool used, a principal component analysis determined the redundancies and duplications both in terms of binders (denoted individuals) and characteristics (denoted variables). Single and multiple linear regression was the model adopted for estimating the observed value (in this case the asphalt performance) by linear combination of binder characteristics.

With regard to relations between asphalt performances, there was little or no redundancy. Only the asphalt complex modulus, an intrinsic property of the asphalt, seems to be related to other measured performance. The fatigue resistance (measured by its ϵ_6) and the moduli and phase angles at 15 °C 10 Hz of the asphalts were determined (Figure 6-2).

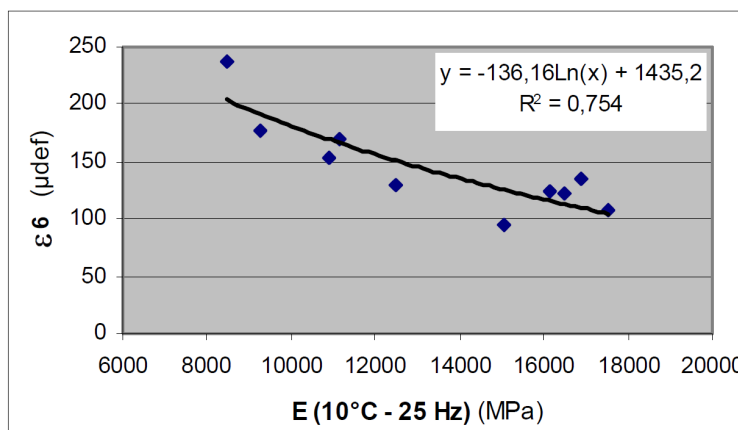


Figure 6-2: Correlation between ϵ_6 and modulus at 15 °C 10Hz

The rutting behaviour of the asphalts cannot be explained solely by examination of the asphalt complex moduli. Both Figure 6-2 and Figure 6-2 present the master curves of the moduli and phase angles of binder A and its asphalt after vertical and horizontal shift.

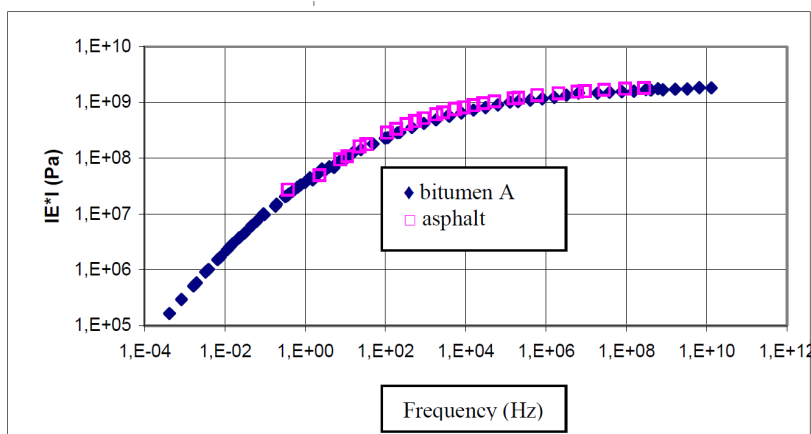


Figure 6-2: Modulus master curves, at 20 °C, of extracted binder A and its asphalt after translations

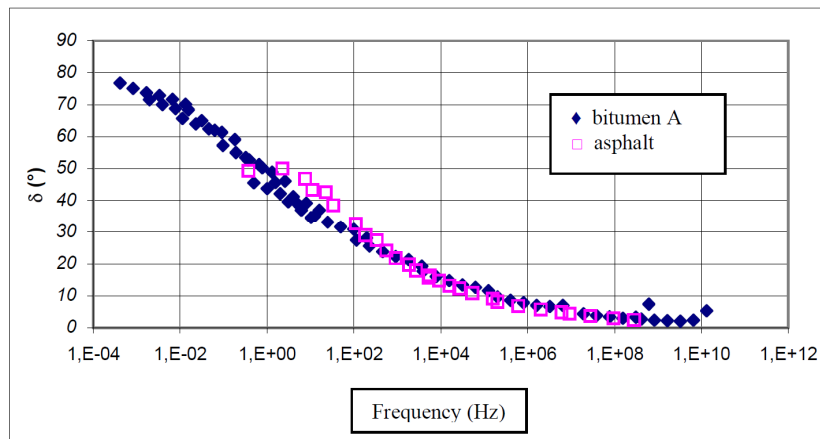
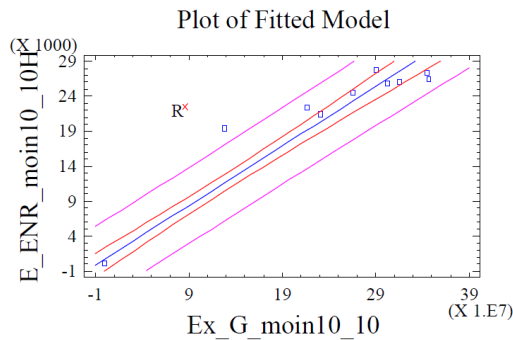


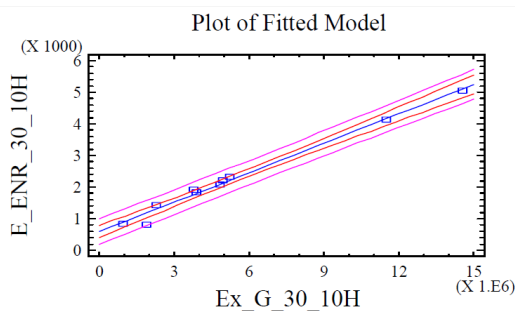
Figure 6-2: Phase angle master curves at 20 °C (ext racted binder A and asphalt after horizontal translation)

It can be noted that there is a correct overlap, and that the **susceptibility difference** between the binder and asphalt is reflected more visibly in the phase angle master curve than on the modulus master curve. For a given asphalt formula, the complex modulus of the asphalt can be deducted directly, to a certain degree. At a given frequency and temperature, multivariate statistical analysis **clearly highlights the correlation between the modulus values of the binder and asphalt**, as illustrated by the figures below for the measured modulus or phase angle points (at -10°C and 10 Hz, 30 °C and 10 Hz, and at 15 °C and 10 Hz).



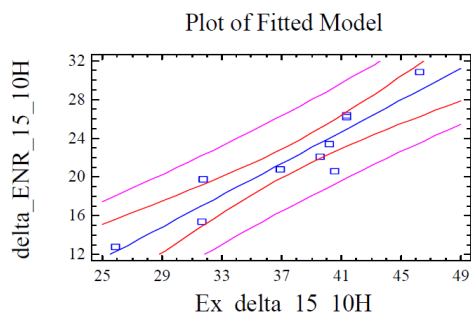
Asphalt Modulus E* vs Binder modulus G* at -10°C 10 Hz

Correlation Coefficient = 0.981536
 R-squared = 96.3412 percent
 Standard Error of Est. = 2509.46



Asphalt Modulus E* vs Binder Modulus G* at 30°C 10 Hz

Correlation Coefficient = 0.993815
 R-squared = 98.7668 percent
 Standard Error of Est. = 158.732



Phase angle of asphalt vs phase angle of binder at 15°C and 10Hz

Correlation Coefficient = 0.932067
 R-squared = 86.8748 percent
 Standard Error of Est. = 2.04726

Figure 6-2: Examples of correlation obtained between the asphalt modulus and binder modulus

Not all these correlations are surprising. In a relatively narrow temperature and frequency area, the asphalt modulus $|E^*_{ENR}|$ can be derived from the binder modulus $|E^*_{bit}|$, either using models (Huet model modified by adding a viscous element), or by relations such the one given by Olard in 2003.

$$\frac{|E^*_{ENR}|}{(E^{\infty}_{ENR} - E^0_{ENR})} = \frac{E^0_{ENR}}{(E^{\infty}_{ENR} - E^0_{ENR})} + b * \frac{|E^*_{bit}|}{E^{\infty}_{bit}}$$

Therefore, asphalt performances are not simply related with binder characteristics. The traditional "simple" binder tests are unable of reproducing the fields of stress and deformation to which asphalts are submitted. Furthermore, these binder tests, especially the "rheological" ones, generally involve only one single type of behaviour at a time, whereas in the asphalt test, the binder is submitted to a variety of stresses (major deformation, minor deformation, tensile - shearing, etc.) **Therefore, it will not be possible to base the framework of future performance specifications solely on tests such as DSR and BBR as currently conducted.**

6.3.1.8 Paper 077 (Azari, 2011)

Effect of laboratory short-term conditioning time on mechanical properties of asphalt mixture was assessed in another study. Recommendations on appropriate laboratory short-term conditioning time for mixture mechanical property testing are provided. The compacted mixtures resulted from the different conditioning schemes were subjected to dynamic modulus and flow number test. For samples conditioned from 0 to 6 hours, at one hour interval, the changes in mechanical properties at every possible pair of conditioning times were statistically tested. The "minimum" allowable short-term conditioning time was determined based on the time of first significant change in a property with respect to the property of an unconditioned mixture. The "maximum" allowable short-term conditioning time was determined based on the time of second significant change in a property with respect to the property of a mixture that has been conditioned for a "minimum" time. The "optimum" conditioning time for a mixture was then determined to be between "minimum" and "maximum" conditioning times. The effect of short-term conditioning on long-term performance of the mixture was used as another tool for determining the "maximum" short-term conditioning time.

The first set of testing was conducted on 39 samples: three replicates of 13 mixtures conditioned at 145 °C at half-hour intervals from zero to six hours. All the samples were subjected to dynamic modulus test at 4 °C; 20 °C and 40 °C (samples denoted "145C-Unaged"). The second set of testing was similar to the first set, with two modifications. It was subjected to the dynamic modulus test at 45°C and to long-term ageing before being tested (sample denoted "145C-Aged"). Two set of testing with 21 samples were conditioned from zero to six hours, on one hour intervals, at 135 °C (samples denoted "135C") and at 145 °C

(samples denoted “145C”). Last set of testing was conducted by a bending beam rheometer (BBR) on small flexure beam samples cut from gyratory compacted cylinders. The mixtures of these samples were conditioned at 135 °C (samples denoted “135C-BBR”).

Sets 1 and 2 were first subjected to dynamic modulus test at multiple frequencies and temperatures at no confinement. The flexural beam samples were prepared and tested according to the new proposed test method for using BBR for mixture flexural creep test teste dat 10°C. For this study, dynamic modulus tests were run at frequencies of 0,5; 1; 2; 5; 10; 20 and 25Hz. A broad spectrum of dynamic modulus values from each of those frequencies and temperatures were used to establish dynamic modulus master curves for the mixtures conditioned for different durations. Analysis of the significance of conditioning time was performed on the test results from the established reference temperature of 20 °C.

The bending beam rheometer (BBR) applies a flexural creep load to a rectangular beam sample 6,25 x 12.5 x 127 mm in size to measure the flexural stiffness (S) and relaxation rate of flexural stress (m). The parameters of the test analyzed were S60 (creep stiffness at 60 s of the test obtained by fitting a second order polynomial to the logarithm of the measured stiffness at 8,0; 15,0; 30,0; 60,0; 120,0 and 240,0 sec and the logarithm of time) and m60 (absolute value of the slope of the logarithm of the estimated stiffness curves versus the logarithm of the time at 60 s of the test).

The master curves for 0 to 6 hours at one half hour interval for “145C-Unaged” samples are presented in Figure 6-2. As with the original dynamic modulus data, there is a positive correlation between conditioning time and the dynamic modulus of the samples. A similar trend was observed for the master curves of the “145C-Aged” mixtures short-term conditioned for 0 to 6 hours. A Scheffé test was performed on dynamic modulus values at 10 Hz interpreted from the master curves of “145C-Unaged” and “145C-Aged” samples. The results of the Scheffé analysis for conditioning time variations at the reference frequency of 10 Hz are in Figure 6-2. The shaded values indicate that the effect of conditioning time was significant for the dynamic modulus of the compared pair of conditioning durations.

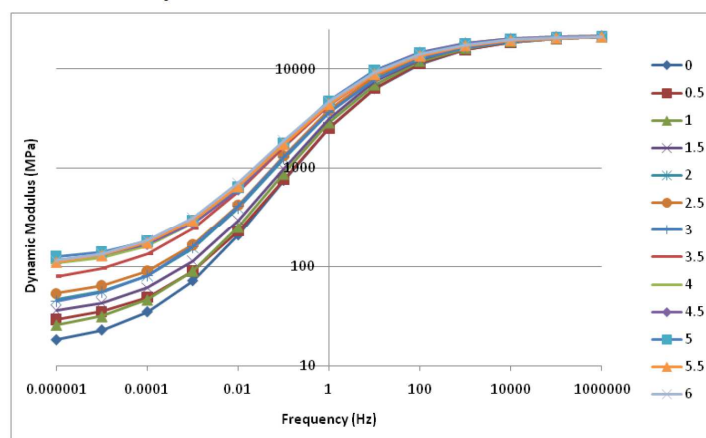


Figure 6-2: “145C-Flow” dynamic modulus master curve data for all conditioning times

The change in intermediate-temperature performance properties of the mixture with change in conditioning time was evaluated as stiffness on BBR. At intermediate temperature, the increase in stiffness can be interpreted as increase in fatigue cracking susceptibility. Using a BBR, the flexural creep stiffness (S) and the rate of stress relaxation (m) of the mixtures conditioned for a range of 1 to 6 hours at 1 hour interval were measured. Figure 6-2 shows the relationship between conditioning time and creep stiffness and Figure 6-2 shows the

relationship between conditioning time and stress relaxation rate. As seen from the graphs, the flexural stiffness increases and the stress relaxation rate decreases with increase in conditioning time. The trends indicate that the mixture is becoming more elastic and less ductile with the increase in conditioning time.

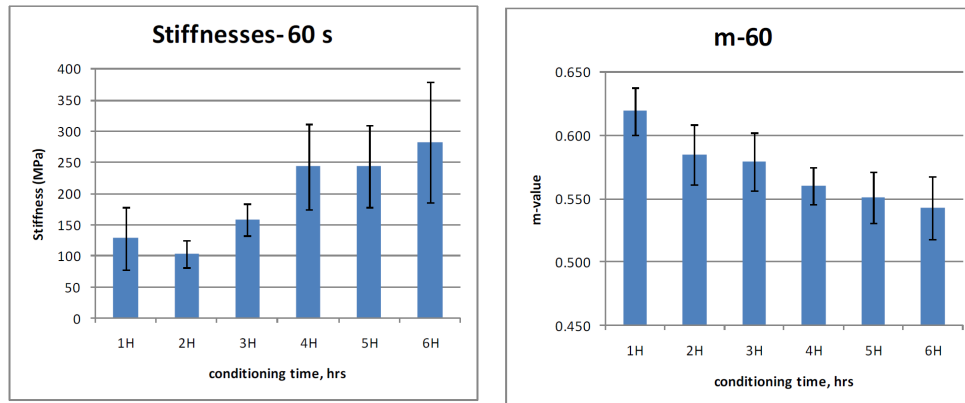


Figure 6-2 and Figure 6-2: Change in BBR stiffness at 60 seconds with increase in conditioning time (left) and change in BBR m-value with increase in conditioning time (right)

Table 6-10 provides the computed F values resulted from the test. Note that the shortest conditioning time for the flexural creep test was 1 hour; therefore the basis of comparison in Table 4 is the properties of the samples conditioned for 1 hour. As indicated from the table, with respect to 1 hour conditioning time, the change in stiffness becomes significant between 4 and 5 hours; however, if correcting for the gained stiffness due to the original one hour of conditioning that was not included in the analysis, the minimum conditioning temperature would be 3 hours. Based on similar reasoning, the second significant change in stiffness would be between 4 and 5 hours of conditioning and therefore, the maximum conditioning time based on flexural creep stiffness would be 4 hours.

The computed F values for comparison of the m-values showed slightly different conditioning times at which the characteristic changes become significant. After correcting for the gained stiffness due to the original conditioning time, the **m-values would be considered significant between 1 and 2 hours of conditioning**, which indicate that the minimum of conditioning time is 2 hours. The change in m-value would be significant for the second time between 4 to 5 hours of conditioning. Therefore, the maximum conditioning time based on creep stress relaxation rate would be 4 hours.

6.3.1.9 Paper 188 (Asphalt mix predictive models) (Pellinen et al., 2007)

The objective of this study was to evaluate the validity of several recent models used to predict asphalt mixture stiffness from the visco-elastic properties of asphalt binders. More specifically, the models by Di Benedetto et al. were compared to the existing Witczak model, which is implemented in the new pavement design guide, and the Hirsch models. The research was conducted using two sets of asphalt mixture dynamic modulus $|E^*|$ and asphalt binder complex shear modulus $|G^*|$ test data from FHWA-ALF and MnROAD studies. Predictions were made using Rolling Thin Film Oven (RTFO) and Pressure Aging Vessel (PAV) aged binder data. Binder modulus was converted to viscosity using existing empirical conversion equations. The results indicate that all three models can be used to estimate the mixture stiffness when certain conditions are met.

The dynamic modulus $|E^*|$ has been tested using either haversine tension (σ) or haversine compression (σ_c) loading, or using combined tension-compression loading (σ/c). In DSR testing, SST shear testing, and axial tension-compression testing, the average measured or

applied shear stress is zero, whereas in the haversine loading the applied stress (or strain) is comprised of constant creep loading superimposed over sinusoidal loading and the average stress deviates from zero. Subsequently, the type of stress or strain introduced or measured in the sinusoidal testing becomes an important variable when comparing test results.

Table 6-11: Most used stiffness predictive models

Model	Predicted	Predictor variables	Sample preparation	Temp. Range °C
Shell Model	S_m ¹	S_b ² , Vol. ³	Lab-no aging slab compactor	-15-30
Asphalt Institute	$ E^* _{mix}$	λ ⁴ , Vol.	Lab-no aging kneading	5-40
Witczak (1996)	$ E^* _{mix}$	η ⁴ , Vol. Grad. ⁵	Lab-no aging kneading	5-40
Witczak (1999)	$ E^* _{mix}$	η Vol. Grad.	Lab-No aging kneading & gyratory	-15-54
Witczak (2006)	$ E^* _{mix}$	$ G^* _{binder}$, Vol. Grad.	Lab-STOA ⁷ , Plant, mostly gyratory	-15-54
Hirsch (2003)	$ E^* _{mix}$ $ G^* _{mix}$	$ G^* _{binder}$, Vol.	Lab-STOA mostly gyratory	-10-54
2S2P1D	$ E^* _{mix}$ $ E^* _{binder}$	τ ⁶	Lab-no aging Slab compactor	-30-45
Global-DB	$E^* _{mix}$	E_{0_mix} , E_{inf_mix}	Lab-no aging Slab compactor	-30-45

NOTE: ¹ S_m is $|E^*|_{mix}$, ² S_b is $|E^*|_{binder}$, ³ Vol. stays for Volumetrics, ⁴ binder viscosity, ⁵ gradation, ⁶ characteristic time, ⁷ short-term aging

The study found that the laboratory-fabricated and aged mixtures were on average 30 % stiffer than plant mixtures compacted in the laboratory and up to 65 % stiffer than pavement cores. However, the variation between mixtures was large and mixture-type dependent. Needed adjustment factors and guidelines for the magnitude are given in a study by Pellinen and Xiao [28]. Table 6-12 shows the average stiffness ratios or adjustment factors for: 1) laboratory-fabricated mixtures (raw) to the plant produced mixtures; 2) plant mixture to one week old pavement cores (first coring); 3) laboratory mixtures (raw) to one week old pavement cores (first coring); and 4) one year old pavement cores (second coring) to one week old pavement cores (first coring).

Table 6-13: Average adjustment factors for mixture stiffness

Mix Type	Raw - Plant	Plant - 1st coring	Raw - 1st coring	2nd forint - 1st coring
All	1,26	1,31	1,65	1,52
DGM	1,36	1,25	1,77	1,68
SMA	1,14	1,38	1,51	1,31

The experimental data obtained for the nine asphalt mixtures and their corresponding binders were used to evaluate the accuracy of the three models that relate asphalt binder stiffness to asphalt mixture stiffness. The FHWA-ALF laboratory mixtures were four-hour short-term oven aged. The binder data were obtained from 15-80 °C for the ALF binders and 34-64 °C for the MnROAD binders. The dynamic modulus $|E^*|$ for mixtures was tested at -9 °C; 4 °C; 21 °C; 38 °C and 54 °C for the ALF mixtures, and at -20 °C; -10 °C; 4 °C; 20 °C; 40 °C and 54 °C for the MnROAD mixtures. As binder and mixture data were obtained at different temperatures and frequencies, master curves were generated to obtain required mixture and binder stiffness combinations. All master curves were generated using a reference temperature of 34 °C. The asphalt binder master curves were generated using the

CAM model and the mixture master curves were generated using the sigmoidal fitting function and allowing free fitting of coefficients. MnROAD binders were designed to be softer at cold temperatures, whereas some ALF binders were extremely elastic as low density polyethylene (LDPE) was used as modifier. Table 6-14 gives the binder PG grades and the A and VTS values obtained from DSR testing. For master curves the glassy modulus for the binders was fixed to $G_g = 1259$ MPa.

Table 6-15: Mixture binder data

Mixture	Binder type	PG-Grade	VTS	A
ALF 5	AC-10	58-22	-3,5569	10,6240
ALF 7	SBS (Styrelf)	82-28	-2,4248	7,5645
ALF 8	LDPE (Novophalt)	76-22	-3,1863	9,6580
ALF 9	AC-5	58-22	-3,4789	10,4084
ALF 10	AC-20	64-22	-3,5091	10,5166
ALF 11	AC-5	58-28	-3,4789	10,4084
ALF 12	AC-20	64-22	-3,5091	10,5166
MR 33-RTFO	Neat	58-28	-3,5633	0,6431
MR 34-PAV	Neat	58-28	-3,2196	9,7442
MR 34-RRFO	SBS	58-34	-2,7113	8,2846
MR 34-PAV	SBS	58-34	-2,8381	8,6804
MR 34-RTRO	SBS	58-40	-2,0682	6,5179
MR 34-PAV	SBS	58-40	-2,2987	7,1990

Figure 6-2 summarizes the predictions for all mixtures and models studied. Overall the most accurate and least variable predictions are produced by the Hirsch model, which is logical since ALF mixtures were included into the calibration dataset of the Hirsch model. However, Hirsch model seems to over-predict at high temperatures where the prediction seems to be confined by the static modulus of the model. Global DB model rotates round the equality line and over- and under-predicts the mixture stiffness.

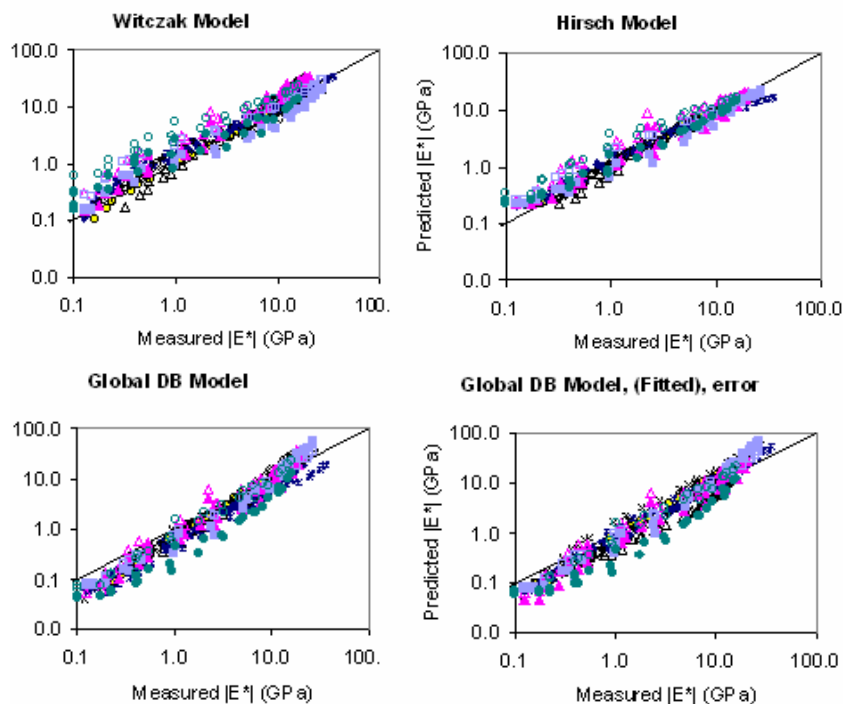


Figure 6-2: Stiffness predictions

Figure 6-2 to Figure 6-2 compares the predicted modulus values to the measured values for all the models at all temperatures. For the ALF mixtures, all the models gave comparable

predictions overall as far as magnitude, but at higher temperatures, the DB model substantially deviated from the Hirsch and Witczak models. Same observations apply to the predictions for the RTFO-MNROAD and PAV-MNROAD data, although the DB model starts to underpredict more already at 20°C. Generally, the DB is underpredicting, and the Hirsch and the Witczak models are overpredicting the stiffness of studied mixtures. The DB model has lower variation in the predictions at high temperatures, and the predictions are somewhat lower than the measured values in contrast to the Witczak and Hirsch models which are overpredicting the stiffness.

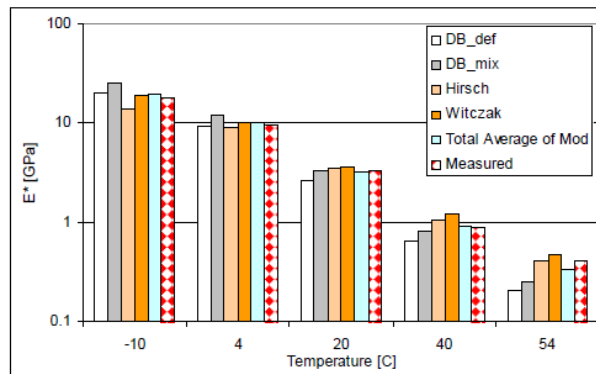


Figure 6-2: Overall model performance ALF-RTFO

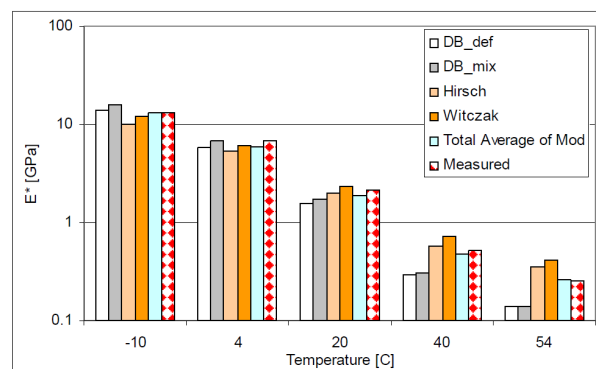


Figure 6-2: Overall model performance MnROAD-RTFO

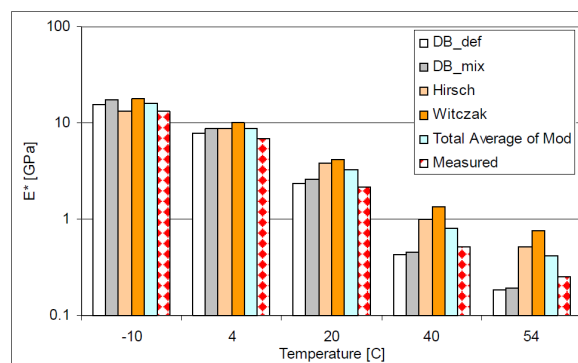


Figure 6-2: Overall model performance, MnROAD-PAV

If a mixture's small strain stiffness is needed for the structural design applications, both the Hirsch and Witczak models may be used. The predictions with the Witczak and Hirsch models were similar and both models gave similar bias and errors for the laboratory mixtures. However, for the plant mixture, the models under-predicted the measured stiffness with the RTFO binder data and drastically over-predicted the stiffness with the PAV binder

data. The results showed that the regression models were more accurate but not as precise as Di Benedetto model. The regression models are probably more accurate on average, but they may be less precise.

6.3.1.10 Paper 478 (Iwański & Mazurek, 2010)

Presented study focused on accelerated failure of pavements in a country with poor pavement conditions due to low performance materials and increased traffic loading. Use of crumb rubber in the bitumen was selected and evaluated as an alternative for increasing mainly the fatigue resistance. For this reason five different mix types of dense or gap gradation prepared with binder content between 5 % and 9 % and void content 5-6 %. As standard binder straight-run bitumen 50/70 was selected. Crumb rubber was applied in the bitumen with content of either 15 % or 20 % applying the wet process (continuous and terminal blends). Resulting optimum content of CR was defined as 17 %.

Stiffness (dynamic modulus) was determined by means of the frequency sweep test evaluating the modulus and phase angle. The test was performed by the 4PB-PR method with a strain level of 100×10^{-6} at seven frequencies: 10; 5; 2; 1; 0,5; 0,2 and 0,1 Hz and at test temperature of 20 °C. To minimize any damage of the beams (used alter for fatigue testing) only 100 cycles were applied for first three frequencies and 10 cycles for the other frequencies. According to the results the dynamic modulus of the conventional mixes shows highest values, because the use of CR reduced in general the stiffness modulus and enhances flexibility of the mixture. This is usually mainly visible for phase angle progression.

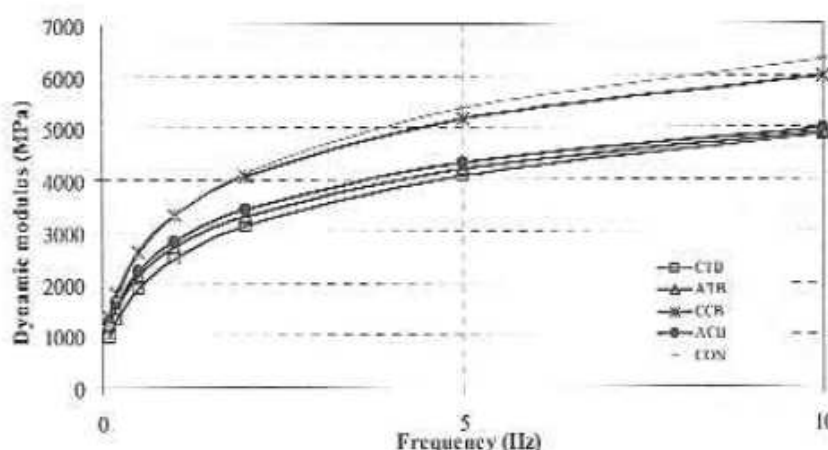


Figure 6-2: Dynamic modulus of assessed mixes as function of loading frequency

6.3.1.11 Paper 479 (Thives et al., 2010)

In this study HMAC16 and SMA16 mixes with four types of binders (3 PMBs and 50/70 bitumen) were evaluated and the effect of PMBs studied. For the binders special elasticity and plasticity was required according to the authors. Stiffness was assessed by 4PB-PR test according to EN 12697-26 at 20 °C for loading frequency 8 Hz in strain controlled modus with 50×10^{-6} .

Table 6-16: Stiffness values for assessed mixes (C is for 50/70)

Type of mixture	Stiffness modulus (MPa)
-----------------	-------------------------

MAMR16-A	8 800
MAMR16-B	6 700
MAMR16-C	11 200
MAMR16-D	9 300
MASF16-A	5 100
MASF16-B	4 700
MASF16-C	9 100
MASF16-D	9 400

6.3.1.12 Paper 496 (Velásquez et al., 2008)

The correlation between the stiffness modulus of bitumen and an asphalt mixture was intensively investigated by BRRC in earlier research. Four bituminous binders and two different grading curves were used. Additionally mixes without and with RAP (25 % and 40 %) were evaluated. It was found that the complex modulus of an asphalt mixture can be calculated using a function that includes the ratio of the volume of dry aggregates to the volume of binder, air voids content, and the complex modulus of the bituminous binder (Francken, 1996). The paper validates this correlation for HMAC mixes. The experimentally determined complex modulus of a series of HMAC mixtures is compared with calculations based on Francken's method. Different calculations are made with different estimations of the stiffness of the bituminous binder (i.e. Van der Poel's method, DSR measurements combined with the Arrhenius equation) and different approximations of the pure elastic modulus of the bituminous binder (i.e. asymptotically approximated from DSR measurements, an average value of 3000 MPa often used for traditional pen grade binders, and a new averaged value of 3640 MPa). It is shown that it is possible to estimate the stiffness of HMAC at different temperatures and frequencies with an accuracy of approximately 10-20 %.

Different methods exist to estimate the stiffness of bitumen. Stiffness can be estimated from its conventional properties by means of Van der Poel's nomogram (VDP). Alternatively, it can be determined with (DSR) measurements. A master curve, giving binder stiffness as a function of temperature and frequency, is experimentally determined. Different methods are available to describe temperature dependency (WLF method and Arrhenius equation).

The stiffness of an asphalt mixture can be estimated with a series of empirical relations as presented below, in which mix composition and the complex modulus of the bituminous binder is considered (Francken, 1996):

$$|E^*|(T, f) = E_{\infty} \cdot R^*(T, f);$$

For G^* evaluation dynamic shear rheometer was used and tests were performed according to EN 12770. Additionally pure elastic modulus of the bitumen $E_{\infty, \text{bit}}^*$ was determined as the asymptotic value of E_{bit}^* towards low X values (low temperatures, high frequencies). Note that $E_{\infty, \text{bit}}^*$ was determined by extrapolation from the DSR measurements, but that the limits of these measurements are lower for high-modulus bitumen than for traditional pen grades. Another method makes use of the Arrhenius relation to determine a master curve from DSR measurements performed on the bituminous binder. The combination with Francken's method is called the Arrhenius-Francken method. Details of the calculations can be found in (BRRC, 2006). The stiffness modulus E^* of the asphalt mixtures was measured with the two-point bending test according to EN 12697-26 (Annex A). This test was performed at various temperatures between -20°C and 30°C and different loading frequencies between 1 Hz and 30 Hz. Stiffness moduli of the different mixtures were presented mainly for 15 °C and 10 Hz.

From the results it was possible to conclude that the various methods are capable of predicting the stiffness of a HMAC mix with an accuracy of 15-20 %, except the Van der Poel-Francken method with $E^*_{\infty, \text{bit}} = 3\,000$ MPa.

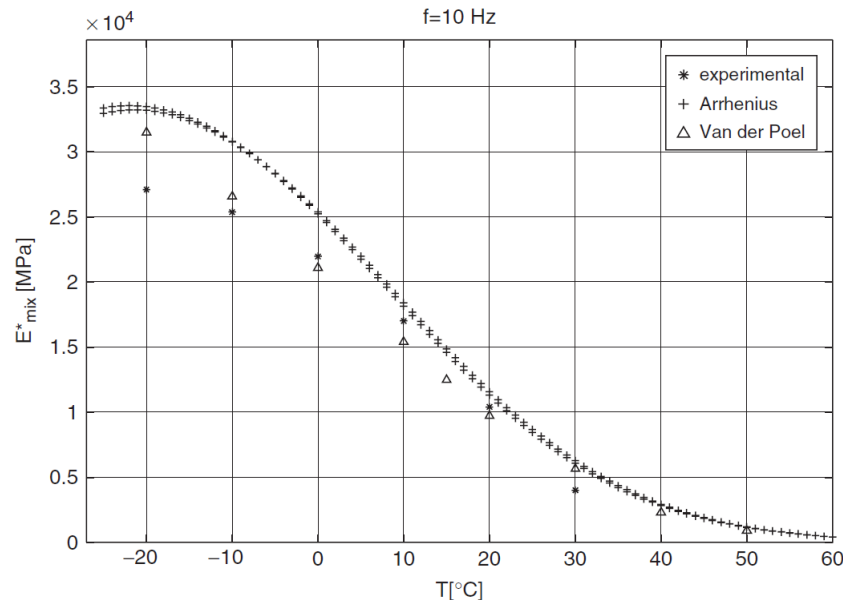


Figure 6-2: Stiffness of bituminous mixture 5 versus temperature

The influence of the skeleton of the asphalt mixture on the accuracy of the stiffness estimation was investigated. No correlation between the skeleton and the accuracy of the stiffness estimation was found (BRRC, 2006).

Separately influence of the HMAC mixture stiffness on structural design was evaluated. Structural design was studied with the software DimMET jointly developed by BRRC and Febelcem on the request of the Walloon Road Administration (DimMET, 2006). This design software makes use of the multilayer model of elastic materials for the structural design of semi-rigid and flexible road pavements with a bituminous surface layer. From gained results it can be inferred that a difference of 30 % in stiffness only has a minor influence on the design life of the road structure. In that case, the life-time decreases from 30 to 27 years, i.e. by approximately 10 %. This reduction in life can be compensated by an increase in layer thickness of 8 mm, or approximately 8 %. For smaller deviations in stiffness, the decrease in life is even smaller. A reduction of approximately 10 % in stiffness shortens the design life by only 3-4 % and requires an increase in layer thickness of only 2-3 % for equal life.

6.3.1.13 Paper 548 (Baptista et al., 2008)

This study focused on inclusion of fundamental approach (performance-based) on CE marking to bituminous mixtures. Assessments are done on 3 different mixes (AC 14 with 5,3 % binder, SMA 11 with 6,5 % binder, AR/Asphalt Rubber 12 with 19,0 % rubber in the bitumen and 9,5 % binder). Test specimens were compacted at 150°C.

- Different types of mixes, with different bitumen content lead to differences in void content. This results in a dissimilar performance of the mixtures during stiffness testing.
- Stiffness was determined at 20 °C by 4PB-PR (EN 12 697-26) with a repetitive sinusoidal loading for the applied test frequencies of 0,1; 0,2; 0,5; 1; 2; 5; 8 and 10 Hz (in growing order).

- AR 10 mix showed smallest frequency susceptibility (given by the CR content according to the authors).

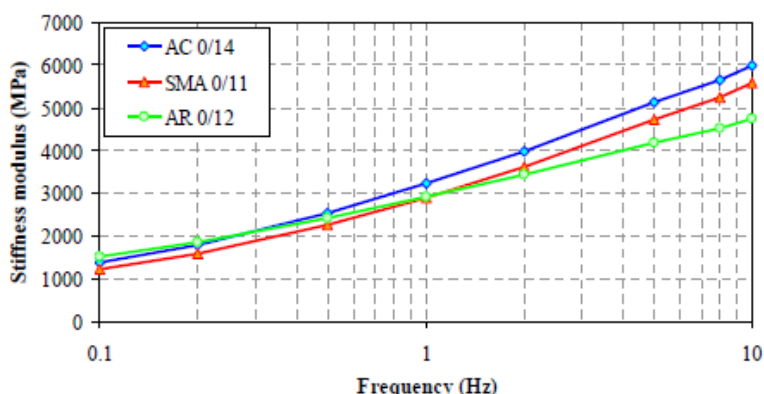


Figure 6-2: Variation of stiffness modulus related to frequency at 20 °C

Table 6-17: Stiffness characteristics and CE marking categories

Bituminous mixture	Average stiffness modulus at 8 Hz and 20°C (MPa)	CE marking category – EN 13108 (MPa)	
		S _{min}	S _{max}
AC 0/14	5600	S _{min} 4500	S _{max} 7000
SMA 0/1	5200	S _{min} 4500	S _{max} 7000
AR 0/12	4400	S _{min} 3600	S _{max} 7000

6.3.1.14 Paper 549 (Silva et al., 2008)

The study provided by this paper focuses on relation between different temperatures and stiffness and fatigue. Assessments are done on 4 different mixes (AC 14 with 5,5 % binder, SMA 12 with 6,8 % binder, AR/Asphalt Rubber 10 with 10,0 % binder and PA 14 with 5,0 % binder). Test specimens were compacted at 150 °C.

- Different types of mixes, with different bitumen content lead to differences in void content. This results in a dissimilar performance of the mixtures during stiffness testing.
- Stiffness was determined at 5°C, 15°C and 25°C by 4PB-PR (EN 12697-26) with a repetitive sinusoidal loading. Impact on pavement layer thickness and thermal susceptibility were evaluated as well.
- Each loading cycle applied a maximum tensile strain of 100×10^{-6} for the applied test frequencies of 0,1; 0,2; 0,5; 1; 2; 5 and 10 Hz (in growing order).
- Variations in stiffness were presented for reference frequency of 10 Hz.
- The laboratory results were used to pavement design at several design temperatures.
- Master curves were calculated for reference temperature of 15 °C.

Specific attention was paid to AC 14 mix focusing on influence of different temperatures. Variation of the stiffness modulus and phase angle was observed when temperature varies 10 °C or when the frequency changes from 10 to 1 Hz. The corresponding change in traffic speed is less common to occur than a temperature variation of 10 °C, meaning that temperature is usually the main parameter that controls the stiffness behavior of bituminous mixtures in road pavements.

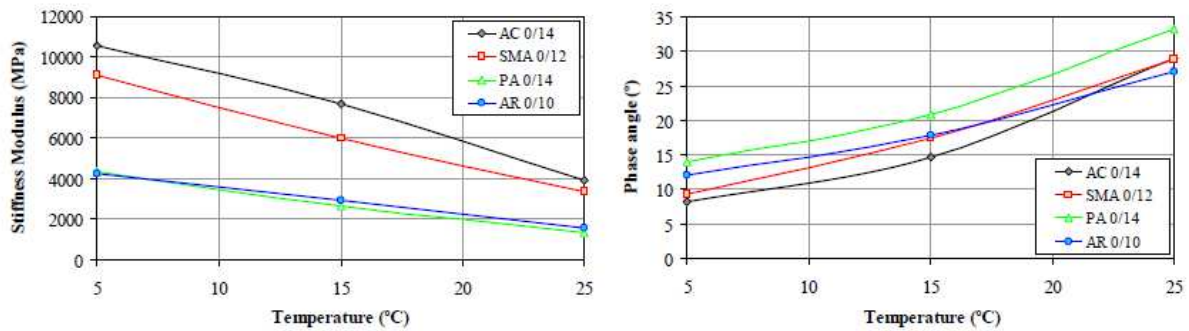


Figure 6-2 – Influence of the temperature on the stiffness modulus and phase angle at 10 Hz for the assessed mixtures

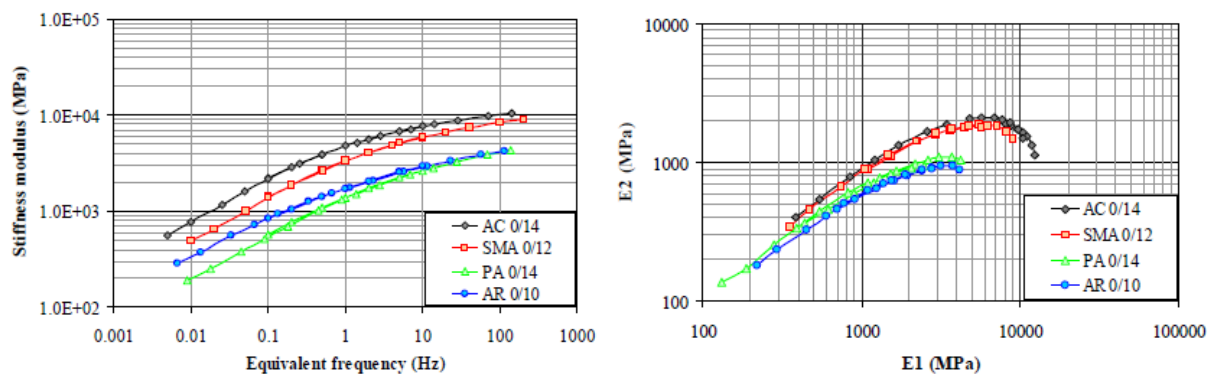


Figure 6-2: Master curves (reference temperature at 15 °C) and complex modulus curves in the Cole-Cole plane

Pavement temperature is an uncontrollable factor. It presents a variability that the design methods cannot transmit in a real way. Hence it is necessary to use a great safety margin in order to overcome that variability (Picado Santos, 1994). Finally, a comparative analysis between the design results of the

6.3.1.15 Paper 563 (Tabatabaee & Tabatabaee, 2010)

In the study done by Wen et al. five bituminous binders (PG70-22, air-blown, SBS LG, CR-TR, terpolymer modified bitumen) and five asphalt mixtures containing these binders with same aggregates sources were tested at intermediate temperatures. Four of the binders were modified with different techniques. The binder content was in the mixes always the same (5,3 %). Complex shear modulus and monotonic constant shear-rates tests were conducted on bituminous binders whereas dynamic modulus was conducted on the corresponding mixtures. The effects of modification techniques on the properties of binders and relationship between properties of binder and asphalt mixture were evaluated study. The results indicated that the modulus of bitumen directly affects that of asphalt mixture, as expected. The failure strain of bitumen controls that of asphalt mixture. However, the shear strength and fracture resistance, critical strain energy density in this case, of bitumen are not directly correlated with those of asphalt mixtures.

It was stated that there is a need to re-evaluate the relationship between the properties of bitumen and those of asphalt mixture such that a proper understanding and selection of asphalt binder can be made to improve the performance of asphalt mixture

Monotonic constant shear-rate test and Complex shear modulus tests

- The laboratory binder tests conducted using a TA Dynamic Shear Rheometer Instrument (AR2000) that allows isothermal loading.
- Binders were aged using the rolling thin film oven (RTFO) prior to the testing.
- Constant strain shear-rate was applied to the binder specimen at 19 °C until the peak stress was reached. Three shear rates were used: 0,005/s, 0,0075/s, and 0,01/s.
- Shear strength, failure strain at shear strength, and critical strain energy density (CSED) were determined. The CSED is the area under the shear stress and shear strain curve up to peak stress, namely shear strength.
- It seems that the increase of failure strain of binder increases the failure strain of HMA. Ductility of the binder dominates the ductility of asphalt mix.
- Frequency sweep tests at selected strains were conducted to obtain the viscoelastic properties in the linear strain range, such as complex shear modulus. Frequency sweep results at 19 °C and 10 Hz were reported.

Results:

- Increasing shear rate also increased the shear strengths (at higher loading rate the binder is stiffer because of its viscoelasticity). Higher shear strain at peak stress found for PMBs.
- Unique relationship between the G^* and shear strength of the binder. There seems to exist a point beyond which the relationship is positive and otherwise is reversed. Two binders might have the same shear strength, but their G^* are significantly different from each other. This indicates that a high modulus binder might not be resistant to fatigue.
- CSED of binders were found to correlate well with field fatigue cracking of asphalt pavements. SBS modified binder showed highest values indicating highest fatigue resistance

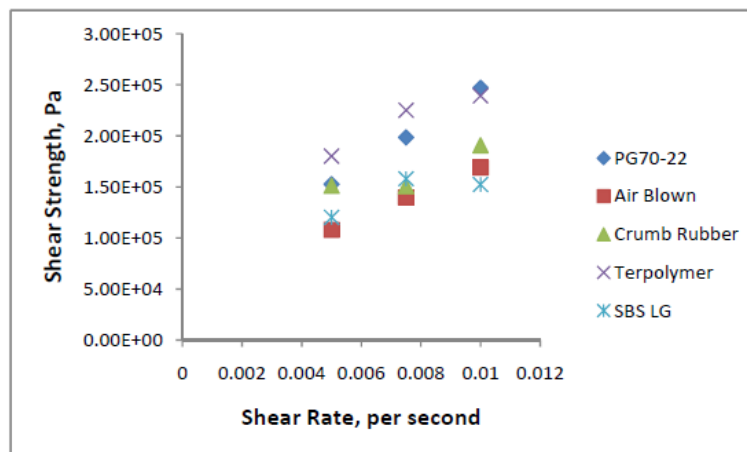


Figure 6-2: Binder effects of shear rates on shear strength

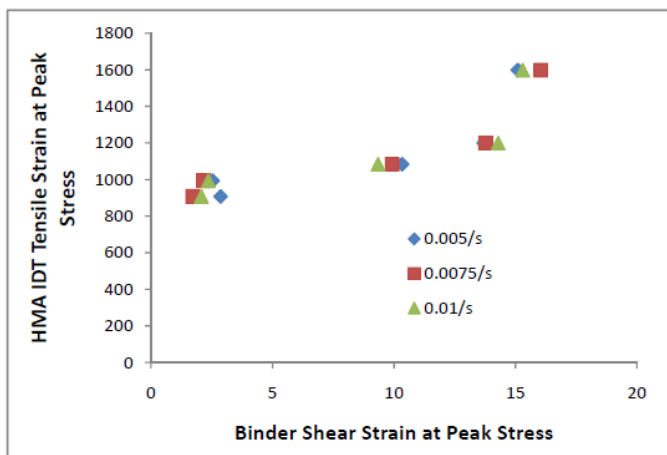


Figure 6-2: Relationship between failure strain of bitumen and asphalt mix

Table 6-18: Complex shear modulus of tested binders

Bitumen	Complex shear Modulus (MPa)
70-22	28,42
Air Blown	16,23
CR TB	9,165
Terpolymer	7,179
SBS LG	10,33

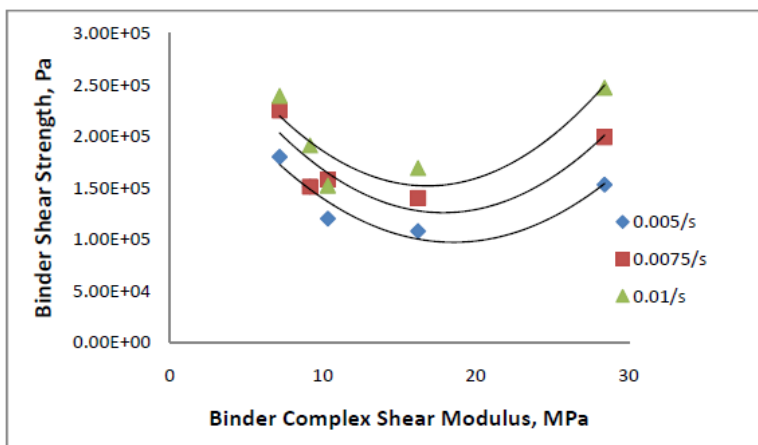


Figure 6-2: Relationship between G* and shear strength of bitumen

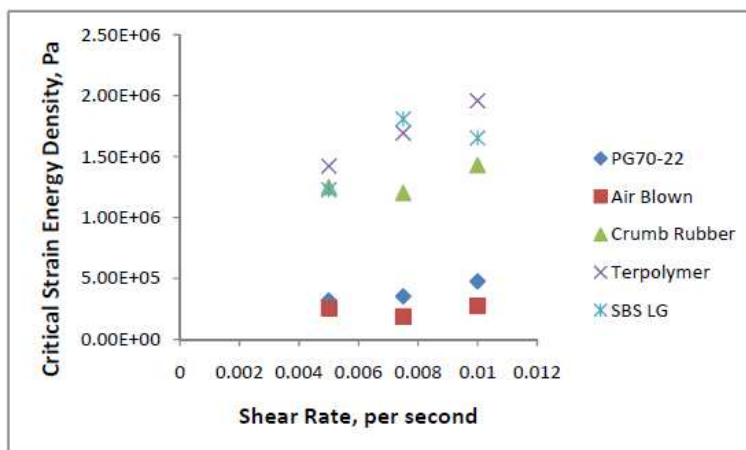


Figure 6-2 Effects of shear rate on CSED of binders

Uniaxial dynamic modulus on asphalt mixes

Dynamic modulus $|E^*|$ master curves of the asphalt specimens were constructed according to the AASHTO TP-62 protocol. The testing temperatures were 4 °C; 19 °C; 31 °C; 46 °C and 58 °C using frequencies of 20; 10; 5; 1; 0,5 and 0,1 Hz. Specimens were prepared in a Superpave gyratory compactor to 180 mm in height and cored to 100 mm in diameter and 150 mm in height. The tests were conducted using the Asphalt Mixture Performance Tester (AMPT). The dynamic modulus of asphalt mixtures at 19 °C and 10 Hz are reported.

Dynamic modulus are different from each other significantly for assessed mixtures (impact of used binder). It further seems that all the modification methods reduced the dynamic modulus of HMA.

Table 6-19: Dynamic modulus test results for HMAs

Binders in HMA	Dynamic Modulus, at MPa(9)	IDT Tensile Strength	IDT Tensile Failure Strain
PG 70-22	7847	1261,02	993,33
Air-Blown	6561	1020,53	907,21
CR-TB	4536	933,96	1082,97
Terpolymer	3726	853,67	1199,39
SBS LG	4467	1032,43	1598,25

In case of evaluating the relationship between the shear strength of bitumen under three shear rates and the tensile strength of the asphalt mix it seems that there is no correlation. This finding is according to the authors unexpected (it was expected that higher strength of bitumen leads to higher strength of the mix). On the other hand there is a clear correlation between complex shear modulus of the bitumen and dynamic modulus of asphalt mixtures. High modulus binder could increase the dynamic modulus of the mixture and lower the tensile strain at the bottom of asphalt mix layer (increasing fatigue resistance).

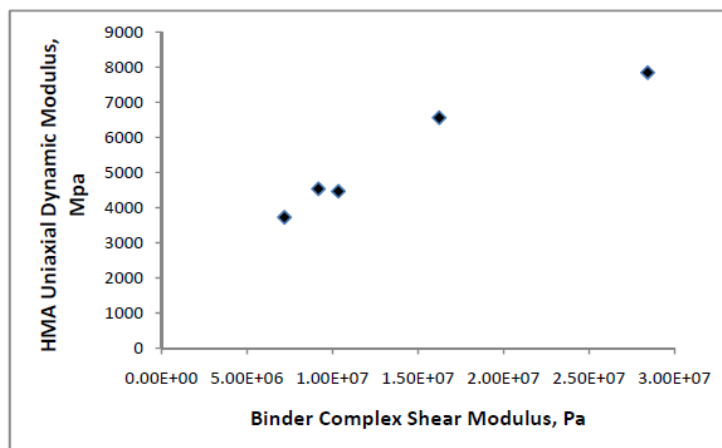


Figure 6-2: Relationship between G^* and E^* of asphalt mix

6.3.2 Dynamic Shear Rheometer (DSR)

6.3.2.1 Paper 025 (Mangiafico *et al.*, 2012)

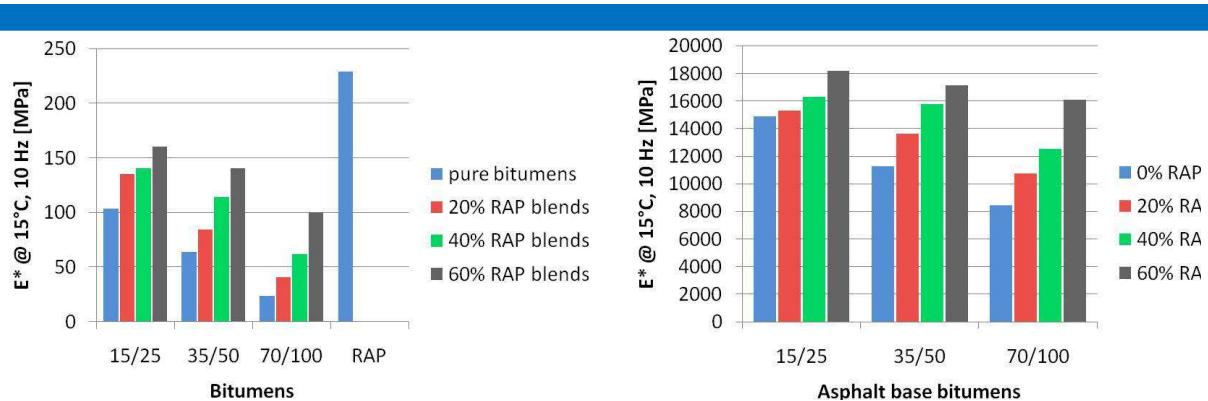


Figure 6-2 – Change in complex modulus with proportion of RA

Figure 6-2 – Change in complex modulus with base bitumen grade

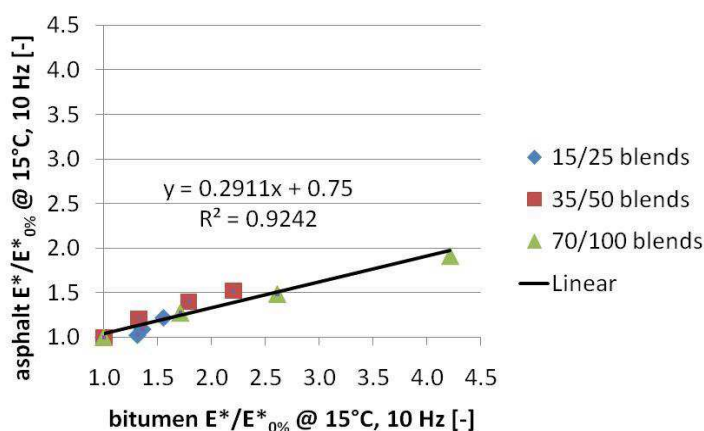


Figure 6-2 – Relationship between normalised stiffness moduli for asphalt and bitumen

Table 6-20: Complex modulus test results at 15 °C and 10 Hz

Bitumen grade	RA (%)	Complex modulus, E* (MPa)		Normalised E*		Air voids content (%)
		Bitumen	Asphalt	Bitumen	Asphalt	
15/25	0	103	14910	1,00	1,00	3,3
	20	136	15282	1,31	1,02	4,2
	40	140	16281	1,36	1,09	3,2
	60	161	18193	1,56	1,22	3,4
35/50	0	64	11268	1,00	1,00	4,1
	20	85	13640	1,32	1,21	4,0
	40	114	15765	1,79	1,40	2,5
	60	141	17129	2,20	2,52	3,9
70/100	0	24	8425	1,00	1,00	3,6
	20	41	10733	1,71	1,27	2,9
	40	62	12506	2,61	1,48	2,7
	60	100	16083	4,21	1,91	2,7

6.3.2.2 Paper 026 (Eckmann et al., 2012)

For the asphalt with 20/30 base bitumen modified with an unnamed cross-linked elastomer polymer, a good correlation was observed between the stiffness moduli measured on the

asphalt at 15 °C and 0.02 s and the $|G^*|$ value measured on the corresponding binders at 15 °C and 10 Hz. This correlation implies that, at higher temperatures, the more elastic behaviour which is conferred to the binder by the polymer modification will also reflect in the asphalt behaviour.

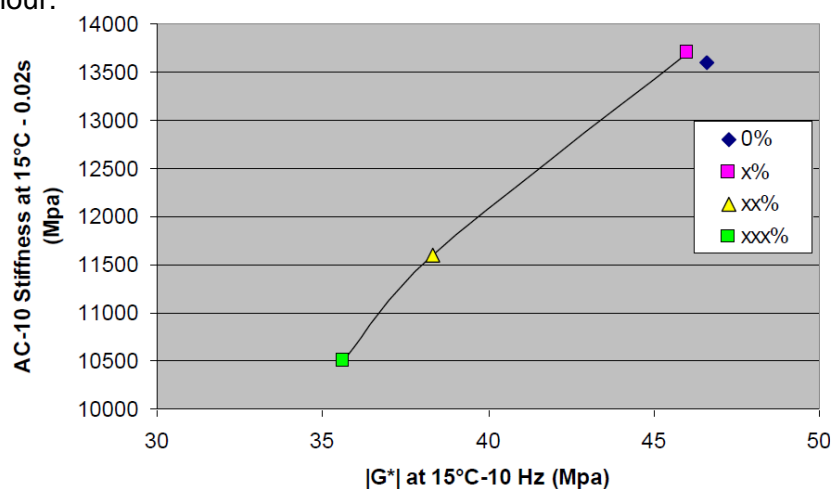


Figure 6-2 Stiffness of AC-10 relative to stiffness of 20/30 bitumen with modification

6.3.2.3 Paper 038 (Valentin *et al.*, 2012)

Table 6-21: Empirical and stiffness results for binders at 60 °C and 1,59 Hz in control-stress mode

Binder	SP (°C)	Pen (0.1 mm)	G' (kPa)	G'' (kPa)	$ G^* $ (kPa)	$\tan(\delta)$	δ (°)	J' (Pa ⁻¹)	J'' (Pa ⁻¹)
50/70	51	51	1 504	8 089	8 228	5,38	79,5	0,00002	0,00012
50/70 + 3 % FTP	76	40	1 246	10 280	10 360	8,25	83,1	0,00001	0,00010
50/70 + 2 % FTP	–	–	2 636	14 100	14 350	5,35	79,4	0,00001	0,00007
50/70 + 0,5 % PPA	53	53	1 233	6 269	6 389	5,09	78,9	0,00003	0,00015
50/70 + 1 % PPA	56	49	5 877	16 990	17 980	2,89	70,9	0,00002	0,00005
50/70 + 0,75 % IT	–	–	569	4 470	4 506	7,86	82,8	0,00003	0,00022
50/70 + 1 % IT	51	40	331	5 058	5 069	15,30	86,3	0,00001	0,00020
50/70 + 0,1 % ZS	50	55	348	4 584	4 597	13,17	85,7	0,00002	0,00022
50/70 + 0,3 % ZS	–	–	253	3 591	3 600	14,19	86,0	0,00002	0,00028
50/70 + 0,5 % DC	–	–	278	4 225	4 234	15,18	86,2	0,00002	0,00024
70/100	46	82	431	6 000	6 015	13,91	85,9	0,00001	0,00017
70/100 + 3 % FTP	91	53	894	7 145	7 200	7,99	82,9	0,00002	0,00014
70/100 + 3 % FAA	95	60	825	7 429	7 475	9,01	83,7	0,00001	0,00013
70/100 + 0,5 % PPA	–	–	777	6 099	6 148	7,85	82,7	0,00002	0,00016
70/100 + 1 % PPA	–	–	1 413	7 098	7 238	5,02	78,7	0,00003	0,00014

Table 6-22: Stiffness moduli of asphalt using IT-CY method

Binder	Process temperature (°C)	Stiffness modulus (MPa) at temperature T (°C)				Thermal susceptibility*
		0 °C	15 °C	27 °C	40 °C	
50/70+3 % FTP	145	25 400	10 600	4 300	1 600	15,88
50/70+3 % FTP	130	14 500	6 900	2 500	500	29,00
CP-M	160	23 700	13 200	4 600	1 800	13,17
CP-M	145	23 200	12 900	6 000	2 200	10,55
50/70+3 % FAA	145	26 800	15 100	5 100	1 200	22,33
50/70+3 % FAA	130	21 700	11 600	3 200	900	24,11
50/70+0,5 % PPA	145	24 100	10 800	3 400	900	26,78
50/70+0,5 % PPA	130	19 900	8 000	2 200	600	33,17

* Calculated as ratio of stiffness modulus at 5 °C and 40 °C.

Table 6-23: Stiffness of moduli of asphalt using 2PB-TR method

Binder	Sample	Stiffness modulus (MPa)				
		5 Hz	10 Hz	15 Hz	20 Hz	25 Hz
50/70+3 % FAA	L1	13 477	14 093	14 614	14 876	15 049
	L2	12 673	13 240	13 653	13 908	14 018
	Mean	13 075	13 667	14 134	14 392	14 534
50/70+1 % PPA	P1	10 929	11 478	11 796	11 985	12 133
	P2	13 003	13 840	14 283	14 565	14 815
	Mean	11 966	12 659	13 040	13 275	13 474
50/70+3 % FTP	T1	12 107	12 887	13 364	13 655	13 773
	T2	11 629	12 220	12 652	12 920	13 016
	Mean	11 868	12 554	13 008	13 288	13 395

6.3.2.4 Paper 128 (Zezelew *et al.*, 2012)

Figure 6-2(a) to Figure 6-2(g) present the comparison of shear modulus $|G^*|$ master curves for the control binder and WMA technologies included in the study. Asphalt binders with higher $|G^*|$ mostly improve shear deformation resistance. It is shown in these figures that the asphalt binders containing the organic additive Sasobit[®] measured high stiffness. The Accu-Shear[®] and Rediset[®] technologies measured slightly higher stiffness as compared to their control binders primarily at the low reduced frequency ranges (i.e., below 10 Hz). The other WMA technologies (Advera[®], Aspha-min[®], and Evotherm[®]) measured comparably similar stiffness values as their control binders when the lower reduced frequency range is considered. For the PA0986 project, the LEA and Gencor technologies demonstrated higher stiffness as compared to the control binder when the high reduced frequency ranges are considered. The differences in the stiffness properties amongst these WMA technologies could be explained from the differences in base binder, dosage rates, the WMA technology used, and the inherent variability in the DSR test procedures.

The dynamic modulus test data was used to construct master curves for each of the test specimen at a reference temperature of 21,1 °C. Data was then shifted along the frequency axis to form a single $|E^*|$ master curve using the sigmoidal function given in ME PDG.

Chyba! Nenalezen zdroj odkazů.(a) through **Chyba! Nenalezen zdroj odkazů.**(g) present comparison of $|E^*|$ master curves of the control HMA and WMA mixtures for all the projects included in the study. Overall, the $|E^*|$ master curve plots exhibited similar shape/trend for a wide range of frequencies. The stiffness properties of all of the asphalt mixtures presented in these figures decreased with an increase in test temperature and increased with an increase in loading frequency. Asphalt mixtures with higher $|E^*|$ mostly improve stability and rutting resistance. In general, compared to the control HMA mixtures, lower stiffness values were observed for the WMA technologies prepared with foaming processes followed by the chemical additives. The reduction in stiffness is more pronounced for the asphalt mixtures with Advera[®] and Aspha-min[®] technologies and therefore these mixes may be more susceptible to rutting. This is a concern during the early life of the pavement if high temperatures are encountered and heavy traffic loading is placed on the pavement before it can age and stiffen in place on the roadway. The WMA mixtures containing organic additive Sasobit[®] exhibited higher stiffness, particularly at lower and intermediate frequency ranges. In these figures, the MATL mix design replicates (MDR) mixtures measured relatively higher stiffness (except for MO0987 project) as compared to the plant produced HMA mixtures due to additional oven conditioning (4 hours at 135°C). The differences in the stiffness properties of these WMA mixtures could be explained through, among others, the differences in volumetric properties, binder rheological properties, WMA dosage rates, aggregate shape properties (e.g. angularity and texture), production temperatures and plant ageing.

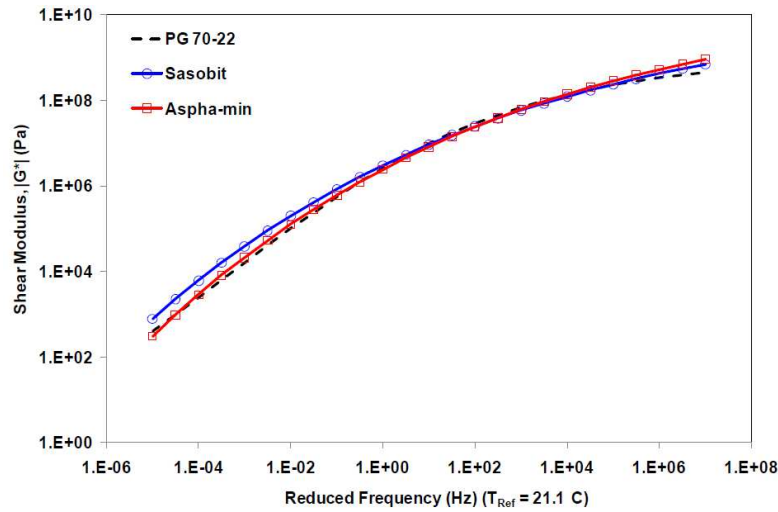


Figure 6-2(a): Shear modulus master curve for MO0672

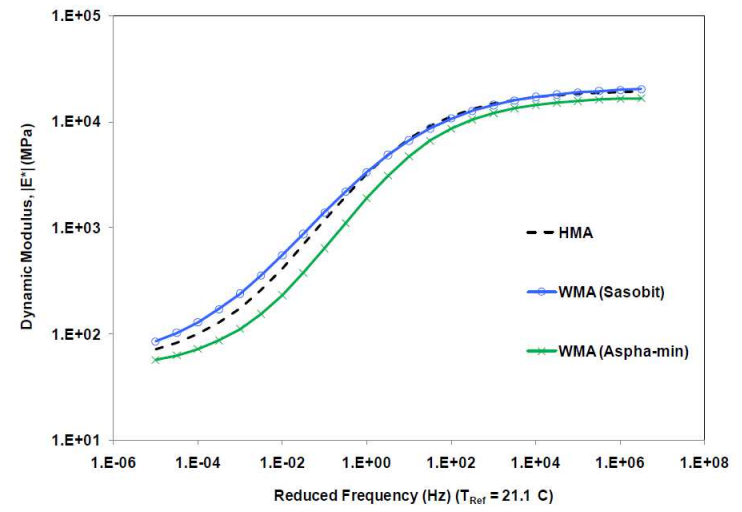


Figure 6-2(a): Dynamic modulus master curve for MO0672

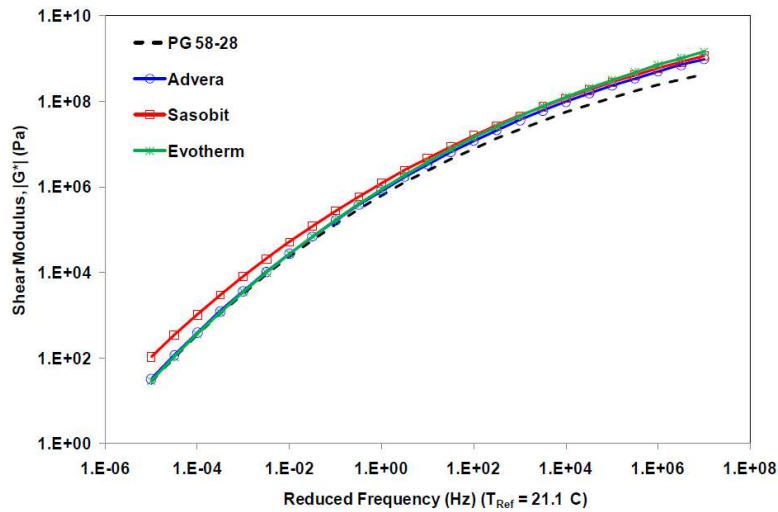


Figure 6-2(b): Shear modulus master curve for CO0777

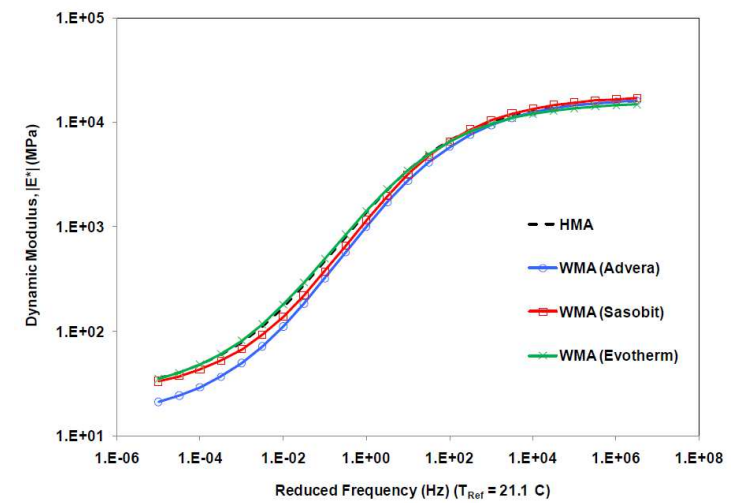


Figure 6-2(b): Dynamic modulus master curve for CO0777

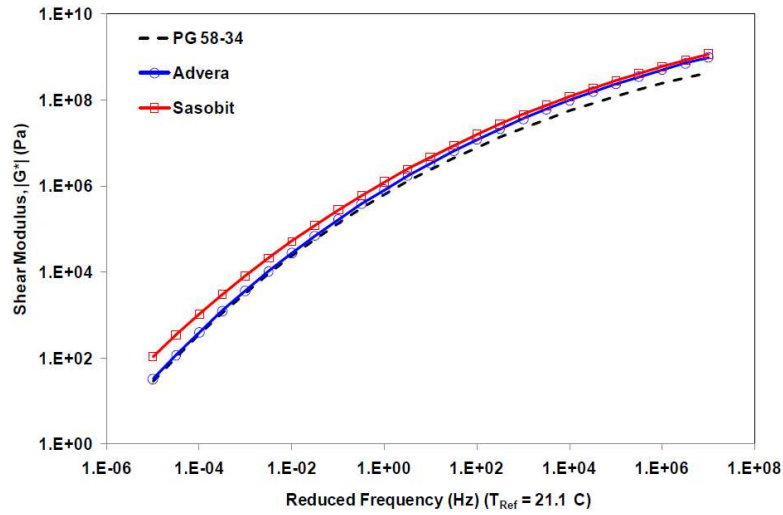


Figure 6-2(c): Shear modulus master curve for WY0778

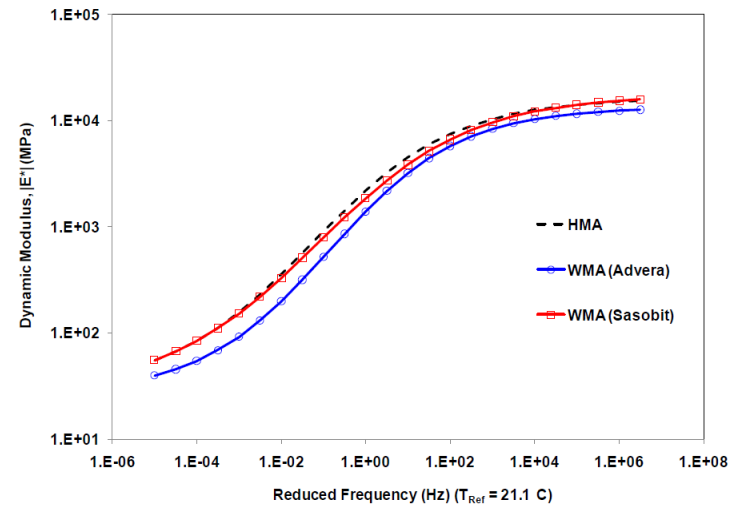


Figure 6-2(c): Dynamic modulus master curve for WY0778

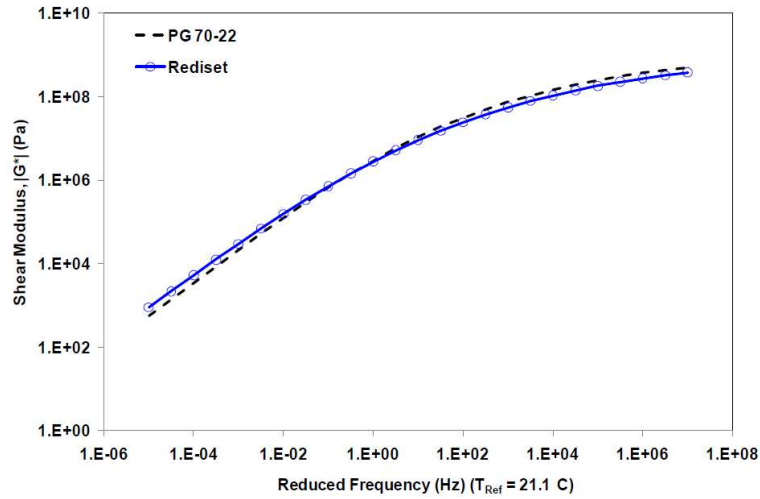


Figure 6-2(d): Shear modulus master curve for TX0985

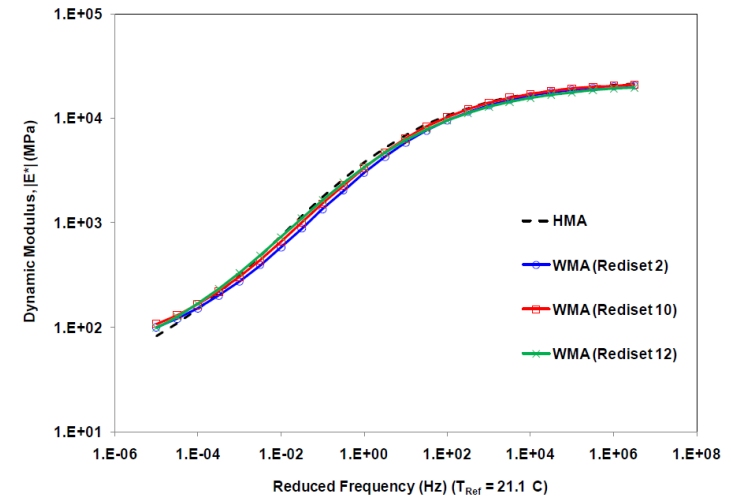


Figure 6-2(d): Dynamic modulus master curve for TX0985

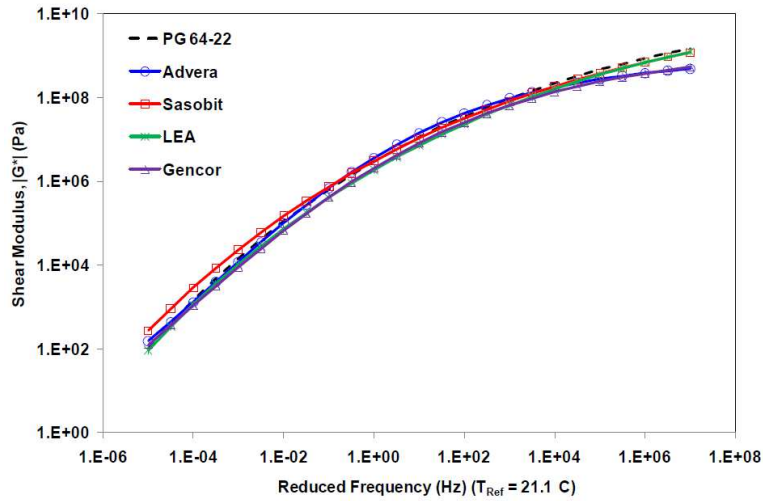


Figure 6-2(e): Shear modulus master curve for PA0986

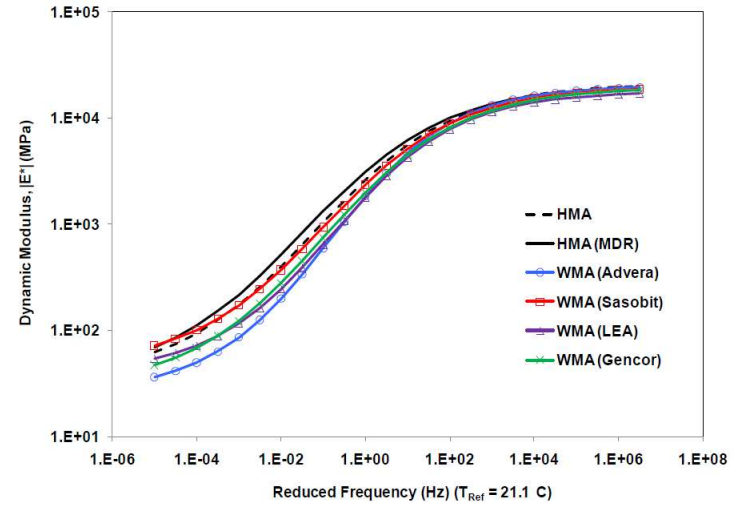


Figure 6-2(e): Dynamic modulus master curve for PA0986

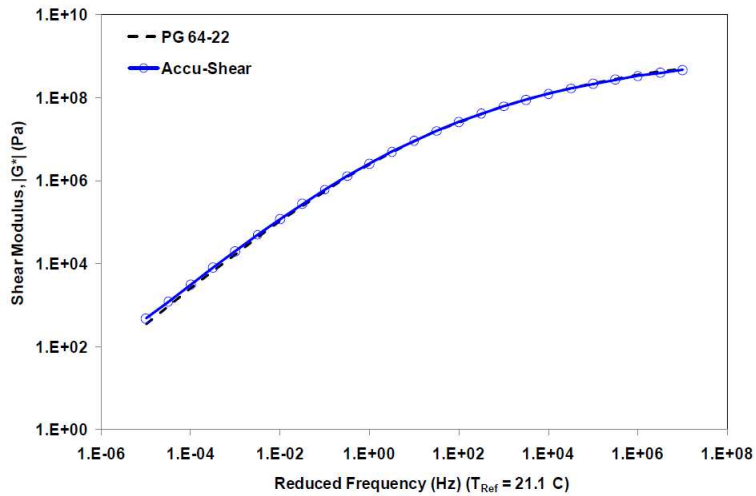


Figure 6-2(f): Shear modulus master curve for LA1088

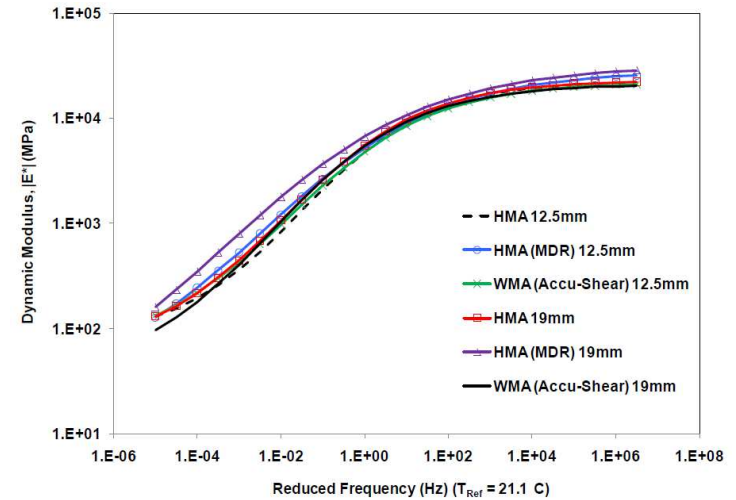


Figure 6-2(f): Dynamic modulus master curve for LA1088

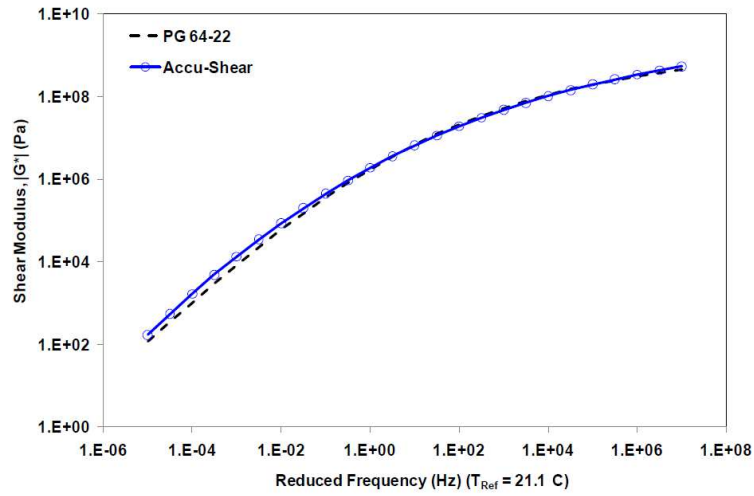


Figure 6-2(g): Shear modulus master curve for IN1099

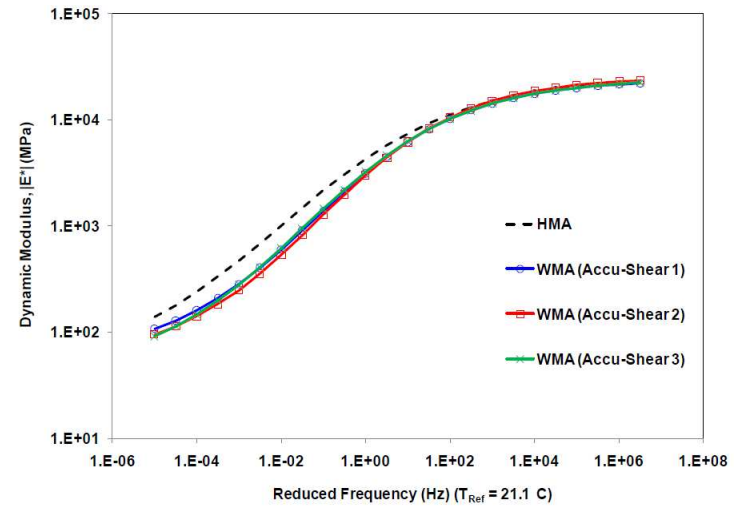


Figure 6-2(g): Dynamic modulus master curve for IN1090

6.3.2.5 Paper 347 (Yang *et al.*, 2014)

The resilient modulus at different age was the average of four specimen cored from the recovered slab. The variability of resilient modulus among the four specimens ranges from the lowest 2 % to the highest 21 %. The variability has been contributed to imperfection positioning of the specimen, different aggregate orientation from one side to the other, or different level of densification/ damage in the field or all three factors. Figure 6-2 shows the results of the average resilient modulus for HMA, WMA-E, and WMA-S cores taken after 0, 2, 4, 8, 24, 36 and 52 weeks of service period. In addition, analysis of variance (ANOVA) at a level of significance of $\alpha = 0.05$ was used to analyse which factors (binder type and age) significantly affect the measured resilient modulus. The binder type was found out to be a significant factor. From the study of the mixture properties it was observed that the WMA-S have no significant effect on the MR values with the exception of the 36th and 52nd week where the MR values were significantly different from that of the HMA mixtures. The WMA-E mixtures were also observed to have no significant differences in MR values compared to the HMA mixtures with the exception of the 0 and 2nd week. These differences could be attributed to testing variability which has been contributed to imperfection positioning of the specimen, different aggregate orientation from one side to the other, or different level of densification/ damage in the field or all three factors. In general, these findings are similar to the observations done by others in which they concluded that the addition of either warm mix process did not affect the resilient modulus of an asphalt mix compared to control mixtures having the same PG binder.

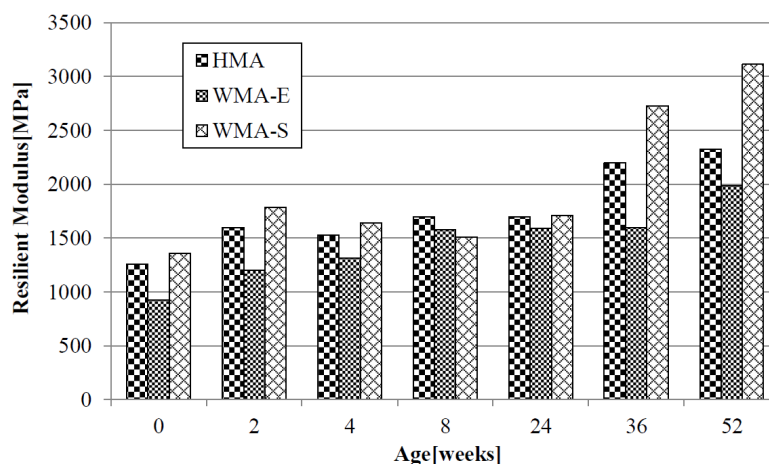


Figure 6-2: Resilient modulus of HMA and WMA at different ages

After the indirect tensile test, the top 25 mm of cylindrical specimen was sawed cut and the binders were extracted from the top inch portion of fractured mixes. This is because most of binder aging happened in the top layer of the pavement surface. The dynamic shear modulus (G^*) and phase angle (δ) of the recovered binder were measured using dynamic shear rheometer (DSR). This test was done using a 25 mm parallel plate setup with a gap of 1 mm and a 2 % strain at 64 °C. The measured G^* of the binders are presented in **Chyba! Nenalezen zdroj odkazů.** From the rheological results it is observed that in most cases the WMA-S binder had a higher complex modulus value than the HMA binder. This implies that Sasobit additive make the binder stiffer at maximum pavement temperature which is a good indication of the binder resistance to rutting. This finding is similar to observations made by Gandhi *et al.* (2010b) in which the results for the $G^*/\sin \delta$ values of the unaged binders increased with the addition of Sasobit. The increase in the $G^*/\sin \delta$ values caused by Sasobit is due to the crystallization effect of the wax after the binders cool. The WMA-E binder had lower G^* values compared to the HMA and WMA-S binders indicating that the lower mixing and compaction temperature reduce the aging of the binder. In general, the complex

modulus; G^* values of the recovered field binders increase with increasing service life due to the effect of aging.

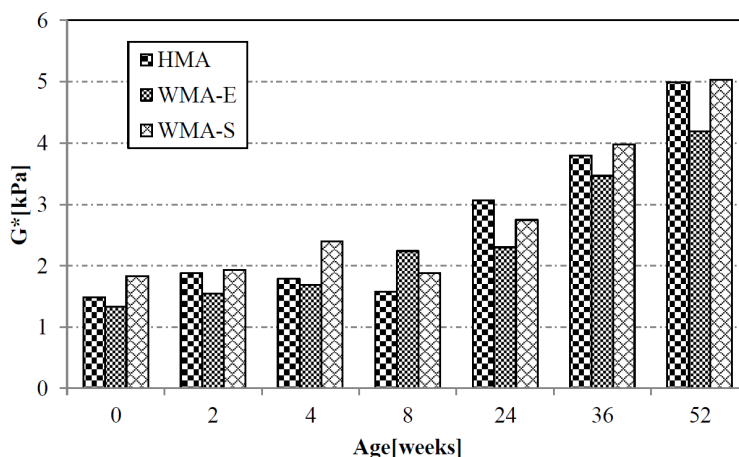


Figure 6-2: G^* values of the extracted HMA and WMA binders

A master curve of an asphalt mix is used to compare the viscoelastic behaviour of materials over a wide loading frequency. The master curves of all binders were constructed at a reference temperature of 25 °C using the principle of time-temperature superposition. The data of various temperatures were shifted with respect to frequency until the curves merge into a single sigmoidal function. **Chyba! Nenalezen zdroj odkazů.**(a) to (c) illustrates the change in G^* and δ values with increasing angular frequencies for the HMA, WMA-E and WMA-S binder respectively for the different service periods. From **Chyba! Nenalezen zdroj odkazů.**(a) to (c) it can be seen that the elasticity of the binders increased with age, indicated by a decrease in the phase angle. However, for the phase angles values, the WMA-S has shown to have lower values especially over all frequency ranges. This show that the addition of WMA-S makes the binder more elastic especially at low frequencies (high temperatures) which is a good indicating that the WMA-S binder will undergo less permanent deformation at these frequencies, and therefore the mixture will be less susceptible to rutting even at high traffic speeds compared to the other binders. On the other hand, the WMA-E shows a more viscous behaviour especially at higher frequencies (low temperature) which implies that the WMA-E has the tendency to reduce thermal cracking.

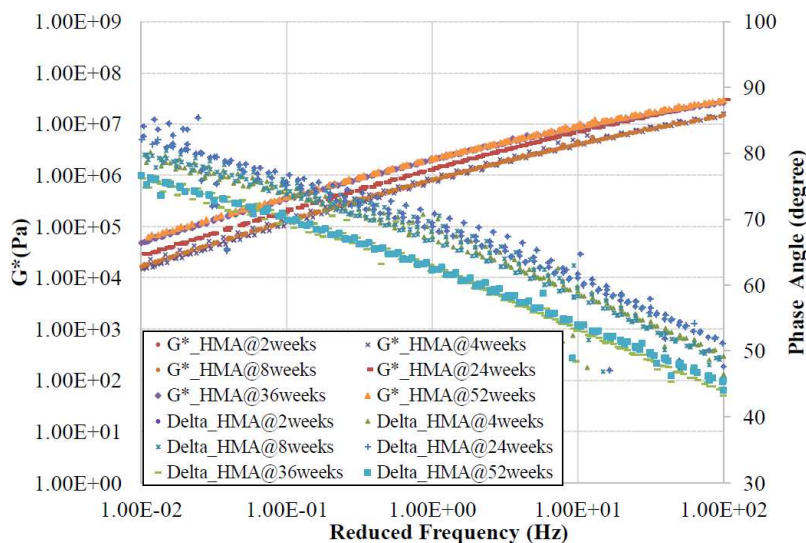


Figure 6-2(a): Complex modulus and phase angle master curves at T = 25°C for HMA binder

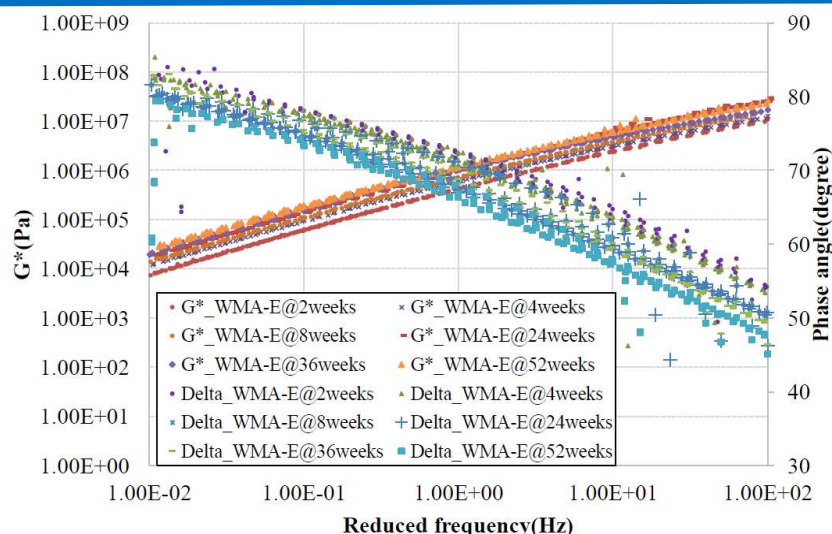


Figure 6-2(b): Complex modulus and phase angle master curves at T = 25°C for WMA-E binder

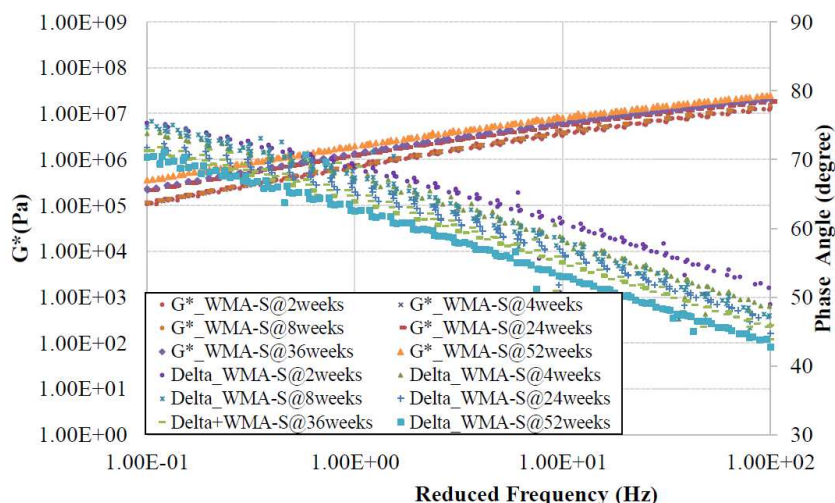


Figure 6-2(c): Complex modulus and phase angle master curves at T = 25°C for WMA-S binder

6.3.2.6 Paper 510 (Hase, 2011)

In the study, 30 % (m/m) RA was added to fresh material. The RA was dried and conditioned at 110 °C for 2 h 30 min before the mixtures were manufactured. Fresh binders (**Chyba! Nenalezen zdroj odkazů.**) were added to the mixture at standard temperature according their viscosity. Asphalt base course mixture EME 0/14 was produced and stiffness of cylindrical specimen was tested at 15 °C according to EN 12697-26. The resulting stiffness moduli are summarised in **Chyba! Nenalezen zdroj odkazů.** When extrapolating the results linearly in order to estimate the resulting stiffness modulus of asphalt containing 100 % RA (last column in **Chyba! Nenalezen zdroj odkazů.**), the resulting stiffness values are similar for all mixtures (8680 ± 1400). This value is close to the stiffness modulus of EME without RAP containing bitumen B 50/70.

Table 6-24: Properties of fresh binders in Colas study (Carbonneau 2012)

Grade of pure binder	Penetration (1/10 mm)	Softening Point (°C)	G* (15°C, 10 Hz) (MPa)
10/20	12	68	98
20/30	20	62	66
35/50	35	54	37
50/70 (1)	49	49	43
50/70 (2)	58	50	20
70/100	81	46	16
160/220	175	40	8

Table 6-25: Stiffness of asphalt specimen in Colas study (Carbonneau 2012)

Grade of fresh binder	Modulus (MPa) of EME without RA	Void content (%) of EME without RA	Modulus (MPa) of EME with 30 % RA	Void content (%) of EME with 30 % RA	Linear extrapolation for modulus (MPa) of 100 % RA
10/20	19251	(4,9)	16303	(5,5)	9424
20/30	11833	(5,2)	11318	(5,7)	10116
35/50	7688	(5,2)	7876	(5,2)	8315
50/70 (1)	8222	(5,1)	8051	(5,8)	7652
50/70 (2)	3344	(5,3)	5255	(5,2)	9714
70/100	3578	(5,5)	5463	(3,8)	9861
160/220	1945	(5,7)	3536	(5,8)	7248

In the second study presented by Carbonneau (2012), asphalt containing RA only with a 50/70(1) pen bitumen (G* value of 43 MPa) was prepared. Asphalt mixture with 20, 30 and 40 % of RA (stiffness are presented in **Chyba! Nenalezen zdroj odkazů.**) were mixed.

There is not a large increase in the modulus value as the proportion of RA increases. The mixture with 30 % of RA even has a slightly lower modulus than the blend with 20 % of RA. Maybe reason can be found in deviation due to measurement uncertainty of the method (reproducibility, limit 95 %: R = 2740 MPa in EN 12697-26:2004) or in optimal ratio between fresh and aged binder.

The results of Colas studies show the contribution of the RA binder to the stiffness of the mixture. Thus, the RA binder is an integral part of the bituminous binder in the mixture. Even if it is not equally distributed it contributes to the mechanical properties of the asphalt mixture.

Table 6-26 – Stiffness of asphalt specimen in second Colas study (Carbonneau 2012)

Proportion of RA	20 % RA		30 % RA		40 % RA	
Test temperature (°C)	10	15	10	15	10	15
Air voids content (%)	5,9	5,9	5,8	5,8	5,4	5,4
Modulus 124 ms (MPa)	14322	10332	13682	8051	16655	10560

6.3.2.7 Paper 543 (Wojceich et al., 2010)

Table 6-27: Binder test results

Test method	Standard	Unit	B 70/100	B 50/70	PmB 25/55-55	PmB 50- 90 S
Penetration at 25 °C	EN 1426	mm/10	74	54	44	68
Softening point (RB)	EN 1427	°C	49,6	54,8	66,8	71,2
Fraass breaking point	EN 12593	°C	-19,5	-18,5	-14	-1 2
Kinematic viscosity 135°C	EN 12595	mm ² /s	416	596	2055	713
Dynamic viscosity at 60°C	EN 12596	Pa.s	181	528	5029	1405
Elastic recovery at 25 °C	EN 13398	%	–	–	88,9	99,3
Deformation energy at 10 °C	EN 13589 EN 13703	J/cm ²	–	–	9,1	4,3
Force at elongation at 10 °C	EN 13589 EN 13703	N	–	–	45,1	24,7
Elongation at break at 10 °C	–	cm	–	–	53,7	92,1
Deformation energy at 25 °C	EN 13589	–	–	–	3,6	2,2
Force at elongation at 25 °C	EN 13589 EN 13703	N	–	–	4,5	1,4
Elongation at break at 25 °C	–	cm	–	–	89,1	69,7

Table 6-28: Asphalt mixture characteristics

Test method	Standard	Unit	B 70/100	B 50/70	PmB 25/55-55	PmB 50- 90 S
Marshall stability (60°C)	–	N	11,6	14,7	19,0	12,9
Marshall flow (60°C)	–	Mm	3,2	3,7	3,8	3,7
Marshall stiffness (60°C)	EN 12697-34	N/mm	3,6	4,0	5,0	3,5
Stiffness modulus (20 °C, 1,28 Hz)	EN 12697-26	MPa	1274	2048	2112	1630
Rut depth at 60 °C after 10 000 cycles	EN 12697-22	%	7,4	2,9	2,4	2,3
Wheel tracking slope		µm/cycle	0,07	0,08	0,03	0,05
Horizontal micro-strain (10 °C, 20 Hz)	EN 12697-24	µdef	387,93	304,55	338,96	331,14
Cracking temperature	–	°C	-29,9	-25,5	-26,8	-27,8
Stress at failure	AASHTO TP10	MPa	4,23	4,03	4,80	4,82

Results of testing showed that asphalt mixture with softer type of binder (B 70/100) has lower Marshall stability value at 60 °C, lower stiffness modulus, lower resistance to permanent deformation but in the same time better fatigue and low temperature resistance in comparison to asphalt mixture with harder type of binder (B 50/70).

Binders with lower penetration (harder bitumen) showed higher stiffness modulus than binders with higher penetration (softer binder), i.e. AC-11 with B 50/70 and PmB 50/90 and PmB 25/55-55) has higher stiffness modulus than AC-11 with B 70/100. Good correlations were found between stiffness modulus of asphalt mixture at 200C and penetration of binders (see Figure 6-2).

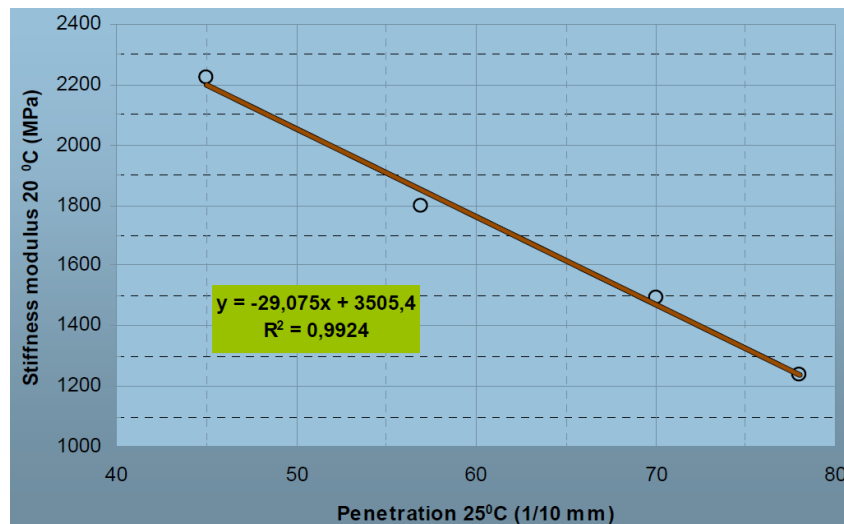


Figure 6-2 – Stiffness modulus of asphalt mixtures vs. penetration of binders

6.3.3 Bending Beam Rheometer (BBR)

No relevant papers found.

6.3.4 Direct Tensile Test (DTT)

No relevant papers found.

6.3.5 Needle penetration

6.3.5.1 Paper 024 (Olard et al., 2012)

Table 6-29: Performances of the materials with 4 % binder content

Binder	Penetration (1/10mm)	Softening Point (°C)	E (MPa) at 15 °C & 10 Hz	ϵ_6 (10^{-6}) at 10 °C & 25 Hz
35/50	38	53,5	16 500 at 2,7 % voids	89
35/50 + 2.5 % SBS	38	62,2	15 600 at 3,2 % voids	110
35/45	37	62,0	13 100 at 2,9 % voids	115
35/45 + 2.5 % SBS	33	71,0	13 700 at 2,5 % voids	130

6.3.5.2 Paper 031 (Nordgren and Olsson, 2012)

Table 6-30: Binder properties of 70/100 pen grade

Characteristic	Bitumen						
	1	2	3	4	5	6	7
Penetration (1/10 mm)	71	83	83	72	83	80	84
Softening point (°C)	47	46	46	46	46	47	46
Fraass breaking point (°C)	-16	-19	-18	-19	-18	-20	-19
Change of mass after RTFOT (%)	0,1	0,0	-0,2	0,1	0,0	0,0	-0,1
Retained penetration after RTFOT (%)	65	67	67	64	48	64	61
Softening point after RTFOT (°C)	51	52	52	51	52	52	51
Increased in softening point after RTFOT (°C)	4	5	5	5	6	5	5

Certain differences in stiffness modulus level at 10 °C between the mixtures were shown, but there was little or no effect from air voids content. Neither laboratory ageing at 60 °C for

50 days nor freeze/thaw conditioning showed any considerable effect on the stiffness modulus. However, after laboratory ageing at 60 °C for 50 days, the stiffness modulus level for asphalt containing Bitumens 1, 4 and 5 were about 2 500 MPa higher than for the rest of the mixtures (**Chyba! Nenalezen zdroj odkazů.**).

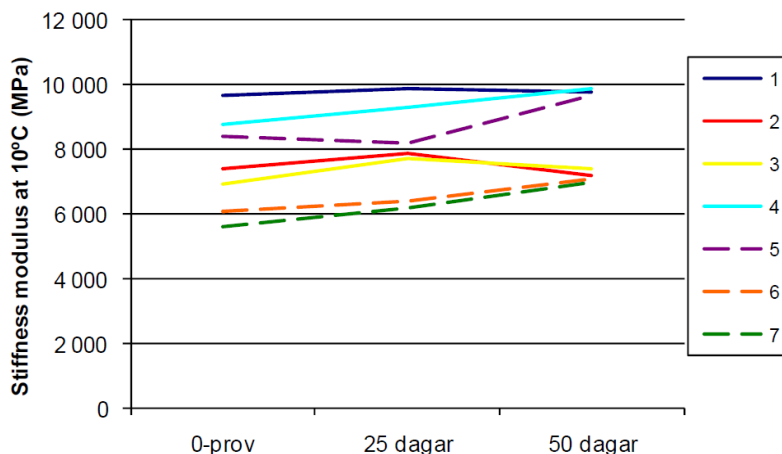


Figure 6-2: Stiffness modulus at 10°C after laboratory ageing at 60 °C

Six cores were drilled out from each mixture type on the road and stiffness modulus was determined, directly as well as after ITSr conditioning for 7 days. The conditioning only had a marginal decreasing effect on stiffness modulus values for all mixtures. In line with laboratory made specimens, the stiffness moduli of asphalt containing Bitumens 1, 4 and 5 were higher than for the remaining asphalts. The stiffness moduli for cores after 1 year in the road are shown in **Chyba! Nenalezen zdroj odkazů.**

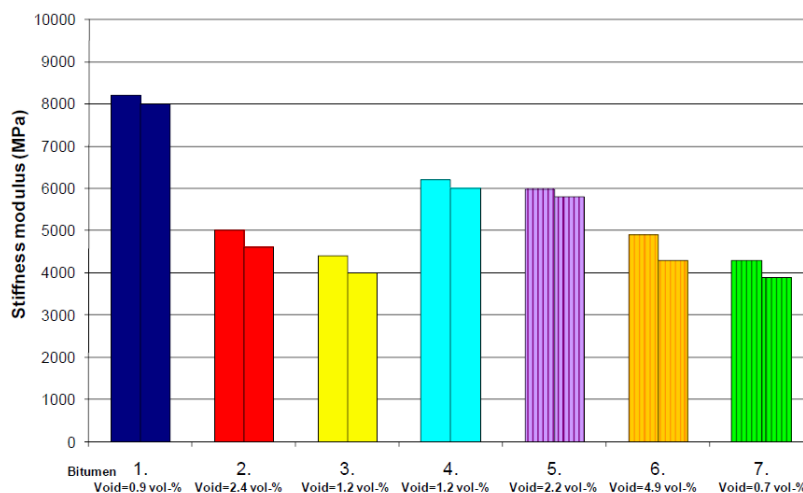


Figure 6-2: Stiffness moduli for cores after one year in the road

6.3.5.3 Paper 074 (de Visscher et al., 2008)

Table 6-317: Empirical characteristics of unaged binder

Binder	Pen (0,1 mm)	R&B (°C)
1	23	66,4
2	18	66,0
3	17	69,8
4	23	68,6

Table 6-32: Results for stiffness modulus

Type	Binder content (%)	Binder type	RA (%)	E* @ 15 °C & 10 Hz (MPa)	E* @ 30 °C & 10 Hz (MPa)
AC 0/14 (porphyry)	4,8	50/70	0	11 010 ± 1070	3 470 ± 700
High-mod. asphalt (porphyry)	5,7	10/15	0	14 770 ± 600	7 090 ± 600
High-mod. asphalt	5,5	3	0	12 740 ± 800	5 340 ± 700
High-mod. asphalt	5,5	3	0	11 860 ± 800	4 740 ± 200
High-mod. asphalt	5,5	3	40	12 830*	5 570*
AC 0/20	4,6	50/70	40	12 860 ± 1700	3 300 ± 400
High-mod. asphalt	6,1	1	0	11 470 ± 800	4 690 ± 80
High-mod. asphalt	4,9	1	0	13 490 ± 300	5 690 ± 600
High-mod. asphalt	5,5	1	0	12 350 ± 600	4 680 ± 600
High-mod. asphalt	5,3	1	0	13 620 ± 700	5 050 ± 100
High-mod. asphalt	5,5	3	0	14 550 ± 30	5 670 ± 300
High-mod. asphalt	5,5	2	0	14 600 ± 50	5 710 ± 700
High-mod. asphalt	5,5	4	0	14 270 ± 300	5 920 ± 400
High-mod. asphalt	5,5	1	25	11 950 ± 100	5 420 ± 150
High-mod. asphalt	5,5	1	25	12 070 ± 200	5 740 ± 700
High-mod. asphalt	5,3	1	25	11 990*	4 410*

The uncertainties represent the differences between both tested samples. * Only one sample tested

6.3.5.4 Paper 171 (Mogawer et al., 2012)

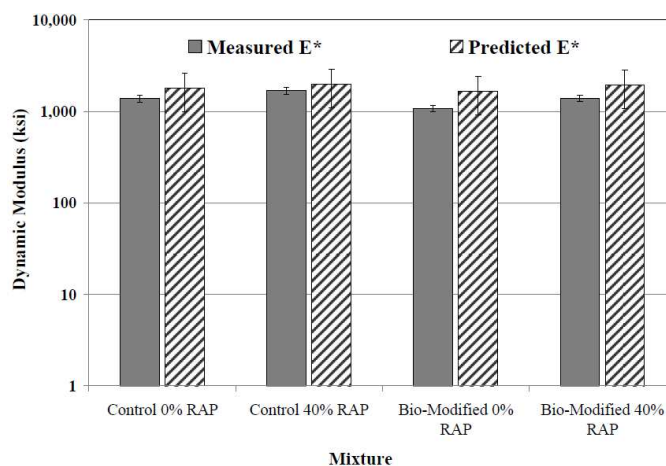


Figure 6-2(a): Degree of blending at a temperature 4 °C and frequency of 10 Hz

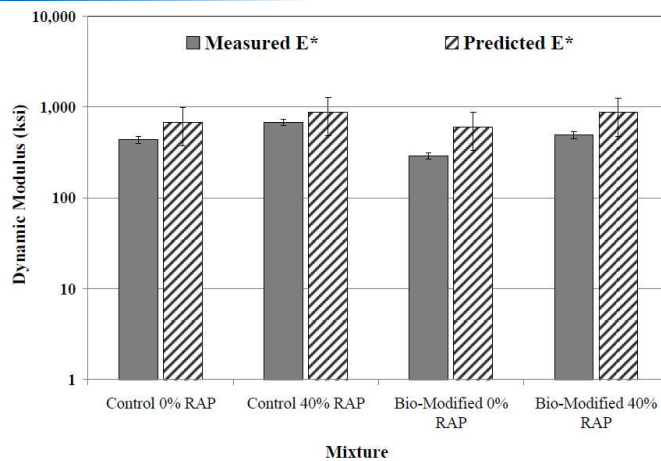


Figure 6-2(b): Degree of blending at a temperature 20 °C and frequency of 10 Hz

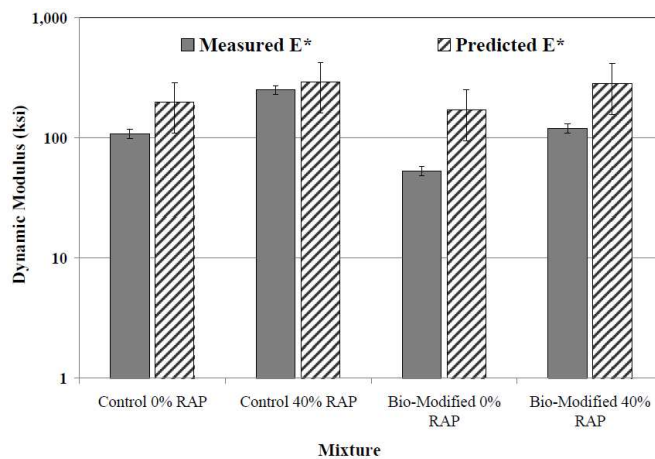


Figure 6-2(c): Degree of blending at a temperature 35 °C and frequency of 10 Hz

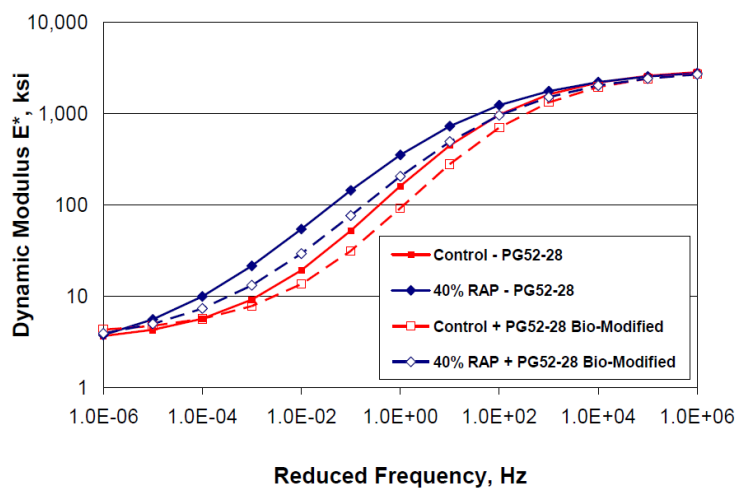


Figure 6-2 – Mixture master curve comparison

6.3.5.5 Paper 487 (Bagampadde et al., 2006)

Two specimens of each asphalt concrete mix were used for complex modulus tests. **Chyba! Nenalezen zdroj odkazů.** shows dynamic modulus and phase angle master curves, respectively, obtained from the three isothermal (at 0 °C; 10 °C and 20 °C) frequency sweeps (0,1–40) Hz. The results indicate certain differences between the mixtures. Adding 6 % of commercial wax increased the modulus and decreased the phase angle, while adding

polyphosphoric acid showed a minor influence. Similar stiffening effects were shown for the binders using DMA (**Chyba! Nenalezen zdroj odkazů.**). Throughout the study, 10 °C was used as reference temperature.

Table 6-33: Conventional rheological characterisation of binders

Binder	Penetration at 25 °C (mm/10)	Softening point (°C)	Dynamic viscosity at 60 °C (Pas)	Kinematic viscosity at 135 °C (mm ² /s)	Pia	PVNb	Fraass breaking point (°C)	Force ductility at 5 °C	
								Max. load (N)	Deformation energy (J)
NB	185	39	52	180	-1,1	-0,8	-	-	-
After mixing treatment									
NB	168	39	55	190	1,5	-0,8	-19	24	1,0
+3 % S	91	64	116	158	3,6	-1,7	-18	55	1,5
+6 % S	71	90	9280	133	6,5	-2,2	-15	98	1,9
+3 % PW	128	47	114	196	0,7	-1,1	-23	32	1,1
+6 % PW	97	62	296	221	3,4	-1,2	-23	40	1,4
+3 % MW	120	64	101	158	4,6	-1,5	-19	56	1,3
+6 % MW	111	87	158	131	7,8	-1,8	-17	75	1,5
+3 % SW	279	35	25	138	-1,1	-0,8	-19	27	0,9
+6 % SW	315	35	12	103	0,1	-1,2	-22	47	0,9
+0,4 % PPA	152	41	74	223	-1,0	-0,7	-20	23	1,0
+1 % PPA	120	44	120	290	0,6	-0,5	-23	25	1,1

Table 6-34: Effects of adding different waxes and PPA on BBR low temperature parameters

Binder	S at -25 °C (MPa)	m at -25 °C	S at -20 °C (MPa)	m at -20 °C	LST (°C)	LmT (°C)	PHI (%)
NB	390,5	0,331	118,0	0,443	-23,3	-26,4	30
+3 % S	452,0	0,297	173,5	0,406	-22,3	-24,9	24
+6 % S	504,5	0,270	219,5	0,338	-21,4	-22,8	24
+3 % PW	416,5	0,316	132,5	0,433	-23,0	-25,7	20
+6 % PW	416,5	0,313	145,5	0,418	-22,9	-25,6	20
+3 % MW	388,5	0,317	141,5	0,392	-23,2	-26,1	34
+6 % MW	421,0	0,275	187,5	0,335	-22,4	-22,9	33
+3 % SW	312,0	0,350	125,0	0,435	-24,7	-27,9	55
+6 % SW	312,5	0,322	143,5	0,344	-24,6	-30,0	56
+0,4 % PPA	372,0	0,343	113,5	0,452	-23,6	-27,0	33
+1 % PPA	334,5	0,350	106,5	0,451	-24,2	-27,5	34

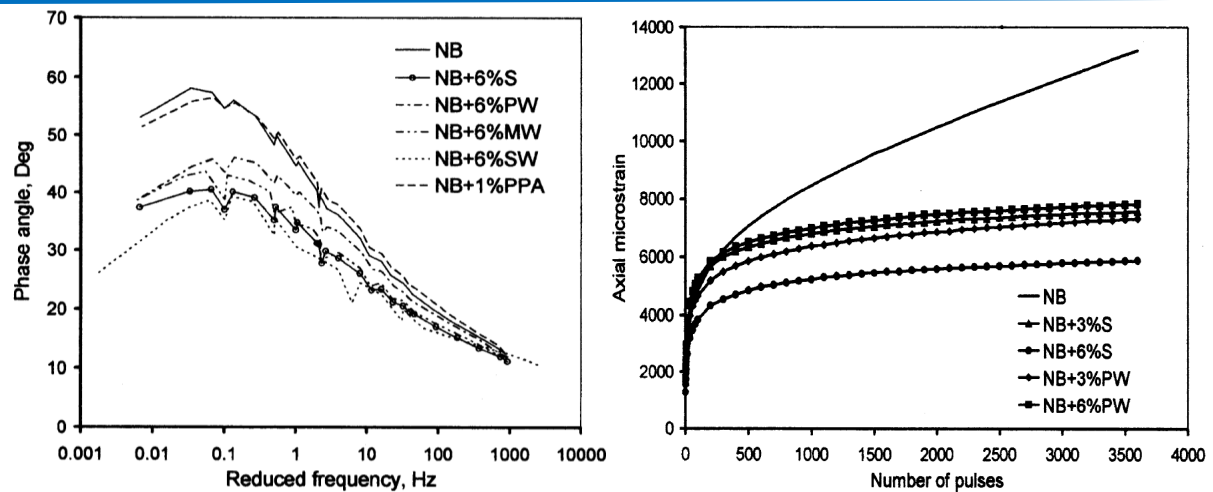


Figure 6-2: Dynamic modulus and phase angle master curves at reference temperature 10 °C

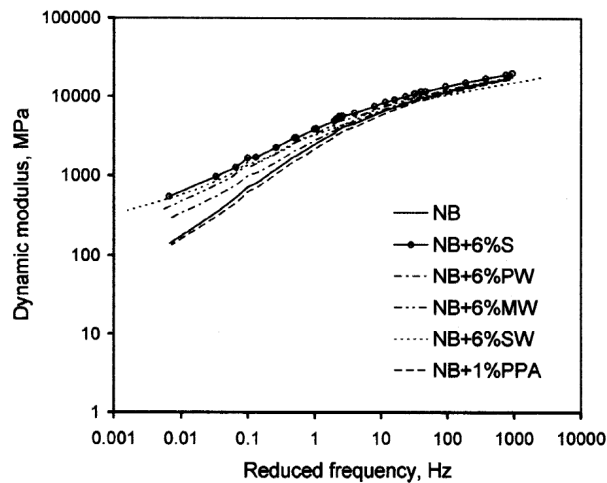


Figure 6-2: Dynamic creep test on asphalt mixtures containing bitumen NB and different levels of wax S and wax PW

6.3.5.6 Paper 504 (Sybilski et al., 2009)

In **Chyba! Nenalezen zdroj odkazů.**, a selection of binder and asphalt mix tests are presented. The asphalt test results were fitted with linear regression to the results of the binder tests. The regression coefficients for these correlations are presented in **Chyba! Nenalezen zdroj odkazů.**

Table 6-35: Selection of binder and asphalt mixture properties

Test	Binder						
	A	B	C	D	E	F	G
Penetration (mm/10)	82	30	29	68	44	74	54
Penetration mod. I (mm/10)	147	43	42	104	66	141	88
Softening point (°C)	47,6	62,2	67,6	71,2	66,8	49,6	54,8
Fraass Break Point (°C)	-17,5	-9,5	-10	-12	-14	-19,5	-18,5
Kinematic viscosity (mm ² /s)	599	1370	2234	713	2055	416	596
Dynamic viscosity (Pas)	271	2697	5184	1405	5029	181	528
Penetration/RTFOT (mm/10)	53	23	25	44	32	51	41
Soft. point/RTFOT (°C)	53,4	68,4	73,6	75,4	75,2	56,2	60,8
Dyn. visc./RTFOT (Pas)	666	7819	15758	1902	8886	825	2373
Elastic recovery (%)	46	–	74	99	89	–	–
Deformation energy II (J/cm ²)	2,2	–	12,6	4,3	9,1	–	–
Deformation energy III (J/cm ²)	0,1	–	1,8	2,2	3,6	–	–
Cone Plate viscosity IV (Pas)	227	2022	3219	1407	2624	141	460
Cone Plate viscosity V (Pas)	0,219	0,587	0,734	0,286	0,691	0,133	0,176
Equiviscous temp. VI (°C)	145	162	167	151	168	138	144
Coaxial cyl. viscosity VII (Pas)	1,69	4,74	6,93	1,89	5,42	1,08	1,97
Coaxial cyl. viscosity VIII (Pas)	0,43	0,80	1,26	0,42	1,17	0,21	0,38
Asphalt test on SMA/basalts							
Wheel tracking rut (mm)	2,45	1,86	1,53	1,54	1,33	2,48	1,98
IT-CY stiffness @ 15 °C (MPa)	1657	4413	4031	2174	3218	1369	2279
Asphalt test on AC/basalts							
IT-CY stiffness @ 15 °C (MPa)	1974	4163	4121	2171	2823	1696	3043
Asphalt test on AC/limestone							
IT-CY stiffness @ 15 °C (MPa)	2494	9132	5297	4320	4572	2225	4934
Asphalt test on PA/basalts							
IT-CY stiffness @ 15 °C (MPa)	838	2670	2889	1435	1975	969	1987

I Penetration at 35 °C with total weight of 50 g

II At 10 °C and speed 50 mm/min

III At 25 °C and speed 50 mm/min

IV At 60 °C

V At 150 °C

VI According to ASTM D 1559 (2382)

VII At 120°C

VIII At 150 °C

The number of binder tested is limited so the data can essentially be used to corroborate for contradict proposed correlations made in other studies. From **Chyba! Nenalezen zdroj odkazů.** it seems to be a fairly good correlation between the wheel tracking rut depth and the softening point even though there are four polymer modified binders in the study. These results are in contrast with the conclusion drawn in the BitVal report, but in line with the current European specification for polymer modified bitumen.

Table 6-36: Correlation coefficient (r^2) in linear regression between of binder and asphalt test results

Binder test	Asphalt test			
	SMA/wheel tracking	AC(basalts)/stiff.	AC(limest.)/stiff.	PA(basalts)/stiff.
Penetration	0,43	0,88	0,67	0,97
Penetration mod. I	0,58	0,87	0,70	0,96
Softening point	0,90	0,23	0,22	0,37
Fraass Break Point	0,5	0,55	0,55	0,57
Kinematic viscosity	0,57	0,50	0,19	0,58
Dynamic viscosity	0,66	0,44	0,18	0,56
Penetration/RTFOT	0,53	0,89	0,72	0,94
Soft. point/RTFOT	0,94	0,25	0,23	0,40
Dyn. visc./RTFOT	0,44	0,67	0,25	0,75
Elastic recovery	0,47	0,00	0,03	0,00
Deformation energy II	0,48	0,93	0,78	0,97
Deformation energy III	0,86	0,08	0,50	0,23
Cone Plate viscosity IV	0,72	0,54	0,30	0,66
Cone Plate viscosity V	0,57	0,57	0,34	0,63
Ekviscous temp. VI	0,68	0,54	0,36	0,61
Coaxial cyl. visk. VII	0,50	0,67	0,32	0,73
Coaxial cyl. visk. VIII	0,55	0,51	0,20	0,58

The stiffness modulus correlates fairly well with penetration tests, but the proportionality constants are different for different mixes (data not shown). The data in **Chyba! Nenalezen zdroj odkazů.** suggest that the deformation energy measured at 10 °C could be a candidate for a performance related test vis à vis the stiffness modulus of asphalt mixes, but the data is very limited.

6.3.6 PG grading

6.3.6.1 Paper 098 (Li et al., 2011)

The high temperatures PG grades of the four modified binders were determined from the Superpave DSR rheological tests. The experimental results for the original, RTFO aged and extracted binder are plotted together for comparison in **Chyba! Nenalezen zdroj odkazů.** The test results show that all four of the binders were similar in stiffness as sampled from the tank and graded as PG 58 with the results from RTFO. Before RTFO aging, the binders' $|G^*|/\sin\delta$ values ranged between 1,52 kPa and 1,71 kPa at 58 °C and after RTFO between 2,09 and 3,90 at 64 °C. When only the properties of the extracted and recovered binder from field mix are considered, the PPA-only and PPA + SBS binders passed PG 70 while the SBS-only and PPA + Elvaloy binder passed PG 64.

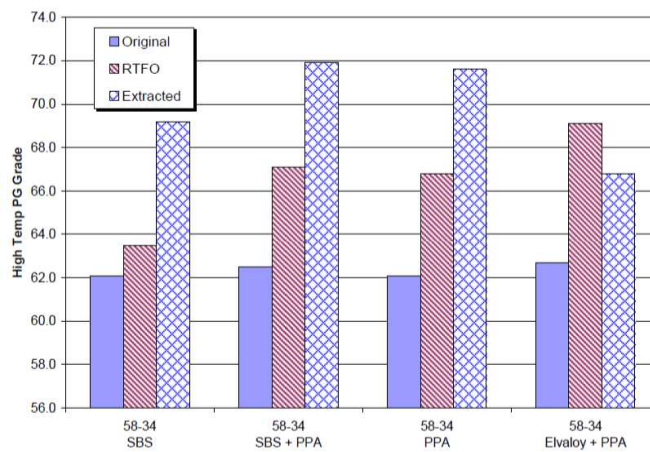


Figure 6-2: High temperature PG grade

The low temperature PG grades of the binders sampled at the time of construction are shown in **Chyba! Nenalezen zdroj odkazů..** All four binders after PAV aging achieved a PG grade of -34. The recovered binders also showed similar low PG temperatures passing PG -34 before PAV aging. Three of the four binders exhibited slightly lower (cooler) PG grades than the laboratory PAV aged original samples. However, different low PG temperatures were obtained when the recovered binders were PAV aged. Specifically, the PPA + Elvaloy and SBS-only binders retained their -34 grade whereas the PPA-only and PPA + SBS binders stiffened enough to have a low PG temperature of -28.

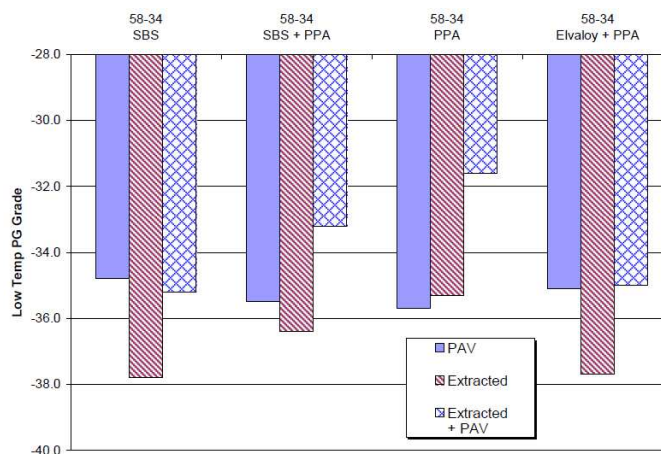


Figure 6-2: Low temperature PG grade

Dynamic modulus and phase angle were tested on three replicates. The dynamic modulus data were then used to build master curves by utilizing a sigmoidal model. The master curves for all four mixtures are shown in **Chyba! Nenalezen zdroj odkazů..** It can be seen that the mixture made with PPA+Elvaloy modified asphalt has the lowest dynamic modulus in the high frequency/low temperature region. However, this same mixture showed the highest dynamic modulus at low frequency/high temperature region by a slight amount. The other three mixtures present similar dynamic modulus at the high frequency/low temperature region. At the low frequency/high temperature region the mixture with PPA-only modification barely has the lowest dynamic modulus. When these test dynamic modulus results are taken into account along with the difference in laboratory RTFO and extracted binder properties, one could infer that the Elvaloy+PPA mix was produced under different conditions (likely lower plant production temperatures) than the other three mixes. This is acknowledged and

not entirely unreasonable given the three other mixes were produced within a three day period about 6 weeks earlier than the Elvaloy+PPA mix in cell 77.

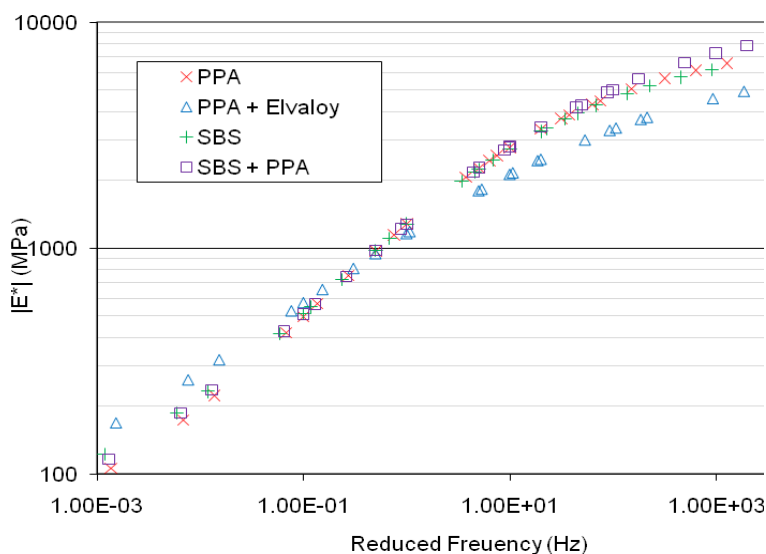


Figure 6-2: Master curve of the dynamic modulus

6.3.6.2 Paper 111 (Mogawer *et al.*, 2011)

Table 6-37: Extracted binder grading results

Mixture	Continuous grade	PG Grade
Control	62,2 - 31,2	58-28
40 % RA	72,4 – 27,9	70-22
5 % RAS	65,6 – 32,2	64-28
35 % RA + 5 % RAS	77,5 – 25,9	76-22
Control + 1 % WMA	56,4 – 32,6	52-28
40 % RA + 1 % WMA	64,2 – 30,9	64-28
5 % RAS + 1 % WMA	60,9 – 32,7	58-28
35 % RA + 5 % RAS + 1 % WMA	71,1 – 27,9	70-22

Test specimens were placed in the Asphalt Mixture Performance Test (AMPT) device and subjected to a sinusoidal (haversine) axial compressive stress at the different temperatures and frequencies. The resultant recoverable axial strain (peak-to-peak) was measured. From this data the dynamic modulus was calculated. Three replicate dynamic modulus specimens were fabricated in the SGC for each mixture at a target air void level of $7,0 \pm 1,0\%$. Each specimen was subsequently prepared for dynamic modulus testing in AMPT in accordance with AASHTO TP62 “Standard Method of Test for Determining Dynamic Modulus of Hot-Mix Asphalt (HMA)” and the draft specification provided in NCHRP Report 614 “Proposed Standard Practice for Preparation of Cylindrical Performance Test Specimens Using the Superpave Gyrotory Compactor”. Each specimen was tested at temperatures of 4 °C, 20 °C and 35 °C and loading frequencies of 10 Hz, 1 Hz, 0,1 Hz and 0,01 Hz (35 °C only). The results of the dynamic modulus testing are shown in **Chyba! Nenalezen zdroj odkazů.**(a) to (c).

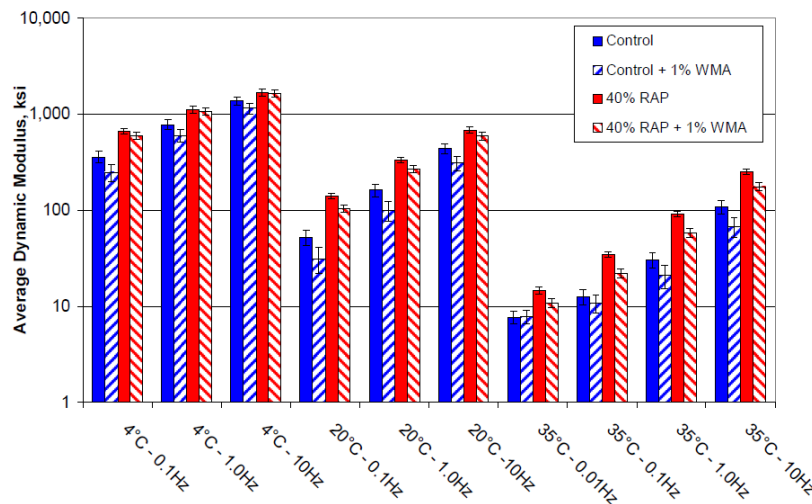


Figure 6-2(a): Dynamic modulus comparison of control and 40 % RA

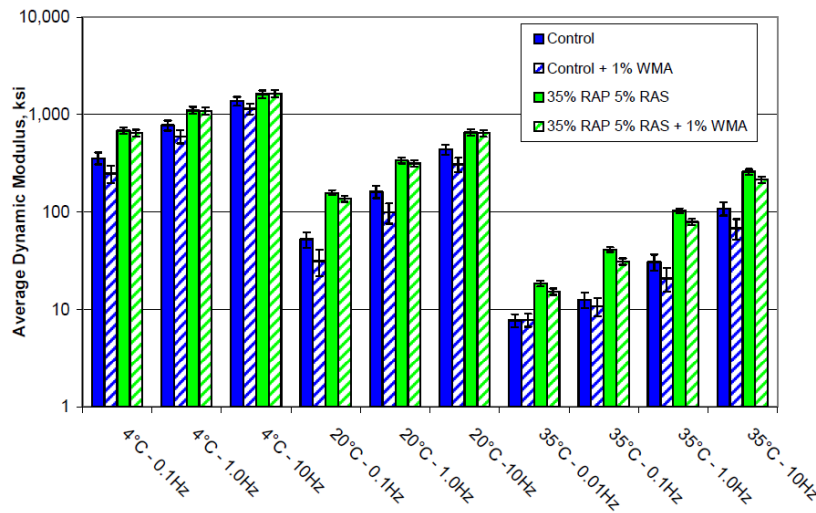


Figure 6-2(b): Dynamic modulus comparison of control and 35 % RA + 5 % RAS

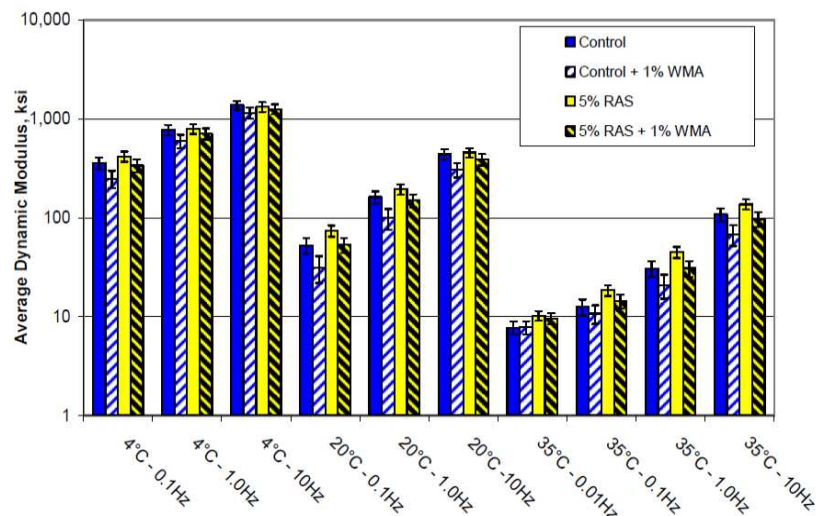


Figure 6-2(c): Dynamic modulus comparison of control and 5 % RAS

The error bars on the dynamic modulus results shown in **Chyba! Nenalezen zdroj odkazů.**(a) to (c) are 95 % confidence intervals. Error bars that overlap indicate that the modulus values are not significantly different. The results indicated, for the majority, that the addition of 40 % RA and 35 % + 5 % RAS increased the mixture stiffness significantly as compared to the control. The 5 % RAS mixture did not show a significant increase in mixture stiffness. This may be attributed to less percent binder replaced for this mixture. Comparing the results for the mixtures with and without the WMA technology indicated, for all mixture tested, that the mixture stiffness decreased for the mixtures incorporating the WMA technology. This is likely a result of less aging due to reduced mixing and compaction (aging) temperatures.

6.3.6.3 Paper 144 (Haij et al., 2012)

The Hirsch model provided reasonable estimates to back-calculate binder shear modulus at high temperature from the measured mixture dynamic modulus. However, some difficulties exist in estimating the high temperature PG grade, particularly when dealing with soft binders like the ones used in this study. The difficulties arise from; first, the difference in temperatures between the dynamic modulus testing and PG grading temperatures; and second, the limitation in the formulation of the Hirsch model at high temperatures and low frequencies. Subsequently, in order to get reasonable estimates, the binder modulus at high temperature was estimated from the back-calculated moduli (using the Hirsch model) at lower temperatures from the mixture dynamic modulus. The modified Huet-Sayegh model was used to estimate the high PG of the asphalt binders from the measured dynamic modulus of the corresponding mixtures. This approach resulted in high critical temperatures that are, respectively, similar and higher than those determined for the recovered binders and using the Hirsch model. The data showed good correlation between the characteristic times of the binders and mixtures, hence, allowing for the determination of the binder properties from the measured dynamic modulus of the mixture. However, this relationship was highly dependent on temperature and need to be verified with other types of mixtures.

6.3.6.4 Paper 153 (Willia et al., 2012)

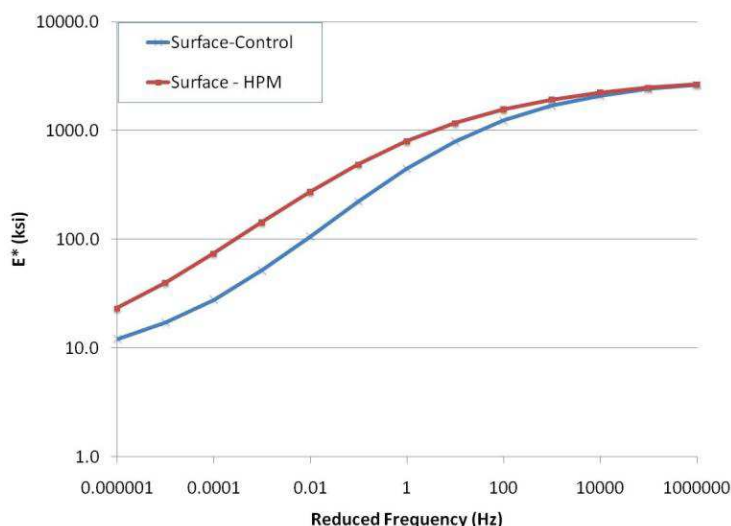


Figure 6-2: Dynamic modulus results for 9,5 mm NMAS mixtures

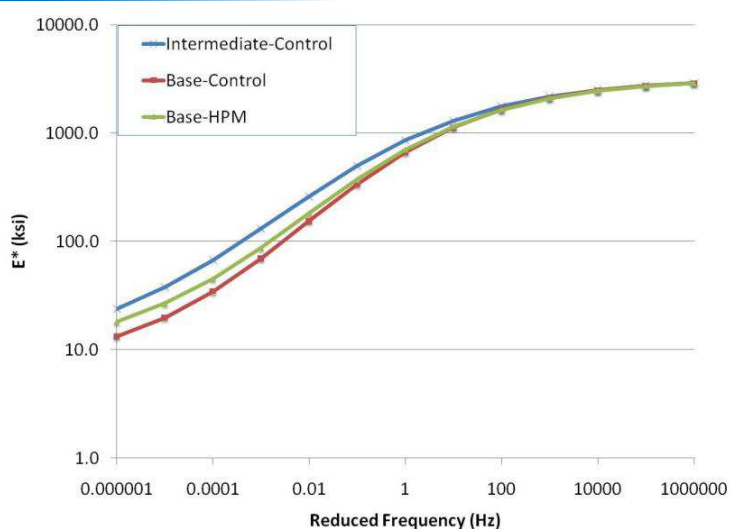


Figure 6-2 Dynamic modulus results for 19 mm NMAS mixtures

Table 6-38: Used grades of bituminous binders

Mixture	True Grade	Performance Grade
9,5 mm Control	81,7 – 24,7	76 – 22
19,0 mm Control	69,5 – 26,0	64 – 22
9,5 mm HPM	93,5 – 26,4	88 – 22
19,0 mm HPM	93,5 – 26,4	88 – 22

6.3.6.5 Paper 171 (Mogawer et al., 2012)

Table 6-39: Performance Grade binder testing results

Property	Standard	PG52-28 Virgin	PG52-28 Bio-Modified
PG Grade	–	PG58-28	PG52-28
Continuous Grade	–	59,4-30,4	56,8-31,3
Viscosity at 135 °C (Pa·S)	AASHTO T316	0,242	0,220
Viscosity at 165 °C (Pa·S)	AASHTO T316	0,077	0,067
G*/sinδ (kPa) Original	AASHTO T315	1,194 @ 58 °C 0,563 @ 64 °C	1,854 @ 52 °C 0,851 @ 58 °C
G*/sinδ (kPa) – RTFO Residue	AASHTO T315	3,028 @ 58 °C 1,360 @ 64 °C	2,347 @ 58 °C 1,085 @ 64 °C
G* sinδ (kPa) – PAV Residue	AASHTO T315	6 210 @ 13 °C 4 547 @ 16 °C	6 006 @ 13 °C 3 969 @ 16 °C
Creep Stiffness @ 60s S (MPa)	AASHTO T313	199 @ -18 °C 411 @ -24 °C	181 @ -18 °C 458 @ -24 °C
Slope @ 60s m-value	AASHTO T313	0,321 @ -18 °C 0,268 @ -24 °C	0,378 @ -18 °C 0,292 @ -24 °C

6.3.6.6 Paper 227 (Tarefder *et al.*, 2007)

The effect of binder PG on modulus at different temperature is depicted in Table 6-40 and Table 6-417. Modulus value does not change significantly due to polymer modification. There are cases where the unmodified binders show higher modulus. In fact, the performance of the modified binder, PG 70-28 will exceed the performance of an unmodified binder, PG 64-22 when tested at high temperatures such as 64°C or above. This study concludes that PG does not affect the modulus at low to medium temperature.

Table 6-426: Modulus values of laboratory mixtures

Test	PG grade	Binder content (%)	Air voids content (%)	Modulus (GPa)		
				0 °C	23 °C	40 °C
1	PG 64-22	4,6	6,5	80,73	25,29	3,08
2	PG 64-22	4,6	3,4	68,56	29,20	14,70
3	PG 64-22	5,1	7,6	74,85	4,23	2,15
4	PG 64-22	5,1	4,5	37,79	5,99	3,09
5	PG 64-22	5,6	3,1	83,07	13,24	7,44
6	PG 64-22	5,6	10,1	33,97	19,47	16,57
7	PG 70-28	4,9	5,5	79,80	9,81	5,21
8	PG 70-28	4,9	7,4	37,71	6,04	2,77
9	PG 70-28	5,4	4,7	80,26	8,51	2,53
10	PG 70-28	5,4	4,2	36,58	22,07	17,72
11	PG 70-28	5,9	12,1	8,71	4,36	2,91
12	PG 70-28	5,9	8,6	9,11	6,21	4,76

Table 6-43: Modulus values of plant mixtures

Test	PG grade	Binder content (%)	Air voids content (%)	Gradation	Max, aggregate size (mm)	Modulus @ 23°C (GPa)
1	PG 64-22	4,6	7,1	ARZ	25	8,67
2	PG 64-22	4,8	6,6	BRZ	19	4,60
3	PG 64-22	5,6	6,9	ARZ	19	12,90
4	PG 64-22	6,3	7,2	TRZ	12,5	9,87
5	PG 70-28	4,9	6,6	TRZ	19	9,20
6	PG 70-28	3,8	7,0	ARZ	25	15,80
7	PG 70-28	4,1	6,3	ARZ	25	6,94
8	PG 70-28	5,2	7,1	ARZ	19	22,60
9	PG 70-28	4,5	6,8	ARZ	19	20,50
10	PG 70-28	4,7	7,0	ARZ	19	6,92

ARZ = above the restricted zone, BRZ = below the restricted zone, TRZ = through the restricted zone

6.3.6.7 Paper 235 (Azari et al., 2008)

Two different structures were considered. One had HMA thickness of 100 mm with base layer of 560 mm and the other had HMA thickness of 150 mm and base layer of 510 mm. Both structures were placed on AASHTO A-4 subgrade soil for each of the six binders listed in **Chyba! Nenalezen zdroj odkazů.**

Table 6-44: Binder types and HMA layer thickness in ALF experiment

Binder	Binder abbreviation	Lane No.	HMA thickness (mm)	PG grade	Binder description
PG 70-22	Control	2	100	70-22	An unmodified PG 70-22 asphalt binder (considered as the Control)
Air Blown	AB	3	100	70-28	An air-blown asphalt binder
SBS LG	SBSLG	4	100	70-28	Styrene-Butadiene-Styrene modified asphalt binder with linear grafting
CR-TB	CR-TB	5	100	76-28	A terminal-blend crumb rubber
Terpolymer	Elvaloy	6	100	70-28	An ethylene terpolymer binder
PG 70-22	Control	8	150	70-22	An unmodified PG 70-22 asphalt binder (considered as the Control)
SBS 64-40	SBS64	9	150	70-34	SB and SBS blended binder
Air Blown	AB	10	150	70-28	An air-blown asphalt binder
SBS LG	SBSLG	11	150	70-28	Styrene-Butadiene-Styrene modified asphalt binder with linear grafting
Terpolymer	Elvaloy	12	150	70-28	An ethylene terpolymer binder

MEPDG software runs were performed at two levels; level 1 and level 3, At level 1, SPT measured E^* values were entered for mix stiffness calculations. The SPT testing for different binders were available for different temperature and frequencies. These values were averaged for all specimen types (LP, PP and FC) and entered into the software for mix stiffness. Because the maximum temperature at which the samples were tested was 58 °C, MEPDG internally extrapolates the data to calculate stiffness at the test temperature of 64 °C (**Chyba! Nenalezen zdroj odkazů.**).

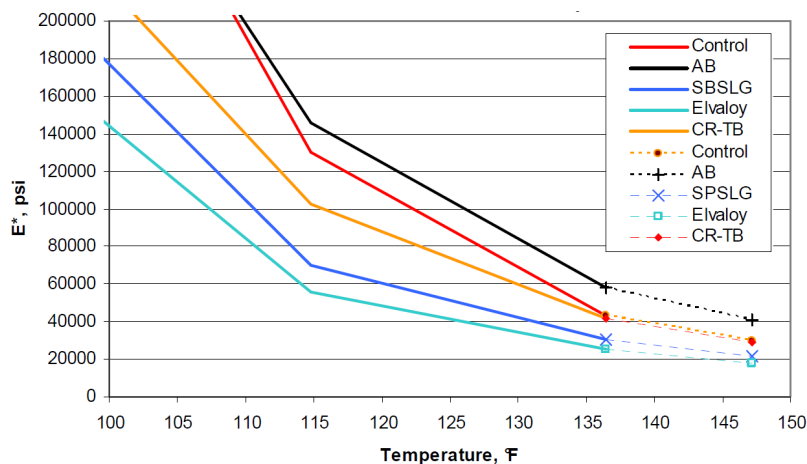


Figure 6-2 – Extrapolation of stiffness data to estimate stiffness at 64 °C

6.3.6.8 Paper 330 (Bower et al., 2014)

Table 6-45: Performance Grades of recovered binders

Modifier	Original PG grade	Recovered PG grade	
		HMA	WMA
Aquablack™	64-28	70-22 (73,5-22,2)	70-22 (71,9-22,6)
Sasobit®	76-28	76-22 (80,6-24,7)	76-22 (80,8-22,5)
Gencor®	64-28	70-22 (74,2-23,9)	70-22 (71,2-22,4)
Water injection	64-28	70-22 (75,6-24,7)	70-22 (70,7-26,7)

Note: The PGs in the parenthesis indicate the continuous PG grades

The WMA binders exhibit consistently lower complex shear modulus values and less resistance to fatigue and rutting than the HMA binders. For thermal cracking, no difference is evident between the water-based foaming WMA binders and their corresponding HMA binders. The Sasobit® binder shows better resistance to thermal cracking than the HMA binder.

Table 6-46: Summary of binder test results

Modifier	G*	Fatigue	Thermal cracking	Rutting
Aquablack™	-	-	=	-
Sasobit®	-	-	+	=
Gencor®	-	-	=	-
Water injection	-	-	=	-

- = No differences between the WMA (or WMA binder) and HMA (or HMA binder)
- The performance of the WMA is adversely affected by the WMA technology
- + The performance of the WMA is positively affected by the WMA technology

Chyba! Nenalezen zdroj odkazů.(a) to (d) presents the binder's complex modulus G* master curves at the reference temperature for each modifier. Analysis of variance (ANOVA) statistical analysis was conducted to aid in evaluating whether there are significant differences in G* between HMA and WMA binder. All four WMA binder samples have significantly lower complex shear modulus values than their corresponding HMA binder samples (p-value < 9 0,05), which may be due to the lower production temperatures and reduced aging for WMA binders.

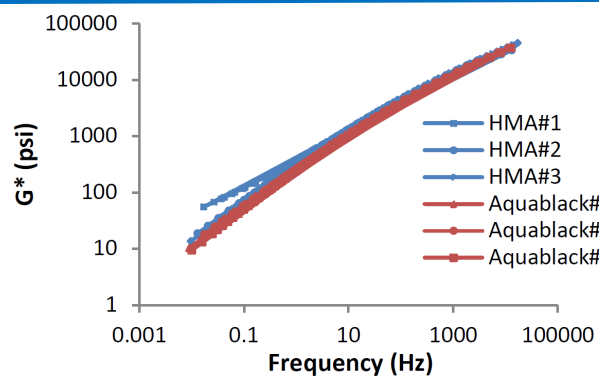


Figure 6-2(a): G* modulus master curve at 25°C with Aquablack™ (p-value = 0,004)

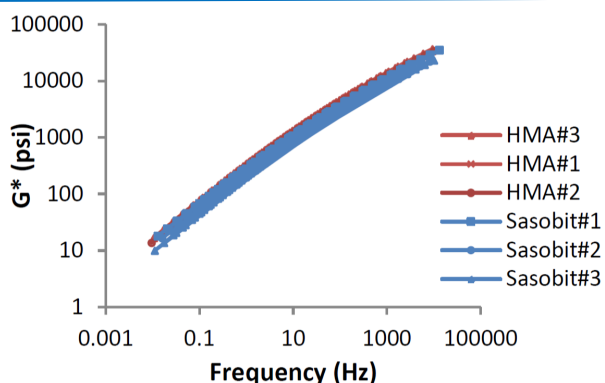


Figure 6-2(b): G* modulus master curve at 25°C with Sasobit® (p-value = 0,000)

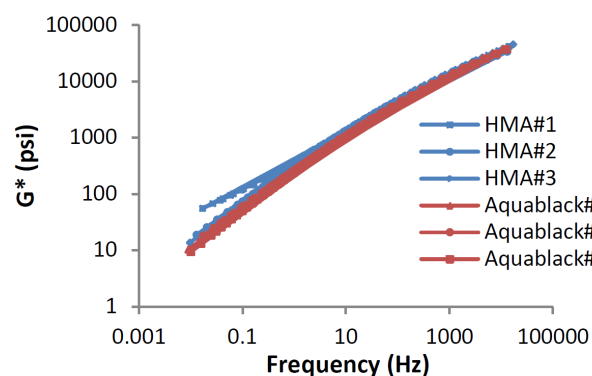


Figure 6-2(c): G* modulus master curve at 25°C with Gencor® (p-value = 0,047)

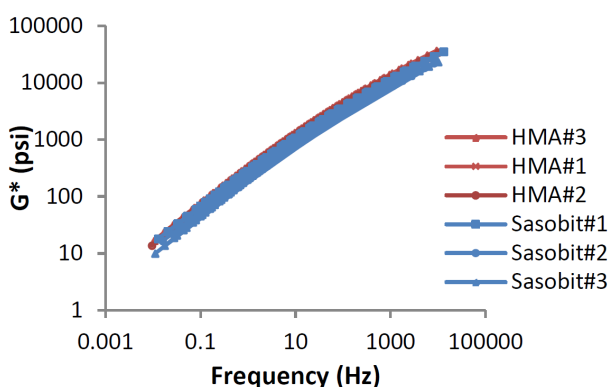


Figure 6-2(d): G* modulus master curve at 25°C with water Injection (p-value = 0,025)

As shown in **Chyba! Nenalezen zdroj odkazů.**(a) to (d), the IDT dynamic modulus master curves for each HMA and WMA mixture pair are similar. However, based on p-value from ANOVA statistical analysis, the dynamic modulus values of the Aquablack™ mixture are significantly lower than those of the HMA mixture, indicating that the Aquablack™ samples are not as strong as the HMA control samples. No statistically significant difference in dynamic modulus values was found between the Sasobit®, Gencor® and water injection mixtures and their corresponding HMA control mixtures. It should be noted that the Aquablack™ mixture has only been in place for one year as of the time of coring, whereas the other WMA mixtures were produced two or three years prior to the time of testing and this value could change with time.

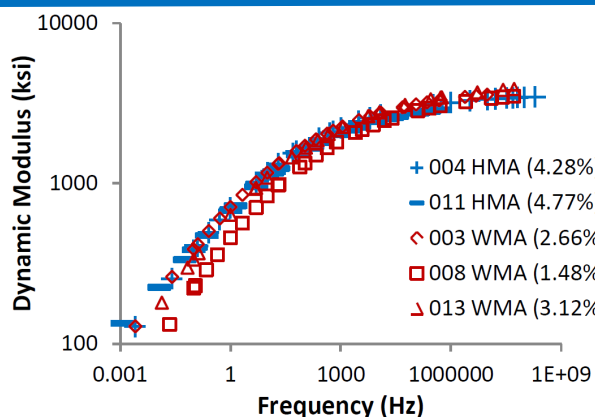


Figure 6-2(a): Dynamic modulus master curves at 20 °C with Aquablack™ (p-value = 0,00)

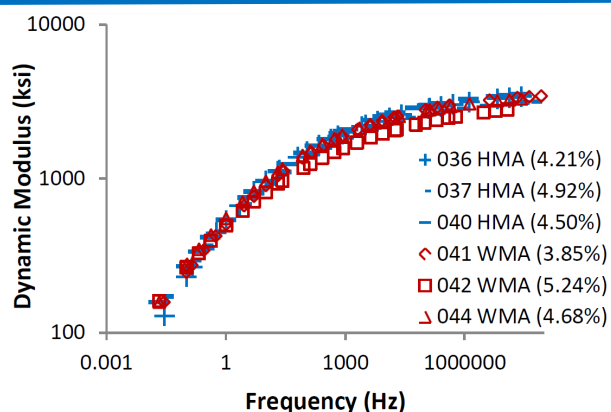


Figure 6-2(b): Dynamic modulus master curves at 20 °C with Sasobit® (p-value = 0,58)

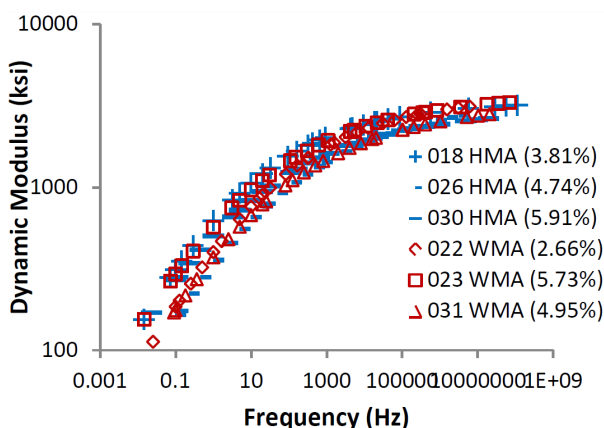


Figure 6-2(c): Dynamic modulus master curves at 20 °C with Gencor® (p-value = 0,96)

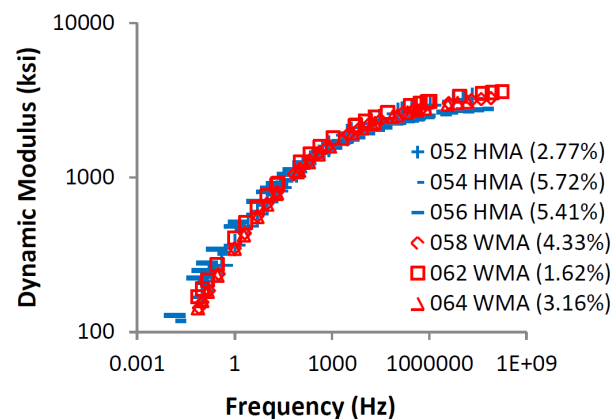


Figure 6-2(d): Dynamic modulus master curves at 20 °C with water Injection (p-value = 0,35)

NOTE: The numbers in parenthesis indicate the air voids of specimen.

6.3.6.9 Paper 456 (Bennert and Martin, 2010)

Table 6-47: Continuous PG grade of binders

Binder type	Continuous PG grade
Neat	PG68,6-23,4 (23,4)
SBS+PPA	PG76,2-25,7 (22,0)
SBS Only	PG76,8-25,2 (21,1)

Dynamic modulus and phase angle data were measured and collected in uniaxial compression following the method outlined in AASHTO TP79. The data were collected at three temperatures; 4 °C; 20 °C and 35 °C (for the neat asphalt binder only) and 45 °C (for both modified asphalt binders), using loading frequencies of 25, 10, 5, 1, 0,5, 0,1, and 0,01 Hz. Samples were tested in triplicate after short-term and long-term following the procedures outlined in AASHTO R30.

The collected modulus values of the varying temperatures and loading frequencies were used to develop Dynamic modulus master stiffness curves and temperature shift factors

using numerical optimisation (AASHTO TP79). The reference temperature used for the generation of the master curves and the shift factors was 20 °C.

The resultant stiffness master curves for the short-term (STOA) and long-term aged (LTOA) samples are shown in **Chyba! Nenalezen zdroj odkazů.**(a) and (b). The short-term aged results in **Chyba! Nenalezen zdroj odkazů.**(a) show that the SBS+PPA modified bitumen obtained higher modulus values at the lower loading frequencies (i.e. at the higher test temperature), while obtaining equivalent modulus values at the higher loading frequencies (i.e. lower test temperature). The neat bitumen obtained similar modulus values until approximately 1,0E-2 Hz for the short-term aged condition, where the modulus values drastically decreased. This was caused by low modulus values at the high test temperature.

The LTOA samples shows a similar trend, except that the SBS modified asphalt binder obtained modulus values much closer to the SBS + PPA modified samples when compared to the STOA condition (**Chyba! Nenalezen zdroj odkazů.**(b)). This indicates that the SBS modified samples underwent greater age hardening due to long-term oven aging than the SBS + PPA modified samples. The extent of aging was further evaluated by comparing the ratio of LTOA to STOA modulus values (**Chyba! Nenalezen zdroj odkazů.**(c)) versus the reduced loading frequency from the master stiffness curves. The aging results showed that:

- The neat asphalt binder accumulated an average increase in modulus due to LTOA of 20 %, with a maximum modulus increase of 65 %.
- The SBS only modified asphalt binder accumulated an average increase in modulus due to LTOA of 9 %, with a maximum modulus increase of 18 %.
- The SBS + PPA modified asphalt binder accumulated an average increase in modulus due to LTOA of 4 %, with a maximum modulus increase of 7 %.

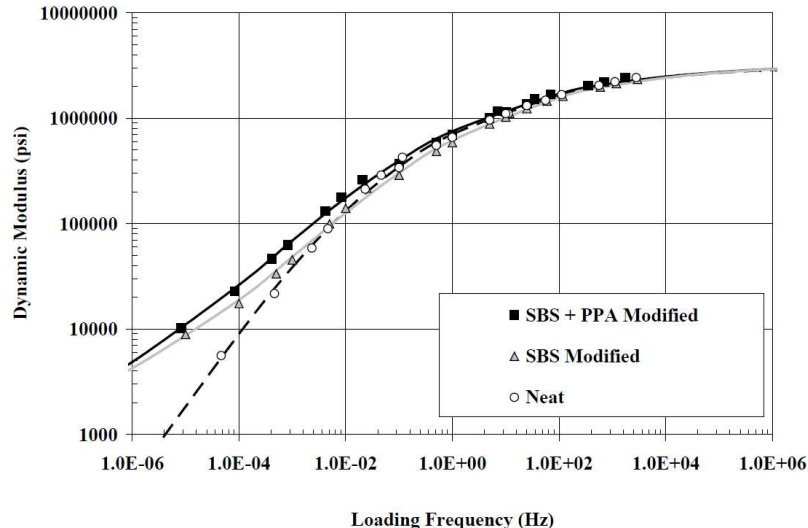
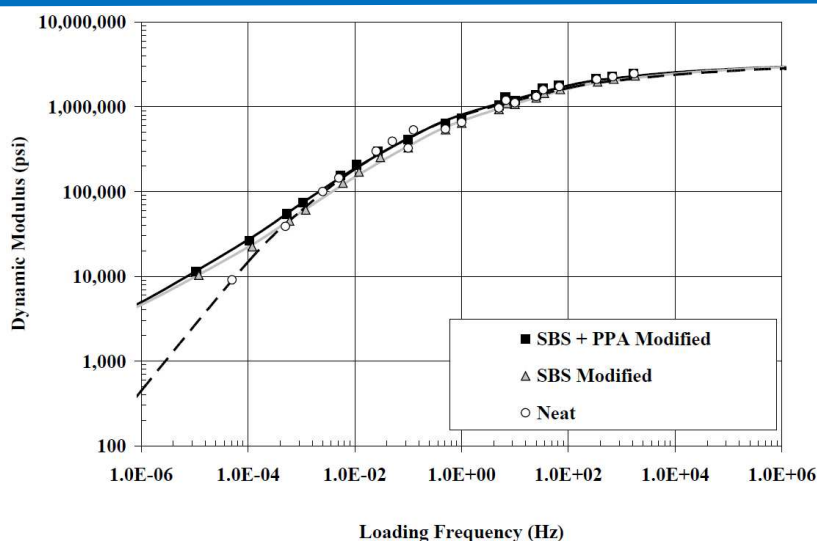
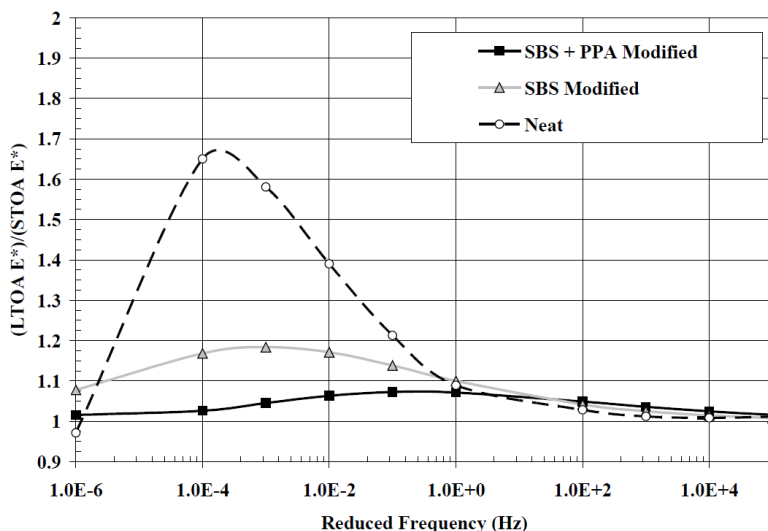


Figure 6-2(a): Master stiffness curves after short-term oven ageing



Chyba! Nenalezen zdroj odkazů.(b): – Master stiffness curves after long-term oven ageing



Chyba! Nenalezen zdroj odkazů.(c): Increase in material stiffness due to long-term oven ageing

6.4 Binder ageing effects on stiffness

6.4.1.1 Paper 272 (Pérez-Jiménez et al., 2014)

A new test procedure, called EBADE, was described. The test method allows characterizing fatigue behaviour of asphalt materials with shorter testing time. The test performs a strain sweep, the strain amplitude increases every 5,000 cycles, providing the complex modulus at low strain amplitude and the maximum strain amplitude the material can sustain. Furthermore, this test procedure allows testing binders, mastics and mixtures at different temperatures using the same loading configuration (used conditions 10 °C, 3 °C and 5 °C with frequency 10 Hz).

The initial complex modulus calculated as an average value of all values registered at the lowest strain amplitude level. There is a clear relationship between the initial modulus obtained in strain sweep tests, and that obtained in conventional time sweep tests, as both of them have the same loading configuration.

Three types of bitumen were studied, before and after RTFOT ageing (see Table 6-48).

Table 6-49: Characteristics of asphalt binders

Properties	Units	Standards	50/70	BC 35/50	PMB 45/80-65
Penetration	0,1 mm	EN 1426	57	46	48
Softening point R&B	°C	EN 1427	50,2	66	62
Penetration Index	-	Annex A	-0,85	1,94	1,31
Elastic recovery @ 25°C	%	EN 13398	**	61	86
Fraass breaking point	°C	EN 12593	**	-11	-17
Residue after RTFOT					
Mass change	%	EN 12607-1	0,02	0,01	0,01
Penetration after RTFOT	0,1 mm	EN 1426	35	36	40
Retained penetration @ 25°C	%	EN 12607-1	61,4	78,3	83,3
Softening point after RTFOT	°C	EN 1427	56,4	72	68,8
Increasing of softening point R&B	°C	EN 12607-1	6,4	6	6,8

Figure 6-2 shows the evolution of the complex modulus with the number of cycles at different temperatures for bitumen PMB 45/80-65. As can be observed, the complex modulus decreases as the number of cycles increases. When the strain amplitude step is increased the speed at which the modulus decreases is also increased. It can be observed that the higher the initial complex modulus, the lower the temperature of the test, this being a more dramatic decrease with lower temperatures and higher numbers of cycles.

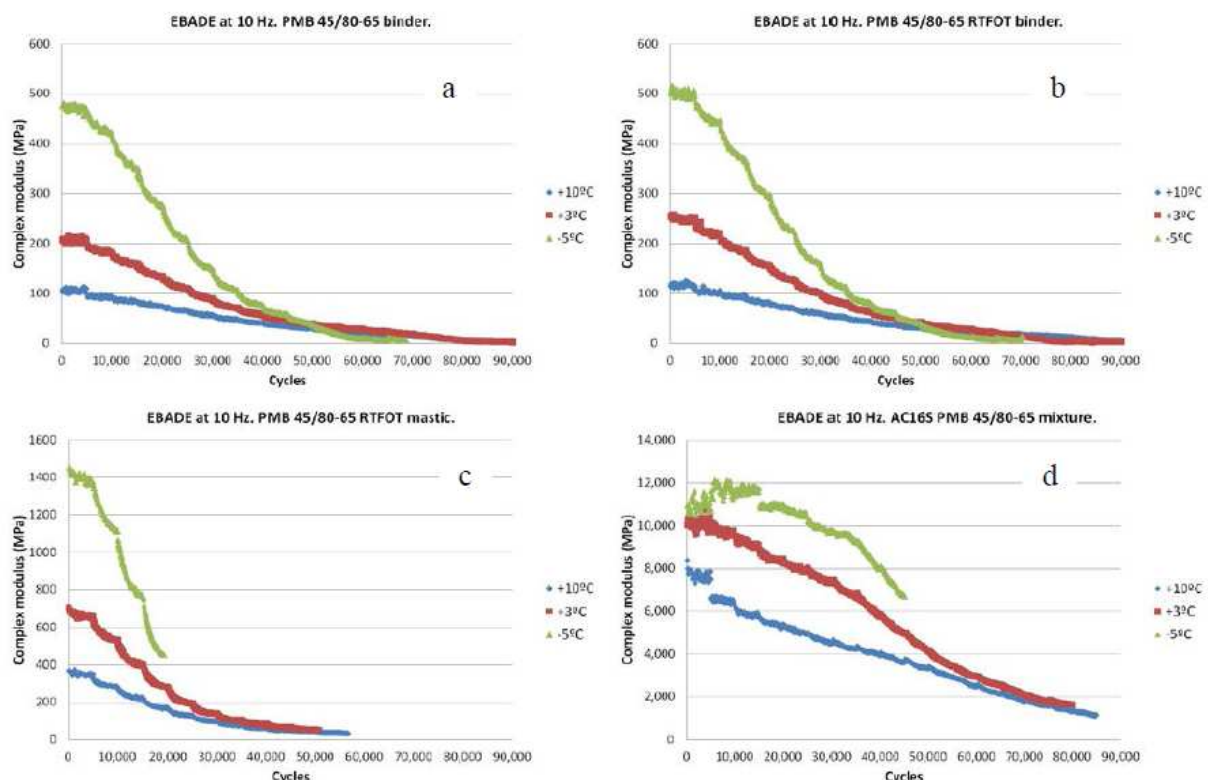


Figure 6-2: Complex modulus evolution with the number of cycles for the PMB 45/80-65 binder before (a) and after RTFOT (b), mastic (c) and mixture (d)

PMB 45/80-65 (aged and unaged) has a quite similar response. This response is not the same for mastics, where the complex modulus value increases at least 3 times with respect

to neat bitumen. The asphalt mixes present then a complex modulus value 80 times higher than neat bitumen at 10 °C. This increase is not so evident at -5 °C, where the increase is of about 24 times. Moreover, the differences between moduli are much slighter from 3 °C to -5 °C, where it exhibits a more elastic behaviour. This fact is more evident for 50/70 bitumen, where the complex modulus remains virtually constant during the test and falls sharply when the failure occurs.

Table 6-50: Numerical values for the initial complex modulus

Binder		Temperature (°C)	Initial complex modulus (MPa)
Binders (unaged)	50/70	10	109
		3	260
		-5	582
	BC 35/50	10	104
		3	196
		-5	466
	PMB 45/80-65	10	106
		3	208
		-5	473
Binders (aged)	50/70 RTFOT	10	160
		3	310
		-5	665
	BC 35/50 RTFOT	10	182
		3	309
		-5	609
	PMB 45/80-65 RTFOT	10	118
		3	251
		-5	503
Mastics (aged)	50/70 RTFOT	10	432
		3	843
		-5	1590
	BC 35/50 RTFOT	10	539
		3	892
		-5	1704
	PMB 45/80-65 RTFOT	10	354
		3	672
		-5	1413
Mixture (unaged)	50/70	10	9368
		3	13343
		-5	14016
	BC 35/50	10	11440
		3	12525
		-5	14619
	PMB 45/80-65	10	6639
		3	8707
		-5	11267

As can be seen in Figure 6-2, the complex modulus increases as the temperature decreases; this fact is emphasised after RTFOT. Modified binders show lower values of complex modulus than conventional bitumen at the three different temperatures studied. RTFO test evidences the ageing effect on the complex modulus, mainly for neat bitumen and the 35/50 crumb rubber modified binder.

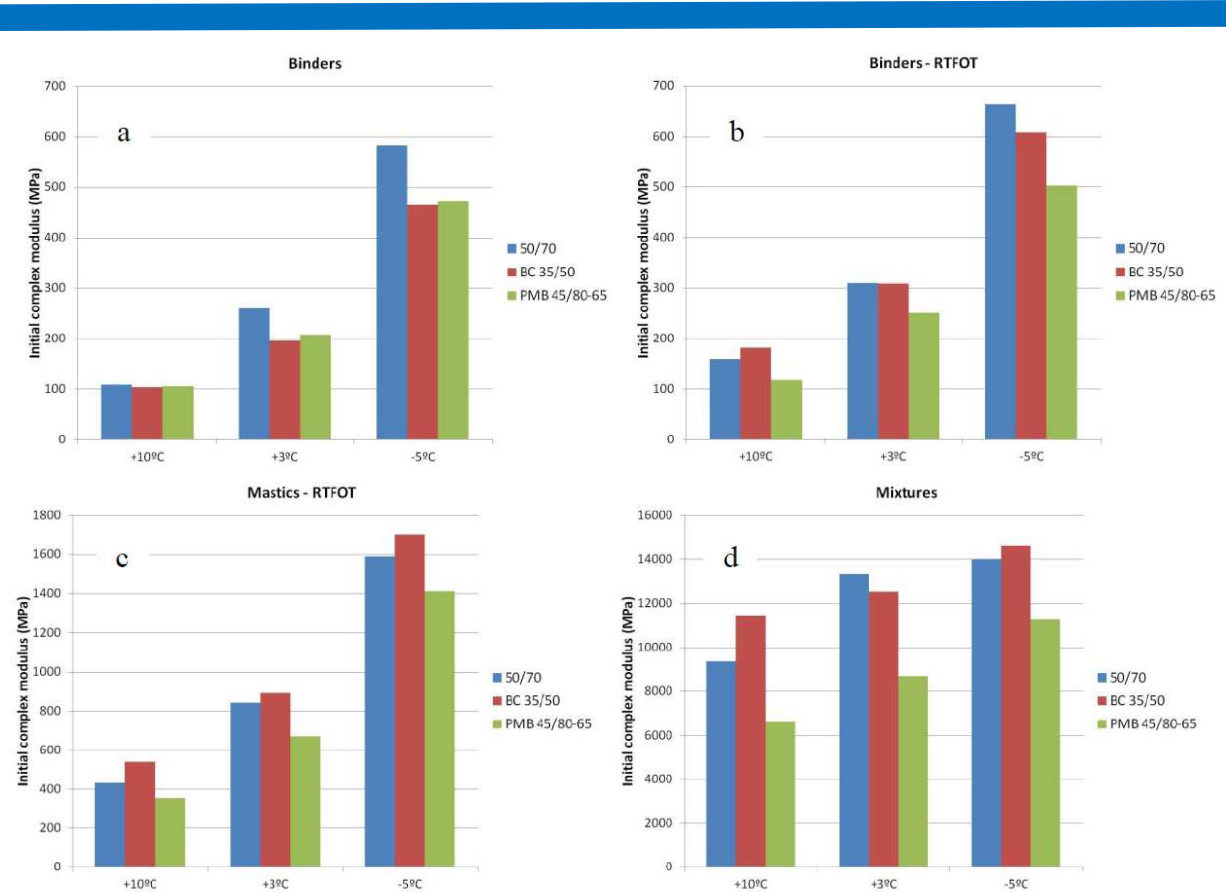


Figure 6-2: Comparison between the initial complex modulus values. Binders (a), binders after RTFOT (b), mastics with binders after RTFOT (c) and mixtures (d)

The effect of temperature variations is more visible between 3 °C and -5 °C, where a significant increase in the complex modulus can be observed, above all for 50/70 and BC 35/50 bitumen.

Figure 6-2 displays the complex modulus for “aged” mastics versus the complex modulus for “aged” binders. As can be observed, there is a linear relationship between both cases, there is only one deviation value for the 50/70 binder at -5°C, due most probably to technical mistakes.

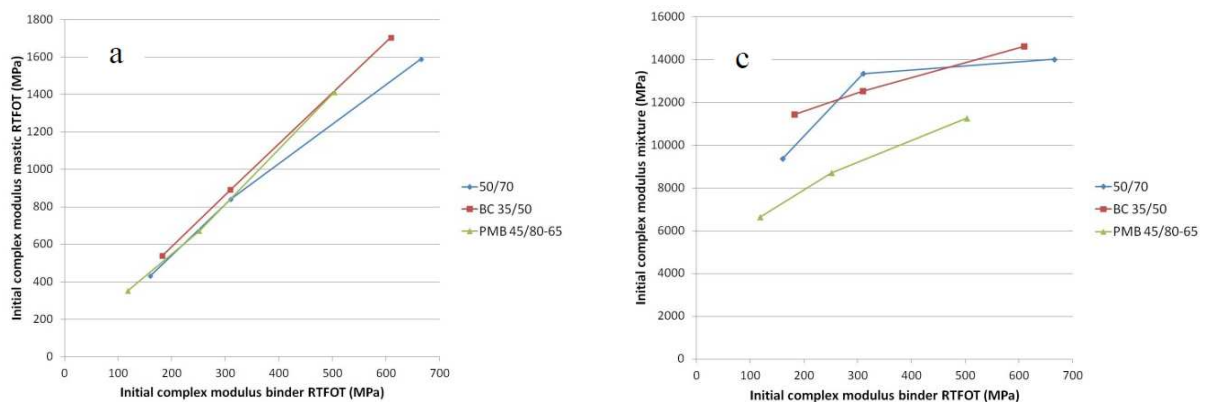


Figure 6-2: Relation between parameters of binder and mastic (a), and binder and mixture (c)

The asphalt mixes yield an increase in the modulus of more than 2 orders of magnitude in relation to their corresponding mastics.

For mixtures with PMB 45/80-65, the complex modulus is lower and is very sensitive to temperature variations. It is clear that the PMB 45/80-65 mixtures have a different response than 50/70 and crumb rubber 35/50 mixtures. As with binders and PMB 45/80-65 mixes, the complex modulus increases as temperature decreases.

6.4.1.2 Paper 481 (Oliveira et al., 2010)

Paper focuses on assessment of fatigue resistance and ageing of asphalt mix used typically in Portugal. Stiffness and fatigue are assessed by means of 4PB-PR test according to EN 12697-26 and EN 12697-24. Tests are performed at frequency of 10 Hz. For fatigue also 30 Hz was evaluated since this value is given in the European standard (EN 13108-20). Additionally ageing was studied since it is considered as an important factor in the performance of asphalt mixtures, particularly in their resistance to fatigue. In order to understand the contribution of ageing phenomenon, the effect of ageing was performed after submitting some test specimens to laboratory simulated ageing according to the long-term oven ageing (LTOA) process – test specimens are aged for 5 days at 85°C.

For the study AC 14 mix was selected and prepared with 35/50 and 50/70 bitumen. Average void content was 2,7 %.

The stiffness test was run in controlled strain modulus with amplitude of 50×10^{-6} at 20 °C. Following loading frequencies were selected: 1; 4; 8; 10; 30 Hz and again 1 Hz.

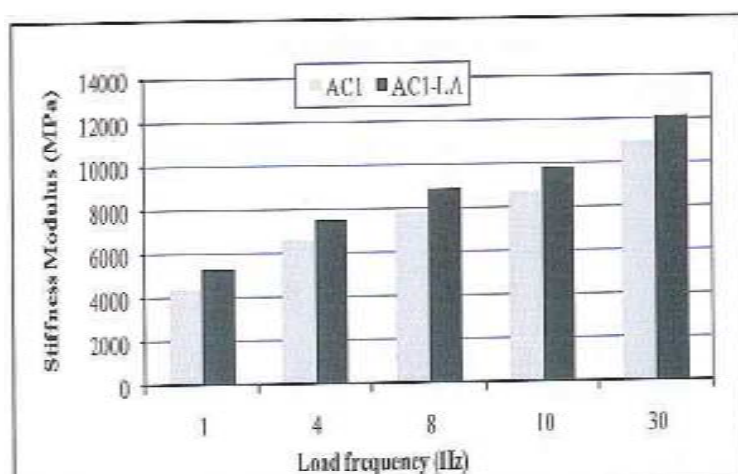


Figure 6-2: Stiffness modulus at 20 °C of aged and un-aged AC14 test specimens (35/50 bitumen)

Table 6-51: Penetration and softening point of assessed AC14 mixes (recovered bitumen)

Mix		Penetration (0,1 mm)	Softening point T_{RB} (°C)
AC1 (35/50)	AC1 (un-aged)	36	54,4
	AC1-LA	34	56,1
AC2 (50/70)	AC2 (un-aged)	63	49,1
	AC2-LA	44	52,5

6.5 Effects of different additives and modifiers

6.5.1.1 Paper 359 (natural asphalt) (Loveček & Schlosser, 2013)

This analysis focused on a comparison of the effects of natural asphalt of various origins on the asphalt mix properties (AC with 50/70 bitumen). Natural asphalt from Trinidad was used for the laboratory applications.

Table 6-525: Natural asphalts from different locations

Natural asphalt property	Location		
	Trinidad	Selenica	Utah
Softening point R&B (°C)	68-78	115-125	132-185
Penetration (25°C) 1/10 mm	3-10	0	0
Asphaltene content (% by mass)	35	45	-
Mineral content (% by mass)	35-46	20	2
Paraffin content (% by mass)	0,2	0,2	0,2

Table 6-53: Change in the properties of bitumen 50/70 with the addition of % PE “Z” 0/8

Natural bitumen Trinidad Epuré (“Z” 0/8)	Road bitumen 50/70	
Content of natural bitumen TE added (%)	Penetration at 25°C (0,1 mm)	Softening point R&B (°C)
0,00	53	46
1,25	40	57
1,85	35	62
2,45	30	67
3,05	25	72

NOTE: TE (Z 0/8) contains 54.0 %-wt. of bitumen and 46 %-wt. mineral particles

Table 6-54: Values of complex stiffness modulus E* (MPa) of mix AC 11 with added TE (Z 0/8)

Mix	T (°C)	FR (Hz)	Complex modulus [MPa]			ϕ (°)	σ_0 (kPa)	E ₀ (10 ⁻⁶)
			E1	E2	E*			
ACO 11 O; 50/70; 2,45 % TE (Z 0/8)	0	5	11381,2	3229,8	11846,0	15,1	429,0	33,3
	0	10	10639,9	2522,0	10,956,0	12,7	.	27,0
	0	15	12851,1	2294,7	13089,0	10,4	458,0	31,9
	0	20	13233,7	1544,2	13324,5	6,7	456,0	31,9
	0	25	14339,2	3035,4	15002,4	10,8	505,0	28,9
	15	5	7517,7	2870,1	8071,2	19,6	316,0	41,9
	15	10	8496,2	1910,1	8731,5	19,5	374,0	42,8
	15	15	8375,4	1136,1	8455,8	7,4	332,0	41,2
	15	20	8490,6	789,1	8529,6	5,1	316,0	38,1
	15	25	8237,7	5965,2	10947,6	36,6	396,0	40,6
	27	5	5387,0	2794,7	6090,7	27,4	193,0	33,3
	27	10	6188,4	1556,4	6390,0	16,8	248,0	41,4
	27	15	6294,4	1337,3	6441,4	11,9	204,0	32,1
	27	20	6396,8	1281,8	6528,8	11,2	181,0	32,1
	27	25	5522,2	3629,7	6880,1	33,5	192,0	34,4

The determining values for the assessment of the mix should be the temperature of 15 °C and frequency of 10 Hz. The loading frequency is determined within the range of 0,1 Hz to 50 Hz, which allows plotting the main curves. The same asphalt mix, AC 11, was used for the functional testing (to determine the complex modulus and fatigue) as in the empirical testing. The impact of bitumen 50/70 modified by natural bitumen TE was demonstrated by higher

complex modulus values under 27 °C. The figure of complex modulus $E^* = 8\,731$ MPa corresponds with the category for minimum stiffness S_{min} 7 000 under the temperature of 15 °C and frequency 10 Hz of the driving force. For the sake of comparison, the value of complex modulus $E^* = 4\,263$ MPa of a classic asphalt mix with road bitumen CA 50/70 and a similar mix composition is given.

Figure 6-2 shows the graphic form of complex modulus dependency on the frequency under various temperatures (-10 °C to +27 °C) with similar doses of asphalt mix components but with road bitumen 70/100. Laboratory testing confirmed the value of complex modulus $E^* = 5938$ MPa.

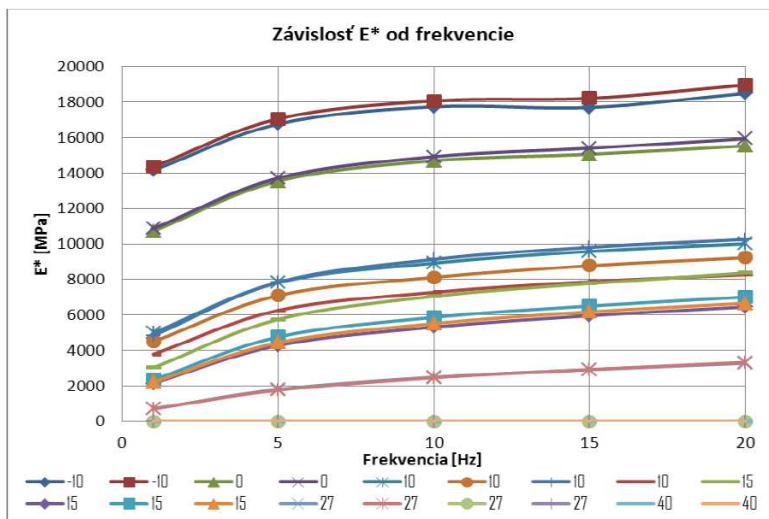


Figure 6-2 Complex modulus dependency on temperature and frequency

6.5.1.2 Paper 378 (crumb rubber) (Sybilski & Ruttmar, 2011)

The objective of the presented study was the comparison of rheological and mechanical properties of asphalt mixes with PMB and with *tecRoad* rubber modified binder. For that purpose, two asphalt mixes, SMA 11 (with PMB 65/105-60 and with *tecRoad*-modified straight-run bitumen 70/100) were chosen for the wearing course while asphalt concrete AC 16 was picked for the base course (with PMB 25/55-60 and *tecRoad*-modified straight-run bitumen 50/70).

The stiffness test of the asphalt mix was carried out according to EN 12697-26 using a four-point beam bending machine (4PB). During each test, the control program recorded the following values: the force, beam deflection, phase shift angle, number of cycles and other data, and the stiffness modulus, strain and deformation were calculated. Temperatures of 0, 10, 20, 30°C were used together with frequencies 0, 5; 1; 2; 5, 8, 10, 20 and 30 Hz with the deformation equal to 50 µm/m and sinusoidal loading.

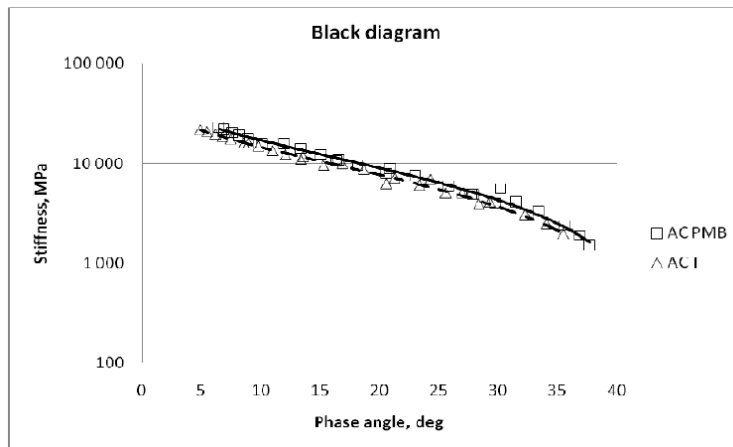


Figure 6-2: Black Diagram of AC mixes

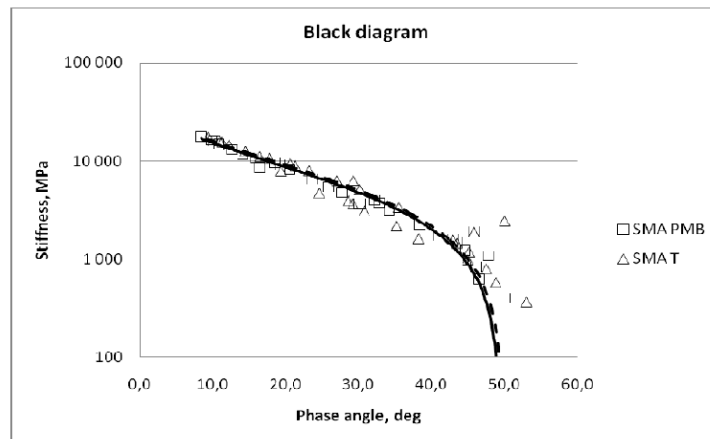


Figure 6-2: Black diagram of SMA mixes

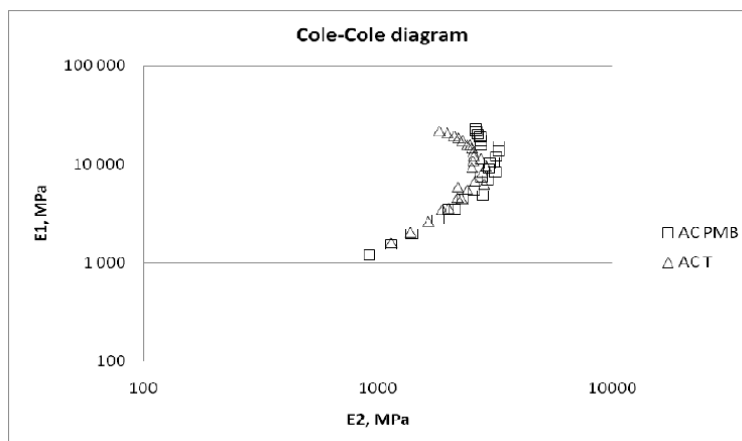


Figure 6-2: Cole-Cole diagram of AC mixes

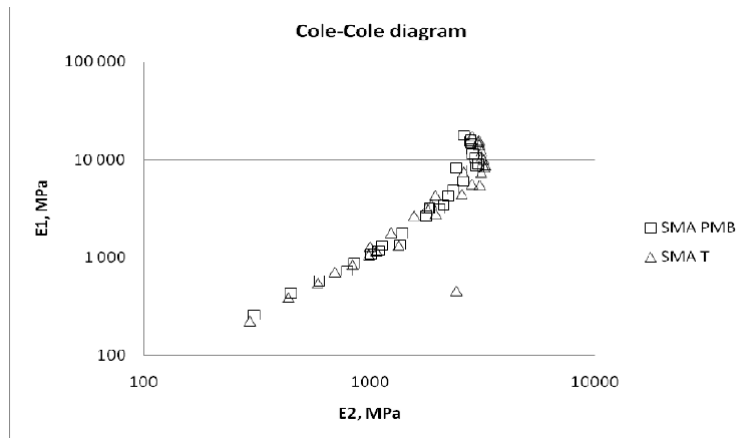


Figure 6-2: Cole-Cole diagram of SMA mixes

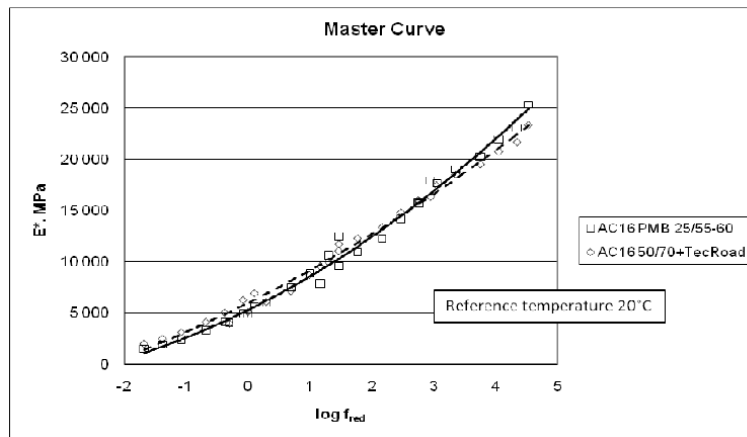


Figure 6-2: Master curve of AC mixes

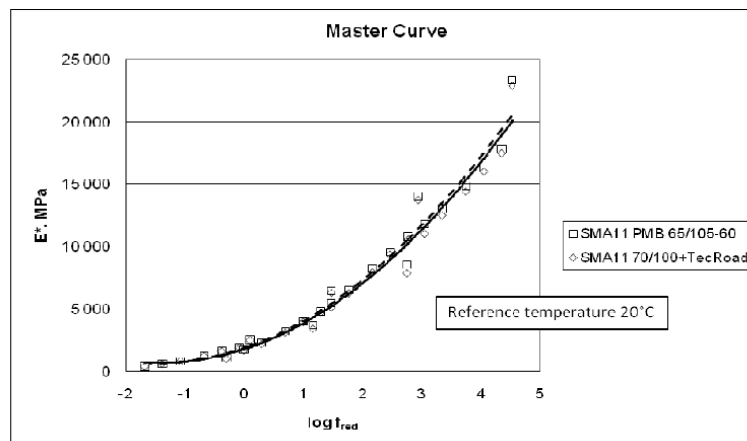
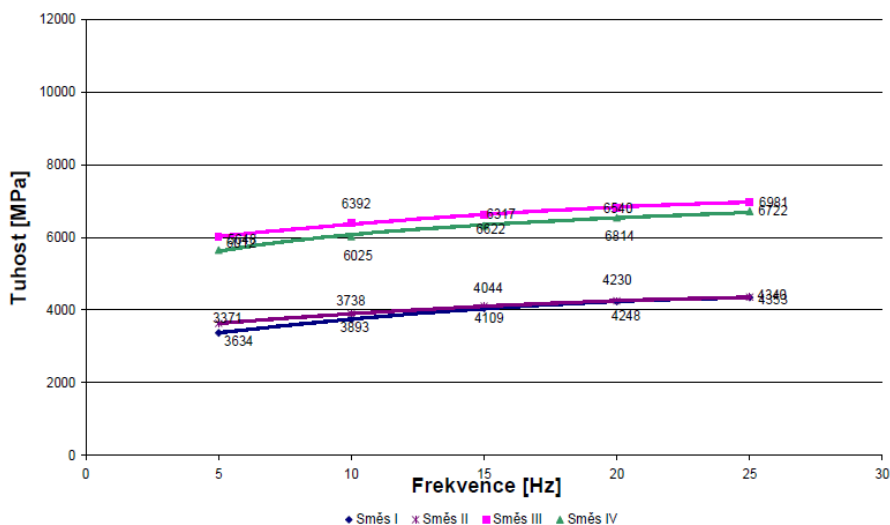


Figure 6-2: Modulus master curve of SMA mix

6.5.1.3 Paper 379 (crumb rubber) (Varaus, 2011)

Two special types of binders were applied: highly modified bitumen with SBS marked PMB 40/100-75 and rubber granulate-modified bitumen (11 % of granulated rubber) marked RmB G 20/60-55 under the German regulations. Both binders were used for the design of both SMA 8 S and SMA 8 LA mixes. In total, four asphalt mixes were designed and tested. In comparison to SMA 8 LA mixes, SMA 8 LA mixes achieve lower stiffness modulus values.



Mix I: SMA 8 LA/ PMB 40/100-75 Mix II: SMA 8 LA/ RmB G 20/60-55
 Mix III: SMA 8 S/ RmB G 20/60-55 Mix IV: SMA 8 LA/ PMB 40/100-75

Figure 6-2 Comparison of the stiffness modules measured

6.5.1.4 Paper 380 (crumb rubber) (Valentin, 2011)

To compare the impact of a CRmB binder, six different options were experimentally designed and produced while the 50/70 bitumen was always the base binder. Addition of synthetic waxes that allow reducing the production temperature were used besides the crumbed rubber (10–15 % of mix) and polyoctenamer or polyphosphoric acid additions. From the point of view of individual representatives, the used binders were CRmB 5 (50/70 + 3 % FTP + 9 % CR), CRmB 7 (50/70 + 1 % additive A + 9 % CR), CRmB 8 (50/70 + 0,5 % additive A + 9 % CR), CRmB 9 (50/70 + 10 % CR with additive B), CRmB 10 (50/70 + 15 % CR with additive B), CRmB 11 (50/70 + 12 % CR with additive B). These versions can be compared to the reference mix, AC16 and AC22.

Non-destructive testing of repeated indirect tensile stress (IT-CY) was conducted and stiffness moduli were determined. The thermal susceptibility is determined by calculating the ratio of stiffness values under 5 °C and 40 °C and, subsequently, in a modified form as the ratio between 5 °C and 27 °C.

Table 6-55: Stiffness modulus values (MPa) for the mixes (ACL16+ and ACP22) as observed

Mix	Binder	5°C	15°C	27°C	40°C	ts_5/40	ts_5/27
REF	50/70	17 000	8 800	2 000	400	42,50	8,50
ACL_HM1	CRmB7	13 200	9 700	2 200	1 300	10,15	6,00
ACL_HM2	CRMB11	16 900	11 400	3 000	1 100	15,36	5,63
ACL_HM3	CRmB8	21 000	11 700	3 700	1 400	15,00	5,68
ACL_HM4	CRMB5	18 100	10 900	4 500	2 500	7,24	4,02
ACP_VA1	CRMB7	24 500	17 100	7 600	3 400	7,21	3,22
ACP_VA2	CRMB9	26 200	18 700	8 400	4 600	5,70	3,12
ACP_VA3	CRMB10	28 400	15 800	7 600	3 000	9,47	3,74

With respect to mixes AC16, the results as indicated demonstrate that, particularly in the interval of 15 °C to 40 °C, CRmB binders improve mix stiffness despite the fact that crumbed rubber should provide a higher degree of elasticity. Thermal susceptibility can be considered very good, primarily from the perspective of the 5/40 °C ratio.

The stiffness modulus results of mixes AC22 differ from mixes AC16 to a certain degree. The most noticeable is a much lower thermal susceptibility of the two ratios used. These are basically half values in the case of the second ratio indicator. In the case of the stiffness modulus values, it is obvious that the AC22 mixes are more than 70 % higher than those of AC16 mixes and the values obtain qualify them as base courses with very good load-bearing properties.

6.5.1.5 Paper 402 (crumb rubber) (Kudrna, 2009)

The properties examined in crumb rubber modified bitumen are indicated in Table 6-56. The measurements were taken after an hour of mixing CRmB under 175 °C in the laboratory.

Table 6-579: Properties of road bitumen and the CRmB prepared

Road bitumen applied	Type II ¹⁾	70/100	70/100	70/100 ³⁾	70/100 ³⁾	50/70	50/70 section 2.1	50/70 Section 2.2
Content of granulate (%) of the bitumen weight	15 - 25	-	18 ²⁾	-	18 ²⁾	-	22	20
Viscosity 175 °C (Pa·s)	1,5-4,0	0,06	2,6	0,085	2,4	-	2,6	3,3
Penetration, 25 °C (0,1 mm)	25-75	91	43	34	24	51	69	33
Softening point (°C)	min. 54	46	69	57,2	88,8	49	58	65,1
Reverse ductility (%)	-	-	65	-	75	-	-	-
Resilience 25 °C (%) ³⁾	min. 20	-	26	-	37	-	22	31

¹⁾ According to ASTM D 6114 (2002), type II is suitable for the weather conditions in Central Europe.

²⁾ Granularity of rubber granulate 0/2 mm

³⁾ Results after the RTFOT and PAV test.

Table 6-58: Properties of mixes with CRmB

Property/ Mix type	AC 11	AC 11	BBTM8	PA 8	Section 1.1	Section 1.2	Section 2.1	Section 2.2
Bitumen applied	70/100	70/100	70/100	70/100	50/70	50/70	50/70	50/70
Content of granulate (%) of the bitumen	-	18	18	18	26	26	22	20
Addition of lime hydrated (% bit.)	-	-	-	-	-	20	20	20
Binder content (% of mix)	6,2	8,5	8,5	9,5	8,3	8,3	8,7	8,7
Stiffness according EN 12697-26 – 10 Hz, 15°C, (MPa)	6640	4110	3800	1490	5120	6020	3070	3820

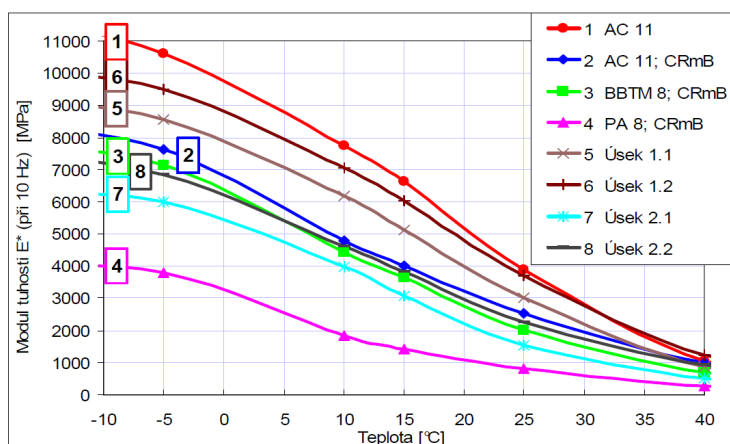


Figure 6-2: Dependence of stiffness on temperature under 10 Hz frequency

Test specimens were cut out of compacted slabs prepared in a plate compactor. The stiffness was determined for truncated wedge-shaped specimens by means of a 2-point test according to standard ČSN EN 12697-26. The stiffness moduli for 15 °C and 10 Hz frequency are recorded in table 4; figure 3 gives a graphic depiction of the dependence of stiffness on temperature.

6.5.1.6 Paper 435 (crumb rubber) (Kudrna & Dašek, 2009)

Rubber modified binders and mainly their use in asphalt mixtures were assessed. Wet process with 0/2 mm rubber granulate was applied in a content of 15-25 % rubber in bitumen. Rubber was mixed with 70/100 or 50/70 bitumen for at least 60 minutes at 175 °C. CRmB was applied in very thin asphalt concrete mix (VTAC11) and in porous asphalt (PA8). VTAC mixes denoted Test 1.1 and 1.2 were taken from the production for trial section No. 1. Similarly VTAC mixes denoted Test 2.1 and 2.2 originate from the trial section No. 2. Unfortunately there is no direct correlation to test specimens from the pavement structure.

Table 6-59: Results for tested mixtures

Mixture type	AC 11	Test 1.1	Test 1.2	PA 8; Laboratory	PA 8; Low traffic	Test 2.1	Test 2.2
Property							
Column	1	2	3	4	5	6	7
Paving bitumen	70/100	50/70	50/70	70/100	50/70	50/70	50/70
Crumb rubber content, [% of bitumen]	-	26	26	18	20	22	20
Hydrated lime addition, [% of bitumen]	-	-	20	-	-	20	20
Binder content, [% of mixture]	6,2	8,3	8,3	9,5	9,2	8,7	8,7
Content of paving bitumen, [% of mixture]	6,2	6,6	6,6	8,1	7,7	7,2	7,2
Air-voids, [%]	3,9	8,9	8,9	19,0	20,8	19,0	19,3
Voids in mineral aggregate, [%]	18,1	26,8	26,8	36,1	38,0	35,6	35,8
Stiffness EN 12697-26; 10 Hz, 15 °C, [MPa]	6640	5120	6020	1490	-	3070	3820

Stiffness was determined according to EN 12697-26 by 2PB-TR test at 15 °C. Additionally tests have been done at -5 °C; 10° C; 26 °C and 40° C. The effect of softer bitumen was shown. At the same time PA8 showed very low stiffness values compared e.g. to AC11 mix. Similarly VTAC with CRmB showed decreased stiffness values.

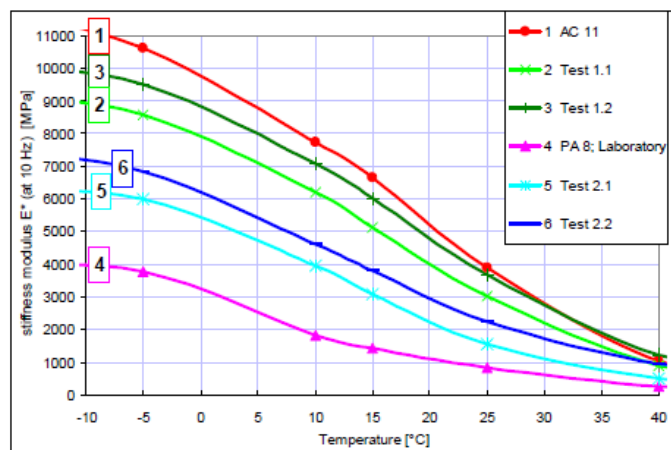


Figure 6-2: Dependence of stiffness on temperature

6.5.1.7 Paper 448 (crumb rubber) (Fontes et al., 2009)

Study on stiffness and fatigue life for four different dense and gap graded asphalt mixes containing terminal blended CRmB with 15-20 % crumb rubber in 50/70 bitumen with penetration around 40 dmm and softening point around 68 °C. Asphalt mixes are designed according to US standards (gap graded ARHM-GG mixture according to Caltrans Standard Special Provisions SSP39-400 and dense graded Asphalt Institute mixture following the Asphalt Handbook Manual Series No. 4), the asphalt mixes might be comparable to AC12.

Dynamic modulus was determined at 15 °C; 20 °C and 25 °C. Test specimens were subjected to different loading frequencies (10; 5; 2; 1; 0,5; 0,2; 0,1 Hz) in 100 cycles. The modulus-temperature dependence was firstly assessed by linear regression. In the second step the regression was extended by bitumen content as another variable.

$$E = K_1 \times B + K_2 \times T + K_3$$

where:

E = dynamic modulus;

B = binder content (%);

T = temperature (°C);

K1, K2, K3 = regression parameters

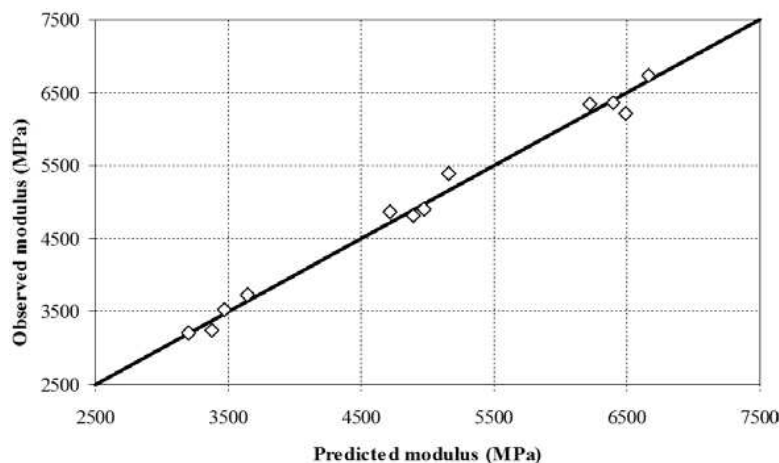


Figure 6-2: Predicted and observed dynamic modulus results

6.5.1.8 Paper 450 (crumb rubber) (Neto et al., 2009)

Paper focuses on specific aspects of asphalt mixes with crumb rubber modified binders (CRmB). For conventional HMAs usually increased stiffness leads to shorter fatigue life, for mixes with CRmB (wet process of using rubber) it was shown that stiffness and fatigue life increased. 4PB-PR test was used to assess resilient modulus. In the study asphalt concrete for wearing course was used and 50/70 bitumen was applied as a basis using additionally 21 % crumb rubber with mixing 60 minutes at 210 °C (question of bitumen degradation at this temperature). Two types of asphalt mixes were studied – dense AC16 and gap graded AC16. Resilient modulus and fatigue life tests were carried out under controlled strain conditions according to AASHTO TP8/96. The specimens obtained from studied asphalt hot mixes were submitted to the long-term aging process normalized by AASTHO PP2/94.

Resilient modulus has been determined on five test specimens at 20 °C for frequencies 0.1; 0.2; 0.5; 1; 2; 5; 10 Hz. Gap graded mix with CRmB showed the highest stiffness values.

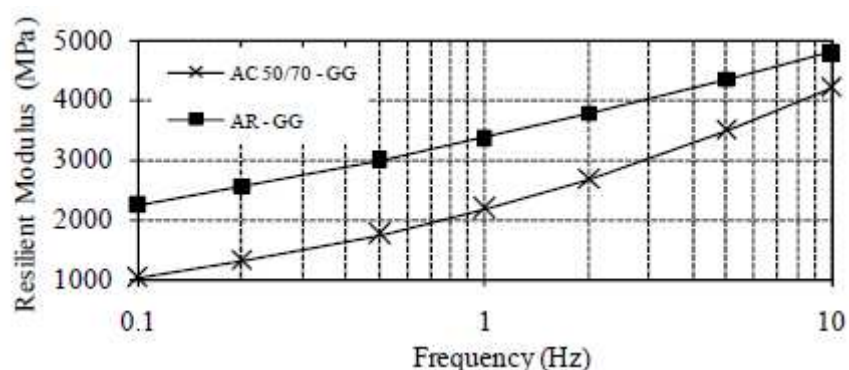


Figure 6-2: Comparison of resilient modulus for gap graded AC with 50/70 and with CRmB

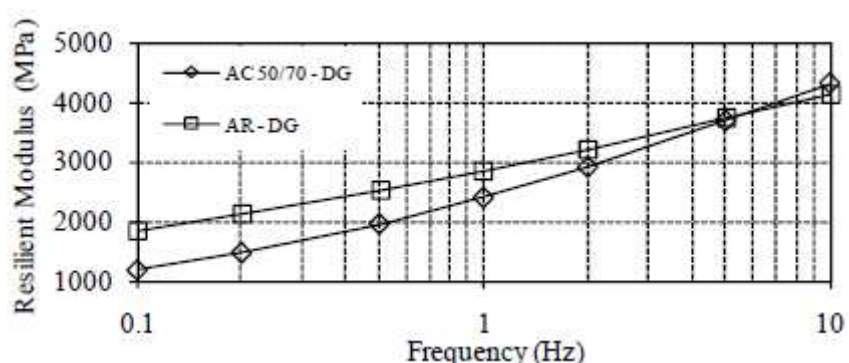


Figure 6-2: Comparison of resilient modulus for dense graded AC with 50/70 and with CRmB

Increased stiffness complies well with reduced penetration (52 dmm for 50/70 and 33 for CRmB) and increased softening point (50,6 °C for 50/70 and 86,4 °C for CRmB).

6.5.1.9 Paper 382 (WMA) (Valentin et al., 2011)

Table 6-60 gives a basic summary of bituminous binders which were applied to the asphalt mixes of three different types – AC_{bin}16 (AC_{bin} 1S) and AC_{base}22, which are utilised primarily in the binding or base layers of the pavement structure. For mix AC_{bin}16S, the binder content was 4,2 % which is shown to be the limit value of bituminous binder that tends to support the general practical trend of using as little bitumen in the mixes as possible. In the case of the mixes AC_{bin}16, the addition of bituminous binder was slightly higher (4,4 %).

Table 6-61: Basic properties of road bitumens 50/70 and 70/100 with different additives to improve viscous behaviour

Basic binder	Additive		Softening point KK, [°C]	Penetration @ 25 °C, [0,1 mm]	Penetration index, [-]
	Type	Content [%]			
70/100	No additive	–	46	82	-1,07
	FTP	3	91	53	5,85
	AMK	3	95	60	6,64
	AMK a PPA	3 + 0,5	99	50	6,55
50/70	No additive	–	51	53	-0,82
	FTP	3	76	40	3,18
	AMK	3	94	41	5,51
	PPA	0,5	53	53	-0,34
	PPA	1,0	56	49	0,14
	PPA	1,5	64	38	1,12
	Zycosoil	0,1	50	55	-0,99
	IterFlow	0,5	51	40	-1,44

The results of the experimentally stipulated stiffness modules, using the IT-CY method according to ČSN EN 12697-26, are indicated in the following Table 6-62 to Table 6-635. For each mix and temperature, the effort was always to determine the value as a mean of the measurements in at least four test specimens. At the same time, an auxiliary characteristic of thermal susceptibility was determined for each specimen. The characteristic shows that a mix can be considered of better quality if the absolute value of thermal susceptibility is lower.

Table 6-64: Stiffness modulus for mix AC_{bin}16 examined (test method IT-CY)

Temperature/Mix	REF	AC16_WMA1	AC16_WMA2	AC16_WMA3	AC16_WMA4
T = 5 °C	17 000	20 300	13 200	11 000	20 500
T = 15 °C	10 600	13 200	9 900	8 300	13 200
T = 27 °C	2 600	3 200	2 100	1 900	5 800
Thermal susceptibility * [-]	6,54	6,34	6,29	5,79	3,53

* Determined as a ratio of the modulus values under 27°C and 5°C.

Table 6-65: Stiffness modulus for mix AC_{bin}16 examined (test method IT-CY)

Mix	REF 2009	2009_2	2009_3	2009_4	2009_5	2009_6	2010_2
Bituminous binder applied	50/70	70/100	50/70	50/70	50/70	50/70	50/70
Additive applied	-	FTP (3%)	PPA (1%)	PPA (0.5%)	AMK (3%)	FTP (3%)	ZT (0.1%)
T = 5 °C	21 400	17 900	17 100	20 600	26 900	27 300	21 600
T = 15 °C	8 800	8 500	9 800	11 200	11 900	13 800	13 600
T = 27 °C	2 000	2 200	3 300	2 800	3 900	5 200	4 000
T = 40 °C	400	600	700	900	1 200	1 600	900
Thermal susceptibility * [-]	10,70	8,14	5,18	7,36	6,90	5,25	5,40
Thermal susceptibility ** [-]	53,50	24,83	24,43	22,89	22,42	17,06	24,00

* Determined as a ratio of the modulus values under 5 and 27 °C;

** Determined as a ratio of the modulus values under 5 and 40 °C.

Table 6-66: Stiffness modulus for mix AC_{base}22 examined (test method IT-CY)

Mix	Binder	Mixing temp. [°C]	Stiffness modulus at T, [MPa]			Thermal susceptibility*
			0 °C	15 °C	40 °C	
AC22+_1a	50/70 + 3 % FTP	145	25 400	10 600	1600	15,88
AC22+_1b	50/70 + 3 % FTP	130	14 500	6900	500	29,00
AC22+_2a	CP-M	160	23 700	13 200	1800	13,17
AC22+_2b	CP-M	145	23 200	12 900	2200	10,55
AC22+_3a	50/70 + 3 % AV	145	26 800	15 100	1200	22,33
AC22+_3b	50/70 + 3 % AV	130	21 700	11 600	900	24,11
AC22+_4a	50/70 + 0,5 % PPA	145	24 100	10 800	900	26,78
AC22+_4b	50/70 + 0,5 % PPA	130	19 900	8000	600	33,17

* Determined as a ratio of the modulus values under 5 and 40 °C.

Based on the results achieved, we can summarise:

- in general, mixes with FTP demonstrated the greatest improvement in stiffness modulus values (approx. 25 % under 15 °C);
- very good comparability of the mixes was discovered for binders 50/70 and 70/100 with FT paraffin, which could suggest that these binders might be practically substitutable when applied in compacted asphalt mixes;

- the effect of viscosity-improving additives is obvious not only in the stiffness modulus values but also in the case of the qualitative indicator of thermal susceptibility. In the case of mixes ACL16, the most appropriate additive seems to be PPA, FTP or ZT. In the case of the set of asphalt mixes AC_{bin}16, an improvement of thermal susceptibility in comparison with the reference mix can be observed within the range of 25–50 %.

Table 6-676: Stiffness determined through a 2-point test in truncated wedge-shaped specimens

Asphalt mix	Stiffness modulus (MPa)					
	Specimen	5 Hz	10 Hz	15 Hz	20 Hz	25 Hz
ACL16 (50/70+3% AMK)	L1	13 477	14 093	14 614	14 876	15 049
	L2	12 673	13 240	13 653	13 908	14 018
	Median	13 075	13 667	14 134	14 392	14 534
ACL16 (50/70+1% PPA)	P1	10 929	11 478	11 796	11 985	12 133
	P2	13 003	13 840	14 283	14 565	14 815
	Median	11 966	12 659	13 040	13 275	13 474
ACL16 (50/70+3% FTP)	T1	12 107	12 887	13 364	13 655	13 773
	T2	11 629	12 220	12 652	12 920	13 016
	Median	11 868	12 554	13 008	13 288	13 395

6.5.1.10 Paper 392 (WMA) (Valentin & Mondschein, 2009)

Another partial experimental assessment of WMAs stiffness was the comparison of individual additives in a single type of asphalt mix. Asphalt mix AC16 with three different additives was chosen as the specimen for this comparison.

Table 6-68: Basic properties of bituminous binders applied

Bituminous binder	Softening point, R&B (°C)	Penetration at 25°C (0,1mm)
50/70	50,5	44
50/70+3% FTP	75,6	40
50/70+3% Licomont	51,3	42
50/70+3% PPA	78,6	27
50/70 + 1,5% PPA	64,3	38

Non-destructive tensile stress test method (IT-CY) according to EN 12697-26 was applied. The stiffness modulus values were obtained from at least three measurements on different test specimens for each temperature.

Table 6-69: Stiffness moduli of the mixes examined

Characteristic	Unit	Mix				
		REF	NTA1	NTA2	NTA3	NTA4
Stiffness modulus @ 5 °C	(MPa)	17 000	20 300	13 200	11 000	20 500
Stiffness modulus @ 15 °C	(MPa)	10 600	13 200	9 900	8 300	13 200
Stiffness modulus @ 27 °C	(MPa)	2 600	3 200	2 100	1 900	5 800
Thermal susceptibility	(-)	6,54	6,34	6,29	5,79	3,53

6.5.1.11 Paper 432 (WMA) (Silva et al., 2009)

In this study, three bituminous mixtures were studied in order to evaluate the characteristics of WMA vs. HMA. One of those was a conventional HMA (control mixture), typically used in Portuguese roads (AC 14 surf 50/70), while the other two were WMA mixtures with the same composition but using binders with Sasobit® and Cecabase®.

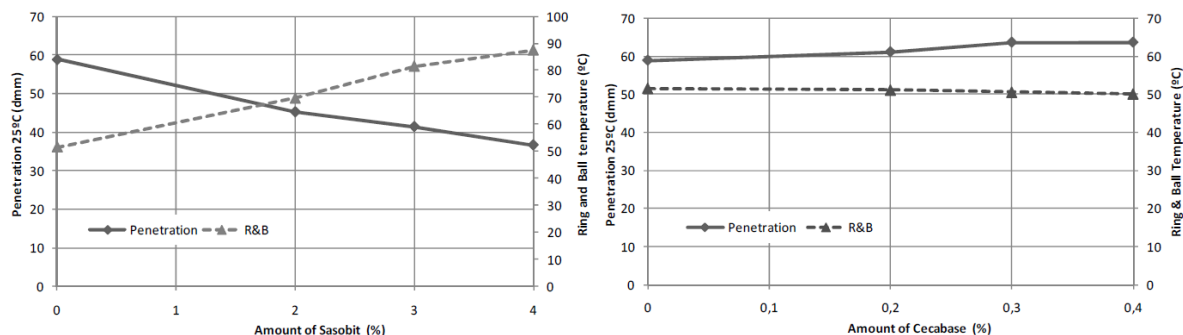


Figure 6-2: Evolution of the penetration and ring & ball values of the binders with the amount of additive

In order to evaluate the properties of the several binders at higher temperatures (100-170°C) in which the asphalt mixtures are mixed and applied, their dynamic viscosity was accessed.

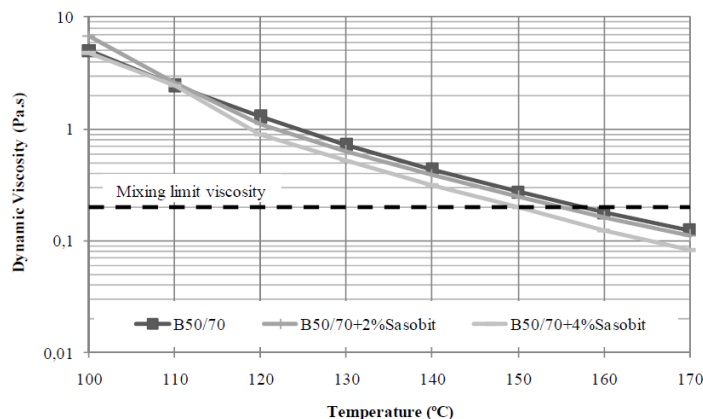


Figure 6-2: Dynamic viscosity of the Sasobit® modified binders (rotating spindle apparatus)

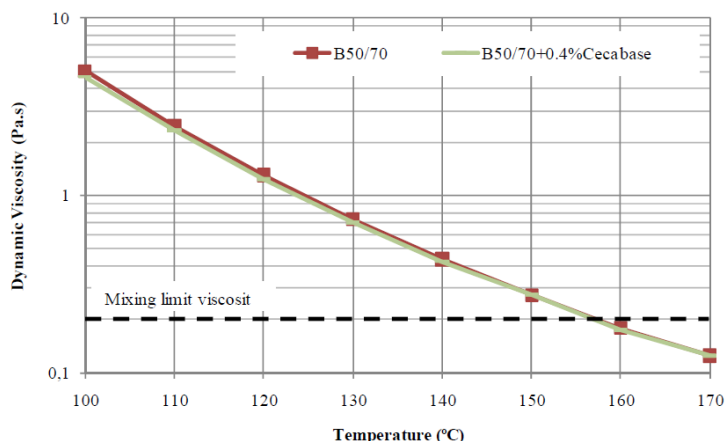


Figure 6-2: Dynamic viscosity of the Cecabase® modified binders (rotating spindle apparatus)

Figure 6-2 shows that the addition of up to 0,4% of Cecabase® to the original bitumen barely changes its dynamic viscosity at the typical application temperatures. In fact, a minor reduction of viscosity can be observed after the addition of 0,4% of Cecabase® that allows a reduction of less than 1°C in the equal-viscosity line of 0,2 Pa.s. It was concluded that a maximum temperature reduction was achieved using 4 % of Sasobit®, while the addition of up to 0,4% of Cecabase® does not reduce the viscosity of the binder.

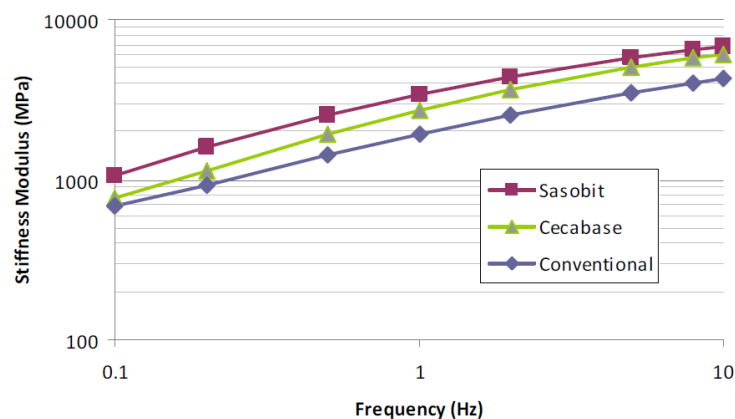


Figure 6-2: Stiffness moduli of the studied mixtures at different frequencies

In terms of stiffness modulus, the mixtures presented values typical for conventional HMA, although the WMAs slightly outperformed the conventional mixture, which confirms that it is possible to produce WMA mixtures without compromising their performance in comparison to HMA mixtures, provided that an adequate quality control is assured.

6.5.1.12 Paper 480 (WMA) (Racanel et al., 2010)

A study was presented comparing traditional hot mix asphalt with two types of warm mix asphalt (WMA) using surfactant and synthetic wax. Standard bitumen 50/70 was used. For optimizing the possible temperature reduction six options of bitumen modification have been prepared (2; 3 and 4 % wax and 0,2; 0,3 and 0,4 % surfactant). Additives mixed for 5 minutes at 130 °C. Standard production temperature 160 °C was reduced by 15 °C for wax and by 30 °C for the surfactant. For stiffness and fatigue testing besides AC14 also option with RAP were prepared with bitumen 160/220 + 6 % wax and temperature reduction of 30 °C as well as bitumen 50/70 + 0,5 % surfactant and 30 °C temperature reduction. Stiffness was measured by 4PB-PR at 20 °C and different frequencies.

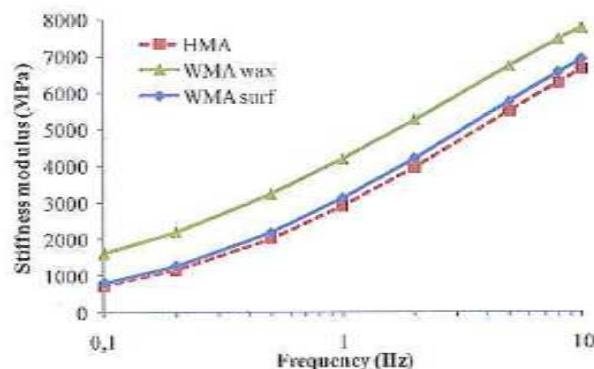


Figure 6-2: Stiffness modulus of HMA and WMA at 20 °C

Fatigue was later evaluated for 20 °C by means of decrease of the stiffness to 50 % of its initial value. WMA show similar behavior and the use of selected additives does not affect fatigue performance.

6.5.1.13 Paper 535 (WMA) (Urquhart et al., 2010)

This study focused on functional characteristics of SMA 9,5 mm and thin SMA mixes containing PMB and special PMBs with warm mix additives. In the SMA mixes 10 % stone dust and 10 % hydrated lime were used together. Mixes were compacted at 110 °C, 135 °C, 145 °C and 160 °C. For performance tests Indirect Tensile Modulus test (ASTM D-4123-82) and Dynamic Creep test (NCHRP-9-19) were used, whereas for indirect tensile modulus

tests temperatures of 15 °C; 25 °C and 35 °C were applied. For creep test temperature of 50 °C used with peak load of 100 kPa and 3600 cycles.

Different binder contents were assessed with very low results on resilient modules. For 15 °C average values of 500-600 MPa. Compaction temperature has a clear impact on the resulting modules (improved resistance to permanent deformations).

Table 6-70: Indirect tensile stiffness modulus test results at various binder and compaction temperatures

Compaction Temperature, °C / Binder Contents	Resilient Modulus at 15°C, MPa			
	5,0%	5,5%	6,0%	6,5%
110	510	445	180	130
130	700	894	621	480
145	531	712	696	566
160	621	758	690	512
Compaction Temperature, °C / Binder Contents	Resilient Modulus at 25°C, MPa			
	5,0%	5,5%	6,0%	6,5%
110	480	685	618	300
130	600	750	629	480
145	602	615	580	520
160	500	515	490	480
Compaction Temperature, °C / Binder Contents	Resilient Modulus at 35°C, MPa			
	5,0%	5,5%	6,0%	6,5%
110	439	585	450	250
130	400	425	382	280
145	430	530	293	260
160	400	514	415	390

Table 6-71: Dynamic creep test results at various binder and compaction temperatures

Compaction temperature, °C / Binder Content	Accumulated Strain, %				Permanent Deformation, mm			
	5,0%	5,5%	6,0%	6,5%	5,0%	5,5%	6,0%	6,5%
110	3,299	2,866	3,177	2,859	2,375	2,603	2,490	2,387
130	3,791	2,865	2,05	1,28	1,80	1,92	2,38	2,255
145	3,459	3,788	1,689	2,102	2,01	1,37	1,13	2,32
160	3,599	3,350	3,468	0,861	1,91	0,86	1,40	0,55

6.5.1.14 Paper 545 (WMA) (Jones et al., 2010)

Paper focused on asphalt mixes (AC) with RAP and with crumb rubber modified bitumen.

- Questions related to possible optimization of asphalt mix behavior with respect to RAP content. Mechanical performance was studied mainly in term of stiffness and fatigue.
- Mixtures with 33 % and 55 % RAP are improved if combined with CRmB containing 9 % of CR. Two types of RAP were used with softening point 65-68 °C and penetration between 12 and 18 dmm. Original binder was 35/50.
- The use of 20 % CR in a mixture with 40 % RAP can be combined with 60% virgin aggregates without incurring in any significant problems during the construction and

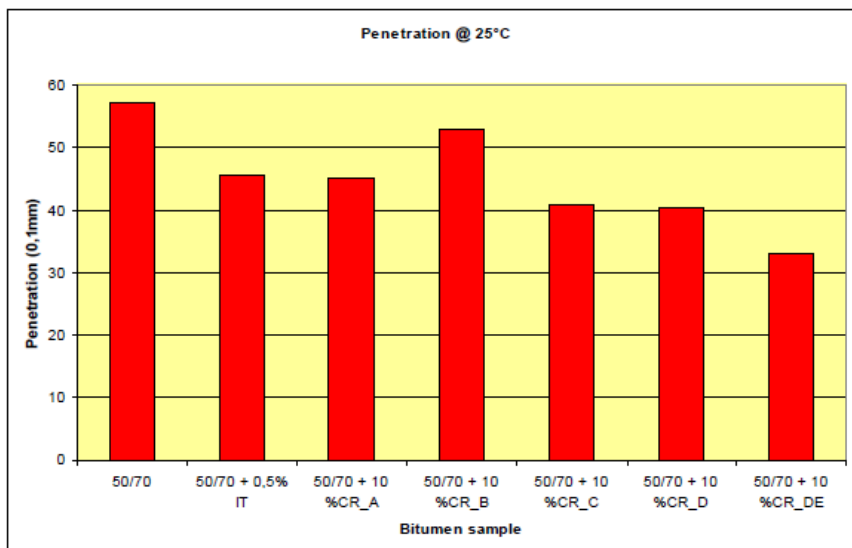
mainly the service performance – it is just important properly to select aggregates. In general CR content of 18-24 % was evaluated together with 35/50 and 50/70 bitumen.

- In terms of bitumen testing CRmB was combined with binders from both RA materials using a ratio of 10-40 %. The softening point was between 70-75°C.
- In the asphalt mixture 8.5 to 10.5 % bitumen was used.
- Preferred CR content was finally recommended 22% for 50/70 and 20% for 35/50.
- The results of the characterization of the recycled binder allowed the conclusion that penetration can exhibit different trends depending on the A as a result of reduced recycling ratios.

Frequency sweep test was applied with frequencies 10; 5; 2; 1; 0.5; 0.2; 0,1 Hz using 4PB-PR test and determining stiffness after 100 cycles. The test temperature was 20 °C. The results have shown that for a mix with 8.5% bitumen content the stiffness at 10 Hz is 4700 MPa (5,0% voids), whereas for 10 % bitumen it was reduced to 4000 MPa (3,6% voids).

6.5.1.15 Paper 361 (Valentin et al., 2013)

In this study experimental findings for acoustic asphalt mixes (SMA LA and LOA type) are presented. In both cases the grading was 0-8 mm or 0-5 mm. PMBs or crumb rubber modified binders were used. The average void content of the assessed mixes was in the range of 8 % to 11 %.



EXPLANATIONS:
 A GL PM5 - 2xJR PV
 B GL PM3 - 2xJR PV
 C GL PM5 - 2xJR PV
 D GL 3M
 DE crumb rubber supplied in 2009 by GENAN

Figure 6-2 Penetration of assessed binders for SMA LA and LOA mixes

These expressions indicate information on the method of high-speed grinding. Since the technology is covered by industrial property protection, the descriptions are not specified in more detail.

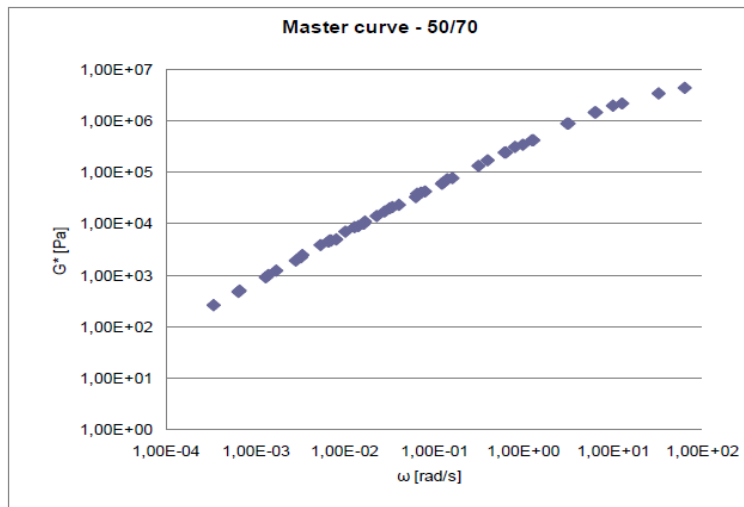


Figure 6-2: Complex shear modulus master curve of 50/70, reference temperature 20 °C

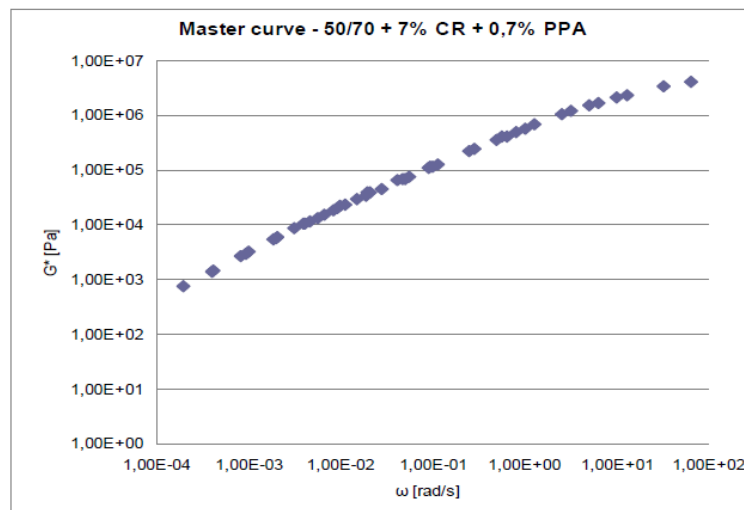


Figure 6-2: Complex shear modulus master curve of 50/70+ 7% CR + PPA bitumen, reference temperature 20 °C

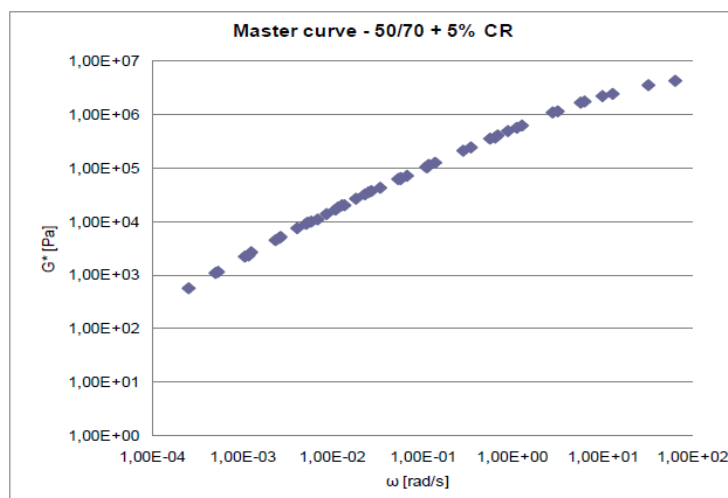


Figure 6-2: Complex shear modulus master curve of 50/70 + 5% CR bitumen, reference temperature 20 °C

Table 6-72: Stiffness moduli of asphalt mixes

Mix	Binder content [%]	Stiffness modulus [MPa] at T		
		0°C	15°C	30°C
BBTM 5 A	7,7 %	10 300	6 300	950
LOA 5 D	6,2 %	12 050	6 400	1 500
	7,5 %	10 100	8 450	2 000
	5,5 %	-	5 600	-
	5,8 %	-	3 650	-
	6,1 %	-	4 350	-
SMA 5 LA	7,2 %	7 700	5 700	1 000
	7,6 %	13 250	8 650	2 100
	7,0 %	-	11 850	-
	7,3 %	-	7 300	-
	7,6 %	-	5 750	-
SMA 8 LA	6,8 %	7 300	3 950	500
	7,2 %	12 300	6 200	1 850

The deformation characteristics were determined both by a permanent deformation resistance test performed in a small test apparatus, in air at 50 °C, and, for some mixes, stiffness modulus was determined by a non-destructive IT-CY test. Three different test temperatures were chosen, namely 5 °C; 15 °C and 30 °C.

From the perspective of stiffness, in most mixes improved values are achieved by the options with different types of CRmB binders applied. It is also obvious that for a number of the versions, the modulus values obtained are relatively low and reach around 6 GPa at the maximum. When compared to the results of the permanent deformation resistance test, as indicated below, this fact documents poor suitability of the stiffness test for the aforementioned types of mixes where the dominant load is pressure.

6.5.1.16 Paper 405 (Bureš & Komínek, 2009)

Polybitume EP (PEN=38 dmm; R&B=74,4°C) as a new alternative to traditional polymer modified bitumen was analyzed. Having selected an appropriate combination of polymers and technology modifications a binder suitable for use in binder and base courses of high (stiffness) modulus mixtures was recommended. Comparison was made with PMB 25/55-60 (PEN=50 dmm; R&B=65,2°C) and bitumen 30/45 (PEN=38 dmm; R&B=58,0°C).

The basic tests were accompanied by the complex modulus G^* and phase shift angle measurement by a shear rheometer within a temperature range of 35°C to 70°C. Based on the data obtained for Polybitume EP, the significantly smaller phase shift angle (characterising more flexible behaviour of the binder) is worth noticing in comparison to the remaining bitumens. In temperatures exceeding 50°C, it will have a positive impact on permanent deformations of the binder.

Table 6-73: Complex shear modulus characteristic for tested binders

Parameter $G^*/\sin\delta$, (kPa)	Test temperature		
	50°C	60°C	70°C
25/55-60	33,2	8,1	2,3
Polybitume EP	44,4	14,1	4,5
30/45	86,4	18,0	4,9

The stiffness moduli of asphalt mixes were determined for cylindrical specimens using the IT-CY method according to EN 12697-26. The stiffness modulus of mix AC16 with PMB 25/55-

60 as ascertained for 15°C only amounted to 8 350 M Pa. Therefore, to improve the stiffness modulus and resistance to permanent deformation, Dolanit AS 18 (0,3 % of the mix weight) and Licomont BS 100 (3 % of bitumen weight) were added.

Table 6-74 Stiffness of tested mixes AC16

Mix	AC16	AC16	AC16+Dolanit	AC16
Binder	30/45		PMB 25/55-60	Polybitume EP
Stiffness modulus (MPa) @15°C	14 510	8 350	9 790	9 350

6.5.1.17 Paper 513 (Šušteršič *et al.*, 2013)

A German study focused on impact of ageing simulation on asphalt mix durability and deterioration. For this reason cores from selected pavements (9-35 years old) were assessed and in parallel to asphalt mixes (extracted binders) standard binders were subjected to accelerated laboratory bitumen ageing. The ageing was done by two methods – Warmbold ageing table and Potschka method with model vessel. With respect to stiffness complex modules in terms of temperature sweep were assessed. The results for aged binders have shown that both ageing methods lead to different impacts. For Warmbold method the modulus increase was 15-104 %, whereas for the second method it was 209-2051 %.

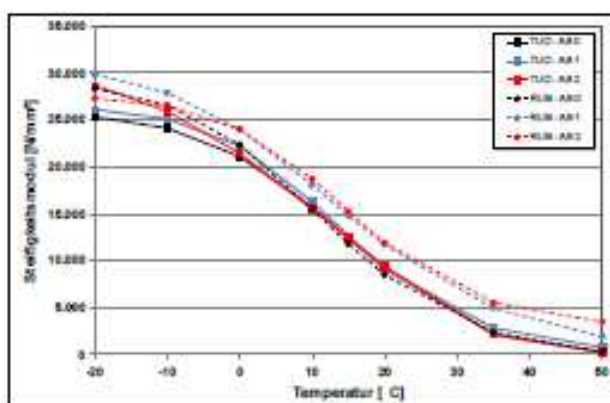


Figure 6-2: Stiffness modulus-temperature relation

6.6 Overall uncertainty of correlations

The ...

6.7 References for stiffness

- Paper 024 **Olard, F, P Huon, S Dupriet, J Dherbecourt and L M Perez (2012).** GB5: Eco-friendly alternative to EME2 for long-life & cost-effective base courses through use of gap-graded curves & SBS modified bitumens. *E&E2012*.
- Paper 025 **Mangiafico, S, H di Benedetto, C Sauzeat, F Olard, S Dupriet, L Planque and R van Rooijen (2012).** Effect of reclaimed asphalt pavement on complex modulus and fatigue resistance of bitumens and asphalts. *E&E2012*.
- Paper 026 **Eckmann, B, M Mazé, S Largeaud and S F Dumont (2012).** The contribution of cross-linked polymer modified binders to asphalt performance. *E&E2012*.
- Paper 031 **Nordgren, T, and K Olsson (2012).** Asphalt concrete test sections containing bitumen of different origins. *E&E2012*.

- Paper 037 **Iwanski, M, and G Mazurek (2012)**. The influence of rheological properties of bitumen with synthetic wax on changing resilient modulus of elasticity of asphalt concrete. *E&E2012*.
- Paper 038 **Valentin, J, P Mondschein, V Souček, O Ryneš, P Hýzl, D Stehlík and M Varaus (2012)**. Selected performance characteristics of warm mix asphalts with various low-viscosity binders. *E&E2012*.
- Paper 074 **de Visscher, J, S Vansteenkiste and A Vanelstraete (2008)**. Test sections in high-modulus asphalt: Mix design and laboratory performing testing. *E&E2008*.
- Paper 098 **Li, X, N H Gibson, T R Clyne, E N Johnson and M E Kutay (2011)**. Laboratory evaluation of asphalt binders and mixtures containing polyphosphoric acid. *TRB2011*.
- Paper 111 **Mogawer, W S, A J Austerman, R Bonaquist and M Roussel (2011)**. Performance characteristics of thin-lift overlay mixtures containing high RAP content, RAS, and warm-mix asphalt technology. *TRB2011*.
- Paper 128 **Zeleeuw, H, M R Corrigan, R Belagutti and J R Reddy (2012)**. Comparative evaluation of stiffness properties of warm-mix asphalt technologies and |E*| predictive models. *TRB2012*.
- Paper 144 **Hajj, E Y, L G Loria and P E Sebaaly (2012)**. Estimating effective performance grade of asphalt binders in high-RAP mixtures using different methodologies: Case study. *TRB2012*.
- Paper 153 **Willis, J R, A J Taylor and N Tran (2012)**. Laboratory evaluation of high polymer plant-produced mixtures. *TRB2012*.
- Paper 171 **Mogawer, W S, E H Fini, A J Austerman, A Booshehrian and B Zada (2012)**. Performance characteristics of high rap bio-modified asphalt mixtures. *TRB2012*.
- Paper 227 **Tarefder, R A, J C Stormont and M Zaman (2007)**. Evaluating laboratory modulus and rutting of asphalt concrete. *TRB2007*.
- Paper 235 **Azari, H, A Mohseni and N Gibson (2008)**. Verification of rutting predictions from mechanistic empirical pavement design guide using accelerated loading facility data. *TRB2008*.
- Paper 330 **Bower, N, H Wen, S Wu, K A Willoughby, J Weston and J DeVol (2014)**. Evaluation of performance of warm-mix asphalt in Washington state. *TRB2014*.
- Paper 347 **Yang, S.H, A Keita and H Wang (2014)**. Comparison of field aging characteristic of warm mix asphalt. *TRB2014*.
- Paper 456 **Bennert, T, and J-V Martin (2010)**. Polyphosphoric acid in combination with styrene-butadiene-styrene block copolymer – Laboratory mixture evaluation. *Asphalt Paving Technology 2010*.
- Paper 487 **Bagampadde, U, U Isacson and B M Kiggundu (2006)**. Impact of bitumen and aggregate composition on stripping in bituminous mixtures. *Materials and Structures 2006*.
- Paper 504 **Syblinski, D, M Gajewski, W Bankowski, H Soenen, E Chailleux and G Gauthier (2009)**. Binder fatigue properties and the results of the Rilem Round Robin Test. *ATCBM2009*.
- Paper 510 **Hase, M (2011)**. Bindemittel und die Gebrauchseigenschaften von Asphalt. *Asphaltstraßentagung 2011*.

Paper 543 **Wojciech, Bańkowski, Marcin, Gajewski, Dariusz and Sybilski (2010).** Full scale testing of high modulus asphalt concrete in Poland. *TRA2010*,

7 Low temperature cracking

7.1 Asphalt test methods for low temperature cracking

7.1.1 General

Low temperature cracking is particularly important for evaluating the low temperature behaviour of asphalt. In this Chapter of Report D1, several test procedures for determining the low temperature cracking properties of asphalt are included. These are:

- tensile stress restrained specimen test (TSRST), as specified in EN 12697-46;
- uniaxial tensile strength test (UTST), as specified in EN 12697-46;
- uniaxial relaxation test (RT), as specified in EN 12697-46;
- unrestrained thermal dilation test (TST),
- Indirect tension test for examining low-temperature strength and creep compliance (IDTC)
- Semi-circular bending tests (SCBT), as specified in EN 12697-44;
- Disk-Shaped Compact tension test (DCTT);
- Acoustic emissions test (AET);
- Uniaxial Thermal stress and strain test (UTSST)

7.1.2 Test procedures with uniaxial loading

Several test procedures, which are used for the assessment of low-temperature cracking resistance, are uniaxial tensile tests. The specimen with rectangular or circular cross-section and a length considerably higher compared to diameter or width/thickness is glued to loading platens in order to introduce tensile forces.

The tensile stress restrained specimen test (**TSRST**) addresses loading conditions occurring in field when the road is cooled down. Therefore, the specimen is cooled down while it is held at constant length. Any movement of the specimen as a consequence of thermal shrinkage is monitored by LVDTs, activating a screw jack that stretches the specimen back to its original length. The restrained thermal shrinkage results in cryogenic stress in the specimen which increases with decreasing temperature. According to EN 12697-46 the *failure temperature* T_f and the associated *failure stress* σ_f are the results of the test. Further the cryogenic stress at predefined temperatures $\sigma_{cry}(T)$ can be assessed. Usually applied test parameters are a temperature rate of $-10\text{ }^\circ\text{C/h}$ starting from a temperature of $20\text{ }^\circ\text{C}$. An illustration of the test procedure of the TSRST is given in Figure 7-1.

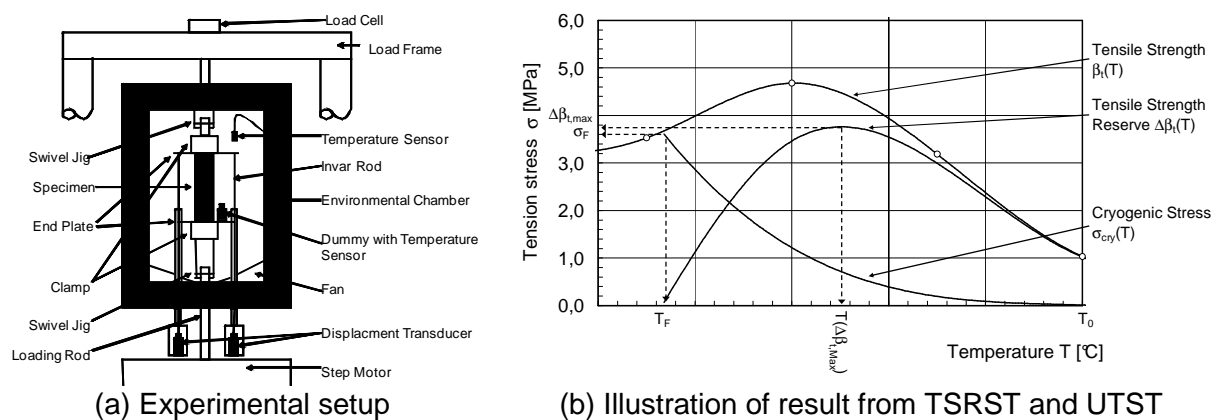


Figure 7-1: Tensile stress restrained specimen test (EN 12697-46)

The uniaxial tensile stress test **UTST** is a monotonic test in which the specimen is loaded with a constant strain rate at constant temperature until specimen failure at low temperatures or until ductile elongation of the specimen at higher temperature. Test results according to EN 12697-46 are the maximum stress, which is interpreted as *tensile strength* β_t and the associated failure strain ε_f . The test is usually conducted at various temperatures in order to assess the tensile strength versus temperature. The standard strain rate is 104 $\mu\text{m}/\text{m}/\text{s}$ resulting from the specimen length of 160 mm and a deformation rate of 1 mm/min.

By combining TSRST and UTST results, the *tensile strength reserve* $\Delta\beta(T)$ can be calculated by the difference of the tensile strength and cryogenic stress from TSRST ($\beta_t(T) - \sigma_{\text{cry}}(T)$). The maximum value of tensile strength reserve $\Delta\beta_{\text{max}}$ and the associated temperature $T(\Delta\beta_{\text{max}})$ are further assessed.

The unrestrained thermal dilation test (**TST**) is applied in order to evaluate the thermal expansion (α_T). Test parameters such as the start temperature and the cooling rate are the same as for the TSRST but the specimen is unrestrained and the thermal induced specimen length is recorded during the test.

The uniaxial thermal stress and strain test (**UTSST**) is a combination of TSRST and TST allowing the evaluation of the thermal cracking resistance with standard test equipment [323].

The relaxation test (**RT**) according to EN 12697-46 is conducted at constant temperature (isothermal condition). Relaxation time (τ) and stiffness (E) are monitored at the considered testing temperatures. The test is performed in three phases. First, the specimen is cooled to the testing temperature (stress-free). A strain increment is then applied so that the instantaneous (elastic) material response can be determined. In the third phase, the strain is kept constant and the relaxation of stress is monitored. In order to avoid damage to the specimen, the stresses induced by the strain increment in step three may not exceed 30 % of the tensile strength of the asphalt at the temperature considered. Commonly, the relaxation test is performed at +20, +5, -10 and -25 °C. The test results are the *time of relaxation* t_{rel} , which is the duration in the third phase until the stress decreased to 36,8 % of its initial value, and/or the remaining tension stress $\sigma_{\text{rem}}(t)$ after a predefined time in phase 3.

The tensile creep test (**TCT**) as specified in EN 12697-46 is a test for assessing the tensile deformation properties. The specimen is loaded with a constant force at constant temperature whereas its creep deformation is measured. In the literature review, no paper discussed this type of low-temperature test.

The uniaxial cyclic tensile stress tests (**UCTST**) assesses the fatigue resistance of an asphalt mix at low temperature for simultaneous loading of a constant tension stress (simulating cryogenic stress) and sinusoidal stress (simulating traffic loading). Result of the test is the number of load cycled until specimen failure.

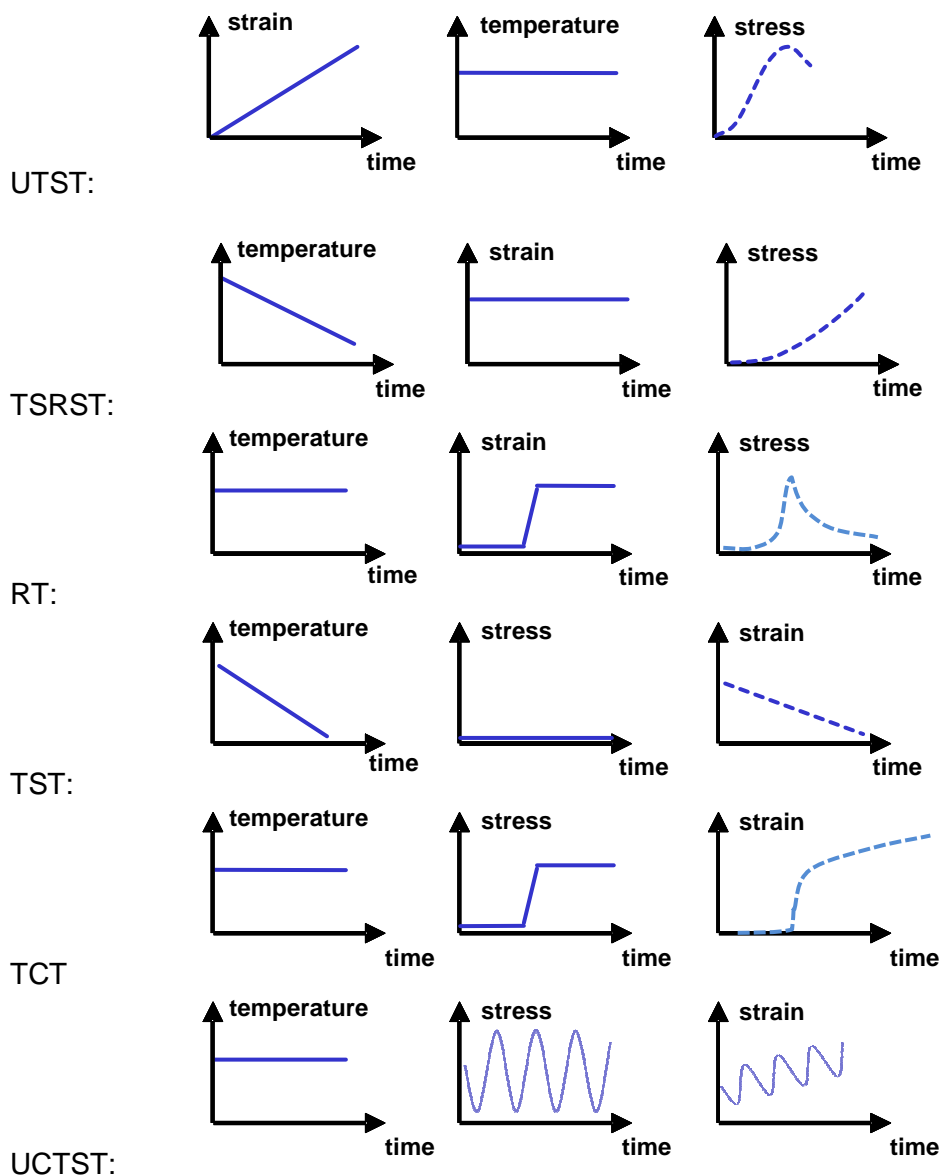


Figure 7-2: Test principles of uniaxial tests for low-temperature cracking assessment (EN 12697-46)

7.1.3 Test procedures with non-uniaxial loading at low temperatures

In addition to uniaxial test procedures, also indirect tensile tests (IDT) are conducted at low temperatures in order to assess the cracking resistance. The IDT with continuous loading as also described in EN 12697-23 is applied for evaluating the indirect tensile strength of the asphalt mix. For this analysis, simple IDT tests were considered as procedure for low-temperature cracking assessment when the test temperature applied was below 10 °C. Though, the sole indirect tensile strength is not a feasible parameter for evaluating the cracking resistance because the value doesn't allow the assessment of the brittleness of the material. Often the increase of strength goes along with an increase in stiffness and therefore with increased brittleness. The jointless construction of asphalt pavements inhibits the danger of thermal constraints. If the thermal stress reaches the tensile strength of the material, cracking occurs even at high strengths.

Therefore, in several contributions, the viscoelastic property of an asphalt mix to endure tensile thermal-induced constraining stress and to even reduce it by relaxation is assessed by indirect tensile creep tests [153]. The creep compliance is assessed by indirect tensile creep tests conducted at 0 °C; -10 °C and -20 °C. A constant vertical load is applied to the specimen for 100 seconds and the horizontal and vertical specimen deformations are measured. Finally the indirect tensile strength is assessed at the lowest temperature. The obtained creep compliance values as well as a calculated thermal coefficient to calculate the increase of tensile stress simulating the stress increase in TSRST. The temperature at which the calculated stress reaches the indirect tensile strength value is evaluated as calculated failure temperature $T_{F,cal}$.

Recently, the AE test for measuring the acoustic emissions of an asphalt specimen while it is cooled down was developed. At a specific temperature, acoustic signals can be registered which can be interpreted as cracking occurring in the bitumen/aggregate contact zone due to large differences in thermal extension parameter and high bitumen viscosity. This temperature can be associated to the temperature at which the tensile strength reaches its maximum value. Above this temperature the bitumen can relax the thermal stress. Below the critical temperature, cracking occurs which weakens the materials tensile strength. In Figure 7-3 a typical results of an AE test is shown.

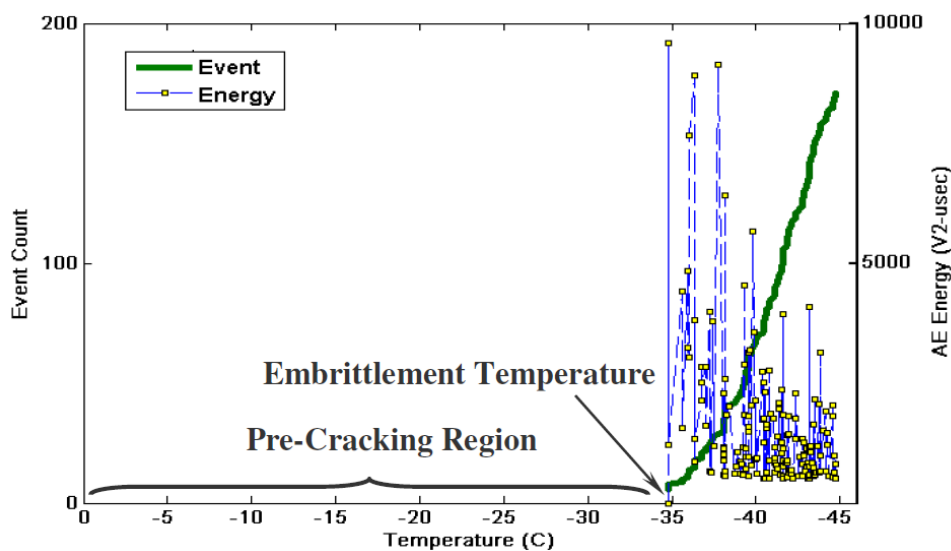


Figure 7-3: Test principle of acoustic emission (AE) test [95]

7.1.4 Test procedures addressing fracture energy approaches

In addition or as an alternative to the uniaxial test procedures the low-temperature cracking resistance of asphalt is assessed by fracture energy approaches. The principle of these tests is that a high cracking resistance is achieved, if an asphalt mixture can endure high deformation energy at low test temperatures. In various test methodologies, the deformation energy is calculated as the area below the stress-strain or force-deflection curve. Most common and already standardised in EN 12697-44 is the semi-circular bending test (SCB) allied on a notched half-cylinder.

7.2 BitVal findings for low temperature cracking

The BitVal project identified and reviewed four binder tests as having a potential relationship with asphalt mixture low temperature cracking. The outcomes of these tests were:

1. The BBR test was covered by many papers which indicated that there is generally a good correlation between the BBR limiting temperature and the TSRST failure temperature. The BBR limiting temperature provides a ranking for the corresponding asphalt's low temperature behaviour. In contrast to the BBR limiting temperature, BBR stiffness S and m -value determined at -24 °C , were not well correlated with the TSRST failure temperature, although the latter data were limited to a single paper. With regard to SBS modified bitumen, it was further reported that the BBR test underestimates the low temperature performance.
2. The results of the DTT were found to correlate reasonably well with mixture low temperature parameters, i.e. derived from TSRST and UTST. Promising candidates for addressing the binder's contribution to the low temperature behaviour of an asphalt mixture were the failure compliance of the binder, the temperature leading to failure at a specific strain rate and a brittle/ductile transition temperature of binders, designated T_{bdb} . It was noted that the DTT data were from three papers, with each paper addressing different characteristic values of DTT testing correlated with asphalt parameters. Despite the promising results, the repeatability of the DTT remained to be improved.
3. The Fraass Breaking Point Test generally had a poor correlation with the asphalt mixture's low temperature behaviour besides a bad precision of the test. Therefore, it was not recommended that Fraass breaking point was used to indicate the contribution of the binder towards the performance of asphalt mixtures in respect to their low temperature properties.
4. The data of the Fracture Toughness Test were limited to data from a single paper and, therefore, the binder fracture toughness K_{Ic} and fracture energy G_{Ic} as performance indicators for low temperature cracking still required further research. The fracture parameters appear to be independent and, thus, may be complementary to other reasonable low temperature binder properties, for example to parameters from the DTT. Both types of parameters need to be combined to adequately reflect and predict low temperature behaviour of asphalt mixtures needed further research. The repeatability of the binder parameters K_{Ic} and G_{Ic} still remained to be improved.

From this point of view, the best options for identifying the potential binder contribution to the low temperature behaviour of asphalt were either BBR limiting temperature or a DTT parameter. An alternative might be the use of the concept of critical cracking temperature, which is a combination of BBR and DTT results to determine a low-temperature parameter called the critical cracking temperature, T_{cr} . In addition, a "real" fracture property, such as the fracture toughness or the fracture energy, could be used to complement the BBR and DTT results. The critical cracking temperature and fracture toughness both show great promise, but needed time to confirm its suitability and it was unlikely to be available in the immediate future.

There were sufficient data from the papers identified to validate the relationship between BBR limiting temperature of the binder and the mixture's failure temperature from TSRST measurements. With regard to both the DTT and the FTT parameters, there were insufficient data from the papers at that time and further research was considered necessary before any definitive conclusion could be drawn. Such research needed to concentrate on the performance characterisation of modified bitumen. Nevertheless, the durability and any relationship to field performance were effectively missing for all tests. Therefore, there was justification to undertake further research to identify field performance, although such research would take some time to come to a robust conclusion.

7.3 Relationship found between bitumen properties and asphalt low temperature cracking

7.3.1 Binder-Mix relationship reported for TSRST

7.3.1.1 Paper 031 (Nordgren and Olsson 2012), TSRST and Fraass

Stone mastic asphalt mixtures (SMA 16) were produced at an asphalt plant using seven different bitumen of penetration grade 70/100. Mixture material for preparing slabs in the laboratory was taken from production at the plant. The production temperature was about 160-165 °C. The results obtained for the bitumen and asphalt mix samples are summarised in Table 7-16 and Table 7-27.

Table 7-1: Binder properties [31]

Property	Unit	1	2	3	4	5	6	7
Penetration	1/10 mm	71	83	83	72	83	80	84
Softening Point $T_{R\&B}$	°C	47	46	46	46	46	47	46
Kinem. Visc.	mm ² /s	357	386	367	336	192	465	366
Dynamic Vis.	Pas	150	137	174	112	105	172	171
Solubility	Vol-%	100,0	99,8	100,0	99,8	99,5	100,0	100,0
Fraass breaking point	°C	-16	-19	-18	-19	-18	-20	-19
Flash Point	°C	352	346	320	356	326	340	284
Change of mass (RTFOT)	%	0,1	0,0	-0,2	0,1	0,0	0,0	-0,1
Pen after RTFOT	1/10 mm	65	67	67	64	48	64	61
$T_{R\&B}$ after RTFOT	°C	51	52	52	51	52	52	51
Density	kg/m ³	1019	1015	1019	1012	1028	1022	1023

Table 7-2: Asphalt properties [31]

	Failure temperature $T_{failure}$ (°C)		Failure tensile stress $\sigma_{cry, failure}$		Air Voids content (%)
	1	-22,1	-21,0	2,54	2,46
2	-20,5	-25,2	2,15	2,76	1,8
3	-23,7	-22,6	2,66	2,08	1,3
4	-22,1	-22,0	2,76	2,52	1,9
5	-22,8	-22,8	2,33	2,56	2,2
6	-24,5	(-17,2)	2,30	(1,70)	1,9
7	-25,7	(-16,1)	3,19	(0,93)	1,1

7.3.1.2 Papers 064 (Hase and Oelkers, 2008) and 502 (Dressen *et al.*, 2009), TSRST – BBR for SMA 8 and AC 16 mixtures

Two asphalt mixtures (SMA 8 and AC 16) were prepared in laboratory with several polymer modified bitumen with same grading and binder content. The results obtained on the bitumen samples are summarised in Table 7-4 whereas the results of TSRST and tensile strength reserve are given in Table 7-5.

The regression analysis undertaken by the authors of the articles give following results:

- The m-values at $T_1 = -10\text{ °C}$, $T_2 = -16\text{ °C}$ and $T_3 = -25\text{ °C}$ shows no correlation regarding the asphalt properties
- The strength values obtained in the asphalt mix tests (tensile strength reserve and σ_{failure}) cannot be correlated to the bitumen properties obtained in BBR.
- Following correlations can be determined between the results of BBR and the low-temperature properties obtained in TSRST and UTST:
 - cryogenic tensile stress $\sigma_{\text{cry}}(T)$, measured at the temperature T and the associated BBR stiffness $S(T)$:

$$\sigma_{\text{cry}} = 0,0053 \cdot S(T) + 0,1873$$
 for the SMA 8 and

$$\sigma_{\text{cry}} = 0,0054 \cdot S(T) + 0,2192$$
 for the AC 16;
 - failure temperature T_{failure} :

$$T_{\text{failure}} = 0,0164 \cdot S(-25\text{°C}) - 38,144$$
 for the SMA 8 and

$$T_{\text{failure}} = 0,0164 \cdot S(-25\text{°C}) - 26,547$$
 for the C 16;
 - temperature at maximum tensile strength reserve $T(\Delta\beta_{\text{max}})$:

$$T(\Delta\beta_{\text{t,max}}) = 0,0092 \cdot S(-25\text{°C}) - 14,542$$
 for the SMA 8 and

$$T(\Delta\beta_{\text{t,max}}) = 0,0174 \cdot S(-25\text{°C}) - 16,482$$
 for the AC 16.

Table 7-3: Binder BBR results

Binder sample	Siffness (MPa) @			M.value @		
	-10 °C	-16 °C	-25 °C	-10 °C	-16 °C	-25 °C
30/45	73,18	160,98	366,55	0,429	0,370	0,244
PmB25A(1)	124,0	247,32	701,08	0,368	0,321	0,193
PmB25A(2)	93,68	147,42	442,42	0,386	0,330	0,218
PmB45A(1)	85,11	224,34	660,09	0,463	0,379	0,240
PmB45A(2)	99,23	217,85	670,42	0,439	0,347	0,217
PmB45A(3)	71,67	146,78	437,92	0,454	0,377	0,250
PmBH(1)	68,47	120,18	288,20	0,383	0,346	0,254
PmBH(2)	28,681	73,58	303,38	0,4852)	0,413	0,308
PmBH(3)	31,611)	97,18	293,80	0,5163)	0,399	0,289
PmBH(4)	66,06	133,27	335,85	0,402	0,345	0,264
PmBNV25	112,26	207,02	554,22	0,346	0,277	0,191
PmBNV45	90,21	206,02	494,60	0,433	0,361	0,227

Table 7-4: Results of TSRST and UTST on SMA 8 samples

SMA 8 with sample binder	TSRST		Tensile strength reserve		TSRST		
	Failure tensile stress ($\sigma_{failure}$)	Failure temp. ($T_{failure}$)	Maximum tensile strength reserve $\Delta\beta t, max$		Cryogenic tensile stress σ_{cry} [MPa] at a temperature of T		
$T_{failure}$	(MPa)	(°C)	(MPa)	(°C)	-10 °C	-16 °C	-25 °C
PmB45A(1)	4,147	-26,9	4,59	-8,7	0,651	1,479	3,667
PmB45A(2)	3,618	-25,5	3,67	-7,4	0,674	1,498	3,501
PmB45A(3)	3,212	-31,6	3,66	-11,2	0,343	0,766	2,005
PmBH(1)	3,547	-34,0	3,94	-11,5	0,338	0,683	1,852
PmBH(2)	4,462	-31,3	5,68	-11,9	0,372	0,922	2,724
PmBH(3)	4,203	-32,4	4,91	-12,2	0,311	0,7612	2,247
PmBH(4)	3,871	-33,2	3,94	-10,3	0,309	0,781	2,128
PmBNV25	4,352	-30,1	5,06	-9,6	0,765	1,455	3,191
PmBNV45	4,654	-32,2	5,92	-10,9	0,490	1,062	2,781

Table 7-5: Results of TSRST and UTST on AC 16 samples

AC 16 with sample binder	TSRST		Tensile strength reserve		TSRST		
	Failure tensile stress ($\sigma_{failure}$)	Failure temperature ($T_{failure}$)	Maximum tensile strength reserve $\Delta\beta t, max$		Cryogenic tensile stress σ_{cry} [MPa] at a temperature of T		
$T_{failure}$	(N/mm ²)	(°C)	(MPa)	(°C)	-10 °C	-16 °C	-25 °C
B 30/45	2,137	-26,5	2,24	-7,8	0,2734	0,6640	1,9057
PmB45A(1)	3,850	-22,5	4,25	-1,9	1,3410	2,3750	3,850
PmB45A(2)	2,811	-28,8	2,92	-6,6	0,3635	0,8545	2,1484
PmB45A(3)	4,076	-26,2	4,34	-4,4	0,7550	1,6030	3,8050
PmBH(1)	3,852	-26,4	4,69	-6,3	0,7220	1,5290	3,6250
PmBH(2)	3,387	-30,5	3,11	-9,0	0,2909	0,7445	2,2254
PmBH(3)	3,378	-35,5	3,57	-13,5	0,2265	0,5052	1,4028
PmBH(4)	4,463	-29,0	4,87	-10,0	0,5290	1,2250	3,1210
PmBNV25	4,516	-28,8	5,00	-8,8	0,8995	1,6385	3,4632
PmBNV45	4,924	-30,4	5,21	-10,9	0,6119	1,2843	3,1296

7.3.1.3 Paper 066 (Beckedahl *et al.*, 2008), 491 (Steinauer, 2007), 498 (Zeghal, 2008) and 505 (Tusar *et al.*, 2009), TSRST, UTST – BBR, Fraass, DSR for SMA 8 mixtures

Stone mastic asphalt mixtures SMA 11 were prepared with seven bitumen samples (1 neat, 6 polymer modified bitumen) and the same grading and bitumen content. The bitumen were analysed in fresh state as well as after RTFOT and RTFOT+PAV ageing. The asphalt

mixtures were evaluated freshly mixed as well as after an ageing procedure (called “Brunswick ageing”), in which the loose mix was stored for 4 days at 80 °C. The unaged and aged asphalt mix was used to compact asphalt samples. The compaction energy was varied in order to achieve similar void content in all mix variations.

The original research report containing all data is written in German (Paper 491), but in Papers 066, 498 and 505 the data are discussed in English articles.

In Table , the quality of the linear correlation between the RTFOT-aged bitumen and the freshly-prepared asphalt mix samples are summarised. For the failure temperature T_f , reasonable correlations can be observed for the penetration, Fraass breaking point as well as the BBR test results $S(-16\text{ °C})$ and the temperature, at which $S = 300\text{ MPa}$ or $m = 0,3$, which are also applied for estimating the bitumen low-temperature properties according to SHRP specification. Additionally, feasible correlations could be obtained between the failure temperature T_f as well as the temperature at maximum tensile strength reserve $T(\Delta\beta_{t,max})$ and a parameter calculated from G^* and δ obtained at 1,59 Hz and 20 °C:

- failure temperature $T_{failure}$: $T_{failure} = 2,0E-6 \cdot G^*/\sin\delta (1,59\text{ Hz } 30\text{ °C}) - 30,374$
- temperature at maximum tensile strength reserve $T(\Delta\beta_{max})$:
 $T(\Delta\beta_{t,max}) = 2E-6 \cdot G^*/\sin\delta (1,59\text{ Hz } 30\text{ °C}) - 11,421$

In [491] the correlations between the RTFOT-aged bitumen parameters and the unaged asphalt mix parameters as well as the RTFOR+PAV-aged bitumen properties and the aged asphalt mix parameters were analysed. For each pair of parameters 14 datasets were available. The resulting correlations with satisfying quality were found as followed:

- for the cryogenic stress at -20 °C:
 - Fraass breaking point: $T_{cry}(-20\text{ °C}) = 0,9701 \cdot T_{Fraass} - 4,0736 (R^2 = 87,8\%)$
 - BBR $S(-16\text{ °C})$: $T_{cry}(-20\text{ °C}) = 1118,941 \cdot S(-16\text{ °C}) - 78,316 (R^2 = 88,1\%)$
 - BBR $T(S = 300\text{ MPa})$ $T_{cry}(-20\text{ °C}) = 4,3604 \cdot T(S=300) - 29,851 (R^2 = 88,4\%)$
 - DSR (60°C, 1,59 Hz) $T_{cry}(-20\text{ °C}) = 3,336e-5 \cdot G^* + 0,0357 \cdot \delta - 0,8009 (R^2 = 88,6\%)$
- for the temperature at maximum strength reserve $T(\Delta\beta_{max})$:
 - $T(\Delta\beta_{t,max}) = 0,9701 \cdot T_{Fraass} - 4,0736 (R^2 = 87,8\%)$

Table 7-6: Low-temperature properties of the SMA 8—mixtures and binders (Paper 498)

Sample		1-2	2-1	2-3	2-5	3-1	4-2	5-1
Binder category		10/40-65	20/60-55	20/60-55	20/60-55	45/80-50	40/100-65H	50/70
Polymer type		SB	SBS	SBS	SB	SBS	SB	-
fresh	T _{R&B} [°C]	64,2	57,2	62,2	58,5	50,0	71,0	48,9
	Pen [1/10 mm]	30	35	43	57	57	62	66
	T _{Fraass} [°C]	-11,5	-11,8	-16,0	-20,9	-17,0	-20,7	-16,5
	El. Rec.(25°C) [%]	74,5	63,0	78,0	75,5	71,0	90,5	15,3
	FD: W _{tot} [J]	2,0691	0,5839	1,0625	0,6618	0,6618	2,7387	0,0488
	FD: W _{0,2-0,4} [J]	0,554	0,111	0,190	0,157	0,006	0,406	0,001
	FD: F _{max} [N]	5,3	3,7	2,5	1,5	1,2	1,4	0,8
	BBR: S(T=-16°C) [MPa]	223,4	254,4	202,3	116,2	111,1	85,1	172,1
	BBR: m (T=-16°C) [-]	0,32	0,33	0,35	0,40	0,43	0,44	0,36
	BBR: T(S=300) [°C]	-18,3	-17,8	-19,5	-21,8	-22,1	-24,8	-20,4
	DSR: G*(T=60°C, f=1,59Hz) [Pa]	25.439	12.242	10.828	9.793	6.377	11.285	2.846
	DSR δ (T=60°C, f=1,59Hz) [°]	66,4	76,7	71,7	68,3	79,0	56,1	86,6
	DSR: G*(T=30°C, f=1,59Hz) [Pa]	1.238.110	1.039.270	850.418	536.887	469.933	290.744	272.627
DSR δ (T=30°C, f=1,59Hz) [°]	39,4	48,3	50,3	55,6	57,4	57,2	67,0	
RTFOT	T _{R&B} [°C]	69,9	64,2	64,8	62,8	56,3	68,9	54,0
	Pen [1/10 mm]	21	24	30	40	48	51	43
	T _{Fraass} [°C]	-8,5	-7,0	-12,0	-14,3	-15,3	-16,6	-13,6
	El. Rec.(25°C) [%]	72,8	65,0	79,3	77,0	59,3	88,8	14,0
	FD: W _{tot} [J]	2,857	2,146	2,883	1,289	0,270	3,416	0,179
	FD: W _{0,2-0,4} [J]	1,062	0,402	0,536	0,392	0,052	0,673	0,016
	FD: F _{max} [N]	10,6	10,5	5,9	3,3	1,9	2,0	2,2
	BBR: S(T=-16°C) [MPa]	241,7	285,5	270,9	160,3	136,5	88,4	138,6
	BBR: m (T=-16°C) [-]	0,303	0,28	0,294	0,364	0,390	0,421	0,384
	BBR: T(S=300) [°C]	-17,8	-16,5	-17,1	-20,9	-23,4	-23,0	-21,1
	DSR: G*(T=60°C, f=1,59Hz) [Pa]	36.620	26.872	16.087	14.828	6.803	11.558	7.355
	DSR δ (T=60°C, f=1,59Hz) [°]	63,6	72,4	69,8	65,7	74,4	57,2	81,7
	DSR: G*(T=30°C, f=1,59Hz) [Pa]	1.474.535	1.655.665	1.097.347	735.852	367.027	296.455	710.232
DSR δ (T=30°C, f=1,59Hz) [°]	33,7	32,8	43,6	49,3	58,5	58,6	52,2	
PAV	T _{R&B} [°C]	83,5	73,8	70,4	72,7	66,0	76,9	62,8
	Pen [1/10 mm]	16	15	21	20	31	32	25
	T _{Fraass} [°C]	-4,0	-2,5	-8,0	-12,8	-12,0	-12,5	-9,8
	El. Rec.(25°C) [%]	68,6	48,4	71,5	61,2	71,0	8,8	16,3
	FD: W _{tot} [J]	4,906	3,893	5,231	1,560	1,613	3,385	0,898
	FD: W _{0,2-0,4} [J]	1,281	0,933	1,314	0,280	0,330	1,452	0,065
	FD: F _{max} [N]	29,4	31,9	16,2	9,3	7,4	7,5	10,9
	BBR: S(T=-16°C) [MPa]	300,8	403,8	298,3	209,2	154,5	119,3	243,8
	BBR: m (T=-16°C) [-]	0,277	0,239	0,260	0,321	0,322	0,370	0,342
	BBR: T(S=300) [°C]	-16,0	-12,5	-16,1	-19,0	-21,0	-22,3	-17,5
	DSR: G*(T=60°C, f=1,59Hz) [Pa]	72.471	72.368	32.739	35.778	19.374	21.289	18.818
	DSR δ (T=60°C, f=1,59Hz) [°]	59,2	65,4	67,4	60,2	68,2	54,6	75,9
	DSR: G*(T=30°C, f=1,59Hz) [Pa]	1.967.800	2.230.633	1.645.897	1.305.590	1.014.771	639.644	1.283.040
DSR δ (T=30°C, f=1,59Hz) [°]	23,1	19,5	30,8	35,4	40,3	48,6	37,6	
Asphalt mix: fresh	UTST: f(-10°C) [MPa]	5,640	4,679	5,241	5,507	4,847	6,465	4,672
	UTST: ε _t (+5°C) [‰]	3,133	2,320	3,350	4,307	3,949	6,131	3,095
	TSRST: σ _f [MPa]	4,561	3,852	4,393	4,603	3,857	5,317	3,945
	TSRST: T _f [°C]	-25,3	-23,9	-27,9	-29,0	-28,1	-34,6	-26,9
	Δf _{max} [MPa]	4,643	4,451	4,362	4,885	4,385	6,191	4,157
	TΔf _{max} [°C]	-6,7	-1,7	-9,2	-9,7	-9,9	-11,9	-9,0
Asphalt mix: aged 4 d @ 85°C	UTST: f(-10°C) [MPa]	5,345	4,586	5,102	5,542	4,399	6,684	4,167
	UTST: ε _t (+5°C) [‰]	2,422	1,549	2,480	3,582	3,024	6,478	2,600
	TSRST: σ _f [MPa]	4,697	3,921	4,661	4,398	3,701	5,053	3,765
	TSRST: T _f [°C]	-24,6	-21,3	-25,5	-26,8	-25,7	-33,8	-23,8
	Δf _{max} [MPa]	4,539	4,819	4,203	4,824	3,773	6,198	3,645
	TΔf _{max} [°C]	-1,9	1,7	-5,2	-8,1	-8,5	-11,0	-3,6

Table 7-7: Coefficients of correlation [%] between bitumen characteristics, evaluated on RTFOT-aged binders and asphalt mix low-temperature tests results evaluated on freshly-compacted SMA 11 mixtures (Paper 505)

Coefficient of correlation between bitumen characteristics (RTFOT) and asphalt characteristics (unaged)		TSRST		UTST								Tensile strength reserve		
				Tensile strength				Tensile strain						
		T_F	σ_F	$\sigma_{br}(-20^\circ\text{C})$	$\beta_1(+20^\circ\text{C})$	$\beta_1(+5^\circ\text{C})$	$\beta_1(-10^\circ\text{C})$	$\beta_1(-25^\circ\text{C})$	$\epsilon_F(+20^\circ\text{C})$	$\epsilon_F(+5^\circ\text{C})$	$\epsilon_F(-10^\circ\text{C})$	$\epsilon_F(-25^\circ\text{C})$	$\Delta\beta_{i,Max}$	$T(\Delta\beta_{i,Max})$
Standard tests	SP R&B	4	51	13	52	12	54	27	6	7	17	17	35	1
	Pen	60	6	97	81	79	6	18	58	55	37	29	19	61
	Fraass BP	71	16	91	76	94	15	30	67	65	40	34	21	86
Force ductility	El. Rec.	16	74	0	11	0	50	23	17	22	23	23	38	1
	Total Energy	8	50	7	41	8	50	36	8	8	24	22	34	0
	Energy (20–40 cm)	0	40	25	61	15	44	18	1	2	7	5	18	1
	F_{Max}	30	0	75	97	80	0	4	25	23	7	7	0	60
DSR	$G^*(60^\circ\text{C}; 1,59 \text{ Hz})$	30	0	80	95	70	1	3	23	20	9	9	0	44
	$\delta(60^\circ\text{C}; 1,59 \text{ Hz})$	33	81	0	11	0	87	54	39	44	49	47	71	7
BBR	$S(-16^\circ\text{C})$	68	22	77	49	66	25	31	73	75	52	40	40	62
	$m(-16^\circ\text{C})$	59	12	83	61	69	13	25	62	60	42	32	27	61
	$T(S = 300 \text{ MPa})$	49	6	78	67	73	8	12	51	53	31	19	18	57
	$m(S = 300 \text{ MPa})$	65	13	82	52	69	16	26	67	65	54	31	33	57

$T(m=0,3)$

7.3.1.4 Paper 112 (Loria *et al.*, 2011), TSRST: PG grade and F-T cycles

HMA mixtures were prepared with 0 %, 15 % and 50% RA and two different neat binders. For these mixtures, TSRST were conducted on field-prepared asphalt mixtures as well as artificially laboratory-aged (4 h @ 135 °C) laboratory-mixed samples. The binders were extracted from the field-prepared and laboratory-mixed samples. After recovery, the binders were RTFOT and PAV-aged. The results obtained are summarised in Table .

Table 7-8: Properties of fresh binders as well as recovered binders from RA and asphalt mix samples (binders RTFOT + PAV-aged after recovery)

Binder		Low PG grade minT(S=300 MPa or T = 0,3) [°C]	TSRST: T _f [°C]	TSRST after frost-thaw- cycles; T _{f,F-T} [°C]
Virgin binder	Pen 150-200	-32,5		
	Pen 200-300	-34,4		
Extracted from RA	RA binder	-14,7		
Field mix: binder extracted and RTFOT+PAV aged	Recovered from F-0%-150	-31,6		
	Recovered from F-15%-150	-29,5	-31	-32
	Recovered from F-50%-150	-21,2	-29	-28
	Recovered from F-50%-200	-25,1	-32	-32
Lab mixed (aged 4 h @ 135 °C);	Recovered from L-0%-150	-32,6	-33	-34
	Recovered from L-15%-150	-30,5	-31	-32
	Recovered from L-50%-150	-22,3	-27	-27
	Recovered from L-50%-200	-26,6	-34	-34

7.3.1.5 Paper 130 (Lee et al., 2012), TSRST: DTT and BBR

Two types of asphalt mixtures (SMA 13 and AC 16) were prepared with three types of bitumen each. The neat bitumen (AH-90), a diatomite modified bitumen DiaMB and an SBS-modified binder are described by penetration, softening point and ductility.

Table 7-9: Properties of fresh binders as well as asphalt mix test results

Asphalt mix type		AC 16			SMA 13		
Bitumen properties	Binder type	AH-90	DiaMB	SBS	AH-90	DiaMB	SBS
	Binder content	4,7	5,4	5,3	6,0	6,5	6,2
	Pen	91	79	95	91	79	95
	Ductility (10 °C)	> 100	36,5	> 100	> 100	36,5	> 100
	Softening point	44,8	47,6	74	44,8	47,6	74
	Sample Mixture	A	B	C	D	E	F
	Penetration [1/10 mm]	91	79	95	91	79	95
	Softening point R&B [°C]	44,8	47,6	71,0	44,8	47,6	71,0
TSRST	Failure temperature [°C]	-21,4	-24,5	-26,1	-23,5	-25,3	-30,1
	Failure stress [MPa]	3,96	4,93	4,96	3,37	4,52	4,56
3PB (-10 °C)	Bending strength [MPa]	9,9	9,7	11,9	7,7	8,9	10,3
	Failure strain [µm/m]	2138	1775	2369	1690	1849	2512
	Critical value of bending strain energy density [KJ/m³]	7,1	8,3	12,3	7,9	11,0	13,4
RT (-10°C)	Relaxation time [s]	4300	12000	7000	3100	10100	3600

For low-temperature cracking assessment, TSRST as well as uniaxial relaxation tests and 3-point-bending strength tests were conducted at -10 °C. The results obtained are summarised in Two types of asphalt mixtures (SMA 13 and AC 16) were prepared with three types of bitumen each. The neat bitumen (AH-90), a diatomite modified bitumen DiaMB and an SBS-modified binder are described by penetration, softening point and ductility.

Table 7-9.

7.3.1.6 Paper 144 (Hajj *et al.*, 2012), TSRST: BBR

The effect of high recycling rates was evaluated in a project on four plant-produced asphalt mixtures. The mixes were sampled on the construction site. Asphalt specimens were prepared by kneading compactor to final air-voids of $7\pm 0,5\%$ and aged for 5 d at 85 °C for simulating long-term ageing. TSRST was conducted on these specimens.

The binders applied were tested after extraction from the asphalt mixture. The results of the tests, including for the PG grades, are summarised in Table 7-10.

Table 7-10: Properties of fresh binders as well as asphalt mix test results

Sample		F-0%-150	F-15%-150	F-50%-150	F-50%-200
RA content		0 %	15 %	50 %	50 %
Virgin Binder	lowPG(BBR)	-32,5	.32,5	-32,5	-34,4
Rec. binder		-31,6	-29,5	-21,2	-25,1
TSRST	T _f [°C]	-33	-31	-29	-32

7.3.1.7 Paper 294 (Bennert *et al.*, 2014), TSRST, IDT – binder properties

For evaluating the possibility to increase the rate of reclaimed asphalt in new pavements, several samples from a trial section were tested. Besides TSRST (starting temperature 4 °C) as well as indirect tensile creep compliance and strength tests were conducted. Regarding the bitumen properties only the PG grades of the added binder are given. Though no details on the resulting binders (extracted from the mix) are identified in the binders, the results can be used for comparing the actual TSRST failure temperature with the critical temperature as evaluated from IDT creep compliance and strength tests. All parameters are summarised in Table 7-11.

Table 7-11: TSRST and IDT compliance and strength test results

Added binder PG		RA content	TSRST: T _f	IDT: T _{crit}
High PG	Low PG	(%)	(°C)	(°C)
64	-22	0	-	-13,8
64	-22	20	-20,4	-15,4
58	-28	30	-23,3	-9,0
64	-22	30	-19,8	-13,4
58	-28	40	-21,5	-9,4
64	-22	40	-17,9	-9,5
52	-34	0	-29,5	-20,4
64	-28	0	-24,8	-20,1
52	-34	20	-30,7	-21,8
64	-28	20	-25,0	-16,4
52	-34	30	-28,6	-22,7
64	-28	30	-24,8	-22,7
52	-34	40	-28,2	-17,3

64	-28	40	-24,0	-16,3
----	-----	----	-------	-------

7.3.1.8 Paper 378 (Sybilski and Ruttmar, 2011), TSRST versus conventional bitumen properties

Four asphalt mixtures with four different binders were tested by TSRST (starting temperature 5 °C). The results are summarised in Table 7-12.

Table 7-12: TSRST and conventional bitumen properties

Asphalt mixture type	50/70	70/100	PMB 25/55-60	PmB 65/105-60
	AC 16	SMA 11	AC 16	SMA 11
Penetration @ 25 °C (1/10 mm)	62	72	33	54
Softening point $T_{R\&B}$ (°C)	49,0	46,4	71,4	68,2
Fraass Breaking Point (°C)	-16	-18	-23	-23
TSRST: T_f (°C)	-26,5	-29	-22,5	-27,9

7.3.1.9 Paper 439 (Butt *et al.*, 2009), TSRST and BBR (bitumen, mastic and asphalt), Fraass for PMB and wax modified bitumen

Two mastic asphalt mixtures were prepared and tested. The bitumen properties were evaluated on RTFOT-aged binders, which were aged for 75 minutes at 200 °C. because of low void content, PAV was not applied. Besides of TSRST (original American device, $T_0 = 2$ °C) on the MA mixtures, also BBR tests were applied on MA samples as well as on mastic samples. The results are summarised in Table 7-13.

Table 7-13: TSRST and bitumen properties for mastic asphalt mixtures

Bitumen		PMB 32	PMB 32+4% wax		
Softening point [°C]		75	93		
Penetration (25 °C) [1/10 mm]		53	45		
Breaking point Fraass [°C]		-14	-11		
Elastic recovery at 10 °C [%]		72,5	53,4		
Viscosity at 135 °C [mPas]		1544	1394		
Viscosity at 180 °C [mPas]		258	192		
After RTFOT at 200 °C	Softening point (°C)	75	94		
	Penetration @ 25 °C (1/10 mm)	23	24		
	Breaking point Fraass (°C)	-9	-8		
	Elastic recovery at 10 °C (%)	55,5	52,2		
BBR test results		S (MPa)	m-value	S (MPa)	m-value
RTFOT-aged bitumen	-24 °C	503	0,234	532	0,202
	-18 °C	281	0,308	311	0,256
	-12 °C	124	0,359	160	0,299
T(S = 300 MPa)		-18,5		-18,0	
T (m = 0,3)		-19,0		-12,0	
BBR test results (mastic)	-24 °C	2753	0,130	3157	0,146
	-18 °C	2061	0,214	2331	0,211
	-12 °C	1158	0,288	1218	0,276
	-6 °C	641	0,357	660	0,319
	0 °C	276	0,438	328	0,398

BBR test results (MA)	-24 °C	6654	0,057	6715	0,066
	-18 °C	5465	0,095	5836	0,098
	-12 °C	4063	0,179	4729	0,133
	-6 °C	2885	0,265	4288	0,203
	0 °C	1386	0,359	2046	0,291
TSRST: T _f (°C)		-35		-30	
TSRST: T _{transition} (°C)		-29		-20	

7.3.1.10 Paper 475 (de Backer *et al.*, 2008), TSRST of wax modified asphalt

Asphalt concrete mixtures AC 11 were prepared with two kinds of binders: a 70/100 bitumen and the same bitumen with 3 % added F-T wax. TSRST was applied with a starting temperature of 5 °C. BBR was assessed on the neat bitumen as well on a binder with 4 % wax added. The results are summarised in Table 7-14.

Table 7-14: TSRST and bitumen properties

Test result	70/100		70/100 + 3 % F-T-wax	70/100 + 3 % F-T-wax	
	Stiffness (S / m)	Creep (m)		Stiffness (S / m)	Creep (m)
BBR: (S / m) -24 °C	620 MPa	0,22		670 MPa	0,17
BBR: (S / m) -18 °C	360 MPa	0,27		420 MPa	0,22
BBR: (S / m) -12 °C	160 MPa	0,34		230 MPa	0,27
BBR: T(S=300 MPa)	-16,5			-14	
BBR: T(m = 0,3)	-20,5			-8,5	
TSRST: T _f (°C) / σ _f (MPa)	-34,2 / 4,90		-30,9 / 4,94		

7.3.1.11 Paper 483 (Nikolaides and Manthos, 2010), TSRST of several laboratory prepared AC 11 mixtures

The neat bitumens were each modified with four different polymers. The bitumen samples were evaluated by BBR and DMA for assessment of glass transition temperature. Asphalt mixtures (AC 11) with crushed granite and a bitumen content of 6,2 % were prepared with the 15 binders and TSRST were conducted. The specimen were compacted by gyratory to a void content of 3,5 %.

The evaluation of the test results indicated a good correlation between TSRST failure temperature and BBR test results. The correlation to Fraass breaking temperature was weak and no correlation was found for the glass transition temperatures evaluated. The results are summarised in Table 7-15.

Table 7-15: TSRST and bitumen properties

Binder sample	Fraass breaking temperature	Pen @ 25 °C	Softening point	BBR: T(S=300MPa)	BBR: T(m=0,3)	TSRST: Tf
	(°C)	(1/10 mm)	(°C)	(°C)	(°C)	(°C)
A - 70/100, Venezuela	-11	84	46,0	-19	-23	-29
A + 6% SBS	-12	49	73,5	-19	-20,5	-28,5
A + 6% SEBS	-16	40	71,8	-18	-18	-22
A + 6% EVA	-14	54	59,5	-20	-23	-25
A + 6% EBA	-13	44	74,8	-19	-21	-26
B - 160/220, Venezuela	-16	183	38,8	-23	-28	-32,5
B + 6% SBS	-17	88	77,2	-23,5	-26	-33
B + 6% SEBS	-18	61	66,8	-22,5	-28	-28
B + 6% EVA	-20	97	53,4	-23	-28,5	-31,8
B + 6% EBA	-18	82	70,2	-24	-27,5	-32
C- 160/220, Mexico	-17	180	41,0	-23,5	-31	-32,5
C + 6% SBS	-20	88	77,2	-25	-24,5	-33
C + 6% SEBS	-17	67	70,5	-23	-24	-29,5
C + 6% EVA	-17	100	57,7	-23,5	-25,5	-34
C + 6% EBA	-20	72	71,0	-24	-25,5	-31,8

7.3.1.12 Paper 485 (Gubler *et al.*, 2005), TSRST and UTST for 4 bitumen and asphalt mixtures

The relationship between bitumen and asphalt mix low-temperature properties were assessed for AC10 mix for which only the bitumen was varied. Four different bitumen binders were used for preparing the asphalt mixtures with diorite aggregates, binder content and 3 % voids content. Results are presented in tables and figures allowing a correlation analysis between bitumen complex shear modulus (obtained from two different tests), bitumen tensile strength tests and creep characteristics from BBR to asphalt mix properties obtained in TSRST and UTST.

Table 7-16: Bitumen and asphalt mix low-temperature properties

Binder sample	Asphalt mix properties				Binder properties			
	TSRST		UTST (dε=12,5 μm/m/s)		BBR		DTT	Complex Modulus test G*
	T _f (°C)	σ _f (Mpa)	β _{t-10 °C} (MPa)	T β _{t,max} (°C)	T _{S=300 Pa} (°C)	T _{m=0,3} (°C)	T _{trans.} (°C)	G* @10 °C & 1 Hz (Pa)
10/20	-21,6	3,8	5,6	-3	-12,2	-14	-10	5,0e7
50/70	-29,5	4,0	6	-13	-19,3	-20,9	-15	1,0e7
PmB1	-34,1	5,5	6,8	-14	-19,3	-21,6	-20	6,3e6
PmB2	-45,2	6,0	5,5	-22	-28,8	-29,1	-30	1,6e6

The TSRST failure temperature correlates well with the three characteristic temperatures obtained from BBR and DTT test on the binders in fresh, unaged condition. Furthermore, an

exponential relationship can be found between the failure temperature and the bitumens shear modulus obtained at 10 °C and 10 Hz. However, four very different binders were used in this study resulting in a large range of test results.

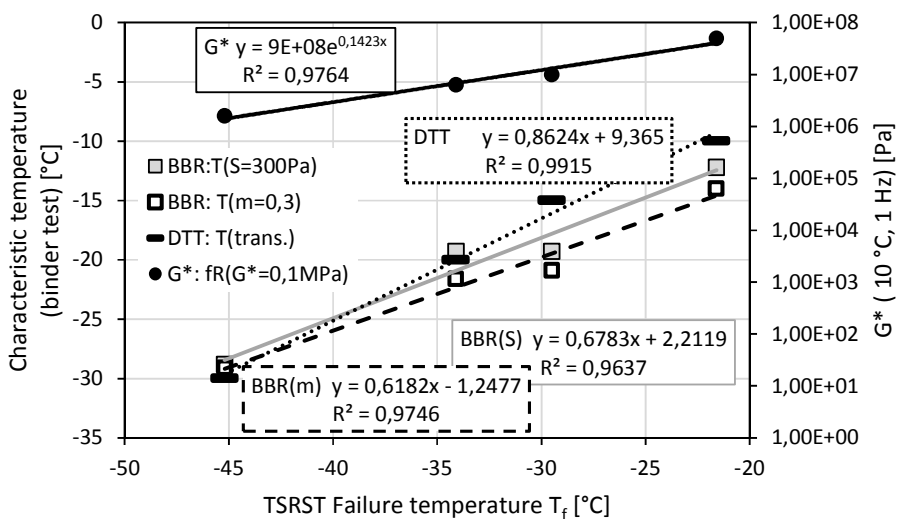


Figure 7-4: Relationship between TSRST failure temperature and characteristic temperatures derived from bitumen tests

7.3.1.13 Paper 487 (Bagampadde *et al.*, 2006), TSRST for AC 11 with varied modifiers (wax, PPA)

A dense graded asphalt concrete with maximum aggregate size of 11 mm was prepared with a crushed granite material and a nominal binder content was 6,2 % by weight. The target air void content was 2,0-3,5 % by volume. Measured air void content was found to vary between 2,1 % and 4,0 %.

Table 7-17: Bitumen and asphalt mix low-temperature properties

	Bitumen	FT-wax		PE wax		Montana wax	Slack wax	Poly-phosphoric acid
	160/220	3% S	6% S	3% PW	6% PW	6% MW	6% SW	1% PPA
Pen @ 25 °C (1/10 mm)	168	91	71	128	97	111	315	120
T _{R&B} (°C)	39	64	90	47	62	87	35	44
PI	1,5	3,6	6,5	0,7	3,4	7,8	0,1	0,6
BP _{Fraass} (°C)	-19	-18	-15	-23	-23	-17	-22	-23
FD: F _{Max} @ 5 °C (NO)	24	55	98	32	40	75	47	25
FD: W @ 5 °C (J)	1,0	1,5	1,9	1,1	1,4	1,5	0,9	1,1
BBR: S @ -25 °C (MPa)	390,5	452	504,5	416,5	416,5	421	3 12,5	334,5
BBR: S @ -20 °C (MPa)	118	173,5	219,5	132,5	145,5	187,5	143,5	106,5
BBR: m @ -25 °C	0,331	0,297	0,270	0,316	0,313	0,275	0,322	0,350
BBR: m @ -20 °C	0,443	0,406	0,338	0,433	0,418	0,335	0,34	0,451
T @ S = 300 MPa	-23,3	-22,3	-21,4	-23,0	-22,9	-22,4	-24,6	-24,2
T @ m = 0,3	-26,4	-24,9	-22,8	-25,7	-25,6	-22,9	-30	-27,5
TSRST: T _f (°C)	-33,6	-33,2	-31,9	-34,0	-33,1	-32,1	-32,9	-36,1
TSRST: T _{trans} (°C)	-27,7	-27,6	-27,2	-27,4	-27,7	-27,4	-27,0	-29,9
TSRST: σ _f (MPa)	3,92	4,31	4,29	4,3	4,23	4,07	4,20	4,09

7.3.1.14 Paper 488 (Edwards *et al.*, 2006), TSRST and UTST results for PA

For evaluating the durability of PA courses on motorways, several asphalt samples were cored 3 to 6 years after construction and TSRST and UTST were conducted. The binders were extracted and were evaluated by DSR, BBR and force ductility tests. From the initially applied bitumen and the aggregates the initial bitumen properties were evaluated in fresh and RTFOT-aged stage. Additionally for some samples asphalt mixtures were laboratory prepared in order to evaluate the initial asphalt properties. The results are summarized in Table 7-18.

7.3.1.15 Paper 489 (Renken, 2007), TSRST and UTST for AC 16 with RA addition and extracted bitumen properties

For evaluating the possibility to add RA in asphalt concrete mixtures AC 16 for binder asphalt courses, for which usually polymer modified bitumen is applied, 36 asphalt mixtures were prepared. The extracted bitumen was analyzed for conventional bitumen properties as well as force ductility and DSR results. From the laboratory-prepared asphalt mixtures the low-temperature cracking properties were evaluated by TSRST and UTST. The asphalt mix and bitumen properties are summarized in Table 7-19.

Table 7-18: Bitumen and asphalt mix low-temperature properties of PA

	No.	1.2n	3.2n	4.3n	6.1s	6.3n	7.1n	A39	256+000	265+550	272+550	257+500	264+000
fresh	T _{R&B}	63,3	75,6	76,5	87	70	68,5	59	75,6	68,5	68,5	75,6	68,5
	Pen	46	85	46	28	44	61	48	85	61	61	85	61
	T _{Fraass}	-13	-15,5	-9	-4,3	-14,5	-16,4	-24	-15,5	-16,4	-16,4	-15,5	-16,4
	FD: W	0,744	0,992	3,743	10,55	1,952	2,661	0,669	0,992	2,661	2,661	0,992	2,661
	DSR:G*(60°C4,Hz)	28700	8420	26890	60100	16260	21550	23090	8420	21550	21550	8420	21550
RTFOT	T _{R&B}	67,1	71	76	82	71,6	71,1	67,6	71	71,1	71,1	71	71,1
	Pen	40	64	35	28	33	50	36	64	50	50	64	50
	T _{Fraass}	-15,2	-22	-10,3	-8,5	-19	-15,3	-22	-22	-15,3	-15,3	-22	-15,3
	FD: W	0,998	0,962	3,219	4,904	1,545	2,654	1,674	0,962	2,654	2,654	0,962	2,654
	DSR:G*(60°C4,Hz)	27090	13300	38400	70140	26060	12120	30450	13300	12120	12120	13300	12120
Extracte d	T _{R&B}	66,4	75,9	77,3	84,5	73,5	89,3	73,5	77,9	87,3	78,8	74,5	80,5
	Pen	29	15	19	14	22	19	14	18	21	20	20	21
	T _{Fraass}	-14	-7	-8,3	-4	-13,5	-11,2	-1,5	-14	-7,8	-13,5	-8,2	-10,2
	FD: W	0,622	2,951	2,719	5,575	1,482	3,277	5,563	3,909	3,775	3,698	3,43	3,382
	DSR:G*(60°C4,Hz)	34420	140170	149900	205200	70590	99610	200900	96320	69320	69540	91060	54710
Asphalt properties													
freshly mixed	f(-10°C)	1,554	1,494		1,461	2,141	1,562	1,687					
	σ _F	1,196	1,219		1,209	2,176	1,455	1,567					
	T _F	-32	-31		-23	-27,8	-30,3	-20,8					
	Δf _{max}	1,477	1,42		1,304	1,833	1,438	1,791					
	TΔf _{max}	-11,5	-12,1		-1,3	-6,1	-9,7	2					
Site aged	f(-10°C)	1,306	1,236	1,605	1,463	1,765	1,606	1,277	1,324	1,304	1,448	1,401	1,398
	σ _F	1,175	1,069	1,296	1,177	1,697	1,342	1,101	1,229	1,209	1,362	1,098	1,202
	T _F	-28,4	-24,7	-24,3	-19,8	-20,5	-25,5	-16,8	-24,2	-27,5	-24,6	-23,6	-27,7
	Δf _{max}	1,063	1,055	1,347	1,309	1,658	1,453	1,199	1,123	1,143	1,258	1,165	1,216
	TΔf _{max}	-5,8	3,5	-2,8	1,4	1,7	-1,3	4,4	0,8	-3,7	-1,6	-1,6	-5,2
	V _m	24,5	26	24	22,6	17,4	24	22,7	24	24,4	24,9	25,7	23,4
	Age [Months]	43	62	42	67	61	51	62	57	49	66	60	66

Table 7-19: Bitumen and asphalt mix low-temperature properties of AC 16 with RA

Sample	Bitumen extracted from lab-prepared asphalt mixture		Asphalt mix properties									
	Pen	T _{R&B}	T _{Fraass}	FD: W	El. Rec.	DSR:G*(60°C1,59,Hz)	DSR:δ(60°C1,59Hz)	V _m	T _f	σ _F	TΔf _{max}	Δf _{max}
O11	43	62,4	-16	0,914	80	10.117	67,1	6,1	-28,3	4,011	-9,0	4,013
O12	34	64,2	-11	0,929	78	13.630	65,2	5,7	-29,2	4,412	-8,8	4,427
S11	33	64,6	-13	0,692	71	14.805	66,2	7,3	-28,7	2,808	-9,0	3,481
S12	30	66,0	-14	1,022	59	19.295	65,2	6,1	-29,8	3,575	-9,8	3,797
S13	37	65,4	-14	0,955	73	13.908	66,6	8,8	-29,9	2,699	-9,6	2,684
S14	32	64,4	-14	0,940	73	13.685	67,1	7,3	-30,9	3,336	-10,0	3,193
S15	36	62,4	-12	0,738	65	12.865	69,9	7,9	-31,1	3,286	-9,6	3,446
S16	32	62,6	-11	0,772	59	14.210	69,4	6,6	-30,0	3,992	-10,0	3,809
S17	29	65,4	-12	0,842	44	20.630	67,1	7,2	-27,6	2,840	-7,7	3,099
S18	28	65,4	-10	0,885	53	17.135	68,2	6,3	-30,7	3,920	-8,8	3,748
P11	33	65,6	-10	1,166	75	18.873	65,3	8,3	-29,2	3,807	-8,9	3,265
P12	35	65,8	-10	1,038	76	20.230	65,0	7,4	-30,5	3,745	-8,4	3,151
P13	28	69,0	-8	1,416	66	25.117	63,4	8,3	-27,2	2,574	-8,7	3,024
P14	31	67,4	-6	1,189	74	22.145	64,4	7,5	-29,8	3,954	-9,1	3,852
P15	36	64,0	-7	0,841	73	14.785	66,4	7,0	-27,0	3,625	-7,2	2,994
P16	30	66,6	-10	1,269	71	18.660	66,7	6,8	-25,7	3,009	-9,0	4,226
P17	28	66,0	-6	1,303	72	17.055	67,5	8,0	-26,8	3,498	-6,7	3,270
P18	27	66,8	-5	0,605	48	20.185	67,3	6,4	-28,2	4,486	-8,0	4,372
O21	29	63,6	-4	1,240	71	22.790	72,0	7,1	-21,9	2,0958	0,1	3,414
O22	25	64,8	-1	1,344	65	24.185	71,2	6,7	-22,7	3,529	0,1	3,946
S21	24	63,2	-8	1,097	64	16.825	73,3	7,0	-21,8	2,848	-2,5	2,943
S22	24	63,4	-6	1,186	61	18.670	72,7	7,2	-23,1	3,087	-3,8	3,653
S23	26	63,0	-7	1,137	66	16.880	73,3	7,4	-21,5	2,541	-2,9	2,468
S24	24	63,4	-7	1,149	62	17.065	73,5	7,1	-23,4	3,561	0,9	3,362
S25	26	63,8	-8	0,972	56	17.920	73,5	7,6	-28,2	3,447	-5,3	3,476
S26	27	63,0	-5	0,903	55	18.040	73,7	6,4	-26,9	3,623	-3,7	3,524
S27	27	62,0	-10	0,896	58	15.450	74,1	7,7	-22,0	2,703	-0,8	2,932
S28	25	64,2	-7	1,009	53	19.635	73,0	6,3	-24,8	3,777	-1,1	3,516
P21	18	67,0	-4	1,922	61	27.910	71,7	7,5	-23,8	2,831	0,0	3,041
P22	18	66,4	-4	1,664	58	26.525	72,1	6,1	-24,0	3,731	-2,8	4,014
P23	20	66,8	-4	1,773	61	28.270	71,7	7,6	-22,9	2,866	-2,1	3,064
P24	20	67,0	-5	1,647	60	28.675	71,8	6,6	-23,0	3,429	-0,8	3,468
P25	23	65,6	-7	1,514	63	21.705	71,3	8,0	-23,6	3,578	-1,9	3,612
P26	23	65,4	-4	1,462	63	26.545	70,9	6,6	-24,2	3,864	-1,8	4,180
P27	22	65,8	-4	1,568	66	24.730	70,5	7,7	-22,8	3,324	-2,3	3,414
P28	22	67,6	-2	1,576	76	28.150	69,3	6,3	-24,4	3,869	-4,5	4,238

7.3.1.16 Paper 495 (van Rooijen and de Bondt, 2008), TSRST – PG bitumen type, void content and aggregate type

Asphalt concrete (AC) mixtures slabs cut from field pavement sections as well as slabs produced in the laboratory, were used to study the influence of binder type, aggregate type, air void content, cooling rate and specimen geometry on the fracture strength and fracture temperature. For the laboratory mixtures, two levels of air void content: 4% and 7%, two levels of binder content: the design value and the design value plus 0,5% and two types of aggregates: limestone and granite were used to prepare the laboratory mixtures.

Table 7-20: Laboratory mixtures description

ID	PG binder	Modifier	Aggregate	Binder content	Target Air voids
58-40:M1:4:GR	58-40	SBS	Granite	opt	4%
58-40:M1:4:GR:+0.5AC	58-40	SBS	Granite	Opt + 0,5 %	4%
58-40:M1:4:LM	58-40	SBS	Limestone	opt	4%
58-34:M1:4:GR	58-34	Elvaloy	Granite	opt	4%
58-34:M1:4:GR:+0.5AC	58-34	Elvaloy	Granite	Opt + 0,5 %	4%
58-34:M1:4:LM	58-34	Elvaloy	Limestone	opt	4%
58-34:M2:4:GR	58-34	SBS	Granite	opt	4%
58-34:M2:4:LM	58-34	SBS	Limestone	opt	4%
58-28:U1:4:GR	58-28	Unmodified	Granite	opt	4%
58-28:U1:4:GR:+0.5AC	58-28	Unmodified	Granite	Opt + 0,5 %	4%
58-28:U1:4:LM	58-28	Unmodified	Limestone	opt	4%
58-28:U1:4:LM:+0.5AC	58-28	Unmodified	Limestone	Opt + 0,5 %	4%
58-28:U1:7:GR	58-28	Unmodified	Granite	opt	7%
58-28:U1:7:GR:+0.5AC	58-28	Unmodified	Granite	Opt + 0,5 %	7%
58-28:U1:7:LM	58-28	Unmodified	Limestone	opt	7%
58-28:U1:7:LM:+0.5AC	58-28	Unmodified	Limestone	Opt + 0,5 %	7%
58-28:U2:4:GR	58-28	Unmodified 2	Granite	opt	4%
58-28:U2:4:LM	58-28	Unmodified 2	Limestone	opt	4%
64-34:M1:4:GR	64-34	Elvaloy	Granite	opt	4%
64-34:M1:4:LM	64-34	Elvaloy	Limestone	opt	4%
64-34:M2:4:GR	64-34	Black Max™	Granite	opt	4%
64-34:M2:4:LM	64-34	Black	Limestone	opt	4%
64-28:U1:4:GR	64-28	Unmodified	Granite	opt	4%
64-28:U1:4:LM	64-28	Unmodified	Limestone	opt	4%
64-28:M1:4:GR	64-28	SBS	Granite	opt	4%
64-28:M1:4:LM	64-28	SBS	Limestone	opt	4%
64-22:U1:4:GR	64-22	Unmodified	Granite	opt	4%
64-22:U1:4:LM	64-22	Unmodified	Limestone	opt	4%

The tested laboratory asphalt mixtures are described in Table 7-20. Results of TSRST tests on field and laboratory prepared specimen including correlation matrix for TSRST test parameters is presented as well.

Based on the experiments performed the following conclusions were drawn:

- As expected, the PG58-40 mixture performed the best while the PG58-28 and PG64-22 mixtures performed the worst in TSRST
- Mixtures with 4% air void content performed better than mixtures with 7% air void.
- On average the granite mixtures performed slightly better than the limestone mixtures.

Table 7-21: TSRST results for field specimens (the last column is for acoustic emission for absorption of the field specimens)

ID	No.	PG	Failure temp. T_F (°C)	Failure stress σ_F (MPa)	cS/dT (MPa/°C)	Transition temp. (°C)	Spec. gravity (Mg/m ³)	Absorption of the field specimens (%)
WI 45	1	58-34	-26,1	3,189	0,137	-10,8	2,37	0,072
WI 45	2	58-34	-15,4	1,145	0,091	-10,0	2,36	0,086
MnROAD 03	1	58-28	-26,8	3,121	0,213	-16,2	2,39	0,058
MnROAD 03	2	58-28	-27,9	3,128	0,187	-15,6	2,37	0,045
MnROAD 19	1	64-22	-22,3	2,239	0,147	-12,6	2,28	0,048
MnROAD 19	2	64-22	-24,4	2,873	0,159	-10,0	2,29	0,061
MnROAD 19	3	64-22	-25,6	2,158	0,120	-11,0	2,30	0,073
MnROAD 19	4	64-22	-26,9	3,139	0,235	-20,2	2,33	0,060
MnROAD 33	1	58-28	-23,3	2,322	0,153	-14,6	2,35	0,079
MnROAD 33	2	58-28	-25,4	2,255	0,138	-14,8	2,36	0,089
MnROAD 33	3	58-28	-26,6	2,802	0,165	-14,6	2,38	0,087
MnROAD 33	4	58-28	-29,0	3,177	0,219	-22,3	2,36	0,069
MnROAD 34	1	58-34	-32,8	3,750	0,291	-25,9	2,35	0,049
MnROAD 34	2	58-34	-32,9	4,014	0,258	-25,2	2,37	0,078
MnROAD 34	3	58-34	-23,8	1,486	0,101	-13,6	2,38	0,039
MnROAD 34	4	58-34	-33,8	3,731	0,237	-23,9	2,36	0,049
MnROAD 35	1	58-40	-26,5	1,698	0,081	-14,8	2,37	0,083
MnROAD 35	2	58-40	-25,5	1,705	0,096	-19,6	2,37	0,052
MnROAD 35	3	58-40	-34,8	1,101	0,037	-14,8	2,36	0,046
MnROAD 35	4	58-40	-31,8	2,716	0,173	-24,2	2,37	0,071

7.3.1.17 Paper 508 (Renken *et al.*, 2010), TSRST for MA 11 and AC 22

For evaluating the applicability of elastic recovery bitumen parameters for practical prognosis of asphalt mix properties, MA 11 and AC 16 asphalt mix samples were prepared and tested by TSRST in freshly mixed stage as well as in short-term ageing stage (MA: storage in mixer at 250 °C for 165 minutes; AC 16: storage as loose mix at 180 °C for 180 minutes). The bitumen properties were evaluated in fresh stage as well as from binders extracted from freshly produced and short-term aged mixtures. The test results are summarised in Table 7-24. The elastic recovery values were obtained at a test temperature of 25 °C.

Table 7-22 TSRST results for laboratory prepared specimens (the last column is for acoustic emission for absorption of the specimens)

ID	No.	Failure temperature T_F (°C)	Failure stress σ_F (MPa)	cS/dT (Mpa/°C)	Transition temperature T_t (°C)	Spec. gravity [g/cm ³]	Absorption of the field specimens (%)
58-40:M1:4:GR	1	-31,0	4,049	0,573	-25,2	2,29	0,113
58-40:M1:4:GR	2	-36,8	4,078	0,543	-31,2	2,33	0,062
58-40:M1:4:GR: +0,5AC	1	-38,9	6,207	0,993	-34,5	2,36	0,044
58-40:M1:4:GR: +0,5AC	2	-29,6	3,557	0,829	-26,2	2,36	0,031
58-40:M1:4:LM	1	-34,8	2,959	0,322	-26,3	2,37	0,159
58-40:M1:4:LM	2	-31,7	4,012	0,673	-27,5	2,33	0,117
58-34:M1:4:GR	1	-30,9	3,005	0,393	-27,1	2,32	0,076
58-34:M1:4:GR	2	-27,9	3,200	0,397	-25,1	2,32	0,051
58-34:M1:4:GR	3	-32,8	4,323	0,303	-24,7	2,28	0,097
58-34:M1:4:GR: +0,5AC	1	-31,6	3,279	0,381	-25,1	2,32	0,085
58-34:M1:4:GR: +0,5AC	2	-28,1	2,040	0,828	-27,0	2,34	0,077
58-34:M1:4:LM	1	-31,1	3,834	0,533	-25,5	2,37	0,112
58-34:M1:4:LM	2	-34,1	3,289	0,322	-25,5	2,36	0,111
58-34:M1:4:LM	3	-32,6	2,862	0,259	-26,7	2,36	0,118
58-34:M1:4:LM	4	-26,6	2,531	1,415	-25,5	2,36	0,111
58-34:M2:4:GR	1	-27,0	3,156	1,704	-25,5	2,30	0,077
58-34:M2:4:GR	2	-34,6	2,764	0,496	-32,0	2,28	0,103
58-34:M2:4:LM	1	-32,3	3,167	0,537	-29,3	2,32	0,139
58-34:M2:4:LM	2	-25,6	1,968	0,986	-24,7	2,30	0,115
58-28:U1:4:GR	1	-28,0	2,636	0,509	-25,7	2,31	0,166
58-28:U1:4:GR	2	-31,1	2,585	0,215	-25,2	2,31	0,095
58-28:U1:4:GR: +0,5AC	1	-31,0	3,020	0,228	-23,0	2,32	0,110
58-28:U1:4:GR: +0,5AC	2	-31,8	3,271	0,224	-22,4	2,33	0,059
58-28:U1:4:LM	1	-25,5	1,136	0,410	-24,9	2,37	0,087
58-28:U1:4:LM	2	-27,3	1,818	0,236	-25,2	2,37	0,088
58-28:U1:4:LM: +0,5AC	1	-27,6	2,555	0,503	-25,9	2,38	0,087
58-28:U1:4:LM: +0,5AC	2	-28,5	2,789	0,502	-26,6	2,40	0,150
58-28:U1:7:GR	1	-34,2	2,293	0,342	-29,9	2,16	2,170
58-28:U1:7:GR	2	-31,5	2,156	0,302	-27,0	2,16	2,126
58-28:U1:7:GR: +0,5AC	1	-27,4	2,104	0,160	-20,7	2,26	0,262
58-28:U1:7:GR: +0,5AC	2	-29,4	2,550	0,293	-25,7	2,26	0,254
58-28:U1:7:LM: +0,5AC	1	-30,8	1,990	0,181	-26,0	2,24	0,570
58-28:U1:7:LM: +0,5AC	2	-27,7	1,351	0,114	-20,1	2,27	0,345
58-28:U2:4:GR	1	-32,7	3,012	0,215	-21,6	2,30	0,212
58-28:U2:4:GR	2	-31,8	2,969	0,201	-21,4	2,31	0,135
58-28:U2:4:LM	1	-26,7	1,670	0,182	-22,1	2,33	0,082
58-28:U2:4:LM	2	-26,8	1,859	0,258	-23,6	2,32	0,084
64-34:M1:4:GR	1	-30,8	3,090	0,197	-20,3	2,32	0,120
64-34:M1:4:GR	2	-26,7	3,268	1,263	-25,5	2,31	0,103
64-34:M1:4:LM	1	-32,7	2,934	0,221	-25,5	2,37	0,088
64-34:M1:4:LM	2	-33,8	3,656	0,321	-28,7	2,36	0,108
64-34:M2:4:GR	1	-26,8	3,184	1,126	-25,1	2,32	0,117
64-34:M2:4:GR	2	-34,3	2,669	0,214	-25,3	2,31	0,155
64-34:M2:4:LM	1	-31,3	3,972	0,702	-27,5	2,32	0,121
64-34:M2:4:LM	2	-33,6	2,992	0,343	-29,5	2,33	0,115
64-28:U1:4:GR	1	-31,0	2,958	0,221	-22,1	2,30	0,169
64-28:U1:4:GR	2	-30,7	3,205	0,229	-21,9	2,31	0,078
64-28:U1:4:LM	1	-28,1	2,468	0,185	-22,7	2,33	0,115
64-28:U1:4:LM	2	-27,7	2,331	0,172	-19,6	2,34	0,096
64-28:M1:4:GR	1	-31,0	3,164	0,475	-26,8	2,31	0,351
64-28:M1:4:GR	2	-29,3	3,032	0,689	-26,6	2,29	0,921
64-28:M1:4:LM	1	-28,3	2,629	0,397	-26,4	2,32	0,135
64-22:U1:4:GR	1	-26,8	2,821	0,209	-19,6	2,30	0,247
64-22:U1:4:GR	2	-25,0	3,023	0,206	-18,5	2,32	0,140

Table 7-23: Correlation matrix for TSRST test parameters

Fracture Str. (MPa)	-0,600	1					
PG-LL	0,499	-0,580	1				
Air void	0,015	-0,367	0,276	1			
Spec. gravity	0,050	0,214	-0,283	-0,736	1		
Absorption of the field specimens	-0,130	-0,220	0,254	0,644	-0,763	1	
dS/dT	0,179	0,290	-0,463	-0,237	0,146	-0,109	1
Trans T. (°C)	0,585	-0,418	0,580	0,039	-0,038	-0,163	-0,383
	Fracture T. (°C)	Fracture Str. (MPa)	PG-LL	Air void	Spec. gravity	Absorption of the field specimens	dS/dT

Table 7-24: TSRST and bitumen parameters for 12 asphalt mix samples

Asphalt mix		AC 22						MA 11					
Bitumen type		10/40-65A			25/55-55A			10/40-65A			25/55-55A		
Bitumen sample		1	3	4	5	6	8	1	2	3	6	7	8
Unaged bitumen	Pen	26	36	28	30	46	48	26	34	36	46	44	48
	T _{R&B}	74,0	64,4	63,8	58,8	56,6	62,0	74,0	67,2	64,4	56,6	58,6	62,0
	T _{Fraass}	-7	-17	-8	-10	-12	-14	-7	-14	-17	-12	-13	-14
	El.Rec.	76	75	74	57	54	83	76	71	75	54	77	83
	FD:W	3,89	7,44	7,38	3,88	2,92	10,54	3,89	6,43	7,44	2,92	4,87	10,54
RTFOT	Pen	83	69	77	67	75	76	83	78	69	75	69	76
	T _{R&B}	78,0	70,4	69,4	62,6	62,4	61,7	78,0	73,6	70,4	62,4	64,4	61,8
	El.Rec.	60	75	74	53	60	77	60	65	75	60	72	77
Freshly mixed	Binder cont.	4,3			4,2			7,3			7,0		
	ρ _b [kg/m ³]	2372	2378	2399	2382	2371	2361	2350	2339	2350	2362	2371	2361
	T _F [°C]	-11,7	-17,9	-17,7	-13,1	-19,8	-20,8	-21,5	-22,3	-22,4	-26,3	-23,9	-25,3
	σ _F [MPa]	2,293	3,029	3,383	2,26	2,379	2,908	4,337	4,471	4,367	5,873	4,687	4,851
	σ(-15°C)							2,705	2,708	2,431	2,12	2,206	1,958
	σ(-3°C)	1,492	1,119	1,162	0,834	0,554	0,43						
Extracted	Pen	25	32	25	25	38	33	26	36	31	42	38	35
	T _{R&B}	70,8	66,6	67,6	63,2	58,4	60,6	69,4	64,2	65,8	57,8	59,6	59,6
	FD:W	5,58	12,65	7,3	18,72	13,58	19,07	5,32	2,71	-	2,47	6,33	6,47
	El. Rec	51	73	76	58	60	80	55	72	73	57	72	75
Aged mixed	ρ _b [kg/m ³]	2371	2381	2383	2355	2375	2363	2363	2351	2361	2368	2369	2365
	T _F [°C]	-4,9	-3,2	-11,8	-9,4	-15,7	-14,5	-19,9	-17,7	-19,1	-21,7	-21,5	-22,5
	σ _F [MPa]	2,127	1,363	3,29	2,134	2,178	2,153	4,669	4,25	3,932	4,663	4,243	4,862
	σ(-15°C)							3,501	3,828	3,243	2,896	2,486	2,947
	σ(-3°C)	2,099	1,286	1,89	1,594	0,954	1,098						
Extr. A	Pen	12	8	14	11	19	18	17	18	19	30	30	31
	T _{R&B}	90	99,2	90	90	79,6	85,6	73,3	79,8	69,3	66	62,6	64,4
	El. Rec	38	49	58	39	41	61	34	44	41	27	39	30

7.3.1.18 Paper 510 (Hase, 2011), TSRST and UTST for several SMA 8 mixtures with RA

For evaluating the multiple recyclability of surface course asphalt with polymer modified bitumen, SMA 8 mixtures were prepared and artificially aged in laboratory. The aged asphalt mix was added to new mixtures in varied percentages.

The mixtures low-temperature properties were evaluated by TSRST and UTST. Furthermore, the bitumen of the prepared mixtures was extracted and analysed. The results are summarised in Table 7-25.

Table 7-25: TSRST, UTST and extracted bitumen parameters for various SMA samples

SMA sample	0A0	0B0	0C0	RA1	1A25	1A50	1B50	1C50	RA2	2C50	RA3	3C50	
$T_{R\&B}$	61,3	65,7	51,1	68,2	63,2	62,1	66,9	59,9	63,6	57,1	63,1	56,7	
Pen	38,3	26,3	67,3	25,3	32,7	32,0	25,7	37,3	26,0	41,3	26,3	42,0	
F_{max}	3,7	8,9	0,8	10,0	4,0	5,0	10,0	3,2	6,5	2,7	7,6	2,4	
W_{tot}	1,21	2,11	0,22	2,59	1,27	1,58	2,42	1,11	1,37	0,79	1,33	0,65	
$W_{0,2-0,4}$	0,24	0,49	0,04	0,64	0,26	0,34	0,63	0,24	0,36	0,17	0,33	0,14	
$G^*(60^\circ\text{C}, 1,59\text{Hz})$	12.050	23.400	3.250	23.750	13.250	16.150	22.950	9.020	15.700	6.720	16.550	6.705	
$\delta(60^\circ\text{C}, 1,59\text{Hz})$	72,2	69,5	78,2	69,8	71,9	71,1	69,3	74,4	73,2	76,0	74,1	76,3	
TSRST	T_F	-24,0	-20,3	-25,5	-19,7	-22,5	-22,3	-22,1	-22,9	-19,5	-23,1	-20,6	-21,8
	σ_F	4,263	4,333	5,039	4,528	4,499	4,450	4,711	4,531	4,931	4,556	4,628	4,801
UTST	$\varepsilon_F(5)$	3,19	2,94	6,44	2,57	3,72	3,56	4,08	4,76	3,63	4,89	3,53	4,78
	$f(5^\circ\text{C})$	2,727	3,080	2,078	4,157	3,121	3,361	3,490	2,956	4,324	3,022	4,318	3,101
	$f(-10^\circ\text{C})$	4,817	5,533	5,930		5,698	5,722	5,943	6,054		6,341		5,857
$T\Delta f_{max}$	-5,9	-6,0	-9,8		-6,4	-5,8	-5,3	-6,7		-7,8		-7,0	
Δf_{max}	3,928	4,131	5,237		4,499	4,655	4,563	4,985		5,266		4,894	

7.3.1.19 Paper 543 (Wojczech *et al.*, 2010), TSRST for AC 11 with varied bitumen types

Asphalt concrete (AC 11) mixtures slabs with 7 % air void content and limestone aggregates were prepared in the laboratory. The properties of bitumen and asphalt mixtures are described in Table 7-26.

Table 7-26: Properties of bitumen

Characteristics	B 70/100	B 50/70	PmB 25/55-55	PmB 50- 90 S
Penetration @ 25 °C (1/10 mm)	74	54	44	68
$T_{R\&B}$ (°C)	49,6	54,8	66,8	71,2
T_{Fraass} (°C)	-19,5	-18,5	-14	-12
Kinematic viscosity @ 135 °C (mm ² /s)	416	596	2055	713
Dynamic viscosity @ 60 °C (Pa·s)	181	528	5029	14 05
TSRST: T_F (°C)	-29,9	-25,5	-26,8	-27,8
TSRST: σ_F [MPa]	4,23	4,03	4,80	4,82

7.3.2 Binder-Mix relationship reported for other uniaxial test methods on asphalt mixtures

In Paper 485 (Gubler *et al.*, 2005), four very different binders were used for the preparation of AC 10 mixtures. The results of UTST can be compared with bitumen characteristics obtained in BBR, G^* and DTT tests. The values obtained are given in Table 7-16. As depicted in Figure 7-5, the bitumen properties correlate well with the temperature at which the asphalt mix indicates maximum tensile strength. The UTST was conducted with a strain

rate of 12,5 µm/m/s and therefore slower compared to the standard strain rate obtained in UTST according to EN 12697-46. This will result in lower characteristic temperatures and strength values.

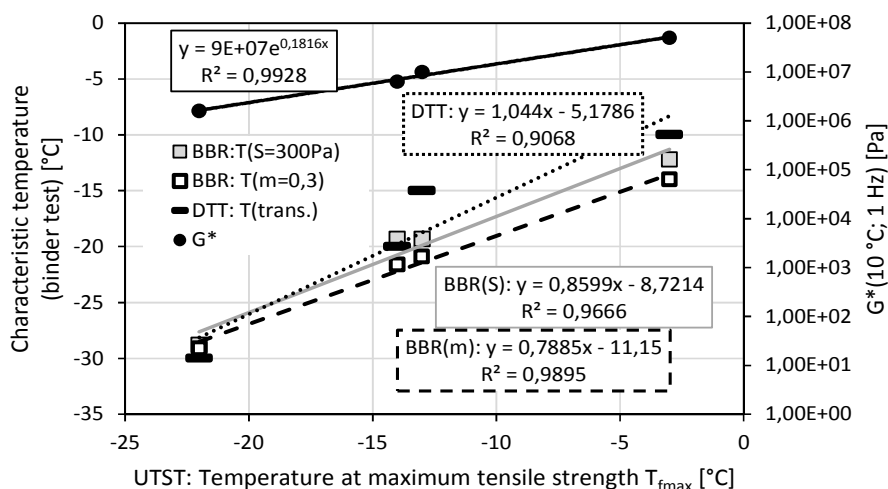


Figure 7-5: Relationship between UTST maximum tensile strength temperature and characteristic temperatures derived from bitumen tests

7.3.3 Binder-Mix relationship reported for results of IDT

7.3.3.1 Paper 193 (Johnson et al., 2009), Effect of WMA additives on IDT strength and fracture energy parameters

The effect of the WMA additives on AC 10 mixtures with neat and two polymer modified bitumens were evaluated. As a result, the indirect tensile strength obtained at various temperatures between 25 °C and -35 °C as well as some bitumen parameters are given in Table 7-27. The binder tests indicate very similar bitumen properties in the low-temperature range resulting in a small BBR limiting temperature range of between -13 and -16 °C. When comparing the binder and asphalt properties, the resulting correlation is low and inconclusive. The lowest lower BBR limiting temperature of the neat binder goes along with comparably bad low-temperature properties of the asphalt mix.

Table 7-27: IDT strength and fracture energy at various temperatures and properties of WMA modified binders

Classification	Binder	Kinematic viscosity (cp)				DSR failure temp. (°C)		High PG	3BR failure temp. (°C)	PG		
		115 °C	Ratio*	135 °C	Ratio*	Orig.	RTFO					
Normal	HMA	NOR0	1392	1	472	1	67.7	66.4	64	-16	64-22	
	WMA	NORE	1083	0.78	366	0.78	65.8	65.6	64	-16	64-22	
		NORP	1033	0.74	408	0.86	67.1	66.8	64	-15	64-22	
		Avg.	1047.0	0.76	385.7	0.82						
PMA	HMA	LVM0	5644	1	1785	1	79.7	77.7	76	-14	76-22	
		LVME	5048	0.89	1758	0.98	79.7	79	76	-14	76-22	
	WMA	LVMP	4517	0.80	1458	0.82	78.2	77.3	76	-13	76-22	
		Avg.	4891.0	0.85	1602.7	0.90						
	HMA	SBS0	4683	1	1519	1	80.5	78.2	76	-14	76-22	
		SBSE	4150	0.89	1417	0.93	76.8	77.2	76	-14	76-22	
		WMA	SBSP	3675	0.78	1258	0.83	80.3	77.9	76	-14	76-22
			Avg.	3972.3	0.84	1361.0	0.88					

* The WMA viscosity ratio to the HMA viscosity.

Type	Binder	Temp. (°C)	HMA		WMA			
			No		Ev WMA		Pe WMA	
			S _i (MPa)	FE (kN·mm)	S _i (MPa)	FE (kN·mm)	S _i (MPa)	FE (kN·mm)
Normal	NOR	-35	4.1	36.4	3.8	34.5	3.5	33.2
		-25	3.7	38.3	4.0	37.8	3.7	34.1
		-15	4.6	48.5	4.8	48.4	5.2	46.0
		-5	4.0	44.2	3.9	39.7	4.4	40.4
		5	2.7	36.1	2.7	38.5	2.9	38.1
		25	0.7	9.7	0.8	13.1	0.8	11.6
PMA	LVM	-35	4.3	38.3	4.0	41.1	4.9	40.0
		-25	4.4	44.9	4.3	45.4	5.7	42.3
		-15	4.9	54.9	4.5	47.5	5.5	42.1
		-5	4.3	57.3	3.6	40.2	4.7	50.6
		5	3.0	38.6	2.5	22.1	2.4	25.4
		25	0.8	12.2	1.0	13.0	1.0	13.5
	SBS	-35	4.3	36.9	4.1	40.2	4.8	41.1
		-25	4.6	41.9	4.7	46.7	4.9	45.4
		-15	5.4	53.6	5.2	48.1	4.8	45.0
		-5	4.5	55.1	4.3	45.2	4.1	42.3
		5	3.1	34.2	2.7	35.8	2.4	29.5
		25	0.9	15.4	0.9	13.2	1.0	15.4

7.3.3.2 Paper 153 (Willis *et al.*, 2012), Calculated mix failure temperature based in IDT and bitumen parameters

For assessing high-polymer mixtures, two asphalt mixtures (surface and base layer mixes) were prepared. Besides low-temperature and creep compliance bitumen tests by BBR and MSCR, indirect tensile strength and creep compliance were assessed at various temperatures for simulating TSRST. The test results are summarised in Table 7-28.

Table 7-28: Fracture energy parameters of asphalt mixtures and bitumen

Mix sample	PG-Grade		MSCR(64°C)			IDT	
	DSR-T	BBR-T	J _{nr,0,1}	J _{nr,3,2}	J _{nr,diff}	IDS(-10 °C)	T _{f(calculated)}
SurfC	81,7	-24,7	0,98	1,37	39,8	4,71	-26,4
BaseC	69,5	-26,0	1,68	1,95	16,1	4,16	-21,4
SurfHPM	93,5	-26,4	0,004	0,013	200,7	4,55	-24,7
BaseHPM	93,5	-26,4	0,004	0,013	200,7	5,27	-26,1

7.3.3.3 Paper 519 (Radenberg, undated), Effect of various rejuvenators for high recycling rates

For evaluating the possibilities to allow high recycling rates in asphalt mixtures by using rejuvenators, seven additives were applied in an AC 10. The low-temperature cracking resistance was evaluated by combined IDT strength and creep compliance tests at -10 °C whereas penetration at 25 °C and 4 °C was conducted and PI was calculated for the extracted binder samples. The results are summarised in Table 7-29.

Table 7-29: Bitumen and asphalt parameters

Sample	Pen @ 25 °C (1/10 mm)	PI	ITD @ -10 °C (kPa)	Creep Compl. @ -10 °C (GPa ⁻¹)
Virgin		-1,29	3650	0,25
RAP	21	2,55	3919	0,06
Wvoil	90	1,56	3058	0,29
Wvgrease	140	1,04	3200	0,24
Organic	95	1,3	3682	0,14
diustilled	85	1,42	3943	0,1
Aromatic	41	0,99	4189	0,13
WEO	65	2,06	2773	0,21

7.3.4 Binder-Mix relationship reported for results of fracture energy assessments

7.3.4.1 Paper 175 (Clopotel et al., 2012), Fracture energy tests on binders and asphalt mixtures

Four bitumens (two neat and two polymer modified) were used to prepare asphalt mix with limestone aggregates and a binder content of 4,75 %. The bitumen fracture energy properties were measured by single edge notched beam test (SENB), similar to bitumen fracture toughness test a specified in EN 15963. The fracture energy properties of asphalt mixtures were assessed by FENIX test, which has some familiarities with SCBT at the same temperatures. The test results obtained are summarised in Table 7-30. According to Figure 7-6 a feasible correlation could be obtained between the asphalt mixture and the bitumen fracture energy parameters.

Table 7-30: Fracture energy parameters of asphalt mixtures and bitumen

	Mixture Fracture Energy (FENIX) (J/m ²)			Binder Fracture Energy (Nm)			Glass transition temperature (°C)
	-15	-5	5	-15	-5	5	
76-22	400	480	550	0,00075	0,0003	0,0017	-12,6
76-28	580	750	820	0,0007	0,0006	0,003	-24,1
64-22	380	400	620	0,00045	0,0002	0,0009	-20,6
64-22	350	400	600	0,0002	0,00025	0,001	-16,7

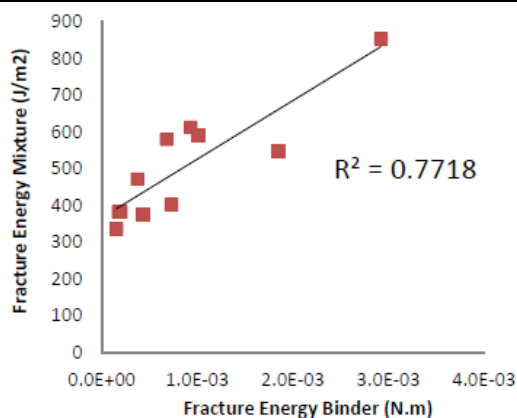


Figure 7-6: Comparison of fracture tests on bitumen (by Fracture Toughness test) and asphalt samples (FENIX test)

7.3.4.2 Paper 219 (Braham *et al.*, 2007), Bitumen effect on fracture toughness of asphalt mixtures assessed by disc-shaped compact tension test

Two types of surface asphalt mixtures (similar to AC 12) were prepared with granite and limestone aggregates as well as ten different types of neat and modified bitumen. For these mixtures, disc-shaped compact tension tests were applied for assessing the fracture energy for three temperatures for each mix. The results of the tests are summarised in Table 7-31.

Table 7-31: Fracture energy parameters of asphalt mixtures

	4% Air Voids				7% Air Voids				
	°C	Granite		Limestone		Granite		Limestone	
		6.0% AC	6.5% AC	6.9% AC	7.4% AC	6.0% AC	6.5% AC	6.9% AC	7.4% AC
PG58-40 SBS	-42	655.4	790.2	440.9					
	-30	1099.6	1377.1	623.1					
	-18	2032.7*	2844.9*	2705.8*					
PG58-34 Elvaloy	-36	455.3	456.2	311.5					
	-24	646.9	632.4	525.5					
	-12	1746.3*	2132.5*						
PG58-34 SBS	-36	459.0		324.9					
	-24	796.0		567.7					
	-12	2640.8*		2717.7*					
PG58-28 Unmodified Source 1	-30	497.1	369.6	316.1	316.9	417.4	445.3	314.7	229.6
	-18	652.8	792.4	422.2	447.3	578.0	653.9	440.4	499.6
	-6		1289.7*	1210.8*	1396.3*		1382.1	935.2	1837.6*
PG58-28 Unmodified Source 2	-30	584.9		265.3					
	-18	822.8		521.0					
	-6	1853.0*		861.1					
PG64-34 Elvaloy	-36	477.9		310.7					
	-24	740.4		493.6					
	-12	2032.8*		2601.4*					
PG64-34 Black Max™	-36	663.8		393.7					
	-24	913.9		579.7					
	-12	3505.7*		3374.9*					
PG64-28 Unmodified	-30	442.7		237.0					
	-18	583.0		425.5					
	-6	1093.8*		488.6					
PG64-28 SBS	-30	456.5		323.3					
	-18	759.8		429.7					
	-6	1361.3		1389.7*					
PG64-22 Unmodified	-24	489.2		332.7					
	-12	738.3		417.1					
	0	1418.8*		1242.0*					

- Asphalt cement modifier is listed beneath PG binder grade in 1st column
- SBS = Styrene-Butadiene-Styrene
- Testing temperature is given in 2nd column
- Fracture energy units are in J/m²
- Blank cells indicate tests which were not performed. (A full-factorial testing matrix was not pursued).
- * indicates extrapolation used, which is described in a later section (Figure 9 and accompanying text).

7.3.5 Relationship between binder low-temperature properties and site cracking

7.3.5.1 Paper 113 (Evans and Hesp, 2011), Bitumen BBR properties from test sections

Cores from seven test sections were taken and the binder extracted. The bitumen properties obtained with BBR (standard method and after prolonged temperature conditioning time) were evaluated. For the test sites the crack parameters were assessed. All results are summarised in

Table 7-32.

Table 7-32: Crack parameters of test sections and BBR critical temperatures for extracted and aged binders

Section	RTFOT/PAV		Extracted from cores		Crack length		Transverse crack count
	BBR-T (low PG)	BBR (longer temp. conditioning)	BBR-T (low PG)	BBR (longer temp. conditioning)	Transverse	Longitudinal	
1	-36	-34,5	-39	-37	1	9	2
2	-36	-28,4	-34	-27	33	176	38
3	-36	-32,5	-34	-26	55	58	50
4	-35	-30,1	-29	-19	137	178	198
5	-35	-31,3	-36	-30	1	33	5
6	-35	-28,7	-32	-21	39	29	91
7	-35	-28,5	-34	-27	61	32	122

7.3.5.2 Paper 131 (Bernier *et al.*, 2012), Low temperature asphalt and bitumen and site cracking properties for warm mix asphalt

For evaluating the possibility of warm-mix asphalt production, three test sites were paved using foamed and wax WMA and a control HMA. From cores asphalt specimen indirect tensile strength tests as well as creep compliance tests were performed and the theoretical failure temperature was calculated. Additionally, semi-circular bending tests were conducted at three temperatures. The crack length after one year of traffic loading was measured. The obtained values are summarised in Table 7-33.

Table 7-33: Crack parameters of test sections and asphalt mix low-temperature properties

Sample		Control	Foam	Sasobit
Transverse cracking	[m/150m]	14	17	21
IDT	ITS (-24°C) [MPa]	4,6	3,4	4,2
	ITS (-12 °C) [MPa]	3,3	3,7	3,5
	ITS (0 °C) [MPa]	2,4	2,2	2,4
	Calculated T_F	-34	-31	-28
SCB	Toughness (-24°C)	1,05	1,1	1,05
	Toughness (-12°C)	0,9	0,7	0,8
	Toughness (0°C)	0,5	0,4	0,48
	Fracture Energy (-24°C)	650	800	620
	Fracture Energy (-12 °C)	1100	1500	1200
	Fracture Energy (0 °C)	1300	1550	1600

7.4 ageing effect on low temperature cracking

In some analysed papers, the ageing effect on test results used for interpretation of low-temperature cracking was systematically evaluated. The synthesis will be included in deliverable report D2.

7.5 Overall uncertainty of low temperature cracking

Currently, the precision of TSRST and other low-temperature asphalt tests is not well evaluated. However several papers identified during this study contain scattering data for the results given. As a first example, in Paper 487 (Bagampadde *et al.*, 2006), eight AC 11 samples were evaluated by TSRST with a start temperature of 23 °C. The standard deviations for the test results can be compared with the standard deviations found on the air void content of the test samples applied. In deliverable D2, the available precision data resulting from test repetitions will be used for evaluating repeatability precision parameters.

Table 7-34: Uncertainty of TSRST results and specimens air voids content

		Bitumen	FT-wax		PE wax		Montane wax	Slack wax	Poly-phosphoric acid
		160/220	3 % S	6 % S	3 % PW	6 % PW	6 % MW	6 % SW	1 % PPA
TSRST: T_f	Mean	-33,6	-33,2	-31,9	-34,0	-33,1	-32,1	-32,9	-36,1
	St. dev.	0,14	0,64	1,06	0,28	1,98	0,42	1,27	1,06
TSRST: σ_f	Mean	3,92	4,31	4,29	4,3	4,23	4,07	4,20	4,09
	St. dev.	0,01	0,11	0,56	0,11	0,35	0,56	0,25	0,20
Air voids content	Mean	2,4	2,8	2,2	3,4	3,0	3,6	2,6	3,5
	St. dev.	0,57	0,0	0,07	0,07	0,35	0,07	0,14	0,0

7.6 References for low temperature cracking

- Paper 031 **Nordgren, T, and K Olsson (2012)**. Asphalt concrete test sections containing bitumen of different origins. *E&E2012*.
- Paper 064 **Hase, M, and C Oelkers (2008)**. The influence of low temperature behaviour of polymer modified binders and of cryogenic tensile stress in asphalt on the life cycle of traffic areas. *E&E2008*.
- Paper 066 **Büchler, S, P Renken and K Mollenhaer (2008)**. Relation between rheological bitumen characteristics and the resistance of asphalt against fatigue and cold temperatures. *E&E2008*.
- Paper 111 **Mogawer, W S, A J Austerman, R Bonaquist and M Roussel (2011)**. Performance characteristics of thin-lift overlay mixtures containing high RAP content, RAS, and warm-mix asphalt technology. *TRB2011*.
- Paper 112 **Loria, L G, E Y Hajj, P E Sebaaly, M Barton, S Kass and T Liske (2011)**. Performance evaluation of asphalt mixtures with high RAP content. *TRB2011*.
- Paper 130 **Yiqiu, T, Z Lei, J Lun and L Shan (2012)**. Comparison of low-temperature performance evaluation methods of asphalt mixtures. *TRB2012*.
- Paper 131 **Bernier, A K, R Josen, A Zofka and M Mahoney (2012)**. Connecticut warm-mix asphalt pilot project. *TRB2012*.
- Paper 144 **Hajj, E Y, L G Loria and P E Sebaaly (2012)**. Estimating effective performance grade of asphalt binders in high-RAP mixtures using different methodologies: Case study. *TRB2012*.

- Paper 153 **Willis, J R, A J Taylor and N Tran (2012).** Laboratory evaluation of high polymer plant-produced mixtures. *TRB2012*.
- Paper 175 **Clopotel, C, R A Velasquez, H U Bahia, F E Perez-Jimenez, R M Recasens and R B Nieto (2012).** Relation between binder and mixture damage resistance at intermediate and 2 low temperatures. *TRB2012*.
- Paper 193 **Kim, S, H J Choi and K W Kim (2013).** Evaluation of tensile property of warm-mix asphalt concretes at low temperatures. *TRB2013*.
- Paper 219 **Braham, A F, W G Buttlar and M O Marasteanu (2007).** Effect of binder type, aggregate, and mixture composition on the fracture energy of hot-mix asphalt in cold climates. *TRB2007*.
- Paper 294 **Bennert, T A, D S Jo and S M Walaa (2014).** Strategies for incorporating higher RAP percentages: Review of northeast states implementation trials. *TRB2014*.
- Paper 377 **Wallin, T (2011).** Long-term effectiveness of adhesion promoters in airfields. *Asfaltové vozovky 2011*.
- Paper 439 **Butt, A A, Y Tasdemir and Y Edwards (2009).** Environmental friendly wax modified mastic asphalt. *Environmentally Friendly Roads (ENVIROAD)*.
- Paper 475 **de Backer, C, J de Visscher, L Glorie, A Vanelstraete, S Vansteenkiste and L Heleven (2008).** A comparative high-modulus asphalt experiment in Belgium. *TRA2008*.
- Paper 483 **Nikolaides, A F, and E Manthos (2010).** Wheel tracking performance of asphalt concrete mixture with conventional and modified bitumen. *iCTi 2010*.
- Paper 485 **Gubler, R, M N Partl, F Canestrari and A Grilli (2005).** Influence of water and temperature on mechanical properties of selected asphalt pavements. *Materials and Structures 2005*.
- Paper 487 **Bagampadde, U, U Isacsson and B M Kiggundu (2006).** Impact of bitumen and aggregate composition on stripping in bituminous mixtures. *Materials and Structures 2006*.
- Paper 488 **Edwards, Y, Y Tasdemir and U Isacsson (2006).** Creep-recovery behavior of bituminous binders and its relation to asphalt mixture rutting influence of commercial waxes and polyphosphoric acid on bitumen and asphalt concrete performance at low and medium temperatures. *Materials and Structures 2006*.
- Paper 489 **Renken, P (2007).** Quality of porous asphalt layers – Optimierung und Qualitätssicherung Offenporiger Asphaltdeckschichten Teil II. *Forschung Straßenbau und Straßneverkehrstechnik*.
- Paper 491 **Steinauer, S (2007).** Comparison of tests procedures for rutting assessment – Vergleich der Prüfverfahren zur Ansprache der Verformungseigenschaften von Asphalt. *Forschung Straßenbau und Straßneverkehrstechnik*.
- Paper 495 **van Rooijen, R C, and A H de Bondt (2008).** Crack propagation performance evaluation of asphaltic mixes using a new procedure based on cyclic semi-circular bending tests. *2008-RILEM-Pavement Cracking*.
- Paper 498 **Zeghal, I (2008).** Thermal cracking prediction using artificial neural network. *2008-RILEM-Pavement Cracking*.
- Paper 502 **Dreessen, S, J P Planche and V Gardel (2009).** A new performance related test method for rutting prediction: MSCRT. *ATCBM2009*.

- Paper 505 **Tusar, M, M R Turk, W Bankowski, L Wiman and B Kalman (2009).** Evaluation of modified bitumen, high modulus asphalt concrete and steel mesh as materials for road upgrading. *ATCBM2009*.
- Paper 508 **Renken, P, M Wistuba, J Grönniger and K Schindler (2010).** Adhesion of bitumen on aggregates. *Forschung Straßenbau und Straßneverkehrstechnik*.
- Paper 510 **Hase, M (2011).** Bindemittel und die Gebrauchseigenschaften von Asphalt. *Asphaltstraßentagung 2011*.
- Paper 519 **Radenberg, M.** Einfluss der chemischen, rheologischen und physikalischen Grundeigenschaften von Straßenbaubitumen auf das Adhäsionsverhalten unterschiedlicher Gesteinskörnungen DAV/DAI, AiF-Forschungsvorhaben Nr. 16639 N/1, http://www.asphalt.de/site/startseite/literatur/infomaterial_download/forschungsberichte/.
- Paper 543 **Wojciech, Bańkowski, Marcin, Gajewski, Dariusz and Sybilski (2010).** Full scale testing of high modulus asphalt concrete in Poland. *TRA2010*,

8 Fatigue cracking

8.1 Asphalt test methods for fatigue cracking

The cracks due to mechanical fatigue depend on the road pavement structures (i.e. thickness of layers, stiffness modulus and the rheological behaviour of the materials), on the traffic (particularly heavy lorries), on the climatic conditions and on the evolution (ageing) of the characteristics of the bitumen.

Fatigue tests on asphalt are undertaken under cyclic loading on specimen cut from pavements or manufactured in the laboratory. Two main types of sinusoidal loading are applied on the specimens:

- Flexural loading on prismatic specimens (applied at three or four points, including restraints, Figure 8-1a) or trapezoidal specimens (applied at two points, Figure 8-1b).
- Push-pull (or tension/compression) loading on cylindrical specimens (Figure 8-1c),
- Diametral loading on cylindrical samples.

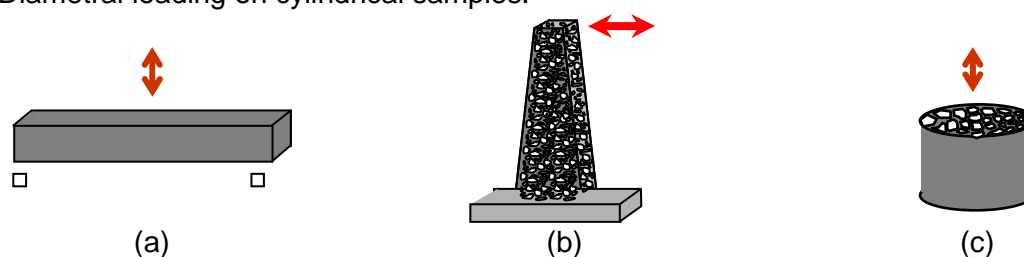


Figure 8-1: Shapes of asphalt specimens for fatigue tests

Cyclic stress or strain displacements are imposed depending on the level of the layer in the pavement to be designed or evaluated. The European standard for fatigue, EN 12697-24:2012, takes into account the two main types of loading, as shown in Figure 8-1. An inter-laboratory investigation on fatigue with eleven different test methods (Table 8-1) included uniaxial push-pull, 2-, 3- and 4-point bending (2PB, 3PB and 4PB) and indirect tension tests was organised by RILEM Committees TC 101 BAT and was completed in 1996. The testing conditions specified were sinusoidal excitation at 10 Hz and 10 °C using controlled strain and stress modes. In total, more than 150 fatigue tests were carried out during the investigation.

The conclusions of the investigation were:

- The fatigue lives determined are significantly affected by the test method employed.
- No correlation was found between the fatigue lives obtained from stress- (load-) and strain- (displacement-) controlled fatigue tests.
- The results of the beam tests (2PB, 3PB and 4PB) appeared to be dependent on the kind of test type used as well as on the size of the sample.
- For a given strain (or stress) amplitude, the beam tests (2PB, 3PB, and 4PB) generally resulted in longer life durations compared to homogeneous tension/compression (T/C) tests. This increase was due to the influence of specimen shape (the stress and strain values are always smaller in the sample). It did not seem possible to transpose results from one test to another or to use the same formula to predict degradation or cracking of roads. Therefore, if a correlation is found between fatigue life and a characteristic of bitumen, it must be relative to a particular asphalt fatigue test.

- The complex modulus obtained at the beginning of the fatigue tests is independent of the type of test.
- A fatigue damage law can be defined and a unique set of parameters derived that accurately describes push-pull (or tension-compression) tests for both strain and stress controlled conditions and describes the controlled strain 2PB tests. However, further work is still needed.
- Biasing effects, which are not fatigue, exist during a fatigue test, which affect the result. One effect is the heat caused by the accumulation of dissipated viscous energy and another, less well known, one appears to be due to the thixotropy of the binder.

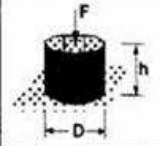
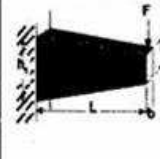
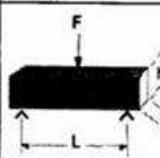

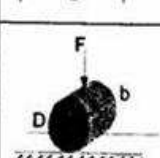
8.1.1 Other test protocols for fatigue testing

8.1.1.1 The strain sweep test (papers 083; 134; 175)

The strain sweep test (Ensayo de BArrido de DEformaciones; EBADE) consists in applying a number of tension-compression load cycles to a prismatic specimen at different strain levels. The aim of this method is to determine the fatigue behavior of mixtures subjected or not to thermal stresses by establishing two critical strain levels, i.e. the limit level, at which no damage in the mixture is observed and the strain level, at which failure occurs, resulting in irreversible damage. A prismatic specimen is used in the test. Two notches are cut in its central area to reduce the specimen area and induce failure. The specimen does not need to have fixed dimensions, as long as the maximum aggregate size is four times smaller than the shortest dimension, and can be obtained either from Marshall or gyratory-compacted specimens, or 5 cm thick plates used in standard plastic deformation or 4-point bending beam tests. In the developing of the research all specimens were carved with the same dimensions, 5 cm wide and thick, and 6 cm high. Both ends of the specimen are fixed to a plate with an epoxy resin to allow clamping. Two extensometers are placed in the failure area of the specimen previously induced to measure strain during testing.

In the EBADE test several displacement amplitudes are applied in ascending order after every 5.000 load cycles at a frequency of 10 Hz. With this protocol, information on material behavior at different strain levels is obtained with a single test, for example, the strain value at which damage to the material occurs and the value at which failure is induced instantaneously. Thus, by limiting the number of cycles at each strain level, the total number of cycles until test termination is considerably reduced both for small and large strains. It is worth noting that the classical failure criterion was used, i.e. failure occurs at the cycle when stress drops to half its maximum value.

Table 8-1: Types of fatigue test

Type	Test Geometry	Type of loading/ Country of the team	Amplitude (10 ⁻⁶ m/m or MPa)
T/C		Tension- Compression "Homogeneous" F ₁ , S ₁	Strain: (80), 100,140, 180 Stress: 0.9
2PB		Two-Point Bending "Non Homogeneous" F ₂ , B ₁ , B ₂	Displacement; max strain: 140, 180, 220 Load; max stress: 1.4
3PB		Three-Point Bending "Non Homogeneous" N ₁	Displacement; max strain: 140, 180, 220 Load; max stress: 1.4
4PB		Four-Point Bending "Non Homogeneous" N ₂ , P, PL, UK	Displacement; max strain: 140, 180, 220 Load; max stress: 1.4
ITT		Indirect Tensile Test "Non Homogeneous" S ₂	Load; max strain: at first cycle: ~25, ~40, ~65

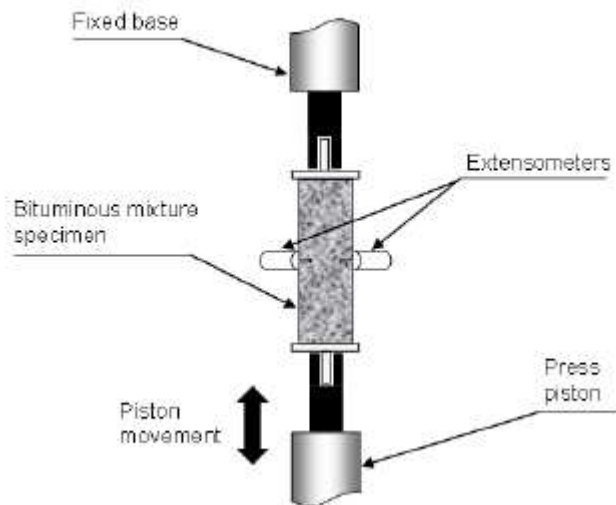


Figure 8-2: EBADE test (Paper 134)

8.1.1.2 Paper 549 (Silva et al., 2008)

Fatigue cracking is one of the main mechanisms of pavement distress and it manifests itself through the appearance of cracks on the surface due to traffic loading. When fatigue tests are carried out in strain control, the fatigue cracking resistance of the bituminous mixture is characterized by the strain applied during the test.

Fatigue life was assessed for 5°C, 15°C and 25°C temperature levels. As failure criterion the 50% reduction of initial stiffness modulus value was used. Tests were carried out at five different tensile strain levels (100×10^{-6} , 150×10^{-6} , 250×10^{-6} , 300×10^{-6} and 350×10^{-6}), with three specimens tested for each strain level. Some correction factors (known as shift factors) should be applied in order to develop a meaningful relationship between the results of laboratory tests and field performance. Shift factor of 20 (Brown et al.)¹ was considered in order to take into account the influence of rest periods. (Rao Tangella et al.)² also adopted a value of 20 as a shift factor, considering high loading rate sinusoidal bending tests carried out without rest periods. An additional factor of 1.1 (Brown et al.)¹ has also been used to simulate the lateral distribution of loads, while the fatigue life associated with the crack propagation phase has been considered by the use of controlled-strain bending tests (Shell)³. Based on these studies, the ultimate value used in the present work was 22.

Evaluated impact of the temperature is further considered in Shell fatigue life equation used in pavement design methodologies. Lundström stated already in 2003 that the classical fatigue evaluation method showed several inadequacies to assess the influence of temperature. The high scattering among fatigue data and the large amount of tests necessary to cover a given temperature range leads to a need for several samples and repetitions in order to obtain an adequate characterization

¹ Brown, S. F., Brunton, J. M., and Stock, A. F. (1985). The Analytical Design of Bituminous Pavements. Proc. Institution of Civil Engineers, Part 2, Vol.79, 1-31.

² Rao Tangella, S.C.S., Craus, J., Deacon, J.A. and Monismith, C.L. (1990). Summary Report on Fatigue Response of Asphalt Mixtures, Prepared for Strategic Highway Research Program, Project A-003-A, Institute of Transportation Studies, University of California, Berkeley.

³ Shell International Oil Products BV, (1998). BISAR 3.0 – Bitumen Stress Analysis in Roads. User Manual. The Hague.

Shell fatigue cracking law (Shell, 1978) and those obtained from the laboratory tests at different temperatures was carried out in order to evaluate the consequences of the lack of temperature information in the Shell fatigue cracking law (Shell, 1978), especially for mixtures commonly used in Portuguese pavement surface layers. The fatigue cracking resistance was given by N_{100} (resistance for tensile strain 100×10^{-6}) and ϵ_6 (resistance of 1×10^{-6}) parameters. According to the authors, the pavement design using *Shell* fatigue life equation is very conservative in some cases leading to the duplication of the bituminous layer thickness design.

It was also proven, that parameter a in relation to temperature is exponential, while the evolution of the parameter b is linear. Thus, the influence of the temperature in the fatigue cracking resistance of the studied AC 0/14 mixture was expressed by following equation. It clearly shows the influence of temperature on fatigue behavior:

$$N = 4.2082E+24 \times e^{-7.2083E-01 \times T} \times \left(\frac{1}{\epsilon_0} \right)^{-0.1290 \times T + 7.6638}$$

The impact of the temperature on fatigue life was further shown also by pavement design calculation done by multilayer linear elastic analysis with BISAR 3.0.

It was possible to observe that temperature may have a massive influence in the asphalt pavement design, mainly for higher traffic design values. In the example of the AC 0/14 design presented in Figure 6, temperature has a greater influence than the foundation class. The reduction of temperature increases the fatigue resistance of the bituminous layer, thus reducing the AC 0/14 thickness needed to bear the traffic loads.

8.1.1.3 Paper 171 (Mogawer et al., 2012)

The first Overlay tester (OT) was designed by Germann and Lytton (1979) in the late 1970s. The key parts of the apparatus, as shown in Figure 8-3, consist of two steel plates, one fixed and the other movable horizontally to simulate the opening and closing of joints or cracks in the old pavements beneath an overlay. Since its development, the OT has been used mainly to evaluate the effectiveness of different geosynthetic materials in retarding reflective cracking (Zou et al., 2001).

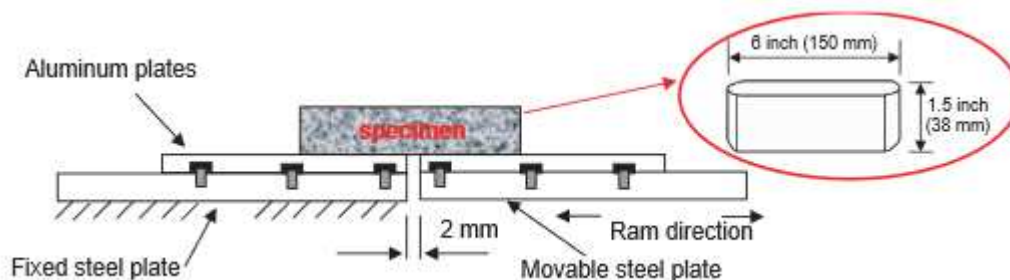


Figure 8-3: Concept of overlay tester OT (Paper 171)

Being an SPT (Simple Performance Tester) means meeting requirements in addition to being highly correlated with field distresses (such as fatigue cracking).

Fatigue is a two-stage process: crack initiation and crack propagation. However, crack initiation is closely related to crack propagation. Therefore, the OT which mainly characterizes crack propagation can be used for fatigue cracking. This finding has been further validated by field FHWA-ALF fatigue test results. Furthermore, the OT also meets

other SPT requirements (such as that of cost of equipment). Finally, it is concluded that the OT can be used as an SPT for fatigue cracking.

For routine operations, it is recommended that the OT be run at room temperature (25 °C) in the controlled displacement mode shown in Figure 8-4. The test is run at a loading rate of one cycle per 10 s, with a maximum opening displacement of 0.63 mm. The loading rate does not represent the field condition, but it was proposed to develop a practical and rapid accelerated crack resistance test. The number of cycles to failure is reported with the failure defined in relation to load reduction from that measured in the first cycle (currently a 93 % reduction is used).

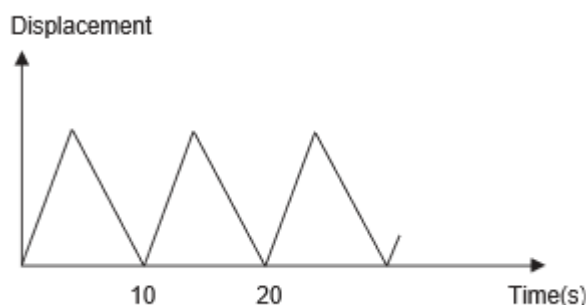


Figure 8-4: Loading form of overlay tester (Paper 171)

8.1.1.4 Paper 559 (Reyes Lizcano *et al.*, 2009); Paper 467 (Hou *et al.*, 2010)

The paper 559 studied the application of viscoelastic continuum damage (VECD) mechanics which has been successfully applied to HMA, to test results of asphalt binders in the shear mode under various loading conditions. The results indicated that VECD can be effectively applicable to asphalt binders, which presents a good potential to characterize asphalt binder and predict its contribution to fatigue resistance using a fundamental approach that parallels some of the advanced work carried on asphalt mixtures. The importance of this potential is it could allow for a unified model for fatigue of mixtures and binders.

In the theory of VECD, pseudo-strain is an essential parameter for applying Schapery's correspondence principle (CP) to the hysteretic stress-strain behavior of asphalt concrete. The damage parameters are found to be independent of test temperature, testing mode, and loading rate. In particular, based on the test results under one condition, the fatigue behaviors under different testing conditions can be predicted, in terms of loading levels, loading frequency, temperature, and mode (e.g. monotonic vs. cyclic).

Three modified asphalt binders used in the Federal Highway Administration (FHWA) accelerated loading facility (ALF) study were selected for this study. Table 8-1 lists the asphalt binders along with its respective PG-grading and modifications.

The laboratory testing was done using a TA Dynamic Shear Rheometer Instrument (AR2000) that allows isothermal loading of asphalt binders. These binders were aged using the rolling thin film oven (RTFO) prior to the testing. Two types of tests were conducted: frequency sweep tests and constant-strain controlled fatigue tests, called here time sweep.

Table 8-2: ALF bituminous binders used in the study

Lane	Type	PG	Notes
3	Air-Blown	70-28	Air Blown Modified
4	SBS LG	70-28	SBS with Linear Grafting
5	CR-TB	76-28	Crumb Rubber-Terminal Blend

Frequency sweep tests were conducted at 10 °C; 16 °C; 19 °C; 22 °C; 26 °C and 30 °C, respectively. For each temperature, 15 frequencies were used, ranging from 0,1 Hz to 60 Hz. Time sweep tests were conducted up to failure, typically beyond 50% reduction of complex modulus. These fatigue tests were performed at 19°C which was the controlled temperature at ALF site. The time sweep tests followed AASHTO TP5 standard procedures. The strain levels used in this study varied for different binders based on the field evaluation of ALF pavement conditions.

In this study, different strain levels were used to test the binders. Figure 8-4 shows the complex shear modulus, G^* , of SBS LG binder as a function of loading cycles. As expected, with the increase of loading cycles, G^* decreased, indicating the occurrence of damage. At about 60% of original G^* value, the decrease rate of G^* accelerated and quickly reached the failure criteria used in this study, 50% of original G^* value. Another observation is the effects of strain level on the fatigue life. Again, as expected, the increase of strain level resulted in shorter fatigue life.

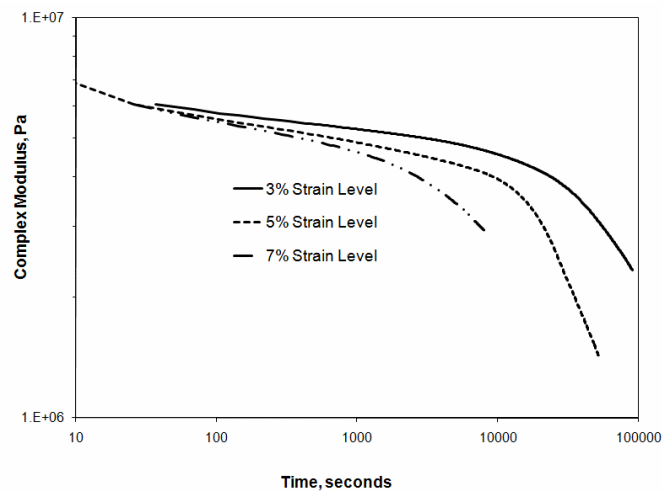


Figure 8-5: Complex shear modulus of SBS-modified bitumen in time sweep test

VECD mechanics uses the correspondence principle and concept of pseudo strain to characterize the damage. Without damage, the stress and pseudo strain curve overlap the line of equality. The deviation of the curve from line of equality indicates damage. The stress and pseudo strain is then regressed to estimate damage evolution parameters C and S.

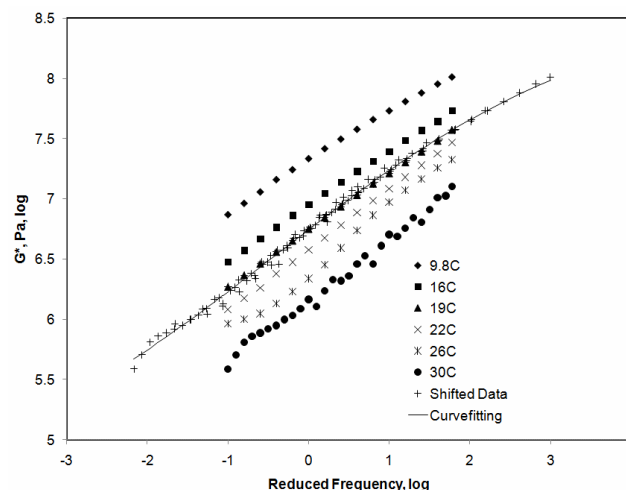


Figure 8-6: Master curve of complex modulus of SBS-modified bitumen

As the first step, the complex shear moduli from frequency sweep testing at each temperature were shifted to form the master curve at the reference temperature (19 °C for this study) based on time-temperature superposition, as shown in Figure 8-4. The master curve was then fitted into a sigmodal function.

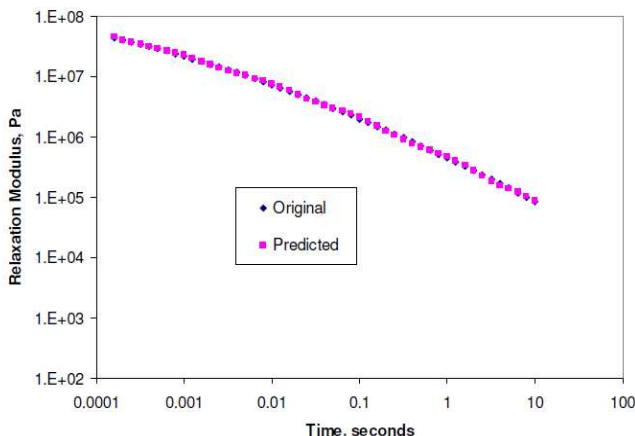


Figure 8-7: Converted and fitted relaxation modulus of SBS-modified bitumen

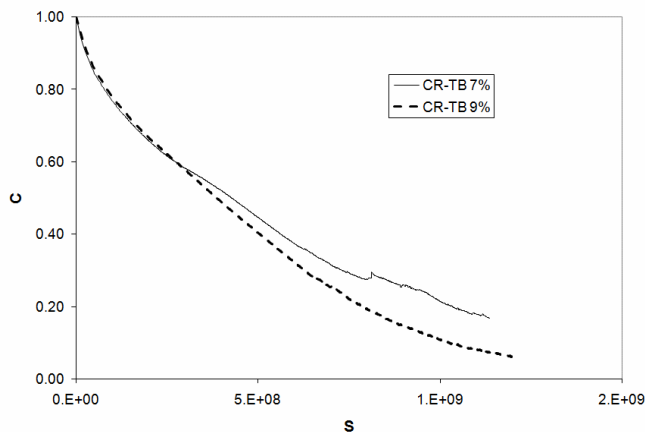


Figure 8-8: Relationship between material integrity (C) and damage intensity (S) for crumb-rubber modified binder

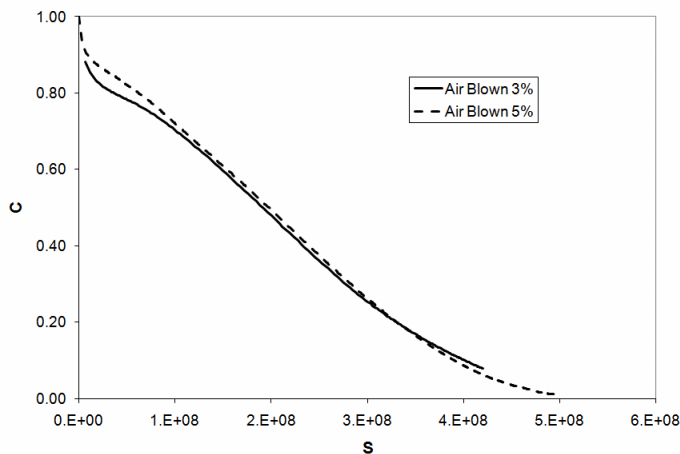


Figure 8-9: Relationship between material integrity (C) and damage intensity (S) for air-blown binder

Figure 8-4 to Figure 8-4 show the relationship between material integrity (C) and damage intensity (S) for crumb-rubber, air-blown, and SBS modified binders, respectively. Figure 8-4 shows the relationships between C and S for all three binders.

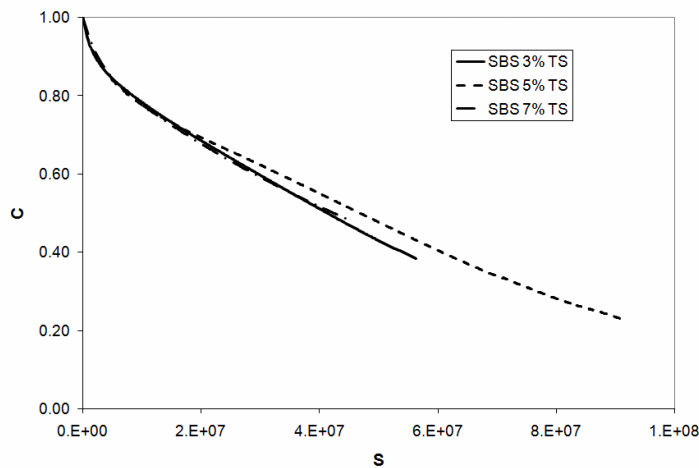


Figure 8-10: Relationship between material integrity (C) and damage intensity (S) for SBS-modified binder

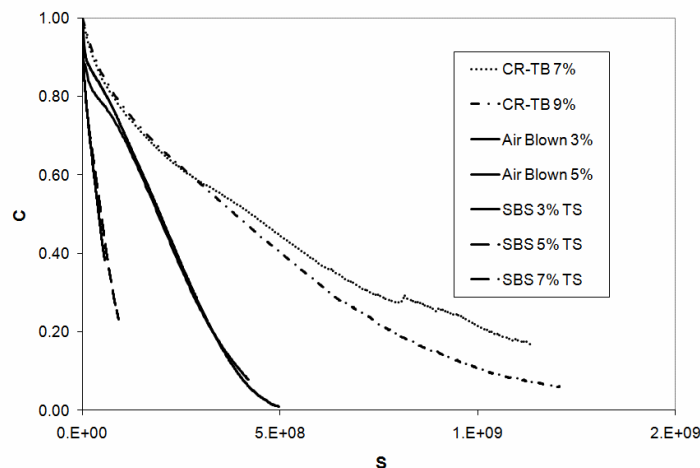


Figure 8-11: Relationship between material integrity (C) and damage intensity (S) for three binders

The results have shown that the relationship between C and S is independent of strain levels used. The C and S curves for different strain levels overlap closely. This indicates that potential of applying the VECD approach to asphalt binders is high and could lead to a unified fatigue approach.

As seen in Figure 8-4, the simulated fatigue behaviours (by using time sweep tests) closely matched those of measured behaviors for this binder. The results demonstrated the advantages of the VECD theory: the fatigue behavior at different strain conditions can be simulated based on the tests results at single strain condition, in this case 5% strain.

Figure 8-4 depicts the comparisons between the values and indicates that there is a close agreement between the simulated and measured fatigue lives.

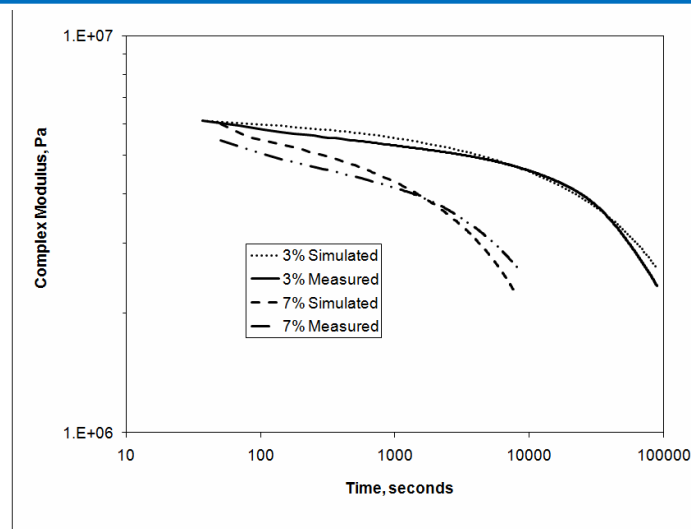


Figure 8-12: Simulated and measured fatigue behavior based on 5% strain level test results (SBS LG)

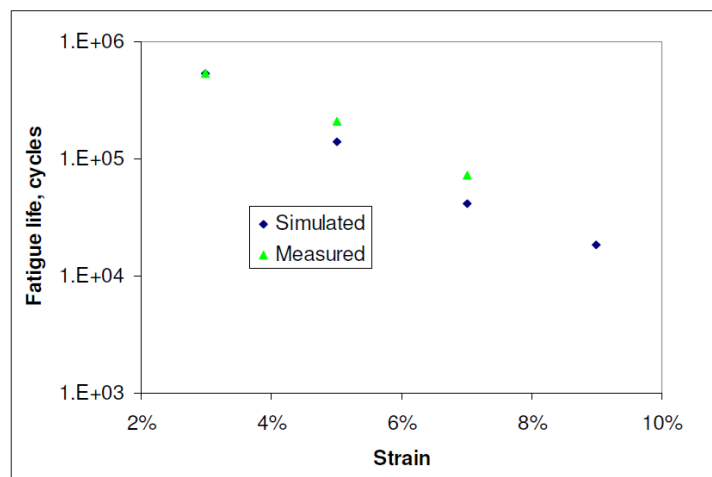


Figure 8-13: Comparison of measured and simulated fatigue life

Overall, this initial trial of applying the VECD principles to binder fatigue results indicates that the VECD approach shows great promise to characterize the fatigue behavior of asphalt binder. The independent relationship between structural integrity (C) and damage intensity (S) is validated. The analysis results in successful prediction of fatigue behavior under different testing conditions in the laboratory, as proved by the comparison to measured values. This understanding of fatigue mechanism can, in turn, be instrumental in estimating the fatigue performance of asphaltic mixtures and in developing a unified fatigue approach for binders and mixtures.

It could be verified that the damage evolution characterization as defined by the relationship between material integrity factor “C” and damage intensity factor “S” is independent of strain levels used in testing binder fatigue.

Similarly paper 467 shows that the simplified VECD model based on the data from a single temperature and a single strain level can predict fatigue test results fairly accurately under various temperature conditions and at various strain levels. The eleven mixtures all use unmodified standard grade binders.

Table 8-3: Bitumen information

Asphalt mixture	Binder grade	Bitumen content (%)
S9.5C	PG 70-22	5,2
S9.5B	PG 64-22	6,1
I19.0C	PG 64-22	4,5
B25.0B	PG 64-22	4,5
RS9.5C	PG 70-22	6,4
S12.5C	PG 70-22	5,5
I19.0B	PG 64-22	4,8
RS12.5C	PG 70-22	4,4
RI19.0B	PG 64-22	4,4
RI19.0C	PG 64-22	4,3
RB25.0B	PG 64-22	4,2

NOTE: Surface (S), Intermediate (I) or Base (B); very high volume (D), high volume (C), standard volume (B) and low volume (A); and prefix R indicating whether the mixture contains reclaimed asphalt pavement (RAP).

Table 8-4: Cyclic test summary (group 1 mixtures)

Material	Test Designation	Initial Strain ^a ($\mu\epsilon$)	Temperature ($^{\circ}\text{C}$)	N_f
S9.5C	27-CX-VH	668	26,8	1600
	27-CX-VH (2)	638	26,8	420
	27-CX-H	437	26,8	17500
	27-CX-L	303	26,6	86100
	27-CX-H2	520	27,0	780
	27-CX-VL2	247	26,8	165000
	27-CX-VL	225	27,4	190000
	19-CX-H	240	19,1	45000
	19-CXVL	190	19,0	311000
	19-CX-VH	402	18,5	2280
	19-CX-H3	425	18,7	3780
	19-CX-H2	332	18,8	12100
	5-CX-H	150	5,0	70000
	5-CX-L	126	4,9	140000
S9.5B	5-CX-VH	213	4,6	1430
	5-CX-H2	189	5,3	1100
	27-CX-H	500	27,4	12100
	19-CX-H	363	19,2	4570
	19-CX-L	266	19,3	47000
	27-CX-L	353	27,3	87900
I19C	5-CX-H	200	5,5	4600
	5-CX-L	166	5,5	198000
	19-CX-H	252	19,2	6500
	27-CX-H	264	27,4	19900
	27-CX-L	236	27,4	217000
B25B	19-CX-L	232	19,5	27000
	5-CX-H	133	5,2	16600
	19-CX-H	240	19,1	4780
	19-CX-L	186	19,1	7160
	5-CX-H	122	5,4	11000
	5-CX-L	112	5,2	73800
RS9.5C	27-CX-L	162	27,5	75000
	27-CX-H	256	27,4	11000
	19-CX-H	287	19,4	44000
	19-CX-L	232	19,6	148000
	27-CX-H	355	27,3	27500
	5-CX-VL-not fail	155	5,2	>168000 ^D
	27-CX-L	318	27,4	79000
5-CX-H	174	5,4	41000	

NOTE: ^a On-specimen strain at the 50th loading cycle

The CX cyclic test is used for fatigue performance characterization. In this test the machine actuator's displacement is programmed to reach a constant peak level at each loading cycle. All the CX tests in this study are conducted at a constant frequency of 10 Hz and at a fixed temperature. In the CX cyclic test, the dynamic modulus and phase angle are tracked throughout the entire fatigue life. The viscoelastic damage characterization is determined by performing CX cyclic tests at different strain levels and under different temperature conditions.

Once the model is verified with the first group of mixtures, it is no longer necessary to perform fatigue tests for the remaining mixtures under so many different conditions. Instead, only two fatigue tests (one at a relatively high input level and the other at a relatively low input level) are performed at a single temperature (19 °C). Using these two tests, the fatigue behavior at all other conditions is predicted with the simplified VECD model. Table 8-1 and Table 8-1 summarize the cyclic test results for all the mixtures used in this study. As mentioned, all tests are performed at a constant frequency of 10 Hz, and failure is defined as the point at which the phase angle starts to drop.

After each cyclic test, the pseudo stiffness (C^*) and damage (S) are computed according to the simplified VECD model. Figure 8-4 shows the damage curves (C^* versus S) for the five model verification mixtures. The results show that the simplified model works well and that most of the 5 °C and 19 °C curves collapse well within each mixture. The exception occurs for the S9.5B mixture where the 5 °C curves are above the 19 °C. In addition, the 5 °C curves are generally shorter than the curves from the 19 °C tests, which is a reflection of the brittleness of the material at low temperatures. Another observation from this figure is that all of the 27 °C curves are below the 5 °C and 19 °C test curves. Due to these reasons, the intermediate temperature, 19 °C, is chosen as the testing temperature for the remaining mixtures after the model has been verified. Figure 8-4 shows the damage curves for the second group mixes.

Table 8-5: Cyclic test summary (group 2 mixtures)

Material	Test Designation	Initial Strain ^a ($\mu\epsilon$)	Temperature (°C)	N_f
S12.5C	19-CX-H	312	19,2	1250
	19-CX-L	192	19,2	74100
I19B	19-CX-H	306	19,0	800
	19-CX-L	181	19,2	19000
RS9.5B	19-CX-H	276	19,4	13000
	19-CX-L	254	19,2	52800
RS12.5C	19-CX-H	186	19,1	9330
	19-CX-L	156	19,0	220000
RI19B	19-CX-H	187	19,5	6000
	19-CX-L	141	19,5	23700
RI19C	19-CX-H	180	19,4	3450
	19-CX-L	122	19,2	68900
RB25B	19-CX-H	175	19,2	950
	19-CX-L	133	19,2	7550

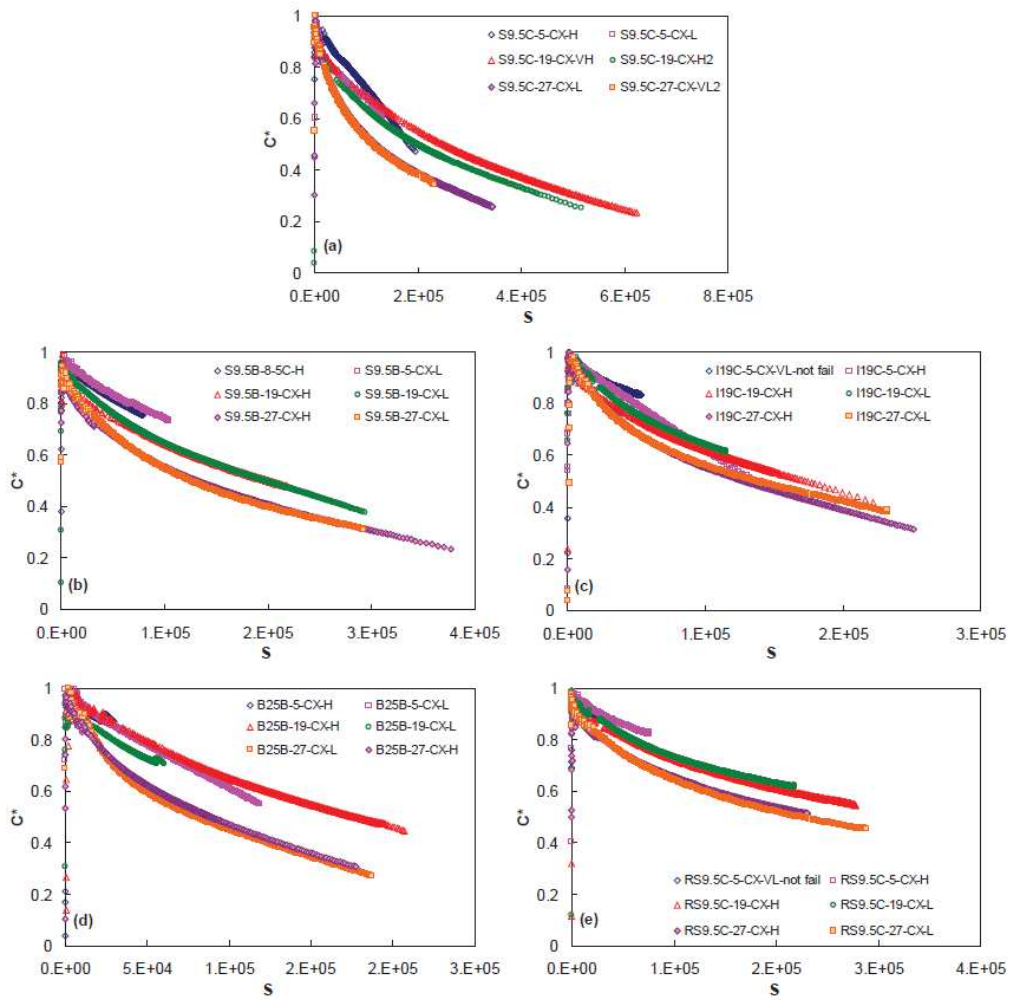


Figure 8-14: Damage curves for selected mixtures

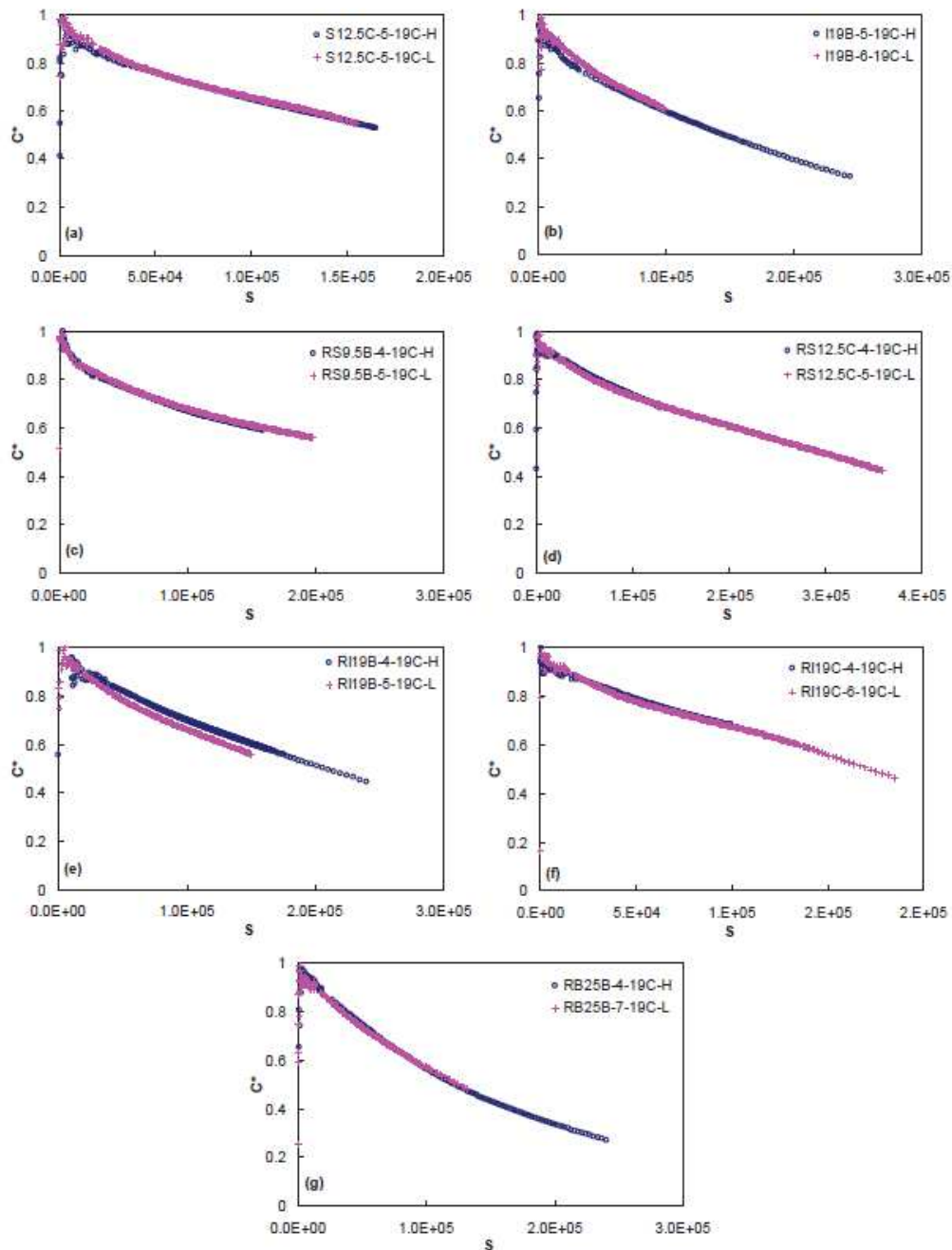


Figure 8-15: Damage curves for selected mixtures

The simulation failure criterion is applied to predict the fatigue life for the mid-failure cyclic tests. The results of this prediction process are shown in the form of line of equality plots in both arithmetic and logarithmic space in Figure 8-4. The relationship shows a high degree of statistical significance as evidenced by the high correlation coefficient in both arithmetic and logarithmic scales. A slight tendency to over-predict in the arithmetic fatigue life prediction is evident, which may be caused by viscoplasticity in some of the high temperature and low strain level tests.

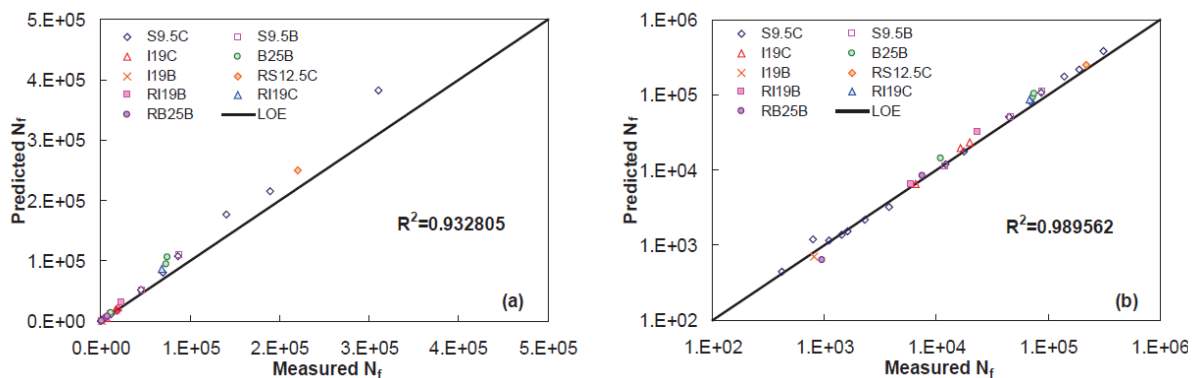


Figure 8-16: Comparison of measured and predicted fatigue life for mid-failure cyclic tests in (A) arithmetic and (B) logarithmic space

Figure 8-4 presents the simulated controlled strain and controlled stress fatigue test envelopes respectively. It is found that the slopes of the fatigue envelopes for the different mixtures are quite close to each other for both the controlled strain and stress tests. Although not performed in pure controlled stress or strain, the experiments also suggest similar slopes for the study mixtures. So, by comparing the vertical positions of those straight lines, it is easy to rank the fatigue life of the different mixtures under the same loading condition.

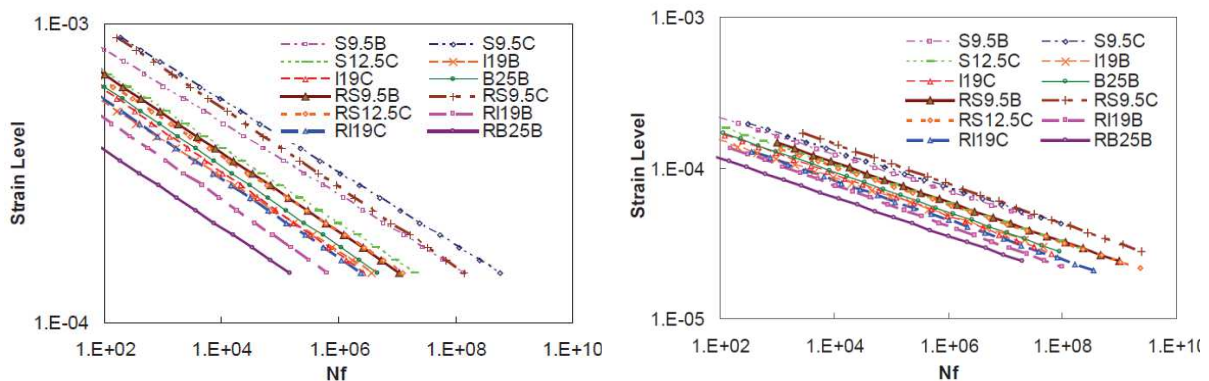


Figure 8-17: Simulated controlled strain fatigue test envelopes for eleven mixtures (10 Hz and 19°C)

It is observed that the two testing modes yield different fatigue performance rankings for most mixtures. In general it is found that mixtures with a smaller NMAS show better performance than mixtures with a larger NMAS. This trend is observed in both the controlled stress and controlled strain simulations but is more pronounced in the latter. In the controlled strain testing mode, the non-RAP mixtures show better fatigue resistance than the RAP mixtures; however, this phenomenon is nearly the opposite under controlled stress mode. The exception to this rule is the 25 mm RAP mixture, which shows the worst performance in both controlled stress and controlled strain simulations. It is possible that other factors, such as asphalt content, could be overwhelming the simple effect of RAP in this mixture. Also it is found, that overall better ranking occurs in the mixtures with higher asphalt contents. This trend is observed in both sets of simulations, but is more pronounced in the controlled strain simulations. Finally, it is found mixtures with a PG 70-22 asphalt binder consistently outperform mixtures with a PG 64-22 binder

The application of the VECD model using this failure criterion results in very good agreement between the measured and predicted fatigue life for the eleven mixtures. The VECD model is also applied to simulate both controlled strain and controlled stress direct tension cyclic tests

under various testing conditions to assess the effects of various mix design factors on the fatigue performance.

8.1.1.5 Paper 555 (Tabatabaee and Bahia, 2014)

Based on knowledge and findings that existing binder tests may not accurately predict cracking performance at intermediate temperatures, this study embarked in the development a new binder fracture energy test (DT test) to fill this void. Nonlinear 3-D finite element analysis (FEA) was used to identify and optimise appropriate specimen geometry to allow for accurate determination of fracture energy. Various binders were tested at multiple temperatures and loading rates using prototype specimens in order to evaluate the feasibility and validity of different specimen geometries. The researchers used nonlinear FEA results to establish a data interpretation system and develop a set of diagrams to simplify calculation procedures. After extensive observation of test results, the researchers concluded that the new fracture energy test and data interpretation system suitably measure unmodified and modified binder fracture energy density. The test results reveal that binder fracture energy is a fundamental property of binder and that characteristic of the true stress-true strain relationship is a good indicator of the presence and relative content of modifiers.

For each test; time, deformation, and load data was acquired using the MTS acquisition software at a rate of 500 points per second. Each specimen was loaded at various displacement rates until failure. Tests were performed not only at various displacement rates, but also at different temperatures. During testing, it was found that any specimen imperfection may result in premature failure at low temperatures and/or faster loading rates. Flawed specimens do not crack at the exact centre, which leads to erroneous test results that must be discarded.

After plotting the new stress-strain calculations, the point of initial fracture is more easily determined (Figure 8-4). The post-peak energy after the point of initial fracture should not be considered when calculating fracture energy, as this measurement is the energy required to separate the specimen in half, rather than the energy used to fracture the binder. Fracture energy should be calculated from the beginning of the true stress-true strain curve to the last stress peak (the point of initial fracture).

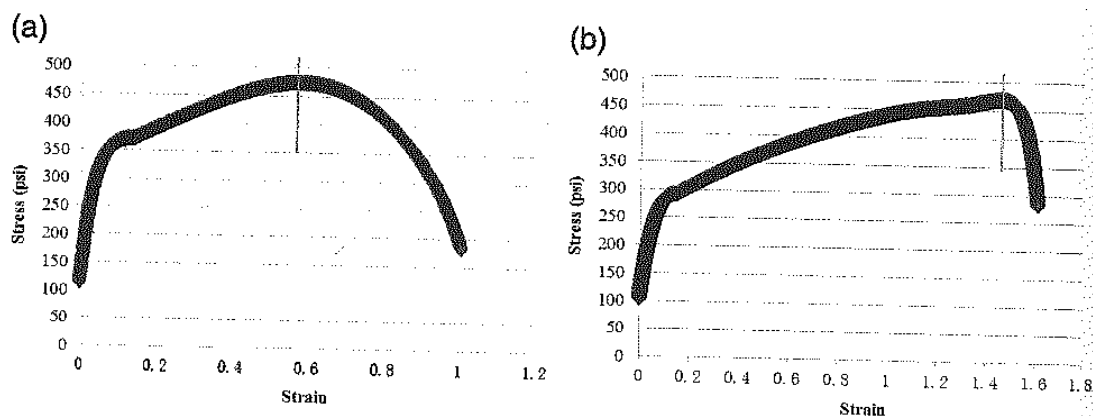


Figure 8-18: True stress-true strain curve by new calculation procedure: (a) PG 67-22, 10 °C, 400mm/min and (b) PG 76-22, 10 °C, 400 mm/min

Different binders, including unmodified binders, SBS modified binders, rubber-modified binders, and hybrid binders were tested and analysed. Both pressure ageing vessel (PAV) residue and recovered binders were prepared. The binders and their modifying additives are listed in Table 8-6. All binders were tested at multiple loading rates in order to determine appropriate loading rates that avoid premature fracture or excessively ductile fracture, both of

which result in erroneous fracture energy. The researchers performed preliminary tests on PG 76-22 (4,25 % SBS), and PG 67-22, a type of unmodified binder (all binders were PAV residues), using the following test temperatures: 0 °C; 5 °C; 10 °C; 15 °C and 20 °C. At 20 °C, specimens become too soft to accurately obtain fracture energy.

As can be seen in Figure 8-4, the fracture energy density at 15°C (test temperature for all tests) was consistent for the same binder at different loading rates, and there was clear distinction between the modified and unmodified binder. Although similar trends occurred at lower test temperatures (10 °C; 5 °C and 0 °C), the least variability and lowest number of premature failures occurred at 15 °C, making this temperature the optimal temperature for determining the fracture energy of most of the binders and conditions evaluated, in this study.

Table 8-6: Binder compositions/formulations

Binder	Modifying components
PG 67-22	None (graded as a PG 69.78-26.50)
PG 64-22	None
AC-30	None
AC-20	None
PG 76-22	4,25% SBS (graded as a PG 76.7-27.16)
PG 82-22	8,5% SBS
Geotech	1% SBS, 8% of Type B ground tyre rubber (GTR) and 1% hydrocarbon
Hudson	3,5% crumb rubber, 2,5% SBS, 0,4%-plus Link PT-743 cross-linking agent
Wright	GTR (digested rubber) and SBS. Unknown content
Marianni	Unclear, possibly 13% GTR, it may contain polymer
ARB-5	5% type B rubber
ARB-12	12% type B rubber

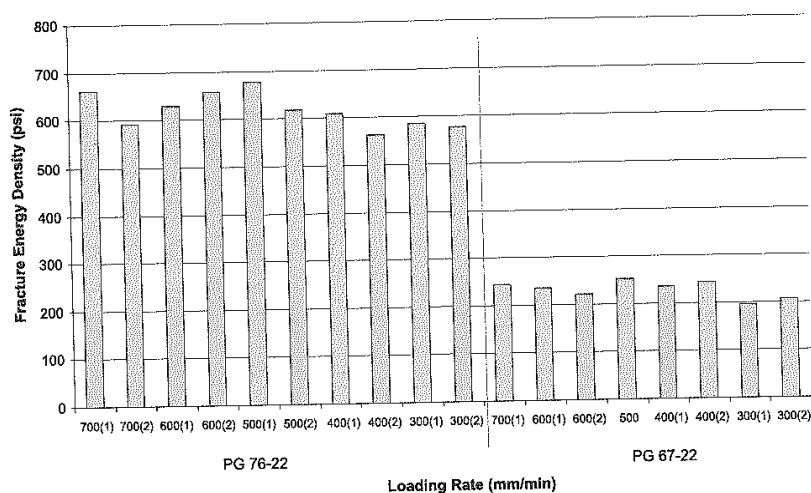


Figure 8-19: Preliminary tests, fracture energy density at 15°C

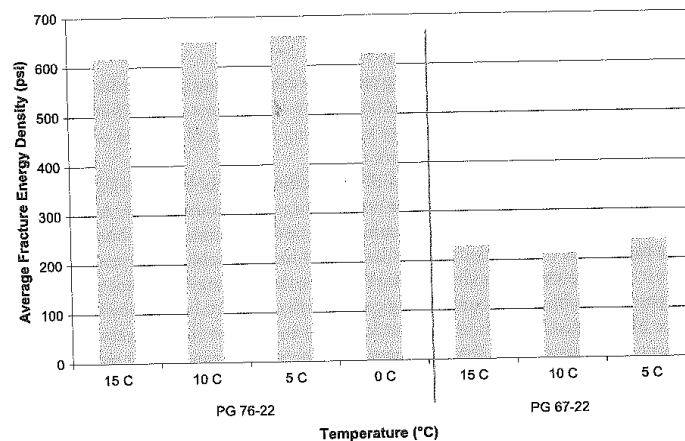


Figure 8-20: Preliminary tests, average fracture energy density at each temperature

The average fracture energy density for the same binder, at each test temperature, is plotted in Figure 8-4. As shown in the figure, the average fracture energy was independent of temperature for each binder, and the difference in fracture energy between binder types is clearly distinct. These results indicate that binder fracture energy is independent of temperature, and that the proposed fracture energy test can capture the expected trend of fracture energy between unmodified and SBS-modified binders.

The average fracture energy is consistent for each binder category, and the difference between binder categories is easily distinguished (Figure 8-4). The fracture energy of recovered PG 76-22 and its PAV equivalent residue were high compared to the unmodified and rubber-modified binders. During the extraction-recovery process, insoluble rubber particles in the binder were caught in the filter paper, causing rubber to be absent from the binder after recovery. Therefore the fracture energy of recovered rubber-modified binder, ARB-5, was similar to that of unmodified binders, as are the true stress-true strain curves. These results bolster the idea or theory that this new fracture energy test may be suitable for identifying binder components.

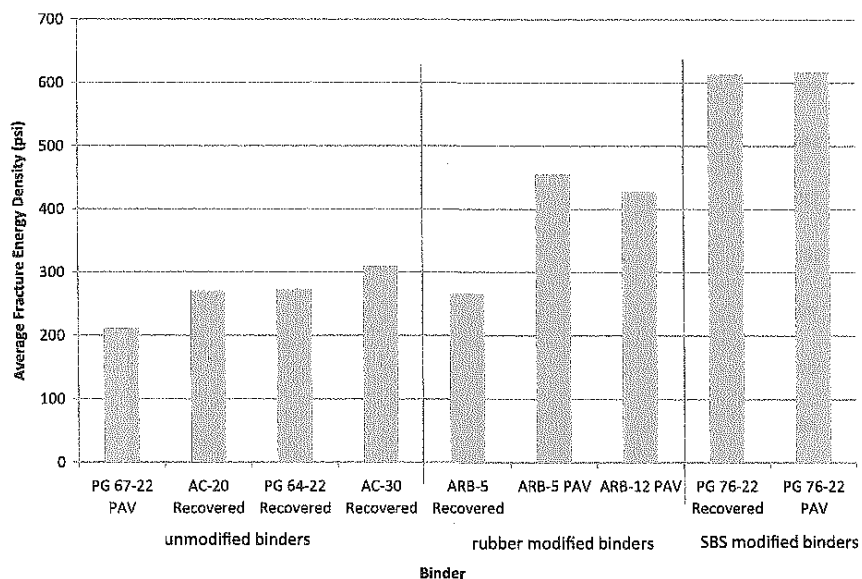


Figure 8-21: Recovered binders test and preliminary test results, fracture energy vs. loading rate

The properties of hybrid binders and highly polymer-modified binders differ from the properties of the more common-modified binders. Since the results of current test methods do not effectively distinguish between the fracture resistance of hybrid binders and that of other modified binders, the new fracture energy test would prove especially useful if it were able to do so.

All tests were conducted at 15 °C, except for the tests on the PG 82-22 binder, which was conducted at both 15 °C and 10 °C. This highly polymer modified binder exhibited excessive ductility at 15 °C, making the tests unsuccessful. The deformation of this binder was excessively high, even at the fastest displacement rate, which resulted in lowering the test temperature by 5 °C. An excessively ductile specimen may make the data interpretation inaccurate and yield incorrect fracture energy.

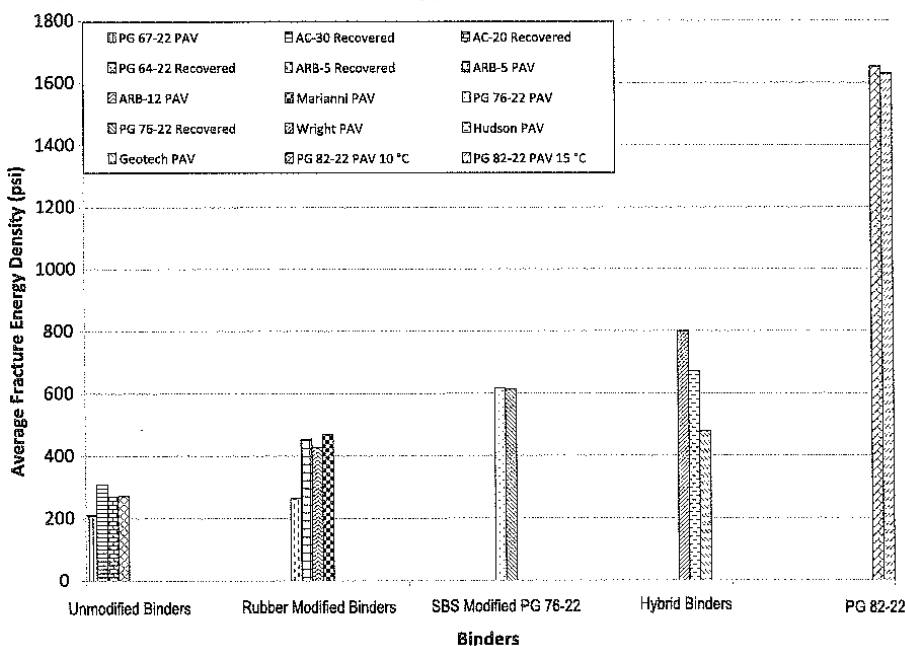


Figure 8-22: Average fracture energy test results of all binders

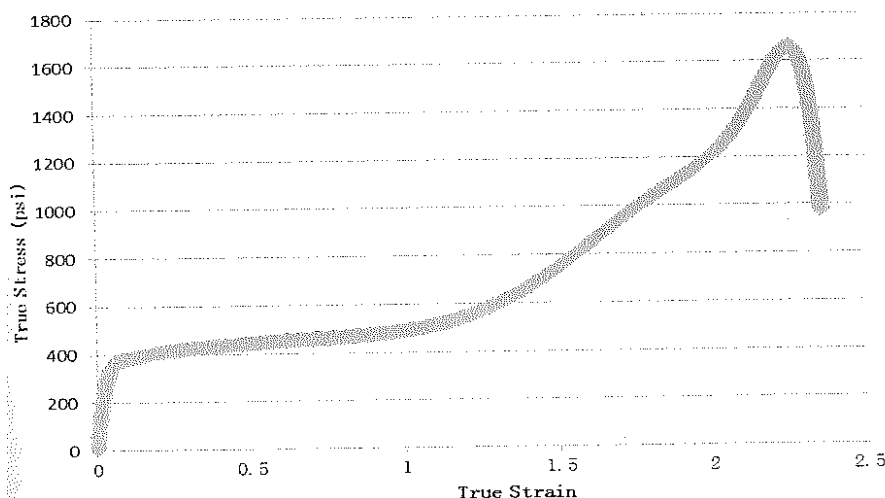


Figure 8-23: PG 82-22 at 15 °C, 900 mm/min, true stress vs. true strain

A unique property of PG 82-22 was that, even at very low displacement rates and with complete true stress-true strain curves, the fracture section consistently resembled that of specimens exhibiting premature failure.

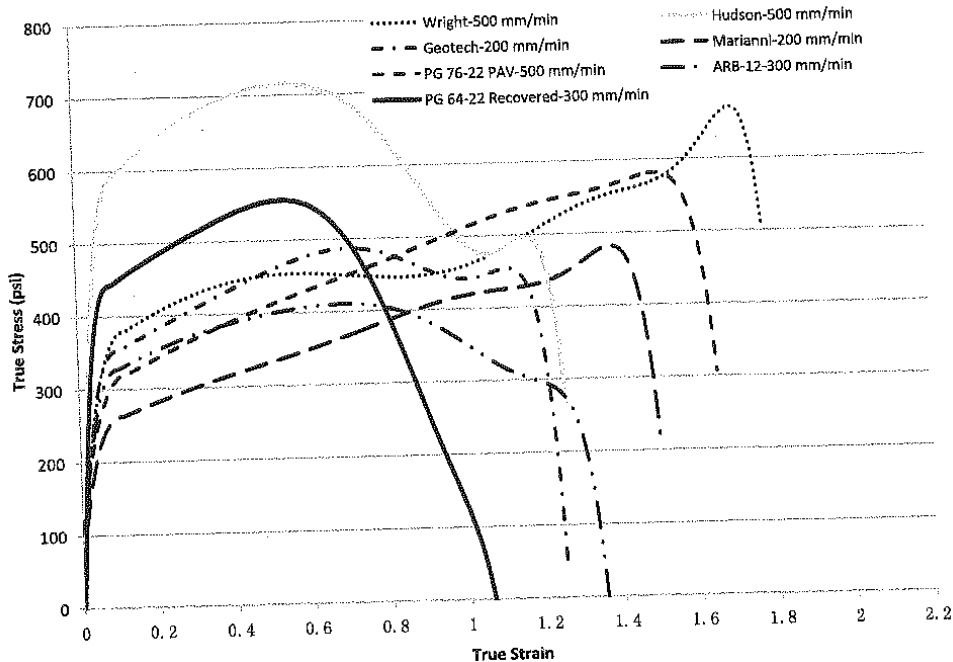


Figure 8-24: Typical true stress-true strain curves

The results of this study indicate that the characteristic shape of failed specimens is not a reliable indicator of premature fracture, and determining the status of the true stress-true strain curve is the only way to identify premature fracture. In order to determine fracture energy, only data from tests that result in complete true stress-true strain curves should be used. The results of statistical analyses indicate that the fracture energy of a binder is independent of displacement rates and temperature (0-15 °C), and that the new fracture energy test significantly differentiates between binders.

8.2 BitVal findings for fatigue cracking

The BitVal project found that further research was needed for a more explicit correlation between the fatigue behaviour of asphalt mixtures and some characteristics of binders. The fatigue of bitumens and typical parameters of complex modulus seemed to be the best properties in relation to the behaviour with the fatigue of the asphalt mixture. While awaiting the results from such research, the basic characteristics (e.g. penetration, softening point or viscosity) and some rheological characteristics, both before and after ageing (e.g. by RCAT or RTFOT and PAV), remained the best criteria to assess the fatigue behaviour of asphalt.

In particular, the relationship between bitumen fatigue and mixture fatigue at the number of cycles to achieve a 50 % reduction in G^* looks particularly promising and it was recommended that this work was continued to include a range of PMBs and other mixture types. The research should involve two aspects:

- Validation with field performance is critical and there was a lack of information relating laboratory fatigue behaviour with performance in practice. More effort was required in this area, particularly in relating the in-situ bitumen properties with fatigue cracking.

- PMBs cover a wide range of polymer types and polymer contents which give them widely differing properties. If further studies were intended to be carried out on asphalt mixtures containing PMBs, it was recommended that a range of the different families of PMBs were examined to ensure that specific conclusions could be attributed to the different families of materials.

The force ductility test showed some promise, but the relationship appeared to be dependent on the type of modifier which makes it of limited use. Furthermore, the research was limited in that it was restricted to a single paper.

8.3 Relationship found between bitumen properties and asphalt fatigue cracking

The performance of asphalt mixes is deeply bitumen dependent. Therefore the binder content and binder type can directly affect the fatigue resistance of asphalt mixtures. In this chapter the effect of binder properties on fatigue cracking of asphalt will be discussed. Since the polymer modified bitumen (PMB) are getting more and more popular in road construction for at least two decades, a subchapter will be dedicated on the discussion on different PMB types and their effects on fatigue performance of asphalt mixtures.

8.3.1 Correlation between binder and asphalt properties in fatigue resistance

8.3.1.1 Paper 025 (Mangiafico et al., 2012)

This study focused on effects of reclaimed asphalt pavement on complex modulus and fatigue resistance of both, bitumen and asphalt mix. The materials used in this study were:

- 3 types of bitumen 15/25; 35/50 and 70/100
- 3 different percentages of RAP 20%; 40% and 60%

Fatigue tests on bitumens were also run as DSR time sweeps: materials were subjected to continuous oscillating loading at a 25 Hz frequency in strain control mode at 10°C.

For fatigue tests on both bitumen and mixes, fatigue life was arbitrarily determined as the number of loading cycles corresponding to a 50% reduction of initial complex modulus.

Fatigue parameters of asphalts appear to reach an optimum for RAP content ranging from 20 to 40 %. In general a 60 % RAP content does not seem to cause a drastic decline of asphalt fatigue response. Although fatigue resistance of asphalts is strongly related to bitumen properties for this limited set of data there is no reliable correlation found between ϵ_6 and b values of asphalts and corresponding bitumens.

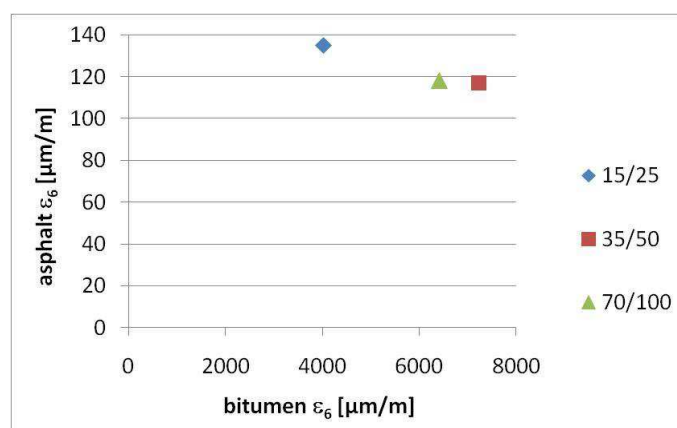


Figure 8-25: Asphalt mixture versus bitumen ϵ_6 values at 10 °C, 25 Hz

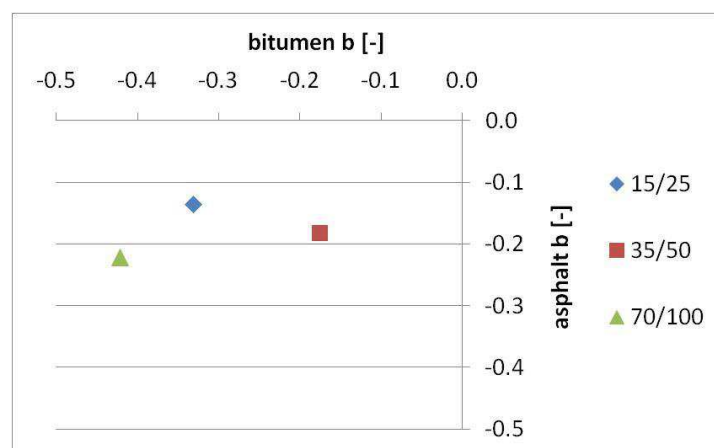


Figure 8-26: Asphalt versus bitumen b values at 10 °C, 25 Hz

Several possible explanations can be advanced. Fatigue characterization for asphalts and bitumens based on classical tests can be erroneous due to the biasing effects existing during such tests. In addition reliability of DSR time sweep as a fatigue test is a non-secondary issue. Finally a limited number of materials were included in the fatigue test experimental campaign.

8.3.1.2 Paper 062 (Pérez Jiménez et al., 2008)

The objective of this study is to relate and to establish a correlation between the fatigue parameters of the bitumen and fatigue parameters of their corresponding mixtures. The results of the laboratory test indicated that, when taking the binders with the same modulus, the higher the critical deformation, the better its behavior under fatigue is. The critical deformation is related with binder's ductility. It is further mentioned by the authors that, the more ductile the binder is, the better its behavior under fatigue will be. As a conclusion, the binder, although it is low in percentage, proves to have a great influence on the fatigue behavior of asphalt mixtures.

8.3.1.3 Paper 070 (Gauthier et al., 2008)

This paper presents an experimental study on stiffness and fatigue evaluation involving six asphalts with the same aggregate size distribution. The effect of bitumen type and content is evaluated. The fatigue tests were performed using two different geometries, and measurements of sample surface temperature were done during all fatigue tests.

It was reported by the authors that thermal effects from tension-compression test was not negligible thus a thermal correction had to be taken into account. However for bending fatigue test this was not the case.

Two different considerations should be taken when choosing a failure criterion for analysing fatigue data:

- Failure criteria based on low stiffness decrease (below 25 %) are not related to fatigue, but only to phase I. Phase I corresponds to a decrease of sample stiffness before thermal equilibrium is reached in the test specimen, related to different phenomena such as damage, heating and thixotropy. They should be avoided.
- Failure criteria based on high stiffness decrease (above 40 %) are hard to achieve. Most specimens break before reaching these levels of stiffness reduction.

It was found that fatigue performance of asphalt is highly dependent on bitumen characteristics. For instance, modified and semi-blown bitumen have better fatigue performance than straight-run bitumen. As expected, asphalt mixes with higher bitumen content were found more resistant to fatigue.

8.3.1.4 Paper 074 (de Visscher et al., 2008)

Two families of high modulus asphalt (French EME) were considered in the project for performance testing. One mix contained a stone skeleton (French mixture type EME) and the other was based on a sand skeleton with low void content. The same binder was used for both families. Fatigue resistance was determined according to BRRC-method. The influence of these parameters was studied:

- High modulus asphalt versus conventional AC-mixes for base layers;
- Sand skeleton vs. stone skeleton;
- Binder content and type;
- Reclaimed asphalt.

All high modulus asphalt mixes show a better resistance to fatigue than traditional asphalt. An increase in binder content leads to a higher resistance to fatigue. High modulus asphalt with porphyry performs less in fatigue than high modulus asphalt with limestone. Limestone adheres better than porphyry to bitumen. Thus the adhesion aggregate-bitumen seems to play an important role for a better fatigue resistance.

The sand skeleton performs better than the stone skeleton. The binder type plays a role. Concerning the use of reclaimed asphalt, mixes with equivalent as well as reduced fatigue performances have been found in this study. Fatigue of high modulus asphalt mixes with RAP depends highly on the properties of the RAP and its binder and on the proportion of new and old binder.

8.3.1.5 Paper 105 (Hintz et al., 2011)

The paper faces the problem of the lack of characterization of asphalt binder damage resistance to fatigue loading focusing on modification and validation of linear amplitude sweep test applicable for bitumen fatigue specification. Starting from the Linear Amplitude Sweep test (LAS) the authors implement the method and find a correlation between the characterization method and the mixtures tests. Based on the experimental results presented in this paper, the following conclusions can be drawn:

- A simplified method that avoids the use of inter-conversion methods for the calculation of “ α ” parameter needed in the Viscoelastic Continuum Damage (VECD) analysis was successfully implemented. Further Equation 8.1 shows the relation between the number of cycles to failure and strain amplitude for defined failure criteria:

$$N = \frac{f(D_f)^k}{k \left(\pi \frac{I_D}{|G^*|} C_1 C_2 \right)^\alpha} |G^*|^{-\alpha} (\gamma_{\max})^{-2\alpha} \quad (8.1)$$

- Viscoelastic Continuum Damage (VECD) coefficients can be easily obtained by applying a logarithmic transformation to the damage curves. The use of this linearization technique eliminates the need of iterative optimization tools that required initial guesses for estimation of the model coefficients.
- It is recommended to modify the current Linear Amplitude Sweep procedure to include strains ranging from 0,1% to 30% due to the fact that significant material degradation is achieved for strain levels above 20%. Moreover, testing time only increases by 100 seconds with respect to the current procedure.

- VECD analysis of LAS test results yields promising correlations between accelerated binder fatigue life and measured cracking in actual pavements constructed as part of the LTPP program. It is believed that this method could be further improved by investigating a method to separate non-linearity from damage accumulation to more accurately predict fatigue lives. Accounting for non-linearity could possibly delineate results from tests using strain amplitudes ranging from 0,1 % to 20 % and tests including strains exceeding 20%.

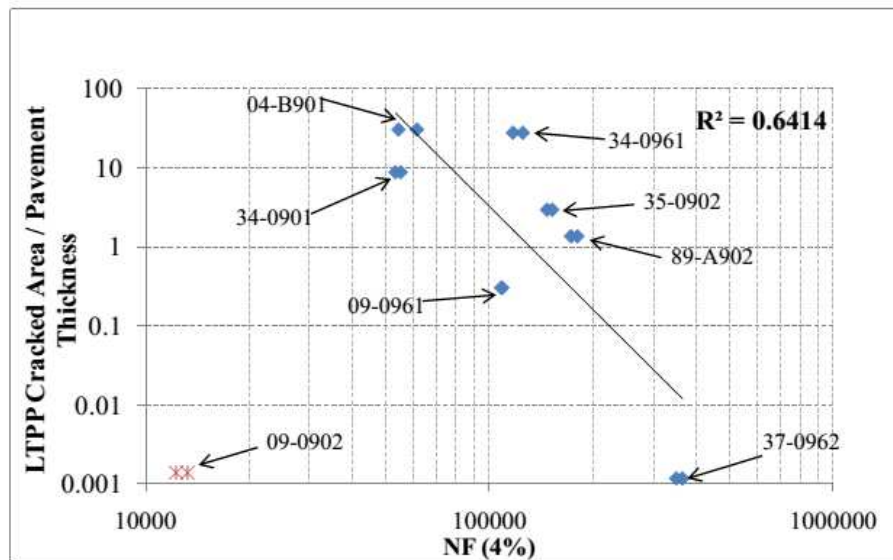


Figure 8-27: Fatigue cracking from LTPP measurements compared to the LAS number of cycles to failure (Paper 105)

8.3.1.6 Paper 125 (Aurangzeb et al., 2012)

This paper focuses on the design and laboratory performance of asphalt mixtures with high amounts of reclaimed asphalt pavement (RAP). The study concluded that including RAP can provide equal or better performance with regards to resistance of asphalt mixtures against moisture susceptibility, rutting, and fatigue failure.

The results of additional 30-40 % RAP to PG 64-22 showed insignificant changes in fatigue performance of the tested mixtures. However the AC mixture with 50 % RAP had an improved resistance against fatigue. The flexural modulus showed approximately 20 % increase with increased RAP content. Examining the effect of PG 58-22 binder on mixture with 30 % RAP showed a significant improvement of fatigue performance while 40 % showed a moderate improvement.

As a conclusion of this paper, it can be said that fatigue life, in general, appeared to improve with the addition of RAP. Single grade bumping proved to be beneficial for fatigue behaviour, while double bumping did not show improvement with respect to single bumping. It is strongly recommended by the authors to perform proper processing and fractionation of the RAP material in order to ensure laboratory production of high quality RAP mixtures.

8.3.1.7 Paper 171 (Mogawer et al., 2012)

The purpose of this study was to evaluate the effect of a bio-modified binder on the performance and workability of asphalt mixtures designed with and without a high RAP content. The four mixtures that were designed and evaluated were: a control mixture incorporating virgin materials, the control mixture incorporating 40 % RAP, the control

mixture incorporating the bio-modified binder and the control mixture incorporating the bio-modified binder and 40 % RAP.

Bio-binder derived from swine manure, in this experiment, was added to the base PG 52-28 asphalt binder at a dosage of 5% by weight of asphalt binder to create the bio-modified binder. Due to the reduced viscosity of the bio-modified binder, the mixture mixing temperature was at 124°C and the compaction temperature was 113°C.

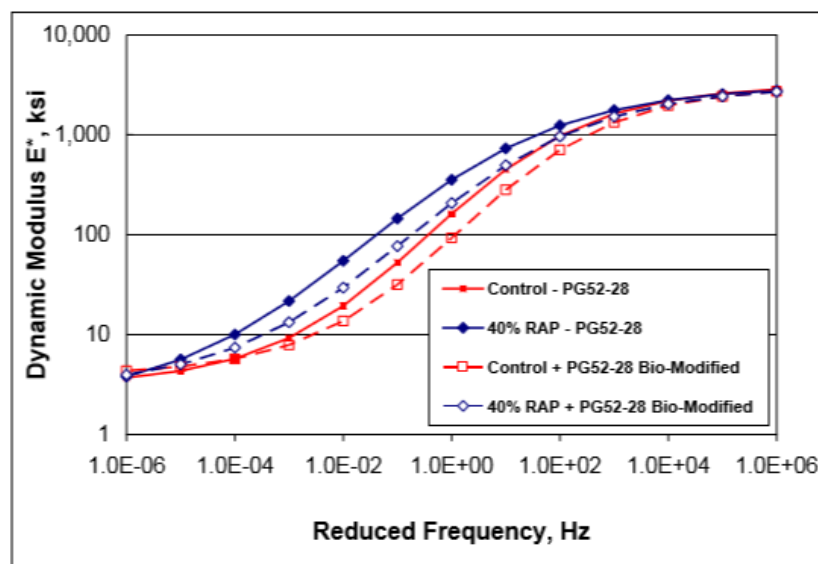


Figure 8-28: Mixture master curve comparison (Paper 171)

A comparison of the mixture master curves is shown in Figure 8-28. The figure showed the expected trend that the incorporation of 40 % RAP to the control mixture increased its stiffness. The introduction of the bio-modified binder decreased the mixture stiffness for both the control and 40 % RAP mixtures as compared to the mixtures fabricated with PG 52-28 binder. This indicated that the bio-modified binder can help reducing the stiffening effects caused by the introduction of high percentages of RAP in the mixture. Moreover, the control mixture with the bio-modified binder master curve indicated that the use of bio-modified binder without the inclusion of RAP should be evaluated on a case by case basis to ensure the mixture does not become too soft, and therefore more susceptible to rutting.

Moreover the Overlay Test (OT) results showed that the addition of 40 % RAP to the control mixture resulted in a mixture that was more susceptible to cracking, as indicated by the smaller amount of OT cycles. This might be related to the increased mixture stiffness due to the incorporation of RAP. The addition of the bio-modified binder to the mixtures showed improvement in the cracking susceptibility of the control and 40 % RAP mixture. As shown with the master curve data, the bio-modified binder reduced the mixture stiffness thereby increasing the cracking resistance of the mixtures. Overall, the use of the bio-modified binder improved the cracking resistance of the 40 % RAP mixtures.

8.3.1.8 Paper 175 (Clopotel *et al.*, 2012)

The importance of binder performance on the mixture response to accelerated fatigue loading and thermal cracking was investigated in this paper focusing on the damage resistance at intermediate and low temperatures. Binder's fatigue performance was measured by means of the Linear Amplitude Sweep test (LAS), while fatigue properties of the mixtures were investigated by performing the EBADE test.

The EBADE test, developed at the Technical University of Catalonia-Spain, measures the fatigue damage resistance of asphalt mixtures that may or may not be subjected to thermal stresses. The test applies a number of tension-compression load cycles to a prismatic specimen at different strain levels. The specimen has two notches in the central area to induce failure and it can be prepared either from the Gyrotory compactor or Marshall samples. The test starts at strain of 2.5×10^{-5} and after 5000 cycles the strain is increased in 2.5×10^{-5} increments until failure. The tests were performed at 20 °C and 5 °C.

Normalized stress vs. strain response of the binders and mixtures to accelerated fatigue loading is very similar (Figure 8-29). The stresses and strains were normalized by their respective maximum values. Significant reduction in the stress happened at about the same normalized strain in the binder and mixture. It can be seen that generally mixtures have remaining strength after reaching peak stress probably due to the aggregate structure.

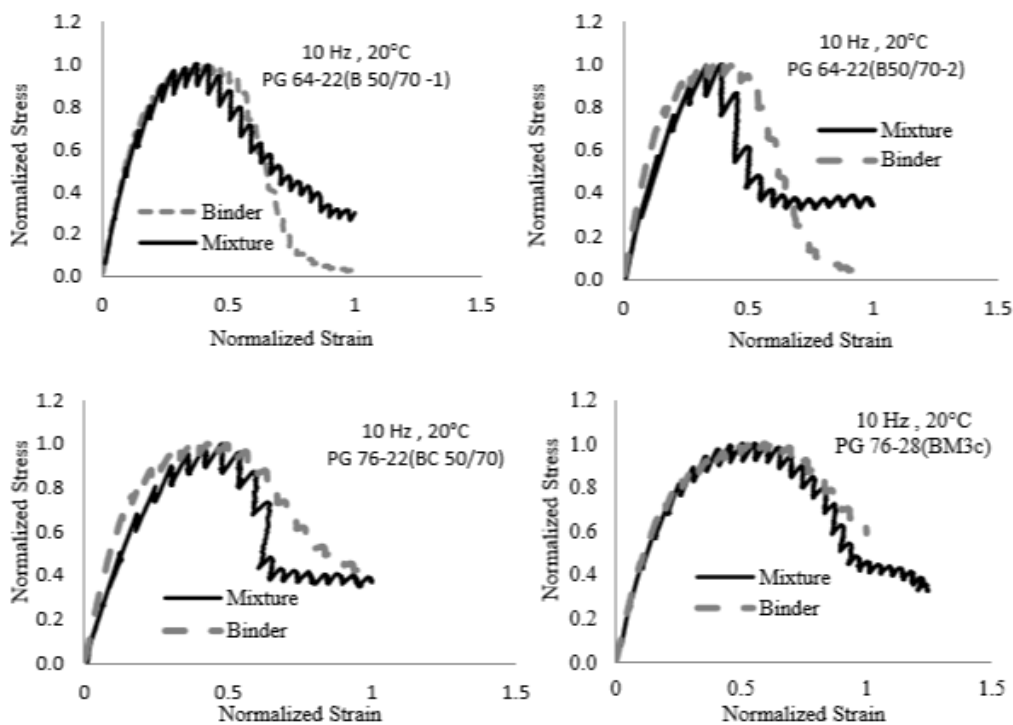


Figure 8-29: Mixture (EBADE) and binder (LAS) normalized stress-strain response to accelerated fatigue (Paper 175)

One may observe in Figure 8-30 that the mixture with polymer modified binder has the best fatigue performance among the tested mixtures.

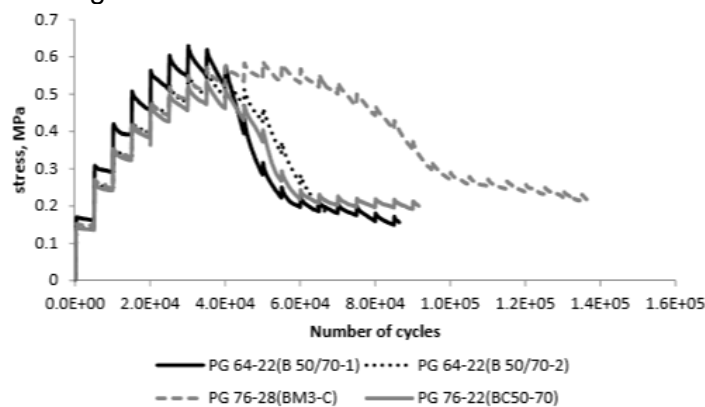


Figure 8-30: Mixture fatigue from EBADE testing at 20°C and 10 Hz (Paper 175)

8.3.1.9 Paper 545 (Jones et al., 2010)

In this study fatigue test was done according to AASHTO TP8-94 using 4PB-PR test. 10 Hz at 20 °C were used for the strain control test. Beam dimensions were 50x63x380 mm. As fatigue criterion the decrease of stiffness to 50 % of initial value was selected. Three strain levels were selected 400×10^{-6} , 600×10^{-6} and 800×10^{-6} . As expected the increase of the binder content in the mixture increases the fatigue resistance. According to the authors the binder content can be defined as a function of the expected traffic. If compared to typical mix with asphalt rubber, the results are comparable (see Table 8-1).

Table 8-7: Coefficients of the fatigue laws

Binder content (%)	a	b	R ²	N ₁₀₀	ε ₆
8,5	9,764E+19	5,419	0,966	1,42E+09	382
9,0	7,246E+14	3,574	0,865	5,16E+07	302
9,5	3,834E+22	6,163	0,859	1,81E+10	491
10,0	1,653E+22	5,940	0,895	2,18E+10	537
10,5	2,130E+19	4,941	0,998	2,79E+09	498

8.3.1.10 Paper 542 (Yang et al., 2010)

Thirteen asphalt beams were tested for fatigue (flexural) at constant strain mode. The study highlights that different empirical fatigue models have different fatigue lives. Densely graded HMA, namely asphalt concrete (AC) 14 using bitumen 60/70, was tested.

Fatigue testing was carried out by a flexural test using a four point loading scheme. Testing was carried out in a controlled temperature cabinet at a surrounding temperature of 20 °C and with a haversine loading pulse (frequency of 10 Hz). Tests were conducted using a controlled strain mode. Five different constant strain levels were applied ranging from 300 micro strains to 600 micro strains. Fatigue failure was defined as a 50 percent reduction in the initial flexural stiffness of each beam. The initial stiffness was determined at the end of the fiftieth loading cycle.

Figure 8-30, shows the relationship between tensile strain level and fatigue life for three different fatigue models (Belgian, TRRL, and Shell) and the measured laboratory fatigue data for AC14 B60/70 HMA. It is clear that each of these models has a different fatigue life prediction and they all under predict the laboratory fatigue life of the tested AC14 B60/70 HMA. Furthermore, the figure shows that the fatigue life of this HMA is considerably greater than what the Shell fatigue transfer function predicts. Table 8-8, gives the average number of times that each model in Figure 8-30 underestimates the fatigue life of the tested mix.

Table 8-8: The number of times each fatigue model underestimates the fatigue life of the AC14 B60/70 HMA

Fatigue Model	Underestimation
Belgian Road Research Centre Model (BRRC)	716.8
Shell fatigue transfer function (SFTF)	5.5
Transport Road and Research Laboratory (TRRL)	6.6

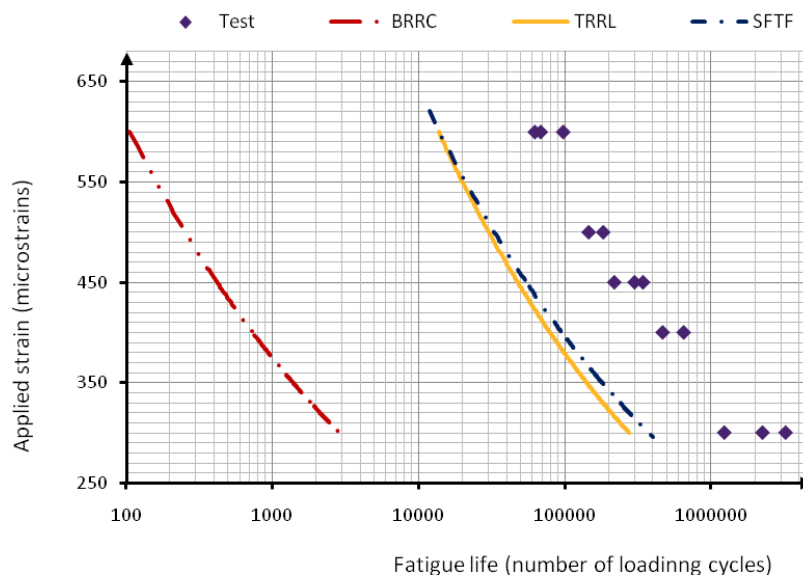


Figure 8-31: Comparison of the different fatigue models, developed under similar conditions against a typical New Zealand roading mix

8.3.1.11 Paper 537 (Kumar and Anand, 2010)

This paper presents the evaluation of the k_1 and k_2 relationship for mixtures based on the results of 53 different asphalt mixtures composed by four different types of aggregate gradations. The results of fatigue tests are expressed in terms of the number of cycles for the tensile strain level applied. Two constants, k_1 and k_2 (Equation 8-2), obtained from a statistical analysis, are involved in this relationship. These constants correspond to the interception and slope of the fatigue line in the log-log scale.

$$N = k_1 \cdot x \quad (8.2)$$

The mixtures for binders and base layers use conventional bitumen, whereas the mixtures for wearing courses use both conventional and modified binders. The binder of asphalt rubber mixtures include some with a low or high content of crumb rubber and various sources of crumb rubber and bitumen. The binder content is identical in each group of mixes.

This study was carried out by analyzing asphalt mixtures tested through four-point bending tests at a temperature of 20 °C and a frequency of 10 Hz. Each mixture was tested using the AASHTO T321-03. The analysis of the results from Table 8-6 allows concluding that the correlation coefficients for all mixtures are extremely high, proving the best fit obtained for the fatigue models. It can be also observed that the mixtures for a specific layer present fatigue behaviors expressed by the different values of the N_{100} and ϵ_6 . The only parameter that seems to have a relatively constancy is the slope of the fatigue model (k_2).

Bearing in mind the form of the relationship between k_1 and k_2 proposed by Pell, Figure 8-30 presents the relationship between k_1 and k_2 for the studied mixtures. The analysis of this figure allows verifying an excellent relationship between k_1 and k_2 for all mixtures.

In spite of the excellent correlation between k_1 and k_2 for all mixtures, which indicates that only one parameter is necessary to characterize the fatigue of asphalt mixtures, the calculation of k_2 using the laboratory fatigue results for the highest strain level (800 microstrain) leads to a set of values that does not represent the fatigue parameters of the asphalt mixtures, as it can be observed in Figure 8-30.

Table 8-9: Fatigue test results

Layer	Mixture	Intercept (k_1)	Slope (k_2)	Correlation coefficient (R^2)	N_{100}	ϵ_6
Wearing course	Mix 01	1,591E+17	4,430	0,984	2,2E+08	338
	Mix 02	2,576E+18	4,762	0,983	7,7E+08	404
	Mix 03	4,784E+17	4,927	0,994	6,7E+07	235
Binder course	Mix 04	8,371E+18	5,021	0,990	7,6E+08	375
	Mix 05	1,591E+17	4,430	0,984	2,2E+08	338
	Mix 06	2,076E+17	4,468	1,000	2,4E+08	341
	Mix 07	5,050E+18	4,907	0,972	7,8E+08	388
	Mix 08	7,837E+16	4,314	0,997	1,8E+08	335
	Mix 09	2,576E+18	4,762	0,983	7,7E+08	404
	Mix 10	6,213E+20	5,604	0,983	3,9E+09	437
	Mix 11	1,563E+19	5,399	0,995	2,5E+08	278
	Mix 12	1,410E+15	4,067	0,976	1,0E+07	178
	Base course	Mix 13	7,977E+17	4,717	0,980	2,9E+08
Mix 14		4,628E+16	4,316	0,960	1,1E+08	296
Mix 15		1,419E+16	4,210	0,996	5,4E+07	258
Mix 16		2,823E+17	4,728	0,979	9,9E+07	264
Mix 17		1,074E+13	3,311	0,968	2,6E+06	133
Mix 18		2,353E+15	4,121	0,977	1,3E+07	188
Mix 19		4,297E+16	4,510	0,993	4,1E+07	228
Mix 20		7,865E+18	5,140	0,995	4,1E+08	323
Mix 21		2,060E+16	4,268	0,959	6,0E+07	261
Mix 22		1,103E+15	3,948	0,954	1,4E+07	195
Mix 23		5,833E+13	3,552	0,949	4,6E+06	154
Mix 24		3,785E+13	3,431	0,990	5,2E+06	162
Mix 25		1,078E+14	3,584	0,986	7,3E+06	174
Mix 26		6,720E+17	4,714	0,968	2,5E+08	323
Mix 27		2,228E+15	4,146	0,984	1,1E+07	180
Mix 28		7,772E+13	3,652	0,992	3,9E+06	145
Base with high Stiffness modulus (10/20 penetration bitumen)	Mix 29	1,113E+23	6,452	0,995	1,4E+10	439
	Mix 30	8,474E+14	3,873	0,997	1,5E+07	202
	Mix 31	3,402E+15	3,975	0,995	3,8E+07	250
	Mix 32	4,511E+20	5,711	0,968	1,7E+09	368
	Mix 33	1,437E+21	5,866	0,993	2,7E+09	384
	Mix 34	7,538E+16	4,452	0,991	9,4E+07	277
Asphalt rubber mixtures	Mix 35	5,361E+15	4,250	0,971	1,7E+07	195
	Mix 36	1,857E+16	4,322	0,973	4,2E+07	237
	Mix 37	1,588E+14	3,592	0,951	1,0E+07	192
	Mix 38	5,305E+11	2,675	0,987	2,4E+06	138
	Mix 39	4,966E+13	3,315	0,977	1,2E+07	210
	Mix 40	4,470E+10	2,275	0,985	1,3E+06	111
	Mix 41	8,704E+13	3,582	0,946	6,0E+06	165
	Mix 42	3,614E+12	2,815	0,979	8,5E+06	214
	Mix 43	6,406E+14	3,567	0,991	4,7E+07	294
	Mix 44	9,747E+10	2,433	0,904	1,3E+06	112
	Mix 45	1,156E+17	4,602	0,988	7,2E+07	253
	Mix 46	3,147E+15	4,086	0,973	2,1E+07	211
	Mix 47	9,878E+14	3,783	0,953	2,7E+07	239
	Mix 48	1,882E+17	4,537	0,974	1,6E+08	305
	Mix 49	1,392E+17	4,564	0,990	1,0E+08	276
	Mix 50	1,330E+15	3,933	0,931	1,8E+07	209
	Mix 51	4,755E+17	4,644	0,984	2,5E+08	327
	Mix 52	2,355E+14	3,652	0,901	1,2E+07	196
	Mix 53	2,279E+16	4,285	0,982	6,1E+07	261

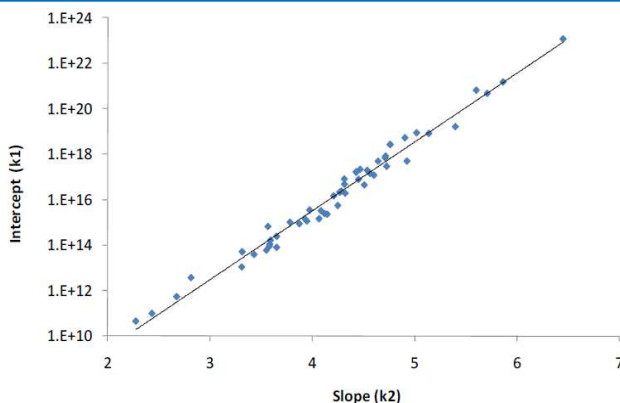


Figure 8-32: Relationship between k_1 and k_2 for all tested mixtures

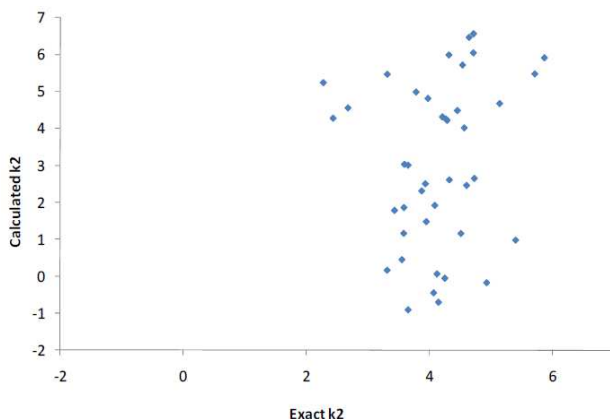


Figure 8-33: Relationship between real k_2 coefficient and the one calculated using the fatigue tests performed at 800 microstrain

The precision of this method continues to be inaccurate even when the results of low strain levels are used, such as 100 microstrain, for which the k_2 calculated using the laboratory results does not represent the exact value, as demonstrated in Figure 8-30. In this case the difference between the exact value of k_2 and the calculated one continues to be very large which produce significant differences in terms of fatigue life when this value of k_2 is used. Furthermore, the use of a strain level of 100 microstrain is not suitable to predict the fatigue life because the fatigue test performed at this strain level lasts longer. The best method to estimate the fatigue life of asphalt mixtures is to perform fatigue tests and to extrapolate the fatigue life for in service strain levels such as 100 microstrain.

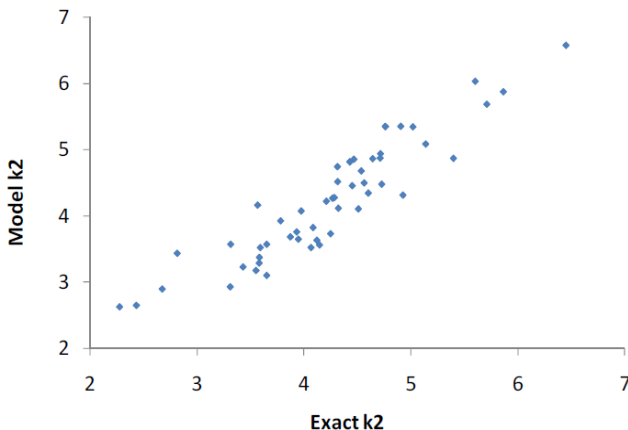


Figure 8-34: Relationship between real k_2 coefficient and the one calculated using the fatigue tests performed at 100 microstrain

The analysis performed in terms of fatigue life produces similar results as the ones obtained in the k_2 comparison. The fatigue life obtained by the k_2 calculated using fatigue results (N , ϵ) for a high strain level, i.e, 800 microstrain, cannot be compared to the exact fatigue obtained using all fatigue tests results, as it can be observed in Figure 8-30. The predicted fatigue life for a 100 microstrain is much greater than the exact one.

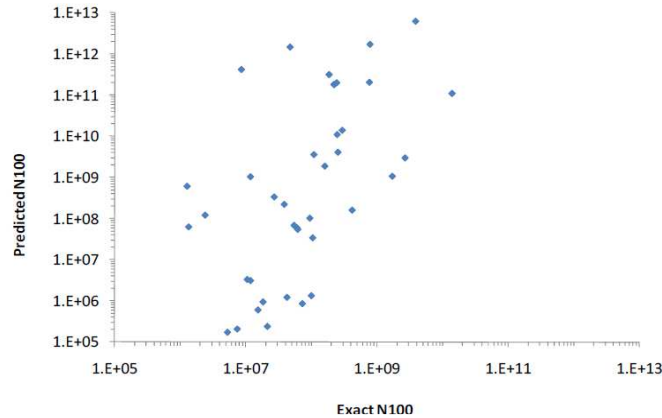


Figure 8-35: Fatigue life at 100 microstrain calculated using k_2 coefficient from fatigue tests at 800 microstrain

An identical analysis using the k_2 coefficient obtained with fatigue tests performed at 400 microstrain is presented in Figure 8-30. In this case the fatigue life for a 100 microstrain strain level also presents a large difference for the exact fatigue life that does not allow using fatigue tests performed at 400 microstrain to predict the fatigue life at 100 microstrain. However, the use of 400 microstrain in comparison to the 800 microstrain reduces significantly the different between the predicted and the exact fatigue life.

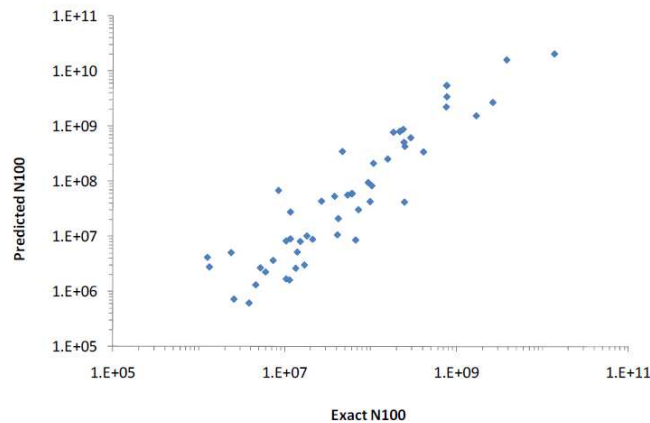


Figure 8-36: Fatigue life at 100 microstrain calculated using k_2 coefficient from fatigue tests at 400 microstrain

The analysis of the fatigue life using the k_2 coefficient obtained from fatigue tests at 200 microstrain produces a fatigue life which is identical to that obtained in the fatigue tests, as it can be observed in Figure 8-30.

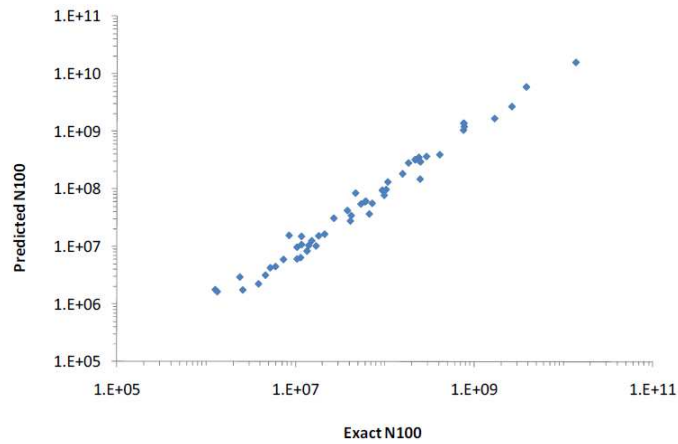


Figure 8-37: Fatigue life at 100 microstrain calculated using k_2 coefficient from fatigue tests at 200 microstrain

This approach can be used to predict fatigue life for other strain levels such as 200 microstrain by using the fatigue results obtained at 400 microstrain (Figure 8-30). In this case, the approach produces fatigue results which follow those obtained by the exact values and the results for a low strain obtained from the fatigue medium level (400 microstrain).

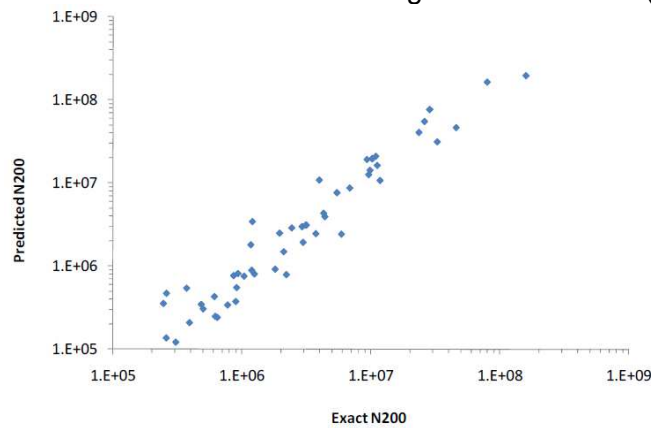


Figure 8-38: Fatigue life at 200 microstrain calculated using k_2 coefficient from fatigue tests at 400 microstrain

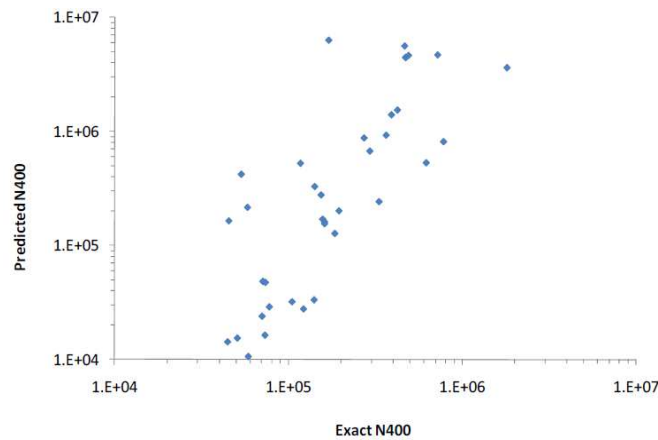


Figure 8-39: Fatigue life at 400 microstrain calculated using k_2 coefficient from fatigue tests at 800 microstrain

The application of the k_2 obtained from fatigue tests performed at high strain levels (800 microstrain) cannot be used to estimate the fatigue life at medium strain levels (400 microstrain), as it can be observed in Figure 8-30.

However, this approach may be used to estimate the fatigue life at lower strain levels using higher strain levels, mainly to estimate the fatigue life for 100 and 200 microstrain using the k_2 obtained for fatigue tests performed respectively at 200 and 400 microstrain.

Relationship between k_1 and k_2 suggests that it can be used to predict the fatigue life of asphalt mixtures due to the good correlation between k_1 and k_2 . The model can be used to produce fatigue testing with only one strain level, once there is only one unknown parameter in the fatigue law (k_1).

Nevertheless, the use of the relationship between k_1 and k_2 for high strain levels does not produce exact values for the in-service fatigue life, such as 100 microstrain. The only valid application of that relationship appears when the k_2 coefficient is calculated for low strain levels around 200 microstrain that do not reduce considerably the testing time.

8.3.1.12 Paper 511 (Mollenhauer *et al.*, 2011)

In this study five different deliveries of bitumen 70/100 at 4 different asphalt mixing plants were anonymously collected and its functional properties were tested to evaluate the overall performance. The used laboratory tests show that especially the fatigue life of the tested bitumen samples vary significantly. Correlations with functional asphalt characteristics indicate that this has influence on the performance of asphalt concrete in the field.

Bitumen fatigue determination was done by means of DSR on the basis of the RILEM test protocol in triplicate at 10°C, 10 Hz and a strain level of 1%, after RTFOT aging. This strain level was chosen because of the test duration of approximately 24 hours, giving the best possibility of scientific understanding. The average curve ($n=3$) of the fatigue data is displayed in Figure 8-30 for each bitumen sample.

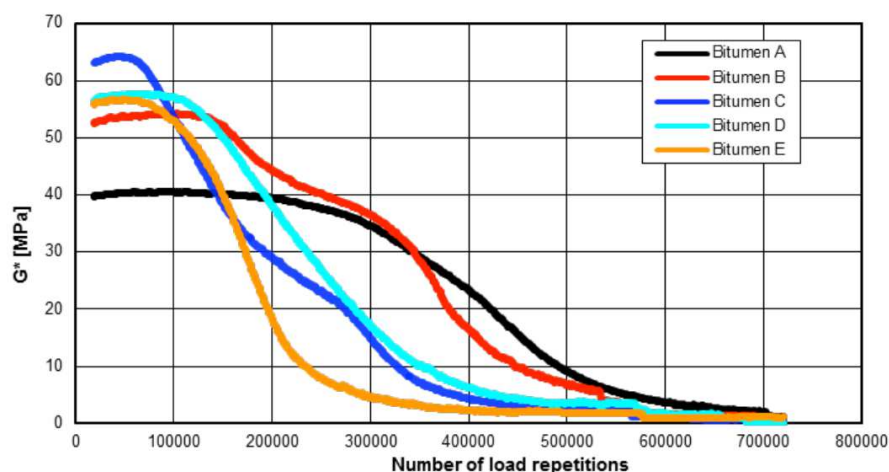


Figure 8-40: Average ($n=3$) fatigue curves at 10 °C and a frequency of 10 Hz

According to RILEM, the fatigue life can be defined in different ways. One definition is the number of load repetitions until halving of the stiffness. Another method is based on dissipated energy ratio (DER). The fatigue life with the latter method can be obtained from the curve in which the number of load repetitions (N) times G^* is plotted against N . The fatigue life is at the maximum of $N \times G^*$ (Figure 8-30).

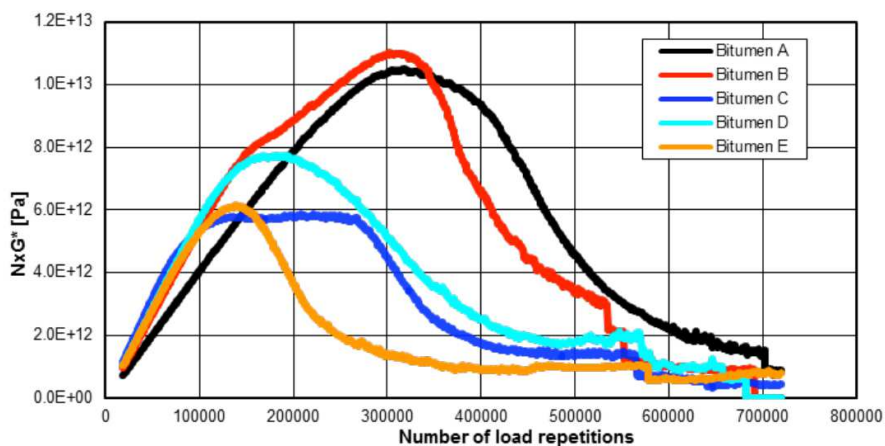


Figure 8-41: Average (n=3) dissipated energy ratio of bitumen samples

The results of both methods of defining fatigue life are displayed in Table 8-10. In this table $N_{50\%}$ is the number of load repetitions until halving of G^* and N_{DERmax} the number of load repetitions until the maximum of $N \times G^*$. Due to the strange curve of bitumen sample C, here the centre of the flat part has been used.

Table 8-10: Fatigue parameters (average lifetimes) tested bitumen samples

Bitumen sample	$N_{50\%}$	N_{DERmax}
A	427 000	319 000
B	364 000	301 000
C	191 000	195 000
D	248 000	184 000
E	179 000	139 000
Average value	281 800	227 600
Coefficient of variation	38,8 %	34,4 %

From the results it can be seen that bitumen samples A and B clearly show better fatigue properties than the other bitumen samples. From the obtained results, it seems as if there is some correlation with the penetration of the bitumen samples as shown in Figure 8-30. However, additional test data of additional suppliers of bitumen 70/100 from work commissioned by an asphalt mix production plant leads to almost no relationship ($R^2=0,36$).

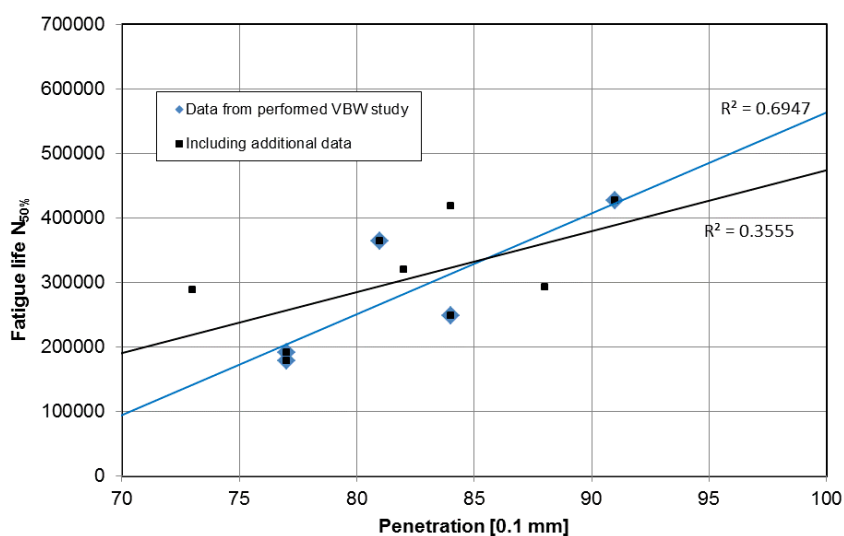


Figure 8-42: Fatigue life bitumen against penetration bitumen

The conventional properties of the tested bitumen samples appear to show little variation (between different suppliers and deliveries). Based on these properties, it would be expected that these bitumen samples will behave similar in an asphalt mixture. However, the functional properties of the tested bitumen samples show some important differences.

Research commissioned by the Transportation Research Board (TRB) in the USA shows a good correlation between the fatigue life of bitumen and an asphalt mixture. In the TRB study this relationship was found to be:

$$N_{50\%,asphalt} = 0,20111 \cdot M_{50\%,bitumen} + 10620 \quad (8.3)$$

Using this relationship the fatigue parameters were calculated for asphalt concrete. The results are shown in Table 8-11. From these results it can be seen that bitumen sample A and B give the best results. Asphalt fatigue tests with these bitumen samples will show a better fatigue curve (the curve moves to the right), resulting in a better fatigue strain level (ϵ_6) in 4-point bending tests according to European standard EN 12967-24.

Table 8-11: Calculated fatigue parameters asphalt at 10 Hz and 10 °C (indicative)

Bitumen sample	N _{50%, bitumen}	N _{50%, asphalt}
A	427 000	96 494
B	364 000	83 824
C	191 000	49 032
D	248 000	60 496
E	179 000	46 619
Average	281 800	67 293
Coefficient of variation	38,8%	32,7%

Additionally performed 4-points bending tests on a specific mixture give an indication on the difference in ϵ_6 . The 4-point bending tests were carried out with bitumen obtained from the supplier of sample A and the supplier of sample C and D. The mixture was an AC 11 surf 70/100 without recycled material. The test conditions were 30 Hz at 20 °C according to the Dutch standard. The results are summarized in Figure 8-30.

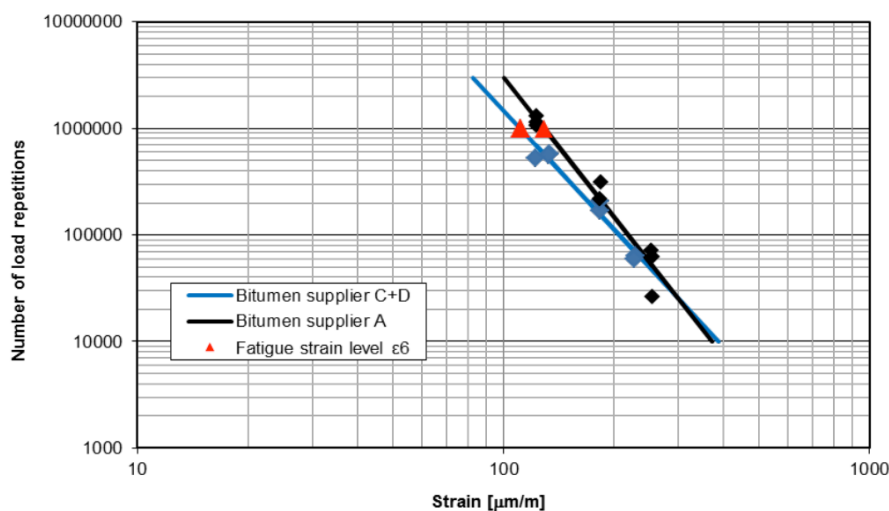


Figure 8-43: Results fatigue tests asphalt for different bitumen suppliers

Despite the limited data set, the graphs clearly show the difference between 2 different suppliers of bitumen. The parameter ϵ_6 was found to be 111 $\mu\text{m}/\text{m}$ (bitumen supplier C and D), respectively 129 $\mu\text{m}/\text{m}$ (bitumen supplier A).

8.3.1.13 Paper 453 (Skotnicki and Szydło, 2009)

The influence of the binder content on fatigue life was studied by paper 453 using HMA samples with unmodified and polymer-modified bituminous binders were used. The first group were mixtures type P1, to base layers as the Asphalt concrete with high stiffness modulus, to heavy load traffic. The second type of analyzed materials, were mixtures W1, to base course layers of road pavement, also as the Asphalt concrete with high stiffness modulus, to heavy load traffic. In base mixtures bitumen D35/50 was used and in base course mixtures a modified asphalt 30B was employed. To improve connection between the aggregate and the asphalt, an adhesive supplement was used (0,3 %).

Table 8-12: Fatigue durability of HMA type P1 and W1

Sample	HMA	Bitumen content [%]	Microstrain ϵ [$\text{m}/\text{m} \cdot 10^{-6}$]	Initial stiffness modulus E [MPa]	Fatigue life N_f /50 [cycles]	Fatigue damage [%]
5	P1-2	4,7	130	13105	946499	~ 52,0
6				12459	>10 ⁶	28,0
7				13538	979303	~ 56,0
9	P1-3	4,8		11954	>10 ⁶	24,1
14	P1-4	5,0		13072	>10 ⁶	37,4
15				12592	>10 ⁶	20,9
16				13373	>10 ⁶	24,4
17	W1-1	4,2		10591	673551	~52
18	W1-2	4,4		10417	512641	~80
21				10781	>10 ⁶	14,7
22				12006	>10 ⁶	19,1
25	W1-3	4,6		11995	>10 ⁶	6,2
26				13242	>10 ⁶	13,3
37	W1-4	4,6		12926	>10 ⁶	11,5
39				13121	>10 ⁶	10,2
41	W1-5	4,6	13345	>10 ⁶	10,8	
42			13187	>10 ⁶	12,1	

Loading each sample, was carried on up to 50% stiffness modulus decrease, or to the moment of 1 million load cycle. In such case in one million load cycle a fatigue damage was recorded. Tests were stopped when fatigue damage obtain 50%, but from the slope of stiffness modulus changes, it was possible to evaluate theoretical value of fatigue damage in 1 million load cycle.

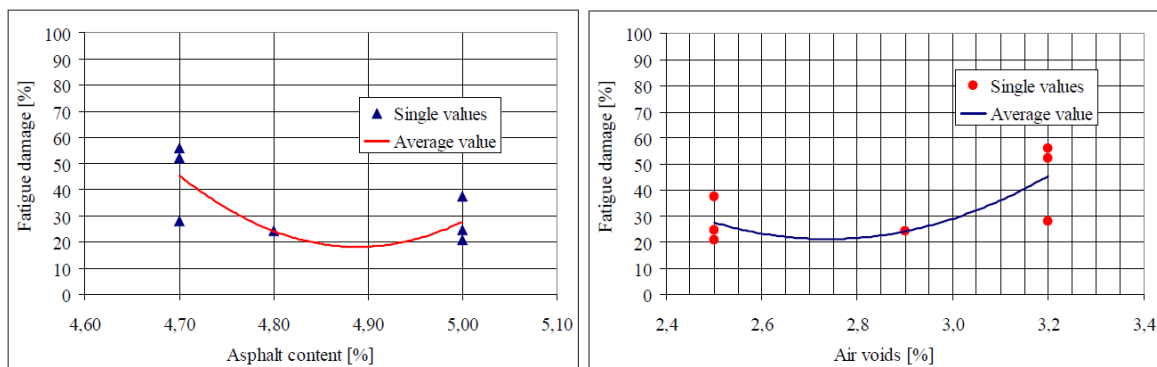


Figure 8-44: Fatigue damage of HMA type P1

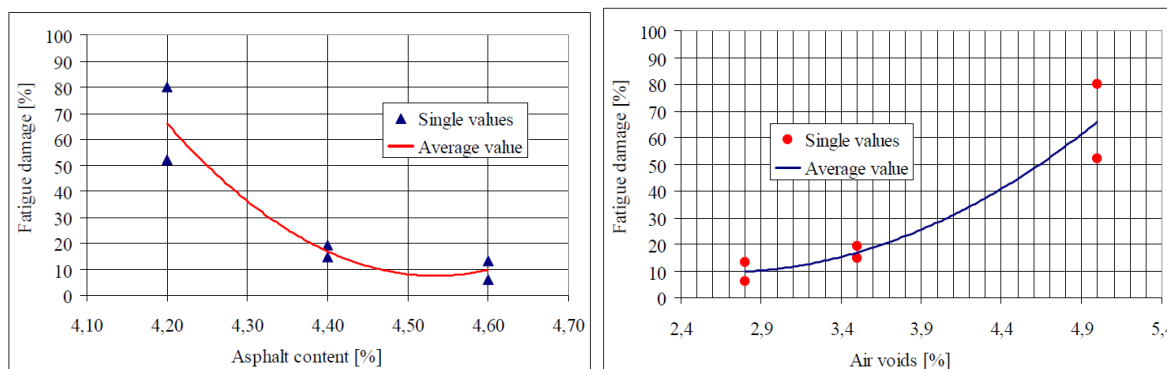


Figure 8-45: Fatigue damage of HMA type W1

An increase of asphalt content only on 0,1% cause forceful increase of fatigue endurance limit, and durability on fatigue and low temperature cracking. At 4,7-4,8 % asphalt content level, the change of fatigue damage value, was about 25 %.

Increasing the asphalt content from 4,2 % to 4,6 %, it is possible to record that fatigue damage fall down from 68 % to only 10 % level. It also can be seen, that the sufficiency fatigue durability, of HMA mixtures with modified binders, is possible to reach, by using about 0,4 % less asphalt, than in HMA with unmodified asphalts. Also the air voids content influence on a fatigue durability of HMA. Slight increase in air voids content causes rapid decrease in fatigue life. Changes in aggregate of HMA mixtures, in good grading field, minimally affecting on the 4PB fatigue durability.

8.3.1.14 Paper 452 (Way et al., 2009)

Another research included SHRP gyratory mixes as well as Marshall design asphalt rubber gap graded (ARAC) and open graded (ARFC) mixes with 15 years of collecting 4PB-PR data and their further analyses.

Table 8-13: 4PBB test results for 1993-1995 projects

Site	Mix Type	Binder Grade	Bind %	Air Voids %	Test Temp °C	k1	k2	Calc. Nf at $\epsilon = 0,0001$
1	SHRP	70-10	4,0	4,0	20	5,56E-17	-6,13	1,84E+08
1	SHRP	70-10	5,0	4,0	20	6,35E-16	-6,04	9,18E+08
1	SHRP H	70-10	4,0	7,4	20	3,48E-11	-4,45	2,13E+07
1	SHRP N	70-10	4,0	10,2	20	1,15E-09	-4,03	1,53E+07
1	SHRP	AC-40	4,2	10,4	20	2,35E-17	-6,13	7,89E+07
2	SHRP	76-10	3,8	7,0	30	4,16E-03	-2,14	1,50E+06
2	SHRP	76-10	4,0	7,0	30	1,95E-04	-2,53	2,46E+06
2	SHRP	76-10	4,3	7,0	30	2,51E-06	-3,07	4,78E+06
2	SHRP	76-10	4,5	7,0	30	9,25E-08	-3,49	8,55E+06
2	SHRP	76-10	4,8	7,0	30	5,47E-10	-4,15	2,18E+07
2	SHRP	76-10	5,2	7,0	30	2,78E-12	-4,80	4,41E+07
2	SHRP	70-10	4,2	5,6	30	5,62E-05	-3,07	1,07E+08
2	SHRP	70-10	4,2	5,6	30	1,06E-04	-3,07	2,02E+08
2	SHRP	70-10	4,2	5,6	30	6,04E-05	-3,07	1,15E+08
2	SHRP	76-16	4,4	5,1	30	6,98E-05	-3,07	1,33E+08
2	SHRP	76-16	4,4	5,1	30	8,55E-05	-3,07	1,63E+08
3	SHRP	70-22	4,3	7,0	15	1,88E-09	-4,25	1,88E+08
3	SHRP	70-22	4,8	7,0	15	6,58E-09	-4,24	6,00E+08
3	SHRP	70-22	5,3	7,0	15	3,62E-07	-3,82	6,90E+08
3	SHRP	70-22	5,3	4,7	15	9,02E-08	-3,82	1,72E+08
3	SHRP	70-22	5,3	4,7	15	6,08E-08	-3,82	1,16E+08
3	SHRP	70-22	5,3	4,7	15	2,52E-08	-3,82	4,81E+07
3	SHRP	70-22	4,8	5,5	15	5,00E-10	-4,24	4,56E+07
3	SHRP	70-22	4,8	5,2	15	9,28E-10	-4,24	8,47E+07

3	SHRP	70-22	4,8	5,2	15	1,43E-09	-4,24	1,31E+08
3	SHRP	70-22	4,7	5,5	15	4,18E-10	-4,24	3,82E+07
3	SHRP	70-22	5,0	5,3	15	2,09E-09	-4,24	1,91E+08
3	SHRP	70-22	5,0	5,3	15	2,56E-09	-4,24	2,34E+08
3	SHRP	70-22	4,9	5,6	15	4,02E-09	-4,24	3,67E+08
3	SHRP	70-22	4,9	5,6	15	5,54E-10	-4,24	5,06E+07
3	SHRP	70-22	4,2	5,7	15	9,09E-10	-4,24	8,29E+07
3	SHRP	70-22	4,2	5,7	15	3,67E-10	-4,24	3,35E+07
3	SHRP	70-22	4,8	5,9	15	2,22E-10	-4,24	2,03E+07
3	SHRP	70-22	4,8	5,9	15	1,06E-09	-4,24	9,73E+07
3	SHRP	70-22	4,2	6,9	15	6,61E-10	-4,24	6,03E+07
3	SHRP	70-22	4,2	6,9	15	1,79E-10	-4,24	1,64E+07
3	SHRP	70-22	4,9	5,7	15	7,81E-10	-4,24	7,13E+07
3	SHRP	70-22	4,9	5,7	15	8,35E-10	-4,24	7,62E+07
3	SHRP	70-22	4,6	6,5	15	1,48E-09	-4,24	1,35E+08
3	SHRP	70-22	4,6	6,5	15	1,11E-09	-4,24	1,02E+08
3	SHRP	70-22	4,7	4,7	15	6,56E-10	-4,24	5,99E+07
3	SHRP	70-22	4,7	4,7	15	1,94E-09	-4,24	1,77E+08
3	SHRP	70-22	4,7	7,3	15	5,30E-10	-4,24	4,84E+07
3	SHRP	70-22	4,6	5,7	15	3,98E-10	-4,24	3,63E+07
3	SHRP	70-22	4,6	6,2	15	9,15E-10	-4,24	8,35E+07
3	SHRP	70-22	4,6	6,2	15	7,46E-10	-4,24	6,81E+07
3	SHRP	70-22	5,1	5,2	15	3,09E-10	-4,24	2,82E+07
3	SHRP	70-22	5,1	5,2	15	2,54E-10	-4,24	2,32E+07
3	SHRP	70-22	5,1	5,2	15	1,06E-09	-4,24	9,69E+07
3	SHRP	70-22	4,6	5,7	15	1,00E-09	-4,24	9,12E+07
3	SHRP	70-22	4,6	5,7	15	4,91E-10	-4,24	4,48E+07
3	SHRP	70-22	4,7	6,4	15	5,87E-10	-4,24	5,36E+07

In reviewing the data in Tables 8-13 and 8-14 the asphalt rubber mixes with higher binder content consistently give a longer fatigue cracking life. As a part of this long term study Consulpav and ASU (Arizona State University) agreed that some degree of comparison between both devices was needed. Comparative results of pertinent 4PBB measurements are shown in Figure 8-30. Although the equipment is made by different manufacturers and samples were transported over the ocean the test results appear reasonably close.

Table 8-14: 4PBB ASU test results

Site	Mix Type	Binder Grade	Bind %	Air Voids %	Test Temp °C	k1	k2	Calc. Nf at $\epsilon = 0,0001$
A	ARFC	58-22	8,8	18,3	4,4	3,00E-14	-5,80	4,76E+09
A	ARFC	58-22	8,8	18,3	21,1	5,00E-15	-6,45	3,16E+11
A	AC	70-10	4,6	7,5	4,4	3,00E-10	-4,29	4,34E+07
A	AC	70-10	4,6	7,6	21,1	3,00E-14	-5,20	1,89E+07
A	AC	70-10	4,6	7,5	37,8	1,00E-10	-4,40	3,98E+07
B	ARFC	58-22	9,3	18,0	4,4	1,00E-17	-6,65	3,98E+09
B	ARFC	58-22	9,3	18,0	21,1	7,00E-12	-5,16	3,06E+09
B	AC	76-16	4,6	7,3	4,4	2,00E-17	-6,24	1,82E+08
B	AC	76-16	4,6	7,5	21,1	3,00E-14	-5,44	1,73E+08
B	AC	76-16	4,6	7,3	37,8	2,01E-10	-4,54	2,90E+08
C	ARAC	58-22	6,8	11,5	4,4	8,00E-20	-7,19	4,60E+09
C	ARAC	58-22	6,8	11,0	21,1	3,00E-08	-3,90	1,19E+08
C	ARAC	58-22	6,8	11,5	37,8	2,00E-07	-4,04	2,89E+09
C	ARFC	58-22	8,8	18,0	4,4	1,00E-13	-5,52	1,20E+09
C	ARFC	58-22	8,8	18,0	21,1	2,00E-07	-3,85	5,02E+08
D	AC	76-16	4,2	7,0	4,4	2,00E-10	-4,17	9,67E+06
D	AC	76-16	4,2	7,0	21,1	1,00E-11	-4,72	7,59E+07
D	AC	76-16	4,2	7,0	37,8	1,00E-10	-4,61	2,75E+08
E	AC	70-22	5,3	7,3	4,4	1,37E-21	-7,20	8,65E+07
E	AC	70-22	5,3	7,2	21,1	1,16E-16	-6,13	3,85E+08
E	AC	70-22	5,3	7,2	37,8	3,73E-14	-5,53	4,92E+08
E	ARFC	58-22	9,5	18,1	4,4	6,73E-20	-7,99	6,14E+12
E	ARFC	58-22	9,5	18,3	21,1	1,75E-29	-10,66	7,64E+13
F	ARAC	58-22	7,8	9,4	4,4	3,97E-13	-5,24	3,62E+08

F	ARAC	58-22	7,8	9,4	21,1	1,56E-14	-6,04	2,25E+10
F	ARAC	58-22	7,8	9,5	37,8	4,82E-15	-6,40	1,92E+11
F	ARFC	58-22	9,0	19,0	4,4	2,84E-13	-5,60	7,14E+09
F	ARFC	58-22	9,0	19,3	21,1	1,18E-09	-4,64	4,29E+09
G	AC-1	64-22	5,4	6,8	4,4	3,08E-16	-5,91	1,34E+08
G	AC-1	64-22	5,4	6,5	21,1	2,62E-11	-4,62	7,91E+07
G	AC-1	64-22	5,4	7,1	37,8	7,59E-09	-4,09	1,74E+08
G	AC-2	76-22TR	5,3	7,5	4,4	2,17E-13	-5,16	9,48E+07
G	AC-2	76-22TR	5,3	7,4	21,1	1,28E-12	-5,21	8,86E+08
G	AC-2	76-22TR	5,3	7,5	37,8	5,04E-11	-5,17	2,41E+10
H	AC	64-22	4,6	6,6	4,4	2,00E-08	-4,01	2,19E+08
H	AC	64-22	4,6	6,4	21,1	1,00E-11	-4,63	3,31E+07
H	AC	64-22	4,6	6,5	37,8	2,00E-17	-6,18	1,05E+08
H	ARAC	58-22	7,0	9,7	4,4	3,00E-14	-5,43	1,57E+08
H	ARAC	58-22	7,0	9,7	21,1	1,00E-14	-5,79	1,45E+09
H	ARAC	58-22	7,0	9,8	37,8	3,00E-14	-5,97	2,28E+10
H	ARFC	58-22	9,4	17,5	4,4	5,00E-10	-4,38	1,66E+08
H	ARFC	58-22	9,4	18,5	21,1	2,00E-06	-3,64	7,26E+08
I	AC	64-22	4,8	7,6	4,4	2,01E-14	-5,40	8,00E+07
I	AC	64-22	4,8	7,6	21,1	1,53E-11	-4,74	1,40E+08
I	AC	64-22	4,8	7,5	37,8	1,88E-07	-3,71	1,30E+08
I	ARAC	58-22	7,3	9,5	4,4	4,45E-17	-6,37	1,34E+09
I	ARAC	58-22	7,3	9,8	21,1	2,29E-16	-6,37	6,92E+09
I	ARAC	58-22	7,3	9,7	37,8	1,62E-10	-4,91	7,07E+09
I	ARFC	58-22	9,3	18,3	4,4	4,09E-17	-6,70	2,58E+10
I	ARFC	58-22	9,3	18,4	21,1	3,05E-19	-8,20	1,92E+14

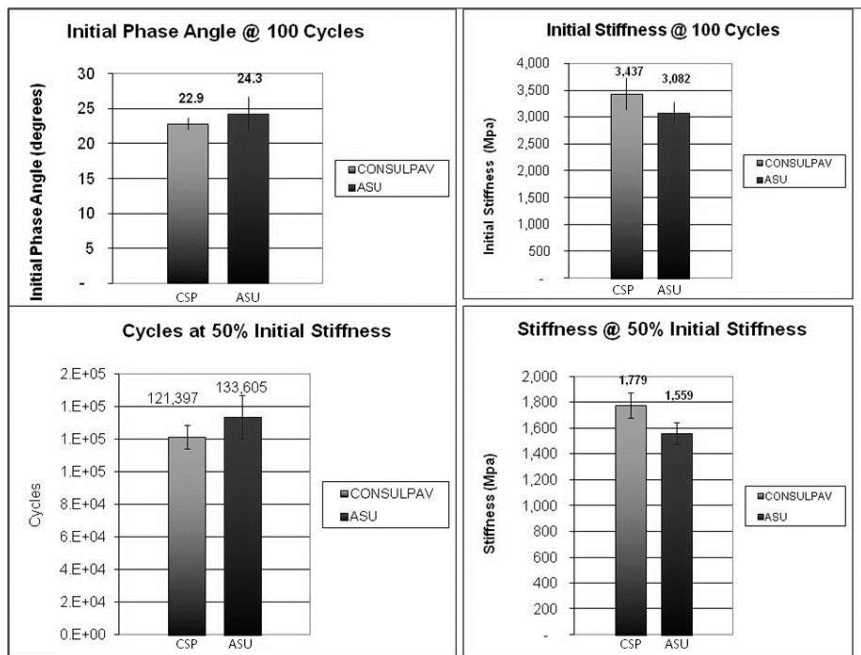


Figure 8-46: 4PBB equipment comparison test results

8.3.1.15 Paper 449 (Johnson et al., 2009)

In another study one mixture gradation and compaction level was used to isolate the relative fatigue performance of three polymer-modified bitumens. This study comparing results from the three binder tests with results from four-point bending of mixtures prepared using the same bitumens. In order to simulate the state of bitumen aging in the mixture specimens, the testing of bitumens was conducted after they were aged in RTFO in accordance with AASHTO T240. The results show that there are no simple correlations, and depending on the loading conditions selected, the ranking of binders could vary by test method.

Table 8-15: Description of bituminous binders

Bitumen PG Grade	Modification Type	Testing Temperature [°C]
64 - 28	Styrene-Butadiene-Styrene Rubber	12,1
58 - 34	Ethylene Ter-polymer	8,6
64 - 34	Ethylene Ter-polymer	6,2

Bitumen time sweep test

The cyclic fatigue testing of the bitumen specimens was performed in strain-control mode at 10 Hz for consistency with the asphalt mixture beam testing. This test is the most direct corollary to the four-point flexural fatigue testing. Results of time sweeps for the three binders are shown in the plots of Figure 8-30 where the complex modulus is shown as a function of number of loading cycles. In this testing the applied strain was kept at 2,5 % strain and at 5 % strain at edge of the parallel plate geometry in the DSR. Based on the dissipated energy ratio, the cycle at which 20 % decrease in the ratio is observed is identified as NP_{20} . The suitability of this test for use in specification is questionable due to the possibility of long testing times. The SBS-modified bitumen shows a substantially higher resistance to fatigue damage than the other two binders. It is also important to note how much increasing applied strain reduces the cycles to failure. The ranking of the three binders does not appear to be affected by the change in strain of testing. Criticality of the results is that although testing is conducted at equal dissipated energy, the cycles to failure are 2 to 7 times different between bitumens depending on type of polymer, PG grade and strain.

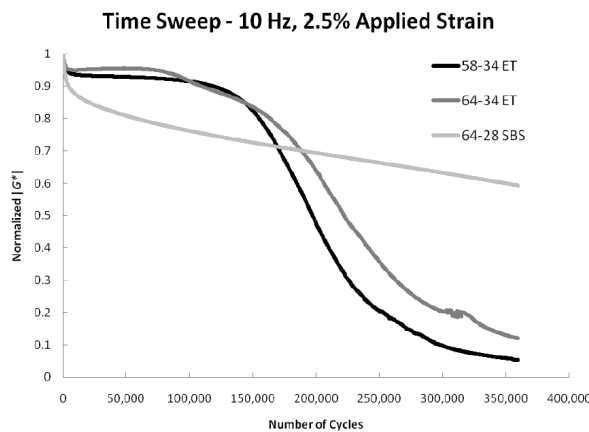


Figure 8-47: Plot of time sweep results for bitumen at 2,5% applied strain

Binder yield energy test (BYET)

Monotonic constant shear rate loading was applied consistent with the procedure described by (Johnson et al. 2009), along with Yield Energy and Strain at Peak Stress being recorded in the same manner (as shown in Figure 8-30).

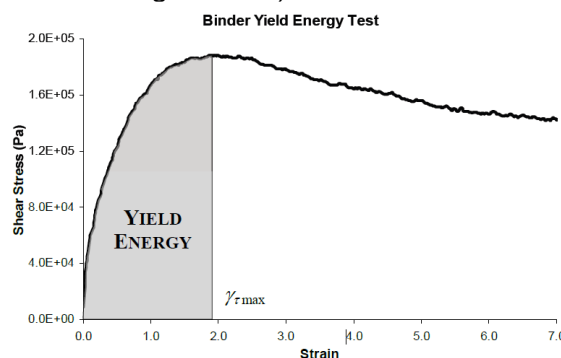


Figure 8-48: Typical BYET results and representation of measured parameters

The BYET provides a novel ability to gain further insight into the mechanical response of polymer modified bitumen. As shown in Figure 8-30, the stress-strain response for the 64-28 SBS material shows a distinct “double-peak” behavior, which is not shown in the bitumens modified with ethylene terpolymer. This trend of response is problematic because it complicates the modeling of the undamaged response using linear viscoelastic (LVE) constitutive equations.

It can be hypothesized that an energy threshold exists, at which point the material loses its ability to resist damage. The ultimate goal of this test is to relate the propensity to absorb applied energy, as denoted by the area under the curve to the maximum value. The data includes the average yield energy, the maximum point of stress-strain curve (EY), and the shear strain at the maximum stress (GTM).

Unlike the time sweep results, the 64-34ET appears to offer the highest yield energy and thus the best resistance to fatigue. However, GTM gives a similar ranking to the time sweep test results; with respect to the SBS modified binder showing the highest strain at failure. Observing the plot in Figure 8-30, it is apparent that the response beyond the maximum peak varies significantly between the binders and, depending on the strain level selected, the binders show different rankings of the stress levels. In fact, comparing Figure 8-30 with Figure 8-30, one can observe some similarity in that the SBS modified binder is showing a higher resistance to cyclic loading in Figure 8-30 at large number of cycles and also showing higher stress at higher strain in Figure 8-30. This similarity may indicate that interpretation of the BYET test should consider the behavior beyond the peak stress, and perhaps the post peak behavior is better related to mixture fatigue under cyclic loading.

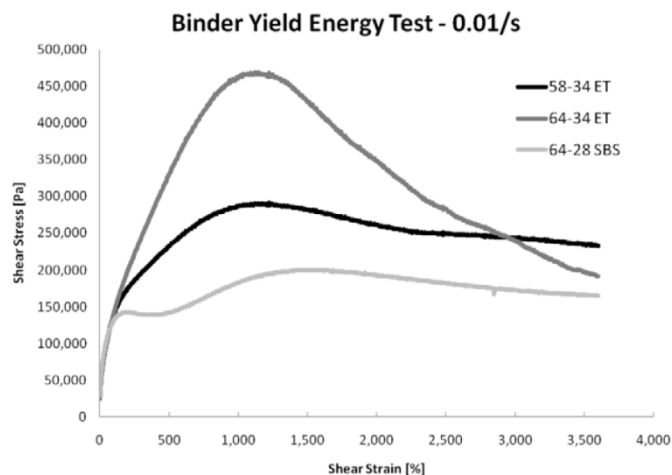


Figure 8-49: BYET results at 1% shear strain per second

Strain sweep test

Cyclic amplitude sweep testing can be thought of as an accelerated fatigue test where the applied loading amplitude is incrementally increased until material failure. A strain-controlled version of the test has been under investigation. All tests were run at 10 Hz frequency, with an initial 100 cycles applied at 0,1 % strain to determine undamaged linear viscoelastic properties. Each subsequent load step consisted of 100 cycles at a rate of increase of 1% applied strain per step for 20 steps, beginning at 1% and ending at 20 % applied strain. The test procedure takes significantly less time than other methods. However, definition of the most appropriate failure criterion for this methodology is not readily apparent.

The stress versus strain plots are shown in Figure 8-30, but determination of a failure criterion remains challenging for this type of test. Recent work at UW-Madison has shown that VECD analysis of time sweep data can successfully indicate the time sweep performance of a given material at different applied strain levels (Wen and Bahia 2009). The benefit of this approach is that it is theoretically independent of the loading conditions, so the characteristic damage curve can be generated from testing at any applied load level.

The failure criterion was selected as the amount of damage at a predetermined percentage of initial undamaged LVE complex modulus. Specifically, the VECD damage parameter D at 25% of the initial complex shear modulus was chosen to ensure a substantial level of damage had occurred in the specimens. The basic idea behind this criterion is that a good-performing material will require higher levels of damage before it reaches 25 % of its initial modulus.

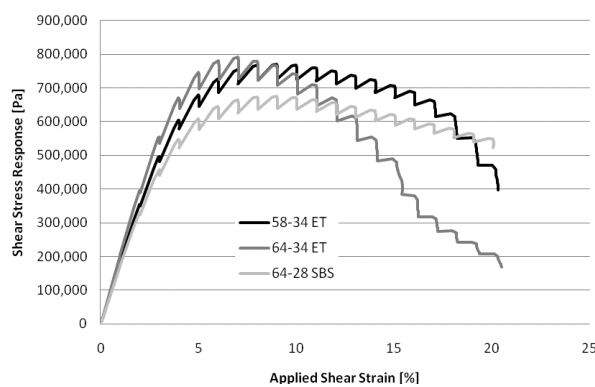


Figure 8-50: Stress versus applied strain from strain sweep test

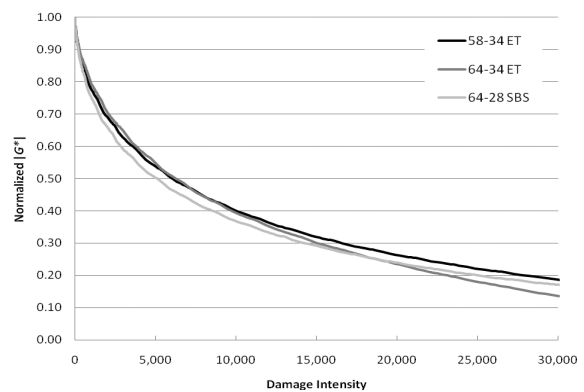


Figure 8-51: Normalized modulus versus damage intensity using VECD analysis for strain sweep

The results show all three binders to have very similar trends in the strain sweep and in the VECD analysis results.

Table 8-16: Bitumen fatigue results

Bitumen	Time sweep test		Yield energy test		Strain sweep test
	N_{P20} - 2.5% strain	N_{P20} - 5.0% strain	Average YE, Pa	Average GTM, %	Damage Parameter at 25% $[G']$
64 – 28 SBS	360 000*	123 100	2 617 000	1 559	18 808
58 – 34 ET	163 500	15 000	2 568 636	1 184	21 654
64 – 34 ET	175 800	32 400	4 024 517	1 093	18 836

*Note: At 2,5 % applied strain, it had reached only a 17.6 % reduction in DER after the preset limit of 10 hrs of testing.

Asphalt mixture flexural beam fatigue test

In order to meet the criteria of both standards, specimens were tested until a reduction of 65% from the initial stiffness was measured, with initial stiffness defined as the stiffness of the specimen at the 50th cycle of loading. Each test was conducted to a minimum of 10 000 loading cycles under strain-control with amplitude of 500 micro-strain.

The terminating criterion of 65 % reduction from initial stiffness allows for data collection beyond the defined failure point. The failure point for this set of testing is defined as the peak value achieved on a graphical representation of Normalized Complex Modulus x Cycles versus Cycles, with the base of normalization as the 50th cycle stiffness value.

Table 8-17: 4PB fatigue results

Bitumen used in mixture	N _f (AASHTO T321)	N _f (50% Stiffness reduction)	N _f (35% Stiffness reduction)
64 – 28 SBS	255 000	177 500	2 500
58 – 34 ET	≥ 5 000 000	N/A	207 500
64 – 34 ET	660 000	660 000	35 000

BYET versus mixture beam fatigue

As shown in Figure 8-30, initial observation shows little relation between the parameters derived from the BYET and beam fatigue cycles to failure. However, upon further investigation into data presented in Figure 8-30, it appears that material behavior after peak stress may play an important role. At roughly 1 000 % strain, there is a clear ranking with the 64-34 ET giving the highest strength. However, as the deformation increases, the ability of that material to withstand additional stress decreases more rapidly in comparison to the other two bitumens. At higher strain levels approaching the end of the test at 3 600 % strain, the ranking of the binders based on the BYET results matches that from the beam fatigue results. This observation is consistent with the findings shown by Jimenez et al. (2003) which stipulates that post peak behavior could be a better indicator of fatigue behavior.

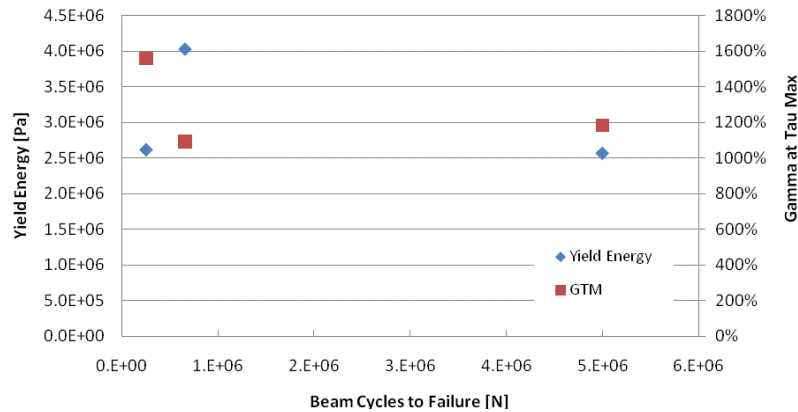


Figure 8-52: Plot of BYET results versus beam fatigue N_f values

Binder Time Sweep versus Mixture Beam Fatigue

Initially, the time sweep data did not appear to have any relation to beam fatigue results. As shown in Figure 8-30, the bitumens appear to follow the same trends at 2,5 % and 5,0 % loading, with neither strain level having an improved relationship with the mixture data.

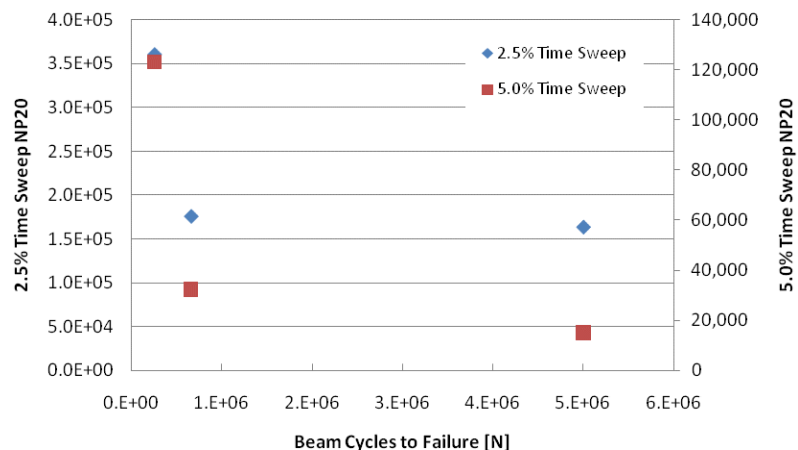


Figure 8-53: Comparison of time sweep N_{P20} versus beam fatigue N_f values

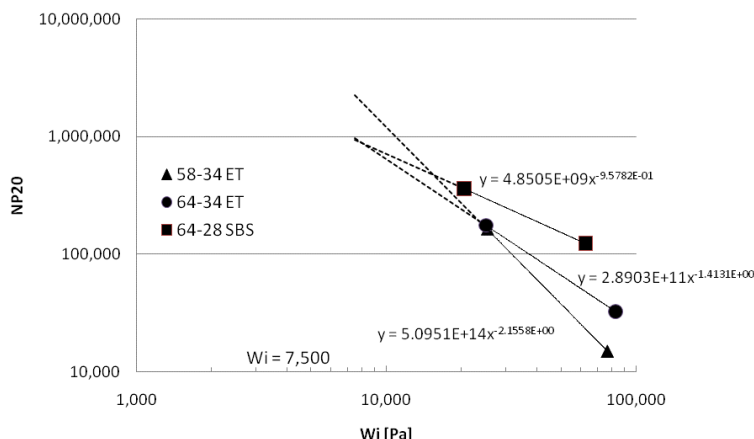


Figure 8-54: Initial dissipated energy (Wi) versus number of cycles to failure

By setting the input Wi value at 7 500 Pa (approximately 1,4-1,5 % applied strain), a favorable correlation between binder time sweep and mixture beam fatigue can be achieved, as shown in Table 8-18 (ranking shown in parentheses). However, when the initial Wi is increased by an order of magnitude to 75 000 Pa, one can see how the ranking changes and results in mismatch with mixture results.

Table 8-18: Predicted Time Sweep NP20 vs. Beam Fatigue Nf (A,B,C = Ranking)

Bitumen	Predicted Time Sweep NP20 at Wi = 7 500 Pa	Beam Fatigue Nf	Predicted Time Sweep NP20 at Wi = 75 000 Pa
64-28 SBS	942 265 (C)	32 499 (C)	103 837 (A)
58-34 ET	2 255 774 (A)	207 499 (A)	15 758 (C)
64-34 ET	966 260 (B)	34 999 (B)	37 324 (B)

Strain Sweep versus Beam Fatigue

As can be seen in Figure 8-30, the binders show very similar damage trends based on the VECD analysis. However using a larger scale at higher damage intensity levels, there appears to be some variations. In fact by selecting 25 % of the initial undamaged modulus as the failure criterion, there is a consistent ranking with beam fatigue results, as shown in Figure 8-30.

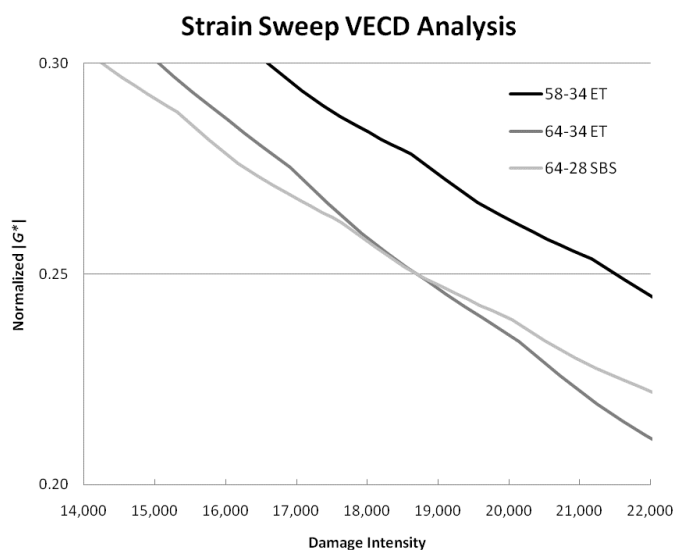


Figure 8-55: Plot of damage intensity from 20-30 % of initial undamaged modulus

The relative ranking of each material for the test methods employed in this study are shown in Table 8-19. It is clear that depending on chosen specification parameters and failure criteria, the rankings vary greatly.

Table 8-19: Ranking of bituminous binders using various fatigue tests

Used bitumen	Beam Fatigue	Time Sweep 2,5 & 5,0 %	Time sweep predict. at $W_i = 7\ 500\ Pa$	BYET – Yield Energy	BYET – GTM	Strain Sweep – $D@0,25M$
64-28 SBS	C	A	C	B	A	C
58-34 ET	A	C	A	C	B	A
64-34 ET	B	B	B	A	C	B

8.3.2 Polymer modified binders effect on asphalt fatigue resistance

8.3.2.1 Paper 479 (Thives et al., 2010)

In this study HMAC16 and SMA16 mixes with four types of binders (3 PMBs and 50/70 bitumen) were evaluated and the effect of PMBs studied. For the binders special elasticity and plasticity was required according to the authors. Fatigue resistance was assessed by 4PB-PR test according to EN 12697-24 at the temperature of 20 °C at 30 Hz and with a strain of 300×10^{-6} . The effect of PMB contribution was clearly shown by this test.

Table 8-20 – Fatigue results for assessed mixes (C is for 50/70)

Type of Mixture	Number of Cycles to Failure	Stiffness Modulus (MPa)		Phase Angle (°)	
		initial	final	initial	final
MAMR16-A	311000	4572	2439	20	30
MAMR16-B	238500	4373	2371	20	36
MAMR16-C	12000	9753	5135	12	25
MASF16-A	224500	7202	3637	13	29
MASF16-B	163000	5462	2792	20	31
MASF16-C	6600	12485	6288	12	25

8.3.2.2 Paper 058 (Baumgardner et al., 2008), Paper 059 (Bennert & Martin, 2008), Paper 069 (Such et al., 2008), Paper 098 (Li et al., 2011)

Polyphosphoric acid (PPA) is one of many additives used for modification and enhancement of paving grade bitumen. For more than 20 years PPA has also been successfully used across the United States in combination with various polymer modifiers. The combined use of PPA and polymers is widely used and has become increasingly popular as state agencies move to PG-Plus specifications including elastic recovery and ductility.

Typically, the use of PPA reduces the penetration value of the bitumen leading to change the penetration classification of the PPA modified binder as well as increasing in various extend its softening point. The PPA modification increases the stiffness of the binder without affecting the low temperature properties. Thus using PPA increases the pavement service life.

In order to quantify the field performance of SBS+PPA bitumen modified asphalt mixtures, several sections on NCAT test track have been monitored over 6 years. The results have been presented in terms of rutting, fatigue cracking and moisture resistance.

Fatigue cracking has been observed in 4 sections, from each, only one section had modified binder. Cores taken from this section revealed top-down cracking with cracks extending only

through the upper two to four inches of the pavement structure. Perhaps low binder content (4,9 %; 6 %) was a contributing factor for fatigue distress mode.

The experimental results of laboratory properties of bitumen modified with and without PPA has also been analysed. The master curve obtained from complex modulus test was given for short term and long term aged samples. The short term aged (STOA) results show that SBS+PPA modified bitumen obtained higher modulus values at the lower loading frequencies. The long term aged (LTOA) results showed a similar trend except that SBS modified bitumen obtained values much closer to SBS+PPA modified samples in comparison with STOA condition. This indicated that SBS modified samples underwent greater age hardening due to long term oven ageing than the SBS+PPA modified samples (Figure 8-56, Figure 8-57).

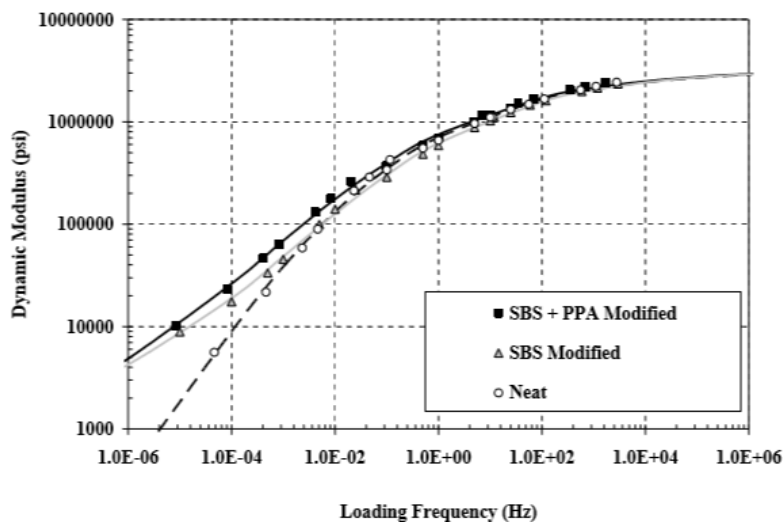


Figure 8-56: Master stiffness curves – short term oven aged (Paper 59)

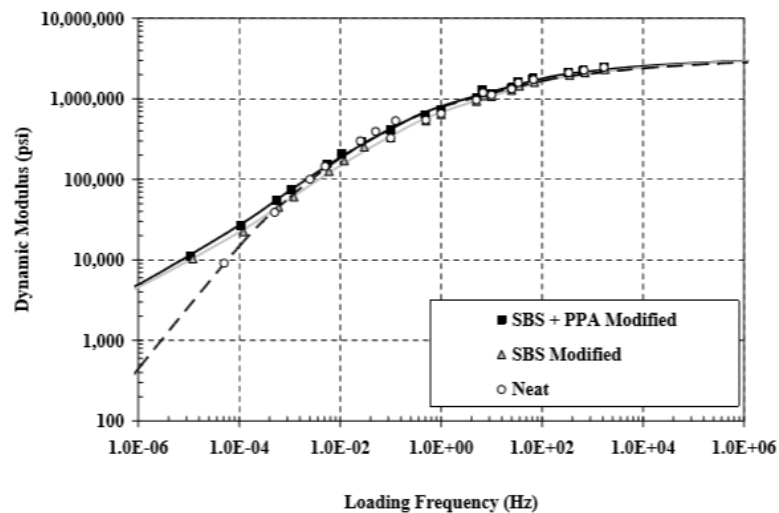


Figure 8-57: Master stiffness curves – long term oven aged (Paper 059)

Based on average results (statistically) of fatigue testing conducted from Flexural Beam Fatigue, the SBS modified bitumen had a slightly higher fatigue resistance than the SBS+PPA modified bitumen. However, when statistically comparing the full set of STOA fatigue results from each tensile strain level, the SBS modified and the SBS + PPA modified bitumens were shown to be statistically equal at a 95% confidence level using the Student t-

test analysis. When statistically comparing the full set of LTOA fatigue results from each tensile strain level, the SBS modified and the SBS + PPA modified bitumens were shown to be statistically equal at a 95 % confidence level at the 250 and 600 micro-strain levels. The SBS modified bitumen had a statistically greater fatigue life at the 400 micro-strain level and the SBS + PPA modified bitumen had a statistically greater fatigue life at the 800 micro-strain level. In both the STOA and LTOA aged conditions, the Neat bitumen achieved the lowest fatigue life (Figure 8-58, Figure 8-59).

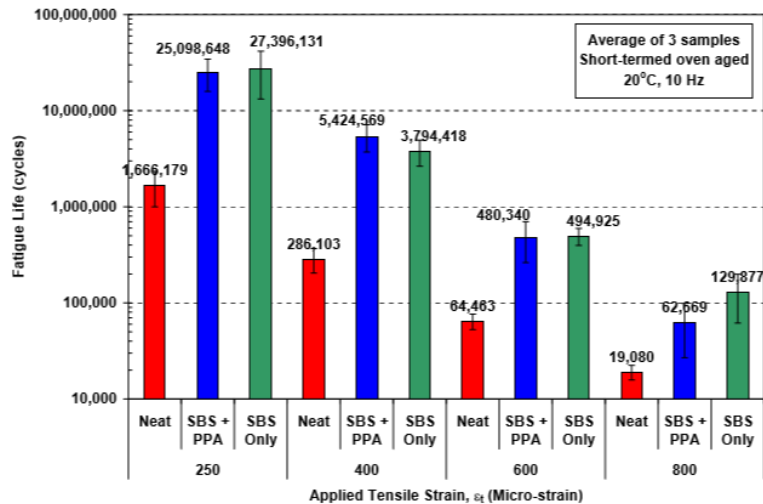


Figure 8-58: Flexural beam fatigue results for short term oven aging (Paper 059)

In conclusion it can be said that SBS+PPA modified bitumens can provide fatigue and durability resistance as well as bitumens solely modified with SBS. Flexural Beam Fatigue test results on short-term and long-term oven aged samples were statistically equal at a 95 % confidence level. Meanwhile, results from the Tensile Strength Ratio (TSR) tests concluded that the SBS+PPA modified bitumen achieved a slightly higher TSR value than the SBS modified samples.

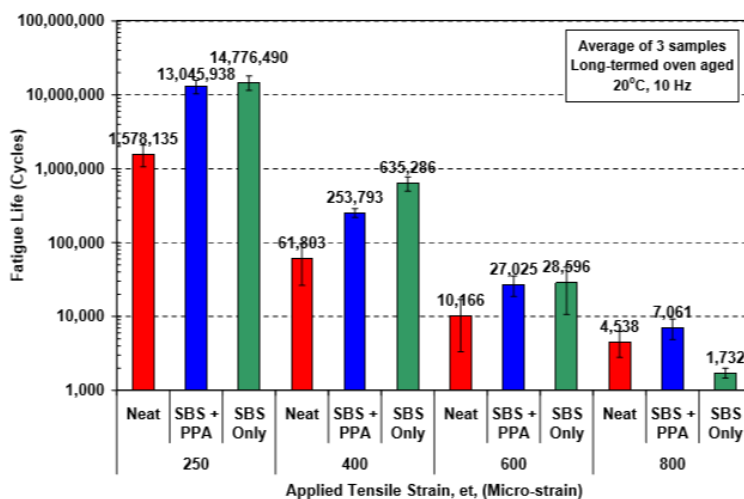


Figure 8-59: Flexural beam fatigue results for long term oven aging (Paper 059)

In a comparable study (Paper 98), the performance of bitumen modified with PPA in combination with other polymers has been tested. For this purpose, four modifications of the same binder with several combinations of polymer and polyphosphoric acid was investigated: PPA; PPA+Elvaloy; SBS; SBS+PPA.

Several tests on binders and mixes were conducted. MSCR data shows that the PPA+Elvaloy modified binder were the most performing with the lowest non-recoverable compliance and highest percentage recovery; this was consistent with VECD strain controlled fatigue analysis. A comparison of the 20 average ranking for the whole fatigue life and fatigue life to 50% loss in modulus before normalization with VECD shows that the PPA modified mixture is the least fatigue resistance and SBS mixture is the best but statistical analysis indicates that some are similar and different within a 95% confidence. This changes when the test data are normalized to constant strain conditions with VECD; the combination of Elvaloy and PPA significantly improved the mixture's fatigue resistance whereas SBS and SBS+PPA were still better than PPA alone. The study also demonstrates that with PPA it is possible to reduce the dosage of SBS obtaining comparable performance as SBS alone.

8.3.2.3 Paper 024 (Olard et al., 2012), Paper 034 (Dreessen et al., 2012), Paper 094 (Olard, 2011), Paper 248 (Scholten et al., 2013)

The ability of SBS polymers to reduce fatigue cracking and aging is well recognized (Baaj, Di Benedetto & Chaverot, 2005) (Dreessen, Ponsardin, Planche, Dumont & Pittet, 2011) but the high modulus required for perpetual pavement base structures usually calls for hard binders (and thus slightly higher binder content to preserve fatigue resistance) that have viscosity and compatibility issues with conventional SBS. Under those circumstances, EIFFAGE Travaux Publics (Paper 024 and Paper 094) was set out to combine both optimal aggregate interlock (using aggregate packing methods initially developed in the field of high-performance cement concretes) and the use of SBS polymers, in order to obtain both very stiff and fatigue-resistant polymer modified base course material in a single formulation. In general, the authors showed that stiffness is hardly influenced by aggregate packing optimization. In contrast the binder nature highly influenced the fatigue resistance. One can also highlight:

- With regards to the High Performance Asphalt (HPA) with Noubleau aggregate (single-gap-graded curve), the polymer modification (2,5 % cross-linked SBS) of the 35/50 neat bitumen leads to an increase of the ϵ_6 value by $21 \cdot 10^{-6}$.
- As regards the reference continuously-graded GB2 material made from Obourg aggregates, moving from the neat 35/50 binder to the blown 35/45B binder brings about an increase of the ϵ_6 value by $20 \cdot 10^{-6}$.
- Regarding the HPA with Obourg aggregates (double-gap-graded curve), the polymer modification (2,5 % cross-linked SBS) of the blown 35/45B bitumen brings about an increase of the ϵ_6 value by $26 \cdot 10^{-6}$, leading to an ϵ_6 value of $140 \cdot 10^{-6}$, which is an "incredibly" high value for an asphalt concrete with only 4 % binder content.

Some other information can be obtained in Paper 034 that concerns a comparative experimental study conducted in canton of Valais in Switzerland where the performance of SBS polymer modified binders have been examined while subjected to harsh weather conditions as well as heavy traffic loading. The period of study for different sites was 2, 8, 14 and 19 years. The binder types are 80/100 and Styrelf 13/80 (TOTAL), which allows a comparison between pure and polymer modified binders (PMB).

The PMB sections in general exhibit a much better ageing resistance throughout the tests carried out. The low evolution of ageing is probably due to the original process of binder reticulation which limits the possibility of oxidation and improves the durability of the surface. Moreover, the polymer network was still present after 19 years of service life reflected on the fact that elastic properties of the PMB were maintained at a very high level in relation to their initial value.

The results from an extensive two years road trial at the NCAT facility and what it means for pavement design are presented in paper 248. Figure 8-60 provides the results of 4 point bending fatigue test. It clearly shows the strong improvement in fatigue resistance that is associated with the continuous polymer rich phase as found in the formulations with 6 % and 7,5 % SBS. The cracks will be hampered by the continuous polymer rich phase.

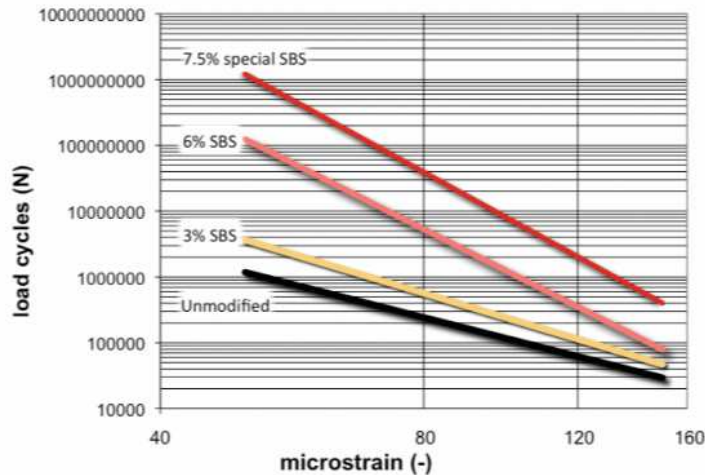


Figure 8-60: Four point bending fatigue results (strain controlled) at 20 °C for a continuously graded base course asphalt concrete with different binders (Paper 248)

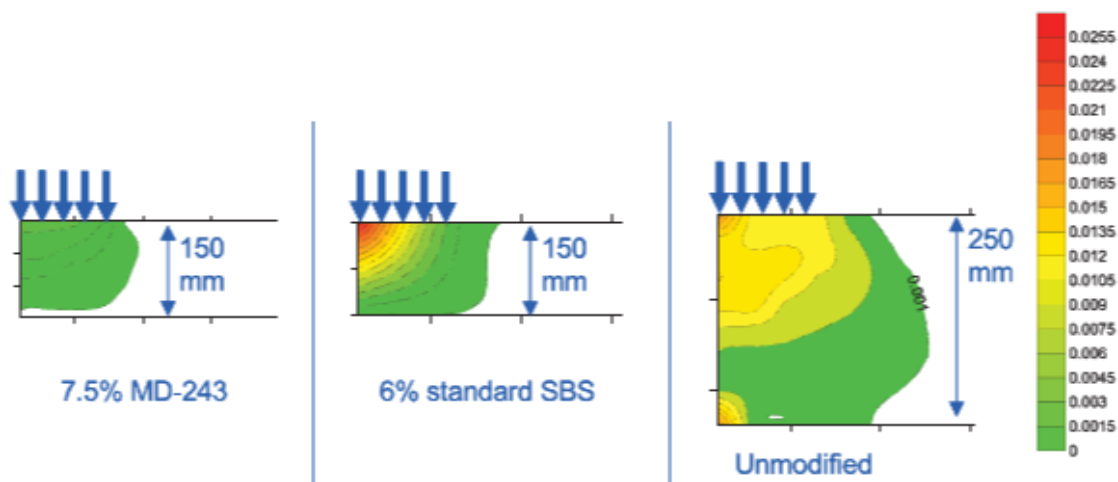


Figure 8-61: Damage development in the asphalt layers after 9000 load repetitions (Paper 248)

Furthermore, a pavement structure has been modeled using CAPA, a finite element program developed in Delft University. In this analysis, the non-polymer modified reference mixture has been compared with two polymer modified mixtures: a mix containing 6 % standard SBS and a mix with contains of 7,5% D0243. Figure 8-61 shows the development of damage after 9000 load repetitions. One may see in the figure below that despite the 40 % reduction in height for the modified structure, the pavement with 7,5 % D0243 shows much less damage. The 6 % SBS modified pavement has a higher intensity of damage directly under loading.

8.3.2.4 Paper 026 (Eckmann *et al.*, 2012)

This paper deals with cross-linked polymer and the optimal dosage to achieve the highest performance in term of rutting resistance, fatigue resistance and thermal cracking. Fatigue was tested on different samples with several amounts of polymer at 10 °C 25 Hz on trapezoidal specimen, in a 2 points bending controlled strain (EN 12697-24). The retained

performance indicator is the ϵ_6 value, i.e. the strain level which leads to conventional failure after 10^6 loading cycles.

The objective of the authors is to propose also a correlation between asphalt and binder properties. The authors claim *“so far there is no consensus on what may be an adequate binder performance indicator for the fatigue behavior of asphalt mixes. In the limited frame of our study, and considering that the ϵ_6 values measured for various polymer modified binders based on the 20/30 are nearly identical the search for meaningful correlations had of course no chance of being successful and has therefore not been attempted.”*

In conclusion the modification with the cross-linked polymer gives a significant contribution to the fatigue resistance but not constantly improved increasing the polymer content. The results suggest a threshold or optimum value above which performance tends to stay level or even decrease slightly. The content of the polymer should not exceed a certain limit.

8.3.2.5 Paper 506 (Wistuba et al., 2009)

The use of polymer-modified bitumen of the same sort from different manufacturers can lead to, as experience shows, different properties of the asphalt mixes produced with it. These differences shall be shown by means of the fatigue behavior of asphalt mixes using the Cyclic Indirect Tensile Test (CITT) on Mastic Asphalt (MA) and Asphalt Concrete (AC). For this purpose, polymer-modified bitumen 25/55-55 A and 10/40-65 A from different manufacturers were analyzed. In addition, chemical properties like chromatography or infrared-spectroscopy were investigated. Afterwards, the bitumen was used for the asphalt mix production for dynamic testing.

During the CITT a sinusoidal loading is applied vertically to a cylindrically shaped specimen. The effective testing force as well as the horizontal strain are recorded. The loading cycle at which fatigue occurs is defined as N_{Macro} and this is the stage of the fatigue test at which macro cracks start to be observed in the specimen. The CITT is performed in a temperature range of $-15\text{ }^{\circ}\text{C}$ to $+20\text{ }^{\circ}\text{C}$. Fatigue functions are determined for dimensioning at $20\text{ }^{\circ}\text{C}$. On the basis of comprehensive investigations with the CITT a testing temperature of $10\text{ }^{\circ}\text{C}$ was chosen for MA specimens, the AC was tested at $20\text{ }^{\circ}\text{C}$.

For each asphalt concrete 0/22 and stone mastic asphalt 0/11, six mix types were produced with PMB 10/40-65 A and PMB 25/55-55 A from four different manufacturers.

Table 8-21: Bitumen volume of the asphalt mixes

Mix		SMA 0/11	AC 0/22
PMB type	10/40-65A	7,3	4,3
	25/55-55A	7,0	4,2

The values of the standard parameters for needle penetration and softening point ring and ball comply with the specifications in the guidelines. The partly big differences for the respective parameters that were obtained for a PmB sort, e.g. for the force ductility test, are due to the different compositions and interlacing of the polymers and the different base bitumen that was used. This was confirmed by gel permeation chromatography and infrared-spectroscopy analyses.

The aim was not to simulate the aging of the asphalts over a specific time on site, but to investigate loading of asphalts at different manufacturing and storage conditions, as well as during transportation. Different loading was chosen to give conditions as close as possible to common practice. After mixing (stage 1) according to the Technical Standards the SMA were

exposed to a temperature of 250 °C and low rotation speeds in a sealed mixer to prevent air entering it for a time of 60 minutes in stage 2 and 165 minutes in stage 3.

Table 8-22: Selected bitumen features or properties at delivery

Property	Unit	PMB	10/40-65 A				25/55-55 A			
		Manufacturer	1	2	3	4	1	2	3	4
Penetration	0,1 mm	DIN EN 1426	26	35	35	28	30	46	44	45
Softening point	°C	DIN EN 1427	74,0	67,2	64,4	63,8	58,5	56,8	58,6	62,0
Force ductility, deformation	J	TL PmB/ DIN 52013	0,813	0,824	1,135	0,866	0,674	0,373	0,516	0,749
Force ductility, Max. force F_{max}	N	TL PmB/ DIN 52013	14,1	6,3	8,9	8,4	6,9	4,7	3,5	2,4
Force ductility deformation at 5 and 10 °C	J/cm ²	DIN EN 13589/ 13703	3,89	6,43	7,44	7,38	3,88	2,92	4,87	10,5
Force ductility, Max. force F_{max} at 5 and 10 °C	N	DIN EN 13589/ 13704	113,9	56,9	75,4	90,3	179,0	112,3	114,6	80,1
Elastic recovery 20 cm/ 25 °C	%	DIN EN 13598	66	74	78	78	57	54	77	83

The asphalt concretes were granulated after mixing and were put into a warming oven on a gauze at 180 °C at a defined air exchange (11 m³/h) and were exposed for a time of 120 minutes in stage 2 and 180 minutes in stage 3. The PmB was reextracted from the asphalt mixes after mixing stage 1 and from each of the mixes after mixing stages 2 and 3. Different bitumen parameters were determined with some tests. To determine the fatigue properties of the asphalt sorts, the CITT was applied in stage 1 and stage 3. For selected options the test was applied additionally in stage 2.

For the CITT of AC, a uniform minimum stress of 0,035 MPa, as well as a stress difference between the minimum and maximum stress of 0,7 MPa was chosen.

The load cycle N_{Macro} after stage 1, showed, as expected, lower values for the types with 25/55-55 A. These were in the range of 770 to 2 426 load cycles. The types with 10/40-65 A achieved 5 460 to 7 576 load cycles. This range in load cycles amongst the PmB sorts shows that the implementation of PmB from different manufacturers has an influence on the results of fatigue tests and thus also on the fatigue properties of asphalt concrete.

The thermal and oxidative exposure in the stages 2 and 3 led to brittleness which was shown e.g. by the bitumen tests softening point ring and ball and by the higher maximum force F_{max} that was achieved during the force-ductility test. The exposure led to an increase in load cycles in all but one sort. The load cycle range for the sorts with 10/40-65 A was 4 351 to 9 455 and for 25/55-55 A sorts it was 1 085 to 3 946. At stage 3 of sort 8 the load cycle dropped and the bitumen tests also showed discrepancies: The softening point in stage 3 lay at 99,2 °C which is an indication for strong brittleness of the PmB and which evidently leads to worsening fatigue properties.

Even though there is a known variance of the single values during dynamic testing for fatigue properties, a clear differentiation of the results and also of single values between the 3 stages, with an average coefficient of variation of 23 %, is possible (Figure 8-61). This was the case for all sorts except type 7.

The change in load cycles from stage 1 to stage 3 differed for each sort. The load cycles in stage 3 are dependent on the changed properties of the exposed PmB. Thus every PmB

reacts with a different intensity to the thermal and oxidative exposure due to the specific composition of the different PmB which have different standards.

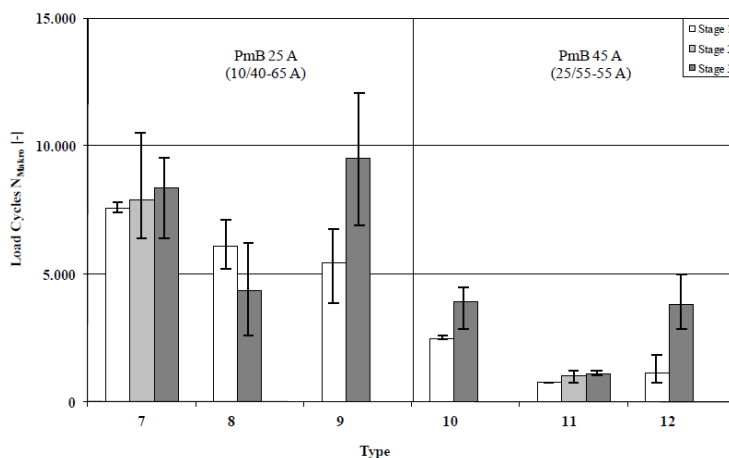


Figure 8-62: Arithmetic averages of the load cycles N_{Macro} with ranges of the three single values for the AC types in the stages 1 to 3 ($\Delta\sigma = 0,7$ MPa)

To determine influences of the PmB properties on the results of fatigue tests, amongst other tests, the maximum force F_{max} was obtained from the force-ductility test. Wear of the PmB was specially noticed when the F_{max} was increased. With type 8 described above, where the load cycle number dropped in stage 3, the largest increase in maximum force from stage 1 to stage 3 could be observed. This force increased more than fourfold. For all stages no correlation could be found between the maximum force F_{max} from the force-ductility test and the load cycle number N_{Macro} .

Further loading of the asphalts beyond stage 3 and the determination of the load cycle number N_{Macro} is theoretically possible, but in practice, investigations of the bitumen properties become increasingly difficult. Experience has however shown that the load cycle numbers decrease because the asphalt becomes increasingly brittle and thus the fatigue properties worsen; i.e. a specific curve with the maximum load cycle number that can be endured, can be drawn.

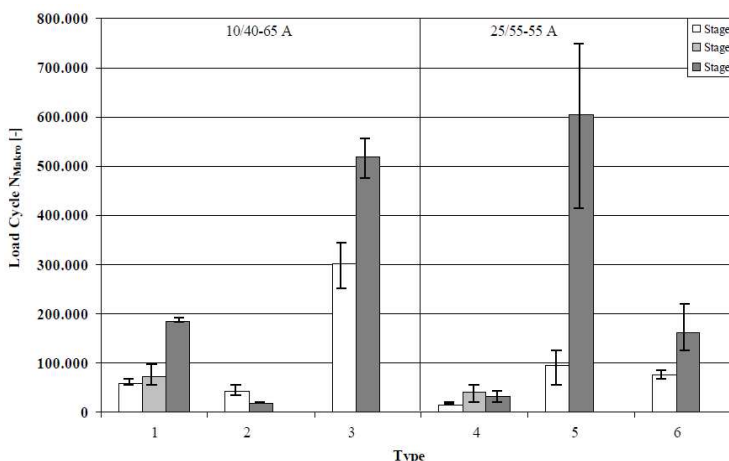


Figure 8-63: Arithmetic averages of the load cycles N_{Macro} with ranges of the three single values of the MA types in the stages 1 to 3 ($\Delta\sigma = 0,7$ MPa with cryogenic minimum stress)

A similar result is observed when trying to obtain a correlation between the values from the softening point ring and ball test and the load cycle number N_{Macro} for all stages. If only stage

1 is taken into consideration, a correlation with a coefficient of determination of $R^2 = 95,3 \%$ can be observed. For the CITT of SMA, specific cryogenic stresses were taken into consideration as the respective minimum stress. These were determined by initially performing cooling tests. For this reason there were different minimum and therefore also different maximum stresses for the respective types and stages due to the chosen constant stress difference of 0,7 MPa.

The load cycle numbers N_{Macro} of stage 1 for the types with Bitumen 10/40-65 A were in the range 41 548 to 301 780 and those for the types with 25/55-55 A were in the range 14 515 to 94 594 (Figure 8-61). Thus a differentiation of the PmB sorts according to the amount of load cycles, is not possible. This is due to the specific properties of the respective PmB and amongst other due to the different occurring minimum stresses. Due to the thermal exposure, the asphalt went brittle and higher cryogenic stresses occurred during the cooling tests. This led to higher minimum and maximum stresses in the stages 2 and 3. An increase in load cycle numbers was observed for all types except types 2 and 4. The highest increase occurred with type 5. Here the load cycle number increased more than fivefold. Also in the case of the SMA the load cycle numbers changed differently for the stages 1 to 3.

No correlation could be found between the softening point and the load cycle number N_{Macro} for all stages. The same findings were obtained during investigations with the maximum force F_{max} from the force-ductility test. If even only stage 1, which showed good correlations in the results of the MA, is considered, no correlation can be found. There is also the possibility of loading the asphalts beyond stage 3 and determining the load cycle number N_{Macro} . However, with this procedure, investigations for bitumen properties become increasingly difficult. Experience shows that therefore a decrease in load cycle numbers can be expected.

The results presented here for the AC and the SMA types were done by respectively choosing one stress condition (stress difference) at one temperature and therefore they represent only one pair of values for, e.g. the fatigue function. The results are strongly influenced by the respective stiffness modulus of the asphalts with the specific PmB under the chosen conditions.

For the range of the temperatures used in this investigation, the oxidative or thermal and oxidative exposure of the asphalts has the effect of increasing the load cycle numbers. Also, smaller strains occur at the same stress difference. These results show that the fatigue property of the exposed asphalts improves.

8.3.2.6 Paper 451 (Jacobs and Sluer, 2009)

A dense asphalt concrete AC 16 surf PMB (5,7 %) with 40/60 penetration grade bitumen and 5 % EVA modification was used in a study focused purely on effect of polymer modification on fatigue asphalt testing. In order to determine the fatigue characteristics of the mix, 18 specimens are tested in a strain controlled test at a temperature of 20 °C. Three different deformation levels are used to achieve life spans of the specimens of 10^4 , $5 \cdot 10^5$ and $2 \cdot 10^6$ load repetitions. In Figure 8-61 a typical result of one of the specimens is presented.

The first phase of the fatigue test on the PMA mix lasts much longer than a fatigue test on a mix with a standard penetration bitumen. With the PMA mix the initial phase takes about 33 % of the total number of load repetitions; with a standard mix between 5 % and 10 %. In the first phase, the stiffness of the PMA mix decreases drastically compared to a standard mix. It should also be mentioned that the fatigue tests on the PMA mix are carried out with a substantial higher deformation level than for the standard asphalt mix.

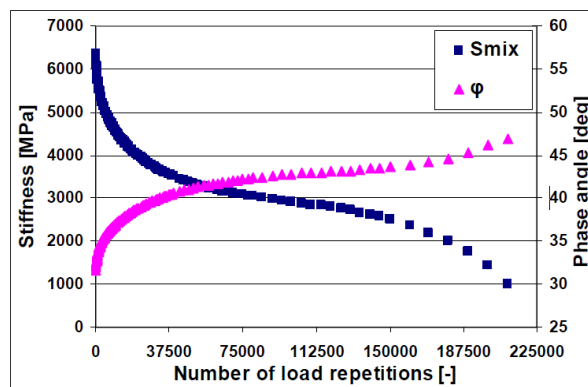


Figure 8-64: A typical result of a fatigue test on a AC 16 surf PMB mix at 20 °C

The large disadvantage of the use of the standard definition of the initial stiffness ($= E_{100}$) is the fact that for almost all of the 18 specimens, the fatigue life occurs in the initial phase of the fatigue process. So using the standard definition, the fatigue life of a polymer modified asphalt mixture is underestimated. This problem can be solved by using the second definition of the initial stiffness ($= E^*$), that is defined as the stiffness found by extrapolation of the secondary phase of the fatigue test to $N=0$. In Table 8-23 the results of this approach are presented, next to the standard definition of the initial stiffness. The life span of the individual specimens with the alternative definition of S_{INI} ($= E^*$) is in average a factor of 2.2 longer than for the standard S_{INI} definition ($= E_{100}$).

In Figure 8-61 both fatigue lines are presented. It can be concluded that there is not a large difference in the ϵ_6 -values of both approaches despite the average factor 2.2 in life span between both sets of data.

Table 8-23: The initial stiffness and fatigue life

Code specimen	ϵ [$\mu\text{m/m}$]	Standard definition S_{INI}		Alternative definition S_{INI}	
		E_{100} [MPa]	N [-]	E^* [MPa]	N [-]
P1B1	342	6356	64528	3544	189463
P1B2	352	6221	52945	4111	82951
P1B3	341	6611	40642	4801	47872
P1B4	301	6227	311472	3600	552717
P1B6	332	6515	76433	3769	197368
P1B7	352	6159	78056	3184	401436
P2B8	332	5695	195938	3192	*)
P2B9	301	6093	213252	3797	292751
P2B10	332	5733	89848	3484	211593
P2B11	333	5430	236838	3122	497168
P2B12	332	5422	199179	3022	499903
P2B13	303	5712	601680	3186	1202885
P2B14	303	6172	263623	3710	409430
P3B15	353	5791	70665	3306	192967
P3B16	272	5648	1278923	3559	1358206
P3B18	301	5575	392258	3397	*)
P3B19	342	5477	141298	3101	*)
P3B21	312	6162	353630	3329	797662
Average value		5944		3512	

*) The test was not long enough to find an appropriate life span value for this specimen

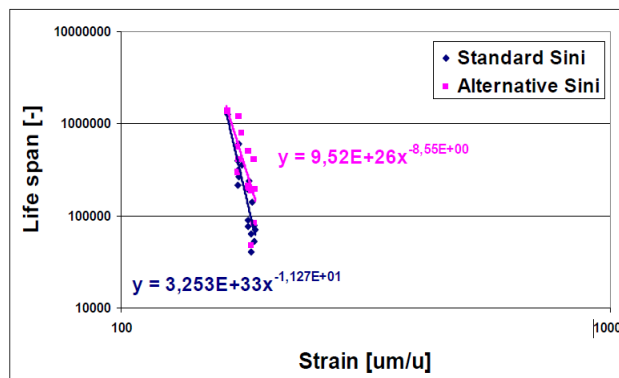


Figure 8-65 – Fatigue lines base on the standard and alternative definition of S_{INI}

During the test not only the standard fatigue parameters were measured, but also the temperature of the beam. These temperature measurements are carried out on the surface of the specimens on two positions on the beam: one at the neutral axis of the beam in the middle between the two inner clamps (=Temp2) and one at the neutral axis of the beam in the middle between the a inner and outer clamp (=Temp1). In figure 5 a typical result of these measurements is shown. The test was carried out with a frequency of 30 Hz at a strain level of 244,8 $\mu\text{m}/\text{m}$.

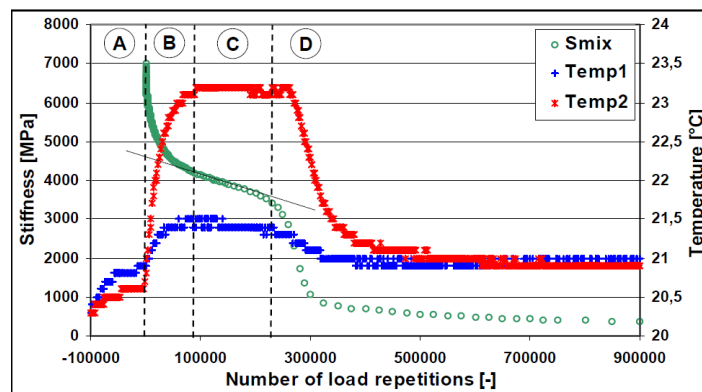


Figure 8-66 – Typical test results of a fatigue test with temperature measurements

During the frequency sweep (between -100 000 and -50 000 load repetitions; phase A) the temperature of the beam increases slightly from 20,3 °C to 20,7 °C. It must be noticed that the frequency sweep was carried out with a strain level of 50 $\mu\text{m}/\text{m}$. After the frequency sweep (between -50.000 and 0 load repetitions), the specimen was in rest in the loading frame. During that time the temperature of the specimen stays constant. After start of the fatigue test at $N=0$, in the initial phase of the fatigue test (phase B) the stiffness of the specimen reduces drastically. On the other hand, the temperature of the part of the specimen between the two inner clamps increases from 20,6 °C to 23,2 °C; the temperature of the asphalt beam between the inner and outer clamp only raises from 20,8 °C to 21,5 °C. This implies that the drastically decrease of the stiffness during the initial phase of the fatigue test is not only caused by mechanically damaging the specimen, but also due to a temperature raise of the specimen. During the second phase of the fatigue test (phase C), the temperature of the specimen remains constant at the elevated level. In the third phase of the fatigue test (phase D), the temperature of the specimen drops significantly to a level just above the temperature at the start of the fatigue test. The specimen keeps this temperature for a long time. From these results, it can be concluded that temperature increase of the specimen has a large effect on the behavior of the specimen during the fatigue test.

The ϵ_6 -value, as it is now in the European product standard for asphalt concrete EN 13108-1, is not a suitable property to describe the fatigue behavior of asphalt mixtures. It would be better if both Wöhler parameters would be used to characterize fatigue of asphalt concrete mixes.

8.3.2.7 Paper 036 (Pasetto & Baldo, 2012), Paper 045 (Vasilica et al., 2012)

The use of crumb rubber modified bitumen, produced with the wet technology, represents an effective option in order to reduce waste tires and, at the same time, to improve the fundamental engineering properties of asphalt mixtures, for road flexible pavements.

The use of crumb rubber modified bitumen has been examined through laboratory tests in order to verify the stiffness properties and the fatigue resistance of bituminous mixtures in base and wearing courses (Paper 036). The mixtures have been prepared with a steel slag content of 89 %. In addition to crumb rubber modified bitumen, hard and soft modified bitumen have been used in sample preparation.

The asphalt rubber concrete presented an increased fatigue life, both before and after aging. Moreover, in each type of mixture, the hard modified bitumen led to an improved fatigue life compared to the soft one. Among the different types of mixtures, the one for base course showed the greatest benefits from the use of the crumb modified bitumen.

In another study coming from Romania (Paper 045), three different forms of rubber powder were used: Simple granulated form (GP); rubber powder mixed with polyoctenamer (OP) and granulated with Bitumen Form (BP). In GP samples, with 1 % addition of rubber powder, the characteristics of dynamic tests (i.e. stiffness, triaxial compression and resistance to fatigue) proved to decrease. In OP samples, for a given temperature, the G^* value increases while the lag angle decreases. This result in higher elasticity thus increases of the resistance to permanent deformation. Moreover, the stiffness value decreases, which shows a better resistance to cracking at low temperature. The authors claim that the fatigue resistance of the sample prepared in the laboratory has also been improved. In case of BP samples, the ratio of G^* to $\sin\delta$ has increased thus resulting in a better resistance to rutting. In addition the $G^* \sin\delta$ has been decreased thus leading to increased fatigue cracking.

8.3.2.8 Paper 435 (Kudrna & Dašek, 2009), Paper 448 (Fontes et al., 2009), Paper 450 (Neto et al., 2009)

There are also other papers focusing on the effect of rubber modified binders on asphalt mixture performance. In paper 435 wet process with 0/2 mm rubber granulate was applied in a content of 15-25 % rubber in bitumen. Rubber was mixed with 70/100 or 50/70 bitumen for at least 60 minutes at 175 °C. CRmB was applied in very thin asphalt concrete mix (VTAC11) and in porous asphalt (PA8). VTAC mixes denoted Test 1.1 and 1.2 were taken from the production for trial section No. 1. Similarly VTAC mixes denoted Test 2.1 and 2.2 originate from the trial section No. 2. Unfortunately there is no direct correlation to test specimens from the pavement structure.

Fatigue test was done according to 12697-24 by 2PB-TR test at the test temperature of 10 °C and frequency of 25 Hz for different strain levels. Higher binder content and modification by CR increased resistance to fatigue in case of similar grading and air voids. Fatigue characteristics according to EN 13108-1 of mixtures with CRmB were determined in the category $\epsilon_{6,190}$ instead of the category $\epsilon_{6,115}$ of AC 11 mixture with straight-run bitumen. Additionally it was proven that mixtures with softer CRmB offer better resistance to fatigue.

Study presented in paper 448 focused on stiffness and fatigue life for four different dense and gap graded asphalt mixes containing terminal blended CRmB with 15-20 % crumb

rubber in 50/70 bitumen with penetration around 40 dmm and softening point around 68 °C. Asphalt mixes are designed according to US standards (gap graded ARHM-GG mixture according to Caltrans Standard Special Provisions SSP39-400 and dense graded Asphalt Institute mixture following the Asphalt Handbook Manual Series No. 4), the asphalt mixes might be comparable to AC12.

Table 8-24: Characteristics of tested mixtures with CRmB binder

Mixture type		AC 11	Test 1.1	Test 1.2	PA 8; Laboratory	PA 8; Low traffic	Test 2.1	Test 2.2
Property		1	2	3	4	5	6	7
Paving bitumen		70/100	50/70	50/70	70/100	50/70	50/70	50/70
Crumb rubber content, [% of bitumen]		-	26	26	18	20	22	20
Hydrated lime addition, [% of bitumen]		-	-	20	-	-	20	20
Binder content, [% of mixture]		6,2	8,3	8,3	9,5	9,2	8,7	8,7
Content of paving bitumen, [% of mixture]		6,2	6,6	6,6	8,1	7,7	7,2	7,2
Air-voids, [%]		3,9	8,9	8,9	19,0	20,8	19,0	19,3
Voids in mineral aggregate, [%]		18,1	26,8	26,8	36,1	38,0	35,6	35,8
Fatigue EN 12697-24	$\epsilon_6 \cdot 10^{-6}$	130	124	148	219	-	216	171
	B	4,55	5,24	4,96	6,68	-	6,58	6,12

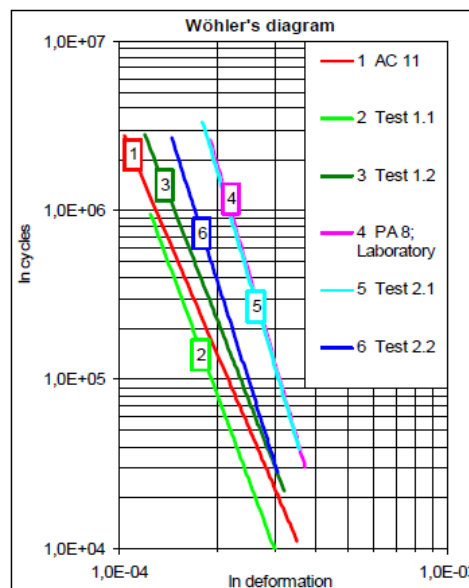


Figure 8-67: Comparison of fatigue life for tested mixes

Fatigue test was performed by 4PB-PR test method (according to AASHTO TP 8-94). All tests were executed at 20 °C and at 10 Hz. For each mixture, three levels of strain were selected (200, 400, 800 $\times 10^{-6}$), with three replicates. Before the fatigue test, the frequency sweep test was conducted in the same equipment, using the same specimen. The dynamic modulus and fatigue tests were carried out under controlled strain conditions in beam specimens with the dimension 380 mm (length) x 50 mm (height) x 63 mm (width).

The development of the fatigue models was based on the model developed by Tayebali et al. (1994), expressed in equation 4, where: N is the fatigue life; e is the Neper's number; VFB is the percentage of voids filled with bitumen; ε is the tensile strain; S'' is the loss stiffness and k₁, k₂ and k₃ are statistical coefficients.

$$N = k_1 \times e^{k_2 \times VFB} \times e^{k_3} \times (S'')^{k_4} \tag{8.4}$$

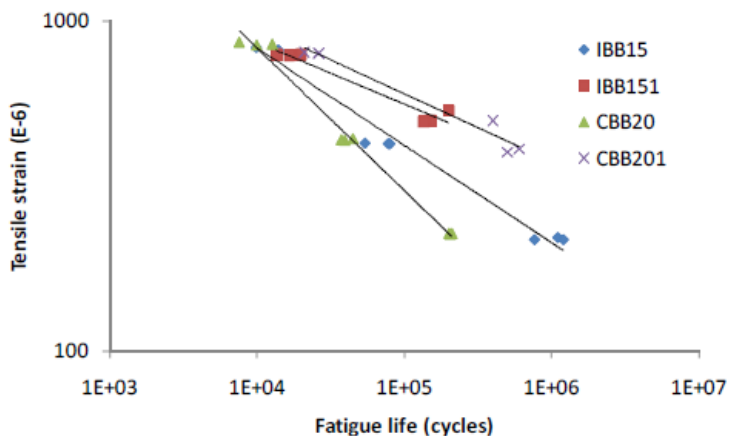


Figure 8-68: Fatigue life for studied dense and gap-graded mixes

Paper 450 focuses on specific aspects of asphalt mixtures with CRmBs. For conventional HMAs usually increased stiffness leads to shorter fatigue life, for mixes with CRmB (wet process of using rubber) it was shown that stiffness and fatigue life increased. 4PB-PR test was used to assess resilient modulus. In the study asphalt concrete for wearing course was used and 50/70 bitumen was applied as a basis using additionally 21 % crumb rubber with mixing 60 minutes at 210 °C (question of bitumen degradation at this temperature). Two types of asphalt mixes were studied – dense AC16 and gap graded AC16. Fatigue life tests were carried out under controlled strain conditions according to AASHTO TP8/96. The specimens obtained from studied asphalt hot mixes were submitted to the long-term aging process normalized by AASTHO PP2/94. Fatigue test has been performed only on three test specimens at 20 °C and 10 Hz.

The fatigue of asphalt hot mixes in wearing courses can be explained by the effect of repeated traffic load acting on the surface of flexible pavement induce tensile stresses or strains in the bottom of the wearing course which works under bending. When the number of applied load cycles is equal to the fatigue life of the asphalt mix a crack is initiated leading to the failure of the wearing course.

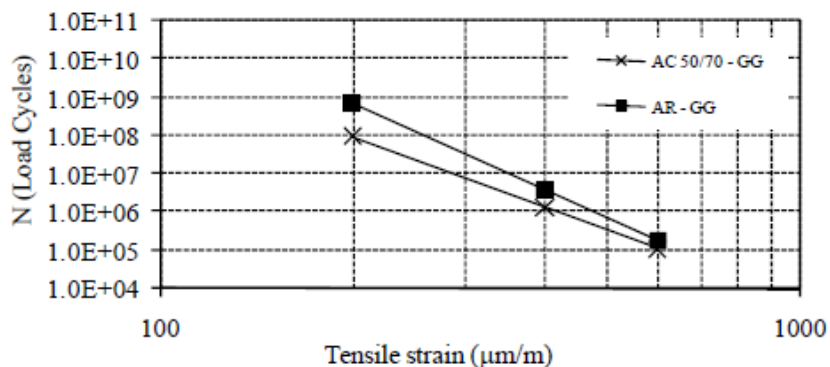


Figure 8-69: Fatigue life comparison for dense graded AC with 50/70 and with CRmB

The laboratory tests used to evaluate the fatigue life of asphalt hot mixes can be performed under conditions usually apply indirect tensile stresses (σ_t). In this type of fatigue life test, the tensile strains increase during the test under constant loading until the complete failure of the specimen. In the case of controlled strain conditions, the tensile strains (ϵ_t) are induced at the bottom of a prismatic specimen (beam) using usually a four bending point loading system. The failure is defined by the number of load cycles applied that reduces the stiffness of the specimen in 50 % of its initial value. The results obtained from fatigue life tests performed under controlled stress conditions are significantly different from those obtained under controlled strain conditions and must be conveniently analyzed. It is important to accent that according to Huang (1993) a complete fatigue life law controlled stress or controlled strain conditions. The tests performed under controlled stress must consider the effect produced in the fatigue life of the asphalt hot mix by its stiffness.

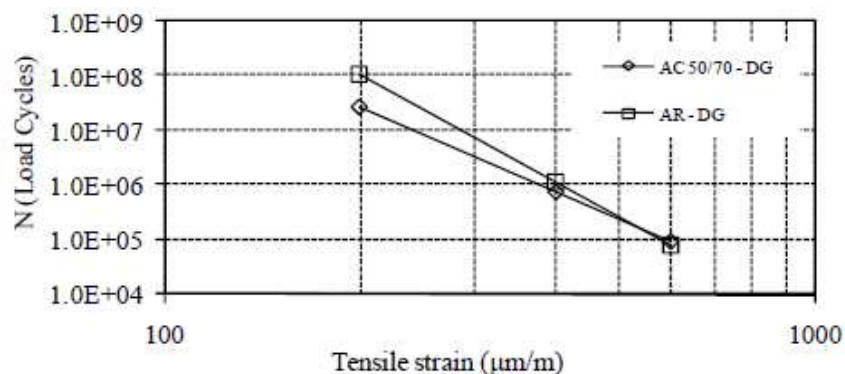


Figure 8-70: Fatigue life comparison for dense graded AC with 50/70 and with CRmB

Study summarized in paper 478 focused on accelerated failure of pavements in a country with poor pavement conditions due to low performance materials and increased traffic loading. Use of crumb rubber in the bitumen was selected and evaluated as an alternative for increasing mainly the fatigue resistance. For this reason five different mix types of dense or gap gradation prepared with binder content between 5 % and 9 % and void content 5-6 %. As standard binder pen grade bitumen 50/70 was selected. Crumb rubber was applied in the bitumen with content of either 15 % or 20 % applying the wet process (continuous and terminal blends). Resulting optimum content of CR was defined as 17 %.

Fatigue is a significant distress as fatigue cracking propagates through the entire asphalt layer, which than allows water infiltration into the unbound layers (Priest)⁴. This causes accelerated surface and structural deterioration as well as pumping of the unbound materials and rutting. The model definition of fatigue theory states that fatigue cracking initiates at the bottom of the flexible pavement layer due to repeated and excessive loading and is associated with the tensile strains at the bottom of the asphalt layer (Romero et al.)⁵. Fatigue cracking is the primary pavement distress at intermediate service temperatures (Roberts et al.)⁶. It is considered as a strain controlled distress in thin pavement layers (≤ 50 mm thickness) because deformations in this asphalt layers are typically the result of a poor subsurface layer and not so much influenced by decreased pavement stiffness. In case of

⁴ Priest A.L., 2005. Calibration of fatigue transfer functions for mechanistic-empirical flexible pavement design. M.S. Thesis, Auburn University, USA.

⁵ Romero P., Stuart K.D., Mogawer W., 2000. Fatigue response of asphalt mixtures tested by the Federal Highway Administration's accelerated loading facility. Journal of the Asphalt Pavement Technologist; vol. 69, p. 212

⁶ Roberts F.I., Kandhal P.S., Brown L.R., Lee D., Kennedy T.W., 1996. Hot mix asphalt materials, mixture design and construction. NAPA Research and Education Foundation, Lanham, MD, USA

thick pavement layers (>150 mm) fatigue cracking is considered a stress controlled distress and the pavement is according to the authors then the main load-carrying constituent. A combination of both stress and strain controlled distresses exists in asphalt pavements with intermediate thickness.

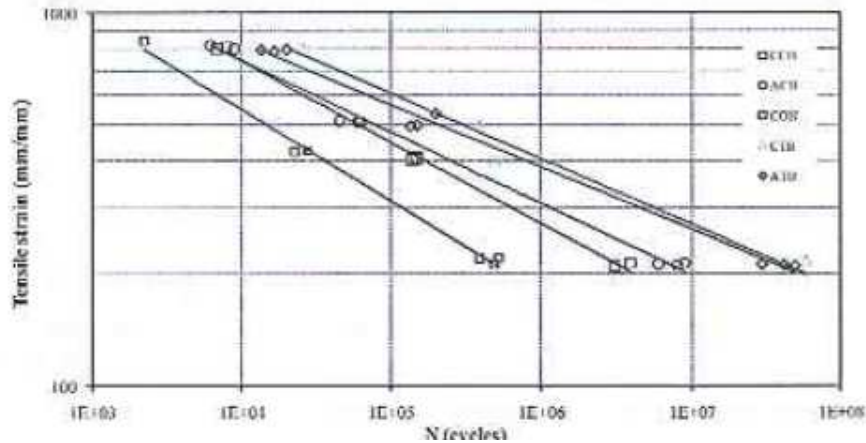


Figure 8-71: Fatigue curves of tested asphalt mixtures

4PB-PR in controlled strain modulus was selected for fatigue testing. Flexural fatigue test was conducted according to AASHTO TP8-94 (Standard Test Method for Determining the Fatigue Life on Compacted HMA Subjected to Repeated Flexural Bending). In this test sinusoidal loading with 10 Hz is used. Further three strain levels of 200×10^{-6} , 400×10^{-6} and 800×10^{-6} were selected. Fatigue failure was assumed to occur when the stiffness is reduced to 50% of its initial value (100^{th} cycle). From the tests following findings can be concluded:

- fatigue life was higher for asphalt mixes with CR (remarkable difference according to the authors considering 5,5 % bitumen for conventional HMA and 7-9 % CRmB for mixes with rubber);
- terminal blended CRmB exhibits better fatigue life;
- asphalt mixtures with terminal blended CRmB require a lower binder content than the mixtures produced with continuous blends.

Further, correlations between fatigue performance and rubber modified bitumen characterization in terms of penetration, softening point, resilience and apparent viscosity were established indicating that the fatigue performance can be predicted through the softening point of the binder. From the correlations only the softening point seems to be a potential indicator of the fatigue performance of asphalt mixtures containing rubber.

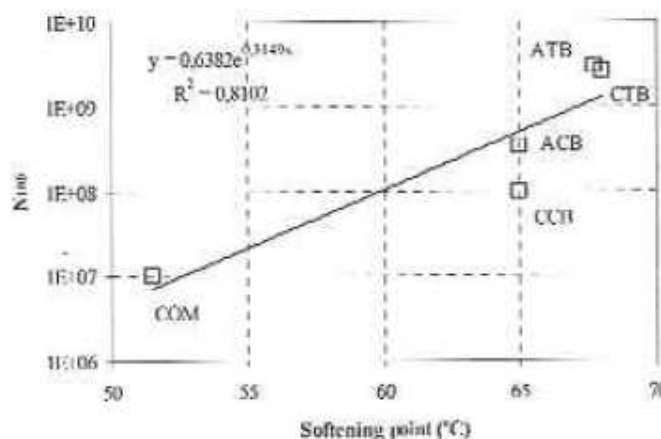


Figure 8-72: Comparison between fatigue life (N100) and softening point

8.3.2.9 Paper 562 (d'Angelo & Dongré, 2009)

In this paper a study on the performance of binders modified with a wide range of crumb rubber content using newly developed test methods such as the time sweep binder fatigue test and the multiple stress creep and recovery (MSCR) test was presented. Additional binder and mixture performance tests were used to compare and validate the results. The results showed that the new tests performed well in predicting performance.

PG 58-22 bitumen (binder A) was selected as the base binder for this study. Binder A was modified by adding 3-15 % ambient ground crumb rubber. The rubber particle gradation was relatively coarse. An optimum binder content of 6,2 % of total mixture weight was determined for binder A. For binders A3%, A6%, A9%, A12% and A15%, optimum binder contents of 6,5 %; 6,8 %; 7,1 %; 7,4 % and 7,8 % of total mixture weight, respectively, were used.

Using a DSR, binder samples 8 mm in diameter and 2 mm thick were subjected to strain-controlled cyclic loading at a strain level of 10 % until the complex shear modulus (G^*) reached 20 % of its initial value. The tests were performed at 15 Hz loading frequency. Tests were also run at 1,59 Hz, but most binders did not fail in a reasonable time and thus this frequency was eliminated. The binders tested were aged using a rolling thin film oven (RTFO) and pressure aging vessel (PAV) to be comparable to current Superpave binder fatigue test specifications. The test temperatures corresponded to IDT mixture test conditions at 30 °C. The indirect tensile (IDT) strength test settings were 30 °C at 0,85 mm/s crosshead displacement rate. Vertical displacement and indirect tensile strength were recorded for each specimen. Lower values of $G^* \cdot \sin \delta$ relate to higher resistance of the binder to fatigue cracking at intermediate temperatures. Results showed that $G^* \cdot \sin \delta$ decreased as the percentage of crumb rubber increased.

The IDT was chosen to predict the fatigue performance of mixtures made with CRM binders used in this study. Tests performed on field cores taken from WesTrack test track sections have shown that the absorbed energy up to the point of failure (fracture energy) calculated from the IDT strength test is an excellent indicator of the resistance of a mixture to fatigue cracking. Thus, the fracture energy parameter was selected to investigate the fatigue resistance of mixtures in the present study.

Results of the tests at 30 °C showed that increasing the rubber content of the binders increased both the absorbed failure energy and the indirect tensile strength of the samples, although the change in the absorbed energy was more pronounced (Figure 8-30). This indicates a greater capacity to flex and absorb the mechanical work induced by repeated tire loading on the pavement. Less work is dissipated through crack formation and accumulated damage, resulting in better resistance to fatigue cracking in pavements using crumb rubber modified binders. These results are consistent with the $G^* \cdot \sin \delta$ results, showing better fatigue resistance in CRM binders.

In the next stage, the CRM binders were subjected to strain controlled time sweep fatigue tests. Tests were done in triplicate for each binder. One property of strain controlled fatigue tests in both binders and mixtures is the lack of a clear failure point. Many criteria have been suggested for determining the point of failure in such tests, the most common being the point where G^* reaches 50% of its initial value, $N_{50\%G^*ini}$. Another criterion, N_p is determined by calculating the cumulative dissipated strain energy ratio (DER) in each cycle and plotting the DER against the number of cycles (N). The point of intersection between the higher and lower asymptotes is defined as N_p .

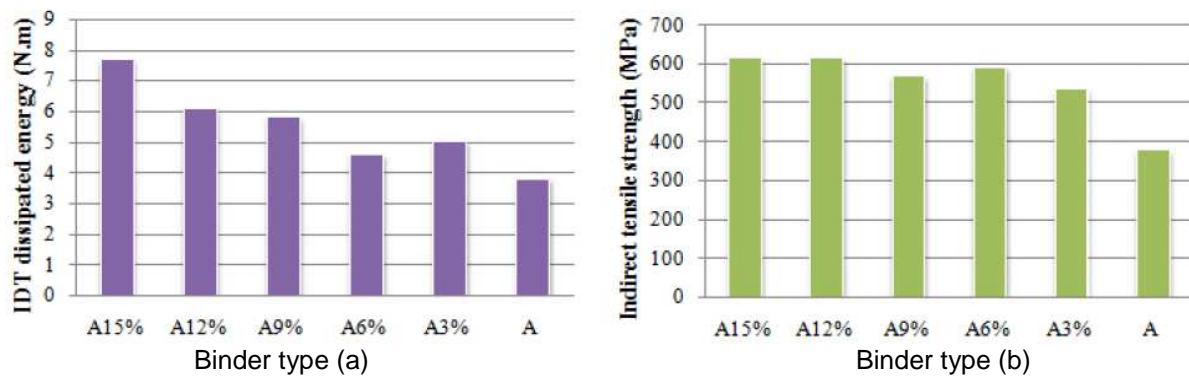


Figure 8-73: (a) absorbed energy to failure and (b) indirect tensile strength, tested at 30°C

The results of the fatigue tests conducted on CRM binders and mixtures, including a time sweep at 15 Hz, are shown in Table 8-25. N_p was observed to increase as the rubber content increased while the results using $N_{50\%G^*ini}$ as the failure criteria followed a different trend. The time sweep showed that crumb rubber modification increased the fatigue life significantly. Judging by the other parameters measured, this is due to the combined effect of decreased stiffness and increased tensile strength and elasticity at intermediate temperatures in CRM binders.

For a completely undamaged binder, the slope of the DER-N curve will remain constant as the amount of dissipated energy in each cycle remains unchanged compared to previous cycles. As fatigue damage occurs, more energy dissipates in the form of micro cracks forming in the binder, causing the DER line to deviate from linearity. In the present study, it was seen that, for binders with relatively low rubber content, the slope of the DER curve increases rapidly. The slope deviation from linearity was less pronounced for the A9% and A12% binders, while the DER slope for A15% remained relatively constant, even after extending the normal duration of the test, indicating the significant improvement in fatigue resistance for high rubber contents.

Table 8-25: Results from binder and mixture laboratory fatigue resistance tests

Binder Type	Time Sweep at 15 Hz and 30°C		$G^* \cdot \sin\delta$ at 30°C	Indirect Tensile Test at 30°C	
	Avg. N_p	Avg. $N_{50\%G^*ini}$	kPa	Strength (MPa)	Diss. Energy (N.m)
A	16 158	9 850	1 087	379	3,8
A3%	22 214	5 775	707	538	5,0
A6%	18 474	3 925	666	593	4,6
A9%	33 495	6 500	765	569	5,8
A12%	41 294	21 267	514	616	6,1
A15%	50 220	52 200	467	616	7,7

The time sweep results and $G^* \cdot \sin\delta$ for all binders tested at 30°C were plotted against the results of the IDT mixture tests to evaluate the conformation of the binder parameter to mixture fatigue (Figure 8-30). In all figures, the data points from left to right correspond to binders with increasing rubber content. According to the R2 values shown in Figure 8-30(a) and (b), $G^* \cdot \sin\delta$ correlates well with IDT tensile strength, but only moderately well with IDT dissipated energy, which is a more relevant parameter to fatigue. But it can be seen that the high R2 value for Figure 8-30(b) is due to the data point at the far left of the graph. Eliminating this data point reduces R2 to 0.688. Note that this correlation is better than results obtained by researchers such as Bahia et.al (3,5) for other types of modified binders.

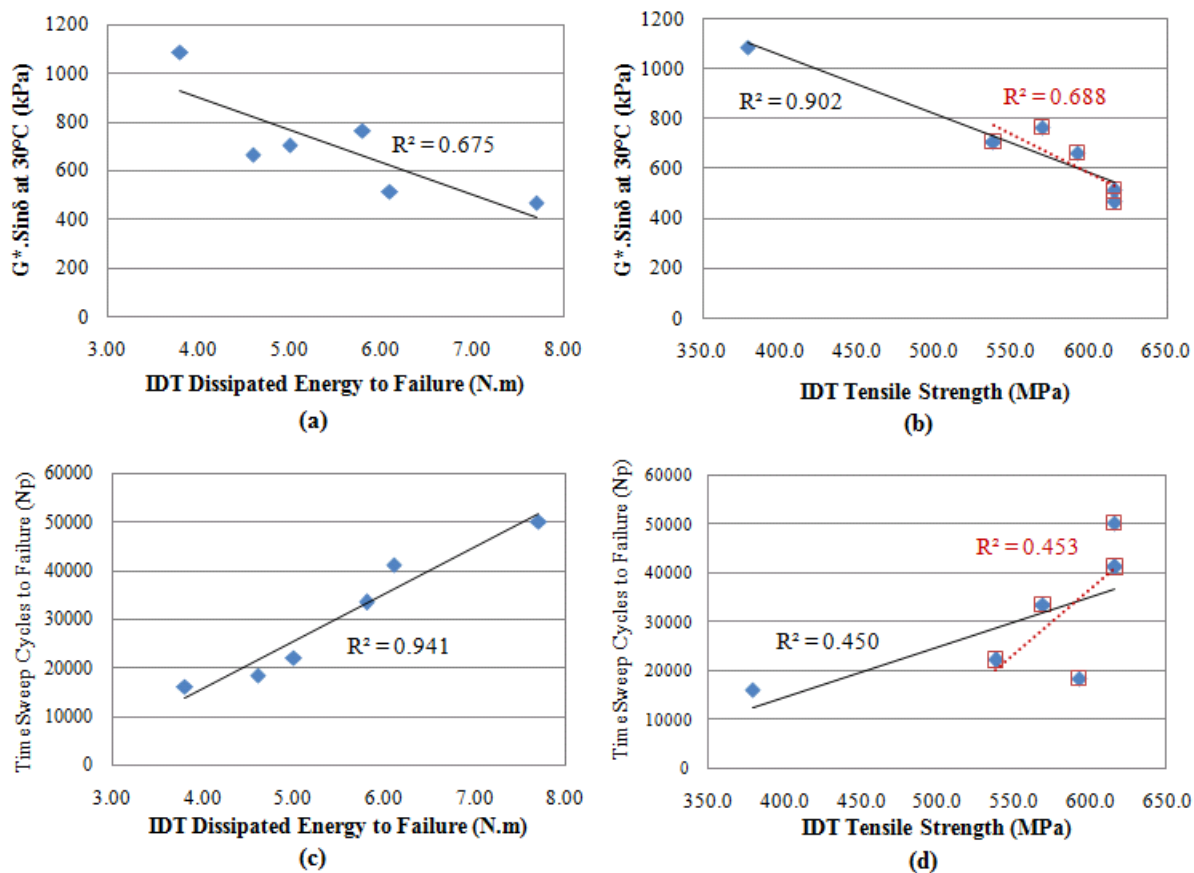


Figure 8-74: Correlation between fatigue binder and mixture test parameters

The results indicate that the time sweep test can be a better indicator of mixture fatigue behavior than the current $G^* \cdot \sin \delta$ specification. DSR linearity tests on CRM binders show that binder response is non-linear at intermediate temperatures. Thus, the $G^* \cdot \sin \delta$ test run at a low strain of 1% cannot properly reflect the behavior at higher strains. Binders may undergo much higher strains under loading in pavements, thus the assumption that fatigue damage occurs within the linear visco-elastic range is not accurate. To take this into account, time sweep tests are usually conducted at 5 % to 10 % strain. Furthermore, unlike the few loading cycles in the $G^* \cdot \sin \delta$ test, the time sweep uses a relatively large number of cycles, which is more similar to actual conditions.

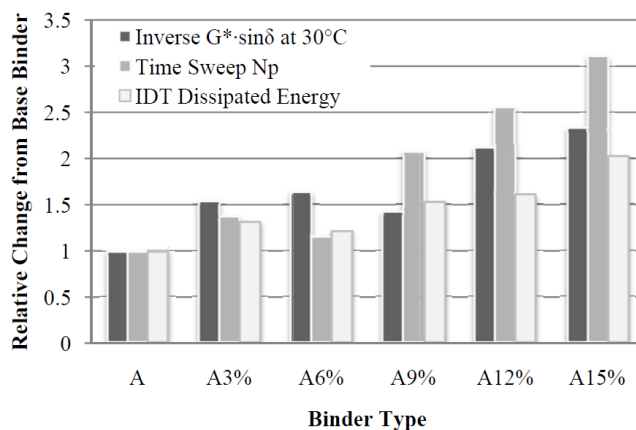


Figure 8-754: Relative change in each parameter compared to unmodified binder (Binder A)

Figure 8-30 shows the relative change in results obtained from each test compared to the test results for unmodified base binder. The inverse of $G^* \cdot \sin \delta$ was used in the figure to accommodate the increasing trend of the other two parameters. The time sweep test shows the highest sensitivity to modification compared to $G^* \cdot \sin \delta$ and IDT dissipated energy. The difference in sensitivity to modification between N_p and $G^* \cdot \sin \delta$, especially in the highly modified binders, shows the advantage of the time sweep test as an indicator of the presence of modification and its effect on binder properties, as well as underlining the tendency of the current Superpave criteria to underestimate the scope of improvement in fatigue performance exhibited by CRM binders.

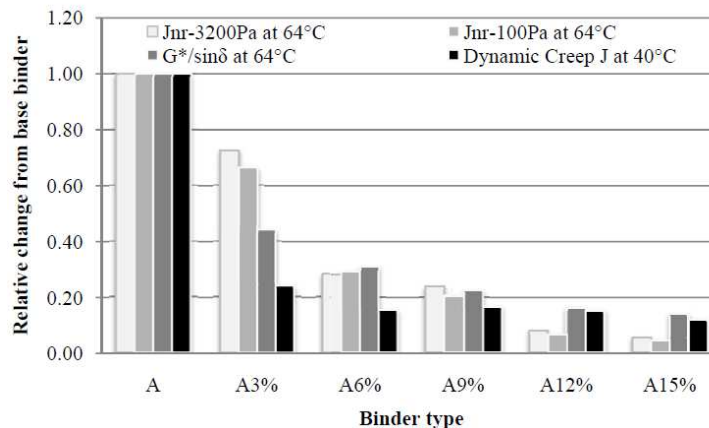


Figure 8-76: Relative change in each parameter compared to unmodified base binder

Comparison of the sensitivity of each test to crumb rubber modification was carried out as shown in Figure 8-30. As expected, the binder tests are more sensitive to binder modification than the mixture test, where factors such as aggregate properties contribute to the results. It can be seen that J_{nr} changed to a greater degree as CRM content increased compared to $G^*/\sin \delta$. Results for binders with 12 % and 15 % rubber content show that $G^*/\sin \delta$ underestimates the performance of highly modified CRM binders. It can be concluded that J_{nr} is a very suitable parameter for comparing modified and unmodified binders and the results are clearly related to the amount of modification.

The time sweep test better predicted fatigue resistance of CRM binders than did the traditional $G^* \cdot \sin \delta$ parameter, although $G^* \cdot \sin \delta$ performed well. However, replacing $G^* \cdot \sin \delta$ with the time sweep test is inefficient because of the long duration of the latter test.

8.3.2.10 Paper 545 (Jones et al., 2010)

For this study two sources of reclaimed asphalt mixtures were obtained from two different pavements under rehabilitation. The reclaimed asphalt mixtures, F1 and F2, were tested in laboratory in order to characterize their physical properties. Recovered bitumen for both types had a penetration between 12 dmm and 18 dmm. Reclaimed asphalt mix F1 presented an asphalt content of 5,9 %, whereas the F2 material exhibited an asphalt content of 5,0 %. The design of the asphalt rubbers to be applied with RAP considered two types of bitumen binders – 35/50 and 50/70.

The crumb rubber from waste tyres used in this study was obtained through the cryogenic process. The rubber has gradation between 0,18 mm and 0,6 mm. The difference in the content of crumb rubber used in two binders results from the fact that the 50/70 is softer than 35/50. The softer binders can be mixed with more crumb rubber without increasing the viscosity of the asphalt rubber. The content of crumb rubber was between 18 % and 24 %.

Table 8-26: Rubber modified bitumen (RMB) characteristics

RMB	Bitumen	Rubber content (%)	Penetration (mm/10)	Softening point (°C)	Viscosity (cP)	Resilience (%)
A1	50/70	18	22	57	2013	53
A2	50/70	20	21	71	2758	58
A3	50/70	22	20	73	4975	61
A4	50/70	24	19	78	8537	64
B1	35/50	18	22	69	2104	55
B2	35/50	19	21	71	2705	56
B3	35/50	20	19	73	3533	56
B4	35/50	21	19	73	5229	59

Based on the obtained results, a content of 22 % crumb rubber may be used to produce asphalt rubber with 50/70 pen asphalt, as it was used in this study (binder A3). For the 35/50 pen asphalt, only 20 % crumb rubber can be used (binder B3).

The next phase of this work aimed at the evaluation of the characteristics of the binder resulting from the addition of asphalt rubber to the recovered asphalt from reclaimed mixes, simulating a recycling process. For this study both asphalt rubbers defined above (A3 and B3) were used. For F1 material, which allows using up to 30 % of reclaimed material, three recycling ratios were defined: 10 %, 20 % and 30 %. For F2 material, which allows using up to 45% of reclaimed material, 10 %, 25 % and 40 % recycling ratios were defined.

As the recycling ratio increases the recycled binder remains less modified by the crumb rubber and the expected performance of the recycled asphalt mixes will be reduced if compared with the performance of typical asphalt rubber mixes.

Table 8-27: Recycled binder characteristics

Bitumen rubber RAP	RAP content (%)	Penetration (mm/10)	Softening point (°C)	Viscosity (cP)	Resilience (%)	Rubber content (%)
A3	10	19	72	3484	53	19,8
F1	20	18	72	2816	48	17,6
	30	15	74	1430	47	15,4
B3	10	19	73	2512	49	18,0
	20	18	72	1549	44	15,0
	30	16	70	966	42	12,0
B3	10	22	76	2275	54	18,0
	20	23	75	1354	50	15,0
	30	24	70	800	44	12,0
A3	10	20	75	3525	56	19,8
	20	21	73	1946	52	17,6
	30	21	71	916	47	15,4

The recycled mixture with 30 % of F1 reclaimed material and B3 was characterized in terms of Marshall properties, stiffness modulus and fatigue resistance for 5 binder contents (8,5 %; 9 %; 9,5 %; 10 % and 10,5 %).

The test configuration employed in this study was the four-point bending test in controlled strain. Flexural fatigue tests were conducted according to the AASHTO TP 8-94. All tests were carried out at 20 °C and at 10 Hz. Fatigue failure was assumed to occur when the flexural stiffness reduces to 50 % the initial value. The fatigue tests were conducted in strain control applying 3 different strain levels (400×10^{-6} , 600×10^{-6} and 800×10^{-6}) and for each one 3 specimens were tested through a sinusoidal loading without rest periods. The mixtures with 9 %, 9,5 % and 10 % binder content were tested with only 2 strain levels. Despite this fact, the results presented a high precision, as illustrated in Figure 8-30. The analysis of this figure

allows the conclusion that, as expected, the increase of the binder content of the asphalt mixture increases the fatigue resistance. This fact allows that the binder content can be defined as a function of the expected traffic.

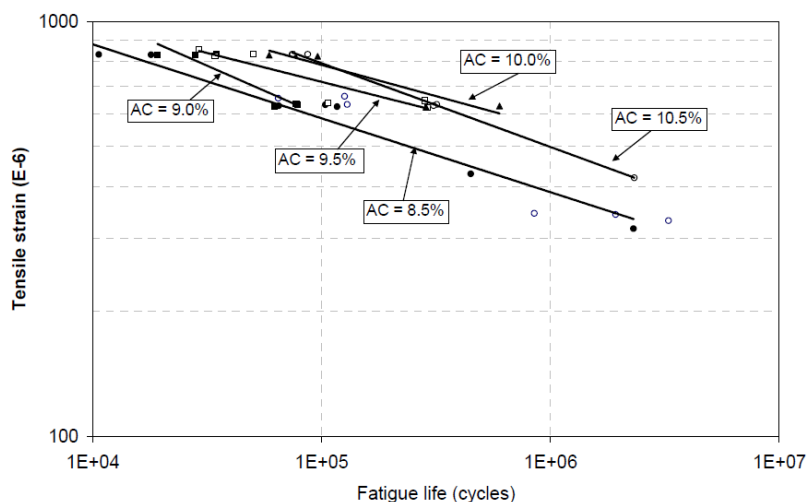


Figure 8-77: Fatigue curves for the recycled mixtures

The fatigue test results expressed in terms of fatigue law are presented in Table 8-128– the N_{100} (fatigue life for a strain of 100×10^{-6}) and ϵ_6 (tensile strain for a fatigue life of 1×10^6).

Table 8-28: Coefficients of the fatigue laws

Binder content (%)	a	b	R ²	N ₁₀₀	ε ₆
8,5	9,76E+19	5,419	0,966	1,42E+09	382
9,0	7,25E+14	3,574	0,865	5,16E+07	302
9,5	3,83E+22	6,163	0,859	1,81E+10	491
10,0	1,65E+22	5,940	0,895	2,18E+10	537
10,5	2,13E+19	4,941	0,998	2,79E+09	498

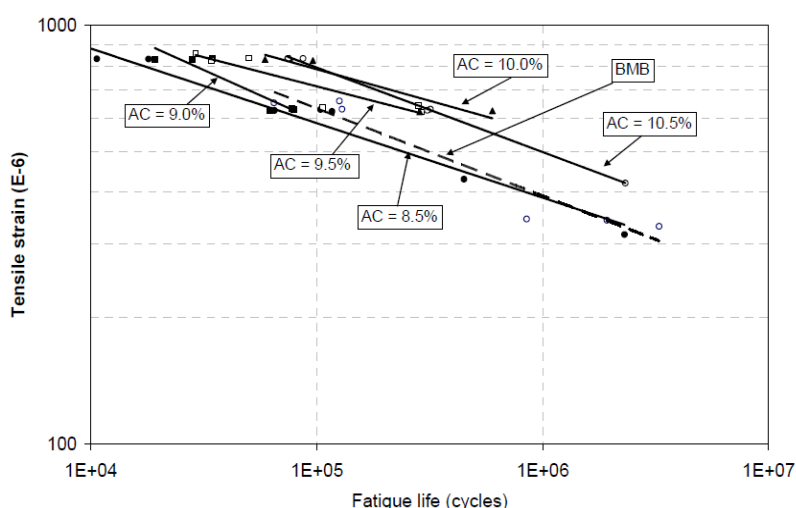


Figure 8-78 – Comparison between recycled mixtures and asphalt rubber mixture

The fatigue resistance of the recycled mixtures was compared to the typical mixtures with asphalt rubber. Thus, it can be concluded that they have an identical performance as the

typical asphalt rubber mixtures (Figure 8-30). Some differences can be found in this comparison due to the binder content. Nevertheless, it can be established that for an average binder content of 9,0-9,5 %, the performance is identical, suggesting that recycling does not affect the fatigue performance.

8.3.2.11 Paper 563 (Tabatabaee & Tabatabaee, 2010)

In the study done by Wen et al. five bituminous binders (PG70-22, air-blown, SBS LG, CR-TR, terpolymer modified bitumen) and five asphalt mixtures containing these binders with same aggregates sources were tested at intermediate temperatures. Four of the binders were modified with different techniques. The binder content was in the mixes always the same (5,3 %). Fatigue resistance was assessed by critical strain energy density of the binder and the resulting asphalt mix.

Bahia et al. reported that there was strong correlation between the fatigue life of bituminous binder and that of asphalt mixture at intermediate temperature and proposed cyclic fatigue test to replace the fatigue parameter in the Superpave Binder Specification. Johnson et al. introduced a new fatigue testing protocol for bitumen, the monotonic constant shear-rate test which has been demonstrated to have great potential to be a fatigue test. For asphalt mixture, current practice relies on Superpave volumetric mix design to produce an asphalt mixture with good performance. However, it has been proposed to supplement the volumetric design with simple performance test, such as dynamic modulus which is also an important parameter in the fatigue model in the mechanistic-empirical pavement design guide (MEPDG). In addition, fracture properties, such as critical strain energy density (CSED), from the indirect tensile (IDT) tests have shown good potential to be a fatigue indicator, which correlated well with the field fatigue performance.

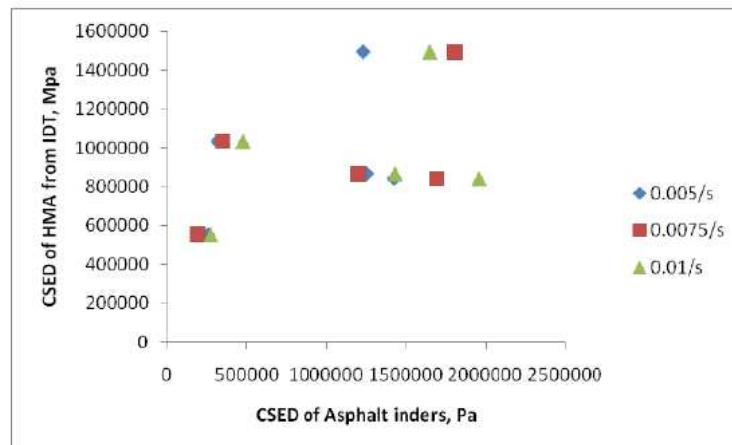


Figure 8-79 – Relationship between CSED of bitumen and asphalt mixture

Following results of the study, HMA with SBS modified binder had the highest CSED. The fatigue resistance of binders and mixtures were studied, in terms of critical strain energy density (CSED). Similar to the findings for the strength characteristics of bitumen and mixtures, there is no direct correlation between the CSEDs of binders and those of mixtures (see Figure 8-30). It indicates that a fatigue-resistant binder does not necessarily cause fatigue-resistant mixtures. As mentioned above, it is believed that the interaction between aggregates and binders probably plays a significant role in the fatigue resistance of mixture.

8.3.2.12 Paper 548 (Baptista et al., 2008)

In this study fatigue was determined by test method 4PB-PR according to EN 12697-24. Tests were carried out at 20 °C on 18 specimens. Loading frequency changed from 30 Hz to

10 Hz (more references). Six strain levels were selected in order to obtain a fatigue rupture between 1×10^4 and 2×10^6 . As failure criterion the 50% reduction of initial stiffness modulus value was used. The fatigue cracking resistance was given by N_{100} (resistance for tensile strain 100×10^{-6}), ϵ_6 (resistance of 1×10^6) parameters and slope p of fatigue line (equal to parameter b).

Table 8-29: Fatigue cracking characteristics and CE marking categories

Bituminous mixture	Fatigue law parameters			N_{100}	EN 12697-24 values		CE marking category ϵ_6
	a	b	R^2		ϵ_6	p	
AC 0/14	1,913E+17	5,099	0,924	1,210E+07	163,076	5,099	ϵ_6 160
SMA 0/11	1,680E+17	4,836	0,936	3,581E+07	209,609	4,836	ϵ_6 190
AR 0/12	1,357E+19	5,568	0,949	9,922E+07	228,405	5,568	ϵ_6 220

8.3.2.13 Paper 463 (Taylor et al., 2010)

The mix design used for the control mixture was a 19 mm NMAS asphalt. A PG 67-22 binder modified by the addition of 0,5 % by bitumen weight of an anti-stripping agent (AD-here® 1500) was used for all the mixes evaluated in this study. For the sulfur-modified warm mixes, this binder was further modified with 1,52 % by the binder weight of a compaction additive. Four asphalt mixtures modified with the sulfur pellets were used for this study. Two mixes each were designed with 30 and 40 % sulfur as a partial replacement for the virgin binder. For each percentage of sulfur, a ‘base’ and a ‘rich bottom’ layer mixture was tested in the laboratory. The base layer mixes were designed with 3,5 % air voids and the rich bottom layer mixes were designed with 2 % air voids.

In the laboratory, the control mixture was short-term aged for two hours at 315 °F and all the sulfur-modified samples were short-term aged in the oven at a temperature of 284 °F for two hours before compaction.

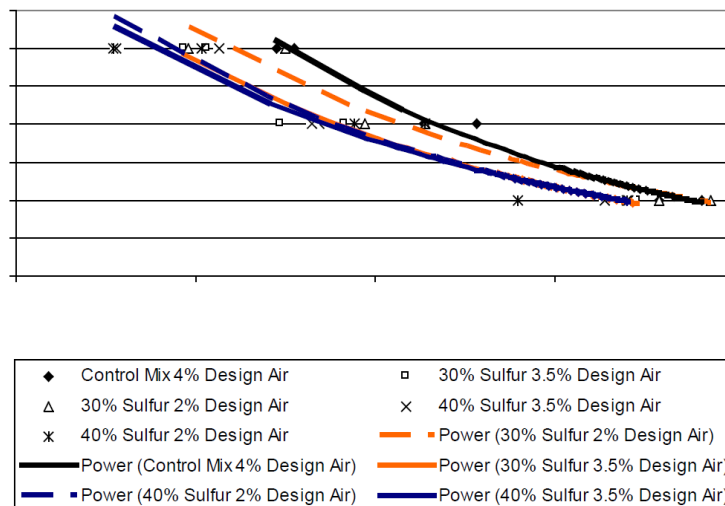


Figure 8-80: Comparison of fatigue resistance (ASTM D7460) for tested mixtures

Six beam specimens were tested for each mix. Within each set of six, two beams each were tested at 200 microstrain, 400 microstrain, and 600 microstrain. The beam fatigue apparatus applies haversine loading at a frequency of 10 Hz. Testing was performed at $68 \pm 0,9$ °F. ASTM D 7460 recommends that the test be terminated when the beam stiffness is reduced to 40 percent of the initial stiffness. To ensure a complete data set for the analysis, the

beams for this project were allowed to run until the beam stiffness was reduced to 30 % of the initial stiffness.

AASHTO T 321 defines failure as the number of cycles after which the initial modulus of the beam has been reduced by 50 %. By running the test to a reduction in initial stiffness of 30 %, both an ASTM and an AASHTO number of cycles to failure could be determined for each beam.

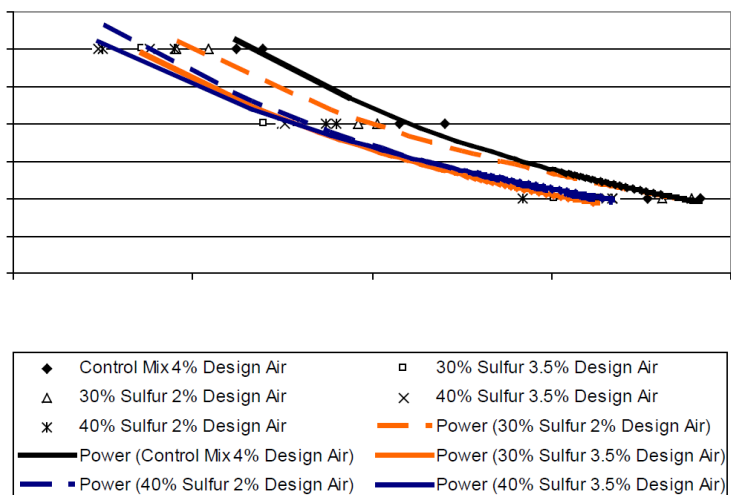


Figure 8-81: Comparison of fatigue resistance (AASHTO T 321) for tested mixture

Figure 8-30 and Figure 8-30 compare the fatigue cracking resistance of the five mixtures determined in accordance with ASTM D 7460 and based on AASHTO T 321, respectively. Both figures show similar relative relationships between the mixtures.

Table 8-30: Fatigue curve fitting coefficients, percentage difference of average cycles to failure for sulfur-modified mixtures versus control mixture and predicted endurance limits

Sulfur content (%)	Voids (%)	ASTM D7460			AASHTO T321			Strain Level			Endurance Limit (Microstrain)*	
		α_1	α_2	R^2	α_1	α_2	R^2	200 ms	400 ms	600 ms	ASTM D7460	AASHTO T321
0	4	5611	-0,22	0,982	4415	-0,20	0,984	-	-	-	99	102
30	3,5	3367	-0,19	0,975	3144	-0,20	0,990	-54%	-82%	-68%	83	79
30	2	3491	-0,18	0,963	3007	-0,18	0,995	8%	-50%	-36%	98	119
40	3,5	2966	-0,18	0,972	2497	-0,17	0,993	-57%	-83%	-73%	84	98
40	2	3211	-0,19	0,890	3180	-0,19	0,957	-70%	-52%	-78%	60	69

Note: * 95% one-sided lower prediction limit

Based on the model coefficients in Table 8-30, there was a significant difference between the magnitude of the intercept (α_1) and slope (α_2) terms between the control mixture and the sulfur-modified mixtures. This table also shows the percentage difference between the average fatigue life of the control mixture and the average fatigue life of the sulfur-modified mixtures at the three strain levels tested in this study using the failure point as defined by the ASTM method. This information helps evaluate important aspects of the material behavior shown in Figure 8-30 as follows:

- At the high strain level of 600 microstrain, the control mixture exhibited the longest fatigue life. The average fatigue life of the control mixture was between 36 % and 78 %

- longer than that of the sulfur-modified mixtures. The 30 % sulfur mix with 2 % air voids had the longest fatigue life among the sulfur-modified mixes at this high strain level.
- At 400 microstrain, the average fatigue life of the control mixture was 82 to 83 % longer than the 30 % and 40 % sulfur mixes with 3,5 % design air voids, respectively. The control mixture had an average 50 % and 52 % longer fatigue life than the sulfur-modified mixtures with 2 % design air voids.
 - At the strain level of 200 microstrain, the control mixture had a significantly longer fatigue life compared to three of the sulfur-modified mixtures (30 % and 40 % sulfur mixes with 3,5 % design air voids, and 40 % sulfur mix with 2 % design air voids). Each of these sulfur-modified mixtures had an average fatigue life between 54 % and 70 % shorter than that of the control mixture. However, the 30 % sulfur mix with 2 % design air voids exhibited an average fatigue life approximately 8 % longer than that of the control mixture.
 - The results suggested that the 30 % sulfur mix with 2 % design air voids was the superior performing sulfur-modified mixture in fatigue across the whole range of strain levels, but most notably at the low strain levels.

Table 8-30 also shows the 95 % one-sided lower prediction of endurance limit based on the number of cycles to failure determined in accordance with ASTM D 7460 and AASHTO T 321. Based on the results, the 30 % sulfur mix with 2 % design air voids had the highest predicted endurance limit among the five mixes tested in this study (according to the AASHTO failure criteria). The control and the 40 % sulfur base layer mixes had the second highest endurance limit according to the AASHTO failure criteria. For the ASTM failure criteria, the control mix and the 30 % sulfur rich bottom layer mix exhibited an equivalent and the highest predicted endurance limits.

8.3.2.14 Paper 456 (Bennert & Martin, 2010)

Another research program was developed to examine and compare the laboratory properties of an asphalt binder modified with and without PPA. Asphalt mixture testing, consisting of Flexural Beam Fatigue tested at both short and long-term aged conditions. A neat PG64-22 asphalt binder was modified under two conditions; 1) 4,25 % SBS polymer (crosslinked) and 2) 2,5 % SBS (crosslinked) + 0,5% polyphosphoric acid (PPA).

Table 8-31: Continuous PG grade of bituminous binders

Bitumen type	Continuous performance graded
Neat	PG68,6-23,4 (23,4)
SBS+PPA	PG76,2-25,7 (22,0)
SBS Only	PG76,8-25,2 (21,1)

The asphalt binders were also characterized using the procedures outlined in the Multiple Stress Creep Recovery (MSCR) test, AASHTO TP70-07. The MSCR results for the asphalt binders are shown in Figure 8-30 and Figure 8-30. The results in Figure 8-30 indicate that SBS Only modified asphalt binder achieved the lowest J_{nr} at each test temperature, while the SBS + PPA modified asphalt binder achieved J_{nr} values approximately 55% higher than the SBS Only modified asphalt binder. Meanwhile, the neat asphalt binder was approximately 525% higher than the SBS + PPA and 850% higher than the SBS Only modified asphalt binders, respectively. The results of Figure 8-30 would indicate that the SBS Only modified binder would have a slightly better resistance to permanent deformation than the SBS + PPA modified binder. Meanwhile, both modified binders should perform significantly better in permanent deformation than the neat asphalt binder.

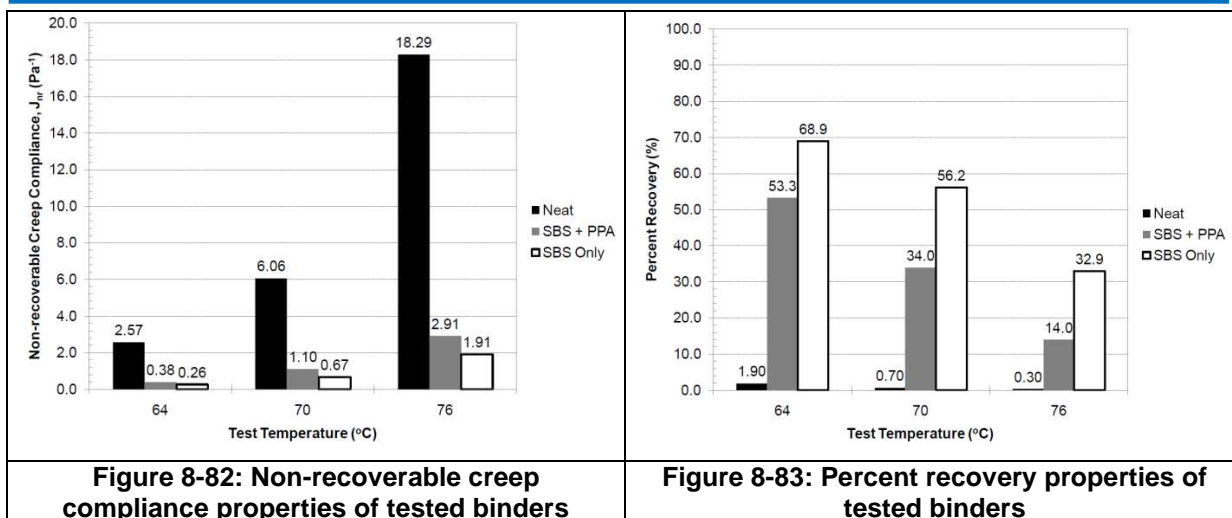


Figure 8-30 shows the Percent Recovery properties of the asphalt binders from the MSCR test. Both modified binders have considerable higher levels of percent recovery than the neat asphalt binder. On average, the SBS Only and SBS + PPA modified binders resulted in Percent Recovery values almost 98 % higher than the neat asphalt binder. Meanwhile, the SBS Only modified binder achieved Percent Recovery values on average 40 % higher than the SBS + PPA modified asphalt binder, with smaller differences found at the 64 °C test temperature and larger differences found at the 76 °C test temperature. This would be expected since the polymer loading in the SBS only asphalt binder was 1,75 % higher than the SBS + PPA modified asphalt binder.

Flexural Beam Fatigue test was done on a coarse-graded, 12,5mm Superspave mixes with 5,3 % binder. The applied tensile strain levels used for the fatigue evaluation were 250, 400, 600, and 800 micro-strains.

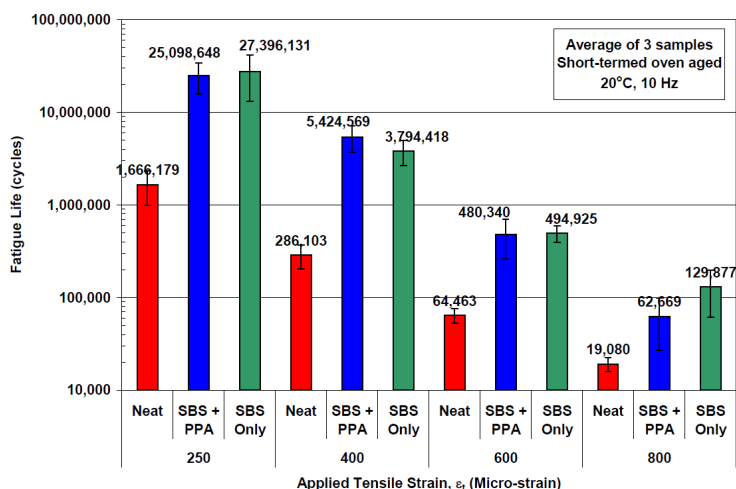


Figure 8-84: Flexural beam fatigue results for short term oven aging

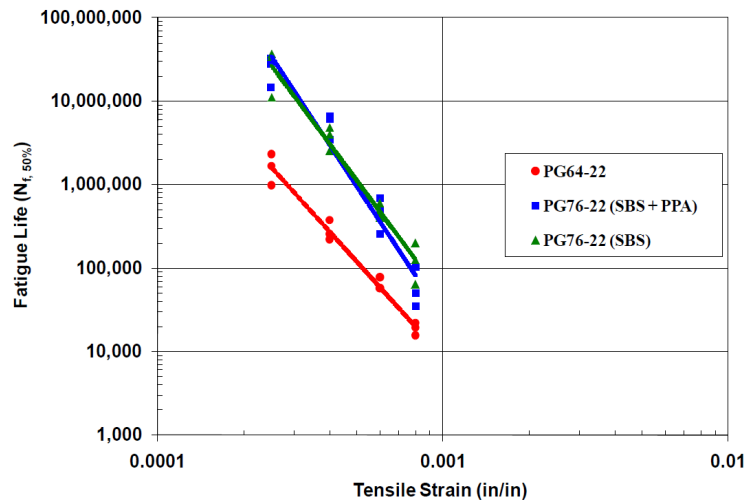


Figure 8-85: Fatigue-life curves for short term oven aged specimens

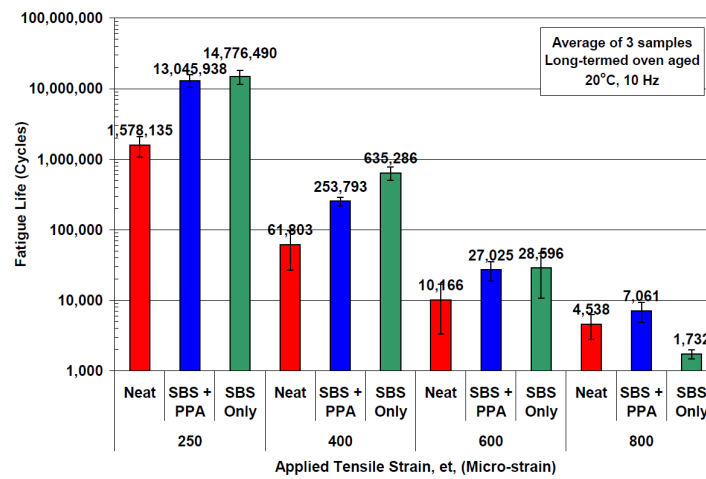


Figure 8-86: Flexural beam fatigue results for long term oven aging

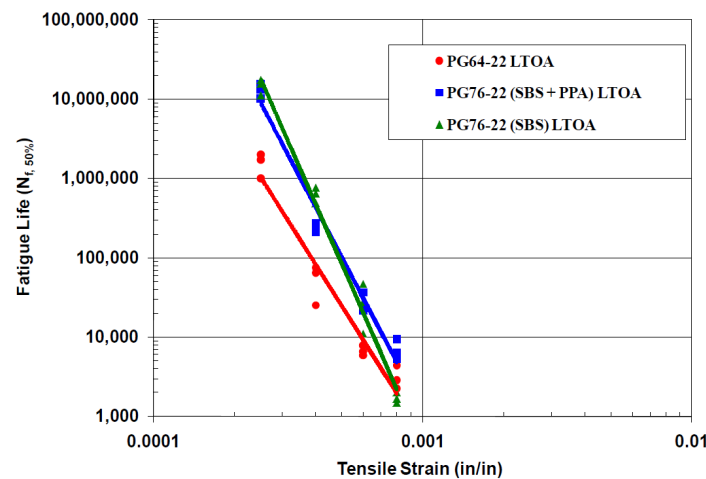


Figure 8-87: Fatigue life curves of long term aged specimens

Figure 8-30 and Figure 8-30 compare the triplicate test results and their measured variability while Figure 8-30 and Figure 8-30 shows the fatigue life regression.

Based on the average results of the STOA and LTOA aged samples, the SBS Only modified asphalt had a slightly greater fatigue resistance than the SBS + PPA modified asphalt. In both the STOA and LTOA aged conditions, the Neat asphalt binder achieved the lowest fatigue life.

8.3.2.15 Paper 085 (Mogawer et al., 2011)

Fatigue resistance was measured on different WMA technologies (Advera®, Evotherm 3G® and Sasobit®) using uniaxial cyclic direct tension-compression fatigue test. The tests results were analyzed using the concept of reduced cycles (N_R) and effective strain. The main aim of the proposed approach is to get plots of the ratio between damaged modulus and undamaged modulus, as a function of the damage parameter “S” “collapse”, by choosing the appropriate value for the continuum damage constant α . Some results are presented in Figure 8-88 and Figure 8-89. Data showed no significant difference in the fatigue crack resistance for the HMA and WMA using 75 and 100 gyrations mix (except for the Advera).

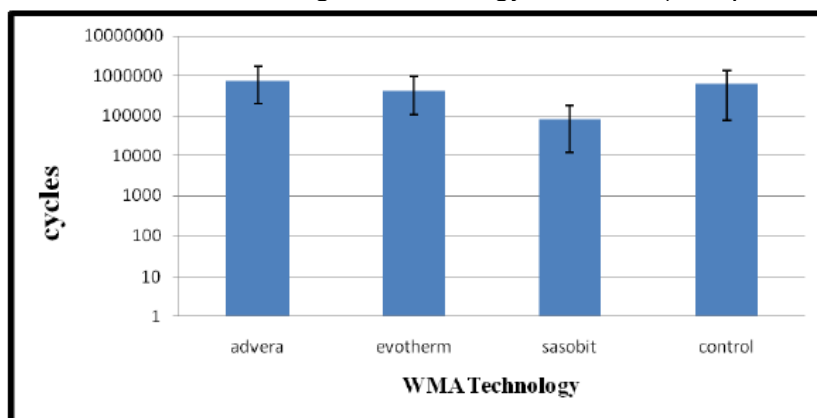


Figure 8-88: Comparison of number of cycles for 50% damage for the 100 gyrations mixtures

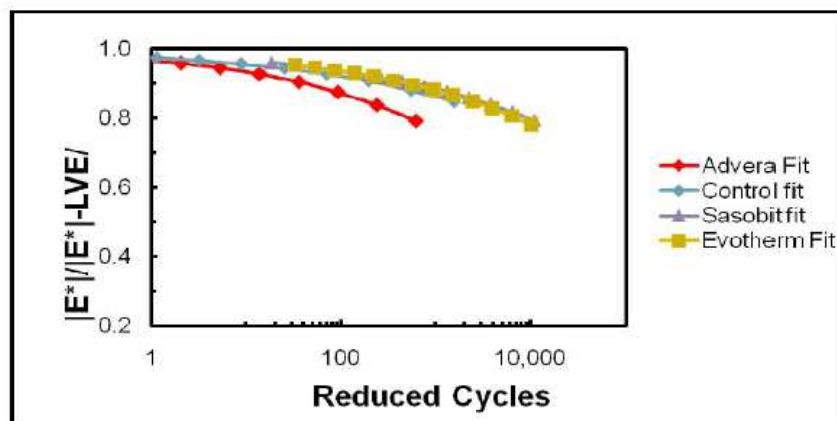


Figure 8-89: Comparison of continuum damage fatigue curves for the 75 gyrations mix

8.3.2.16 Paper 137 (Baek et al., 2012)

The performance of Warm-Mix Asphalt (WMA) with wax-based additives, named low energy and low carbon dioxide asphalt pavement (LEADCAP) and developed in Korea, have been studied in this paper. LEADCAP is an organic additive of a wax-based composition including crystal controller and artificial materials. The LEADCAP allows producing and paving WMA at 30°C lower temperature than HMA. Three different mixtures have been tested: WMA with LEADCAP; WMA with Sasobit® additives; and a conventional HMA mixture.

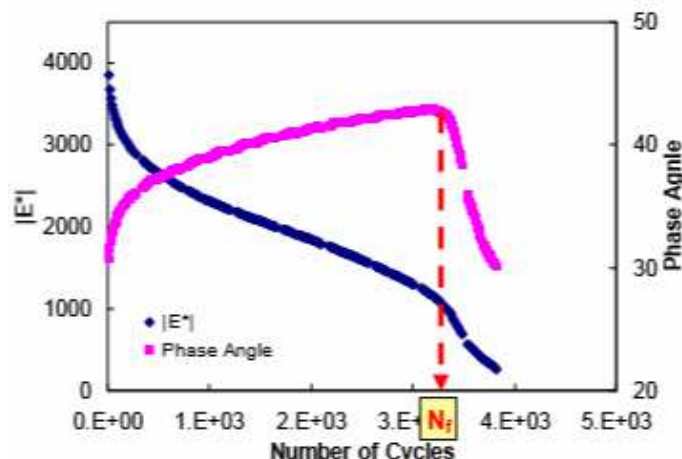


Figure 8-90: Changes in dynamic modulus and phase angle as the cyclic loading continues

Fatigue tests have been performed on cylindrical specimens with controlled crosshead cyclic testing (CX) condition. To define the failure of specimen, the phase angle criterion has been chosen in which sudden change of phase angle means failure. An example is depicted in Figure 8-90.

From Figure 8-91, it can be observed that HMA proved to have the better fatigue resistance (*i.e.* number of cycles to failure), followed next by WLC (WMA with LEADCAP) and, finally, by WSA (WMA with Sasobit®). Care should be taken in concluding from these observations that HMA is the most performing asphalt mixture tested and WSA the less performing. The fatigue performance must be evaluated by considering both resistance to deformation (stiffness) and resistance to damage, which is possible through the pavement evaluation.

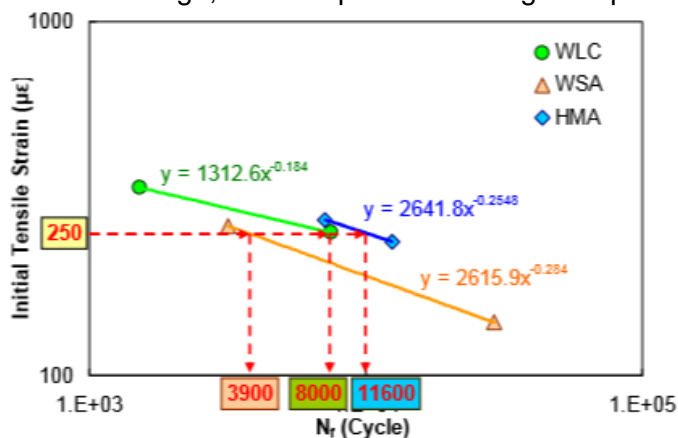


Figure 8-91: Initial tensile strain versus the number of cycles to failure

8.3.2.17 Paper 480 (Racanel et al., 2010)

A study was presented comparing traditional hot mix asphalt with two types of warm mix asphalt (WMA) using surfactant and synthetic wax. Standard bitumen 50/70 was used. For optimizing the possible temperature reduction six options of bitumen modification have been prepared (2 %; 3 % and 4 % wax and 0,2 %; 0,3 % and 0,4 % surfactant). Additives mixed for 5 minutes at 130 °C. Standard production temperature 160°C was reduced by 15 °C for wax and by 30 °C for the surfactant. For stiffness and fatigue testing besides AC14 also option with RAP were prepared with bitumen 160/220 + 6 % wax and temperature reduction of 30 °C as well as bitumen 50/70 + 0,5 % surfactant and 30 °C temperature reduction. Fatigue was evaluated for 20°C by means of decrease of the stiffness to 50% of its initial

value. WMA show similar behavior and the use of selected additives do not affect fatigue performance.

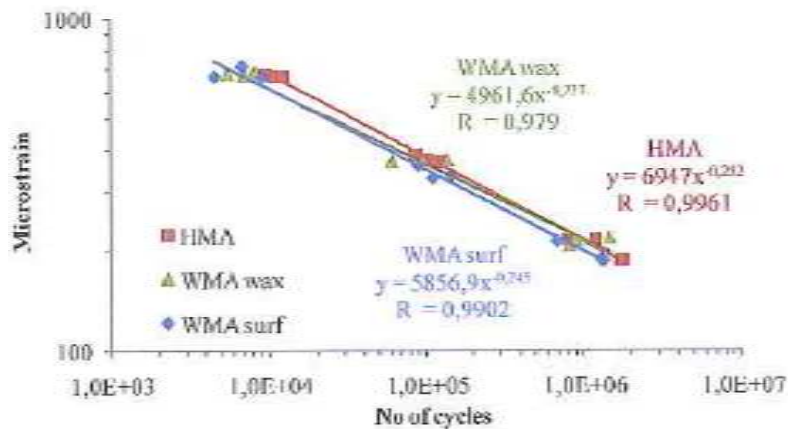


Figure 8-92: Fatigue curves of HMA and WMA at 20 °C

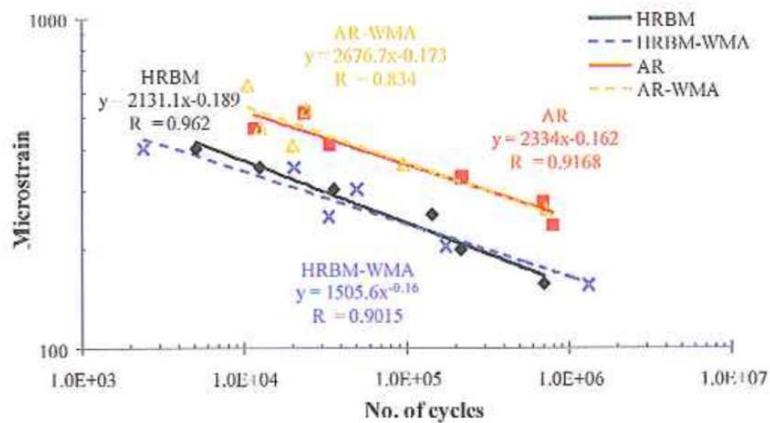


Figure 8-93: Fatigue cracking resistance of AR and HRBM (HMA and WMA) mixtures at 20 °C

8.3.2.18 Paper 565 (Haritonovs et al., 2012)

In this study laboratory tests were performed in order to establish which viscosity modifying additive should be used. It was intended to not affect any mechanical engineering modifications at the asphalt mixing plants required by LT asphalt tests, we selected organic additives. Fatty acid amides were selected. The properties of three different fatty acid amides were compared in the laboratory. One sample was from Ireland, while the other two samples came from two different manufacturers in Italy. In the course of the laboratory tests, the three additives were mixed with bitumen 50/70 and viscosity was tested at various temperatures. Asphalt mixes were produced as well.

The focus of the tests was to establish the rate the three additives reduces the viscosity of the 50/70 bitumen used most frequently in Hungarian road construction. For that reason the three additives were mixed in a 0,4 % ratio. Viscosity was tested between 90-150 °C. The bitumen containing the additive from Ireland is marked 1/I, while the bitumen containing the two additives from Italy are marked 2/O and 3/O, respectively. Additive 1/I is a fatty acid amide. Figure 8-91 presents viscosity test results.

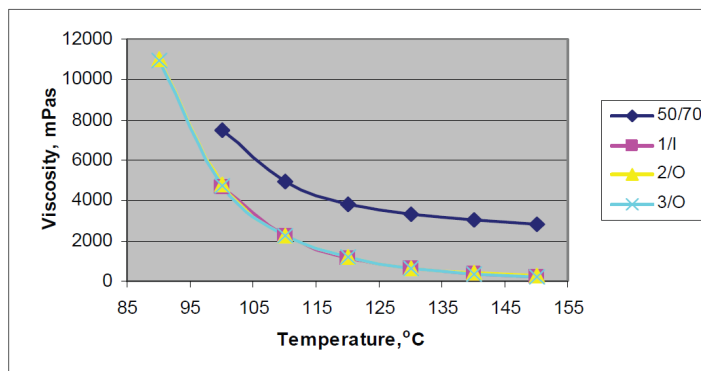


Figure 8-94: Viscosity of bitumens with additive

Figure 8-30 shows that the tested additives significantly reduce bitumen viscosity in the 100-150 °C temperature range. There is no considerable difference between the three additive types with respect to the rate of viscosity reduction. As a result of the laboratory tests additive 1/1 was selected to use in the course of laying a trial sections. Four of the trial sections were paved with 50/70 type bitumen and one with modified bitumen. The test results obtained from the core samples taken from one of the trial sections (low traffic road on the state public road network) are summarised in Table 8-32.

Table 8-32: AC 11 wearing 50/70 LT asphalt mix test results

Property	Test method	With additive	Without additive
Bitumen content, %	EN 12697-1	5,6	5,5
Fatigue, PB-TR 10 °C 25 Hz	EN 12697-24	107	87

Fatigue tests have shown that WMA has better fatigue characteristics than conventional mix.

8.3.2.19 Paper 552 (Kringos et al., 2010)

Two WMA technologies are considered: foaming by water injection and Evotherm 3G modification. For this study, the asphalt mixtures were subjected to laboratory conditioning in a forced air convection oven to simulate long-term field ageing according AASHTO R30. The asphalt mixtures and extracted binders were subjected to linear viscoelastic and fatigue characterisation following ageing using AASHTO R 30, samples were conditioned at 85 °C for two days and at 85 °C for eight days as the LTA Level 1 (LTA1) and Level 3 (LTA3) respectively. LTA1 corresponds to approximately four years of ageing in the field and LTA3 corresponds to approximately 18 years of ageing in the field. Cyclic direct tension tests were used to measure the fatigue resistance of the asphalt mixtures, and the linear amplitude sweep (LAS) test was used to measure the fatigue resistance of the binders. Simplified viscoelastic continuum damage (S-VECD) analysis was performed to interpret the fatigue test results and predict the fatigue performance of the binders and mixtures using a pavement structural model. The results demonstrate that after substantial long-term ageing, differences between the fatigue performance of WMA and HMA become insignificant. The results also demonstrate good agreement between the binder and mixture results, indicating that the LAS test coupled with S-VECD analysis is able to capture the binder’s contribution to mixture fatigue.

The mechanical testing of the asphalt binders were conducted using DSR with 8 mm plate. The linear viscoelastic characterisation considered of measuring the dynamic shear modulus ($|G^*|$) of the asphalt binders using frequency sweep tests at 1 % shear strain amplitude at 64 °C; 50 °C; 30 °C; 20 °C and 5 °C and a range of 0,1 -30 Hz loading frequency. The fatigue characterisation of the asphalt binders was measured using LAS tests at 19 °C. The LAS

test, AASHTO TP 101, is an oscillatory strain sweep test consisting of linearly increasing strain from 0,1 % to 30 % effective strain amplitude at a constant frequency of 10 Hz over the course of 310 s. A VECD framework can be applied to predict the fatigue life at any strain amplitude from the LAS test results.

Dynamic modulus and controlled crosshead (CX) cyclic direct tension tests were used to evaluate the linear viscoelastic properties and fatigue of the asphalt mixtures in this study. Dynamic modulus testing was performed in load-controlled mode in axial compression following the protocol given in AASHTO PP 61-09 using the Asphalt Mixture Performance Tester. Tests were completed for all mixtures at 5 °C, 20 °C and 40 °C and at frequencies of 25; 10; 5; 1; 0,5 and 0,1 Hz. Cyclic and direct tension tests were carried out in the CX mode in axial tension using a closed-loop servohydraulic material test system to measure the fatigue resistance of the asphalt mixtures.

Figure 8-30 presents the dynamic modulus and VECD damage characteristic curves for the binder and mixtures after STA. As expected, Figure 8-30(a) and Figure 8-30(b) shows that the HMA binder and corresponding mix are stiffer than both the WMA binders and mixtures due to reduced STA.

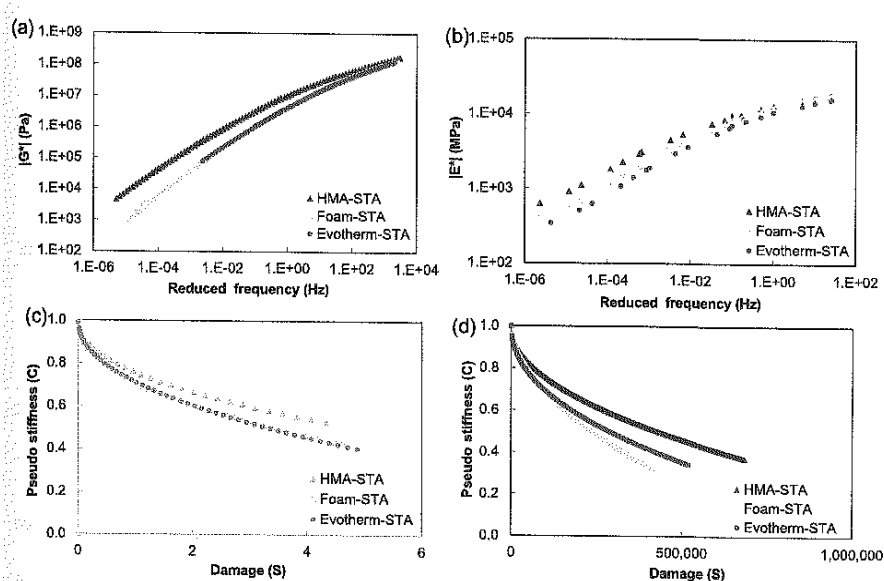


Figure 8-95 – STA master curves for (a) binders (b) mixtures, damage characteristic curves at a reference temperature of 19 °C for (c) binders (d) mixtures

For LTA1 trends in the dynamic modulus values are similar to those observed after STA. The WMA mixtures and corresponding binders have similar dynamic modulus values and are softer than the HMA mixtures and binder. The VECD damage characteristic curves are also similar. For LTA3 the results still indicate that the HMA binder is stiffer and, hence, more aged than WMA binders as a consequence of increased production temperatures. The C versus S curves of the WMA and HMA binders and mixtures have a similar pattern, indicating the important role of binder on mixture response (Figure 8-30).

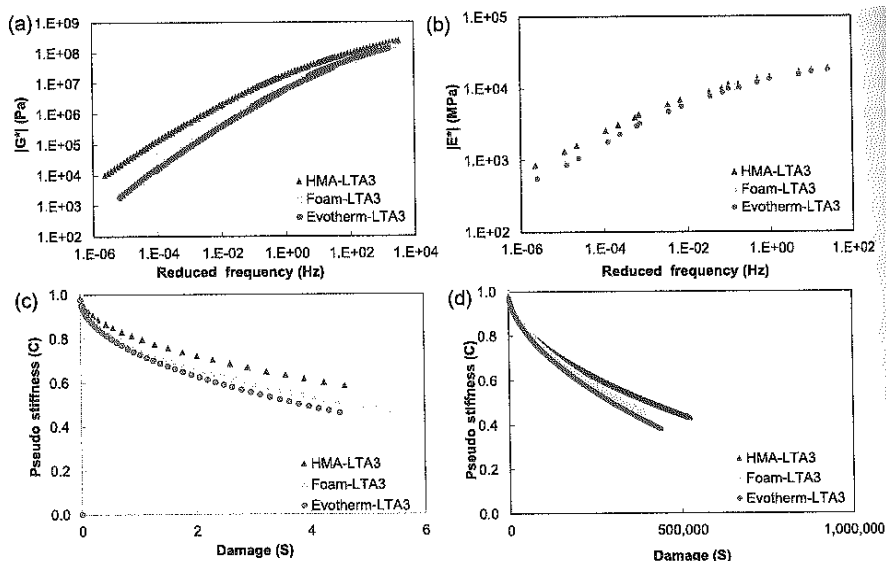


Figure 8-96: LTA3 master curves for (a) binders (b) mixtures, damage characteristic curves at a reference temperature of 19 °C for (c) binders (d) mixtures

In addition to the damage characteristic curves that are used to define fatigue resistance, the damage and material integrity (i.e. C value) at failure is also important in defining fatigue resistance. In this study, the fatigue life of asphalt mixture specimens tested in cyclic direct tension was determined by trends in the phase angle. It has been demonstrated that the phase angle increases until the point of damage localisation and, hence, the onset of macrocracking, and then decreases during the remainder of the test.

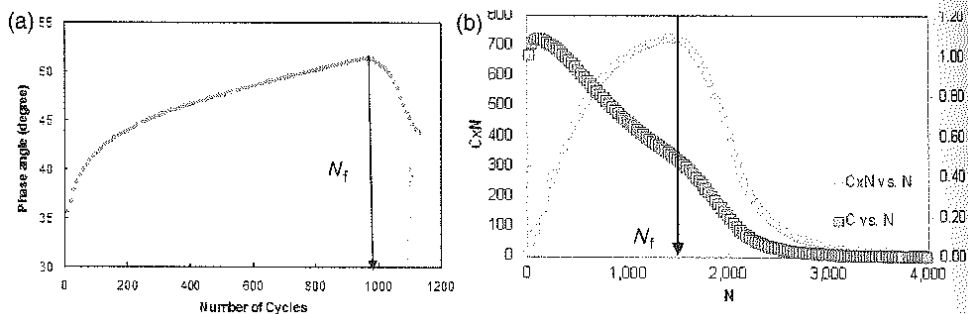


Figure 8-97: Fatigue definitions for (a) asphalt mixtures and (b) asphalt binders

Figure 8-30 presents the results of C value at failure (C_f) for the HMA and WMA mixtures and binders tested at all levels of ageing. Similar trends are observed for C_f for both the binders and mixtures, indicating the ability of the LAS test to capture the binder’s contribution to mixture fatigue and the important role that asphalt binder plays in determining mixture fatigue resistance. It can be seen that the relative magnitude of C_f does not change substantially, indicating C_f is not terribly sensitive to ageing. The C_f value generally increases as the ageing level increases, which is intuitive, because an increase in C_f implies damage localisation at a high material integrity level and, hence, increased brittleness, which is expected as the oxidation level increases. Also, the binder C_f values are higher than those for the mixtures and appear to be somewhat more sensitive to material type in general. However, there is some discrepancy in material ranking between the binder and mixture results at LTA3.

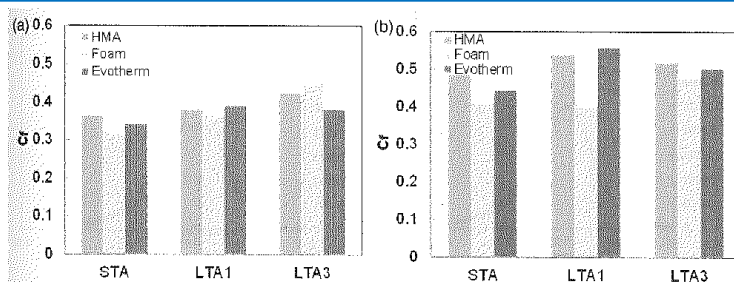


Figure 8-98: C value at failure for (a) mixtures and (b) binders

The fatigue performance of pavements is a function of the material’s ability to resist damage and also a function of the strain that the material experiences. Thus, it is important to consider both the loading that a given material will undergo in a given pavement structure as well as the material’s damage resistance characteristics to predict how an asphalt mixture will perform in the field. In this study, the fatigue performance of the asphalt mixtures was evaluated by combining the VECD model and the pavement responses determined from the structural analysis of the pavement. Because fatigue is the accumulation of damage over time, these results suggest that the HMA mixtures perform better than the WMA mixtures due to the superior performance of the HMA during the first two levels of ageing. Figure 8-30 shows that STA and LTA1, the HMA shows superior fatigue performance compared with the WMA. However, at LTA3, the differences in fatigue performance between the WMA and HMA become negligible, indicating that the effects of reduced short-term ageing in WMA compared with HMA diminish with increasing LTA for this pavement structure.

A similar approach was taken to evaluate asphalt binder fatigue performance using the pavement response strain kernels. However, it is not straightforward to convert the strain kernel results into equivalent asphalt binder strain levels.

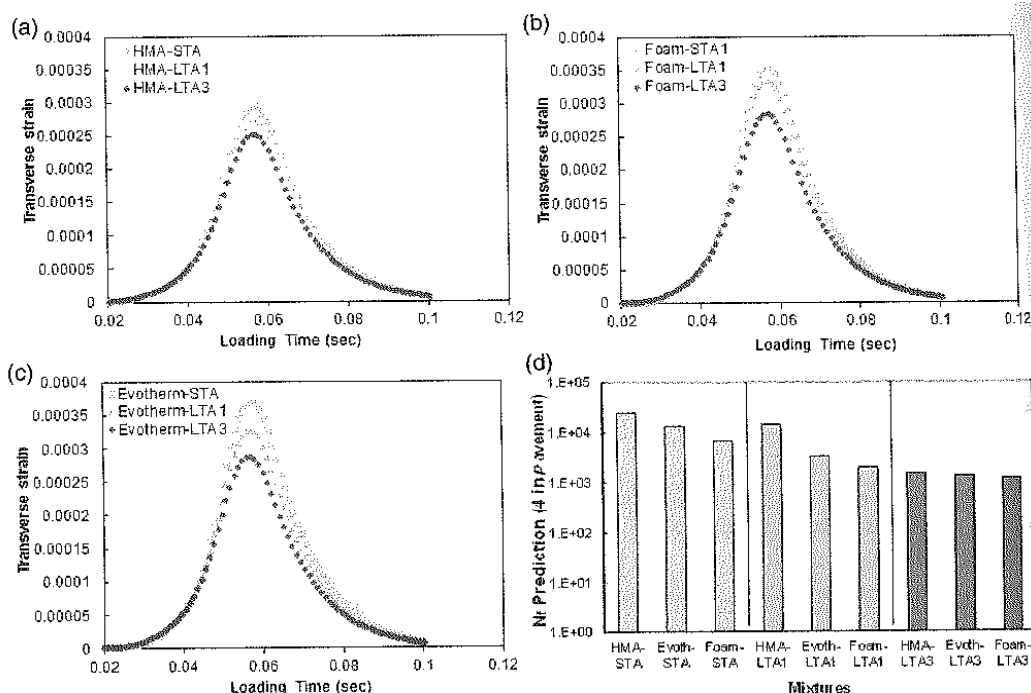


Figure 8-99: Fatigue performance analysis results for asphalt mixtures: (a) HMA, (b) foam WMA, (c) Evotherm WMA, and (d) fatigue life comparison of the mixtures

Figure 8-30 presents the correlation between binder and mixture fatigue life using a binder-to-mixture strain ratio of 80. Although there is a fair amount of scatter around the line of equality, the results demonstrate reasonable agreement (R^2 of 0,84) between the mixture and binder fatigue life predictions. The results promise that the LAS test coupled with S-VECD analysis can capture the asphalt binder's contribution to mixture fatigue.

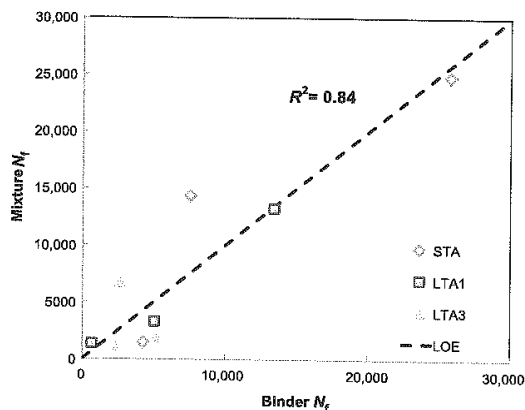


Figure 8-100: Comparison between mixture and binder fatigue life

8.3.2.20 Paper 544 (Pap, 2010)

In California a comprehensive warm-mix asphalt study was done, which compared the performance of a control mix, produced and constructed at conventional hot-mix asphalt temperatures, with three mixes produced with three warm-mix additives (Advera – chemical foam, Evotherm – surfactant and Sasobit – wax), produced and compacted at approximately 35°C lower than the control. The binder was rated as PG 64-22. After mixing, one of the additives (Sasobit) changed the PG grading from PG 64-22 to PG 70-22. The recommended bitumen content was 5,1-5,4 % by mass of aggregate. The binder content of the Sasobit mix was 0,62 % below the lowest permissible content. This discrepancy was considered likely to influence behaviour of the mix. Test specimens were cored from 500x500 mm slabs.

Conventional fatigue life is defined as the number of load repetitions when 50 percent stiffness reduction has been reached. The side-by-side fatigue life comparison of dry and wet tests is plotted in Figure 8-30. The following observations were made:

- Fatigue life was both strain- and temperature-dependent. In general, lower strains and higher temperatures will result in higher fatigue life and vice versa.
- Soaking generally resulted in a lower fatigue life compared to the unsoaked specimens. Inconsistent results were obtained across the mixes at the higher temperatures (i.e., 200 microstrain and 30 °C). It is not clear why this occurred.
- There was no significant difference between the four mixes in terms of fatigue life at 50 % stiffness reduction indicating that the addition of the additives and lower production and compaction temperatures did not significantly influence the performance of the mix in this test.

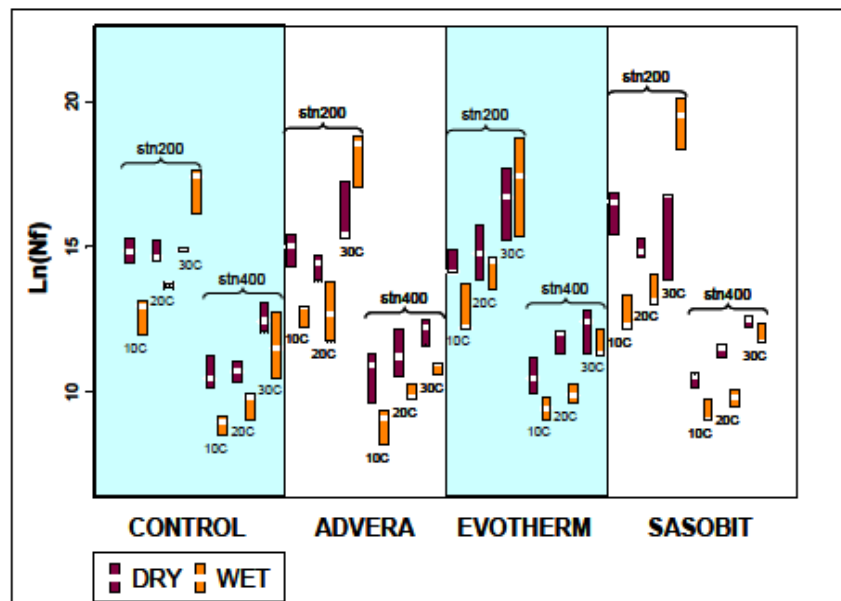


Figure 8-101: Summary boxplot of fatigue life

Figure 8-30 to Figure 8-30 show the shifted master curves with Gamma-fitted lines and the temperature-shifting relationships for the dry and wet frequency sweep tests. The temperature-shifting relationships were obtained during the construction of the complex modulus master curve and can be used to correct the temperature effect on initial stiffness.

The following observations were made from the frequency sweep test results.

Dry Tests:

- There was no apparent difference between the complex modulus master curves of the Control and Advera and Sasobit mixes. The curve for the Evotherm mix was below those of the other three mixes, possibly due to the higher air-void contents of tested beams.
- The temperature-shifting relationships indicate that the Advera mix was the most temperature-sensitive in extreme temperatures and that the Control mix was the least temperature-sensitive on average. Higher temperature-sensitivity implies that a per unit change of temperature will cause a larger change of stiffness.

Wet Tests:

- The complex modulus curves of the Control and Sasobit mixes were essentially the same, while the curves for the Advera and Evotherm mixes showed lower stiffness.
- There were no apparent temperature-sensitivity differences between the four mixes at higher temperatures (higher than 20 °C). At lower temperatures (lower than 20 °C), there was no significant difference in temperature-sensitivity between the Control and Advera mixes, but some temperature sensitivity in the Evotherm and Sasobit mixes.
- A loss of stiffness attributed to moisture damage was apparent in all four mixes.

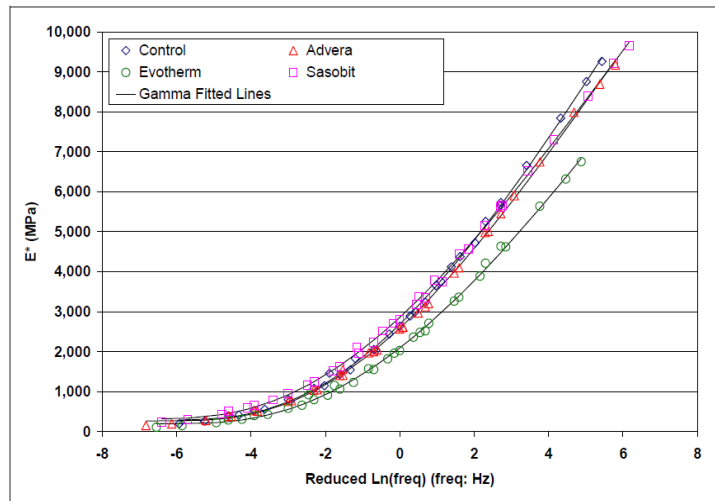


Figure 8-102: Dry complex modulus (E^*) master curves (fatigue beam)

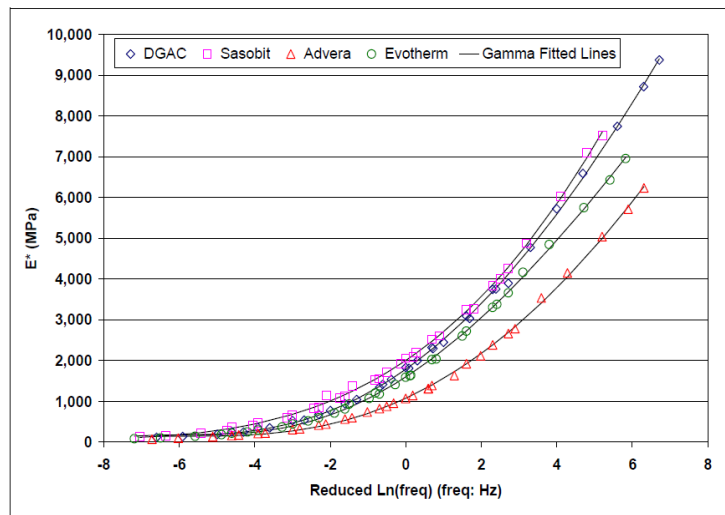


Figure 8-103: Wet complex modulus (E^*) master curves (fatigue beam)

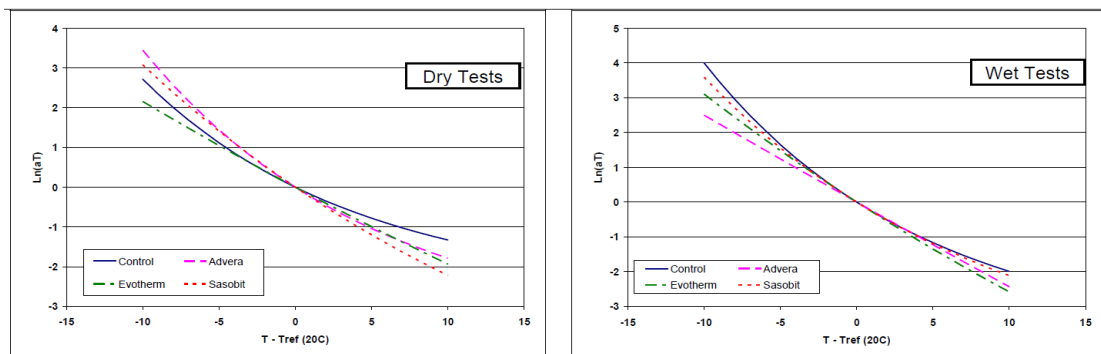


Figure 8-104: Temperature-shifting relationships (fatigue beam)

8.3.2.21 Paper 153 (Willis *et al.*, 2012)

The objective of this work was to fully characterize the high polymer plant-produced mixtures that were placed at the 2009 National Center for Asphalt Technology (NCAT) Test Track. The laboratory performance of the high polymer mixtures (HPM) were compared to the standard Test Track control mixtures.

The 4PB-PR fatigue test with strain controlled condition had been conducted in this study in order to define the fatigue life of the mixtures. The reduction of 50 % in beam stiffness was defined as failure criteria. In order to ensure a complete data set, the beams used in the study were allowed to run until the beam stiffness was reduced to 25 % of the initial stiffness.

The difference between fatigue resistance of the control mix and the mixture with high polymer mix can be seen in Figure 8-30. From the Figure it can be said that:

- At the highest strain magnitude, the HPM was able to withstand almost 4 times more loading cycles than the control mixture.
- At 400 $\mu\epsilon$, the average fatigue life of the HPM was greater than the control mixture. The average cycles until failure for the control mixture was 186 193 and while the HPM averaged 6 043 907 loading cycles.

The calculated fatigue endurance limit for the control base mixtures was 77 $\mu\epsilon$ while the endurance limit for the HPM base mixtures was 231 $\mu\epsilon$. Thus, the HPM base mixture could theoretically withstand three times the strain magnitudes without accruing damage when compared to the control base mixture.

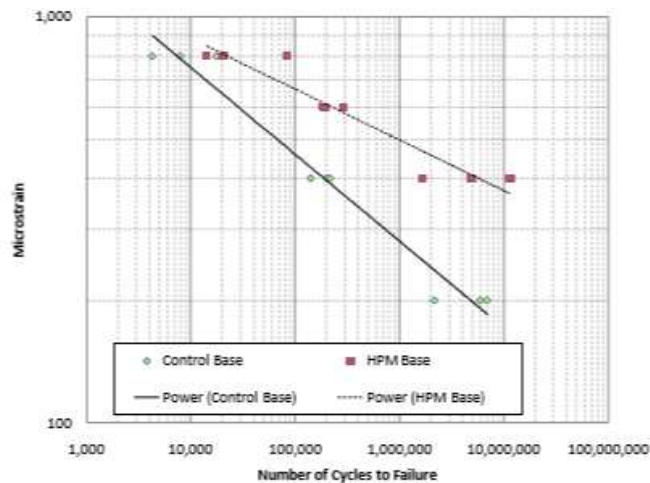


Figure 8-105: Comparison of fatigue resistance of mixtures

8.3.2.22 Paper 558 (Shen et al., 2009)

Mixes prepared with binders with varying percentages (3 %; 5 %; 7 %; 9 %; 11 % and 13 %) of SBS were studied. An oil-based additive was necessary to lower the mixing temperature to a manageable level for polymer contents above 3 %.

In terms of thermal susceptibility, the penetration index increases with increasing percentages of polymer in the asphalt; however, M6 asphalt presents a slight reduction. The modified binders have very different penetration and softening point characteristics. In general, the penetration and the softening point increase as the additive content is increased. The rheologic curves show that in order to reach the same viscosity, modified asphalts require greater temperatures, which translates into higher mix and compacting temperatures for modified asphalts (around 15°C) than for conventional asphalt and asphalt with additive. The elastic recovery of the polymer-modified binders is superior to that of conventional asphalt. This is due to the fact that the polymer used (SBS) is an elastomer that enhances the virgin asphalt elastic properties.

Eight different mixtures were prepared, each one applying a different binder. For asphalts C and A the percentage of asphalt used was 6,4 %, and for mixtures containing asphalts M1, M2, M3, M4, M5, and M6; 6,1 % bitumen was used.

Table 8-33: Characteristics of all the binders used in the study

Characteristic	Bitumen							with additive A
	Conventional	Modified						
	C	M1	M2	M3	M4	M5	M6	
Polymer Content (%)	-	3	5	7	9	11	13	-
Additive Content (%)	-	5	15	30	40	55	65	1,7
Penetration 100 g, 5 s, at 25°C, (0.1 mm)	72	66	84	117	124	150	147	75
Cinematic Viscosity at 135°C, (cSt)	291,9	633,2	713,7	475,7	572,4	778,6	867,4	269,1
Softening Point [Ball and Ring], (°C)	48,6	53,8	57,8	59,8	61,8	61,0	60,0	47,0
IP* [INV E-724]	-0,6	0,4	2,1	3,7	4,3	5,0	4,7	-1,0
Elastic Recovery using a Ductilometer (%)	0	67,1	77,6	81,4	83,3	82,9	82,4	0
Specific Weight at 25°C	1,0177	1,0166	1,0159	1,0126	1,0105	1,0046	1,0008	1,0163
Residual Penetration at 25°C after the RTFOT (0.1 mm)	33	39	47	67	79	98	104	38
Mass Reduction (%)	1,95	1,84	1,66	1,78	1,84	1,94	1,78	2,27
Retained Penetration (%)	46	59	56	57	64	66	71	51
Softening Point of the Residual after the RTOFT (°C)	58,0	62,0	63,0	65,8	65,0	63,5	62,0	55,5
Absolute Viscosity at 60°C (cP)	159000	412000	499000	482000	432000	193000	146000	135000
Absolute Viscosity at 80°C (cP)	14167	31567	32500	24706	20636	16417	16133	12571
Absolute Viscosity at 100°C, (cP)	2420	5261	5400	4046	4175	3783	3912	2217
Absolute Viscosity at 120°C, (cP)	668	1322	1487	1270	1388	1350	1430	605
Absolute Viscosity at 140°C, (cP)	238	505	575	520	620	613	655	220
Absolute Viscosity at 160°C, (cP)	115	210	260	260	310	320	345	90
Absolute Viscosity at 180°C, (cP)	-	110	153	155	195	190	210	-

The term "Penetration Index" is not applicable to modified asphalts, since by definition its use is limited to conventional asphalts (Newtonian). However, in this study the term is used as an empirical method to show the reduction in the thermal susceptibility of asphalts.

The procedure for the fatigue test was conducted under the parameters of the British Standard DD AFB (method for the determination of the fatigue characteristics of bituminous mixtures using indirect tensile fatigue-ITFT). The fatigue tests were conducted on specimens with asphalts C, M1, M2, and A. The stress levels used were 400, 450, and 500 kPa at a temperature of 20 °C and a frequency of 2,5 Hz. Two samples were tested for each stress level, for a total of 24 fatigue tests. The greatest horizontal strain (ϵ_x) in the center of the specimen (microstrain) was calculated.

The results are summarized in Table 8-34. The maximum horizontal strain ($\epsilon_{x, \max}$) was graphed as a function of the number of cycles that presented a sample failure (Nf), using a logarithmic scale in both axes (Figure 8-30). A linear regression analysis was applied to $\log(\epsilon_{x, \max})$ and $\log(Nf)$ data using the method of least squares. It is noted that initially, asphalt type M1 behavior was better than that of all other asphalt types; however, at greater loads asphalt type C presented a better behavior.

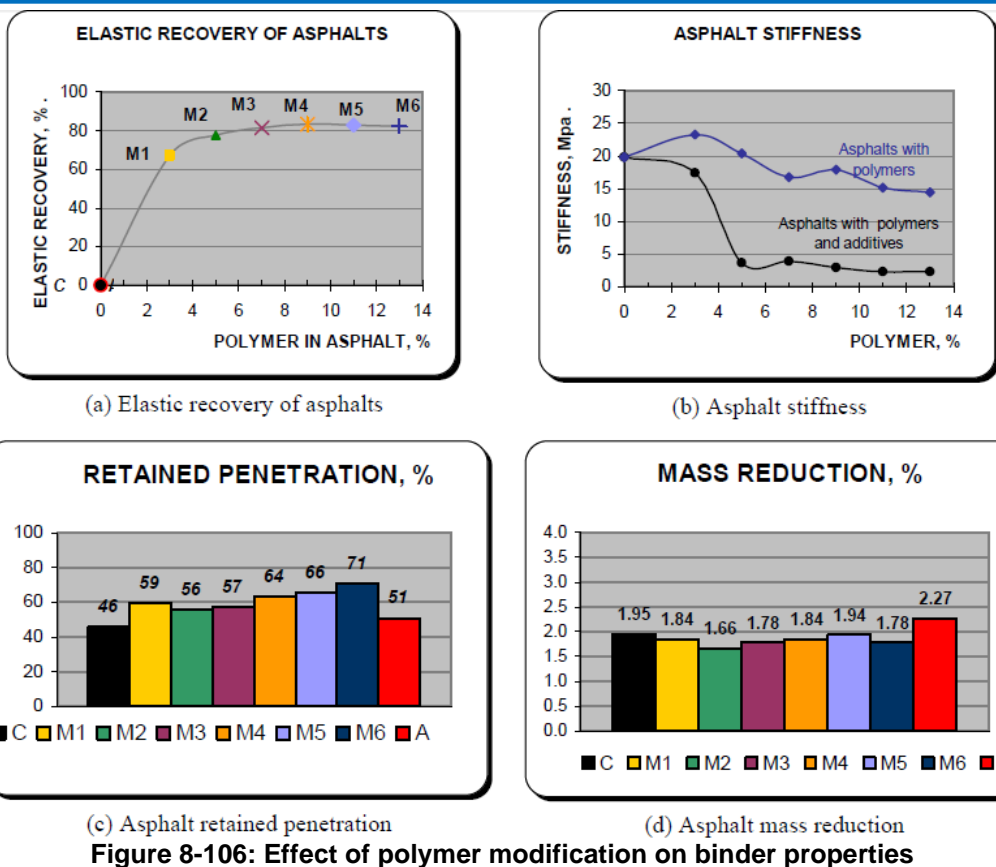


Figure 8-106: Effect of polymer modification on binder properties

The maximum tensile stress $\sigma_{x, max}$ was plotted against the number of cycles that presented a sample failure (N_f), as shown in Figure 8-30. In terms of the life of the fatigue, the behavior is linear. The movement of the lines upward indicates a better response of the mixture to tension. It was observed that for a similar tensile load, asphalt mixture M1 presented a better response to fatigue produced by load repetitions in comparison to the other mixtures. Initially, the behavior of asphalt A was better than that of M2; however, at greater loads M2 ended up presenting a better response.

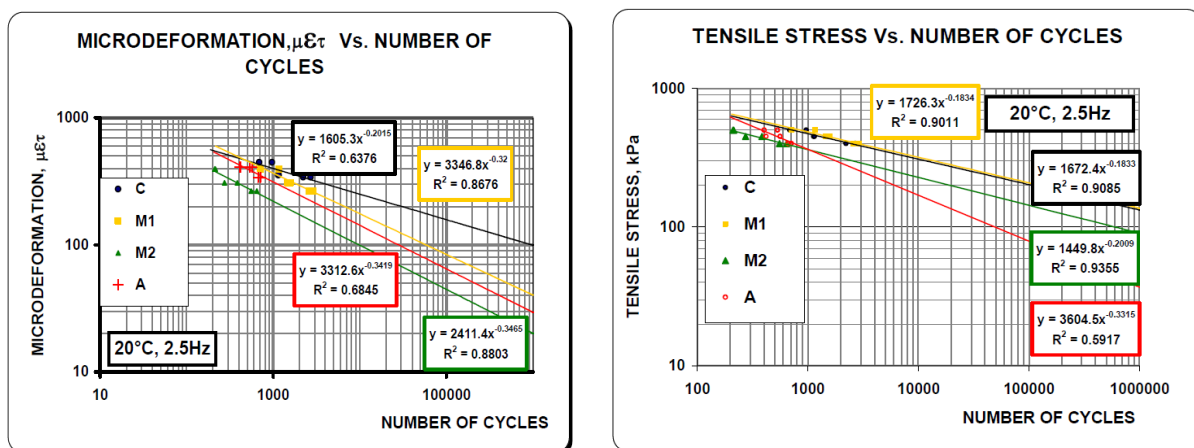


Figure 8-107: Controlled-strain fatigue test results (2,5 Hz; 20 °C)

The study shows that adding SBS polymer in amounts greater than or equal to 3 % in weight to conventional asphalt yields asphalt with greater stiffness and rigidity, affecting its level of

manageability and necessitating the use of additives. The increment in the stiffness becomes more pronounced as the percentage of additive exceeds 5% of the polymer. This translates into high additive content, which in turn considerably affects the rigidity modulus of the asphalts, producing low dynamic modulus and poorer behavior under fatigue tests. The fatigue test showed that type A HMA modified mixes are the most likely to develop loadrelated cracking.

Table 8-34: Fatigue test results

Asphalt	Stress (kPa)	Sm (MPa)	Cycles to Failure (Nf)	ex, max
C	400	2411	2219	340
C	400	2411	2706	340
C	450	2605	1134	354
C	450	2605	1154	354
C	500	2297	687	446
C	500	2297	970	446
M1	400	3081	2581	266
M1	400	3081	2898	266
M1	450	3003	1461	307
M1	450	3003	1585	307
M1	500	2602	714	394
M1	500	2602	1170	394
M2	400	2089	643	393
M2	400	2089	556	393
M2	450	2015	386	458
M2	450	2015	274	458
M2	500	1929	210	531
M2	500	1929	214	531
A	400	2405	711	341
A	400	2405	669	341
A	450	2259	421	408
A	450	2259	565	408
A	500	2487	535	412
A	500	2487	405	412

8.3.2.23 Paper 458 (Prowell et al., 2010)

This study focused on endurance limit assessment for HMA with SBS modified binder. The endurance limit was used as a criterion for prevention of bottom-up fatigue cracking. The tested mixes were a 19,0 mm NMAS granite mixture at optimum asphalt content (4,6 %) with both neat PG 67-22 and SBS modified PG 76-22 binder. All mixtures underwent short-term aging for four hours at 135 °C before compaction according to AASHTO R30. Two additional binder grades, PG 58-28 and PG 64-22, were utilized in the previously described mixture at optimum asphalt content.

Beam specimens were loaded under strain-controlled conditions using sinusoidal loading at 10 Hz at a temperature of 20 °C. Testing was conducted in constant strain mode. Each of the cells in the experimental plan was tested at strain levels beginning on the high side: 800, 400, 200 and 100 micro-strain. Testing was conducted to failure (a reduction in stiffness of 50 %) or a minimum of 50 million cycles. AASHTO T321 specifies an exponential model for the calculation of cycles to 50 percent initial stiffness

For the PG 67-22 mix at optimum asphalt content, samples tested at 200 and 170 micro-strain were used to investigate extrapolation techniques. Four techniques were investigated for extrapolation: exponential model, Weibull function, three-stage Weibull function, and ratio of dissipated energy change (RDEC).

Failure data can often be modeled using a Weibull distribution. The stiffness ratio is the stiffness measured at cycle n , divided by the initial stiffness, determined at the 50th cycle. Figure 8-30 shows an example of the data from the two 100 micro-strain samples from the PG 67-22 at optimum mixture. Tsai⁷ observed that the concave down shape, exhibited by Sample 13, “implied that the fatigue damage rate is slowed down and flattens out with increased repetitions and thus causes no further damage after a certain number of repetitions.” This behavior is believed to be indicative of the endurance limit. The single-stage Weibull function generally provides a good estimate of a sample’s fatigue life. There are, however, cases for which the single-stage Weibull function apparently under predicts fatigue life. Sample 13 in Figure 8-30 is one such example.

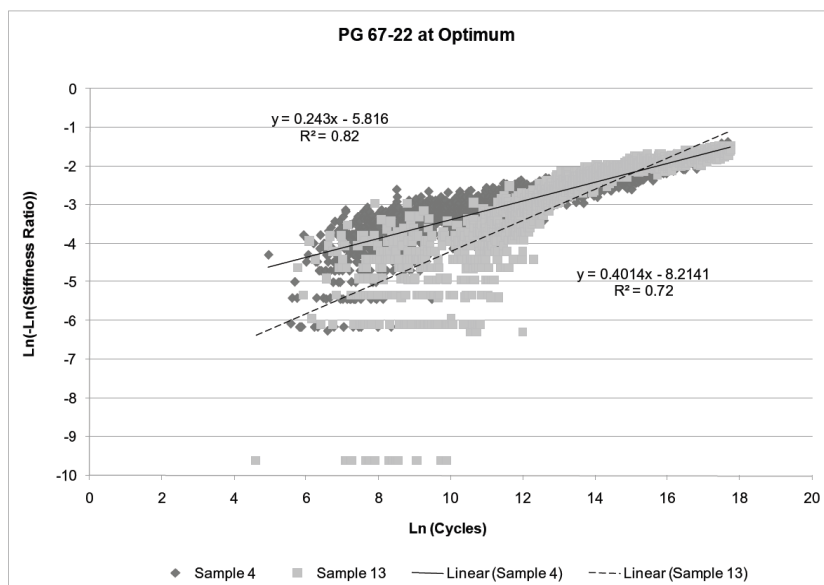


Figure 8-108: Weibull survivor function for PG 67-22 at optimum 100 microstrain samples

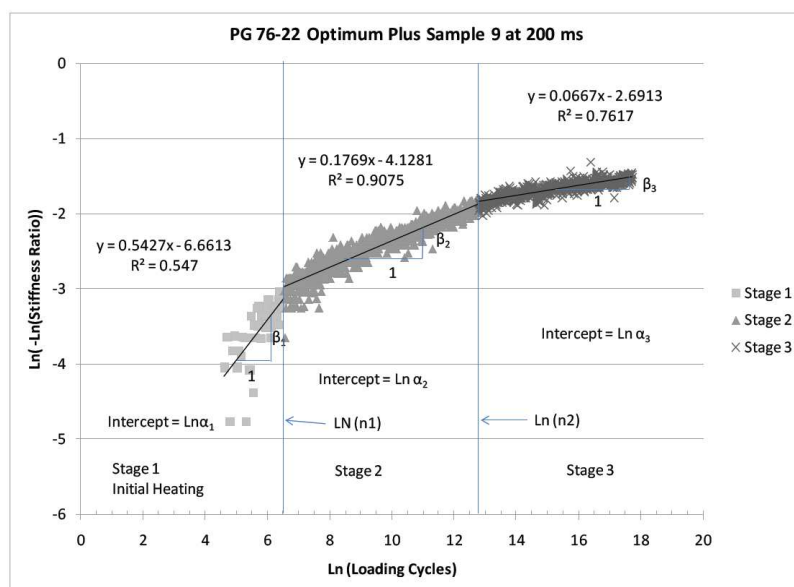


Figure 8-109: Three-stage Weibull curve definitions

⁷ Tsai, B.W., Harvey, J.T., Monismith, C.L.: High Temperature Fatigue and Fatigue Damage Process of Aggregate-Asphalt Mixes. In: Journal of the Association of Asphalt Paving Technologists, Vol. 71, 2002.

To improve upon the accuracy of the single-stage Weibull function, Tsai⁸ developed a methodology for fitting a three-stage Weibull curve. Tsai⁸ theorized that a plot of loading cycles versus stiffness ratio could be divided into three stages: initial heating and temperature equilibrium, crack initiation, and crack propagation.

Figure 8-30 shows an example of the three-stage Weibull fit. This methodology provides a good fit to both normal and low strain fatigue data.

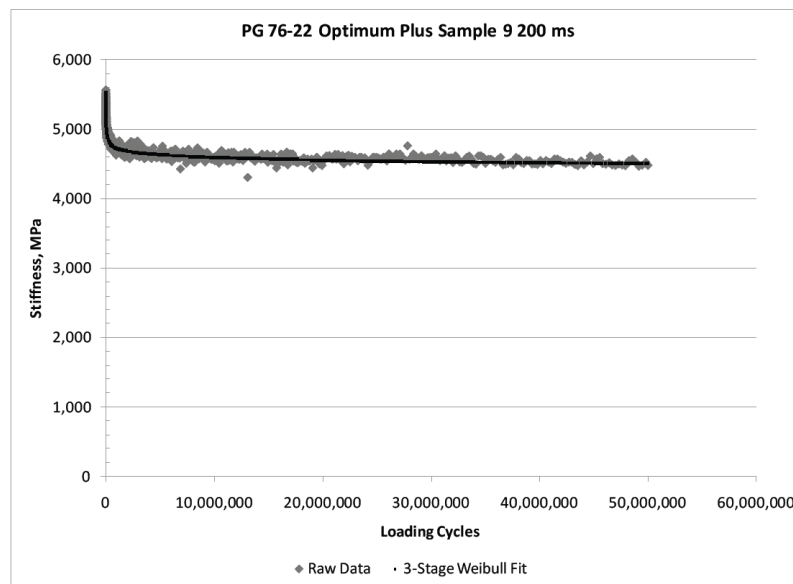


Figure 8-110: Three-stage Weibull fit to stiffness data

Dissipated energy is a measure of the energy that is lost to the material or altered through mechanical work, heat generation, or damage to the sample. Other researchers have used cumulative dissipated energy to define damage within a specimen, assuming that all of the dissipated energy is responsible for the damage.

Table 8-35 shows the fatigue life predictions for the five samples using four different extrapolation methods: exponential model, power model, single-stage Weibull, three-stage Weibull, and RDEC. This procedure consistently overestimates the samples fatigue lives by three to seven orders of magnitude. The power model also consistently overestimates fatigue life by two to seven orders of magnitude.

For the remaining methods, with the exception of the exponential model, the fatigue life of Sample 5 of the PG 67-22 at optimum asphalt content was overestimated by a larger degree than for the other samples. Sample 5 was tested at 170 micro-strain. The three-stage Weibull model overestimated fatigue life of Sample 5 by three or four orders of magnitude based on the data from 4 million and 10 million loading cycles, respectively. However for the remaining samples, the three-stage Weibull function overestimated fatigue life by zero to two orders of magnitude. Sample 23 of the same mix was also tested at 170 micro-strain. It was tested to 60 million cycles without reaching 50 percent of its initial stiffness.

The exponential and single-stage Weibull function produced the most accurate fatigue life predictions.

⁸ Tsai, B.W., Harvey, J.T., Monismith, C.L.: Using the Three-Stage Weibull Equation and Tree-Based Model to Characterize the Mix Fatigue Damage Process. In: Transportation Research Record No. 1929, Transportation Research Board, Washington, DC, 2005, Pp 227-237.

In summary, the Weibull functions were selected for extrapolating fatigue tests that did not fail within 50 million cycles or when the test was interrupted prior to failure (as occurred with Sample 6 of the PG 67-22 mix at optimum asphalt content). For long-life fatigue tests, at strain levels slightly above the endurance limit, the single-stage Weibull function appears to provide the most accurate extrapolation of fatigue life. The three-stage Weibull function, however, provides the best fit to the stiffness versus loading cycle data.

Table 8-35: Comparison of fatigue life extrapolations

Mix	Sample	Cycles used for extrapolation	Actual	Exponential	Power (used in RDEC)	Single-stage Weibull	Three-stage Weibull	RDEC
PG 67-22 Optimum	2	4 E+06	2,60E+07	7.89E+06	3.80E+10	3.31E+07	1.41E+08	6.78E+11
		10 E+06		1.87E+07	3.43E+10	5.59E+07	1.89E+08	3.08E+11
	21	4 E+06	2,08E+07	4.94E+06	4.19E+09	1.44E+07	4.43E+07	5.53E+10
		10 E+06		9.88E+06	1.78E+09	1.91E+07	5.04E+07	1.92E+09
	5	4 E+06	3,47E+07	1.27E+07	2.15E+14	3.87E+08	7.23E+11	1.66E+14
		10 E+06		2.88E+07	2.15E+14	7.24E+08	1.92E+10	8.02E+13
PG 67-22 Optimum+	4	4 E+06	3,90E+07	8.62E+06	1.58E+11	3.11E+07	1.20E+09	2.26E+15
		10 E+06		1.84E+07	2.97E+10	4.97E+07	3.39E+09	1.06E+11
PG 76-22 Optimum+	10	4	3,96E+07	7.69E+06	7.16E+09	1.13E+07	3.28E+08	2.56E+12
		10		1.73E+07	7.41E+09	2.01E+07	4.54E+08	1.71E+10

Testing was only conducted to 50 million cycles. Therefore, the failure point of these samples needed to be extrapolated. Two techniques were used to extrapolate the stiffness versus loading cycle data, the single- and three-stage Weibull functions. Additionally, the data were analyzed using the RDEC procedures to determine the plateau value.

The results for the PG 67-22 mix tested at optimum asphalt content are presented in Table 8-27. The PG 67-22 mix at optimum asphalt content was tested by NCAT. Samples 4 and 13, tested at 100 micro-strain produced extrapolated Nf using the single-stage Weibull function of 5,49E+09 and 3,00E+08, respectively. Although both of these numbers represent extraordinarily long fatigue lives, Sample 13 would be expected to have a longer fatigue life. The best fit line for the Weibull function for Sample 13 has a steeper slope, resulting in the prediction of a shorter fatigue life.

Table 8-36: Granite 19,0 mm NMAS mix with PG 67-22 at optimum bitumen content

Beam ID	Initial flexural stiffness, MPa	Micro-Strain	Cycles tested	Extrapolated cycles to 50% initial stiffness		PV	Cycles to 50% initial stiffness	Avg. cycles to failure
				Single-stage Weibull	Three-stage Weibull			
18	5 175	800	6 000	NA	NA	3,66 E 5	6 000	6 377
3	4 686	800	7 130	NA	NA	2,06 E 5	7 130	
7	4 522	800	6 000	NA	NA	2,63 E 5	6 000	
10	5 153	400	246 220	NA	NA	6,25 E 7	246 220	252 136
46	5 239	400	57 000	NA	NA	2,24 E 7	267 808 ¹	
1	5 868	400	242 380	NA	NA	3,17 E 7	242 380	20 445 922
2	5 175	200	26 029 000	NA	NA	5,33 E 9 ⁴	26 029 000	
6	6 435	200	12 930 000	NA	NA	6,19 E 9 ⁴	14 537 186 ²	
21	6 240	200	20 771 580	NA	NA	6,35 E 9 ⁴	20 771 580	
5	4 519	170	34 724 500	NA	NA	2,30 E 9 ⁴	34 724 500	69 362 250
23	5 645	170	60 000 000	1,04E+08	9,16E+07	5,37 E	1,04E+08 ³	
4	6 602	100	50 000 000	5,49E+09	5,52E+09	9,25 E	5,49E+09 ³	2,90E+09

¹ Failure extrapolated. Testing suspended at 58 percent of initial stiffness at 57 000 due to computer problem.
² Software froze. Result extrapolated using linear regression of latter cycles.
³ Results extrapolated using single-stage Weibull model.
⁴ Less than 8,57E-9 proposed by Shen and Carpenter as indicative of long-life pavement.

Table 8-37: Granite 19,0 mm NMAS mix with PG 76-22 at optimum bitumen content

Beam ID	Initial flexural stiffness, MPa	Micro-Strain	Cycles tested	Extrapolated cycles to 50% initial stiffness		PV	Cycles to 50% initial stiffness	Avg. cycles to failure
				Single-stage Weibull	Three-stage Weibull			
4	3 025	800	42 240	NA	NA	4,02E-	42 240	26 160
7	5 445	800	10 080	NA	NA	1,58E-	10 080	
2	4 191	400	3 609 470	NA	NA	1,66E-	3 609 470	1 664 400
8	4 976	400	591 770	NA	NA	2,87E-	591 770	
13	3 675	400	791 960	NA	NA	2,15E-	791 960	
1	4 637	250	1 483 745	NA	NA	3,30E-	14 837 45	NA
11	4 148	250	5 000 000	2,91E+	1,31E+	2,22E ⁻²	2,91E+09 ¹	
5	4 460	200	5 000 000	2,75E+	1,53E+	0,00 ²	2,75E+09 ¹	2,72E+09
3	4 062	200	5 000 000	2,68E+	2,61E+	0,00E ²	2,68E+09 ¹	

¹ Results extrapolated using single-stage Weibull model.
² Less than 8.57E-9 proposed by Shen and Carpenter as indicative of long-life pavement.

Table 8-38: Granite 19,0 mm NMAS mix with PG 67-22 at optimum plus asphalt

Beam ID	Initial Flexural Stiffness (MPa)	Micro-Strain	Cycles Tested	Single-Stage Weibull	Three-Stage Weibull	PV	Cycles to 50% Initial Stiffness	Avg. Cycles to Failure
Cox and Son's fixture in Interlaken load frame except as noted								
8	5 054	800	15 464	NA	NA		15 464	403 232
14	5 306	800	34 500	NA	NA		34 500	
10	5 896	400	468 343	NA	NA		468 343	
15	6 698	400	338 121	24 944	NA		338 121	
9	6 094	200	100 000	NA	1.14E+		24 944 621	62 310 044
4 ²	6 923	200	389 855	1,23E+	NA		38 985 510	
1 ³	6 219	200	500 000	1,23E+	9.95E+		1,23E+081	
IPC Global fatigue device								
6	6 862	800	5 570	NA	NA	4,17E-	5 570	94 615
3	7 472	800	5 230	NA	NA	3,99E-	5 230	
7	7 675	400	131 390	NA	NA	1,49E-	131 390	
4	7 653	400	57 840	NA	NA	6,26E-	57 840	
2	7 512	200	358 474	NA	NA	1,58E-	358 474	3 584 740
6a	8 605	100	153 500	5,81E+	NA ⁴	NA	5,81E+08 ¹	5,81E+08

¹ Results extrapolated using single-stage Weibull model.
² Testing conducted by University of Rutgers on an IPC Global fatigue device.
³ Tested on Asphalt Institute IPC Global fatigue device.
⁴ No solution.

Table 8-39: Granite 19.0 mm NMAS mix with PG 76-22 at optimum plus asphalt

Beam ID	Initial Flexural Stiffness (MPa)	Micro-Strain	Cycles Tested	Extrapolated Cycles to 50% Initial Stiffness		PV	Cycles to 50% Initial Stiffness	Avg. Cycles to Failure
				Single-Stage Weibull	Three-Stage Weibull			
8	3 520	800	252 450	NA	NA	2,61E-	252 450 ¹	48 050
5	5 451	800	32 520	NA	NA	3,12E-	32 520	
14	5 764	800	63 580	NA	NA	1,09E-	63 580	
1	5 532	400	28 600	NA	NA	1,17E-	2 860 000	6 257 500
4	5 532	400	96 550	NA	NA	2,05E-	9 655 000	
10	4 308	300	39 624	NA	NA	1,71E-	3 962 400	7,57E+07
2	5 427	300	88 118 ⁴	4,88E+7	5,63E+	1,84E-	4,88E+7 ²	
12	4 105	300	20 080 ⁴	1,47E+8	2,46E+	7,33E-	1,47E+8 ²	
11	5 162	300	50 000	6,75E+7	4,50E+	1,25E-	6,75E+7 ²	
13	6 841	200	50 000	5,96E+9	6,79E+	2,22E-	5,96E+9 ²	1,85E+10
9	5 609	200	50 000	3,10E+1	1,58E+	0,00E+0 ³	3,10E+10 ²	

¹ Not included in average.
² Results extrapolated using single-stage Weibull model.
³ Less than 8,57E-9 proposed by Shen and Carpenter as indicative of long-life pavement.
⁴ Sample did not fail, extrapolated using single-stage Weibull model.

The ratio of dissipated energy change plateau values were calculated for each of the PG 67-22 at optimum samples. The results are shown in Table 8-36. The samples tested at 200, 170 and 100 micro-strain produce plateau values lower than the critical value, $8,57E-9$ recommended by Shen and Carpenter⁹ as indicative of long-life pavements. Although all three strain levels appear to provide a long fatigue life, 170 micro-strain appears to be at or slightly above the endurance limit based on the other analyses. The recommended plateau value may not define the endurance limit, but rather a long fatigue life.

The results for the PG 76-22 mix tested at optimum asphalt content were presented in Table 8-37. The PG 76-22 mix at optimum asphalt content was tested by NCAT. One sample at 250 micro-strain and both samples at 200 micro-strain produced plateau values less than the critical value indicated by Shen and Carpenter to be indicative of long fatigue life.

Testing for the PG 67-22 mix at optimum plus asphalt content was initially conducted on the Asphalt Institute Interlaken servo-hydraulic frame using a Cox and Son's fixture. Due to problems with the Interlaken system, low-strain beams were later tested on IPC Global beam fatigue devices operated by the Asphalt Institute. The initial results from the machines and the retests using the IPC Global machine were presented in Table 8-38.

The fatigue lives for the retests are significantly shorter than for the original mix. The initial stiffness for the original set of beams averaged 6 027 MPa; the initial stiffness of the replacement beams averaged 7 435 MPa.

Clear indications of the endurance limit were indicated for three of four mixes (not PG 67-22 at optimum plus). Visually, the endurance limit appears to be more sensitive to binder properties than to asphalt content/air void content. An endurance limit of approximately 170 micro-strain was determined for the PG 67-22 mix at optimum asphalt content. The endurance limit for the PG 76- 22 mixture appears to be on the order of 220 micro-strain, and approximately 300 micro-strain for the PG 76-22 at optimum plus. The Weibull function appears to be the best technique for extrapolation of low strain stiffness results.

The 19,0 mm NMAS granite Test Track mix was replicated using a true grade PG 64-22 and PG 58-28. Three beams were tested at 800 microstrain and three beams were tested at 400 micro-strain for each mixture. The fatigue testing was conducted by NCAT. The endurance limit was estimated using the one-sided 95% lower prediction interval for a strain level corresponding to 50 million cycles.

Table 8-40: Summary of Estimates of the Endurance Limit (micro-strain)

Mix	Beam fatigue		Beam fatigue round robin (28)		
	Predicted	95% lower confidence limit	Predicted ¹	95% lower confidence limit ²	Average 95% lower confidence limit ²
PG 58-22	107	82	NA	NA	NA
PG 64-22	89	75	NA	NA	NA
PG 67-22	172	151	182	130	103
PG 67-22 Opt. +	184	158	176	141	121
PG 76-22	220	146	195	148	126
PG 76-22 Opt. +	303	200	NA	NA	NA

¹ Calculated using the pooled data from the round robin.
² Average of the 95% lower confidence limit calculated by each individual lab.

Table 8-40 summarizes the endurance limit predictions from the beam fatigue tests. There appears to be good correlation between the beam fatigue estimates of the endurance limit

⁹ Shen, S., Carpenter, S.H.: Application of Dissipated Energy Concept in Fatigue Endurance Limit Testing. In: Transportation Research Record 1929, Transportation Research Board, Washington, DC, 2005, pp. 165-173.

determined in Phase I and those determined during the mini-round-robin analysis. Based on the predicted values determined from testing at NCAT and the Asphalt Institute, stiffer hightemperature binder grades and optimum plus asphalt contents produce higher endurance limit values. The 95 percent lower prediction limit samples follow the same general trend.

A practical definition of the endurance limit or long-life pavement would be a pavement able to withstand 500 million design load repetitions in a 40 year period.

8.3.3 *Fatigue life of unconventional mixtures*

8.3.3.1 **Paper 046 (Güngör et al., 2012)**

The performance of asphalt mixes containing volcanic aggregates and PMB, which is a common practice in Turkey, has been examined in this paper. Rutting and fatigue life of different asphalt samples with use of PMB and 50/70 bitumen has been tested with four point testing method as well as cyclic compression. The four point beam test has been performed under strain controlled condition with three different strains levels. As a conclusion it has been shown that stone mastic asphalt mixtures (SMA) with PMB performed better regarding plastic deformation and fatigue life. Although it was observed that the stiffness of AC wearing course was a bit higher than SMA mixtures, AC mixtures lost half of the initial stiffness in a shorter time in comparison with SMA mixtures.

8.3.3.2 **Paper 050 (Haritonovs et al., 2014)**

Similarly performance of asphalt mixtures with dolomite aggregates (relatively weak) and different binder types was analysed. In order to achieve resistance against deformation at high temperatures, hard grade bitumen has been used for sample preparation. However, in order to achieve workability as well as prolonged fatigue life, lower porosity (3-5 %) and higher binder content in comparison with traditional asphalt mixtures were required. A reference mixture (70/100) has been designed in this study, for comparison purpose. It was shown that while the results of wheel tracking test has been approximately the same for the reference mixtures and unconventional ones, the fatigue life of unconventional mixtures have been notably higher than the reference mixture. This can be explained by higher bitumen content used in these mixtures.

8.3.3.3 **Paper 061 (Beckedahl et al., 2008)**

Another paper describes the effect of the compaction degree on the performance and properties (temperature dependent resilient modulus, resistance against rutting and/or fatigue) of asphalt base layer, asphalt binder layer and stone mastic asphalt surface layer by means of laboratory tests. Asphalt slabs with compaction degrees between 94 % and 103 % of Marshall density were prepared using a laboratory roller compaction machine. A significant lower rutting trend and a much higher fatigue resistance with decreasing compaction degree can be observed for innovative asphalt compared to conventional asphalt mixtures with respect to different compaction degrees. The innovative asphalt mixtures with PMB 25H with a compaction degree of 94 % have a higher resilient modulus as well as fatigue resistance than the asphalt mixtures with 50/70 and PMB 45A with a compaction degree of 100 % (at 20 °C). Thus the innovative asphalt provides at a high and low compaction degree a high resistance against permanent deformation and a high bearing capacity with low strain at the bottom of the asphalt base layer.

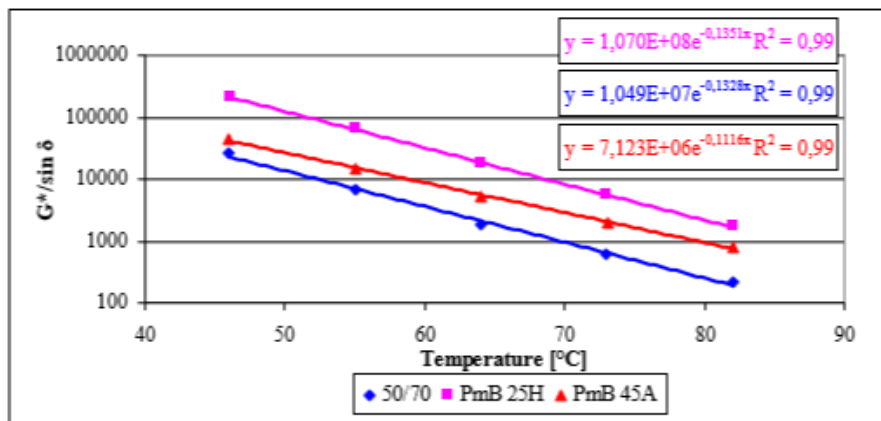


Figure 8-111 Comparison of Relation $G^*/\sin\delta$ (25 mm plate; 1,59 Hz)

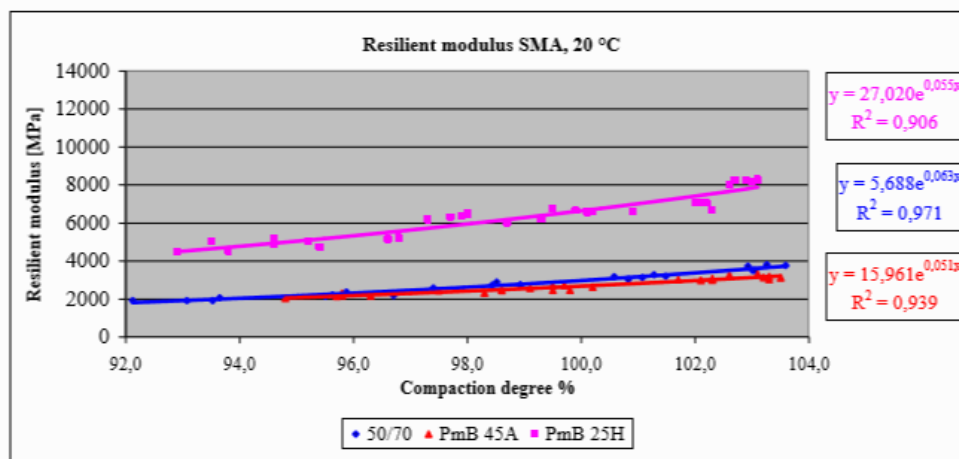


Figure 8-112 Resilient modulus versus compaction degree at 20 °C for SMA

8.3.3.4 Paper 542 (Yang *et al.*, 2010)

The test section was divided into four parts of the same layer thickness, but with two different bituminous mixes. The section A has high modulus asphalt concrete HMAC 16 20/30, while section B has conventional asphalt concrete AC 16 35/50 in the binder course. Sections C has composite mix (porous asphalt with cement mortar) in the wearing course. In case of other three sections A, B and D wearing course is made of SMA 8 mix with Orbiton 80C (PMB 45/80-65). The crucial feature of structure D is an application of anti-fatigue layer (AP AF). Bituminous mixes were designed according to the series EN-13108-x and requirements for heavy traffic category specified in the Polish national document WT NA 2008.

Table 8-41: Properties of bituminous mixtures designed for test sections

Properties	SMA 8 DE80C	AC 16 35/50	ACWMS 16 20/30	PA 11 50/70	AP AF
Binder content, % m/m	7,1	4,3	5,5	4,7	7,4
Fatigue (4PB, 10°C, 10Hz), ϵ_6 , $\mu\text{m/m}$	-	116	180	-	279

In the Table 8-42 results of the fatigue obtained in 4PB tests according to PN-EN 12697-26 (10 °C, 10Hz) for mixes HMAC 16 20/30 and AC 16 W 35/50 on specimens taken from tested sections (taken from loading line A, B, C, D and next to it A', B', C', D') and specimens prepared in the laboratory conditions (Lab) during mix design are presented.

Table 8-42: Results of the fatigue tests carried out on mix HMAC 16 20/30 and AC 16 35/50

	HMAC 16 20/30					AC 16 35/50				
	Lab	A	A'	D	D'	Lab	B	B'	C	C'
A	4,4E+25	3,1E+23	1,6E+23	7,9E+20	9,7E+19	3,1E+18	3,8E+19	9,1E+19	3,8E+17	1,4E+17
b	-8,71	-7,79	-7,59	-6,60	-6,22	-6,05	-5,55	-6,56	-5,52	-5,32
R ²	0,92	0,85	0,89	0,91	0,84	0,91	0,91	0,89	0,88	0,91
ε ₆	180	176	185	181	179	116	131	134	126	124
ε _{6max}	189	190	195	190	194	129	141	147	141	136
ε _{6min}	172	163	176	173	166	104	121	122	111	114

8.3.3.5 Paper 541 (Adnan et al., 2010)

In this study, four types of additives were targeted in laboratory research to select the optimal additive for the pavement. Four types of widely used polymer modifiers, all of which have shown desirable impact on rutting resistance of asphalt mixes were selected in this study and mixed with bitumen Esso AH-70, listed as SBS (Styrene Butadiene Styrene, China), PR (PR PLAST.S, France), Domix (Germany) and RS (Rad Spunrie, China).

The gradation of Sup-20 was designed according to the Superpave volumetric mix design procedure, and its optimum asphalt content was determined as 4,2 %. At the same time 0,4 % by the total weight of asphalt mix of PR, RS and Domix is added. However, SBS was mixed with Esso AH-70 before mixing with aggregate, and the ratio of SBS and Esso AH-70 is 5:95.

Four-point bending beam test was chosen for fatigue resistance analysis. Strain-controlled loading mode was applied. A continuous haversine axial compressive load was applied to the specimen at the loading rate of 10 Hz. The test temperature was 15 °C. The strain is controlled at 400 µε and 700 µε, and the results are shown in Table 8-43. It can be found that both the fatigue life and the cumulative strain energy of the asphalt mixture with PR are greater than those of the asphalt mixture without any additive. Use of PR can enhance the fatigue resistance of asphalt mixture.

Table 8-43: Results of the fatigue test

Mix	Microstrain (µε)	Initial stiffness (MPa)	Finish stiffness (MPa)	Fatigue life (Cycles)	Cumulative strain energy (MPa)
Base asphalt	400	2 965	1 486	21 609	36,21
	700	3 682	1 802	1 979	12,35
PR	400	5 989	2 990	30 253	61,35
	700	8 527	4 229	4 040	20,86

8.3.3.6 Paper 530 (Mangiafico et al., 2013)

The investigation was carried out in two steps. Section A consisted in a qualitative evaluation of the influence of the variation of some mix design parameters on fatigue properties (ε₆ and 1/b at 10 °C, 25 Hz) of asphalt mixes containing 20 % of RAP material. Factors used for analysis were aggregate nature (limestone vs. basalt), filler nature (limestone vs. hydrated lime), binder content (4,35 % vs. 5,35 %) and binder nature (35–50 vs. 35–50 B). Section B was focused on quantitatively estimating of the impact of RAP content and fresh added pen grade bitumen on fatigue properties of asphalt mixes with RAP (0 %, 20 %, 40 % and 60 %). Experimental data were obtained from tests performed using two-point bending configuration. Samples were cut from slabs compacted.

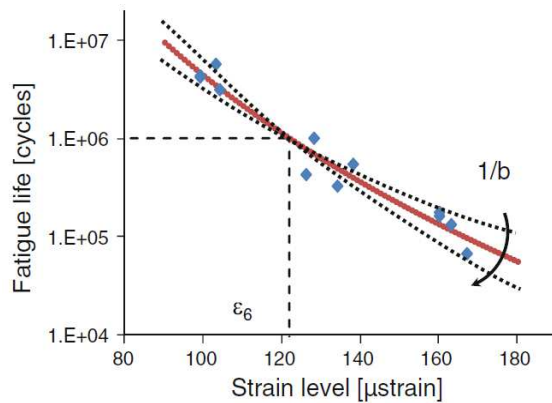


Figure 8-113: Example of fatigue life data fitting obtained with 12 samples (Section A)

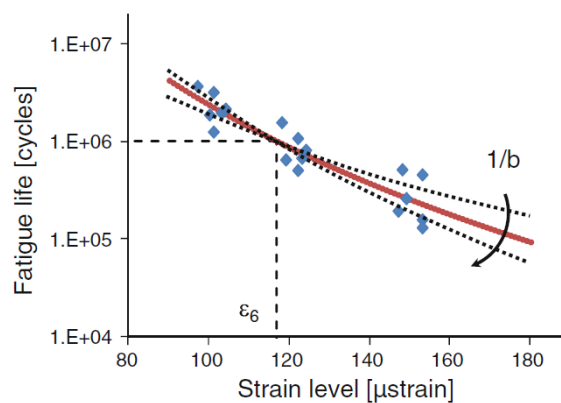


Figure 8-114: Example of fatigue life data fitting obtained with 18 samples (Section B)

Table 8-44 shows the eight combinations of factors corresponding to the tested mixes.

Table 8-44: Varying factors of mixes tested in Section A

Mix	Aggregate nature	Filler nature	Binder content (%)	Binder nature
Mix 1	Limestone	Hydrated lime	5,35	35–50 B
Mix 2	Basalt	Limestone	5,35	35–50 B
Mix 3	Basalt	Hydrated lime	4,35	35–50
Mix 4	Limestone	Limestone	4,35	35–50
Mix 5	Limestone	Limestone	5,35	35–50
Mix 6	Basalt	Limestone	4,35	35–50 B
Mix 7	Basalt	Hydrated lime	5,35	35–50
Mix 8	Limestone	Hydrated lime	4,35	35–50 B

Table 8-45: Results of fatigue tests (mixes of Section A); different strain levels at 10 °C, 25 Hz

Mix	ϵ_6 (µm/m)	1/b (-)	$\Delta\epsilon_6$ (µm/m)	Void content (%)
Mix 1	131	-6.28	4	5,3
Mix 2	155	-8.01	6	3,1
Mix 3	115	-5.66	4	5,1
Mix 4	102	-4.94	5	4,5
Mix 5	115	-5.94	4	5,1
Mix 6	122	-7.74	3	5,8
Mix 7	112	-4.99	6	4,9
Mix 8	111	-3.25	10	4,3

All mixes of Section B have the following common characteristics with fixed continuous 0/14 gradation curve of HIMA type, silica-limestone aggregate and 5,35 % total binder content by weight of the final mix. Fatigue life was determined as the number of loading cycles corresponding to a 50 % reduction of the initial complex modulus value.

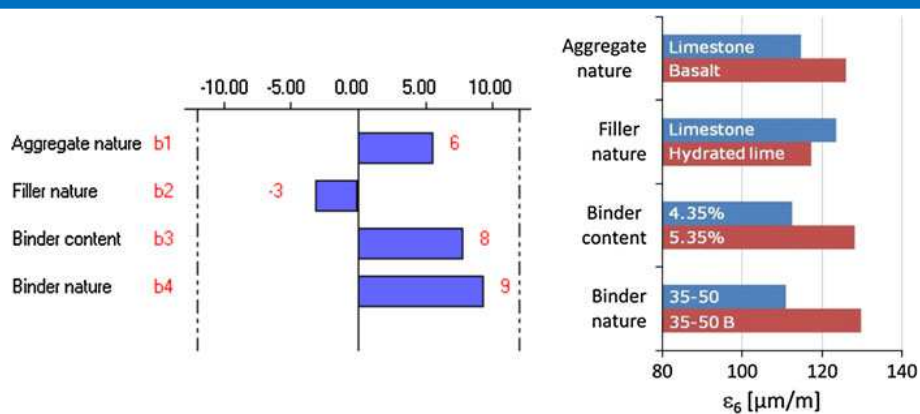


Figure 8-115: Histogram of ϵ_6 model coefficients of Eq (left); factor level variation on ϵ_6 (right) (Section A)

According to the histogram in Figure 8-30, using basalt instead of limestone aggregates, increasing binder content and adding 35–50 B instead of 35–50 seem to improve fatigue life of mixes. Although less importantly, the use of hydrated lime as so-called “active” filler does not improve ϵ_6 with respect to the addition of limestone filler. As for ϵ_6 , no factor level variation is identified by the software as statistically significant for $1/b$, although, as observed for the other two factors, some non-negligible differences are observed for different levels. In particular, $1/b$ is smaller in absolute value (therefore fatigue life of mixes varies less with strain level) when limestone aggregates are used instead of basalt ones, hydrated lime instead of limestone filler is added, a 4,35 % instead of 5,35 % binder content is fixed or 35-50 fresh binder is used instead of 35-50 B.

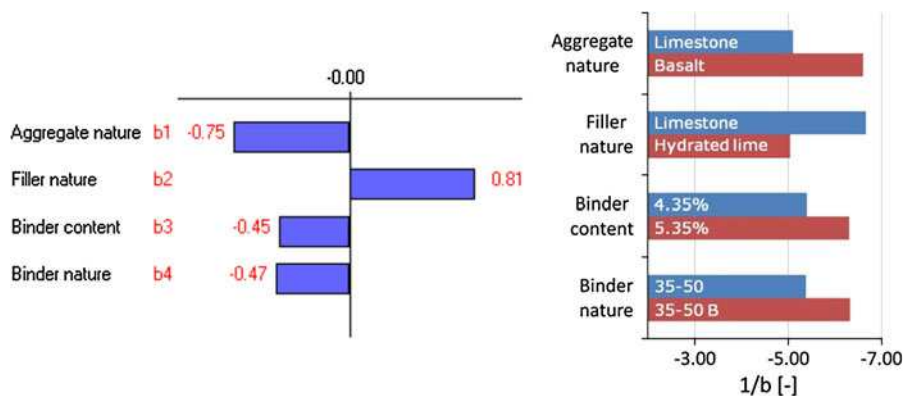


Figure 8-116: Histogram of $1/b$ model coefficients of Eq (left); factor level variation on $1/b$ (right) (Section A)

In section B ϵ_6 appears to increase with RAP content, reaching a peak value for RAP between 20 % and 40 % for mixes produced with 35-50 fresh binder. This observation confirms field experience. The parameter $1/b$ appears to increase with RAP content as well. An unexpected tendency is observed for ϵ_6 of mix produced with fresh binder 15-25. In particular, the mix containing 40 % of RAP shows an oddly low value compared to mixes with 20 % and 60 % of RAP. For these reason fatigue measurements were repeated on mixes containing 40 % and 60 % RAP. A good repeatability is observed for ϵ_6 , while $1/b$ values show a large variation. The authors hypothesize that the cause could be related to an incomplete blending of RAP and fresh binder within the mix when mixes with hard binders and high recycling rates (such as 40 % or 60 %) are produced.

Penetration values of bitumen blends corresponding to produced mixes decrease as RAP extracted binder content increases. Fatigue parameter ϵ_6 does not appear to follow a well-defined trend with bitumen blend penetration.

Table 8-46: Fatigue results obtained for mixes and corresponding binder blends of Section B; testing at different strain levels

Mix	ϵ_6 ($\mu\text{m/m}$)	1/b (-)	$\Delta\epsilon_6$ ($\mu\text{m/m}$)	Penetration (dmm) ^a
15–25 + 0 % RAP	135	-7,35	6	16
15–25 + 20 % RAP	147	-7,65	7	16
15–25 + 40 % RAP	121 (123)	-4,35 (-6,90)	14 (11)	12
	124	-9,44	7	
15–25 + 60 % RAP	138 (140)	-11,76 -9,40	4 (4)	11
	142	-7,04	3	
35–50 + 0 % RAP	117	-5,49	4	34
35–50 + 20 % RAP	130	-5,92	5	24
35–50 + 40 % RAP	131	-5,59	5	19
35–50 + 60 % RAP	121	-6,58	5	16
70–100 + 0 % RAP	118	-4,50	5	73
70–100 + 20 % RAP	129	-5,56	5	42
70–100 + 40 % RAP	128	-5,78	6	33
70–100 + 60 % RAP	135	-6,94	6	22

^a Penetration value obtained on bitumen blends (virgin binder + recovered RAP binder)

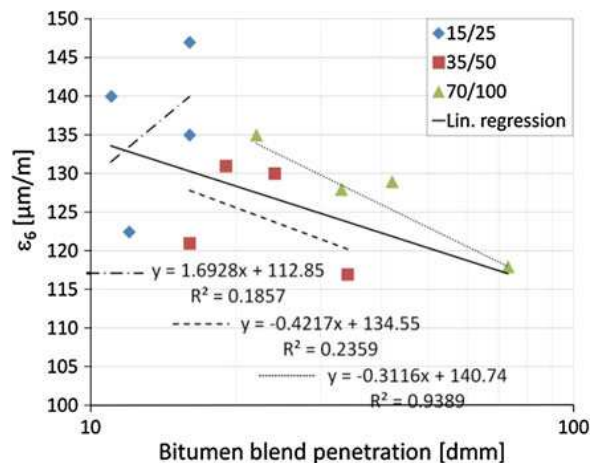


Figure 8-117 – ϵ_6 of mixes of Section B against penetration of corresponding bitumen blends in logarithmic scale

No factor was identified as significant for ϵ_6 and 1/b. Binder content and nature appear to have noticeable influence on fatigue life of mixes. Therefore, a partial conclusion extracted from Section A is the importance of bitumen nature and content, among the considered mix design factors, with regards to mixture performances. The only discrepancies are observed for mixes produced with a hard binder and high recycling rates, probably because of blending issues between binders. Observed fatigue performances of mixes containing up to 60 % RAP material are encouraging from technical, economical and environmental points of view.

8.3.3.7 Paper 461 (Blankenship and Anderson, 2010)

A laboratory study was proposed to investigate the effect of density ranging from 88,5 % (11,5 % air voids) to 96,0 % (4,0 % air voids) of G_{mm} . It was assumed and later proven, that an increase in 1,5 % density can increase the fatigue life by 8 %. The use of a 9,5mm nominal maximum aggregate size mixture that serves as surface layer was selected. A Performance Grade (PG) 64-22 was selected as for the laboratory standard binder.

All test samples were made using optimum 5,4 % bitumen. The optimum bitumen content plus 0,5 % and 1,0 % mixtures were made. Samples for this limited testing were made at 93 % of G_{mm} . Six sets of specimens representing different density levels were prepared for beam testing at 1,5 % density increments. Five beams were fabricated for each density increment. The aggregates and asphalt were mixed and aged according to AASHTO R30.

Beam fatigue samples were tested in a 4-point beam fatigue apparatus using constant strain at a typical 20°C test temperature. The strains were varied from 300 to 800 microstrain to produce resulting cycles to failure (Nf) in the range of 10 000 to 1 000 000. The cycles to failure were calculated using the cycles x modulus numerical method.

The trend was as expected. As the air voids decreased, the cycles to failure increased especially at lower test strains. This was true until the fatigue cycles to failure hit a maximum at about 6.0 % air voids. Other observations from this data were:

- A decrease in air voids from 8,5 % to 7,0 % yield fatigue life increases of 4, 8, and 10 % at 500, 450, and 350 microstrain.
- The effect of air voids on the fatigue life of the asphalt mixture became more pronounced at lower strain levels. This may represent a pavement section with lesser load or deeper in the pavement cross section.
- The lack of response at the high strain may indicate that regardless of the air voids, high movements will quickly fail this mixture. This lack of response to high strain may be seen when overlaying a severely cracked pavement or concrete joint with low load transfer (high potential movements that result in reflective cracking, sometimes regardless of the HMA quality).
- The peak at the 6,0 % air voids and the lower cycles to failure to the left of the curve is most likely the result of crushed aggregates that were noted in the specimen preparation. If the mixture had been optimized to a lower air void level, such as two or three percent, the fatigue life should have continued to increase as air voids decreased.

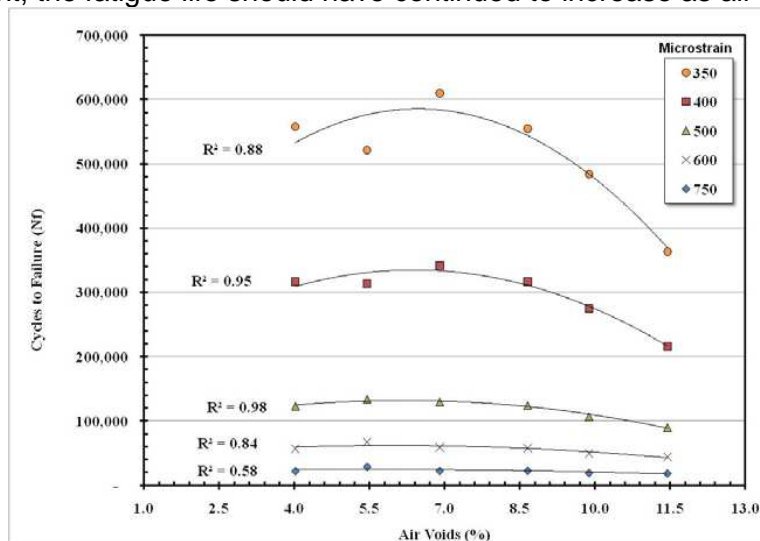


Figure 8-118: Beam fatigue cycles to failure for varying air voids and strains

Table 8-47: Sample results of varying bitumen content with similar air voids

Bitumen content (%)	5.5	5.9	6.4
Beam fatigue cycles to failure at 20°C and 500 $\mu\epsilon$, Nf	110,745	123,450	263,805

As asphalt content increased, the fatigue life increased. Note the fatigue life did not change much with the 0,5 % bitumen.

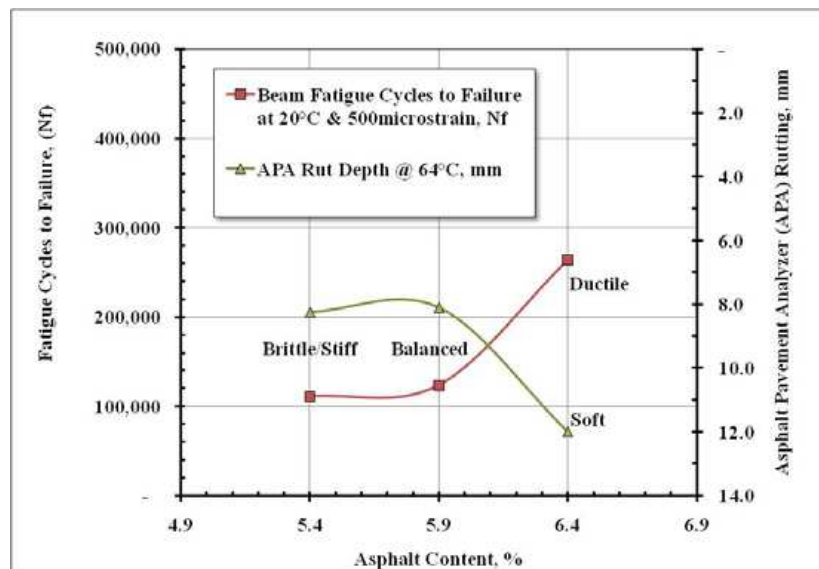


Figure 8-119: Effect of bitumen content on flexural fatigue and APA rutting

If the fatigue and APA rutting data are shown together as in Figure 8-30, one can see that this mixture could possibly be designed with more asphalt binder without causing much change if the air voids were held constant.

8.3.3.8 Paper 519 (Radenberg et al., 2014)

The potential of differently originated recycling agents was evaluated in another study to restore the desired binder properties and the results were compared with performance-related test results of 100 % RAP mixture. Binder test results showed that application of organic products require much lower dose to provide the same softening effect as petroleum products. Organic oil and both waste vegetable products provided the best performance in binder and mixture fatigue resistance tests as measured by linear amplitude sweep and fracture work density respectively. It was observed that penetration test may be a good indicator for initial selection of optimum dose since the results provide indication of rut resistance as well as fatigue performance of mixture and can be easily predicted using an exponential relationship that was developed in the research.

The mixture were crushed to nominal maximum aggregate size of 9,5 mm. The RAP had a relatively high binder content (6,2 %). The binder content was 5,94 % after the addition of the recycling agents and was kept constant for the different mixtures. Used bitumen had penetration of 68 dmm and softening point of 51 °C.

Six different recycling agents were added to extracted RAP binder at 12 % dose and changes in consistency as well as fatigue characteristics using the linear amplitude sweep (LAS) test were determined and compared to those obtained from tests on the virgin binder. The recycling agents that were used in the study: waste vegetable oil (WV oil), waste vegetable grease (WV grease), organic oil - Hydrogreen STM, distilled tall oil, aromatic extract and waste engine oil (WEO).

To evaluate benefit of simply increasing binder dose rather than adding recycling agents, virgin binder was added to the RAP at 12 % from binder mass (equal to dose of recycling agents). This mixture is named "RAP mix". To quantify performance of this 9.5 mm gradation

as a virgin mixture aggregates were mixed with 5,94 % of virgin bitumen which is equal to that of the rejuvenated samples. The aggregates for this mixture were obtained by removing binder from the re-graded RAP in an ignition oven. This mixture is named “Virgin Mix”.

Binder was extracted from RAP using toluene. To determine the softening efficiency of these products, penetration was determined at 25 °C and additionally at 4 °C to calculate the penetration index (PI). The LAS (AASHTO TP-101) test has been proposed as a replacement to currently used PG grading intermediate temperature parameter $G^* \cdot \sin \delta$. The LAS procedure uses DSR testing unit with 8 mm plate and 2 mm gap setting. To allow direct comparison to $G^* \cdot \sin \delta$ the test was performed at 25 °C after short plus long term aging. The test is conducted in two steps. First, a frequency sweep is run from 0,1 to 30 Hz at a strain level of 0,1 % to determine undamaged linear viscoelastic properties of asphalt binder (complex shear modulus and phase angle). This data is used to calculate the slope m of the best-fit linear log-log plot of storage modulus versus frequency. The material constant α is then calculated. Secondly, a strain sweep test is performed in strain-controlled mode at a constant frequency of 10 Hz with linearly increasing strain from 0,1 to 30 %. At each strain level mean G^* , phase angle, and oscillatory shear stress is recorded. A typical plot of damage accumulation is illustrated in Figure 8-30. It is used to calculate the curve fit coefficients for calculation of damage accumulation in the specimen at any strain level using the viscoelastic continuum damage (VECD) approach. The results are expressed as cycles to failure (N_f), where the failure is defined as 35 % reduction from undamaged $G^* \cdot \sin \delta$.

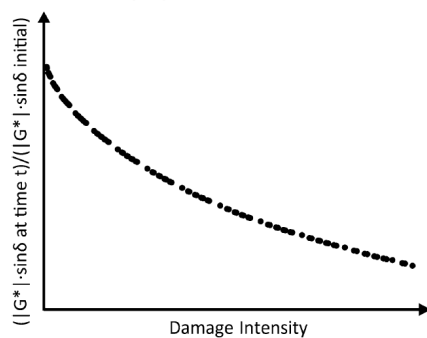


Figure 8-120: $|G^*| \cdot \sin \delta$ at time t divided by initial $|G^*| \cdot \sin \delta$ versus damage plot for linear amplitude sweep test (AASHTO TP 101)

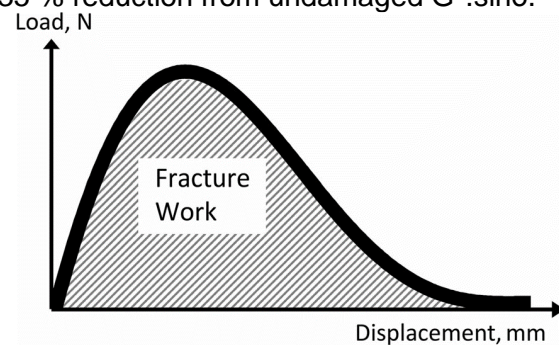


Figure 8-121: Schematic diagram of fracture work

Fracture work density (FWD) is conducted at a constant ram movement of 50,4 mm/min at 19 °C temperature. Since fatigue damage is likely to occur later in pavement life, before testing FWD, additional long term aging at 85 °C for 5 days was conducted. The fracture work is determined by measuring the area under the load-vertical deformation curve until the load returns to zero as illustrated in Figure 8-30. The work done by the machine ram is dissipated by the specimen, and therefore the fracture work can be determined based only on the load and vertical ram movement. The FWD is then calculated by dividing the fracture work by the volume of the specimen.

The binder LAS test results in Figure 8-30 on a logarithmic scale demonstrate cycles to failure at four different strain levels. Interestingly at the lowest strain level, RAP binder has the highest fatigue life compared to other samples but as the strain increases its performance gradually decreases until it has the lowest cycles to failure at 10 % strain. Virgin binder has the opposite trend: at high strain level it performs better than at low strain level relative to most other samples. Since the strain level can be attributed to pavement response, this suggests that RAP binder would perform better at lower loads or thicker pavements while the virgin binder would be superior at higher loads or thinner pavements.

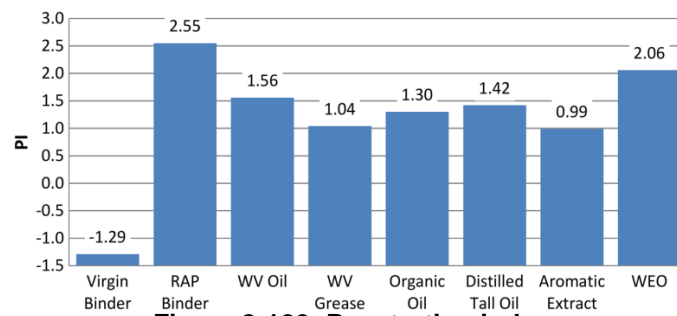


Figure 8-122: Penetration index

At 5 % strain level, unexpectedly, WEO and aromatic extract have almost no effect compared to RAP binder. This is surprising considering that these products have been extensively used for rejuvenation and provided good field performance. Addition of tall oil and organic oil has increased the number of cycles to fatigue failure compared to extracted binder, but the result is lower than that of virgin binder. The use of WV grease and WV oil provides performance that is similar to the virgin mix. Predictably this confirms that a reduced binder viscosity provides longer fatigue life.

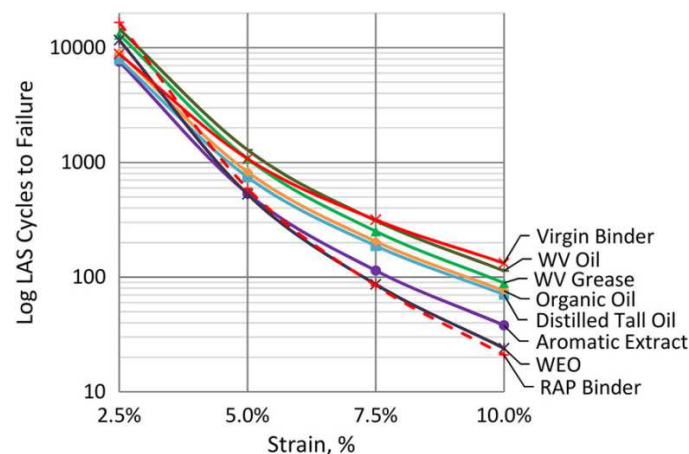


Figure 8-123: Linear amplitude sweep test results

The mixture FWD results in Figure 8-30 demonstrate that most recycling agents provide FWD similar or slightly higher than that of the RAP mix. The only exception is WEO, thus suggesting negative effect on bottom-up fatigue resistance. The virgin mix has the highest FWD which is a result of high strain before failure.

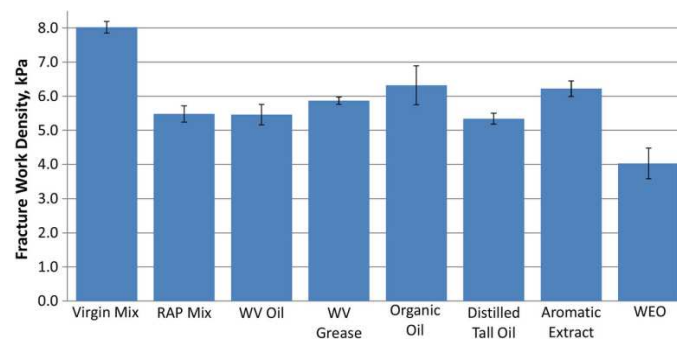


Figure 8-124: Fracture workdensity

Although both are designed to demonstrate fatigue performance, the binder LAS tests results correlate poorly with FWD results. This is likely due to the very different loading modes between the tests methods.

8.3.4 Fatigue life and healing effect

8.3.4.1 Paper 557 (Pérez-Jiménez et al., 2007)

This study conducted an analysis of binder's fatigue and healing using laboratory Dynamic Shear Rheometer (DSR) testing and a specifically designed intermittent loading sequence. Based on fundamental dissipated energy concept, the ratio of dissipated energy change (RDEC) approach which has been successfully applied in the mixtures' fatigue and healing study is adopted for the binder.

The previous work by Carpenter and Shen (11, 17, and 19) demonstrated that not all dissipated energy is responsible for fatigue damage. Only the relative amount of energy dissipation coming from each additional load cycle, while excluding the energy dissipated through passive behaviors such as plastic dissipated energy, visco-elastic damping, and thermal energy, will produce further damage. This incremental value has a direct relation to damage accumulation. Similar description by Delgadillo and Bahia (20) also suggested that the relative change of dissipated energy due to repeated cycling is a good direct physical indicator of the fatigue damage initiation and propagation. A low amount of relative energy dissipation can be found either in high fatigue resistant materials, low external loading amplitude, or both (17). This relative energy dissipation has been well related to fatigue damage of HMA mixtures which uses the ratio of dissipated energy change (RDEC) to describe fatigue.

The plateau value (PV), the representative value of the ratio of dissipated energy change (RDEC) parameter, is defined as the RDEC value that corresponds to the number of loading cycle at the 50 % initial modulus reduction. This plateau value (PV) has been demonstrated in the previous study (17, 22) to be a unique parameter which can be fundamentally related to the fatigue life of HMA mixtures, regardless of the material type, loading modes and testing conditions. The unique curve PV (plateau value) vs. Nf (fatigue life) has been constructed as $PV = 0,539Nf^{1,038}$ with an R^2 value of 0,9831 and a standard error of estimate of 0,123 (in logPV) for the 19 typical Illinois HMA mixtures.

A similar intermittent loading sequence as used in the mixture's fatigue and healing study (11) is adopted in this study for binder testing. A short constant rest period varying from zero to 6 seconds is inserted after every ten load pulses to simulate a rest period between loads. Such design of loading sequence provides better simulation to the field loading condition comparing with interrupted loading sequence (continuous loading – full stop for longer rest period – resume continuous loading). At the same time it maintains the continuous loading nature so that the dissipated energy can still be calculated for each load cycle, which enables us to perform dissipated energy analysis.

Two types of bitumen PG64-28 and PG70-28 were used in this study. They represent neat binder and polymer modified binder, respectively. Both binders were tested at two different temperatures (25 °C and 15 °C), 10 Hz frequency, with constant stress loading mode and with various rest periods. The tests used 8 mm spindle with 2 mm gap setup. Constant stress loading mode was selected because under constant stress mode the DSR equipment can have quicker response and thus maintain a nice sinusoidal loading wave when a rest period is introduced. For the failure criteria, the traditional 50% stiffness reduction approach is used to be consistent with asphalt mixture fatigue tests.

In order to be comparable with most existing fatigue study results, the traditional strain-fatigue life (Nf) relationship was developed for the binders' controlled stress fatigue testing with no rest period added. In the controlled stress loading modes, the initial strain, an average of the strain from cycle 170 to 300, was selected as representative strain. As shown in Figure 8-30, under the log-log plot, the strain-Nf follows a linear relationship for each binder and testing condition. Specifically, lower temperature produced shorter fatigue life at the same initial strain level.

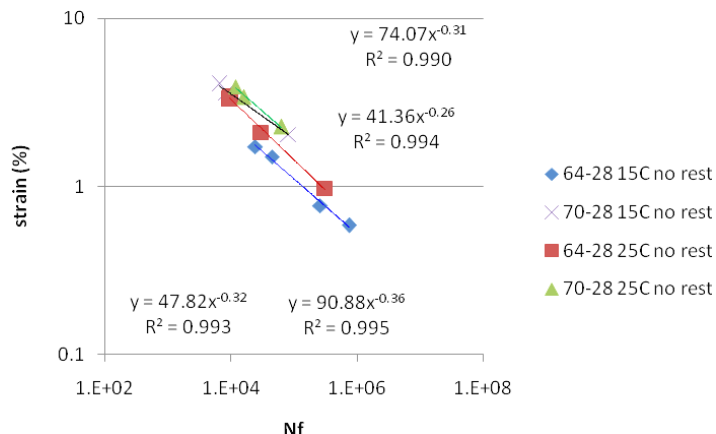


Figure 8-125: Traditional strain-Nf relationship for binder's fatigue testing results

As observed in this study and other studies (13), phase angle is not very sensitive to fatigue damage. During the fatigue test, the phase angle only has marginal (limited to few degrees) increase. Therefore, the complex shear modulus (G^*) can be used to represent the deterioration of material performance due to fatigue effect. As shown, although starting from almost the same initial complex modulus G^* value, the ones with longer rest periods travelled much longer before they reached the 50% initial G^* reduction.

The ratio of dissipated energy change (RDEC) and the plateau value (PV) for all binders tested at different conditions are then. The results are plotted versus fatigue life Nf in Figure 8-30. As shown, no matter the binder type (PG64-28 and PG70-28), temperature (15 °C and 25 °C), stress levels (varies from 60 kPa to 230 kPa), and with or without rest period (0-6sec), all data points follow a unique PV-Nf line with R² value of 0,975. This provides more substantiation that the dissipated energy based RDEC approach and the unique PV-Nf relationship which has been validated for HMA mixtures is also applicable for bitumen.

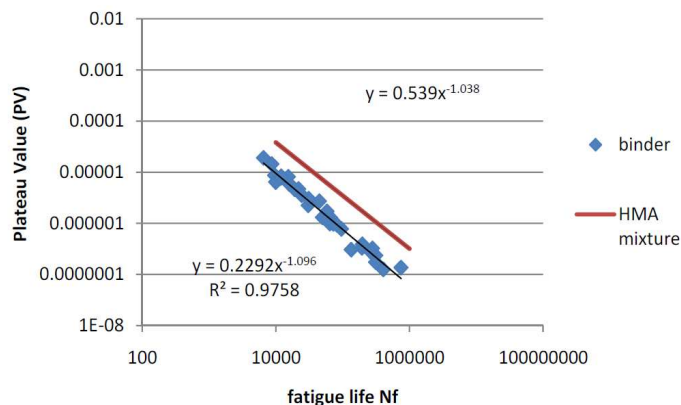


Figure 8-126: Plateau Value (PV) vs. fatigue life (Nf) plot for all tested binders

Also indicated in Figure 8-30 is the PV-Nf unique curve developed for 19 typical Illinois HMA mixtures using linear regression method. As shown, the binder's PV-Nf curve has the similar slope as the mixture's but with different interception. The effect of aggregate-binder interaction is hypothesized to be responsible for the difference of the two curves, which requires further evaluation.

Table 8-48: Results for different testing conditions

Binder type	Temperature (°C)	Stress (kPa)	Initial Strain (%)	initial G* (MPa)	Initial DE
PG64-28	25	60	3,27	1,95	5,33
PG64-28	25	70	3,45	2,14	6,56
PG64-28	15	180	1,74	10,85	7,88
PG70-28	25	60	3,30	1,95	5,20
PG70-28	25	70	3,75	2,00	6,90
PG70-28	15	230	3,50	6,75	20

The fundamental energy based RDEC approach is applicable for evaluating the fatigue and healing behavior of asphalt binder. It produces a unique PV-Nf curve for asphalt binder regardless of the binder type, stress/strain levels, temperatures, and with or without rest periods.

8.4 Binder ageing effect on fatigue cracking

8.4.1.1 Paper 143 (Baek et al., 2012)

In this paper, the phenomenon of oxidative aging is examined in terms of its effects on the dynamic modulus and fatigue performance of asphalt mixtures. For this purpose, an asphalt mixture is aged in the laboratory at four different aging levels namely short-term aging STA (135 °C for 4 hours before compaction), long-term aging LTA1 (STA+ conditioning at 85 °C for 2 days before testing), LTA2 (STA+ conditioning at 85 °C for 4 days before testing) and LTA3 (STA+ conditioning at 85 °C for 8 days before testing). Mechanical tests for the four aged mixtures are performed to characterize the linear viscoelastic and damage properties.

In Figure 8-127, the master curve for different levels of aged mixtures is depicted. It is observed that, in general, the stiffness increases with aging time over all of the frequency ranges. Moreover, a clearer trend with regards to aging time is observed at low reduced frequencies (physically representing warm temperatures and/or slow loading frequencies).

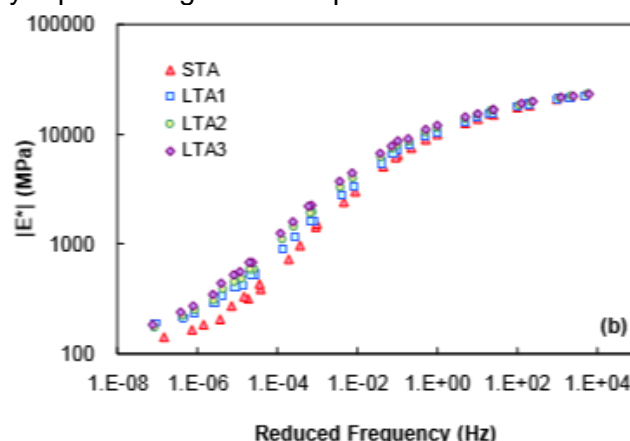


Figure 8-127: LVE properties of STA and LTA aged mixtures: $|E^*|$ mastercurves in log-log space

Cyclic fatigue tests were conducted for all four aged mixtures under CS (controlled stress) and CX (controlled crosshead) cyclic conditions. The phase angle criterion has been chosen

in order to define the fatigue life the mixtures. The reason for choosing this criterion is that phase angle criterion works well under both CX and CS test.

Comparisons of the cyclic test results lead to the following conclusions:

- Regardless of testing mode, temperature, and aging level, fatigue resistance decreases as the magnitude of the input increases;
- From the CX test results and from comparisons at a similar initial strain magnitude, as the temperature decreases or the aging time increases, the resulting initial stress magnitude increases and the N_f decreases;
- From the CS test results and from comparisons at a similar initial stress magnitude, as the temperature decreases or the aging time increases, the resulting initial strain magnitude decreases and the N_f increases.

Overall, the different testing modes result in the opposite fatigue performance; e.g., the STA mix shows better performance in the CX tests, but the LTA3 mix shows better performance in the CS tests. It is known, based on energy principles that stiff materials tend to perform better in CS test protocols, whereas soft materials yield better performance in CX tests, all other factors being equal. Depending on the mode of loading (i.e., stress- or strain-controlled), the ranking of the mixtures can be quite different. Stress-controlled push pull tests reveal a reverse trend when compared to field fatigue data obtained from the Federal Highway Administration's Accelerated Load Facility (FHWA-ALF) whereas strain-controlled tests provide the correct trend.

8.4.1.2 Paper 034 (Dreessen et al., 2012)

A comparative experimental study has been conducted using a highway located in canton of Valais in Switzerland. The aim was to evaluate the performance of PMB if in-situ aged. Site has been subjected to heavy traffic loading as well as harsh weather conditions. The period of study for different sites was 2, 8, 14 and 19 years. The binder types are 80/100 and Styrelf 13/80 from TOTAL allowing a comparison between pure and polymer modified binders. The PMB sections in general exhibit a much better ageing resistance throughout the tests carried out. The low evolution of ageing is probably due to the original process of binder reticulation which limits the possibility of oxidation and improves the durability of the surface. Moreover, the polymer network was still present after 19 years of service life reflected by elastic properties of the PMB which were maintained at a high level in relation to their initial value.

8.4.1.3 Paper 272 (Pérez-Jiménez et al., 2014)

In this study, three types of bitumen were used, before and after ageing: a conventional 50/70 binder, a crumb rubber modified BC 35/50 binder and a polymer modified PMB 45/80-65 binder. With use of these three binder type, 6 mastics were fabricated, 3 with regular binders, and 3 with aged binders. Six different mixtures were manufactured with the same strategie as the mastics. Using EBADE test, the performance of binders, mastics and mixtures have been evaluated for three different temperatures (i.e. -5 °C; 3 °C and 10 °C). In Figure 8-128 the performance of PMB are shown. One may observe that the ageing has very limited impact on the binder complex modulus evolution.

Moreover, the relationship between the complex modulus of «aged» mastic versus the complex modulus for “aged” binders have been studied. One may see in Figure 8-129 that a linear relationship exists for both cases. There is only one deviation value for the 50/70 binder at -5 °C, due most probably to technical mis takes.

In conclusion, it has been shown in this paper that the fatigue behaviour of asphalt materials could be characterized using their initial complex modulus and their failure strain, extracted

from EBADE tests. For asphalt materials with the same modulus, the higher their failure strain, the better their fatigue behaviour. Moreover the results showed that the modified polymer binder has a better fatigue response than any other binders studied. This fact was observed for binders as well as mastic and asphalt mixtures.

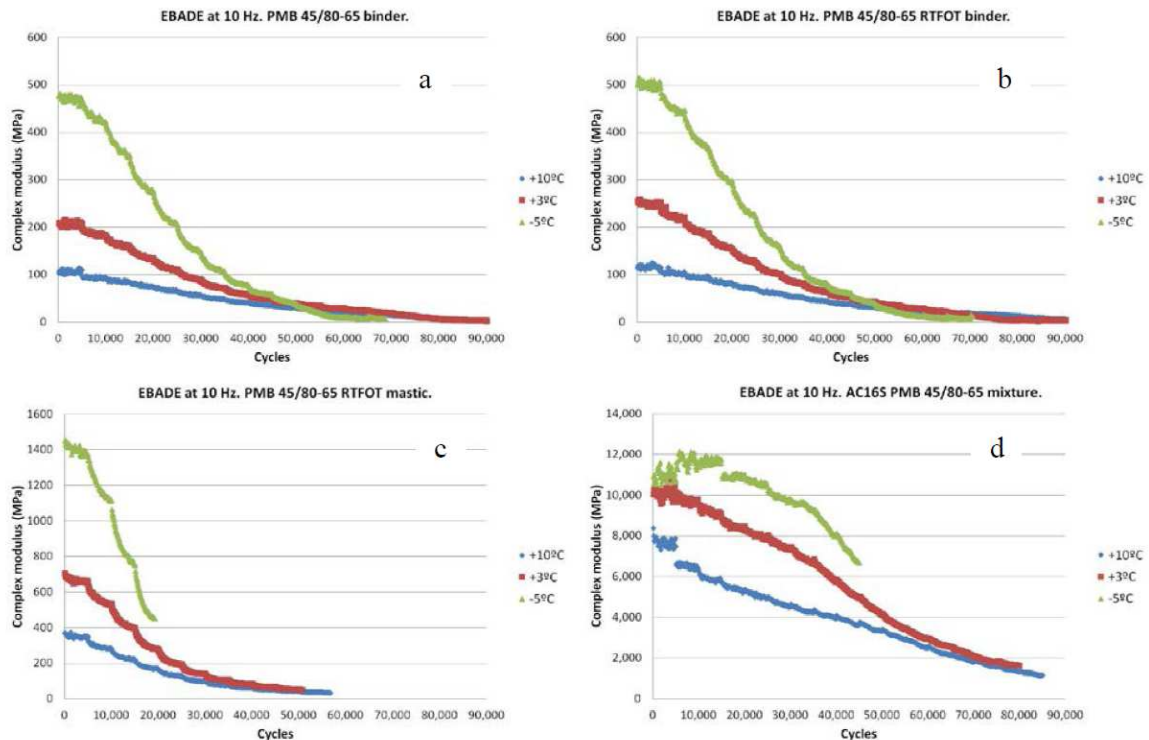


Figure 8-128: Complex modulus evolution with the number of cycles for the PMB 45/80-65 binder before (a) and after RTFOT (b), mastic (c) and mixture (d)

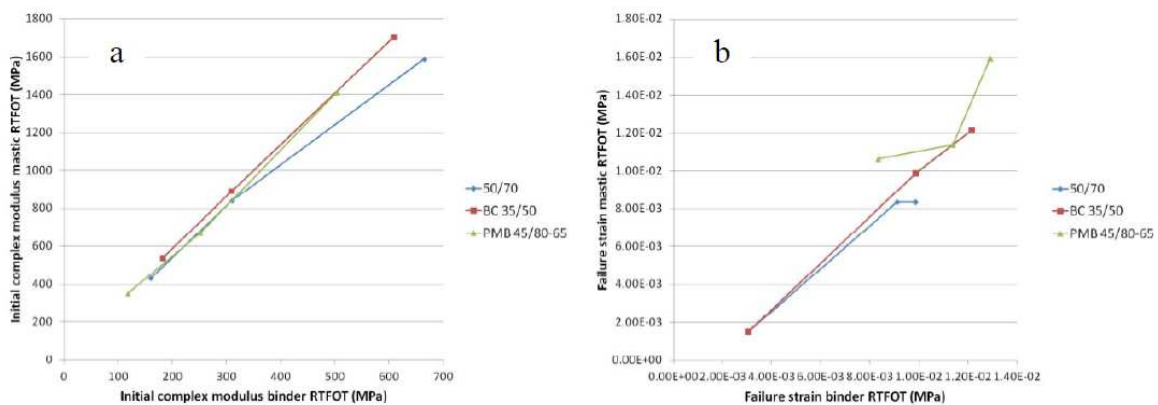


Figure 8-129: Comparison between the failure strain values; binders (a), binder after RTFOT (b)

8.4.1.4 Paper 297 (Farhana et al., 2014)

This paper focuses on structural characteristics of aged asphalt concrete pavements. If asphalt layers are overlaid, their structural characteristics change due to ageing of asphalt. In order to evaluate the fatigue performance of these structures, six pavement test sections in Kansas has been tested, using Direct Tension Fatigue testing method. The fatigue results were expressed in terms of traditional fatigue relationship as follows:

$$N_f = k_1 (1/\varepsilon_i)^{k_2}$$

The summary of fatigue test results are given in Table 8-48 with their corresponding binder and air contents. The older layers usually have higher binder contents than the range of 5%-7% which is the range encountered in the Superpave mixture design in Kansas. Some of the higher binder contents in the older layers might be the result of pavement surface maintenance (e.g. surface recycling, chip seal, etc).

In general, the higher the value of k_2 , the more fatigue susceptible the mixture would be. Overall, according to the results presented in Table 8-48 the older layers show a higher k_2 values. However the test results revealed some exceptions as it can be seen in this table. Furthermore, the fatigue results were also statistically analyzed on a project-by-project basis. The dependent variable was the maximum strain or the strain at failure. The independent variables were the initial strain, resilient modulus (M_r), asphalt content (AC), air void (VA), and age of the layer. The results show that no consistent, statistically significant factor was identified for all projects. However, all significant factors, such as, initial strain (or resilient modulus for one project), air voids, and asphalt content, are already known to affect the fatigue life of an AC pavement. The study reconfirms the importance of these factors. It is recommended that these factors, initial strain, binder content and air voids are strictly controlled during the pavement design, AC mix design, and construction process.

Table 8-49: Summary of fatigue test results

Projects	Layer	Year	NMAS (in)	Data points	k1	k2	Pb (%)	Pa (%)
I-70	BM1T, SRECYL	2000	0,75	9	7126,2	0,2717	4,68	8,12
	CRECYL	2000	0,75	12	1391,6	0,0892	4,23	7,43
	HM3A	1960	1	0			6,53	
US-56	SM125A, SRECYL	2006	0,5	6	588,08	-0,039	5,01	5,88
	BM2A, CRECYL	1999	0,5	7	5796,7	0,2068	5,64	4,56
	HRECYL	1992	0,75	9	10093	0,2726	5,64	5,43
	BC1	1968	0,75	2	19847	0,637	5,68	8,55
US-59	SM95A, HRECYL	1993		10	1481,3	0,0617	6,12	6,60
	BM3, HM3B	1976		5	5681,8	0,332	6,39	6,08
	ACB3	1961		0			5,81	
	AB3	1960		1			5,93	7,90
US-169	SM95T, SR190B	2002	0,75	8	2124,4	0,0611	6,51	7,09
	SR-190A	2002	0,75	9	751,97	-0,0139	5,94	7,73
	ACB3	1973	0,75	28	3734,8	0,1627	5,86	3,24
K-4	SR95T, SRECYL	2002		3	1263,5	0,0834	5,91	7,37
	HRECYL, BM2	1995		3	703,17	0,0125	6,63	5,33
	HMSP	1965		7	2537,3	0,2166	6,35	5,01
	ACB2R	1965		7	2997,5	0,2695	6,89	6,94
K-141	SM125A, BM2A	1995	0,5	8	2762	0,239	5,11	6,09
	BM2	1987	0,5	6	1881,2	0,1498	5,87	6,33
	BITCOV	1962	0,5	2	6165,4	0,446	5,69	7,75

*Highlight cells: Lower number of data points

8.4.1.5 Paper 481 (Oliveira et al., 2010)

Paper focuses on assessment of fatigue resistance and ageing of asphalt mix used typically in Portugal. Stiffness and fatigue are assessed by means of 4PB-PR test according to EN 12697-26 and EN 12697-24. Tests are performed at frequency of 10 Hz. For fatigue also 30 Hz was evaluated since this value is given in the European standard (EN 13108-20). Additionally ageing was studied since it is considered as an important factor for the performance of asphalt mixtures, particularly in their resistance to fatigue. In order to understand the contribution of ageing phenomenon, the effect of ageing was performed after submitting some test specimens to laboratory simulated ageing according to the long-term oven ageing (LTOA) process – test specimens are aged for 5 days at 85 °C.

The fatigue life was defined as the number of repeated load cycles corresponding to a 50% reduction in initial stiffness. Resulting values show relatively low ϵ_6 (resistance of 1×10^6) around 60 and 70 microstrains. Higher values are expected if the frequency is reduced to 10 Hz. The values are similar for aged and un-aged test specimens, which is different from the findings gained for stiffness where the modulus increased for aged test specimens.

8.5 Overall uncertainty of fatigue cracking

One of the main issues concerning the uncertainty in fatigue cracking is the uncertainty in fatigue testing of bitumen as well as asphalt mixtures. In this chapter some important points, regarding this issue that has been raised by different researchers will be discussed.

8.5.1.1 Paper 052 (Qi et al., 2008)

In this paper, asphalt binder fatigue parameters obtained from three different procedures have been compared and validated with pavement performance data from FHWA Accelerated Loading Facility (ALF) testing. The three procedures used are as follows: stress sweep based test, strain sweep and conventional based test. Unlike conventional fatigue test, both strain and stress sweep tests take much less time and failure is reached rapidly due to increased energy input as the strain or stress is increased. New fatigue parameters have been identified in this study, in order to match well to pavement performance. The new fatigue parameters are “shear stress at failure” and “loss modulus ($|G^*| \sin \delta$) at 2% strain level” which can be obtained from either strain sweep test or stress sweep test.

8.5.1.2 Paper 071 (Ballié et al., 2008)

Ten bituminous binders from various origins (conventional, polymer modified and special bitumens) were characterised in terms of their physical and mechanical properties in three different conditioning states (fresh, artificially RTFOT aged and extracted from laboratory formulated asphalts). The characteristics of dense asphalts (French BBSG) formulated for standard usage with these binders, were also determined in accordance with the procedures in force at the time of the study.

The classical "simple" binder tests are unable of reproducing the fields of stress and deformation to which asphalts are submitted. Furthermore, these binder tests, especially the "rheological" ones, generally involve only one single type of behaviour at a time, whereas in the asphalt test, the binder is submitted to a variety of stresses (major deformation, minor deformation, tensile - shearing, etc.). Finally, the measurement uncertainty of the asphalt tests also includes the uncertainty in the specimen production. Therefore it is no surprise that one often needs to use multi-criteria type correlations based on tests, which, taken individually, only imperfectly reflect one aspect of the behaviour of the binder in the mixture.

It was found in this paper that, it will not be possible to base the framework of future performance specifications solely on tests such as DSR and BBR as currently conducted. In

general terms, we can conclude that the study underlined the shortcoming of rheological tests restricted to the domain of linear behaviour under small deformation. This is indeed demonstrated by the characteristics derived from the tensile test or the pendulum test, which appear in the correlations with the asphalt performances. So the range of tests currently covered for the performance approach should be completed with additional indicators.

8.5.1.3 Paper 083 (Perez-Jimenez et al., 2011)

The paper has the specific aim of testing the effect of thermal stress on fatigue performance through the EBADE test using two mixes AC 16 S with two different bitumen (13/22 and 60/70). The fatigue behavior was determined at 20°C and 5°C, during a period of 12 hours lowering the temperature (from 20°C to 5°C) showed in Figure 8-128 and after a period of 1 hour lowering the temperature showed in Figure 8-128.

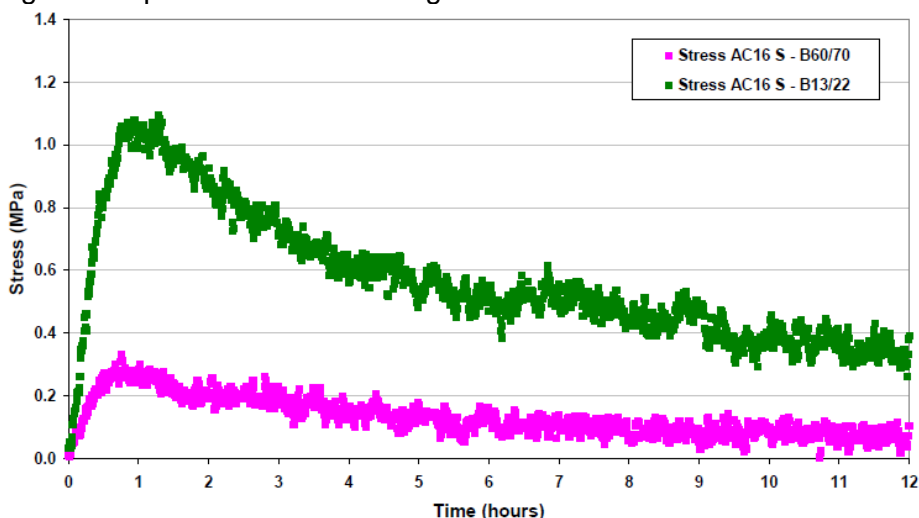


Figure 8-130: Thermal stresses recorded during a 12h period, 60/70 and 13/22 AC mixture

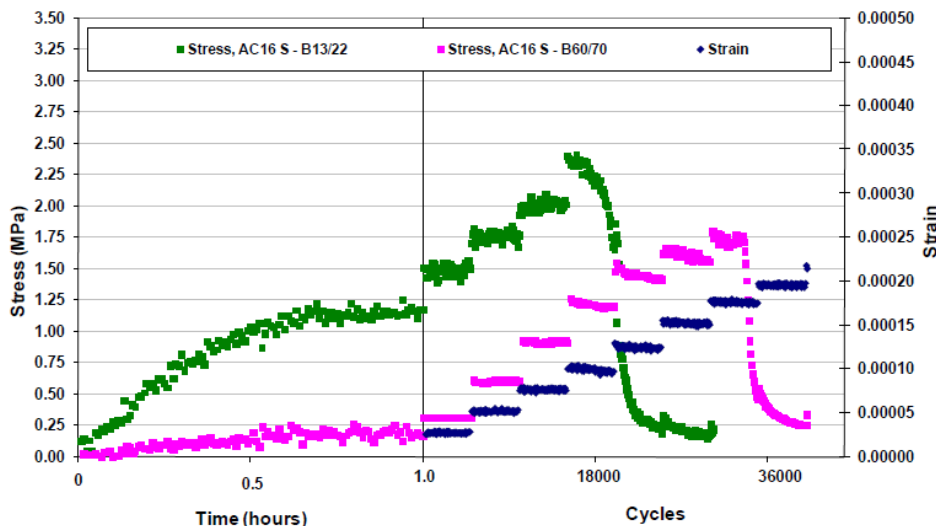


Figure 8-131: Thermal stresses recorded during a 1h period, T (°C) from 20 °C to 5 °C, subsequent application of EBADE method, 60/70 and 13/22 AC mixture

The fatigue resistance of both mixes depends on the initial thermal stress induced. The EBADE test allows the evaluation of the fatigue behavior in the combined presence of traffic load and environmental conditions.

$$\epsilon_T = \epsilon_T + \epsilon_C$$

ϵ_T = total strain

ϵ_t = thermal strain

ϵ_C = traffic loads strain

8.5.2 Paper 089 (Timm et al., 2011)

The objective of the paper is to correlate the full-scale structural and fatigue characteristics of WMA mixes with high content of RAP. The main results highlighted that:

- There is no need of a special treatment in the load response modeling for pavement design when WMA and RAP are used.
- None of the experimental sections were statistically different from the control (ANOVA) with respect to the strain at lower temperature. The situation is different for higher T.
- At 110 °F RAP section has the lowest strain, the WMA the intermediate and the HMA the highest.
- Combining temperature-corrected strain responses with laboratory-derived beam fatigue transfer functions indicated that the RAP – WMA section would have the best performance at 68°F. The number of cycles to failure was approximately 3,6 times greater than the control.
- Caution should be exercised when considering the fatigue performance estimates. They were made using laboratory-determined transfer functions combined with strains corrected to the corresponding laboratory temperature and were extrapolated below that which was tested. Actual field performance may differ and was one of the primary motivations in building the sections to evaluate the full-scale field performance of these materials.

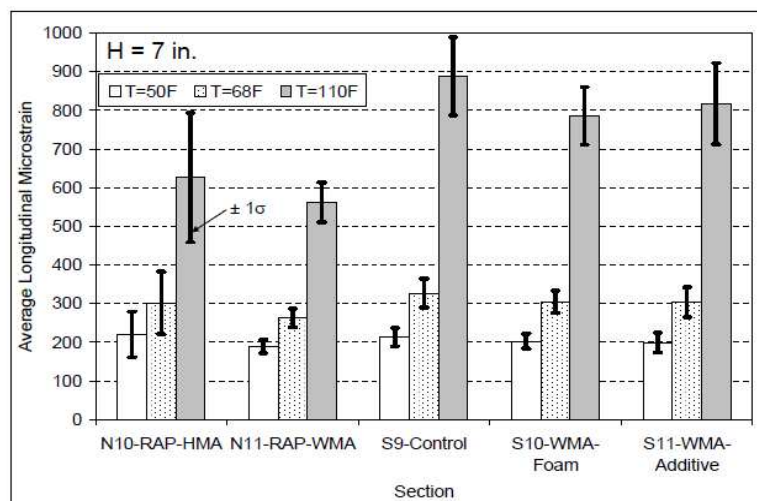


Figure 8-132 Temperature and thickness-corrected microstrain

8.5.3 Paper 134 (Perez-Jimenez et al., 2012)

It is accepted that the fatigue process of asphalt mixtures and binders subjected to cyclic constant amplitude loading is divided into three stages. In the first cycles, stiffness of the material drops rapidly because of thixotropy and/or a temperature increase. In the second stage, stiffness starts to decrease linearly. Finally, in the third stage macrocracks propagate and complete failure of the material occurs. This kind of test is called time sweep test

It is very important to differentiate between the real damage in fatigue tests and changes in viscoelastic behaviour and thixotropy. It is also crucial to account for the healing properties of the asphalt material that act after rest periods. This paper shows that in many cases, what is taken for fatigue failure during testing for asphalt binders, i.e. decrease in the complex

modulus below half its initial value is thixotropy. However for asphalt mixtures this matter has less importance.

Three different test modalities have been performed: time sweeps (i.e. constant strain amplitude until failure); increasing strain sweeps (i.e. increase in strain amplitude every 5000 cycle); up and down strain sweeps (increase and decrease in strain amplitude alternately). It was shown by the authors that most part of the mechanical properties loss experienced by the asphalt materials in fatigue tests is due to its viscoelastic behaviour and thixotropy, instead of irreversible damage. In this connection the complex modulus can be recovered by reducing the loading or, in our case, the strain applied. The study analyzed the failure criteria currently used in fatigue testing of asphalt mixtures and binders, and evaluates the parameters chosen, namely complex modulus, G^* , and phase angle, δ , to characterize asphalt binders ($G^* \sin \delta$). A cyclic uniaxial tension-compression test under strain controlled conditions, i.e., EBADE test, was performed.

The up&down strain sweep tests performed on asphalt binders show that these materials can experience up to a 60 % complex modulus reduction and recover it completely when the strain applied is decreased. Each binder has a strain level at which it fails under cyclic loading in a small number of load applications, showing a fast and continuous drop in the complex modulus. Below that strain level the binder either does not fail, or fails at a large number of cycles after having maintained its complex modulus almost constant during the most part of the test. It is easy to determine that strain level in a cyclic strain sweep test and the initial complex modulus. These two parameters allow defining and differentiating the behavior under cyclic loading of the asphalt binders. A significant part of the complex modulus loss observed in asphalt mixtures is also caused by thixotropy. However, in this case, there is a part of the modulus that cannot be recovered when the strain applied is decreased in the up&down strain sweep tests. Although it is clear that the mixture suffers some amount of irreversible damage during the test, a great part of the modulus loss is recovered at the unloading. In some cases, after dropping below 60% the initial value, the complex modulus recovered over 90 % this value when the strain was decreased.

8.5.4 Paper 139 (Stimilli et al., 2012)

Nine different binders, both neat and modified have been tested in this paper in order to quantify the effect of healing on the fatigue damage. This paper highlights the challenges of using few rest periods to predict healing potential. Studying the effect of rest on fatigue law parameters is thought to provide useful insight to the healing capabilities of asphalt binders.

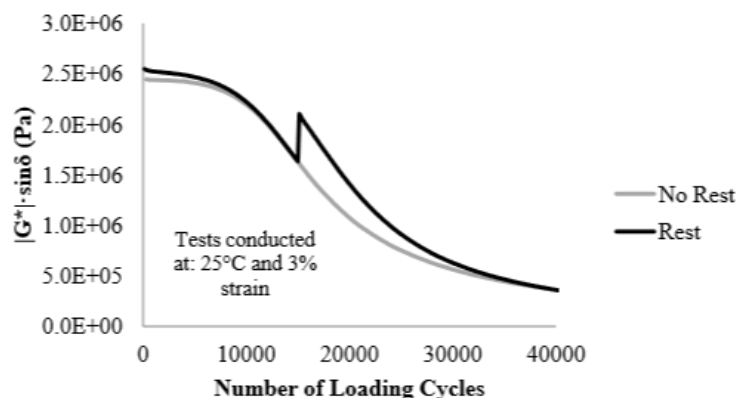


Figure 8-133: Typical results; (a) 37-0901 (un-aged): effect of rest

Figure 8-128 presents typical binder healing test results. Results demonstrate a significant increase in $|G^*| \cdot \sin \delta$ due to the rest period. After the rest period, $|G^*| \cdot \sin \delta$ decreases at a rate similar to that before the rest period. Thus, a single rest period only has a marginal effect on fatigue life. Moreover the test results indicated that for a single rest period, the effect of duration of resting period is insignificant. Moreover, based on testing of one binder, increasing the number of rest periods from one to ten shows a vertical shift in fatigue life. This implies fatigue law parameter: A changes with number of rest periods and B does not. In terms of healing, increasing the number of rest periods is more significant than increasing the duration of the rest time.

8.5.5 Paper 169 (Mamlouk et al., 2012)

This study attempts to optimize the test conditions such as waveform type (haversine vs. sinusoidal), incorporated rest periods between loading cycles and the effect of rest period on healing of the HMA to minimize the errors in the data analysis of the fatigue test result. Although the continuous loading cycles without rest periods do not accurately simulate actual traffic loading, it has been the most dominant procedure due to testing time constraints. In order to better simulate the traffic loading in the field a typical loading pulse of 0,1 sec. and typical rest periods range from 0,1-19 sec. can be applied in the fatigue test. Introducing rest periods during the fatigue test allows the HMA material to heal some of micro cracks caused by the load due to the viscous nature of the material. Figure 8-128 shows schematically the stiffness ratio (current stiffness/initial stiffness) versus loading cycles with and without rest period. The difference between the two curves can be used as a measure of healing.

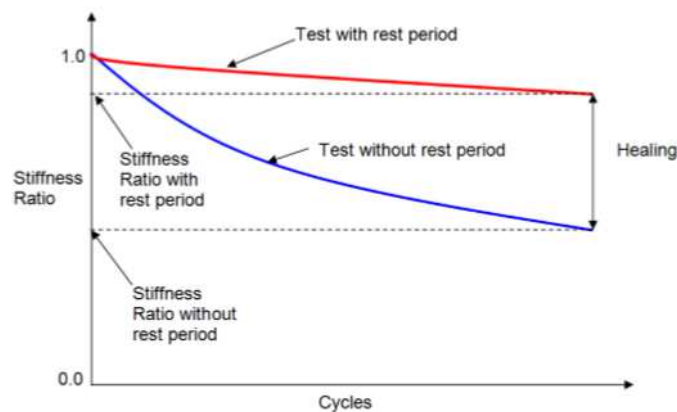
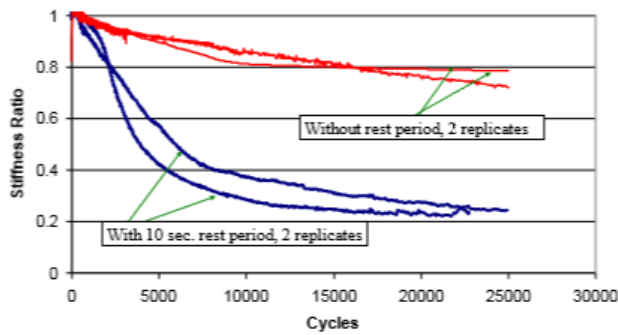
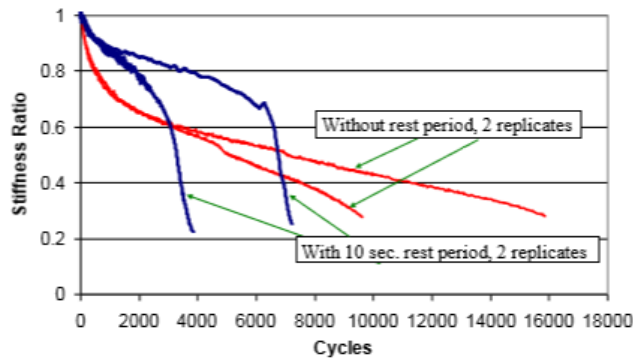


Figure 8-134: Number of cycles vs. stiffness ratio with and without rest periods

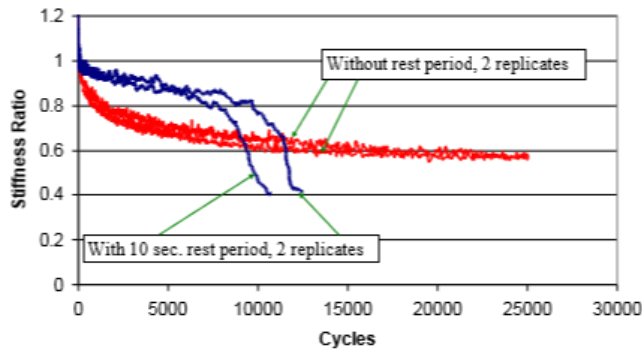
The use of a haversine deflection-controlled fatigue test without rest period (ASTM D-7460) produces inconsistent waveforms, which might produce erroneous fatigue results. A more serious effect happens during the healing analysis when the results of the test with rest period are compared to those of tests without rest period. Figure 8-128 shows examples of fatigue test results using haversine deflection control with and without rest periods. Part (a) of the figure shows that the test with a rest period, in some cases, resulted in faster damage (smaller stress ratios) and lower fatigue life than the test without rest period, producing “negative healing.” This, of course, is completely opposite to the main hypothesis of healing, which is based on the premise that it is the rest period that “heals” the damage in the HMA and extends its fatigue life. In other cases, beams subjected to rest periods started in the proper trend, where they had less damage than beams without rest periods. However, these beams failed during the test as shown in part (b) and (c) of the figure, which is opposite to what is expected.



(a) 400 microstrains, 4°C

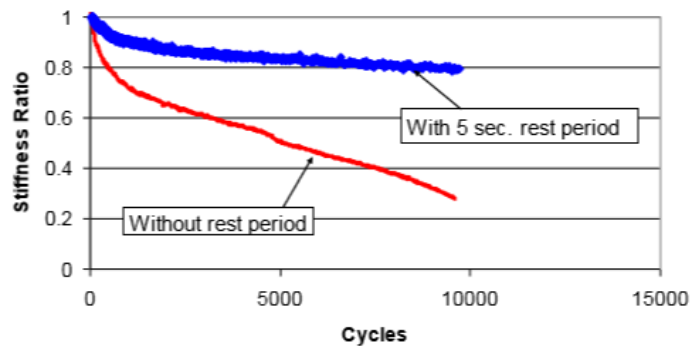


(b) 800 microstrains, 21°C

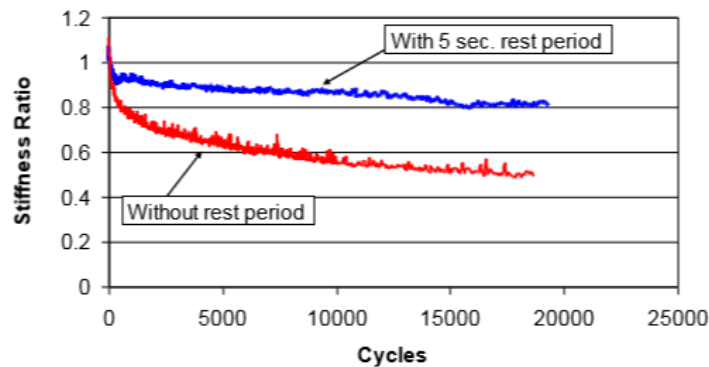


(c) 800 microstrains, 38°C

Figure 8-135: Example of beam fatigue test results using haversine deflection-control with and without rest periods



(a) 800 microstrains, 21°C



(b) 800 microstrains, 38°C

Figure 8-136: Example of beam fatigue test results using sinusoidal deflection-control with and without rest periods

Figure 8-128 shows examples of fatigue test results using sinusoidal deflection control. Unlike the case of haversine waveforms, the figure shows that there is always less damage for the test with a rest period as compared to the test without a rest period (positive healing). The figure also shows that the test with rest period results in a longer fatigue life than the test without rest period as expected.

As a conclusion, the authors strongly recommend that the American Society of Testing and Materials (ASTM) changes the ASTM D-7460 designation and test procedure to eliminate the deflection-controlled haversine waveform and replace it with the deflection-controlled sinusoidal waveform ensuring consistent and more accurate test procedure.

8.5.6 Paper 104 (Wen et al., 2011)

This study attempted to develop a model to account for the effects of loading rate and temperature on critical strain energy density, based on time-temperature superposition principle. The time-temperature superposition principle was evaluated to construct master curve of damage properties of HMA, such as IDT strength, failure strain, and critical strain energy density, as well viscoelastic property, such as dynamic modulus. It was found that the time-temperature superposition principle is valid for IDT strength at both low and intermediate temperatures, and for failure strain and critical strain energy density at intermediate temperatures only. The shift factors for dynamic modulus were about the same as those of IDT strength and close to those of critical strain energy density. However, there seems to be a discrepancy between shift factors of dynamic modulus and those of failure strain.

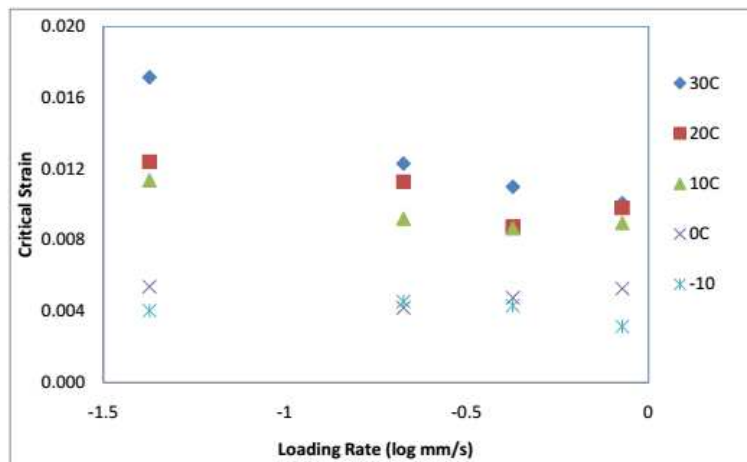


Figure 8-137: Strain at different temperatures and loading rates

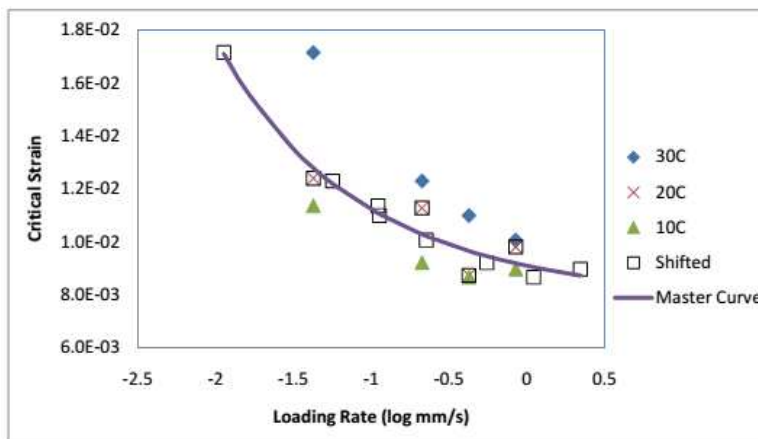


Figure 8-138: Master curve of failure strain

8.5.7 Paper 117 (Mateos et al., 2011)

The objective of this paper is mainly to understand the fatigue deterioration mechanism along the life a flexible pavement by performing field measurements (full-scale testing). Moreover some efforts regarding to correlation of fatigue test results in the lab and fatigue deterioration in the field has been performed. For this reason, 4 sections have been tested at CEDEX full scale facility.

As a result of the test, most of the damage has been observed during medium to low temperature, which is contrary to most of the design procedures, where damage is predicted to mostly occur when it is warm.

It is important to establish a shift factor which relates the laboratory test results to pavement behaviour in the field. In this study a variable shift factor was successfully applied where the beneficial effect of rest periods are incorporated.

8.5.8 Paper 291 (Kanaan et al., 2014)

In this paper two fatigue testing modes (i.e. stress-controlled and strain controlled) has been applied on asphalt specimens with different percentages of recycled asphalt shingles (RAS). The results of the different tests modes revealed to be exactly oposit. Fatigue test results under strain control at the mixture and fine aggregate level showed a decreasing trend in the fatigue life with increasing RAS content (Figure 8-139).

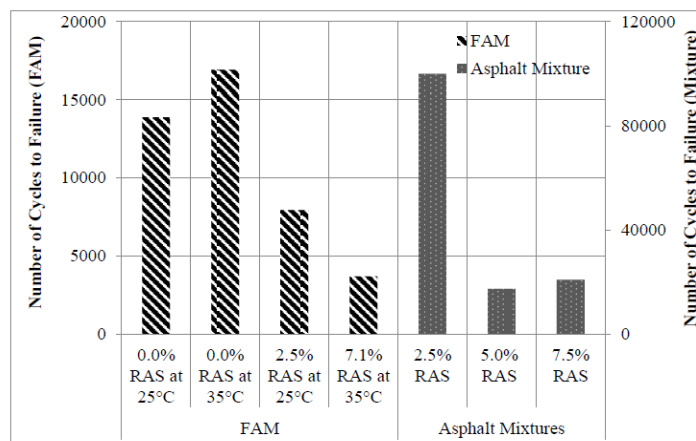


Figure 8-139: Modulus degradation chart from strain-controlled fatigue tests for FAM

However, when the fatigue testing was conducted in stress-controlled mode, the number of cycles to failure increased for materials with higher RAS (Figure 8-140). This result was due to smaller initial strain in mixes with higher RAS, which had higher stiffness.

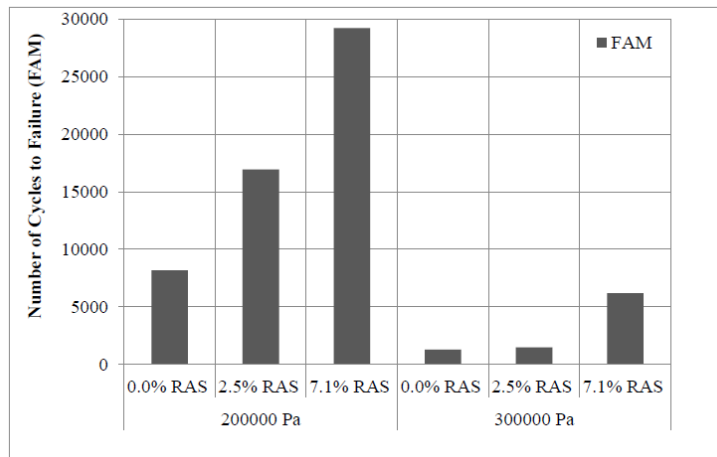


Figure 8-140: Modulus degradation chart from the stress-controlled fatigue test

It has to be noted that the stress-controlled fatigue test simulates field vehicular loading, especially for thin structures and lower traffic loadings. The strain-controlled fatigue test is appropriate for evaluating displacement boundary conditions such as thermal expansion and contraction.

8.5.9 Paper 503 (Hase and Oelkers, 2009)

Data of binder fatigue RILEM Round Robin Test were received from 11 participating laboratories. In a first stage, the RRT consisted of three binders, two unmodified binders and one polymer modified binder. These three binders had almost the same stiffness level at the testing conditions, 10 °C and 10 Hz. Fatigue tests were conducted in controlled strain mode at three strain levels 2,5 %; 1,8 % and 0,8 %, and each strain level was measured in three repeats. For each test it was asked to follow the small strain stiffness during an equilibration time of 30 minutes. The same three binders were also tested in two and in four point bending mix fatigue tests. The analysis was separated into two parts, in a first part the repeatability and reproducibility of the small strain equilibrium stiffness was evaluated and in a second part the fatigue data were analyzed. Small strain stiffness data showed that the repeatability and reproducibility of G^* is still not very high, and possible reasons are under evaluation. The analysis of the fatigue data showed that the overall reproducibility was not good. But when all participants that did in some way not follow the preparation procedure or that had problems with recording, were excluded, it was found that for 6 of the participating laboratories the fatigue properties gave good repeatability and reproducibility levels, for the two unmodified binders in this study. Each laboratory could distinguish the better fatigue life of the polymer modified binder compared to the unmodified binders as was also confirmed by mixture tests.

Used asphalt mix was a 0/6 BBC (according to NF 98-133), with a binder content of 6,88 %.

Complex modulus measurements are performed by two laboratories using respectively a two point bending (2PB) test on trapezoidal samples (NF EN 12697-26) and four point bending (4PB) on prismatic beams (PN-EN 12697-26). It can be noted in Figure 8-140(right), that the visco-elastic behaviors of mixes, are quasi identical, contrary to rheological behaviors of the binders which are relatively different (especially at high temperature). At 10 °C, 10 Hz, the mechanical properties of the mixes are closely related to each other as it can be seen in

Table 8-49. It can also be observed that results from 2PB and 4PB are very close to each other especially when phase angle is concerned. Stiffness from 2PB is 12-15 % higher than for 4PB, but for both methods, taking into account the standard deviations it is impossible to rank the mixes according to their stiffness (binders have almost the same values of $|G^*|$).

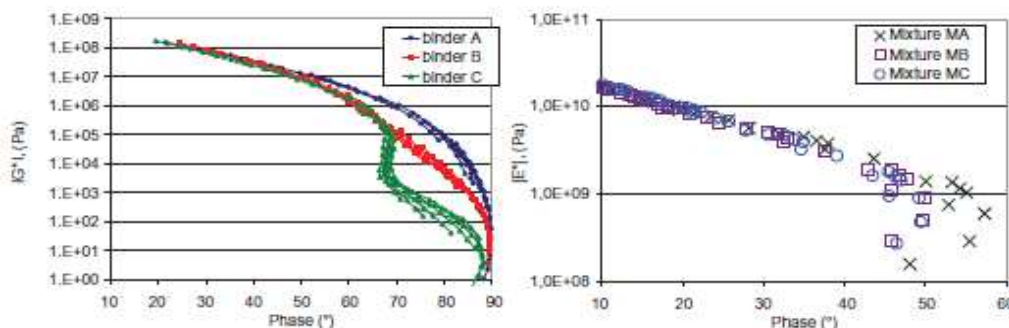


Figure 8-141: Black curves of three binders selected for the first phase testing (left). Black curves of three mixtures prepared with binder A, B and C (right).

Table 8-50: Mechanical properties of the mixture at 10 °C, 10 Hz

	Binder	$ E^* $ (MPa)	Phase angle (°)	Std of $ E^* $ (MPa)
Mixture MA	A	13741 (2PB)	13.4° (2PB)	978 (4PB)
		12193 (4PB)	13.3° (4PB)	
Mixture MB	B	12941 (2PB)	15.3° (2PB)	703 (4PB)
		11606 (4PB)	15.4° (4PB)	
Mixture MC	C	14162 (2PB)	12.4° (2PB)	793 (4PB)
		12282 (4PB)	13.0° (4PB)	

Almost all participants used the 8 mm plate-plate DSR equipment, only one laboratory used a diabolo-shaped sample in a tension compression type of equipment.

The fatigue properties of the mixes MA, MB and MC were measured by two laboratories, LCPC and IBDM, according to the standard EN 12697-24. Two modes of loading were used: four points bending on rectangular beams, and two points bending on trapezoidal samples. Tests were carried out in strain controlled mode. Considering the usual scatter of these fatigue tests, a minimum of six samples, for each strain level was used. Fatigue life is defined as the number of cycles which corresponds to 50% decrease of the initial stiffness modulus. The fatigue tests are performed at three strain levels. The lowest strain is chosen in such way that the rupture time reaches one million cycles. The test conditions in the mixture tests were chosen to be the same as in the binder fatigue test: 10 °C and 10 Hz.

In Figure 8-140 and Figure 8-140, the evolution of $|G^*|$ and phase angle in the equilibration period is shown for sample A (only one repeat). For lab-M, the only laboratory that did not use a plate-plate rheometer but a tension compression device, the $|E^*|$ data are divided by three to obtain $|G^*|$ values. Although statistical procedures do not find outliers, some problems become clear from figure 2 & 3: for lab-B, thermal equilibrium is not obtained within the 30 minutes period. The data from lab-T indicate a temperature problem, since $|G^*|$ values are slightly lower and phase angles are slightly higher. For lab-E, the stiffness seems to be rather low, while the phase angle is similar as for the other laboratories.

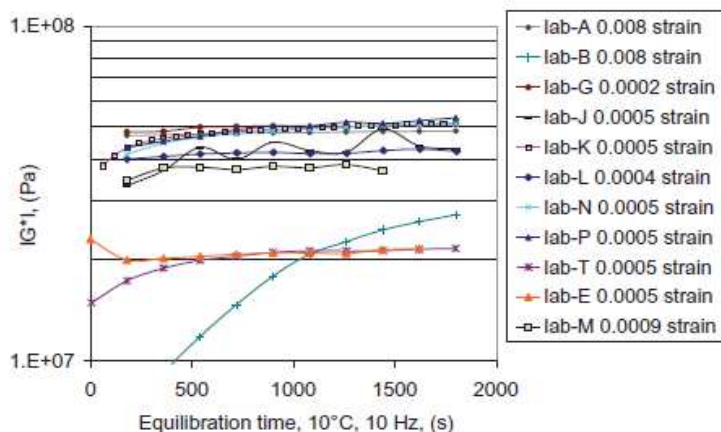


Figure 8-142: Evolution of complex modulus norm during the equilibration period (binder A)

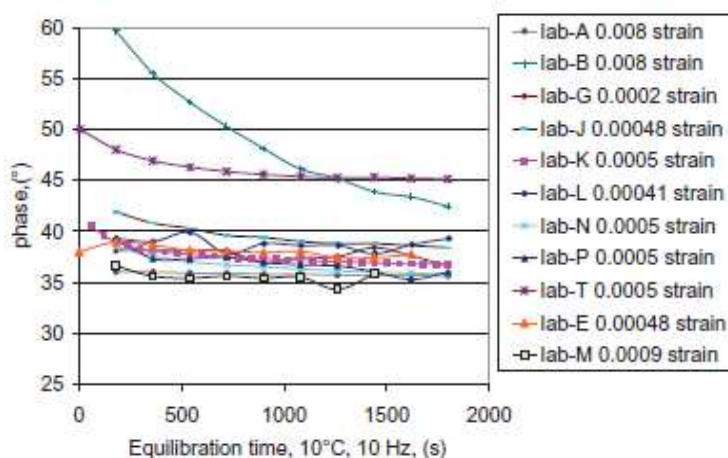


Figure 8-143: Evolution of phase angle during the equilibration period (binder A)

In Table 8-50, statistics of the repeats within each of the respective laboratories are provided for binder A. COV refers to the coefficient of variation. The variation between the repeats, within a fixed laboratory is rather good, for stiffness as well as for the phase angle. The behavior for binder B and binder C is not shown separately, since it was very similar to binder A. In Table 8-51, statistics of the averages between the various laboratories are provided, for all three binders. Since the sample loading and equilibration times were fixed, the presence of physical hardening (binder A and C) does not influence the reproducibility.

Table 8-51: Overview of average values of low strain $|G^*|$ and low strain phase angle. Data relate to binder A only

Lab	av.- $ G^* $ (Pa)	cov%	av.- δ (°)	cov%	Nr. repeats	Strain (%)	Notes
Lab-A	4,85E+07	2,1	35,5	1,7	4	0,8	
Lab-B	2,39E+07	8,8	43,6	1,1	9	0,8	no thermal equilibrium
Lab-G	4,98E+07	3,8	37,3	1,9	9	0,22	
Lab-J	4,59E+07	8,2	28,4	1,8	9	0,048	
Lab-K	5,18E+07	3,5	36,4	1,0	9	0,05	
Lab-L	4,25E+07	7,1	38,3	2,2	9	0,041	
Lab-N	5,54E+07	6,7	34,8	2,6	9	0,05	
Lab-P	5,32E+07	4,3	37,0	5,2	9	0,05	
Lab-T	2,19E+07	7,1	44,7	2,5	9	0,05	
Lab-E	3,16E+07	18,6	35,8	4,6	9	0,048	
Lab-M	3,94E+07	4,6	35,3	1,3	8	0,09	$ G^* $ derived from $ E^* /3$

Table 8-52: Overview of average values of low strain $|G^*|$ and low strain phase angle data, for all binders

	All data		Excluding data from lab-B & T		Excluding data from lab-B, T & E	
	$ G^* $ (Pa)	δ (°)	$ G^* $ (Pa)	δ (°)	$ G^* $ (Pa)	δ (°)
Binder A						
average	4.22E+07	37.9	4.64E+07	36.6	4.83E+07	36.6
Std dev	1.17E+07	3.3	7.55E+06	1.3	5.44E+06	1.3
cov %	27.7	8.7	16.3	3.5	11.3	3.7
Binder B						
average	4.28E+07	38.9	4.65E+07	38.0	4.77E+07	38.4
Std dev	1.07E+07	2.1	7.60E+06	1.2	7.20E+06	0.8
cov %	24.9	5.4	16.4	3.2	15.1	2.0
Binder C						
average	4.80E+07	34.1	5.20E+07	32.9	5.36E+07	33.2
Std dev	1.22E+07	2.9	9.19E+06	1.3	8.35E+06	1.2
cov %	25.3	8.5	17.7	4.1	15.6	3.5

The fatigue life was evaluated using the number of cycles needed to reduce the low strain level stiffness $|G^*|$ to half its value. The result of the fatigue life for binder A, including all data, is given in Figure 8-140. In order to compare the fatigue data, it was necessary to recalculate the fatigue life at certain strain levels or the strain level at a certain life time, since each laboratory used slightly different strain levels. Since although stiffness is geometry independent, from this figure fatigue results seem to be geometry dependent.

The fatigue lines of binder C are shown in Figure 8-140. Binder C is quite different from the other two, its fatigue resistance is clearly higher, and therefore most participants did not get a failure at the lowest strain level. Even though the error bars for binder C are large, it is still obvious that this binder is better in this fatigue test compared to the other two binders. The behavior of binder A and B with regard to fatigue testing can be considered as identical.

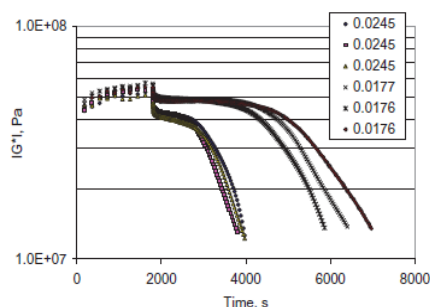


Figure 8-144: Example of a typical fatigue curve (two strain levels, with three repeats; binder A)

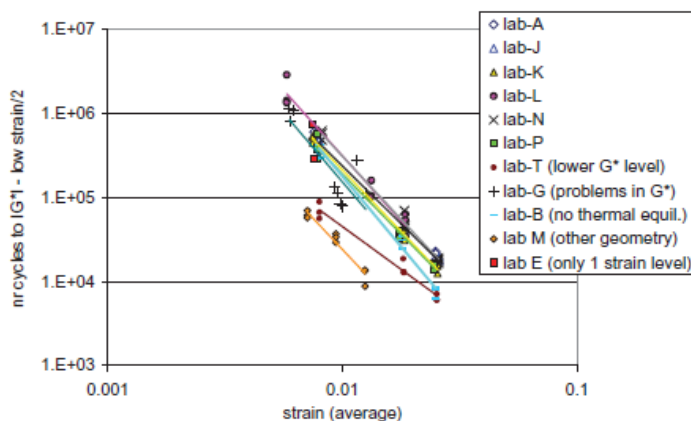


Figure 8-145: Fatigue lines, based on $|G^*|$ low strain level /2 for all data received, for binder A

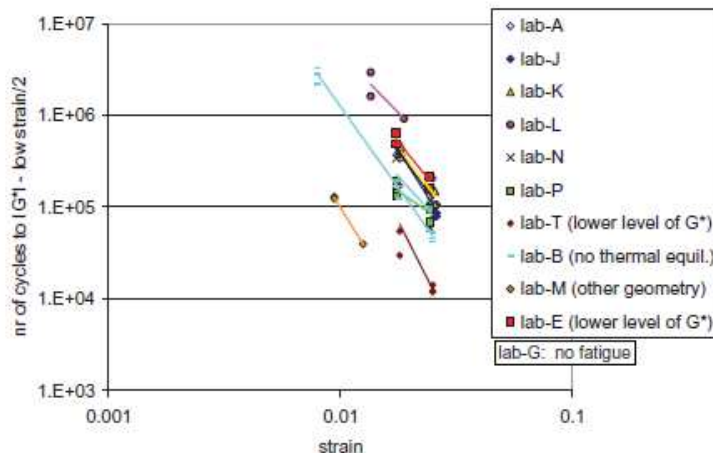


Figure 8-146: Fatigue lines, based on $|G^*|$ low strain level/2 for all data received for binder C

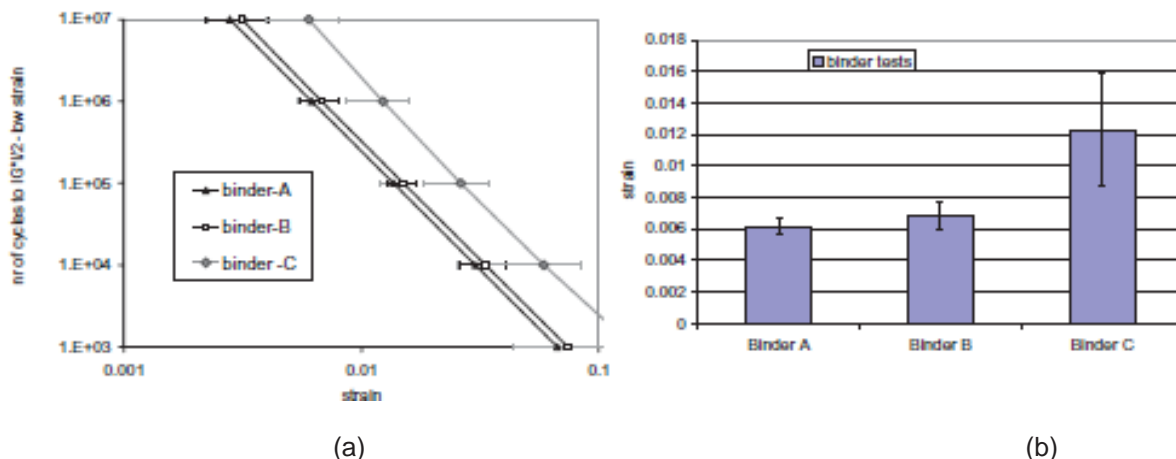


Figure 8-147: Fatigue lines for the three binders based on average values using data from 6 laboratories, error bars are derived from the standard deviation (a). Values of ϵ_6 with confidence intervals (b)

Fatigue test results on the MA, MB and MC mixes are depicted in Figure 8-140. Mix MC, whatever the procedure used (2PB or 4PB) shows clearly a better behavior in fatigue (ϵ_6 20 % higher than the others). It is interesting to note that the ϵ_6 given by 2PB and 4PB fatigue tests, are similar whereas the slope of the fatigue line seems to be “procedure dependent”.

Table 8-53: Outcome of the two mixture fatigue tests

Mix	ϵ_6 -2PB	Slope-2PB	ϵ_6 -4PB	Slope-4PB
MA	152	-5,23	142	-5,25
MB	159	-6,43	154	-5,73
MC	196	-6,30	190	-4,99

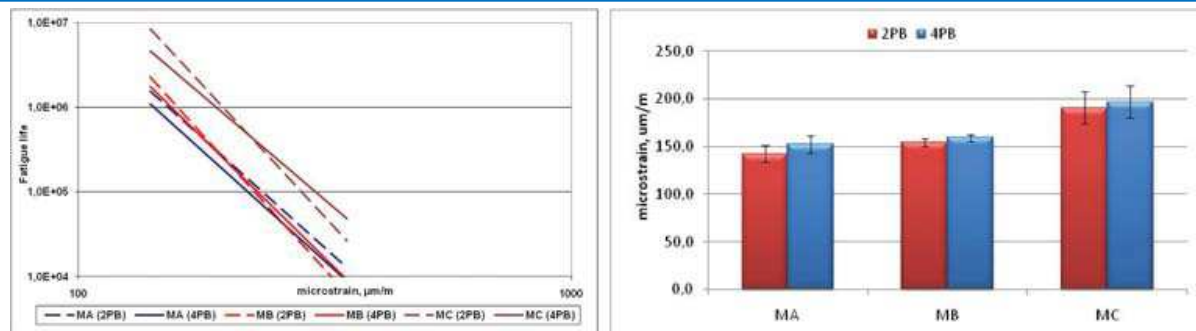


Figure 8-148: Fatigue lines for the three mixes MA, MB and MC using the two fatigue test (2PB and 4PB). 8b. Values of ϵ_6 with confidence intervals for the mixes

The repeatability levels for binder A and B were less good compared to the reproducibility levels, this is a strange finding and may indicate that three repeats per strain level are not enough. In mixture fatigue tests it is also common to use 6 repeats per strain level. The results of binder C are of low repeatability and reproducibility, but the fatigue life of this binder was much higher, and it seems to be more difficult to measure longer fatigue life.

8.5.10 Paper 556 (Niu et al. 2014)

This paper shows the results of fatigue tests on different types of binders, using a Dynamic Shear Rheometer (DSR). The tests were carried out under controlled stress conditions at 20 °C. The stress input signal was a sinusoidal wave of constant amplitude and a frequency of 1,59 Hz. Failure was defined as the point where Dissipated Energy Ratio (DER) dropped 10 % after peaking. A new parameter, named crack failure energy, was defined.

Several conventional binders were tested together with polymer modified bitumen. The conventional bitumens had different ranges of penetration (B-13/22, B-40/50, B-60/70, B-80/100 and B-150/200). The modified binder was a BM-3c. The samples were cylinders measuring 8 mm in diameter and 2 mm height. The applied stress varied between 1 kPa and 9 kPa. The variables recorded were strain, complex modulus (G^*), dissipated energy and dissipated energy ratio. In Figure 8-140, strain is plotted with number of cycles for a conventional binder B-80/100. The test was maintained until the slope increased sharply.

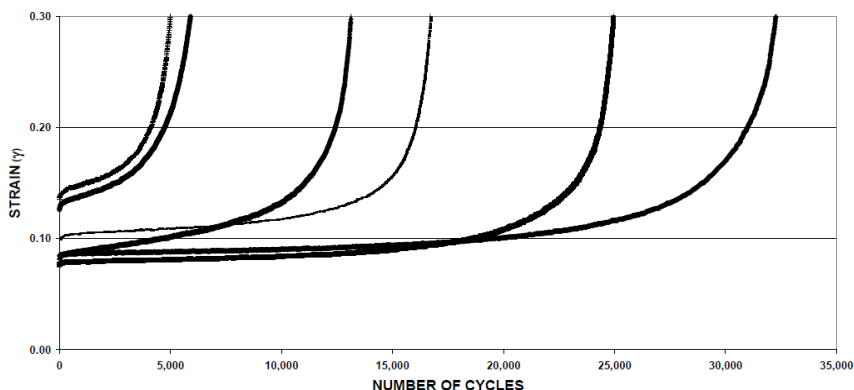


Figure 8-149: Modulus Strain vs. number of cycles example curve; bitumen B-80/100

In Figure 8-140 to Figure 8-140 strain variation along load cycles is shown for all bitumens. Each curve belongs to different applied stress values. During the first part of the test, strain increased slowly until a certain number of cycles, when strain begins to increase dramatically. Tests showed that samples belonging to a same type of bitumen failed in the same strain range, defined as failure strain range. This strain range increased with penetration of binders. Polymer modified binders had the highest in failure strain range magnitude of all binders tested.

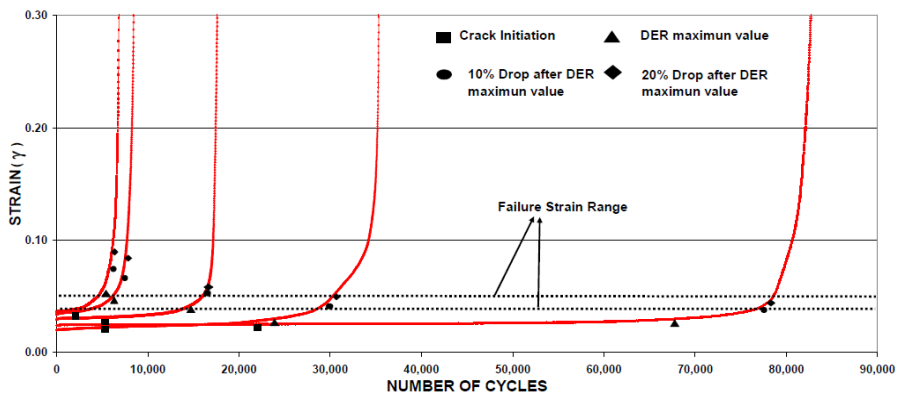


Figure 8-150: Strain variation vs. number of cycles; bitumen B-13/22

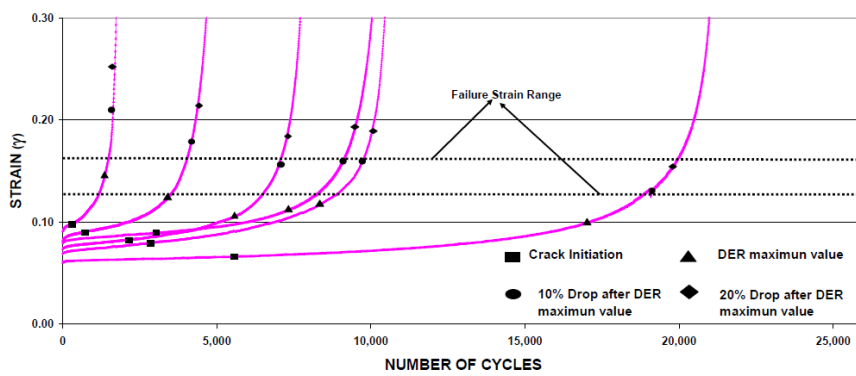


Figure 8-151: Strain variation vs. number of cycles; bitumen B-60/70

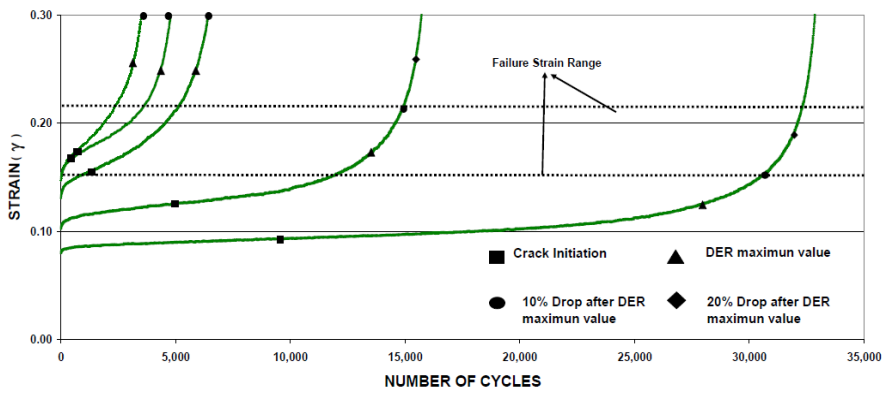


Figure 8-152: Strain variation vs. number of cycles; bitumen B-150/200

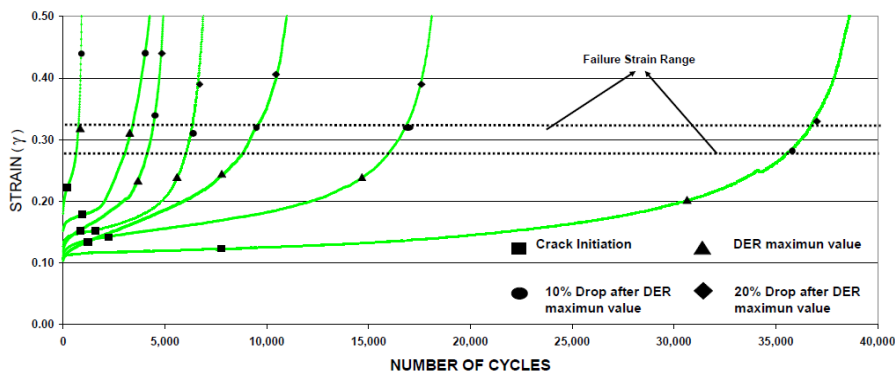


Figure 8-153: Strain variation vs. number of cycles. Polymer modified Binder BM3c

Figure 8-140 shows the variation of DER along the load cycles for the same binders.

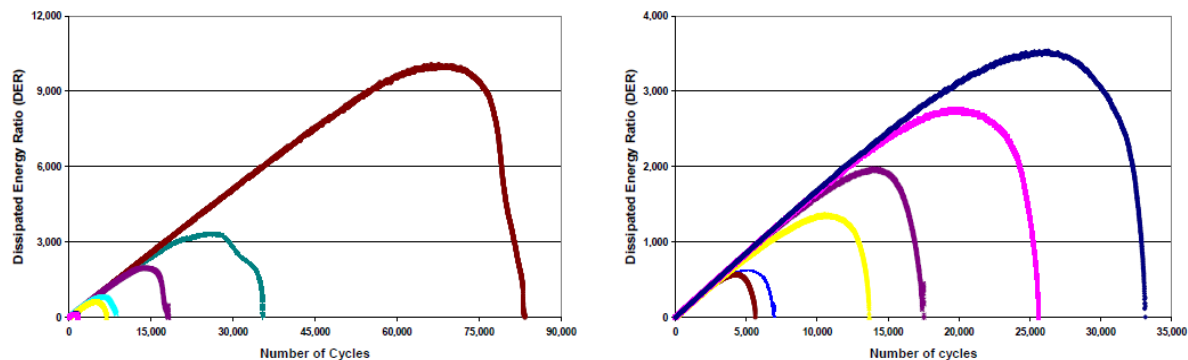


Figure 8-154: DER vs. number of cycles; (a) bitumen B-13/22 and (b) bitumen B-80/100

On the basis of these curves, the number of cycles at which failure occurred was computed using four different criteria:

1. DER deviation from the path
2. DER’s maximum value
3. 10% drop from DER’s maximum value
4. 20% drop from DER’s maximum value

Criterion 1 proved to be too conservative, as strain, established by the criterion, appeared at a much lower value than the failure strain range. In other words, it appeared much before actual fatigue failure occurred. Criterion 3 and 4 were more suitable for soft and polymer modified binders, or, more precisely, when a high number cycles was required to produce significant damage. Finally, criterion 2 was best suited to low numbers of cycles. Given that a high number of cycles is necessary to obtain a reliable fatigue test, criterion 3 should be the parameter for determining failure.

In Figure 8-140 strain range at which samples failed, under criterion 3 conditions, is represented. Strain at which failure took place was higher for binders with higher penetration range, and it was even higher for the polymer modified bitumen.

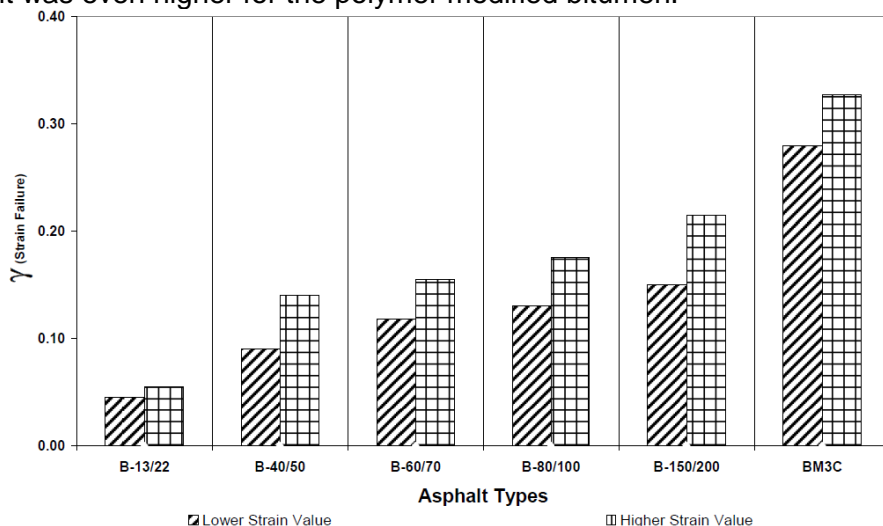


Figure 8-155: Failure strain range vs. binders types

Using this new criterion, the fatigue laws for each binder have been determined (Figure 8-140). The relationship between the vertical position of fatigue law and failure strain has been observed. Binders with higher failure strain have their fatigue laws in a higher position

on the graph, while, bitumens with higher complex modulus have fatigue laws with less slope.

Using strain value corresponding to the 10% drop after DER peak value, (the criterion used to determine binders failure) it is possible to determine a new parameter, *crack failure energy* (E_{cf}), defined as the product of stress (τ) and strain (γ_f) at the moment of failure.

$$E_{cf} = \gamma_f \tau$$

Crack failure energy parameter is related with the amount of energy used to open the crack. That is due to parameter's dependence on stress applied and crack width.

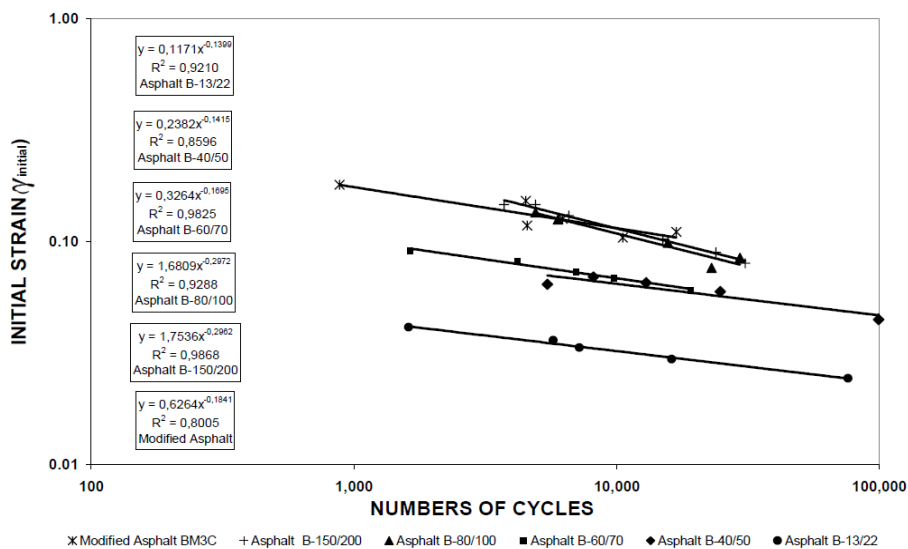


Figure 8-156: – Fatigue law using criterion 3

In Figure 8-140 crack failure energy has been plotted with initial complex modulus. Each bitumen type was tested using DSR at varying degrees of stress. The higher the stress applied, the higher the crack failure energy value, and the lower the number of cycles. In other words, the amount of energy required to break the sample is higher when the process is shorter (Table 8-52).

Table 8-54: Crack failure energy for asphalt B-13/22 and asphalt B-60/70

Bitumen B-13/22			Bitumen B-60/70		
Torque (Pa)	γ_f	Energy (E_{cf})	Torque (Pa)	γ_f	Energy (E_{cf})
1750	0,093	163	2750	0,0373	103
2250	0,116	262	3000	0,0423	127
2500	0,126	315	3500	0,0525	184
2600	0,139	360	3750	0,0689	258
3000	0,159	476	4000	0,0741	296

In the case of conventional binders, medium penetration binders (B-40/50 and B-60/70) had the highest energy value. In other words, these binders required a higher degree of applied energy to break. On the other hand, low penetration binders were more fragile and failed at lower rates of energy. The high penetration binders failed at lower rates of energy as well. The researchers found that the modified binder required the highest amount of energy to fail.

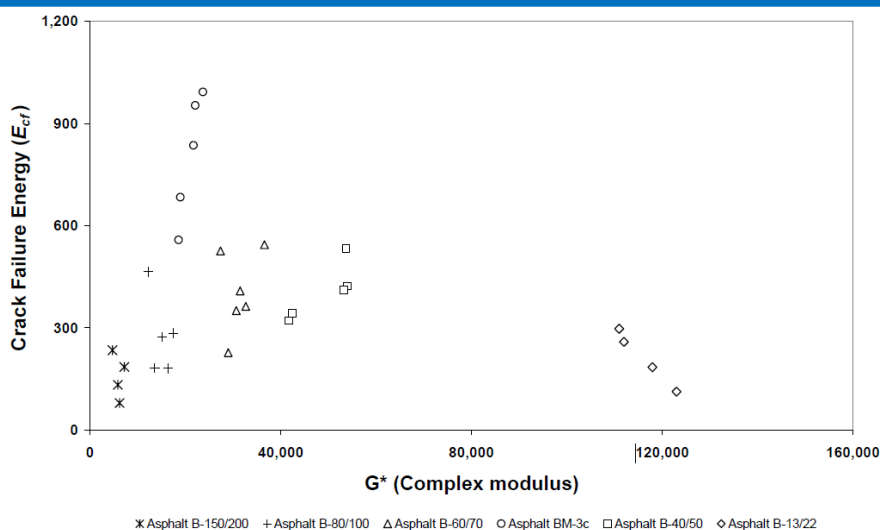


Figure 8-157: Crack failure energy vs. initial complex modulus

8.5.11 Paper 549 (Silva et al., 2008)

The influence of temperature on the fatigue life of the bituminous mixtures is empirically considered in Shell fatigue life equation normally used in the pavement design. A35/50 bitumen, with penetration of 35 dmm and a softening point of 54,2 °C was used in the AC 0/14. Optimum binder content for the mixture AC 0/14 was 5,5 % by mass of mixture.

Fatigue cracking resistance was obtained through four-point bending tests, with a repetitive sinusoidal loading configuration without resting periods. These tests were carried out at three different temperatures (5 °C; 15 °C and 25 °C) and at a loading frequency of 10 Hz in fifteen specimens per temperature. Tests were carried out at five different tensile strain levels (100×10^{-6} , 150×10^{-6} , 250×10^{-6} , 300×10^{-6} and 350×10^{-6}), with three specimens tested for each strain level.

The fatigue cracking laws at different temperatures, presented in Figure 8-140, were drawn and determined based on all fatigue tests results, after applying the shift factor of 22 to estimate the field fatigue performance. Figure 5 also presents the Shell fatigue cracking law (Shell, 1978) for the AC 0/14 mixture ($V_b=11,7\%$ and $S_{Mix}=5\,450\text{ MPa}$) usually used in pavement design, in order to have a reference indicator.

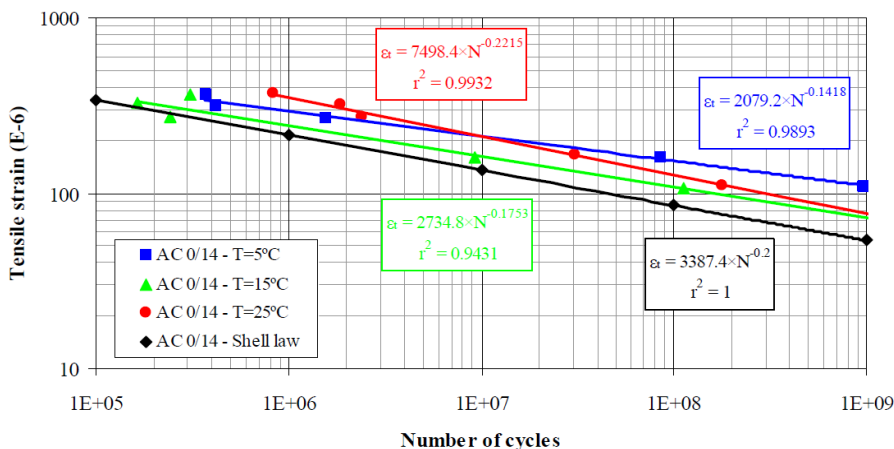


Figure 8-158: Laboratory fatigue cracking laws at different temperatures and Shell fatigue law obtained for the AC 0/14 mixture

It was observed that, at high strain levels (above 200×10^{-6}), the AC 0/14 mixture presents the highest fatigue cracking resistance at a temperature of 25 °C, since the mixture is more flexible at elevated temperatures, and thus it supports high strain levels that would easily fracture the mixture if the behaviour were more rigid (at lower temperatures). In contrast, at lower strain levels the AC 0/14 mixture presents the highest fatigue cracking resistance at a temperature of 5 °C, probably because the strain level is very small and it is applied in the elastic domain of a mixture with a higher stiffness modulus, thus delaying the beginning of the fatigue cracking phenomenon. The AC 0/14 mixture shows the lowest fatigue cracking resistance at 15 °C. Fatigue cracking resistance obtained in the laboratory was superior to that calculated with the Shell fatigue life equation, given that the latter was obtained with probabilistic values that are usually more conservative.

The variation of fatigue cracking resistance with the strain level, given by the slope of the fatigue laws, reduces with the increase of the temperature, since the flexible behaviour at higher temperatures is less sensitive to strain level changes. This variation is similar in the laboratory and in the Shell fatigue cracking laws at an approximate temperature of 20 °C. The parameters of the fatigue laws were N_{100} – fatigue cracking resistance for a tensile strain of 100×10^{-6} (usual value in pavements) and ϵ_6 – tensile strain which causes a fatigue cracking resistance of 1×10^6 cycles (this is the main result required by the European Standard EN 12697-24).

Table 8-55: Fatigue cracking law parameters used to calculate N_{100} and ϵ_6 values

Temperature	a	b	R^2	N_{100}	ϵ_6
5 °C	$2,5028 \times 10^{23}$	7,052	0,989	$1,968 \times 10^9$	293
15 °C	$4,0361 \times 10^{19}$	5,705	0,943	$1,574 \times 10^8$	243
25 °C	$3,1204 \times 10^{17}$	4,515	0,993	$2,917 \times 10^8$	352
Shell – 20 °C	$4,4600 \times 10^{17}$	5,000	1,000	$4,460 \times 10^7$	214

8.5.12 Paper 548 (Baptista et al., 2008)

In another study three different bituminous mixtures for surface layers were selected for experimental characterisation and assessment of consequences of affixing the CE marking to asphalt mixtures, namely: Asphalt Concrete 0/14 (AC 0/14); Stone Mastic Asphalt 0/11 (SMA 0/11) and Asphalt Rubber 0/12 (AR 0/12). Two types of binders were used – 35/50 bitumen, with penetration of 35 dmm and a softening point of 54.2°C (AC 0/14 and SMA 0/11) and a rubber modified binder (RMB) with 35/50 bitumen and 19% of crumb rubber for AR 0/12. It was observed that the optimum binder content of the studied mixture was 5,3 %, 6,5 % and 9,5 % for AC 0/14, SMA 0/11 and AR 0/12 respectively.

In this work, the fatigue cracking resistance of the studied mixtures was obtained through fatigue four point-bending tests, with a repetitive sinusoidal loading configuration without resting periods. These tests were carried out at 20 °C, in 18 specimens per mixture. A loading frequency of 10 Hz was used. The tests were carried out in strain control, at three different tensile strain levels, with six repetitions for each strain level. Following EN 12697-24, the strain levels were selected in order to obtain a fatigue rupture between $1E+04$ and $2E+06$ cycles. The moment when the stiffness modulus decreases up to 50% compared with its initial value was registered, thus obtaining the fatigue life of each tested specimen (number of cycles that causes the fatigue rupture of the specimen). The fatigue laws of the studied mixtures (Figure 8-140) were drawn and determined based on all fatigue tests results.

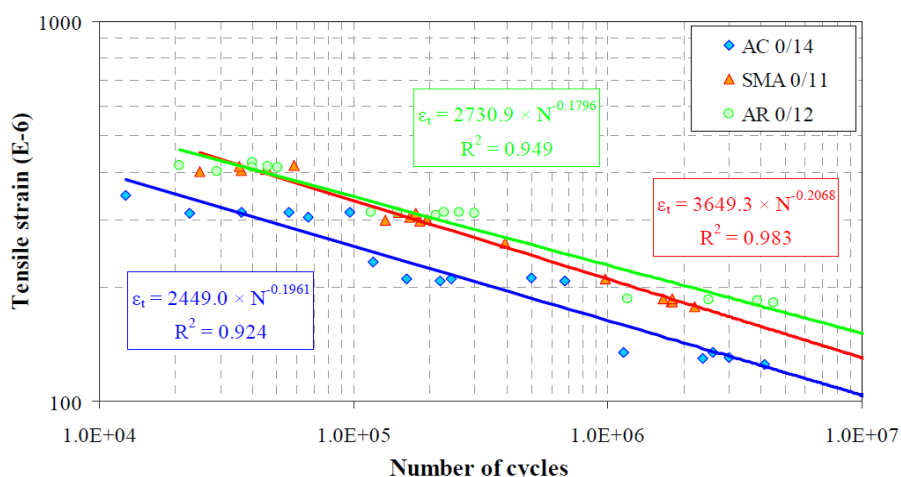


Figure 8-159: Fatigue cracking laws obtained in laboratory

The fatigue cracking resistance of the AR 0/12 and SMA 0/11 mixtures is visibly higher than the one of the traditional AC 0/14 mixture, what shows that the fundamental evaluation of these mixtures is much more explanatory regarding their advantages than the traditional empirical specifications. The parameters of the fatigue laws of each mixture and their CE marking categories are presented in Table 8-54, as well as two essential variables for the evaluation of the fatigue cracking resistance, namely:

- N_{100} – fatigue cracking resistance for a tensile strain of 100E-06 (usual in pavements);
- ϵ_6 – tensile strain which causes a fatigue cracking resistance of 1E+06 cycles;
- ρ – slope of the fatigue line, equal to b .

Table 8-56: Fatigue cracking characteristics and CE marking categories of the mixtures

Asphalt mixture	Fatigue law parameters			N_{100}	EN 12697-24 values		CE marking category ϵ_6 (EN 13108)
	a	b	R^2		ϵ_6	ρ	
AC 0/14	1,91E+17	5,099	0,924	1,21E+07	163	5,099	ϵ_6 160
SMA 0/11	1,68E+17	4,836	0,938	3,58E+07	210	4,836	ϵ_6 190
AR 0/12	1,36E+19	5,568	0,949	9,92E+07	228	5,568	ϵ_6 220

The AR 0/12 mixture presented the best CE marking category for fatigue cracking resistance properties (since it supports a higher strain in each loading cycle for equivalent traffic levels), followed by the SMA 0/11 mixture and finally by the AC 0/14 mixture categories. These differences in the CE marking category are significant if fatigue cracking is an important criterion concerning the use of these mixtures in the pavement. Actually, it was observed that the AR 0/12 mixture presented a N_{100} fatigue resistance 2,8 times superior to the SMA 0/11 mixture and 8,2 times superior than the traditional AC 0/14 mixture.

8.5.13 Paper 547 (Aksoy et al., 2008)

The study focused on performance-based mix design process of hot-mix recycled in plant (HMR). It took into consideration 30 % and 40 % of milled material incorporated in the mixture and a reference traditional mixture without recycled material. In the reclaimed material 4,1 % bitumen was determined.

The recovered bitumen was hard, with a high softening point (71 °C). For further tests bitumen 35/50 and 50/70 was applied for combination with the reclaimed asphalt material. The penetration was then improved depending on the RAP content by 15 dmm to 25 dmm.

Table 8-57: Designation of the mixtures applied in trial sections and fatigue parameters

Mixture	A1	A2	A3	C1	C2	C3	D1	D2	D3
TR (%)	0	0	0	30	30	30	40	40	40
total bitumen content (%)	-	-	-	3.9	4.4	4.9	4.2	4.7	5.2
new bitumen added (%)	3.7	4.2	4.7	2.7	3.2	3.7	2.6	3.1	3.6
A	7263	6102	6697	6782	4252	7651	10072	12346	11151
B	-0,289	-0,259	-0,266	-0,261	-0,220	-0,257	-0,282	-0,299	-0,281
ϵ_6 (microns)	134	170	171	184	202	220	204	199	230

Fatigue resistance of mixtures were evaluated from four-point bending tests. The chosen fatigue resistance criterion was 50 % loss of the initial stiffness modulus. Fatigue tests were performed at 25°C, typical for the Portuguese climatic conditions and using a sine wave load with a frequency of 10 Hz. The fatigue laws ($\epsilon = A \times N^B$) obtained from prismatic beams extracted from trial sections are shown in Table 8-55. The parameter ϵ_6 (strain which induces specimen ruin after 1 million load cycles) derived from those fatigue laws are also presented. Both trial sections mixtures have presented better fatigue performance than the reference mixture.

8.6 References for fatigue cracking

- Paper 024 **Olard, F, P Huon, S Dupriet, J Dherbecourt and L M Perez (2012)**. GB5: Eco-friendly alternative to EME2 for long-life & cost-effective base courses through use of gap-graded curves & SBS modified bitumens. *E&E2012*.
- Paper 025 **Mangiafico, S, H di Benedetto, C Sauzeat, F Olard, S Dupriet, L Planque and R van Rooijen (2012)**. Effect of reclaimed asphalt pavement on complex modulus and fatigue resistance of bitumens and asphalts. *E&E2012*.
- Paper 026 **Eckmann, B, M Mazé, S Largeaud and S F Dumont (2012)**. The contribution of cross-linked polymer modified binders to asphalt performance. *E&E2012*.
- Paper 034 **Dressen, S, T Gallet, A G Dumont and M Pittet (2012)**. Durability study: field experience of long-term evolution of SBS polymer modified binder. *E&E2012*.
- Paper 036 **Pasetto, M, and N Baldo (2012)**. Fatigue behaviour and stiffness properties of asphalt rubber mixtures made with steel slags. *E&E2012*.
- Paper 045 **Vasilica, B, G Georgeta and S Elisabeta (2012)**. The effects of rubber powder on the performance of pavement asphalt. *E&E2012*.
- Paper 046 **Güngör, A G, F Orhan and S Kaşak (2012)**. The determination of performance of wearing course mixtures using advanced asphalt tests. *E&E2012*.
- Paper 050 **Haritonovs, V, J Tihonovs, M Zaumanis and A Krasnikovs (2014)**. High modulus asphalt concrete with dolomite aggregates. *TRA2014*.
- Paper 052 **Qi, D, A Shenoy and X Qi (2008)**. Validation of asphalt binder fatigue parameters with ALF pavements. *LJMU2008*.
- Paper 058 **Baumgardner, G, J V Martin, R B Powell and P Turner (2008)**. Polyphosphoric acid and styrene-butadiene-styrene block co-polymer modified asphalt: Evaluation of paved section at the NCAT test track built in 2000 and 2003. *E&E2008*.

- Paper 059 **Bennert, T, and J V Martin (2008)**. Polyphosphoric acid in combination with styrene-butadiene-styrene co-polymer: Mix fatigue resistance and permanent deformation evaluation. *E&E2008*.
- Paper 061 **Beckedahl, H J, P Sivapatham and L Neutag (2008)**. Impacts of the compaction degree of asphalt mixes on the asphalt pavement performance. *E&E2008*.
- Paper 062 **Pérez Jiménez, F, O J Reyes-Ortiz, R Miró Recasens and A Hernández-Noguers (2008)**. Relation between the fatigue behavior of asphalt binders and bituminous mixtures. *E&E2008*.
- Paper 069 **Such, C, J-V Martin, S Périgois and N Picard (2008)**. Properties and performances of asphalt binders and asphalt mixes modified with polyphosphoric acid. *E&E2008*.
- Paper 070 **Gauthier, G, D Bodin and R Chkir (2008)**. Stiffness and fatigue properties of asphalt: Effect of the bitumen type and the bitumen content. *E&E2008*.
- Paper 071 **Ballié, M, E Chailleux, P Dumas, B Eckmann, C Leroux, B Lombardi, J-P Planche, C Such and J-C Vaniscote (2008)**. Characteristics of bituminous binders and their consequences on the mechanical performance of asphalts. *E&E2008*.
- Paper 074 **de Visscher, J, S Vansteenkiste and A Vanelstraete (2008)**. Test sections in high-modulus asphalt: Mix design and laboratory performing testing. *E&E2008*.
- Paper 083 **Perez-Jimenez, F E, G V Vidal, R Miró, R B Nieto and J M Campana (2011)**. Effect of thermal stresses on fatigue behavior of bituminous mixes. *TRB2011*.
- Paper 085 **Mogawer, W S, M M Haggag and R Bonaquist (2011)**. Fatigue evaluation of warm-mix asphalt mixtures using uniaxial cyclic direct tension compression test. *TRB2011*.
- Paper 089 **Timm, D H, J R Willis and A Kvasnak (2011)**. Full-scale structural evaluation of fatigue characteristics in high RAP and warm-mix asphalt. *TRB2011*.
- Paper 094 **Olard, F (2011)**. Innovative design approach to high-performance asphalt concretes with long-life base and binder courses by use of aggregate packing concepts and polymer-modified binders. *TRB2011*.
- Paper 098 **Li, X, N H Gibson, T R Clyne, E N Johnson and M E Kutay (2011)**. Laboratory evaluation of asphalt binders and mixtures containing polyphosphoric acid. *TRB2011*.
- Paper 104 **Wen, H, X Li and S Bhusal (2011)**. Modeling effects of temperature and loading rate on fatigue properties of hot-mix asphalt. *TRB2011*.
- Paper 105 **Hintz, C A, R A Velasquez, C Johnson and H U Bahia (2011)**. Modification and validation of linear amplitude sweep test for binder fatigue specification. *TRB2011*.
- Paper 117 **Mateos, A, J P Ayuso and B C Jáuregui (2011)**. Shift factors for asphalt fatigue from full-scale testing. *TRB2011*.
- Paper 125 **Aurangzeb, Q, I L Al-Qadi, I M Abuawad, W Pine and J Trepanier (2012)**. Achieving desired volumetrics and performance for high-RAP mixtures. *TRB2012*.
- Paper 134 **Perez-Jimenez, F E, R B Nieto and R Miró (2012)**. Damage and thixotropy in asphalt mixture and binder fatigue tests. *TRB2012*.

- Paper 137 **Baek, C, S Yang, J Lee, S Hwang and S A Kwon (2012).** Development of warm-mix asphalt additive and evaluation of its performance. *TRB2012*.
- Paper 139 **Stimilli, A, C A Hintz, Z Li, R A Velasquez and H U Bahia (2012).** Effect of healing on fatigue law parameters of asphalt binders. *TRB2012*.
- Paper 143 **Baek, C, B S Underwood and Y R Kim (2012).** Effects of oxidative aging on asphalt mixture properties. *TRB2012*.
- Paper 153 **Willis, J R, A J Taylor and N Tran (2012).** Laboratory evaluation of high polymer plant-produced mixtures. *TRB2012*.
- Paper 169 **Mamlouk, M S, M I Souliman and W A Zeiada (2012).** Optimum testing conditions to measure hma fatigue and healing using flexural bending test. *TRB2012*.
- Paper 171 **Mogawer, W S, E H Fini, A J Austerman, A Booshehrian and B Zada (2012).** Performance characteristics of high rap bio-modified asphalt mixtures. *TRB2012*.
- Paper 175 **Clopotel, C, R A Velasquez, H U Bahia, F E Perez-Jimenez, R M Recasens and R B Nieto (2012).** Relation between binder and mixture damage resistance at intermediate and 2 low temperatures. *TRB2012*.
- Paper 248 **Scholten, E, W Vonk and R Kluttz (2013).** The dawning of a new era of pavement design. *REAAA2013*.
- Paper 272 **Pérez-Jiménez, F, R Botella, R Miró, A Paez-Dueñas, F J Barceló-Martínez and V Carrera (2014).** Binder, mastic and mixture fatigue characterization using a cyclic uniaxial strain sweep test. *TRB2014*.
- Paper 285 **Boriack, P, S W Katicha and G W Flintsch (2014).** A laboratory study of the effect of high RAP and high asphalt binder content on the stiffness, fatigue resistance and rutting resistance of asphalt concrete. *TRB2014*.
- Paper 291 **Kanaan, A I, H Ozer and I L Al-Qadi (2014).** Quantification of asphalt binder replacement effectiveness using recycled shingles through fine asphalt mixture level testing. *TRB2014*.
- Paper 294 **Bennert, T A, D S Jo and S M Walaa (2014).** Strategies for incorporating higher RAP percentages: Review of northeast states implementation trials. *TRB2014*.
- Paper 297 **Farhana, R, T Jeremiah T, H Mustaque and G Schieber (2014).** Structural characteristics of aged asphalt concrete pavements. *TRB2014*.

9 Binder/aggregate interaction

9.1 Asphalt test methods for binder/aggregate interaction

It is generally accepted that adhesion is the property which characterises the bond between two materials. In the case of asphalt mixtures, it reflects the interaction of the binder or bitumen and the aggregate material. Adhesion is an interface phenomenon because it occurs at the surface of materials (e.g. binder, aggregates and fillers). The term adhesivity is the ability or capacity of a material such as bitumen to form a bond that results in adhesion. While the term adhesion (also referred to, less precisely, as affinity or compatibility) is wide spread, its direct quantitative measure is less evident. Often, it is far easier to define the lack of adhesion because that phenomenon is directly correlated with failure or in situ damage (e.g. ravelling). Moreover, water has a detrimental effect on adhesion. Therefore, the susceptibility to moisture or the resistance towards debonding is considered to be a good indirect indicator of the power of a binder to adhere to aggregates. In this context, it is frequently referred to as a stripping phenomenon. This idea has already been taken up in the European standards EN 12697-11:2012. Determination of the affinity between aggregates and binder, and EN 13697-12:2008. Determination of the water sensitivity of bituminous specimens, dealing with the assessment of the adhesion of asphalt mixtures. Frequently in such procedures, a ratio (expressed in per cent) of a mechanical property (e.g. strength or modulus) of an asphalt mixture is calculated from a series of measurements conducted before (dry specimens) and after water conditioning.

Although, adhesion is defined as the bond between only two materials, the situation is more complex in the case of composite materials such as asphalt mixtures. There are often difficulties in the interpretation of test results or failure mechanisms because the separation of adhesion characteristics within the asphalt mixture is hampered by other binder or mixture properties such as cohesion and the mix design. As a consequence, researchers have developed test procedures that focus both on a single binder/aggregate pair as well as compacted asphalt specimens. However, because adhesion is an interface event, generally all test procedures include both the binder and the aggregate.

Stripping is known to be a demonstration of interfacial tension between bitumen and aggregate in the presence of water and could, therefore, be explained and estimated by thermodynamic theories. Several research studies report the measurement and use of such thermodynamic characteristics (e.g. surface tension) to develop quantitative models describing interface phenomena such as adhesion or stripping (the lack of adhesion). Such studies require a more fundamental insight into material characteristics governing adhesion.

The development of tests to determine adhesion began in the 1930s. Since then, numerous tests have been developed in an attempt to identify and quantify adhesion properties. The moisture susceptibility tests can be divided in two major categories:

- Test conducted on loose coated aggregate (e.g. rolling bottle, boiling test and immersion test),
- Test conducted on compacted mixtures (e.g. Cantabro, Indirect Tensile Strength (ITS) and abrasion tests).

The first family of tests makes use of simpler equipment and is less time consuming to perform. However, the results are often qualitative and more difficult to interpret in relationship with the adhesion phenomenon. The second family of tests, when conducted with conditioning, is considered as an indirect measure for adhesion. They take into consideration the traffic, environment and mixture properties but need more elaborate testing equipment, longer testing time and/or laborious test procedures. Specific test methods to

evaluate the role of the mastic (mixture of filler and bitumen) on the adhesion properties of a mixture are currently not available.

9.2 *BitVal findings for binder/aggregate interaction*

The BitVal project (Paper 000, Nicholls, 2007) recognised that the primary function of bitumen is to act as an adhesive and, as a consequence, has been the subject of numerous investigations in recent decades. The range of descriptions of the various test methods devised to assess the adhesive properties of binders illustrated the research efforts in this area. Furthermore, it was appreciated that the list of test methods taken up in that project was not comprehensive. However, other methods reported often only vary in the choice of test parameters or experimental set up.

Tests such as the freeze-thaw pedestal test, the immersion wheel tracking test, the Hamburg wheel tracking device with water conditioning and the environmental conditioning system (ECS) had been omitted from the overview. The latter test methods could be related only indirectly to adhesion phenomena (immersion in water while carrying out the tests) but were otherwise not developed as adhesion test for binders or mixtures. Therefore, such tests were considered as not really relevant to the topic of adhesion and, consequently, not discussed further.

The conclusions for adhesion were not straightforward. Although, research on this topic had been going on for a long time, both the understanding as well as the assessment of the adhesive properties of bitumen was still an area of focus. An attempt was made to clarify some of the issues in Table 9-1 by reviewing both the advantages as well as the limitations of several test methods considered. However, Table 9-1 was not comprehensive (as noted above) but it did illustrate some of the unanswered questions relating to adhesion.

The review given in Table 9-1 serves as a guide to formulate the following general conclusions with respect to adhesion:

- Adhesion is an interface phenomenon and, therefore, applies to material combinations (e.g. binder/aggregate or mastic/aggregate). Water has to be included into the relationship because of the durability issues with asphalt mixtures. As a result, the direct assessment of adhesion is complicated (a variety of test specimens ranging from a bitumen/aggregate pair to compacted asphalt mixtures subjected to water conditioning and/or traffic).
- The surface properties of a sample (e.g. of bitumen) could differ significantly from the bulk material. All materials will tend to minimise their surface energy if possible (depending on their capacity to rearrange at a given temperature).
- The approach of using surface energies of materials enables some fundamental insights about adhesion to be gained. However, equilibrium in an asphalt mixture is probably never realised.
- The interpretation of test results with respect to adhesion is often hampered by the interference of other phenomena. The occurrence of a cohesive failure mode often accompanies the observations made during an experiment. Moreover, water conditioning could introduce a change in the failure mechanism and, hence, lead to inconclusive test results (e.g. PATTI).
- The effect of the water conditioning can vary with the accessibility of the asphalt mixture (e.g. voids content) and, therefore, the mix design itself could interfere with the test result (e.g. ITS).

Table 9-1: Summary of advantages/limitations of test methods assessing adhesion

Test method	Advantages	Limitations
Rolling bottle test	Simple and easy to perform	Visual and, therefore, subjective evaluation of test result, making it a screening technique
Boiling water stripping test	Objective test	Need for chemicals
Ultrasonic method	High sensitivity	Highly dependant of experimental set up
Net adsorption test	Thermodynamic basis (Langmuir isotherms)	Further research needed in order to predict the in service performance
Vialit plate test	Considerable experience	Interpretation in terms of adhesion hampered by other parameters such as cohesion and ductility
Indirect tensile strength	Takes into account the effect of water conditioning Test carried out on a asphalt mixture	Validation with in situ performance not straightforward Interpretation of test results by the use of a single parameter (moisture) is questionable
PATTI	Well established test used in coating industry	Mode of failure changes with water conditioning (cohesive to adhesive)
SATS	Replicates observed loss of adhesion	Limited experience Results highly dependent on aggregate
Surface energies of materials	Based on solid thermodynamic principles	Sophisticated instrumentation needed Theoretical model only valid for systems in equilibrium
Water immersion test, aggregate method	–	Designed specifically for bitumen emulsions only
Shaking abrasion test	–	Designed specifically for bitumen emulsions in slurry surfacings only

- An asphalt mixture is a dynamic system (e.g. ageing and/or traffic introduced damage) and, therefore, its susceptibility to moisture damage or loss in adhesive properties could vary over time (e.g. introducing cracks enables water to penetrate the system).
- The majority of the tests lack in situ experience. Validation with in-service performance needs to be evaluated.

In contrast to other tests, interfacial properties and, therefore, adhesion is possibly the most difficult one to conceive. It has to describe the suitability of binders to adhere to various pavement components such as aggregates, sand and fillers. Although a lot of interesting ideas were included in the tests described, the subject of adhesion still needed future research in order to establish well validated and performance-based specification.

9.3 Bitumen tests correlating with binder/aggregate interaction

9.3.1 General

Although a large number (> 100) of papers from the database were identified with respect to the interaction of bituminous binders with aggregates (which includes also articles evaluating the water sensitivity of asphalt mixtures), only in a limited number of publications a possible relation between the nature of the bitumen and its adhesive properties and/or its impact on the water sensitivity of a corresponding asphalt mixture is discussed. In a majority of the papers the water sensitivity of asphalt mixtures is probed for in a more general context of performance testing, often to study the impact of additives, the use of RAP or the evaluation of new production techniques such as Warm Mix Asphalt (WMA). Therefore, latter papers are not discussed in this report, although it is envisioned to include any relevant information from these papers in the final report.

Since a wide variety of tests are used to determine the adhesion between bitumen and aggregates literature will be discussed, in analogy with the BitVal report, in two major parts. In a first part tests conducted on compacted asphalt mixtures are reviewed (e.g. according to EN 12697-12 and the AASHTO T283 method used in the US), while in a second part tests on loose coated aggregate are discussed (e.g. boiling water test and PATTI test).

In order to interpret the results of the tests discussed in this report, it is the reviewers' opinion that a more fundamental understanding of adhesion of bitumen with aggregates is also required. Typical issues relevant in this field include studies discussing the importance of surface energy of materials involved (both bitumen as well as aggregates), the possible impact of the chemical (e.g. generic composition) and/or physical properties (e.g. viscosity) of bitumen. It is recognized that latter research areas are outside the objective of current report D1 but will be taken up in the final report.

9.3.2 Tests conducted on compacted mixtures

9.3.2.1 Paper 031 (Nordgren et al., 2012)

Nordgren et al reported the results of a large scale project where the impact of the source of a paving grade bitumen 70/100 (7 different suppliers) was investigated on functional properties of a SMA16 mix such as: instance wear resistance, water sensitivity, low temperature performance and permanent deformation (rutting).

None of the seven tested mixtures showed low ITSR values (high water sensitivity). The variation in tensile strength between mixtures may be linked to binder stiffness as well as the addition of cement additive and small differences in compaction and composition. The special freeze/thaw conditioning used for half of the specimens showed, in this case, no decisive effect compared to the conventional testing procedure for water sensitivity. Ranking of the different types of bitumen according to ITSR is different from that of the rolling bottle test (see below). The ITSR method takes into account the total mixture, while in the rolling bottle test only adhesion between quartz aggregate fraction and binder is involved.

Water sensitivity results at 10°C after winter conditioning are shown in Figure 9-1.

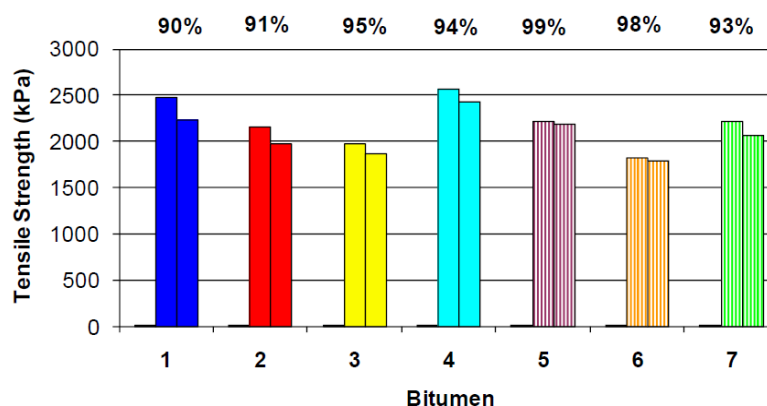


Figure 9-1: Water sensitivity results at 10 °C after winter conditioning

All binders showed 0 % of bitumen coverage on the aggregate after 24 hours. Adding cement as adhesion agent showed little effect, except in combination with bitumen 3 and 7, respectively (about 60 % bitumen coverage).

9.3.2.2 Paper 041 (Deniz et al., 2012)

Deniz et al reported the results of the effect of salt solution on both AC20 wearing course as well as SMA11 mixes (including both a 50/70 binder as well as a PmB). Test specimens were conditioned over a long time (5 days) at 5°C before probing for the water sensitivity of the mixes (applying EN12697-12). The test results are summarized in Table 9-2.

Table 9-2: Indirect tensile strength values for mixtures

Specimen Type	Water Conditioning	Salt Solution Conditioning
Surface Course Type 1 0/20 (50/70 Bitumen)	68,6	73,6
Surface Course Type 1 0/20 (Modified Bitumen)	74,2	87,6
SMA Type 2 (Modified Bitumen)	81,0	86,6

It could be concluded that there was no negative effect of the salt solutions on all mixes independently of the aggregate (limestone or basalt) or binder used.

9.3.2.3 Paper 076 (Ishai et al., 2011)

Ishai *et al.* reported the results of a study comprising:

- 1) practical development of a more efficient and user friendly binder-stabilizer for preventing the bitumen draindown in SMA mixes;
- 2) identifying some positive added values of the role of the active bitumen-stabilizer in the compacted SMA also under service condition;
- 3) Verification of these advantages by a comprehensive laboratory study, as compared to the cellulose fibres.

In preliminary laboratory studies it was found that SMA11 mixes, combined with the new bitumen stabilizer (powered silica activated with a surface-active agent), exhibit low acceptable bitumen draindown values which are comparable to those with the fibers. As a result of systematic mix designs, European and American SMA mixes also show comparable and better mechanical properties related to: resistance to water damage (ITSR values > 80%), wear resistance, indirect tensile strength, and rutting resistance.

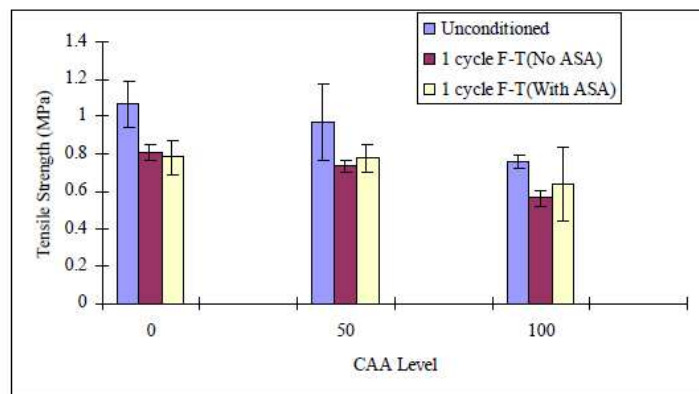
9.3.2.4 Paper 225 (Chen et al., 2007)

Chen *et al.* reported the results of an extensive laboratory study, evaluating the moisture damage of a dense-graded surface HMA mixture using simple performance test (SPT) and Superpave™ indirect tension test (IDT). Asphalt binders (PG 64-22) with and without amine-based antistripping additive (ASA) were used to make mixtures for laboratory moisture damage evaluations. Specimens were conditioned by four different methods: 1) one cycle of freeze-thaw (F-T), 2) two cycles of F-T, 3) 500 cycles of pore pressure pulses with Moisture Induced Stress Tester (MIST), and 4) 1000 cycles with MIST. The dynamic modulus, Superpave IDT creep, resilient modulus and strength tests were performed on conditioned and unconditioned specimens. As an example, the results for the ITSR values are presented in Figure 9-2.

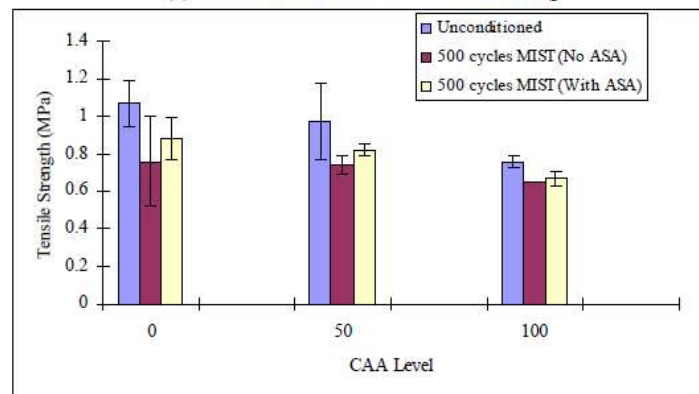
Based on the laboratory experiments and analyses, the following can be summarised and concluded:

- a. The SPT Dynamic Modulus Test and Superpave IDT combining F-T or MIST conditionings were effective to characterize lab-measured moisture susceptibility for HMA mixtures.
- b. The change in HMA mixture dynamic modulus was effective to identify lab-measured moisture damage of HMA mixtures.

- c. The results from the Superpave IDT resilient modulus, creep, and strength testing indicated that the lab-measured moisture damage of mixtures include changes in multiple parameters.
- d. Increase F-T or MIST cycles increased lab-measured moisture damage in HMA mixtures.
- e. Amine-based antistripping additive was effective to decrease the lab-measured moisture susceptibility of HMA mixtures.
- f. Increase CAA levels could increase the dynamic modulus E^* , however, it seemed that CAA had not significant effects on the lab-measured moisture resistance of HMA mixtures.



(a) Unconditioned and F-T Conditioning



(b) Unconditioned and MIST Conditioning

Figure 9-2 Tensile strength of mixtures

9.3.2.5 Paper 242 (Varveri *et al.*, 2014)

In the paper by Varveri *et al.* a new moisture conditioning protocol which attempts to distinguish the contributions of long- and short-term moisture damage, i.e. moisture diffusion and cyclic pore pressure generation, namely MIST (Moisture Induced Sensitivity Tester), in asphalt mixtures is presented. It is shown that the use of cyclic pore pressures has a significant effect and can be used as an accelerated moisture conditioning procedure.

In this study, six PA16 (porous asphalt mixture compositions) were tested. The mixtures differed in terms of the type of aggregates and bitumen used. The specimens were produced using either granite (known to be prone to moisture damage) or sandstone (with known good field moisture damage performance) aggregates. a conventional bitumen Pen 70/100, a moderately polymer modified bitumen with 50/80 pen grade and a highly polymer modified one with 65/105 pen grade. A target bitumen content of 4.5% by total mixture mass was selected for all the specimens. Hydrated lime filler was added at 4.8% by mass of total

aggregate. The different mixtures are denoted as: GP, GM, GH, SP, SM, SH, with the letters G and S denoting Granite and Sandstone aggregates respectively, while the letters P, M and H denote the bitumen types used (Pen 70/100, moderately and highly modified bitumen).

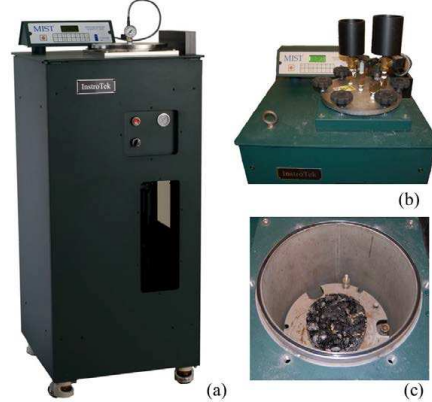


Figure 9-3: Moisture induced sensitivity tester or MIST

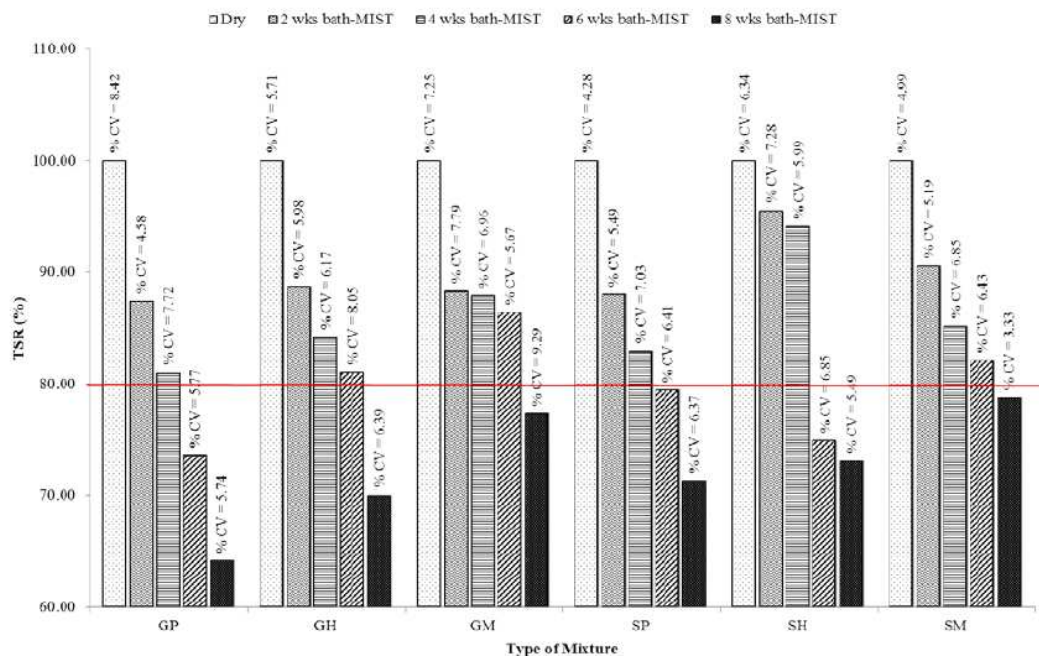


Figure 9-4: Mean TSR values after each conditioning period

The evaluation of the proposed protocol for its ability to discriminate amongst mixtures in terms of moisture sensitivity was attained via the Tensile Strength Ratio (TSR). The mean TSR values (out of 3 replicas) after each conditioning period are shown in Figure 9-4. Also, the coefficient of variation for every mix, at each conditioning level, was calculated and is presented on the top of the bars. It is observed that the TSR values decrease over conditioning time for all asphalt mixtures, which is in accordance with the expectations. The solid red line represents the threshold value below which an asphalt mixture is considered to be more susceptible to moisture damage, according to the Dutch standards.

The effect of the aggregate type was investigated by replacing the granite aggregate with a sandstone one, whilst keeping the same binder type for the various mixtures. Results show that for all three binders, the sandstone aggregate mixtures have demonstrated better moisture damage performance than those containing granite aggregates. In an earlier study

by Kringos et al., in which the same materials were used, field observations showed that sandstone aggregates have better moisture performance than granite ones and this is in agreement with the findings of this research.

Also, the effect of polymer modification on moisture susceptibility has been investigated. It has been reported that polymer modified binders are less susceptible to moisture damage compared to the non-modified. In this study, by comparing the mixtures in terms of the type of binder used, it is shown that the use of polymer modified bitumen increases the resistance of the mixture to moisture damage. Moreover, it is observed that moisture sensitivity increased when binders prepared with softer bitumen are used.

From this research, it can be concluded that the conditioning procedure developed can be used to evaluate the moisture susceptibility of asphalt mixtures and distinguish among mixtures with different moisture damage potential. Furthermore, the developed protocol enables the quantitative determination of the individual short- and long-term contribution to the overall specimen damage. In addition, it is shown that the use of cyclic pore pressures has a significant effect and can be used as an accelerated moisture conditioning procedure. Because the protocol was decided on the basis of porous asphalt mixtures, further research is needed to determine the conditions for testing mixtures with lower air void content.

9.3.2.6 Paper 287 (Amelian et al., 2014)

Amelian et al identified moisture damage in hot mix asphalt is one of the major concerns in durability of flexible pavements. In their research, a digital image analysis approach was utilized to convert boiling water test (ASTM D3625) from visual rating to objective evaluation. Digital images captured from mixtures were processed and analyzed to identify the amount of stripping percentages. Some laboratory tests were conducted on specimens prepared from different types of aggregates to compare the stripping percentages obtained from image analysis of the boiling water test and modified Lottman test (AASHTO T283) results. In AASHTO T283 test, in addition to indirect tensile strength, the Dynamic Modulus E^* test and the Marshall Stability test were performed; therefore, three criteria including tensile strength ratio (TSR), E^* stiffness ratio (ESR) and retained marshall stability (RMS) were used to compare the results of two methods. The dynamic modulus test was conducted in indirect tension mode by assumption of Poisson's ratio and a linear viscoelastic solution was used for the E^* calculation. Findings showed that the results of boiling water test have significant relationship with TSR and ESR. Good correlation was found between three tests (see Figure 9-5); however, the results of boiling test did not show significant relationship with RMS.

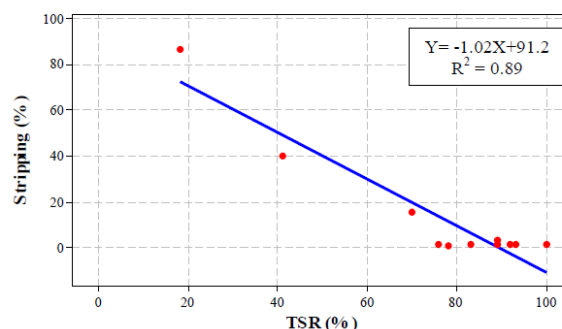


Figure 9-5: The correlation between tensile strength ratios limited to 100 % and stripping percentages in boiling test

9.3.2.7 Paper 484 (Gubler et al., 2005)

In the paper by Gubler et al different test methods are compared to evaluate moisture susceptibility. This is of special importance because of the insufficient effectiveness of the

test procedures currently used. In this research, experiments were conducted to investigate the effects of water and temperature on mechanical properties of mixtures with different air void content. The evaluation of such properties concentrates on the following three approaches: innovative (Coaxial Shear Test), traditional (Indirect Tensile Test) and empirical (Cantabro Test). Specimens were prepared by means of Superpave Gyratory Compactor (SGC) and divided in two different subsets for controlled dry and wet conditioned testing. Test results indicated that the Indirect Tensile Test (IDT) is not able to discriminate between wet and dry condition as the Coaxial Shear Test (CAST) does. The CAST method reproduces closest the real field conditions and indicates clearly the risk of water damage for open graded mixtures (high air void content). Dense graded mixtures (low air void content) showed less influence probably due to the reduced amount of penetrating water. Cantabro Tests (CAT) provided also significant results in good correlation with air void content and material properties of asphalt mixes.

The IDT is able to discriminate between mixtures with modified and unmodified bitumen, while modified bitumen improved the Cantabro abrasion resistance on both dry and wet conditioned specimens.

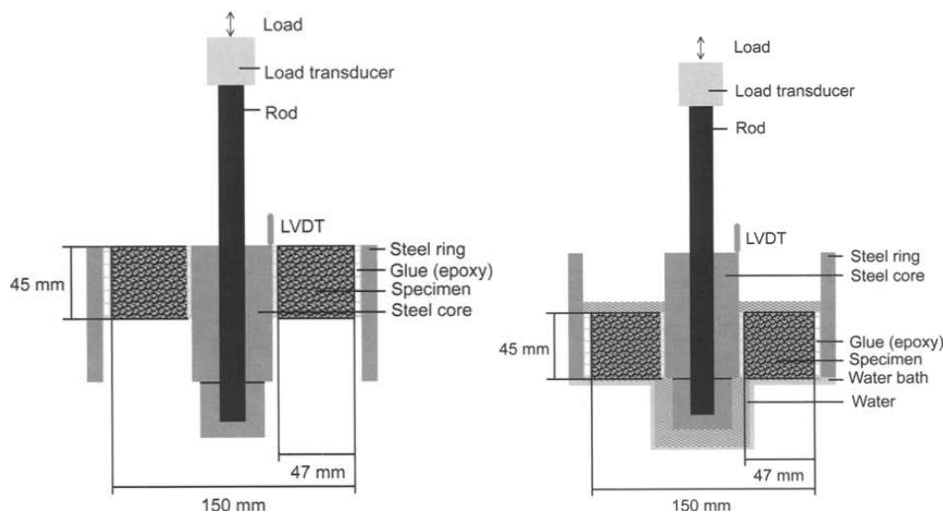


Figure 9-6: Setup of both dry (left) as well as wet (right) test using CAST

9.3.2.8 Paper 507 (Renken *et al.*, 2010)

In the paper by Renken the results of an extensive test program on the adhesion of bitumen on aggregates, comprising combinations of 6 bitumens (four 50/70 from different producers and two PmB's) and 5 aggregates are reported. On these combinations the affinity of bitumen and aggregate was tested according the three options of EN 12697-11 (rolling bottle, boiling and static water). Moreover, by carrying out contact angle measurements, the surface energy of all binders was probed for. Four asphalt mixtures (AC 11, AC 16, SMA 11, PA 8) were prepared using four bitumens and 2 aggregates. The water sensitivity for latter mixtures was measured both by applying the conventional indirect tensile strength test as well as by a direct tensile test. The advantages and disadvantages of all testing methods were investigated. Furthermore, a rating regarding the adequacy for routine testing is given. Finally, in this study possible correlations between material properties such as bitumen or aggregates and the water sensitivity of the corresponding asphalt mixtures are established.

9.3.2.9 Paper 508 (Roos *et al.*, 2010)

In the report by Roos *et al.*, the results of an extensive test program including MA 11 and AC 22 asphalt mixtures which were prepared with two different PmBs, namely 25/55-55A and 10/40-65A (for each bitumen and mix type 4 bitumen originating from different suppliers were

used). The asphalt mixes were laboratory aged (MA: 60 and 165 minutes in a mixer; AC: 2 and 3 h in a heating cabinet). Binders were tested in 4 stages: freshly produced, recovered from the freshly-mixed asphalt mix; recovered after short short-term conditioning and recovered after long short-term conditioning. From the freshly produced as well as from the short-term ageing conditioned asphalt samples specimens were prepared and a series of (performance) tests were conducted on both binders as well as asphalt mixtures. Special attention was given to the relationship of the elastic recovery. Moreover, static splitting tensile tests to determine adhesion behavior were conducted. However, no systematic correlations between the different ageing regimes and ITSR values could be established; results varied from one PmB binder to another (see Figure 9-7).

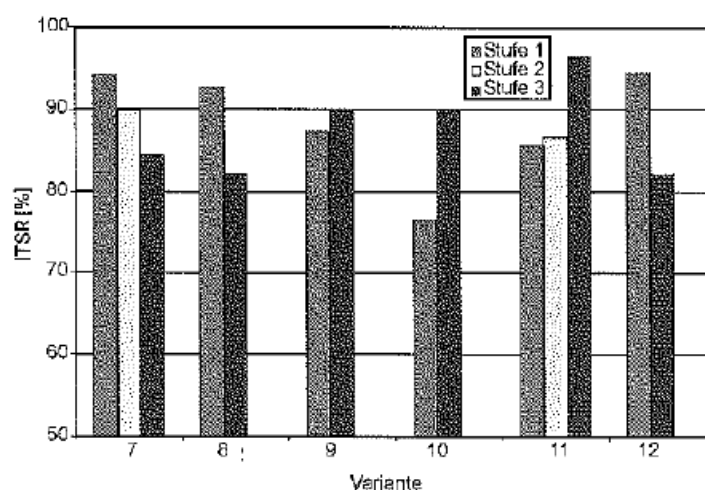


Figure 9-7: ITSR values of asphalt binder variants of stages 1, 2 and 3

9.3.2.10 Paper 542 (Yang *et al.*, 2010)

Yang et al evaluated the water sensitivity of asphalt base layer mixtures (Sup-20) containing anti-rutting additives by carrying out the freeze-thaw splitting test. The specimens of 150mm (diameter)×95mm (height) with a void ratio of about 7% were fabricated using the Superpave Gyration Compactor, and 101.6mm (diameter)×63.5mm (height) specimens were cored from gyration specimens for the freeze-thaw splitting test. The specimens were divided into two groups, each group had four specimens. One group was conserved at room temperature, the other was processed by a standard freeze-thaw process, and then both groups were researched in the splitting test.

Table 9-3 - Results of the freeze-thaw splitting test

	RT1 (MPa)	RT2 (MPa)	TSR (%)	Code Requirement (%)
Base asphalt	1,218	1,012	83,1	≥80
PR	1,361	1,256	92,3	≥80

It was found that adding PR could both enhance the water sensitivity as well as the high temperature stability of asphalt mixtures.

9.3.2.11 Paper 566 (Puchard *et al.*, 2012)

Puchard et al reported the results of efforts to introduce LT asphalt in Hungary, in particular by conducting comparative performance laboratory tests on a series of AC11 wearing course variants containing viscosity modifying additives (fatty acid amides). Following laboratory testing, test sections were constructed while using a fatty acid amide with a dosing rate of 0.4% to both conventional 50/70 binder as well as a PmB (25/55-65 type). Mixing temperatures of LT variants was about 40°C lower as compared to the reference mix (without

additive). The mechanical tests carried out on the produced asphalt mixes showed that water sensitivity of the mixes was adequate, being 92-96% (reference mix: 88%). Visual inspections demonstrated no defects up to now (2-3 years following construction) of any of the test sections.

9.3.3 Tests conducted on loose coated aggregate

9.3.3.1 Paper 014 (Aguiar *et al.*, 2013)

In the paper by Aguiar *et al.* the performance of asphalt mixtures applied in Costa Rica in terms of moisture damage is addressed. Because of the geographic location of Costa Rica, the country is subjected to one of the highest levels of precipitation in the world. As such, it is to be expected that moisture damage is the most common type of pavement failure in the country. Consequently, the present study consists of an effort to characterize the strength in the bond between the asphalt binder that is used locally (PG64-22) and several types of aggregates from different parts of the country (1 limestone and 4 distinct river gravels from several locations). Additionally, the neat asphalt binder was also modified with a commercial SBR, a modifier commonly used in Costa Rica since it is supposed to promote adhesion. To evaluate the strength of the bond between the asphalt binder and the various aggregate combinations, the Bitumen Bond Strength (BBS) test was used. The results were checked by means of a goniometer that measures the contact angle between the asphalt binder and the aggregate surface, which corresponds to a measure of wettability. Finally, a subset of the analyzed asphalt binder and aggregate combinations were used to prepare an HMA mixture and evaluate it under the Hamburg Wheel Tracking Device (HWTd). The BBS results showed differences in behavior due to the effect of moisture on bond strength when changing the aggregate source. Additionally, depending on the aggregate type, different types of failure were observed: cohesive versus adhesive. A decrease was identified in the bond strength when the SBR was used. However, when using the modifier, the effect of moisture on bond strength was reduced. The BBS results were consistent with the contact angle measurements and with the HWTd results, showing that the test can eventually be implemented as a screening tool.

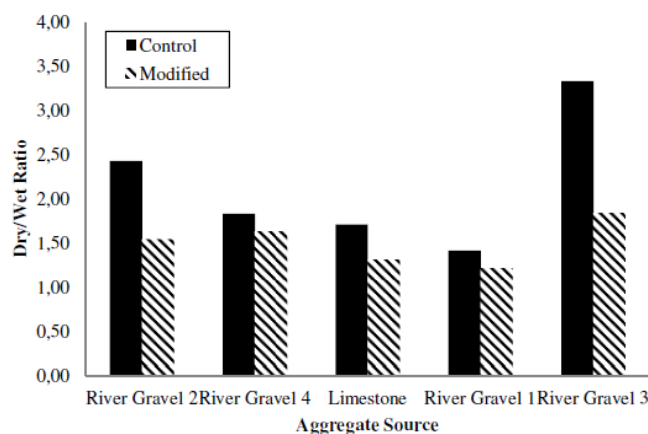


Figure 9-8: POTS dry/wet ratio

9.3.3.2 Paper 232 (Bhasin *et al.*, 2007)

An important material property that influences the performance of an asphalt mixture is the surface free energy of the asphalt binder and the aggregate. Surface free energy governs the adhesive bond strength between the asphalt binder and the aggregate as well as the cohesive bond strength of the asphalt binder. These bond energies in turn influence the resistance of the asphalt mixture to distresses such as fatigue cracking and moisture induced damage. Asphalt binders undergo several different types of engineering and/or natural

modifications that influence their chemical and mechanical properties. Three common examples of modifications are addition of polymers, addition of additives (e.g. anti-strip agents), and oxidative aging of the asphalt binder. This paper by Bhasin et al is part of a study conducted to examine the effect of different types of modifications on the surface free energy components of the asphalt binder. The change in surface free energy was used to calculate parameters that are related to the performance of the asphalt mixtures. Results from this study demonstrate that the magnitude and nature of change to the surface free energy and concomitant performance related parameters varied significantly among different asphalt binders. For example, certain modifications improved the performance of some binders while adversely affecting the performance of other binders. The experiment and analysis methods presented in this study can be used to examine the influence of modifications on performance and optimize the engineering properties of binders and asphalt mixtures.

9.3.3.3 Paper 236 (Copeland et al., 2007)

Copeland et al stated that the bond strength is a critical parameter in evaluating a binder's ability to resist moisture-induced damage. The influence of polymer modification and long-term aging in combination with moisture conditioning on bond strength of asphalt binders was measured using the modified pull off test method that has previously been developed to measure adhesive strength and evaluate moisture sensitivity of asphalt binders using the Pneumatic Adhesion Tensile Testing Instrument (PATTI). The pull-off tensile strength of dry specimens is a measure of cohesive failure strength whereas adhesive failure strength may be determined after moisture conditioning (see Figure 9-9). The pull-off test is able to distinguish among binders with the same performance grade but different chemical properties. However, the exact effect of modification on bond strength cannot be determined without consideration of the binder's physical properties. Moisture conditioning was the most influential factor on bond strength. Long-term laboratory aging increased cohesive strength of asphalt binders. However, aging combined with moisture conditioning decreased adhesive strength of binders. Comparisons of binder resistance to permanent deformation with pull-off tensile strength highlight the need for a test method that measures adhesive properties, namely bond strength, of asphalt binder and mastics. Finally, recommendations are provided to improve ability of pull-off test method for determining bond strength.

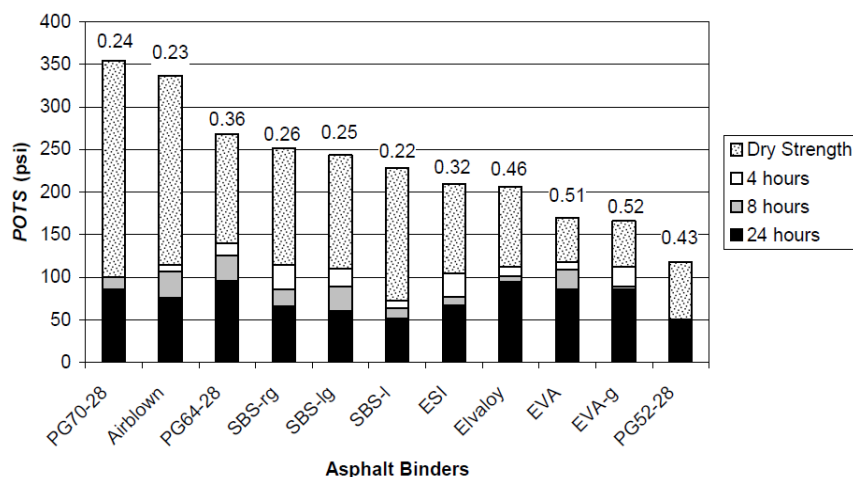


Figure 9-9: Pull-off test results

9.3.3.4 Paper 317 (Canestrari et al., 2014)

Canestrari et al stated that the durability of asphalt mixtures is strongly related to the adhesion properties developed at the interface between binder and aggregates. The loss of adhesion implies a rapid deterioration (e.g. stripping, raveling) of pavement layers under

traffic loads, especially when the pavement is affected by the presence of moisture. Adhesion is a complex phenomenon related to the mineralogical and morphological nature of aggregates, as well as to the chemical binder composition and the environmental conditions. Nowadays, its evaluation becomes even more complicated as an increasing percentage of Reclaimed Asphalt is used in the production of new asphalt mixes. Therefore, adhesion properties are also related to the mechanisms developed at the interface between virgin binder and aged binder that coats the Reclaimed Asphalt aggregate surface. An innovative procedure to evaluate the compatibility of the system virgin binder/Reclaimed Asphalt aggregate is proposed in this study. This procedure allows to simulate in laboratory the substrate of a Reclaimed Asphalt aggregate and can integrate the Binder Bond Strength test currently used to investigate bonding properties and water sensitivity of the system binder-virgin aggregates. Tests were conducted using different aggregate sources, several modified binders and two conditioning types (dry, wet). It was found that this procedure is able to catch the differences between different test configurations and variables. In particular, the artificial reclaimed aggregate substrate ensured higher adhesion performance compared to the virgin aggregate, especially in wet condition, regardless the modification level of the virgin bitumen adopted.

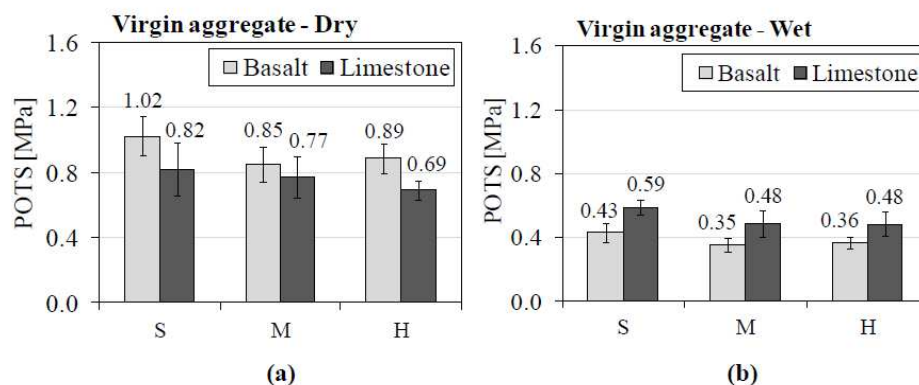


Figure 9-10: Pull-off tensile strength results: comparison between basalt and limestone virgin aggregate (that show failure at the interface) in (a) dry condition and (b) wet condition

9.3.3.5 Paper 519 (Radenberg *et al.*, 2014)

Radenberg *et al.* recently reported on a large study carried out in Germany dealing with the adhesion of paving grade binders with a variety of aggregates. In total the adhesion of 90 bitumens with 8 different aggregates was evaluated while using the Rolling Bottle test (EN 12697-11). In order to rationalize the test results, bitumens were extensively characterized by a series of both empirical as well as rheological test methods. Additionally, some physico-chemical properties of bitumens were assessed such as contact angle or generic composition (by SARA analysis). Also, the characteristics of the used aggregates were determined. Finally, a possible correlation with the water sensitivity of an asphalt mixture (SMA11) was probed for.

Although, a large number of parameters were identified to play a major role in the adhesion of paving grade bitumens with different aggregates, it was not possible to establish a systematic correlation for all bitumen – aggregate combinations.

9.3.3.6 Paper 533 (Renken *et al.*, 2012)

In the paper by Renken the results of an extensive test program on the use of 3 different waxes for the production of asphalt at lower temperature are discussed. Although, the study comprises in the first place the possible impact of latter additives on the performance (e.g. low temperature and fatigue behavior) of several asphalt mixtures such as AC11 and SMA 11 while using both paving grade as well as polymer modified binders, it is also stated that

the adhesion of the bitumen with the aggregate (as probed by the Rolling bottle test) is not negatively influenced.

9.4 Binder ageing effect on binder/aggregate interaction

The effect of ageing on the binder/aggregate interaction has been discussed in only a very limited number of publications. In the paper by Bhasin *et al.* (Paper 232), the possible impact of both short as well as long term ageing was evaluated on the cohesive and the adhesive properties of bitumen. A link was studied with the evolution of physical characteristics of binders (e.g. surface energies). Finally, a possible correlation with water sensitivity was explored.

In a paper by Copeland *et al.* (Paper 236) the bond strength of a wide range of different types of bitumen is studied while using the PATTI test (Pneumatic Adhesion Tensile Testing Instrument). It was demonstrated that the long-term ageing of bituminous binders increased their cohesive strength. However, ageing combined with moisture conditioning decreased significantly their adhesive performance.

A similar research approach was followed by Canestrari *et al.* (Paper 317) in order to study the adhesion of fresh and ‘old’ or aged bitumen originating from RAP. In latter way, the compatibility between both binders was assessed.

Drawing conclusions of the above sited papers in terms of adhesion of bituminous binders is clearly complex (also due to conflicting results) and poses a challenge within the deepened discussion foreseen in deliverable D2.

9.5 Overall uncertainty for binder/aggregate interaction

It is recognized that the uncertainty for binder/aggregate interaction is largely arising from the fact that while assessing the water sensitivity of asphalt mixtures other parameters/factors than adhesion also play a role in the outcome of the test such as choice and grading of the mixtures, sample preparation (e.g. air void content) and conditioning method. Therefore, interpretation in term of adhesion is often hampered.

On the other hand, the precision of the test methods themselves is sometime unsatisfactory. A typical example is the water sensitivity test according to EN 12697-12 where a R = 23% is stated in the standard. Also tests carried out on loose mixtures such as the Rolling Bottle method (EN 12697-11) rely on a visual assessment of the stripping percentage. Consequently, the discriminating power of latter test methods is rather poor.

In Deliverable 2, the impact of the precision data will be discussed further in more detail with respect to the evaluation of binder/aggregate interaction and the possible correlation with asphalt performance, in particular the water sensitivity.

9.6 References for binder/aggregate interaction

Paper 000: **Nicholls, J C (Editor) (2007)**. Analysis of available data for validation of bitumen tests. Report on Phase 1 of the BiTVal Project. Brussels: FEHRL. <http://bitval.fehrl.org/index.php?id=16&dir=Library>.

Paper 014 **Aguiar-Moya, J P, L Loria-Salazar, J Salazar, J Corrales-Azofeifa, E Villegas and E Y Hajj (2013)**. Evaluation of adhesion properties of Costa Rican asphalt mixtures using bitumen bond strength and contact-angle measurement tests. *TRB2013*.

- Paper 031 **Nordgren, T, and K Olsson (2012)**. Asphalt concrete test sections containing bitumen of different origins. *E&E2012*.
- Paper 041 **Deniz, M T, B K Eren, S A Yildirim and A Topcu (2012)**. The effect of salt solution on asphalt pavements and road materials. *E&E2012*.
- Paper 076 **Ishai, I, J B Sousa and G Svehchinsky (2011)**. Activated minerals as binder stabilizers in SMA paving mixtures. *TRB2011*.
- Paper 225 **Chen, X, and B Huang (2007)**. Evaluation of moisture damage in hot mix asphalt using simple performance and Superpave indirect tension tests. *TRB2007*.
- Paper 232 **Bhasin, A, J Howson, E Masad, D N Little and R L Lytton (2007)**. Effect of modification processes on bond energy of asphalt binders. *TRB2007*.
- Paper 236 **Copeland, A R, J Youtcheff and A Shenoy (2007)**. Moisture sensitivity of modified asphalt binders: factors influencing bond strength. *TRB2007*.
- Paper 242 **Varveri, A, S Avgerinopoulos, A Scarpas, A Collop and S Erkens (2014)**. On the combined effect of moisture diffusion and cyclic pore pressure generation in asphalt concrete. *Infradagen 2014 – Netherlands & TRB2014*.
- Paper 287 **Amelian, S, and S M Abtahi (2014)**. Moisture susceptibility evaluation of asphalt mixes based on image analysis. *TRB2014*.
- Paper 317 **Canestrari, F, G Ferrotti, F Cardone and A Stimilli (2014)**. Innovative testing protocol for evaluation of binder-reclaimed aggregate bond strength. *TRB2014*.
- Paper 484 **Lu, X, U Isacson and J Ekblad (2003)**. Influence of polymer modification on low temperature behaviour of bituminous binders and mixtures. *Materials and Structures 2003*.
- Paper 507 **Karcher (2010)**. Effect of different polymer-modified bitumen of the same sort on the fatigue behavior of asphalt. *USAP2010*.
- Paper 508 **Renken, P, M Wistuba, J Grönniger and K Schindler (2010)**. Adhesion of bitumen on aggregates. *Forschung Straßenbau und StraÙneverkehrstechnik*.
- Paper 519 **Radenberg, M**. Einfluss der chemischen, rheologischen und physikalischen Grundeigenschaften von StraÙenbaubitumen auf das Adhäsionsverhalten unterschiedlicher Gesteinskörnungen DAV/DAI, AiF-Forschungsvorhaben Nr. 16639 N/1, http://www.asphalt.de/site/startseite/literatur/infomaterial_download/forschungsberichte/
- Paper 533 **Renken, P**. Wachsadditivierung zur Viskositätsveränderung von Bitumen – Produkteigenschaften und Einfluss auf die Gebrauchseigenschaften von Asphalt DAV/DAI, AiF-Forschungsvorhaben Nr. 15589 N, http://www.asphalt.de/site/startseite/literatur/infomaterial_download/forschungsberichte/
- Paper 542 **Yang, J, X Zhang, H Zhu, Z Chen, W Tian and X Zhang (2010)**. Performance evaluation of superpave asphalt mixture with anti-rutting additives. *TRA2010*,
- Paper 566 **Puchard, G (2012)**. Experiences on low temperature (LT) asphalt in Hungarian road building. *TRA2012*.

10 Conclusions

An extensive review of potential papers has been carried out from conferences and published journals, from which 555 have been found containing details of both bitumen and asphalt properties which could be of use in understanding the relationship between those properties. From these papers, those related to the asphalt properties of permanent deformation (rutting), stiffness, low temperature cracking, fatigue cracking and binder/aggregate interaction have been identified and the data from them extracted in this report. The next stage is to study in detail that data in order to try to select the best bitumen tests to predict the asphalt properties of mixtures made with them. However, it must be appreciated that any such predictions are also dependant on the mixture design (in particular grading, binder content and aggregate type) and the compaction so that perfect correlation is not feasible.

11 Acknowledgement

The research presented in this report/paper/deliverable was carried out as part of the CEDR Transnational Road Research Programme Call 2013. The funding for the research was provided by the national road administrations of Denmark, Germany, Ireland, the Netherlands, the United Kingdom and Slovenia.

Annex A: Relevant papers identified

- Paper 001: **Huang, S-C, T Turner and F Thomas (2013)**. Aging characteristics of RAP-modified binders: Rheological properties. *TRB2013*.
- Paper 002 **Li, X, and N H Gibson (2013)**. Analysis of RAP with known source history and influence on fatigue performance. *TRB2013*.
- Paper 003 **Perez-Jimenez, F E, R Botella Nieto, R Miró and A H Martinez (2013)**. Analysis of temperature effect on bituminous mixture fatigue behaviour using the EBADE test. *TRB2013*.
- Paper 004 **Hanz, A, and H U Bahia (2013)**. Asphalt binder contribution to mixture workability and application of asphalt lubricity test to estimate compactability temperatures for warm-mix asphalt. *TRB2013*.
- Paper 005 **Kim, Y, J Lim, M Lee, S-A Kwon, S Hwang and L Wei (2013)**. Comprehensive evaluation of polymer-modified sma mixture produced with new polyethylene wax-based WMA additive with adhesion promoter. *TRB2013*.
- Paper 006 **Leiva-Villacorta, F, L Loria-Salazar and J P Aguiar-Moya (2013)**. Development of improved and more effective dynamic modulus E^* model for mixtures in Costa Rica by means of artificial neural networks. *TRB2013*.
- Paper 007 **Charmot, S, A Braham and K Zheng (2013)**. Effect of emulsion content and cement loading on cold recycling mixture fracture energy measured using semicircular bending fracture test. *TRB2013*.
- Paper 008 **Leatherman, K, and J R Willis (2013)**. Effect of warm-mix technologies and testing protocol on moisture susceptibility of asphalt mixtures. *TRB2013*.
- Paper 009 **Watson, D E., J R Moore, A J Taylor and P Y Wu (2013)**. Effectiveness of antistripping agents in asphalt mixtures. *TRB2013*.
- Paper 010 **Willis, J R, P Turner, F R de G Padula, N Tran and G Julian (2013)**. Effects of changing virgin binder grade and content on rap mixture properties. *TRB2013*.
- Paper 011 **Geng, H, C Clopotel and H U Bahia (2013)**. Effects of high-modulus asphalt binders on performance of typical asphalt pavement structures. *TRB2013*.
- Paper 012 **Zeida, W A, M I Souliman, K E Kaloush and M S Mamlouk (2013)**. Endurance limit for hot-mix asphalt based on healing-damage balance criterion using viscoelastic continuum damage analysis. *TRB2013*.
- Paper 013 **Ragab, M S, M Abdelrahman and A Ghavibazoo (2013)**. Enhancing performance of crumb rubber-modified asphalts through controlling internal network structure. *TRB2013*.
- Paper 014 **Aguiar-Moya, J P, L Loria-Salazar, J Salazar, J Corrales-Azofeifa, E Villegas and E Y Hajj (2013)**. Evaluation of adhesion properties of Costa Rican asphalt mixtures using bitumen bond strength and contact-angle measurement tests. *TRB2013*.
- Paper 015 **Hesami, E, N Bidewell, B Birgisson and N Kringos (2013)**. Evaluation of environmental susceptibility of bituminous mastic viscosity as a function of mineral and biomass fillers. *TRB2013*.
- Paper 016 **Premkumar, L, G R Chehab and M Solaimanian (2013)**. Evaluation of low-temperature properties of asphalt binders and mixtures. *TRB2013*.

- Paper 017 **Zaumanis, M, R B Mallick and R Frank (2013).** Evaluation of rejuvenator's effectiveness with conventional mix testing for 100% RAP mixtures. *TRB2013*.
- Paper 018 **Yang, S-H, T Suciptan and Y-H Chang (2013).** Investigation of rheological behaviour of Japanese cedar-based biobinder as partial replacement for bituminous binder. *TRB2013*.
- Paper 019 **Onochie, A C, E H Fini, X Yang, J Mills-Beale and Z You (2013).** Rheological characterization of nanoparticle-based biomodified binder. *TRB2013*.
- Paper 020 **Morian, N, E Y Hajj and P E Sebaaly (2013).** Significance of mixture parameters on binder aging in hot-mix asphalt mixtures. *TRB2013*.
- Paper 021 **Zhao, S, B F Bowers, B Huang, X Shu and M Woods (2013).** Using gel permeation chromatography to predict viscoelastic properties of recycled asphalt shingle binder and its use in RAS blending efficiency. *TRB2013*.
- Paper 022 **M Cope, B Allen and S E Zoorob (2007).** A study of the effect of bitumen / vegetable oil blends on asphalt mixture performance. *ICBMP2007*.
- Paper 023 **Dueñas, A P, A P Lepe, E M Martinez and V C Ibañez (2012).** Relationships between zero shear viscosity, low shear viscosity and MSCRT tests and EN 12697-22 rutting test. *E&E2012*.
- Paper 024 **Olard, F, P Huon, S Dupriet, J Dherbecourt and L M Perez (2012).** GB5: Eco-friendly alternative to EME2 for long-life & cost-effective base courses through use of gap-graded curves & SBS modified bitumens. *E&E2012*.
- Paper 025 **Mangiafico, S, H di Benedetto, C Sauzeat, F Olard, S Dupriet, L Planque and R van Rooijen (2012).** Effect of reclaimed asphalt pavement on complex modulus and fatigue resistance of bitumens and asphalts. *E&E2012*.
- Paper 026 **Eckmann, B, M Mazé, S Largeaud and S F Dumont (2012).** The contribution of cross-linked polymer modified binders to asphalt performance. *E&E2012*.
- Paper 027 **Nazarbeygi, E A, and A R Moeini (2012).** Sulfur extended asphalt investigation - laboratory and field trial. *E&E2012*.
- Paper 028 **Hase, M, C Oelkers and K Schindler (2012).** Influence of differences in quality polymer modified bituminous binder same variety on the mechanical behaviour of asphalt, Part 1: Deformation behaviour under heat. *E&E2012*.
- Paper 029 **Pouget, S, CSauzeat, H Di Benedetto and F Olard (2012).** Prediction of isotropic linear viscoelastic behaviour for bituminous materials – forward and inverse problems. *E&E2012*.
- Paper 030 **Jensen, B B, and J B Andersen (2012).** 15 years experience adding polymer powder directly into the asphalt mixer. *E&E2012*.
- Paper 031 **Nordgren, T, and K Olsson (2012).** Asphalt concrete test sections containing bitumen of different origins. *E&E2012*.
- Paper 032 **Haritonovs, V, M Zaumanis, G Brencis and J Smirnovs (2012).** Research on the use of bof steel slag aggregates with dolomite sand waste to develop high performance asphalt concrete. *E&E2012*.
- Paper 033 **Plug, K, A de Bondt and C Smits (2012).** Development of a durable noise reducing thin surfacing for heavy traffic. *E&E2012*.

- Paper 034 **Dreessen, S, T Gallet, A G Dumont and M Pittet (2012)**. Durability study: field experience of long-term evolution of SBS polymer modified binder. *E&E2012*.
- Paper 035 **Dreessen, S, and T Gallet (2012)**. MSCRT: Performance related test method for rutting prediction of asphalt mixtures from binder rheological characteristics. *E&E2012*.
- Paper 036 **Pasetto, M, and N Baldo (2012)**. Fatigue behaviour and stiffness properties of asphalt rubber mixtures made with steel slags. *E&E2012*.
- Paper 037 **Iwanski, M, and G Mazurek (2012)**. The influence of rheological properties of bitumen with synthetic wax on changing resilient modulus of elasticity of asphalt concrete. *E&E2012*.
- Paper 038 **Valentin, J, P Mondschein, V Souček, O Ryneš, P Hýzl, D Stehlík and M Varaus (2012)**. Selected performance characteristics of warm mix asphalts with various low-viscosity binders. *E&E2012*.
- Paper 039 **Bahia, H, R Moraes and R Velasquez 92012)**. The effect of bitumen stiffness on the adhesive strength measured by the bitumen bond strength test. *E&E2012*.
- Paper 040 **Morea, F, and R Marcozzi (2012)**. Rheological properties of asphalt binders with chemical tensoactive additives used in warm mix asphalts (WMA). *E&E2012*.
- Paper 041 **Deniz, M T, B K Eren, S A Yildirim and A Topcu (2012)**. The effect of salt solution on asphalt pavements and road materials. *E&E2012*.
- Paper 042 **Robertus, C, R van Rooijen and L Thimm 92012)**. A comparison of binder tests that relate to asphalt mixture deformation. *E&E2012*.
- Paper 043 **Morea, F (2012)**. Performance of asphalt mixtures at different temperatures and load, their relation with the asphalt low shear viscosity (LSV). *E&E2012*.
- Paper 044 **Deniz, M T, S A Yildirim, B K Eren, A Topcu, S Girit and I Sonmez (2012)**. The effect of different agents on warm mix asphalt pavements. *E&E2012*.
- Paper 045 **Vasilica, B, G Georgeta and S Elisabeta (2012)**. The effects of rubber powder on the performance of pavement asphalt. *E&E2012*.
- Paper 046 **Güngör, A G, F Orhan and S Kaşak (2012)**. The determination of performance of wearing course mixtures using advanced asphalt tests. *E&E2012*.
- Paper 047 **Gungor, A G, and A Sağlık (2012)**. Evaluation of rutting performance of neat and modified binders using zero shear viscosity. *E&E2012*.
- Paper 048 **Nikolova, S, and A Nikolov (2012)**. Study on the plastic deformations of the asphalt mixtures. *E&E2012*.
- Paper 049 **Kamal, M A, A Rahat and I Hafeez (2010)**. Effects of polymer modified bitumen on rutting with varying aggregate gradations. *LJMU2010*.
- Paper 050 **Haritonovs, V, J Tihonovs, M Zaumanis and A Krasnikovs (2014)**. High modulus asphalt concrete with dolomite aggregates. *TRA2014*.
- Paper 051 **Fakhri, M, and N B Jommor (2008)**. The effect of SBS polymer modified bitumen on indirect tensile strength (IDT) of porous friction coarse mixes and conventional hot mix asphalt. *LJMU2008*.

- Paper 052 **Qi, D, A Shenoy and X Qi (2008)**. Validation of asphalt binder fatigue parameters with ALF pavements. *LJMU2008*.
- Paper 053 **Beckedahl, H J, P Sivapatham and L Neutag (2008)**. Performance of asphalt pavements with high polymer modified bitumen - a life-cycle study. *E&E2008*.
- Paper 054 **De Visscher, J, S Vansteenkiste and A Vanelstraete (2008)**. Test sections in high-modulus asphalt: Mix design and laboratory performing testing. *E&E2008*.
- Paper 055 **Edwards, Y (2008)**. Influence of waxes on bitumen and asphalt concrete mixture performance. *E&E2008*.
- Paper 056 **Edwards, Y (2008)**. Influence of waxes on bitumen and asphalt concrete mixture performance. *E&E2008*.
- Paper 057 **Wasage, T L J, M Ryes, J Stastna and L Zanzotto (2008)**. Creep characteristics of conventional, oxidized, polymer and tire crumb rubber modified asphalt binders and mixtures. *E&E2008*.
- Paper 058 **Baumgardner, G, J V Martin, R B Powell and P Turner (2008)**. Polyphosphoric acid and styrene-butadiene-styrene block co-polymer modified asphalt: Evaluation of paved section at the NCAT test track built in 2000 and 2003. *E&E2008*.
- Paper 059 **Bennert, T, and J V Martin (2008)**. Polyphosphoric acid in combination with styrene-butadiene-styrene co-polymer: Mix fatigue resistance and permanent deformation evaluation. *E&E2008*.
- Paper 060 **Zolotarev, V A, S V Kudryavtseva and S V Yefremov (2008)**. Influence of joint introduction of polymers and adhesive agents on bitumens properties. *E&E2008*.
- Paper 061 **Beckedahl, H J, P Sivapatham and L Neutag (2008)**. Impacts of the compaction degree of asphalt mixes on the asphalt pavement performance. *E&E2008*.
- Paper 062 **Pérez Jiménez, F, O J Reyes-Ortiz, R Miró Recasens and A Hernández-Noguers (2008)**. Relation between the fatigue behavior of asphalt binders and bituminous mixtures. *E&E2008*.
- Paper 063 **Pérez Jiménez, F, M Barral, J A Soto Sánchez and J A Navro Jansoro (2008)**. Effect of the nature and filler content on cohesion, adhesion and rheological behaviour of the bituminous mastics. *E&E2008*.
- Paper 064 **Hase, M, and C Oelkers (2008)**. The influence of low temperature behaviour of polymer modified binders and of cryogenic tensile stress in asphalt on the life cycle of traffic areas. *E&E2008*.
- Paper 065 **Mollenhauer, K, S Buechler and P Reinken (2008)**. Testing of cold characteristics of asphalt. *E&E2008*.
- Paper 066 **Büchler, S, P Renken and K Mollenhaer (2008)**. Relation between rheological bitumen characteristics and the resistance of asphalt against fatigue and cold temperatures. *E&E2008*.
- Paper 067 **Guericke, R, and K Schlame (2008)**. A new "Softening Point" - Based on asphalt pavement performance figures. *E&E2008*.
- Paper 068 **Hammoum, F, S Hamlat, P-Y Hicher and J-P Terrier (2008)**. Laboratory evaluation of the resistance to tangential forces of bituminous surfacing. *E&E2008*.

- Paper 069 **Such, C, J-V Martin, S Périgois and N Picard (2008)**. Properties and performances of asphalt binders and asphalt mixes modified with polyphosphoric acid. *E&E2008*.
- Paper 070 **Gauthier, G, D Bodin and R Chkir (2008)**. Stiffness and fatigue properties of asphalt: Effect of the bitumen type and the bitumen content. *E&E2008*.
- Paper 071 **Ballié, M, E Chailleux, P Dumas, B Eckmann, C Leroux, B Lombardi, J-P Planche, C Such and J-C Vaniscote (2008)**. Characteristics of bituminous binders and their consequences on the mechanical performance of asphalts. *E&E2008*.
- Paper 072 **Reinke, G, S Engber, D Herlitzka, D Tranberg and J Jorgenson (2008)**. Utilization of binder stress sensitivity to investigate the impact of applied load, binder type and aggregate structure on the rutting behaviour of bituminous mixtures. *E&E2008*.
- Paper 073 **Stephan, F, and L Drüschner (2008)**. Recycling of reclaimed asphalt from porous asphalt. *E&E2008*.
- Paper 074 **de Visscher, J, S Vansteenkiste and A Vanelstraete (2008)**. Test sections in high-modulus asphalt: Mix design and laboratory performing testing. *E&E2008*.
- Paper 075 **Soenen, H, T Tanghe, P Redelius, J de Visscher, F Vervaecke and A Vanelstraete (2008)**. Laboratory study on the use of waxes to reduce paving temperatures. *E&E2008*.
- Paper 076 **Ishai, I, J B Sousa and G Svehinsky (2011)**. Activated minerals as binder stabilizers in SMA paving mixtures. *TRB2011*.
- Paper 077 **Azari, H (2011)**. Analysis of the effect of laboratory short-term conditioning on mechanical properties of asphalt mixture. *TRB2011*.
- Paper 078 **Huber, G A, M Beeson and M Prather (2011)**. Characterization of reclaimed asphalt pavement in Indiana: Changing INDOT specifications for RAP. *TRB2011*.
- Paper 079 **Harnsberger, P M, M J Farrar, S-C Huang and R E Robertson (2011)**. Comparative field performance using asphalts from multiple crude oil sources. *TRB2011*.
- Paper 080 **Wen, H (2011)**. Development of a damage-based phenomenological fatigue model for asphalt pavement. *TRB2011*.
- Paper 081 **Marchildon, R P and S A M Hesp (2011)**. Development of microindentation tests for specification grading of asphalt cements. *TRB2011*.
- Paper 082 **Wang, H, I L Al-Qadi, A F Faheem, H U Bahia, S-H Yang and G H Reinke (2011)**. Effect of mineral filler characteristics on asphalt mastic and mixture rutting potential. *TRB2011*.
- Paper 083 **Perez-Jimenez, F E, G V Vidal, R Miró, R B Nieto and J M Campana (2011)**. Effect of thermal stresses on fatigue behavior of bituminous mixes. *TRB2011*.
- Paper 084 **Swiertz, D, E Mahmoud and H U Bahia (2011)**. Estimating effect of recycled asphalt pavement and recycled asphalt shingles on fresh binder low-temperature properties without extraction and recovery. *TRB2011*.
- Paper 085 **Mogawer, W S, M M Haggag and R Bonaquist (2011)**. Fatigue evaluation of warm-mix asphalt mixtures using uniaxial cyclic direct tension compression test. *TRB2011*.

- Paper 086 **Islam, R U L, S J Ddamba, S L Tighe, R Essex and N Hanasoge (2011).** Field and laboratory evaluation of recycled asphalt shingle mixes: Canadian study. *TRB2011.*
- Paper 087 **Scholz, T, L Hunt and N Shippen (2011).** Forensic investigation of moisture-related pavement failures on interstate highways in Oregon. *TRB2011.*
- Paper 088 **Timm, D H, M M Robbins and R Q Kluttz (2011).** Full-scale structural characterization of a highly polymer-modified asphalt pavement. *TRB2011.*
- Paper 089 **Timm, D H, J R Willis and A Kvasnak (2011).** Full-scale structural evaluation of fatigue characteristics in high RAP and warm-mix asphalt. *TRB2011.*
- Paper 090 **Yu, H, and S Shen (2011).** Impact of aggregate packing on dynamic modulus of hot-mix asphalt mixtures using discrete element method. *TRB2011.*
- Paper 091 **Hatami, K (2011).** In-aggregate performance of unitized and woven geogrids in open-graded and dense-graded aggregates. *TRB2011.*
- Paper 092 **Awed, A, S M El-Badawy, F M Bayomy and M J Santi (2011).** Influence of MEPDG binder characterization input level on predicted dynamic modulus for idaho asphalt concrete mixtures. *TRB2011.*
- Paper 093 **Bennert, T A, A Maher and R W Ali (2011).** Influence of production temperature and aggregate moisture content on performance of warm-mix asphalt. *TRB2011.*
- Paper 094 **Olard, F (2011).** Innovative design approach to high-performance asphalt concretes with long-life base and binder courses by use of aggregate packing concepts and polymer-modified binders. *TRB2011.*
- Paper 095 **Behnia, B, E V Dave, S Ahmed, W G Buttlar and H Reis (2011).** Investigation of effects of recycled asphalt pavement amounts on low-temperature cracking performance of asphalt mixtures using acoustic emissions. *TRB2011.*
- Paper 096 **Bayat, A, H Akbarzadeh and H R Soleymani (2011).** Investigation of temperature dependency of asphalt concrete using laboratory dynamic modulus and field deflection testing. *TRB2011.*
- Paper 097 **Buss, A F, R C Williams, S A Schram and A Kvasnak (2011).** Investigation of warm-mix asphalt using Iowa aggregates. *TRB2011.*
- Paper 098 **Li, X, N H Gibson, T R Clyne, E N Johnson and M E Kutay (2011).** Laboratory evaluation of asphalt binders and mixtures containing polyphosphoric acid. *TRB2011.*
- Paper 099 **Lu, Qi, and J Harvey (2011).** Laboratory evaluation of open-graded asphalt mixes with small aggregates and various binders and additives. *TRB2011.*
- Paper 100 **Hossain, Z (2011).** Laboratory evaluation of water-bearing additive for warm-mix asphalt. *TRB2011.*
- Paper 101 **Kim, K W (2011).** Low-temperature fracture characteristics of selected warm-mix asphalt concretes. *TRB2011.*
- Paper 102 **Xiao, F, V S Punith and S N Amirkhanian (2011).** Low-volume warm-mix asphalt mixtures: moisture susceptibility of mixtures containing coal ash and roofing shingle with moist aggregate. *TRB2011.*

- Paper 103 **Moraes, R, R A Velasquez and H U Bahia (2011).** Measuring effect of moisture on asphalt-aggregate bond with bitumen bond strength test. *TRB2011.*
- Paper 104 **Wen, H, X Li and S Bhusal (2011).** Modeling effects of temperature and loading rate on fatigue properties of hot-mix asphalt. *TRB2011.*
- Paper 105 **Hintz, C A, R A Velasquez, C Johnson and H U Bahia (2011).** Modification and validation of linear amplitude sweep test for binder fatigue specification. *TRB2011.*
- Paper 106 **Sui, C, M J Farrar, P M Harnsberger, W H Tuminello and T F Turner (2011).** New low-temperature performance grading method using 4-mm parallel plates on a dynamic shear rheometer. *TRB2011.*
- Paper 107 **Sui, C, M J Farrar, P M Harnsberger, W H Tuminello and T F Turner (2011).** New low-temperature performance grading method using 4-mm parallel plates on a dynamic shear rheometer. *TRB2011.*
- Paper 108 **Wasiuddin, N M, N E Saltibus and L N Mohammad (2011).** Novel Moisture-conditioning method for adhesive failure of hot- and warm-mix asphalt binders. *TRB2011.*
- Paper 109 **Morian, N, E Y Hajj, C J Glover and P E Sebaaly (2011).** Oxidative aging of asphalt binders in hot-mix asphalt mixtures. *TRB2011.*
- Paper 110 **Buddhavarapu, P N V S R, A de F Smit and J A Prozzi (2011).** Parametric procedure to evaluate fracture sensitivity of hot-mix asphalt. *TRB2011.*
- Paper 111 **Mogawer, W S, A J Austerman, R Bonaquist and M Roussel (2011).** Performance characteristics of thin-lift overlay mixtures containing high RAP content, RAS, and warm-mix asphalt technology. *TRB2011.*
- Paper 112 **Loria, L G, E Y Hajj, P E Sebaaly, M Barton, S Kass and T Liske (2011).** Performance evaluation of asphalt mixtures with high RAP content. *TRB2011.*
- Paper 113 **Evans, M, and S A M Hesp (2011).** Physical hardening effects on stress relaxation in asphalt cements and implications for pavement performance. *TRB2011.*
- Paper 114 **Falchetto, A C, M Turos, K H Moon, M O Marasteanu and R N Dongre (2011).** Physical hardening: from binders to mixtures. *TRB2011.*
- Paper 115 **Marasteanu, M O, E Z Teshale, K H Moon, Ki Hoon and M Turos (2011).** Pressure aging vessel and low-temperature fracture properties of asphalt binders. *TRB2011.*
- Paper 116 **Apeageyi, A, B K Diefenderfer and S Diefenderfer (2011).** Rutting resistance of asphalt concrete mixtures containing recycled asphalt pavement. *TRB2011.*
- Paper 117 **Mateos, A, J P Ayuso and B C Jáuregui (2011).** Shift factors for asphalt fatigue from full-scale testing. *TRB2011.*
- Paper 118 **Zeida, W A, K E Kaloush, K P Biligiri, J Reed and J J Stempihar (2011).** Significance of confined dynamic modulus laboratory testing for dense and gap- and open-graded asphalt concrete mixtures. *TRB2011.*
- Paper 119 **Yang, E, W C V Ping, Y Xiao and Y Qiu (2011).** Simplified predictive model of dynamic modulus for characterizing Florida hot-mix asphalt mixtures. *TRB2011.*

- Paper 120 **Palma, G R S (2011).** Stiffness modulus behavior in hot-mix asphalt. *TRB2011.*
- Paper 121 **Khosla, N P, H Nair, B Visintine and G Malpass (2011).** Study on rheological behavior of reclaimed asphalt binder blends. *TRB2011.*
- Paper 122 **Howard, I L, J D Doyle, M Hemsley, G L Baumgardner and L A Cooley (2011).** Use of hot-mix warm-compacted asphalt in construction. *TRB2011.*
- Paper 123 **Xiao, F, V S Punith, B Putman and S N Amirkhanian (2011).** Utilization of foaming technology in warm-mix asphalt mixtures containing moist aggregates. *TRB2011.*
- Paper 124 **Zezelew, H, C Paugh and M R Corrigan (2011).** Warm-mix asphalt laboratory permanent deformation performance in state of Pennsylvania: Case study. *TRB2011.*
- Paper 125 **Aurangzeb, Q, I L Al-Qadi, I M Abuawad, W Pine and J Trepanier (2012).** Achieving desired volumetrics and performance for high-RAP mixtures. *TRB2012.*
- Paper 126 **La Torre, F, and M Meocci (2012).** Calibration of mechanistic-empirical pavement design guide model for nonconventional asphalt concrete materials. *TRB2012.*
- Paper 127 **Merusi, F, and F Giuliani (2012).** Chromatic and rheological characteristics of clear road binders. *TRB2012.*
- Paper 128 **Zezelew, H, M R Corrigan, R Belagutti and J R Reddy (2012).** Comparative evaluation of stiffness properties of warm-mix asphalt technologies and |E*| predictive models. *TRB2012.*
- Paper 129 **Walubita, L F, J Zhang, G Das, X Hu, C Mushota, A E Alvarez and T Scullion (2012).** Comparison of Hamburg, dynamic modulus, and repeated-load tests for evaluation of hot-mix asphalt permanent deformation. *TRB2012.*
- Paper 130 **Yiqiu, T, Z Lei, J Lun and L Shan (2012).** Comparison of low-temperature performance evaluation methods of asphalt mixtures. *TRB2012.*
- Paper 131 **Bernier, A K, R Josen, A Zofka and M Mahoney (2012).** Connecticut warm-mix asphalt pilot project. *TRB2012.*
- Paper 132 **Lee, H S, S Kim, B Choubane and P B Upshaw (2012).** Construction of dynamic modulus master curves using resilient modulus and creep test data. *TRB2012.*
- Paper 133 **Walubita, L F, A N Faruk, G Das, R H Izzo, B Haggerty and T Scullion (2012).** Continuing search for a hot-mix asphalt cracking test: single shot versus repeated-load testing. *TRB2012.*
- Paper 134 **Perez-Jimenez, F E, R B Nieto and R Miró (2012).** Damage and thixotropy in asphalt mixture and binder fatigue tests. *TRB2012.*
- Paper 135 **Mogawer, W S, A J Austerman and R Bonaquist (2012).** Determining influence of plant type and production parameters on performance of plant-produced RAP mixtures. *TRB2012.*
- Paper 136 **Qiu, J, A Molenaar, M F C van de Ven and S Wu (2012).** Development of autonomous setup for evaluating self-healing capability of asphalt mixtures. *TRB2012.*

- Paper 137 **Baek, C, S Yang, J Lee, S Hwang and S A Kwon (2012).** Development of warm-mix asphalt additive and evaluation of its performance. *TRB2012.*
- Paper 138 **Lu, Q, and J Harvey (2012).** Effect of aggregate type on noise and durability performance of open-graded asphalt mixes. *TRB2012.*
- Paper 139 **Stimilli, A, C A Hintz, Z Li, R A Velasquez and H U Bahia (2012).** Effect of healing on fatigue law parameters of asphalt binders. *TRB2012.*
- Paper 140 **Swamy, K A, and J S Daniel (2012).** Effect of mode of loading on viscoelastic and damage properties of asphalt concrete. *TRB2012.*
- Paper 141 **Yu, X, J Wu, Y Liu and J Wu (2012).** Effects of aging on rheological properties of crumb rubber modified asphalts with and without warm additives. *TRB2012.*
- Paper 142 **Daniel, J S, and S Tarbox (2012).** Effects of long-term oven aging on RAP mixtures. *TRB2012.*
- Paper 143 **Baek, C, B S Underwood and Y R Kim (2012).** Effects of oxidative aging on asphalt mixture properties. *TRB2012.*
- Paper 144 **Hajj, E Y, L G Loria and P E Sebaaly (2012).** Estimating effective performance grade of asphalt binders in high-RAP mixtures using different methodologies: Case study. *TRB2012.*
- Paper 145 **Alavi, M Z, E Y Hajj, A Hanz and U Hussain (2012).** Evaluating adhesion properties and moisture damage susceptibility of warm-mix asphalts using bitumen bond strength and dynamic modulus ratio tests. *TRB2012.*
- Paper 146 **Roberts, L, P Romero and K van Frank (2012).** Evaluation of asphalt mixture performance tester: Utah experience. *TRB2012.*
- Paper 147 **Ali, H A, and R Bonaquist (2012).** Evaluation of binder grade and recycling agent blending for hot in-place recycled pavement. *TRB2012.*
- Paper 148 **Hakimzadeh, S, W G Buttlar and R Santarromana (2012).** Evaluation of bonding between hot-mix asphalt layers produced with different tack coat application rates using shear-type and tension-type tests. *TRB2012.*
- Paper 149 **Wang, H, Z You, S W Goh, P Hao and X Huang (2012).** Evaluation of high-temperature rheological properties of rubber asphalt by dynamic shear rheometer test and master curve. *TRB2012.*
- Paper 150 **Hossain, Z, and M Zaman (2012).** Evaluation of high-temperature viscoelastic characteristics of warm-mix additive-modified binders and prediction of dynamic modulus of mixes. *TRB2012.*
- Paper 151 **Hill, B, B Behnia, S Hakimzadeh, W G Buttlar and H Reis (2012).** Evaluation of Low-Temperature Cracking Performance of Warm-Mix Asphalt Mixtures *TRB2012*
- Paper 152 **Rashwan, M, and R C Williams (2012).** An evaluation of warm mix asphalt additives and reclaimed asphalt pavement on performance properties of asphalt mixtures. *TRB2012.*
- Paper 153 **Willis, J R, A J Taylor and N Tran (2012).** Laboratory evaluation of high polymer plant-produced mixtures. *TRB2012.*
- Paper 154 **Shannon, C, Y Kim, G Thomas and H Lee (2012).** Fractionation of high recycled asphalt pavement content in asphalt mixtures for Superpave mix design compliance. *TRB2012.*

- Paper 155 **Alvarez, A E, J S Carvajal, O Reyes-Ortiz, L F Walubita and C K Estakhri (2012).** Image analysis of the internal structure of warm mix asphalt 1 (WMA) mixtures. *TRB2012.*
- Paper 156 **Choi, Y-T, V Subramanian, M N Guddati and Y R Kim (2012).** An incremental model for the prediction of permanent deformation of asphalt concrete in compression. *TRB2012.*
- Paper 157 **Azari, H, and A Mohseni (2012).** Incremental repeated load permanent deformation testing of asphalt mixtures. *TRB2012.*
- Paper 158 **Faheem, A F, C A Hintz, H U Bahia and I L Al-Qadi (2012).** Influence of filler fractional voids on mastic and mixture performance. *TRB2012.*
- Paper 159 **Gong, W, M Tao, R B Mallick and T El-Korchi (2012).** Investigation of moisture susceptibility of warm mix asphalt (wma) mixes through laboratory mechanical testing. *TRB2012.*
- Paper 160 **Wurst, J, and B Putman (2012).** Laboratory evaluation of the use of warm-mix technology to produce ogfc mixtures without fibers. *TRB2012.*
- Paper 161 **Zhao, S, B Huang, X Shu, X Jia and M Woods (2012).** Laboratory performance evaluation of warm mix asphalt containing high percentages of RAP. *TRB2012.*
- Paper 162 **Powell, R L, and S Buchanan (2012).** Long term performance of a thin asphalt overlay on the NCAT pavement test track. *TRB2012.*
- Paper 163 **Palvadi, S, A Bhasin and D N Little (2012).** A method to quantify healing in asphalt composites using continuum damage approach. *TRB2012.*
- Paper 164 **Aragao, F T S, Y-R Kim and M H Javaherian (2012).** Modeling rate-dependent fracture behavior of asphalt mixtures. *TRB2012.*
- Paper 165 **Tabatabaee, H A, R A Velasquez and H U Bahia (2012).** Modeling thermal stress in asphalt mixtures undergoing glass transition and physical hardening. *TRB2012.*
- Paper 166 **Kim, Y-R, J Zhang and H Ban (2012).** Moisture damage characterization of warm-mix asphalt mixtures based on laboratory-field evaluation. *TRB2012.*
- Paper 167 **Shivaprasad, P V, F Xiao, D W Wingard, B A Putman and N M Aziz (2012).** Moisture susceptibility and rutting resistance evaluation of foamed half warm asphalt mixtures. *TRB2012.*
- Paper 168 **Ali, H A. and K Sobhan (2012).** On the road to sustainability: properties of hot in-place recycled superpave mix. *TRB2012.*
- Paper 169 **Mamlouk, M S, M I Souliman and W A Zeiada (2012).** Optimum testing conditions to measure hma fatigue and healing using flexural bending test. *TRB2012.*
- Paper 170 **Mogawer, W S, A J Austerman, R Q Kluttz and M Roussel (2012).** Performance and workability characteristics of high performance thin lift overlays incorporating high RAP content and warm mix asphalt technology. *TRB2012.*
- Paper 171 **Mogawer, W S, E H Fini, A J Austerman, A Booshehrian and B Zada (2012).** Performance characteristics of high rap bio-modified asphalt mixtures. *TRB2012.*

- Paper 172 **Porras, J, E Y Hajj, P E Sebaaly, S Kass and T Liske (2012).** Performance evaluation of field-produced WMA mixtures in Manitoba. *TRB2012.*
- Paper 173 **Giuliana, G, V Nicolosi and B Festa (2012).** Predictive formulas of complex modulus for high air void content mixes. *TRB2012.*
- Paper 174 **Zeida, W A, K E Kaloush and M S Mamlouk (2012).** Rational approach for adjusting hot-mix asphalt dynamic modulus due to changes in air voids and asphalt content. *TRB2012.*
- Paper 175 **Clopotel, C, R A Velasquez, H U Bahia, F E Perez-Jimenez, R M Recasens and R B Nieto (2012).** Relation between binder and mixture damage resistance at intermediate and 2 low temperatures. *TRB2012.*
- Paper 176 **Coleri, E, R Wu, J M Signore and J Harvey (2012).** Rutting of rubberized gap graded and polymer modified dense graded asphalt overlays in composite pavements. *TRB2012.*
- Paper 177 **Gonzalez, A A, M Cubrinovski, B D Pidwerbesky and D Alabaster (2012).** Study on elastic strains, modulus, and permanent deformation of foamed bitumen pavements in accelerated testing facility. *TRB2012.*
- Paper 178 **Miller, C, D N Little and A Bhasin (2012).** Surface energy characteristics of natural minerals and their impact of aggregate-bitumen bond strengths and asphalt mixture durability. *TRB2012.*
- Paper 179 **Dawson, A R, P K Dehdezi, M Hall, J Wang and R Isola (2012).** Thermo-physical optimisation of asphalt paving materials. *TRB2012.*
- Paper 180 **Rushing, J F, D N Little and N Garg (2012).** Using the asphalt pavement analyzer to assess rutting susceptibility of 1 HMA designed for high tire pressure aircraft. *TRB2012.*
- Paper 181 **Zhang, D-Y (2012).** Virtual rutting test of asphalt mixture based on discrete element method. *TRB2012.*
- Paper 182 **Stempihar, J J (2012).** Use of fiber reinforced asphalt concrete as a sustainable paving material for airfields. *TRB2012.*
- Paper 183 **Ho, C-H, and P Romero (2012).** Using asphalt mixture beams in bending beam rheometer for quality control: Utah experience. *TRB2012.*
- Paper 184 **Bhattacharjee, S, and R B Mallick (2012).** Use of continuum damage mechanics with small scale accelerated pavement testing to determine damage development in hot mix asphalt. *TRB2012.*
- Paper 185 **d'Angelo, J, R Kluttz, R Dongré, K Stephens and L Zanzotto (2007).** Revision of the Superpave high temperature binder specification: The multiple stress creep recovery test. *AAPT2007.*
- Paper 186 **Kvasnak, A N, and R C Williams (2007).** Evaluation of the interaction effects between asphalt binders and fillers using a moisture susceptibility test. *AAPT2007.*
- Paper 187 **Bodley, T, A Andriescu, S Hesp and K Tam (2007).** Comparison between binder and hot mix asphalt properties and early top-down wheel path cracking in a Northern Ontario pavement trial. *AAPT2007.*
- Paper 188 **Pellinen, T, A Zofka, M Marasteanu and N Funk (2007).** Asphalt mixture stiffness predictive models. *AAPT2007.*

- Paper 189 **Ozer, H, I L Al-Qadi, S H Carpenter, Q Aurangzeb, G L Roberts and J Trepanier (2009).** Evaluation of RAP impact on hot-mix asphalt design and performance. *AAPT2009*.
- Paper 190 **Daniel, J S, G R Chehab and D Ayyala (2009).** Sensitivity of RAP binder grade on performance predictions in the MEPDG. *AAPT2009*.
- Paper 191 **Masad, E, C-W Huang, J d'Angelo and D Little (2009).** Characterization of asphalt binder resistance to permanent deformation based on nonlinear viscoelastic analysis of multiple stress creep recovery (MSCR) test. *AAPT2009*.
- Paper 192 **Johnson, C M, H Wen and H U Bahia (2009).** Practical application of viscoelastic continuum damage theory to asphalt binder fatigue characterization. *AAPT2009*.
- Paper 193 **Kim, S, H J Choi and K W Kim (2013).** Evaluation of tensile property of warm-mix asphalt concretes at low temperatures. *TRB2013*.
- Paper 194 **Farrar, M J, T F Turner, J-P Planche, J F Schabron and P M Harnsberger (2013).** Evolution of crossover modulus with oxidative aging: Method to estimate change in viscoelastic properties of asphalt binder with time and depth on the road. *TRB2013*.
- Paper 195 **Lee, S-J, J Park, J-P Hong and K W Kim (2013).** Fracture resistance of warm-mix asphalt concretes at low temperatures. *TRB2013*.
- Paper 196 **Apeageyi, A K, K K McGhee and T Clark (2013).** Influence of aggregate packing and asphalt binder characteristics on performance of stone matrix asphalt. *TRB2013*.
- Paper 197 **da Silva, A H M, K L Vasconcelos, A L Aranha, L B Bernucci and J M Chaves (2013).** Laboratory and field evaluation of cold-in-place RAP recycling. *TRB2013*.
- Paper 198 **Mohammad, L N, M A Elseifi, S Cooper, H Challa and P Naidoo (2013).** Laboratory evaluation of asphalt mixtures containing bio-binder technologies. *TRB2013*.
- Paper 199 **Walubita, L F, A N Faruk, A E Alvarez, R Izzo, B Haggerty and T Scullion (2013).** Laboratory HMA cracking testing: evaluation of three repeated loading crack tests. *TRB2013*.
- Paper 200 **Woldekidan, M F, M Huurman and A Pronk (2013).** Linear and nonlinear viscoelastic analysis of bituminous mortar. *TRB2013*.
- Paper 201 **Hill, B, D J Oldham, B Behnia, E H Fini, W G Buttlar and H Reis (2013).** Low-temperature performance characterization of biomodified asphalt mixtures containing reclaimed asphalt pavement. *TRB2013*.
- Paper 202 **Calderon, A E U, E Y Hajj and P E Sebaaly (2013).** Mechanistic-based approach to evaluate rutting susceptibility of hot-mix asphalt mixtures using dynamic triaxial testing. *TRB2013*.
- Paper 203 **Azari, H, and A Mohseni (2013).** Permanent deformation characterization of asphalt mixtures using incremental repeated load testing. *TRB2013*.
- Paper 204 **Hou, Y, P Yue, L Wang, W Sun, A T Pauli, D Wang, W Zhou and M Hu (2013).** Phase field modeling of mode I cracking failure in asphalt binder. *TRB2013*.
- Paper 205 **Sousa, J B, G M Rowe, A Vorobiev and I Ishai (2013).** Reacted and activated rubber: elastomeric asphalt extender. *TRB2013*.

- Paper 206 **Wasiuddin, N M, S S Ashani, Md S Kabir, C D Abadie, W King and L N Mohammad (2013)**. Rheology of asphalt emulsion residues and its relationship to elastic recovery in AASHTO T301. *TRB2013*.
- Paper 207 **Hintz, C, R Velasquez, Z Li and H Bahia (2011)**. Effect of oxidative aging on binder fatigue performance. *AAPT-2011*.
- Paper 208 **Kim, Y-R, F A C de Freitas and D H Allen (2011)**. Experimental characterization of ductile fracture-damage properties of asphalt binders and mastics. *TRB2008*.
- Paper 209 **Velasquez, R, H Tabatabaee and H Bahia (2011)**. Low temperature cracking characterization of asphalt binders by means of the Single -edge notch bending test. *AAPT-2011*.
- Paper 210 **Anderson, R M, G N King, D I Hanson and P B Blankenship (2011)**. Evaluation of the relationship between asphalt binder properties and non-load related cracking. *AAPT-2011*.
- Paper 211 **Howson, J, E Masad, D Little and E Kassem (2012)**. Relationship between bond energy and total work of fracture for asphalt binder-aggregate systems. *AAPT-2012*.
- Paper 212 **Clopotel, C, R Velasquez, and H Bahia (2012)**. Measuring physico-chemical interaction in mastics using glass transition. *AAPT-2012*.
- Paper 213 **Yut, I, A Bernier, and A Zofka (2012)**. Development of a compact laboratory aging procedure for asphalt binders. *AAPT-2012*.
- Paper 214 **Centeno, M, I Sandoval, I Cremades and J Alarcón (2008)**. Assessing rutting susceptibility of five different modified asphalts in bituminous mixtures using rheology and wheel tracking test. *TRB2008*.
- Paper 215 **Wasage, T, M Cantu, J Stastna, G Polacco and L Zanzotto (2007)**. The role of viscosity in dynamic creep tests in conventional, oxidized and polymer modified asphalts. *TRB2007*.
- Paper 216 **Bianchetto, H, R Miró, F Pérez-Jiménez and A Martínez (2007)**. Effect of calcareous fillers on bituminous mix aging. *TRB2007*.
- Paper 217 **Kodrat, I, D Sohn and S A M Hesp (2007)**. How polyphosphoric acid-modified asphalt binders compare to straight and polymer-modified materials. *TRB2007*.
- Paper 218 **Ni, F, Z Wu, R Chen, X Gu and D Qiao (2007)**. Fatigue and anti-reflective cracking properties of binder course mixtures used in China. *TRB2007*.
- Paper 219 **Braham, A F, W G Buttlar and M O Marasteanu (2007)**. Effect of binder type, aggregate, and mixture composition on the fracture energy of hot-mix asphalt in cold climates. *TRB2007*.
- Paper 220 **Atud, T J, K Kanitpong and W Martono (2007)**. Laboratory evaluation of hydrated lime application process in asphalt mixture for moisture damage and rutting resistance. *TRB2007*.
- Paper 221 **Bhasin, A, D N Little, K L Vasconcelos and E Masad (2007)**. Use of surface free energy to identify moisture sensitivity of materials for asphalt mixes. *TRB2007*.
- Paper 222 **Zhou, F, S Hu, D-H Chen and T Scullion (2007)**. Overlay tester: a simple performance test for fatigue cracking. *TRB2007*.

- Paper 223 **Cho, D W, and H U Bahia (2007)**. Effects of aggregates' surface and water on rheology of asphalt films. *TRB2007*.
- Paper 224 **Castro-Fernandez, P, P E Sebaaly and P Chavarria-Salas (2007)**. Optimization of fatigue cracking resistance of Costa Rican asphalt concrete mixes. *TRB2007*.
- Paper 225 **Chen, X, and B Huang (2007)**. Evaluation of moisture damage in hot mix asphalt using simple performance and Superpave indirect tension tests. *TRB2007*.
- Paper 226 **Lee, S-J, S Amirkhanian, B Putman and K W Kim (2007)**. Laboratory Investigation of volumetric and rutting properties of CRM asphalt mixtures due to compaction conditions. *TRB2007*.
- Paper 227 **Tarefder, R A, J C Stormont and M Zaman (2007)**. Evaluating laboratory modulus and rutting of asphalt concrete. *TRB2007*.
- Paper 228 **Bennert, T, and J-V Martin (2008)**. Polyphosphoric acid in combination with styrene-butadiene-styrene block copolymer: laboratory mixture evaluation. *TRB2008*.
- Paper 229 **Middleton, B, and L C Falls (2007)**. Long-term performance investigation of Superpave™ using the LTPP SPS-9A experiment. *TRB2007*.
- Paper 230 **Alvarez, A E, A E Martin, C Estakhri and R Izzo (2008)**. Evaluation of durability tools for porous friction courses. *TRB2008*.
- Paper 231 **Jung, S H, L F Walubita, A E Martin and C J Glover (2007)**. Mixture versus neat-film binder oxidation and hardening and the impact of binder oxidation on estimated mixture fatigue life. *TRB2007*.
- Paper 232 **Bhasin, A, J Howson, E Masad, D N Little and R L Lytton (2007)**. Effect of modification processes on bond energy of asphalt binders. *TRB2007*.
- Paper 233 **Wasiuddin, N M, M M Zaman and E E O'Rear (2008)**. Effect of Sasobit® and Aspha-min® on wettability and adhesion between asphalt binders and aggregates. *TRB2008*.
- Paper 234 **Hrdlicka, G M, and V Tandon (2007)**. Estimation of hot mix asphalt concrete rutting potential from repeated creep binder tests. *TRB2007*.
- Paper 235 **Azari, H, A Mohseni and N Gibson (2008)**. Verification of rutting predictions from mechanistic empirical pavement design guide using accelerated loading facility data. *TRB2008*.
- Paper 236 **Copeland, A R, J Youtcheff and A Shenoy (2007)**. Moisture sensitivity of modified asphalt binders: factors influencing bond strength. *TRB2007*.
- Paper 237 **Sluer, J (2012)**. Bepaling van de healingeigenschappen van asfaltmengsels met de CMSE-benadering [Determination of the healingcapacity of asphalt mixes using the CMSE approach].
<http://www.crow.nl/vakgebieden/infrastructuur/wegaanleg/bijeenkomsten-ontwerp-en-aanleg/eerdere-edities-infradagen/crow-infradagen-2012>.
- Paper 238 **Jacobs, M, C Gharabaghy, C Schulze and R van den Beemt (2012)**. Bepaling van de rafelingeigenschappen van open asfaltmengsels met de ARTe [Measurement of raveling of porous mixes using the ARTE test].
<http://www.crow.nl/vakgebieden/infrastructuur/wegaanleg/bijeenkomsten-ontwerp-en-aanleg/eerdere-edities-infradagen/crow-infradagen-2012>.

- Paper 239 **Besamusca, J, A Volkers, J van de Water and B Gaarkeuken (2012)**. De verschillen tussen laboratorium veroudering van bitumen 70/100 en asfalt toepassing in ZOAB [Differences accelerated aging tests and aging of a B70/100 in an open porous asphalt]. <http://www.crow.nl/vakgebieden/infrastructuur/wegaanleg/bijeenkomsten-ontwerp-en-aanleg/eerdere-edities-infradagen/crow-infradagen-2012>.
- Paper 240 **Erkens, S, A van Dommelen, D van Vliet, G Leegwater and M Jacobs (2012)**. Bepaling van de Healingscapaciteit van een asfaltmengsel [Determination of the healing capacity of an asphalt mix]. <http://www.crow.nl/vakgebieden/infrastructuur/wegaanleg/bijeenkomsten-ontwerp-en-aanleg/eerdere-edities-infradagen/crow-infradagen-2012>.
- Paper 241 **Leegwater, G, T Scarpas and S Erkens (2014)**. Verkenning en toetsing van het Amerikaanse convolutie healing model voor asfalt [Exploration and check-up of the American convolution healing model for asphalt]. *Infradagen 2014 – Netherlands*.
- Paper 242 **Varveri, A, S Avgerinopoulos, A Scarpas, A Collop and S Erkens (2014)**. On the combined effect of moisture diffusion and cyclic pore pressure generation in asphalt concrete. *Infradagen 2014 – Netherlands & TRB2014*.
- Paper 243 **Jacobs, M M J, and D AJ van Duin (2014)**. Rafelingsproeven en textuurmetingen in het lab [Raveling test and texture measurements in the lab]. *Infradagen 2014 – Netherlands*.
- Paper 244 **Mookhoek, S D, D van Vliet, D Q van Lent and S M J G Erkens (2014)**. Eerste resultaten op basis van type onderzoek (RAW proef 62) en bindmiddel onderzoekproef 62) en bindmiddel onderzoek voor asfaltbeton [First results of introducing type testing on asphalt concrete and on bituminous binders]. *Infradagen 2014 – Netherlands*.
- Paper 245 **Poeran, N, B Sluer and B Andeweg (2014)**. Verwerkbaarheid van asfaltmengsels [Workability of asphalt mixes]. *Infradagen 2014 – Netherlands*.
- Paper 246 **Ambika, B, K Gajendra and K Jain (2013)**. Performance of low energy crumb rubber modified bituminous mixes. *REAAA2013*.
- Paper 247 **Zdrálek, P, and P Hýzl (2009)**. Influence of different factors on the testing asphalt mixtures by triaxial compression test. *Asfaltové vozovky 2009*.
- Paper 248 **Scholten, E, W Vonk and R Kluttz (2013)**. The dawning of a new era of pavement design. *REAAA2013*.
- Paper 249 **Moazami, D, R Muniandy and H Hamid (2013)**. Effect of new and old generations of wide-base tires on HMA rutting. *REAAA2013*.
- Paper 250 **Králová, E (2009)**. The improvement of the binder adhesion to the aggregate with the use of Licomont BS 100 – the current results of the research. *Asfaltové vozovky 2009*.
- Paper 251 **Morova, N, S Serin, S Terzi, M Saltan and M Karaşahin (2013)**. Determining marshall stability of asphalt concretes reinforced using steel fiber with artificial neural networks. *REAAA2013*.
- Paper 252 **Sakamoto, T, and K Saito (2013)**. The characteristics and durability of the long life asphalt mixture. *REAAA2013*.
- Paper 253 **Abe, N (2013)**. The development and the performance of the asphalt mixture for the heavy loading. *REAAA2013*.

- Paper 254 **Kawakami, A, H Nitta, K Kubo, T Nukui, Y Inaba and Y Arai (2013)**. Development of new evaluation method for recycled aggregate in Japan. *REAAA2013*.
- Paper 255 **Valentin, J, P Mondschein and J Vavricka (2013)**. Assesment of behaviour of warm mix asphalts in the low-temperature range. *REAAA2013*.
- Paper 256 **Michito, K, and M Takahiro (2013)**. Development and field application of in-site road surface maintenance method with the simple surface recycling machine. *REAAA2013*.
- Paper 257 **Florian, A, and L Ševelová (2013)**. Cyclic-load triaxial testing of materials used in computer simulation of the low volume roads. *REAAA2013*.
- Paper 258 **Hirato, T, M Iwama, H Hanitta, A K Kawakami and Y Masuyama (2013)**. The present conditions and problem of the porous asphalt pavement in Japan. *REAAA2013*.
- Paper 259 **Yongjoo, K, L Munseop, L Jinwook and C Dongwoo (2013)**. Evaluation of warm-recycled asphalt mixtures containing polyethylene wax-based WMA additive. *REAAA2013*.
- Paper 260 **Hasegawa, J, and H Fujita (2013)**. Development of the surface treatment method with hot mix aphalt which contribute to the life extension of pavement. *REAAA2013*.
- Paper 261 **Kedoudja, S, S Samia and H Smail (2013)**. Influence of the modification process of the bituminous concrete by the NBR on the mechanical characteristics. *REAAA2013*.
- Paper 262 **Hasnan, N H, and M H Harun (2013)**. Quality control on bitumen delivered to road construction sites. *REAAA2013*.
- Paper 263 **Sakata, F, J Tanaka and T Okamoto (2013)**. Improving durability of pavement on expressways in snowy area (Hokkaido region). *REAAA2013*.
- Paper 264 **Yamin, A, K Kubo, I Sasaki and S Ueno (2013)**. Japan-Indonesia cooperation on the research in Asbuton. *REAAA2013*.
- Paper 265 **Kedoudja, S, S Samia and H Smail (2013)**. Influence of the modification process of the bituminous concrete by the NBR on the mechanical characteristics. *REAAA2013*.
- Paper 266 **Gagandeep, S, P Satish, M N Nagabhusana and P K Jain (2013)**. Studies on reduction of flexible pavement thickness by use of polymer modified binder. *REAAA2013*.
- Paper 267 **Koc, M, and R Bulut (2014)**. Characterization of warm mix asphalt additives using direct contact angle measurements and surface free energies. *TRB2014*.
- Paper 268 **Sprinkel, M M, and A K Apegyei (2014)**. Evaluation of the installation and initial condition of thermoplastic polymer-modified asphalt overlays on bridge decks. *TRB2014*.
- Paper 269 **Guercio, M C H, L M McCarthy and Y Mehta (2014)**. Mechanical responses and viscoelastic properties of asphalt mixtures under heavy static and dynamic aircraft loads. *TRB2014*.
- Paper 270 **Bureš, P, J Fiedler and Z Komínek (2011)**. Rheological properties of asphalt binders and mixtures at medium and high temperatures. *Asfaltové vozovky 2011*.

- Paper 271 **Faisal, H M, R A Tarefde and M T Weldegiorgis (2014)**. Characterization of asphalt mastic and aggregate phases for moisture damage. *TRB2014*.
- Paper 272 **Pérez-Jiménez, F, R Botella, R Miró, A Paez-Dueñas, F J Barceló-Martínez and V Carrera (2014)**. Binder, mastic and mixture fatigue characterization using a cyclic uniaxial strain sweep test. *TRB2014*.
- Paper 273 **Yin, H, and D Barbagallo (2014)**. Full-scale test of thermally-induced reflective cracking. *TRB2014*.
- Paper 274 **Doyle, J D, and I L Howard (2014)**. Characterizing dense-graded asphalt concrete with the Cantabro test. *TRB2014*.
- Paper 275 **Araya-Zamorano, L, D Hernández-Barrera, F Pérez-Jiméne, A H Martínez and R Miró (2014)**. Analysis of the effect of the compaction procedure of asphalt specimens with marshall and gyratory compactor on the volumetric and mechanical properties. *TRB2014*.
- Paper 276 **Ai, C, Y Qiu, J Q Li, K C P Wang and E Yang (2014)**. Bending characteristics for asphalt concrete beams with bond interface. *TRB2014*.
- Paper 277 **Xiao, F, and S N Amirkhanian (2014)**. Moisture susceptibility and rut resistance of RAP mixtures with high percentage of natural sand. *TRB2014*.
- Paper 278 **LaCroix, A T, and Y R Kim (2014)**. Performance predictions of rutting for NCAT test track. *TRB2014*.
- Paper 279 **Abuawad, I M, Q Aurangzeb, I L Al-Qadi and H Ozer (2014)**. Potential moisture damage of asphalt mixtures with additives using various test mechanisms. *TRB2014*.
- Paper 280 **Buss, A F, Y Kuang, R C Williams, J Bausano, A Cascione and S A Schram (2014)**. Influence of warm-mix asphalt additive and dosage rate on construction and performance of bituminous pavements. *TRB2014*.
- Paper 281 **Cheng, D, R G Hicks, B Fraser and M Garcia (2014)**. Evaluating performance of asphalt rubber used in California. *TRB2014*.
- Paper 282 **Qian, Z, and Q Lu (2014)**. Design and laboratory evaluation of small particle porous epoxy asphalt concrete. *TRB2014*.
- Paper 283 **Rowe, G M, C Ericson and A Cooper (2014)**. The Vialit cohesion pendulum as a tool for asphalt binder evaluation . *TRB2014*.
- Paper 284 **Cooper, S B, L N Mohammad and M A Elseifi (2014)**. Laboratory performance of asphalt mixtures containing recycled asphalt shingles. *TRB2014*.
- Paper 285 **Boriack, P, S W Katicha and G W Flintsch (2014)**. A laboratory study of the effect of high RAP and high asphalt binder content on the stiffness, fatigue resistance and rutting resistance of asphalt concrete. *TRB2014*.
- Paper 286 **Charmot, S, C Ye, Z Zhu and Y Yang (2014)**. Measurements of the effectiveness of fiber reinforced micro surfacing mixtures. *TRB2014*.
- Paper 287 **Amelian, S, and S M Abtahi (2014)**. Moisture susceptibility evaluation of asphalt mixes based on image analysis. *TRB2014*.
- Paper 288 **Poulikakos, L D, S dos Santos J Lee and M N Partl (2014)**. Moisture susceptibility of recycled asphalt concrete: A multi-scale approach. *TRB2014*.
- Paper 289 **Li, J, F Ni and Y Huang (2014)**. New additive used in hot in-place recycling to improve performance of RAP mix. *TRB2014*.

- Paper 290 **Mohammadi, M A, A Aghasoltan and A Kavusi (2014)**. An optimal grading model to improve the rut resistance of stone mastic asphalt. *TRB2014*.
- Paper 291 **Kanaan, A I, H Ozer and I L Al-Qadi (2014)**. Quantification of asphalt binder replacement effectiveness using recycled shingles through fine asphalt mixture level testing. *TRB2014*.
- Paper 292 **Lacroix, A, and Y R Kim (2014)**. Performance Predictions of Rutting for the NCAT Test Track. *TRB2014*.
- Paper 293 **Grünner, K, and M Luknár (2011)**. Possibilities of utilization of waste materials gained from asphalt pavements into bituminous mixtures. *Asfaltové vozovky 2011*.
- Paper 294 **Bennert, T A, D S Jo and S M Walaa (2014)**. Strategies for incorporating higher RAP percentages: Review of northeast states implementation trials. *TRB2014*.
- Paper 295 **Bleakley, A M, and P J Cosentino (2014)**. Strength and deformation testing of chemically stabilized RAP-Limerock base course blends. *TRB2014*.
- Paper 296 **You, T, A M Eyad R K A Al-Rub, E Kassem and D N Little (2014)**. A systematic approach for calibration and validation of a comprehensive constitutive model for asphalt mixtures. *TRB2014*.
- Paper 297 **Farhana, R, T Jeremiah T, H Mustaque and G Schieber (2014)**. Structural characteristics of aged asphalt concrete pavements. *TRB2014*.
- Paper 298 **Kuna, K, G Airey and N Thom (2014)**. A laboratory mix design procedure for foamed bitumen mixtures (FBM). *TRB2014*.
- Paper 299 **Mogawer, W S, A J Austerman, R Q Klutz and L N Mohammad (2014)**. Performance-based specifications for high-performance thin overlay mixtures incorporating reclaimed asphalt pavement. *TRB2014*.
- Paper 300 **Coleri, E, and J Harvey (2014)**. Prediction of rutting performance using laboratory measured and strain gauge backcalculated asphalt concrete stiffnesses. *TRB2014*.
- Paper 301 **Byung, S O, Y C Ji and J Y Pyeong (2014)**. Fiber's interfacial bond strength analysis using direct tensile loading tests. *TRB2014*.
- Paper 302 **Solanki, P, H Ozer, S S Yousefi and I L Al-Qadi (2014)**. Field validation of laboratory-predicted low-temperature performance of hot-poured crack sealants. *TRB2014*.
- Paper 303 **Motta, R, L Bernucci, P Vasconcellos, V Faria and J F Leal (2014)**. Laboratory and field evaluation of warm mix asphalt in Brazil. *TRB2014*.
- Paper 304 **Putman, B J, and K R Lyons (2014)**. Laboratory evaluation of long-term in draindown of porous asphalt mixtures. *TRB2014*.
- Paper 305 **Zhao, S, B Huang, X Shu and P Ye (2014)**. Laboratory Investigation of Bio-Char Modified Asphalt Mixture. *TRB2014*.
- Paper 306 **Ahmed, A W, and S Erlingsson (2014)**. Evaluation of permanent deformation model for asphalt concrete mixtures using wheel tracking and heavy vehicle simulator tests. *TRB2014*.
- Paper 307 **Rahman, F, M Hossain, C Hobson and G Schieber (2014)**. Performance of Superpave overlay mixtures with high RAP content. *TRB2014*.

- Paper 308 **Yiqiu, T, L Shan and X Li (2014)**. Unified evaluation index for high- and low-temperature performance of asphalt binder. *TRB2014*.
- Paper 309 **Ma, W, N Tran, A J Taylor and X LI (2014)**. Proposed improvements to overlay test for determining cracking resistance of asphalt mixtures. *TRB2014*.
- Paper 310 **Wen, H, and S Bhusal (2014)**. Toward development of asphaltic materials to resist studded tire wear. *TRB2014*.
- Paper 311 **Nahar, S N, J Qiu, A J M Schmets, E Schlangen, M Shirazi, M F C van de Ven, G Schitter and A Scarpas (2014)**. Turning back time: rheological and microstructural assessment of rejuvenated bitumen. *TRB2014*.
- Paper 312 **Saleh, M F (2014)**. Utilization of vertical and horizontal measurements in determination of indirect resilient modulus and effect on accuracy of interconversion to dynamic modulus. *TRB2014*.
- Paper 313 **Jamrah, A, M E Kutay and H I Ozturk (2014)**. Characterization of asphalt materials common to Michigan in support of the implementation of the "Mechanistic-Empirical Pavement Design Guide". *TRB2014*.
- Paper 314 **Willis, J R, T Rosenmayer and D Carlson (2014)**. Effect of ground tire rubber on open-graded mixture performance. *TRB2014*.
- Paper 315 **Son, S, and I L Al-Qadi (2014)**. Engineering cost-benefit analysis of thin durable asphalt overlays. *TRB2014*.
- Paper 316 **Greene, J, S Chun and B Choubane (2014)**. Enhanced gradation guidelines to improve asphalt mixture performance. *TRB2014*.
- Paper 317 **Canestrari, F, G Ferrotti, F Cardone and A Stimilli (2014)**. Innovative testing protocol for evaluation of binder-reclaimed aggregate bond strength. *TRB2014*.
- Paper 318 **Oldham, D J, E H Fini and T Abu-Lebdeh (2014)**. Investigating the rejuvenating effect of bio-binder on recycled asphalt shingles. *TRB2014*.
- Paper 319 **Wu, S, K Zhang, H Wen, J DeVol and K Kelsey (2014)**. Performance evaluation of hot-mix asphalt containing recycled asphalt shingles in Washington State. *TRB2014*.
- Paper 320 **Kodippily, S, G Holleran, I Holleran, T F P Henning and D J Wilson (2014)**. Performance of recycled asphalt pavement mixes: comparing New Zealand experience with American experience. *TRB2014*.
- Paper 321 **Sabahfar, N, S R Aziz, M Hossain and G Schieber (2014)**. Evaluation of Superpave mixtures with high percentages of reclaimed asphalt pavement. *TRB2014*.
- Paper 322 **Putman, B J, and K R Lyons (2014)**. Evaluation of warm-mix and rubber-modified open-graded friction course test sections made without fibers in South Carolina. *TRB2014*.
- Paper 323 **Morian, N, M Z Alavi, E Y Hajj and P E Sebaaly (2014)**. Evolution of thermo-viscoelastic properties of asphalt mixtures with oxidative aging. *TRB2014*.
- Paper 324 **Mohseni, A, and H Azari (2014)**. High-temperature characterization of highly modified asphalt binders and mixtures. *TRB2014*.
- Paper 325 **El-Hakim, M, and S L Tighe (2014)**. Impact of freeze-thaw cycles on mechanical properties of asphalt mixes. *TRB2014*.

- Paper 326 **Ling, C, A Hanz and H U Bahia (2014)**. Evaluating moisture susceptibility of cold-mix asphalt. *TRB2014*.
- Paper 327 **Zeinali, A, P B Blankenship and K C Mahboub (2014)**. Evaluation of effect of density on asphalt pavement durability through performance testing. *TRB2014*.
- Paper 328 **Diefenderfer, S, and H Nair (2014)**. Evaluation of high RAP mixture production, construction, and properties. *TRB2014*.
- Paper 329 **Kim, S, S-J Lee, Y Youn and K-W Kim (2014)**. Evaluation of optimum short-term aging temperature for SBS-modified warm-mix asphalt mixtures. *TRB2014*.
- Paper 330 **Bower, N, H Wen, S Wu, K A Willoughby, J Weston and J DeVol (2014)**. Evaluation of performance of warm-mix asphalt in Washington state. *TRB2014*.
- Paper 331 **Soleimanbeigi, A, R F Shedivy, J M Tinjum and T B Edil (2014)**. Effect of temperature on resilient modulus of recycled unbound aggregates. *TRB2014*.
- Paper 332 **Johnson, K-A, and S Hesp (2014)**. Effect of waste engine oil residue on quality and durability of SHRP materials reference library binders. *TRB2014*.
- Paper 333 **Islam, M R, U A Mannan, A A Rahman and R A Tarefder (2014)**. Effects of recycled asphalt pavement on mix and binder properties and performance in the laboratory. *TRB2014*.
- Paper 334 **Motamed, A, D R Salomon, N Sakib and A Bhasin (2014)**. Emulsified asphalt residue recovery and characterization using combined moisture analyzer balance-dynamic shear rheometer procedure. *TRB2014*.
- Paper 335 **Isola, M, S Chun, R Roque, J Zou, C Koh and G Lopp (2014)**. Development and evaluation of laboratory conditioning procedures to effectively simulate mixture property changes in the field. *TRB2014*.
- Paper 336 **Ge, Z, H Wang, Y Wang and X Hu (2014)**. Development of a new test method for evaluating fatigue behavior of asphalt mixtures under tension-compression loading mode. *TRB2014*.
- Paper 337 **Apeagyei, A K, J R A Grenfell and G D Airey (2014)**. Durability of asphalt mixtures exposed to long-term moisture conditioning. *TRB2014*.
- Paper 338 **Hesp, S A M, K A N Johnson, R G McEwan, S K P Samy, S Ritchie and M Thomas (2014)**. Effect of ten commercial warm mix additives on the quality and durability of cold lake asphalt cement. *TRB2014*.
- Paper 339 **Leiva-Villacorta, F, R E Villegas-Villegas, J P Aguiar-Moya, J Salazar-Delgado and L G L Salazar (2014)**. Effect of aging on rheological, chemical and thermodynamic properties of asphalt components. *TRB2014*.
- Paper 340 **Ghavibazoo, A, and M Abdelrahman (2014)**. Effect of crumb rubber dissolution on low-temperature performance and aging of asphalt-rubber binder. *TRB2014*.
- Paper 341 **Ozturk, H I, and M E Kutay (2014)**. Effect of foamed binder characteristics on warm-mix asphalt performance. *TRB2014*.
- Paper 342 **Zeinali, A, P B Blankenship and K C Mahboub (2014)**. Effect of laboratory mixing and compaction temperatures on asphalt mixture volumetrics and dynamic modulus. *TRB2014*.
- Paper 343 **Zeinali, A, P B Blankenship and K C Mahboub (2014)**. Effect of long-term ambient storage of compacted asphalt mixtures on laboratory-measured dynamic modulus and flow number. *TRB2014*.

- Paper 344 **Florio, E, C Berti, C Kasbergen, M M Villani, A Scarpas, S M J G Erkens, C Sangiorgi C Lantieri (2014).** Combining the American and European mix design approaches: Utilization of NCHRP performance indicators for analysis of CEN-test results. *TRB2014*.
- Paper 345 **Islam, M R, and R A Tarefder (2014).** Comparing temperature induced fatigue damage to traffic induced fatigue damage in asphalt concrete. *TRB2014*.
- Paper 346 **Zeida, W A, M I Souliman, K E Kaloush, M Mamlouk and B S Underwood (2014).** Comparison of fatigue damage, healing, and endurance limit using beam and uniaxial fatigue tests. *TRB2014*.
- Paper 347 **Yang, S.H, A Keita and H Wang (2014).** Comparison of field aging characteristic of warm mix asphalt. *TRB2014*.
- Paper 348 **Brandon, J, S Hines, D M Jared, B H Bui and Y Ahmed (2014).** Comparison of procedures to predict moisture susceptibility characteristics in warm mix asphalt. *TRB2014*.
- Paper 349 **Domingos, M D I, and A L Faxina (2014).** Creep-recovery behavior of modified asphalt binders with similar high-temperature performance grades. *TRB2014*.
- Paper 350 **Islam, M R, M U Ahmed and R A Tarefder (2014).** Cross-anisotropy of laboratory and field compacted asphalt concrete samples. *TRB2014*.
- Paper 351 **Hosseinezhad, S, D Holmes and E H Fini (2014).** Decoupling the physical filler effect and the time dependent dissolution effect of crumb rubber on asphalt matrix rheology. *TRB2014*.
- Paper 352 **Mueller, M, A K Singh and K W Lee (2014).** Cold in-place recycling for sustainable streets and highways. *TRB2014*.
- Paper 353 **Li, P, Z Ding and Z Zhang (2014).** A new approach to evaluating aggregate slip shear resistance in HMA. *TRB2014*.
- Paper 354 **Dašek, O, P Coufalík, P Hýzl, M Varaus, P Špaček, Z Hegr and S Stoklásek (2013).** New test methods allowing to predict the life extension of asphalt pavements. *Asfaltové vozovky 2013*.
- Paper 355 **Mondschein, P, and J Valentin (2013).** Compaction of hot asphalt mixtures in laboratory: influence of compaction on the behaviour of asphalt mixtures. *Asfaltové vozovky 2013*.
- Paper 356 **Mahmud, M, H Yacob, R Jaya and N Hassan (2013).** Investigation on the effects of flaky aggregates on creep and resilient modulus of asphalt mixture. *Asfaltové vozovky 2013*.
- Paper 357 **Valentin, J, J Suda, M Faltus and G Karra'a (2013).** Is mechano-chemical activation a solution for new types of fine grained materials in civil engineering? *Asfaltové vozovky 2013*.
- Paper 358 **Králová, E (2013).** Evaluation of selected additives of binders in mastic asphalts. *Asfaltové vozovky 2013*.
- Paper 359 **Loveček, Z, and F Schlosser (2013).** The empirical and functional tests of the asphalt concrete adjusted with native bitumen (TE). *Asfaltové vozovky 2013*.
- Paper 360 **Gschwendt, I, S Štefunková and A Zuzulová (2013).** Development of technologies and their influence on energy consumption. *Asfaltové vozovky 2013*.

- Paper 361 **Valentin, J, P Mondschein, M Varaus, P Hýzl and D Stehlík (2013)**. Selected laboratory experience with design and assessment of SMA LA and LOA asphalt mixture. *Asfaltové vozovky 2013*.
- Paper 362 **Hanzík, V, and M Rosenbaum (2013)**. The possibility of reducing production temperatures of asphalt mixtures for asphalt plant DM 55. *Asfaltové vozovky 2013*.
- Paper 363 **Jamshidi, A, M Hamzah and A Yahya (2013)**. Analysis of the resilient behavior of warm mix asphalt incorporating Sasobit®. *Asfaltové vozovky 2013*.
- Paper 364 **Varaus, M, P Hýzl, P Mondschein, J Valentin, R Pazyna, P Svoboda and D Matoušek (2013)**. Recycling of asphalt mixtures in parallel drying drum with the use of rejuvenators and additives for the reduction of manufacturing temperature. *Asfaltové vozovky 2013*.
- Paper 365 **Kachtík, J, and J Kudrna (2013)**. Experience with production of the crumb rubber modified bitumen (CRmB) in the Czech Republic. *Asfaltové vozovky 2013*.
- Paper 366 **Řikovský, V (2013)**. Asphalt mixture tests for fulfilment of fundamental requirements. *Asfaltové vozovky 2013*.
- Paper 367 **Fiedler, J, and P Mondschein (2013)**. Notes on the fatigue properties of asphalt mixtures and the pavement design. *Asfaltové vozovky 2013*.
- Paper 368 **Adorjányi, K, and P Füleki (2011)**. Stiffness and creep properties of paving grade, hard and polymer modified bitumens. *Asfaltové vozovky 2011*.
- Paper 369 **Báčová, K, and S Štefunková (2011)**. Impact of asphalt mixtures quality on road traffic safety. *Asfaltové vozovky 2011*.
- Paper 370 **Zdrálek, P, and P Hýzl (2011)**. Testing of bituminous mixtures resistance to permanent deformations using cyclic load triaxial test method. *Asfaltové vozovky 2011*.
- Paper 371 **Mondschein, P (2011)**. Composition of bituminous mixtures – basic aspect of quality. *Asfaltové vozovky 2011*.
- Paper 372 **Oylumluoglu, J, B Sengoz, A Topal and C Gorkem (2011)**. Experimental study of recycled asphalt mixtures with Sasobit®. *Asfaltové vozovky 2011*.
- Paper 373 **Dražan, L, and F Luxemburk (2011)**. Impact of air-voids and compaction rate on selected bituminous mixtures rheology properties (stiffness modulus, fatigue resistance). *Asfaltové vozovky 2011*.
- Paper 374 **Hanzík, V, and D Sova (2011)**. The possibility of expanding the knowledge of low- temperature properties of asphalts and asphalt mixtures. *Asfaltové vozovky 2011*.
- Paper 375 **Fiedler, J, P Bureš, J Kašpar and Z Komínek (2011)**. Experience with technology reducing reflective cracking propagations to the pavement surface. *Asfaltové vozovky 2011*.
- Paper 376 **Vavříčka, J, J Žák and P Mondschein (2011)**. Utilization of various types microfiber iterfibra for improving properties of asphalt mixture. *Asfaltové vozovky 2011*.
- Paper 377 **Wallin, T (2011)**. Long-term effectiveness of adhesion promoters in airfields. *Asfaltové vozovky 2011*.

- Paper 378 **Sybilski, D, and I Ruttmar (2011)**. Use of innovative rubber-bitumen granulates in Poland. *Asfaltové vozovky 2011*.
- Paper 379 **Varaus, M (2011)**. Low-noise stone mastic asphalts. *Asfaltové vozovky 2011*.
- Paper 380 **Valentin, J, P Mondschein and M Holík (2011)**. Selected performance characteristics of asphalt mixes containing crumb binders with lower content of crumb rubber. *Asfaltové vozovky 2011*.
- Paper 381 **Dašek, O, and J Kudrna (2011)**. Evaluation of crumb rubber modified bitumen storage stability. *Asfaltové vozovky 2011*.
- Paper 382 **Valentin, J, P Mondschein, V Souček, M Varaus, P Hýzl and D Stehlík (2011)**. Performance characteristics of selected warm mix asphalts. *Asfaltové vozovky 2011*.
- Paper 383 **Plitz, J, and D Švadlák (2011)**. New grades of mofalt – modified binders for lower noise wearing courses. *Asfaltové vozovky 2011*.
- Paper 384 **Mondschein, P, and J Valentin (2011)**. The problems of the usage of reclaimed asphalt in hot mix asphalt. *Asfaltové vozovky 2011*.
- Paper 385 **Suda, J, D Matoušek and J Valentin (2011)**. Alternative binders from energetic by-products in stabilized cold recycled mixtures. *Asfaltové vozovky 2011*.
- Paper 386 **Mondschein, P, and E Márová (2009)**. Influence of compacting energy on water resistance of asphalt mixture. *Asfaltové vozovky 2009*.
- Paper 387 **Varaus, M, P Hýzl and O Vacín (2009)**. Determination of asphalt mixtures stiffness modulus by 2-point and 4-point bending test according to ČSN EN 12697-26. *Asfaltové vozovky 2009*.
- Paper 388 **Černý, R, and M Zbuzek (2009)**. Evaluation of the quality of bituminous binders by means of DSR and BBR rheological parameters. *Asfaltové vozovky 2009*.
- Paper 389 **Olenočinová, P, C Denayer and O Dašek (2009)**. Hydrated lime as a chemical active filler: research of hydrated lime effect on rutting resistance. *Asfaltové vozovky 2009*.
- Paper 390 **Bežilla, T, J Komačka and E Remišová (2009)**. Does cyclic compression test enable to differentiate asphalts from resistance to rutting point of view? *Asfaltové vozovky 2009*.
- Paper 391 **Mazé, M, F Delfosse, S Dumont, E Crews and C Giorgi (2009)**. European development of the Tempera®/Evotherm Dat® process. *Asfaltové vozovky 2009*.
- Paper 392 **Valentin, J, and P Mondschein (2009)**. Selected experience of experimental assessment of warm asphalt mixes characteristics and behaviour. *Asfaltové vozovky 2009*.
- Paper 393 **Valentin, J, and P Mondschein (2009)**. Assessment of stiffness modulus characteristic for selected mixes of cold recycling mixes. *Asfaltové vozovky 2009*.
- Paper 394 **Hýzl, P, D Stehlík and M Varaus (2009)**. Functional characteristics of asphalt mixtures with additives enabling the lowering of temperatures. *Asfaltové vozovky 2009*.
- Paper 395 **Hanzík, V, J Plitz and P Sokol (2009)**. Report on the production of low temperature stone mastic asphalts. *Asfaltové vozovky 2009*.

- Paper 396 **Valentin, J, M Macko and P Mondschein (2009)**. Present results of fatigue testing of cold recycling mixes. *Asfaltové vozovky 2009*.
- Paper 397 **Beer, F, K Damm, C Schmeisser and S Stoklásek (2009)**. Evaluation of the application of bituminous crumb rubber modified binder in a German road project. *Asfaltové vozovky 2009*.
- Paper 398 **Eckmann, B, and S Soliman (2009)**. Performance assessment of cold recycling in place. *Asfaltové vozovky 2009*.
- Paper 399 **Polakovič, L, and Z Loveček (2009)**. Utilization of scrap tyres for asphalt pavement courses. *Asfaltové vozovky 2009*.
- Paper 400 **Marcant, B, and J Martin (2009)**. A new technology of rubber modified bitumen meeting performance and environmental requirements. *Asfaltové vozovky 2009*.
- Paper 401 **Žalman, L (2009)**. Hot mix asphalt rubber material. *Asfaltové vozovky 2009*.
- Paper 402 **Kudrna, J, O Dašek and O Burian (2009)**. Properties of asphalt mixtures with crumb rubber modified bitumen. *Asfaltové vozovky 2009*.
- Paper 403 **Stoklásek, S, and C Schmeisser (2009)**. New concept for polymer modified binder from Shell for use in hot mix asphalt with high content of reclaimed asphalt pavement (R-material). *Asfaltové vozovky 2009*.
- Paper 404 **Fiedler, J, and P Bureš (2009)**. Deformation properties of bituminous binders. *Asfaltové vozovky 2009*.
- Paper 405 **Bureš, P, and K Komínek (2009)**. Modified bituminous binder for high (stiffness) modulus mixtures. *Asfaltové vozovky 2009*.
- Paper 406 **Černý, R, J Plitz, D Švadlák and D Maxa (2007)**. New EU testing methods for paving grade bitumens. *Asfaltové vozovky 2007*.
- Paper 407 **Báčová, K, P Gábor and I Gschwendt (2007)**. Deformation characteristics of recycled materials and their use in the pavement structure. *Asfaltové vozovky 2007*.
- Paper 408 **Klaus (2007)**. Experience with low-temperature mixtures in Germany. *Asfaltové vozovky 2007*.
- Paper 409 **Racek, I, J Fiedler, Z Komínek and P Bureš (2007)**. Improvement of rutting resistance of asphalt mixes by modified bitumen. *Asfaltové vozovky 2007*.
- Paper 410 **Zdrálek, P (2007)**. Application of triaxial cyclic compression in testing of asphalt mixtures. *Asfaltové vozovky 2007*.
- Paper 411 **Vacín, O (2007)**. Comparison of cyclic loading tests at CVUT. *Asfaltové vozovky 2007*.
- Paper 412 **Adorjányi, K (2007)**. Fundamental properties of stone mastic asphalt with modifiers. *Asfaltové vozovky 2007*.
- Paper 413 **Zdrálek, P (2007)**. Comparison of different methods for testing permanent deformation. *Asfaltové vozovky 2007*.
- Paper 414 **Svoboda, F, and P Bureš (2007)**. Assessment of the influence of fines. *Asfaltové vozovky 2007*.
- Paper 415 **Králová, E (2007)**. Acrylic fibres Dolanit®AS – properties and use in highway engineering. *Asfaltové vozovky 2007*.

- Paper 416 **Králová, E, J Štěpánek and L Žalman (2007)**. Influence of the additive Licomont BS 100 on the properties of bituminous binders. *Asfaltové vozovky 2007*.
- Paper 417 **Fiedler, J, I Racek, K Komínek and P Pospíšil (2007)**. Chemically cross-linked binder for waterproofing system on bridges. *Asfaltové vozovky 2007*.
- Paper 418 **Sokol, P (2007)**. Comparison of the methods for short-term ageing of bitumens – RTFOT, RFT, TFOT. *Asfaltové vozovky 2007*.
- Paper 419 **Ahmed, S, E V Dave, B Behnia, W G Buttlar and M K Exline (2009)**. Fracture characterization of gap-graded thin bonded wearing course. *Environmentally Friendly Roads (ENVIROAD)*.
- Paper 420 **Eckmann, B, and S Soliman (2009)**. Performance assessment of cold recycling in place. *Environmentally Friendly Roads (ENVIROAD)*.
- Paper 421 **Sybilski, D, W Bańkowski and M Krajewski (2009)**. Applicability of limestone aggregates for high modulus asphalt concrete. *Environmentally Friendly Roads (ENVIROAD)*.
- Paper 422 **Kravchenko, S E (2009)**. Structural stability of asphalt concrete. *Environmentally Friendly Roads (ENVIROAD)*.
- Paper 423 **Bańkowski, W, K Błażejowski, M Gajewski, R Horodecka, I Ruttmar and D Sybilski (2009)**. Validation of innovative pavement structures on test section with use of accelerated loading test. *Environmentally Friendly Roads (ENVIROAD)*.
- Paper 424 **Scholten, E J, W Vonk and J Korenstra (2009)**. Towards green pavements with novel class of SBS polymers for enhanced effectiveness in bitumen and pavement performance. *Environmentally Friendly Roads (ENVIROAD)*.
- Paper 425 **Dreessen, S, J P Pascal (2009)**. Seeking for a relevant binder test method for rutting prediction. *Environmentally Friendly Roads (ENVIROAD)*.
- Paper 426 **Utterodt, R, and R Egervári (2009)**. Effectiveness of the Compactasphalt® technology. *Environmentally Friendly Roads (ENVIROAD)*.
- Paper 427 **Soenen, H, J de Visscher, F Vervaecke, A Vanelstraete, T Tanghe and P Redelius (2009)**. Foamed bitumen in half-warm asphalt: A laboratory study. *Environmentally Friendly Roads (ENVIROAD)*.
- Paper 428 **Beckedahl, H.J, P Sivapatham and S Janssen (2009)**. Heavy loaded asphalt bus lane test sections in the city of Wuppertal - comparison of in situ and lab-test rutting. *Environmentally Friendly Roads (ENVIROAD)*.
- Paper 429 **Zofka, A, I Yut and D Nener-Plante (2009)**. RAP study for asphalt mixtures used in Connecticut. *Environmentally Friendly Roads (ENVIROAD)*.
- Paper 430 **Scherer, J (2009)**. Durable asphalt surfaces with high crack resistance. *Environmentally Friendly Roads (ENVIROAD)*.
- Paper 431 **Van den Bergh, W, and J Stoop (2009)**. The development of an aged-bitumen bound base structure with roofing waste and reclaimed asphalt pavement: State of the Art 2009. *Environmentally Friendly Roads (ENVIROAD)*.
- Paper 432 **Silva, H M R D, J R M Oliveira, C I G Ferreira and P A A Pereira (2009)**. Assessment of the performance of warm mix asphalts in road pavements. *Environmentally Friendly Roads (ENVIROAD)*.

- Paper 433 **Metzker, K, and M P Wistuba (2009).** Comparative study on wax modified bitumen. *Environmentally Friendly Roads (ENVIROAD)*.
- Paper 434 **Neutag, L, U Zieke, H J Beckedahl and K Johannsen (2009).** Crumb rubber modified binders for flexible pavements. *Environmentally Friendly Roads (ENVIROAD)*.
- Paper 435 **Kudrna, J, and O Dašek (2009).** Scrap tyres used in pavement reduce traffic noise. *Environmentally Friendly Roads (ENVIROAD)*
- Paper 436 **Mazé, M, F Delfosse, S F Dumont, E Crews and C Giorgi (2009).** European development of the Tempera[®]/Evotherm DAT[®] process. *Environmentally Friendly Roads (ENVIROAD)*.
- Paper 437 **Behnia, B, E V Dave and W G Buttler (2009).** Fracture characterization of asphalt mixtures with reclaimed asphalt pavement (RAP). *Environmentally Friendly Roads (ENVIROAD)*.
- Paper 438 **Evgenyeva, A G (2009).** Ultrasound and bitumen: new results. *Environmentally Friendly Roads (ENVIROAD)*.
- Paper 439 **Butt, A A, Y Tasdemir and Y Edwards (2009).** Environmental friendly wax modified mastic asphalt. *Environmentally Friendly Roads (ENVIROAD)*.
- Paper 440 **Raab, C H, and M N Partl (2009).** Influence of the gap width between the shearing rings on interlayer shear bond testing. *Environmentally Friendly Roads (ENVIROAD)*.
- Paper 441 **Kischinskiy, S (2009).** Influence of modifier Polydom, and also other types of polymeric additions on properties of bitumen and asphalt-concretes. *Environmentally Friendly Roads (ENVIROAD)*.
- Paper 442 **González, J A L, S Ligier, P Caujolle and G Barreto (2009).** Warm mix asphalts with chemical additives: properties and advantages. *Environmentally Friendly Roads (ENVIROAD)*.
- Paper 443 **Van den Bergh, W, and M F C van de Ven (2009).** Hot recycling of asphalt: experiences in Flanders and the Netherlands. *Environmentally Friendly Roads (ENVIROAD)*.
- Paper 444 **Zhdanyuk, V, Y Prusenko, O Volovyk and K Zhdanyuk (2009).** Rut resistance of asphalt concretes of different aggregate gradation. *Environmentally Friendly Roads (ENVIROAD)*.
- Paper 445 **Tušar, M (2009).** Performance of composite dust in asphalt mixture as an additive to filler. *Environmentally Friendly Roads (ENVIROAD)*.
- Paper 446 **Tóth, C, and J Ureczky (2009).** Determination of master curves for asphalt mixtures by means of IT-CY tests. *Environmentally Friendly Roads (ENVIROAD)*.
- Paper 447 **Sebaaly, H K, E Y Hajj, P E Sebaaly and E Hitti (2009).** Fatigue properties of rubber modified asphalt mixtures. *2nd Workshop on Four Point Bending*.
- Paper 448 **Fontes, L, G. Trichês, J Pais and P Pereira (2009).** Fatigue laws for brazilians asphalt rubber mixtures obtained in 4 point bending tests. *2nd Workshop on Four Point Bending*.
- Paper 449 **Johnson, C M, H U Bahia and A Coenen (2009).** Comparison of bitumen fatigue testing procedures measured in shear and correlations with four-point bending mixture fatigue rubber binders. *2nd Workshop on Four Point Bending*.

- Paper 450 **Neto, S A D, M M Farias and J C Pais (2009)**. Change in fatigue behavior of asphalt hot mixes produced with asphalt rubber binders. *2nd Workshop on Four Point Bending*.
- Paper 451 **Jacobs, M M J, and B W Sluer (2009)**. Fatigue testing of polymer modified asphalt mixtures. *2nd Workshop on Four Point Bending*.
- Paper 452 **Way, G B, K E Kaloush, J M B Sousa and A Zareh (2009)**. Arizona's 15 years of experience using the four point bending beam test. *2nd Workshop on Four Point Bending*.
- Paper 453 **Skotnicki, L, and A Szydło (2009)**. Analysis of HMA stiffness modulus and resistance to fatigue in function of composition. *2nd Workshop on Four Point Bending*.
- Paper 454 **Capitão, S D, A Baptista and L Picado-Santos (2009)**. Statistical analysis of unconventional bituminous mixtures' performance based on 4PB tests. *2nd Workshop on Four Point Bending*.
- Paper 455 **Romagosa, E E, R Maldonado, D Fee, R Dongré and G Reinke (2010)**. Polyphosphoric acid binder modification. *Asphalt Paving Technology 2010*.
- Paper 456 **Bennert, T, and J-V Martin (2010)**. Polyphosphoric acid in combination with styrene-butadiene-styrene block copolymer – Laboratory mixture evaluation. *Asphalt Paving Technology 2010*.
- Paper 457 **d'Angelo, J A (2010)**. Effect of poly phosphoric acid on asphalt binder properties. *Asphalt Paving Technology 2010*.
- Paper 458 **Prowell, B D, E R Brown, R M Anderson, S Shen and S H Carpenter (2010)**. Endurance limit of hot mix asphalt mixtures to prevent bottom-up fatigue cracking. *Asphalt Paving Technology 2010*.
- Paper 459 **Reinke, G, and S Glidden (2010)**. Analytical procedures for determining phosphorus content in asphalt binders and impact of aggregate on quantitative recovery of phosphorus from asphalt binders. *Asphalt Paving Technology 2010*.
- Paper 460 **Ahmed, S, E V Dave, W G Buttlar and M K Exline (2010)**. Fracture properties of gap & dense graded thin bonded overlays. *Asphalt Paving Technology 2010*.
- Paper 461 **Blankenship, P B, and R M Anderson (2010)**. Laboratory investigation of HMA modulus, flow number and flexural fatigue on samples of varying density. *Asphalt Paving Technology 2010*.
- Paper 462 **Ma, T, H U Bahia, E Mahmoud and E Y Hajj (2010)**. Estimating allowable RAP in asphalt mixes to meet target low temperature PG requirements. *Asphalt Paving Technology 2010*.
- Paper 463 **Taylor, A, N Tran, R May, D Timm, M Robbins and B Powell (2010)**. Laboratory evaluation of sulfur-modified warm mix. *Asphalt Paving Technology 2010*.
- Paper 464 **Huurman, M, L T Mo, and M F Woldekidan (2010)**. Mechanistic design of silent asphalt mixtures and its validation. *Asphalt Paving Technology 2010*.
- Paper 465 **Velasquez, R, M Marasteanu, J Labuz and M Turos (2010)**. Evaluation of bending beam rheometer for characterization of asphalt mixtures. *Asphalt Paving Technology 2010*.
- Paper 466 **Archilla, A R (2010)**. Developing master curve predictive equation models for local conditions: A case study for Hawaii. *Asphalt Paving Technology 2010*.

- Paper 467 **Hou, T, B S Underwood and Y R Kim (2010)**. Fatigue performance prediction of North Carolina mixtures using the simplified viscoelastic continuum damage model. *Asphalt Paving Technology 2010*.
- Paper 468 **McGennis, R B (2010)**. Implementation of polyphosphoric acid modification of asphalt binders and related experience. *Asphalt Paving Technology 2010*.
- Paper 469 **Kim, S-S, A Wargo and D Powers (2010)**. Asphalt concrete cracking device to evaluate low temperature performance of HMA. *Asphalt Paving Technology 2010*.
- Paper 470 **Haji, E Y, A Ulloa, R Siddharthan and P E Sebaaly (2010)**. Characteristics of the loading pulse for the flow number performance test. *Asphalt Paving Technology 2010*.
- Paper 471 **Dave, E V, S Ahmed, W G Buttlar, J Bausano and T Lynn (2010)**. Investigation of strain tolerant mixture reflective crack relief systems: an integrated approach. *Asphalt Paving Technology 2010*.
- Paper 472 **Reinke, G, S Glidden, D Herlitzka and S Veglahn (2010)**. PPA modified binders and mixtures: aggregate and binder interactions, rutting and moisture sensitivity of mixtures. *Asphalt Paving Technology 2010*.
- Paper 473 **Masad, E, J Howson, A Bhasin, S Caro and D Little (2010)**. Relationship of ideal work of fracture to practical work of fracture: background and experimental results. *Asphalt Paving Technology 2010*.
- Paper 474 **Masad, E, J Howson, A Bhasin, S Caro and D Little (2010)**. Relationship of ideal work of fracture to practical work of fracture: background and experimental results. *Asphalt Paving Technology 2010*.
- Paper 475 **de Backer, C, J de Visscher, L Glorie, A Vanelstraete, S Vansteenkiste and L Heleven (2008)**. A comparative high-modulus asphalt experiment in Belgium. *TRA2008*.
- Paper 476 **Wagner, M, M P Wistuba and R Blab (2008)**. Low viscous asphalt mixtures – A critical review of FT paraffin modified mixture properties using performance-based test methods. *TRA2008*.
- Paper 477 **Dubois, V, C de la Roche and S Buisson (2008)**. Sensitivity of some asphalts to the wheel tracking test. *TRA2008*.
- Paper 478 **Iwański, M, and G Mazurek (2010)**, Asphalt concrete with low-viscosity modifier. *ICTi 2010*.
- Paper 479 **Thives, L P, G Trichês, P Pereira and J Pais (2010)**. Use of tire rubber to improve fatigue performance of asphalt mixtures. *ICTi 2010*.
- Paper 480 **Racanel, C, A Burlacu and C Surlea (2010)**. Laboratory results obtained on new asphalt mixtures with polymer modified bitumen. *ICTi 2010*.
- Paper 481 **Oliveira, J, H Silva, P Pereira and L Moreno (2010)**. A laboratory study on the fatigue performance of warm mix asphalt mixtures. *ICTi 2010*.
- Paper 482 **Dias, J, F A Batista and M G Lopes (2010)**. Assessment of fatigue resistance and aging of asphalt mixtures in Portugal. *ICTi 2010*.
- Paper 483 **Nikolaides, A F, and E Manthos (2010)**. Wheel tracking performance of asphalt concrete mixture with conventional and modified bitumen. *ICTi 2010*.

- Paper 484 **Lu, X, U Isacsson and J Ekblad (2003)**. Influence of polymer modification on low temperature behaviour of bituminous binders and mixtures. *Materials and Structures 2003*.
- Paper 485 **Gubler, R, M N Partl, F Canestrari and A Grilli (2005)**. Influence of water and temperature on mechanical properties of selected asphalt pavements. *Materials and Structures 2005*.
- Paper 486 **Olard, F, H di Benedetto, A Dony and J-C Vaniscote (2005)**. Properties of bituminous mixtures at low temperatures and relations with binder characteristics. *Materials and Structures 2005*.
- Paper 487 **Bagampadde, U, U Isacsson and B M Kiggundu (2006)**. Impact of bitumen and aggregate composition on stripping in bituminous mixtures. *Materials and Structures 2006*.
- Paper 488 **Edwards, Y, Y Tasdemir and U Isacsson (2006)**. Creep-recovery behavior of bituminous binders and its relation to asphalt mixture rutting influence of commercial waxes and polyphosphoric acid on bitumen and asphalt concrete performance at low and medium temperatures. *Materials and Structures 2006*.
- Paper 489 **Renken, P (2007)**. Quality of porous asphalt layers – Optimierung und Qualitätssicherung Offenporiger Asphaltdeckschichten Teil II. *Forschung Straßenbau und Straßneverkehrstechnik*.
- Paper 490 **Renken, P, and T Lobach (2007)**. Effect of RA in asphalt mixes for binder courses with PmB – Einfluss der zugabe von Ausbauasphalten in Asphaltbinderemischgut mit PmB 45. *Forschung Straßenbau und Straßneverkehrstechnik*.
- Paper 491 **Steinauer, S (2007)**. Comparison of tests procedures for rutting assessment – Vergleich der Prüfverfahren zur Ansprache der Verformungseigenschaften von Asphalt. *Forschung Straßenbau und Straßneverkehrstechnik*.
- Paper 492 **Büchler, Mollenhauer and Renken (2008)**. The influence of polymer modified binders on the results of low temperature and fatigue tests and their change during service life. *Forschung Straßenbau und Straßneverkehrstechnik*.
- Paper 493 **Khedoe, R N, A A A Molenaar and M F C van de Ven (2008)**. Low temperature behavior of very hard bituminous binder material for road applications. *2008-RILEM-Pavement Cracking*.
- Paper 494 **Mohammad, L N, M D Kabir and S Saadeh (2008)**. Evaluation of fracture properties of hot mix asphalt. *2008-RILEM-Pavement Cracking*.
- Paper 495 **van Rooijen, R C, and A H de Bondt (2008)**. Crack propagation performance evaluation of asphaltic mixes using a new procedure based on cyclic semi-circular bending tests. *2008-RILEM-Pavement Cracking*.
- Paper 496 **Velásquez, R, M Turos, M Marasteanu, N Gibson and T Clyne (2008)**. Investigation of low temperature cracking in asphalt mixtures using TSRST. *2008-RILEM-Pavement Cracking*.
- Paper 497 **Vervaecke, F, J Maeck and A Vanelstraete (2008)**. Comparison of the modulus of high-modulus asphalt mixtures – experimental determination and calculation. *2008-RILEM-Pavement Cracking*.
- Paper 498 **Zeghal, I (2008)**. Thermal cracking prediction using artificial neural network. *2008-RILEM-Pavement Cracking*.

- Paper 499 **Büchler, Mollenhauer, Wistuba and Renken (2009)**. Ageing of stone mastic asphalt and evaluation of cracking resistance. *Bearing Capacity of Roads, Railways and Airfields*.
- Paper 500 **de Visscher, J, and A Vanelstraete (2009)**. Equiviscous temperature based on low shear viscosity: Evaluation as binder indicator for rutting and critical discussion of the test procedure. *ATCBM2009*.
- Paper 501 **de Visscher, J, A Vanelstraete, A Leuridan, N Pierard, E Schelkens and P du Bus de Warnaffe (2009)**. New tests for polymer-modified binders: Results of a Belgian round robin test. *ATCBM2009*.
- Paper 502 **Dreessen, S, J P Planche and V Gardel (2009)**. A new performance related test method for rutting prediction: MSCRT. *ATCBM2009*.
- Paper 503 **Hase, M, and C Oelkers (2009)**. Influence of low temperature behaviour of PmB on life cycle. *2009-RILEM-Advanced Testing and Characterisation of Bituminous Materials*.
- Paper 504 **Syblinski, D, M Gajewski, W Bankowski, H Soenen, E Chailleux and G Gauthier (2009)**. Binder fatigue properties and the results of the Rilem Round Robin Test. *ATCBM2009*.
- Paper 505 **Tusar, M, M R Turk, W Bankowski, L Wiman and B Kalman (2009)**. Evaluation of modified bitumen, high modulus asphalt concrete and steel mesh as materials for road upgrading. *ATCBM2009*.
- Paper 506 **Wistuba, M, K Mollenhauer and K Metzker (2009)**. Assessing low temperature properties of asphalt materials by means of static testing techniques. *Bearing Capacity of Roads, Railways and Airfields*.
- Paper 507 **Karcher (2010)**. Effect of different polymer-modified bitumen of the same sort on the fatigue behavior of asphalt. *USAP2010*.
- Paper 508 **Renken, P, M Wistuba, J Grönniger and K Schindler (2010)**. Adhesion of bitumen on aggregates. *Forschung Straßenbau und Straßneverkehrstechnik*.
- Paper 509 **Roos, R, C Karcher, A Wittenberg and P Plachkova (2010)**. Relationship between the elastic recovery of recycled PmB and the properties of the asphalt mixture. *Forschung Straßenbau und Straßneverkehrstechnik*,
- Paper 510 **Hase, M (2011)**. Bindemittel und die Gebrauchseigenschaften von Asphalt. *Asphaltstraßentagung 2011*.
- Paper 511 **Mollenhauer, K, V Mouillet, N Piérard, T Gabet, M Tušar and A Vanelstraete (2011) & De Visscher, J.; Mollenhauer, K.; Raaberg, J.; Khan, R. (2012)**. Chemical and physical compatibility of new and aged binders from RA % Mix design and performance of asphalt with RA. *Re-Road Deliverables D2.3 and D2.4, 2011 & 2012*.
- Paper 512 **Plug, C P, A H de Bondt and H Roos (2013)**. Performance of bitumen 70/100 obtained from different suppliers. *2013-EATA*.
- Paper 513 **Šušteršič, E; M Tusar, A Zupanciv (2013)**. Asphalt concrete modification with waste PMMA/ATH. *Materials and Structures 2013*.
- Paper 514 **Wellner, F, M Radenberg, D Ascher and R Cetinkaya (2013)**. Determination of the ageing properties of asphalt mixtures as a general basis of pavement design and prognosis of the service life/development of damages (In German). *Forschung Straßenbau und Straßneverkehrstechnik*.

- Paper 515 **Xiao, Newton, Putman, Punith and Amirkhanian (2013)**. A long-term ultra-violet aging procedure on foamed WMA mixtures. *Materials and Structures 2013*.
- Paper 516 **Bueno, Hugener and Partl (2014)**. Fracture toughness evaluation of bituminous binders at low temperatures. *Material & Structures 2014*.
- Paper 517 **Laukkanen, O-V, H Soenen, T Pellinen, S Heyrman and G Lemoine (2014)**. Creep-recovery behavior of bituminous binders and its relation to asphalt mixture rutting. *Materials and Structures 2014*.
- Paper 518 **Njead, Gholami, Naderi and Rahi (2014)**. Evaluation of rutting properties of high density polyethylene modified binders. *Material and Structures 2014*.
- Paper 519 **Radenberg, M.** Einfluss der chemischen, rheologischen und physikalischen Grundeigenschaften von Straßenbaubitumen auf das Adhäsionsverhalten unterschiedlicher Gesteinskörnungen DAV/DAI, AiF-Forschungsvorhaben Nr. 16639 N/1, http://www.asphalt.de/site/startseite/literatur/infomaterial_download/forschungsberichte/.
- Paper 520 **Zaumanis, Mallick and Frank (2014)**. Evaluation of different recycling agents for restoring aged asphalt binder and performance of 100 % recycled asphalt. *Materials and Structures 2014*.
- Paper 531 **Mangiafico, S, H di Benedetto, C Sauzéat, F Olard, S Pouget, S Dupriet, L Planque and R Van Rooijen (2013)**. Statistical analysis of the influence of RAP and mix composition on viscoelastic and fatigue properties of asphalt mixes. *Materials and Structures 2013*.
- Paper 532 **Tan, Y-Q, H-N Xu, Z-J Dong and W-Q Gong (2008)**. Effect of aggregate grading on low temperature cracking resistance in asphalt mixtures base on mathematical statistic. *2008-RILEM-Pavement Cracking*.
- Paper 533 **Renken, P (2012)**. Walzasphalte mit viskositätsabsenkenden Additiven – Entwicklung und Optimierung der Eignungs- und Kontrollprüfungsverfahren und Bestimmung der Einflüsse auf die performance-orientierten Asphalteigenschaften. DAV/DAI, AiF-Forschungsvorhaben Nr. 15589 N, http://www.asphalt.de/site/startseite/literatur/infomaterial_download/forschungsberichte/.
- Paper 534 **Binh, T T, R A Hassan, T M Boral (2010)**. Effects of increased reclaimed asphalt pavement on the performance of a recycled hot asphalt mix. *ARRB2010*.
- Paper 535 **Urquhart, R, M Budija and G Wilson (2010)**. Investigations into the relationship between binder consistency/underlying viscosity and asphalt rutting. *ARRB2010*.
- Paper 536 **Kamaraj, C, M N Naghabhushana, P K Jain, B M Sharma, S Gangopadhyay, Prashant, M S Amarnath and D India (2010)**. Laboratory investigation on the performance of warm mix based thin stone matrix asphalt mix for urban roads. *ARRB2010*.
- Paper 537 **Kumar, P, and M P Anand (2010)**. Laboratory study on performance of mastic asphalt. *ARRB2010*.
- Paper 538 **Pais, J C, and M J C Minhoto (2010)**. The prediction of fatigue life of asphalt mixtures using four-point bending tests. *ARRB2010*.

- Paper 539 **Stubbs, A, M Saleh and H Jeffery-Wright (2010)**. An investigation of viscoelastic and fatigue behaviour of hot mix asphalt. *ARRB2010*.
- Paper 540 **de Vischer, J (2010)**. Performance of asphalt produced at reduced temperatures. *TRA2010*.
- Paper 541 **Adnan, Qadir, Murat and Guler (2010)**. Effect of aggregate type and rate of temperature change on fracture strength of asphalt concrete. *TRA2010*,
- Paper 542 **Yang, J, X Zhang, H Zhu, Z Chen, W Tian and X Zhang (2010)**. Performance evaluation of superpave asphalt mixture with anti-rutting additives. *TRA2010*,
- Paper 543 **Wojciech, Bańkowski, Marcin, Gajewski, Dariusz and Sybilski (2010)**. Full scale testing of high modulus asphalt concrete in Poland. *TRA2010*,
- Paper 544 **Pap, I (2010)**. Investigation of asphalt mixture behaviour at low and high air temperatures. *TRA2010*,
- Paper 545 **Jones, D, R Wu and C Barros (2010)**. Interim results from the California warm mix asphalt study. *ARRB2010*.
- Paper 546 **Pais, J, P Pereira, M Minhoto and A Baptista (2008)**. Recycling of asphalt pavements with asphalt rubber. *EPAM 3*.
- Paper 547 **Aksoy, A, E Iskender and H Ozen (2008)**. Rutting comparison of laboratory and field samples with verified repeated creep tests in asphalt mixtures. *EPAM 3*.
- Paper 548 **Baptista, A M C, P-S Luís, D C Silvino and J Oliveira (2008)**. Performance-based mix design method for bituminous hot-mix recycling in plant. *EPAM 3*.
- Paper 549 **Silva, H M R D, C A O F Palha, D Gardete and S D Capitão (2008)**. Study on the consequences of affixing the CE marking to bituminous mixtures. *EPAM 3*.
- Paper 550 **Silva, H M R D, J R M Oliveira and L G Picado-Santos (2008)**. Influence of temperature on the fatigue life of flexible pavements. *EPAM 3*.
- Paper 551 **Gaarkeuken, B (2010)**. Quality control on open porous asphalt (Dutch). *Infradagen 2010*.
- Paper 552 **Kringos, N, et al. (2010)**. Simulation of frost damage in asphalt mixtures (Dutch). *Infradagen 2010*.
- Paper 553 **Safaei, S, et al. (2014)**. Implications of warm mix asphalt on the long term oxidative aging and fatigue performance of asphalt binders and mixtures. *RMPD-2014*.
- Paper 554 **Mensching, D J, et al. (2014)**. Low temperature properties of plant produced RAP mixtures in the North East. *RMPD-2014*.
- Paper 555 **Tabatabaee, H A, H U Bahia (2014)**. Establishing use of asphalt binder cracking tests, for prevention of pavement cracking. *RMPD 2014*.
- Paper 556 **Niu, T, R Roque and G A Lopp (2014)**. Development of a binder fracture test to determine fracture energy properties. *RMPD 2014*.
- Paper 557 **Pérez-Jiménez, F, O Reyes-Ortiz, R Miró and A H Martínez (2009)**. Fatigue behaviour of bituminous binders, as measured in the laboratory. *TRB2009*.
- Paper 558 **Shen, S, H-M Chiu and H Huang (2009)**. Fatigue and healing in asphalt binders. *TRB2009*.

- Paper 559 **Reyes Lizcano, F, C Lizarazo, A Figueroa, M Candia, G Flintsch and S W Katicha (2009).** Dynamic characterization of hot-mix asphalt mixtures using modified and conventional asphalts in Colombia. *TRB2009*.
- Paper 560 **Wen, H, and H Bahia (2009).** Characterizing fatigue of asphalt binders using viscoelastic continuum damage mechanics. *TRB2009*.
- Paper 561 **Reyes, M, I B Kazatchkov, J Stastna and L Zanzotto (2009).** Modelling of repeated creep and recovery experiments in asphalt binders. *TRB2009*.
- Paper 562 **d'Angelo, J, and R Dongré (2009).** Practical use of the mscr test: characterization of SBS dispersion and other additives in PMA binders. *TRB2009*.
- Paper 563 **Tabatabaee, N, and H A Tabatabaee (2010).** Multiple stress creep and recovery and time sweep fatigue tests: Crumb rubber modified binder and mixture performance. *TRB2010*.
- Paper 564 **Wen, H, M E Kutay and S Shen (2010).** Evaluation of the effects of asphalt binder on the properties of hot mix asphalt at intermediate temperatures. *TRB2010*.
- Paper 565 **Haritonovs, V, M Zaumanis, G Brencis and J Smirnovs (2012).** Performance based evaluation on the use of different waste materials in asphalt. *TRA2012*.
- Paper 566 **Puchard, G (2012).** Experiences on low temperature (LT) asphalts in Hungarian road building. *TRA2012*.